frontiers | Research Topics

Cross-reactive immunity and COVID-19

Edited by
Alberto Beretta, Ahmed Yaqinuddin, Aristo Vojdani and Pedro A. Reche

Published in
Frontiers in Immunology

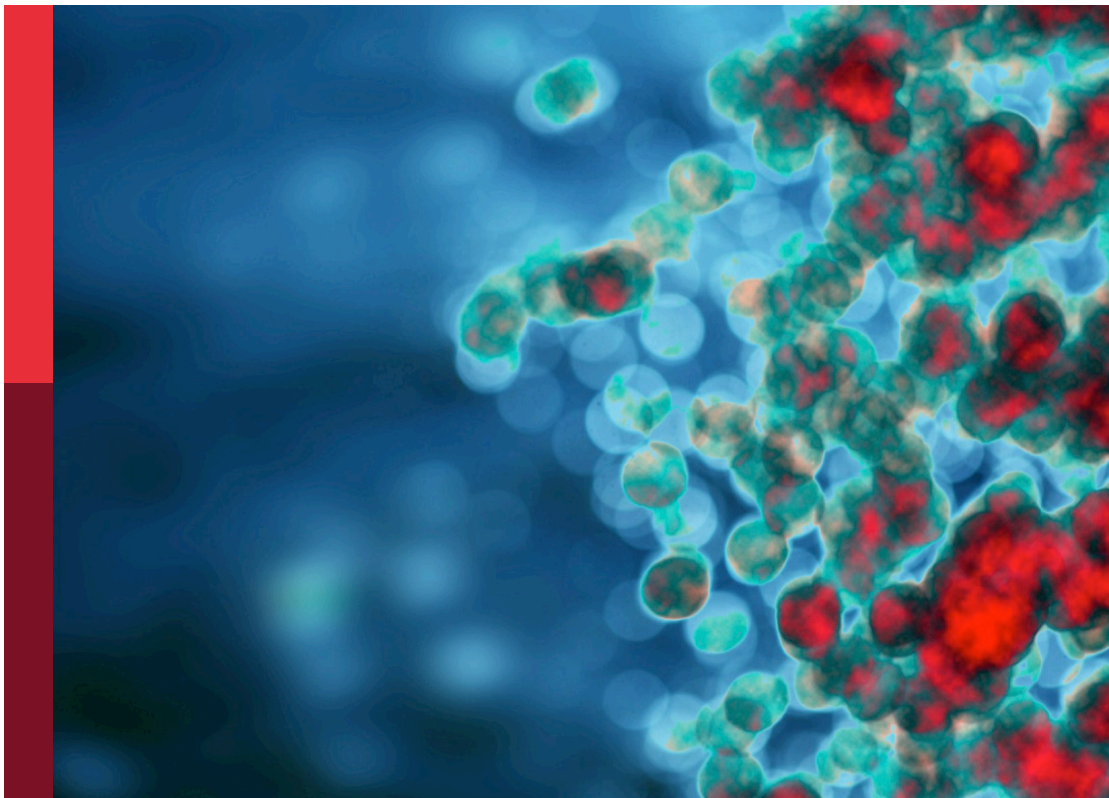

ISSN 1664-8714
ISBN 978-2-8325-5878-2
DOI 10.3389/978-2-8325-5878-2

About Frontiers

Frontiers is more than just an open access publisher of scholarly articles: it is a pioneering approach to the world of academia, radically improving the way scholarly research is managed. The grand vision of Frontiers is a world where all people have an equal opportunity to seek, share and generate knowledge. Frontiers provides immediate and permanent online open access to all its publications, but this alone is not enough to realize our grand goals.

Frontiers journal series

The Frontiers journal series is a multi-tier and interdisciplinary set of open-access, online journals, promising a paradigm shift from the current review, selection and dissemination processes in academic publishing. All Frontiers journals are driven by researchers for researchers; therefore, they constitute a service to the scholarly community. At the same time, the *Frontiers journal series* operates on a revolutionary invention, the tiered publishing system, initially addressing specific communities of scholars, and gradually climbing up to broader public understanding, thus serving the interests of the lay society, too.

Dedication to quality

Each Frontiers article is a landmark of the highest quality, thanks to genuinely collaborative interactions between authors and review editors, who include some of the world's best academicians. Research must be certified by peers before entering a stream of knowledge that may eventually reach the public - and shape society; therefore, Frontiers only applies the most rigorous and unbiased reviews. Frontiers revolutionizes research publishing by freely delivering the most outstanding research, evaluated with no bias from both the academic and social point of view. By applying the most advanced information technologies, Frontiers is catapulting scholarly publishing into a new generation.

What are Frontiers Research Topics?

Frontiers Research Topics are very popular trademarks of the *Frontiers journals series*: they are collections of at least ten articles, all centered on a particular subject. With their unique mix of varied contributions from Original Research to Review Articles, Frontiers Research Topics unify the most influential researchers, the latest key findings and historical advances in a hot research area.

Find out more on how to host your own Frontiers Research Topic or contribute to one as an author by contacting the Frontiers editorial office: frontiersin.org/about/contact

Cross-reactive immunity and COVID-19

Topic editors

Alberto Beretta — Independent researcher, Milano, Italy
Ahmed Yaqinuddin — Alfaisal University, Saudi Arabia
Aristo Vojdani — Immuno Sciences Lab Inc, United States
Pedro A. Reche — Complutense University of Madrid, Spain

Citation

Beretta, A., Yaqinuddin, A., Vojdani, A., Reche, P. A., eds. (2025). *Cross-reactive immunity and COVID-19*. Lausanne: Frontiers Media SA.
doi: 10.3389/978-2-8325-5878-2

Table of contents

frontiers | Frontiers in Immunology

TYPE Editorial
PUBLISHED 09 December 2024
DOI 10.3389/fimmu.2024.1509379

OPEN ACCESS

EDITED AND REVIEWED BY
Randi Vita,
La Jolla Institute for Immunology (LJI), United States

*CORRESPONDENCE
Aristo Vojdani
drari@msn.com

RECEIVED 10 October 2024
ACCEPTED 25 November 2024
PUBLISHED 09 December 2024

CITATION
Vojdani A, Yaqinuddin A, Beretta A and Reche PA (2024) Editorial: Cross-reactive immunity and COVID-19.
Front. Immunol. 15:1509379.
doi: 10.3389/fimmu.2024.1509379

Editorial: Cross-reactive immunity and COVID-19

Aristo Vojdani[1,2]*, Ahmed Yaqinuddin[3], Alberto Beretta[4] and Pedro A. Reche[5]

[1]Laboratory, Immunosciences Lab., Inc., Los Angeles, CA, United States, [2]Administration, Cyrex Labs, LLC, Phoenix, AZ, United States, [3]Research and Graduate Studies, Graduate Programs, College of Medicine, Alfaisal University, Riyadh, Saudi Arabia, [4]Solongevity Research, SoLongevity Healthcenters, Milano, Italy, [5]Dpto de Immunologia, Facultad de Medicina, U. Complutense de Madrid, Madrid, Spain

KEYWORDS

cross-reactivity, COVID-19, long COVID, SARS-CoV-2, vaccines, pre-existing immunity

Editorial on the Research Topic
Cross-reactive immunity and COVID-19

SARS-CoV-2 and COVID-19 impacted the world like a modern plague, stretching icy fingers across the globe. Humanity was even more horrified upon finding that this new plague came with variants, and surviving one version of the virus did not automatically grant immunity to all variants. But as has happened with previous pandemics, the deadliness and reach of COVID-19 has subsided into a slightly worrisome status quo due to the advancements of medical science and the virus' own evolution into less harmful forms. The intense scrutiny that SARS-CoV-2 and COVID-19 received during the height of their deadly assault on the world has revealed things that are now used to combat this pandemic.

We now know that, unlike us, our immune system was not so surprised by SARS-CoV-2 since cross-reactive immunity to SARS-CoV-2 existed prior to the COVID-19 pandemic. Cross-reactive immunity is mediated by antibodies and memory B and T cells elicited by a specific pathogen or antigen that can also react to other pathogens or antigens (1) Cross-reactivity is a main feature of adaptive immunity, which is highly favored by the recognition of small portions within protein antigens (epitopes) (2) and the poly-specificity of cognate B and T cell receptors (3, 4). Human common cold coronaviruses (hCoVs) have received major attention as potential sources of cross-reactive immunity to SARS-CoV-2 (5). However, immune cross-reactivity has also been reported between SARS-CoV-2 and unrelated viruses (6), bacteria (7), vaccines (8, 9) and even food antigens (9). Activation of cross-reactive immunity is not always protective and can also produce immunopathology (10). Moreover, immune cross-reactivity is a two-way road and SARS-CoV-2 infection as well as COVID-19 vaccines can also induce cross-reactive immunity. Indeed, immune cross-reactivity between SARS-CoV-2 and COVID-19 vaccines with human tissues has been shown, raising the possibility that autoimmune reactivity can result from SARS-CoV-2 infection and COVID-19 vaccines (see Figure 1) (11).

Clearly, pre-existing cross-reactive immunity must have a major impact in shaping the immune response to the virus and to COVID-19 vaccines, but to what extent and its contribution to protection is still undetermined. Likewise, SARS-CoV-2 and COVID-vaccines can have profound cross-reactive immunological consequences that need to be investigated. In this Research Topic of Frontiers in Immunology about "*Cross-Reactive*

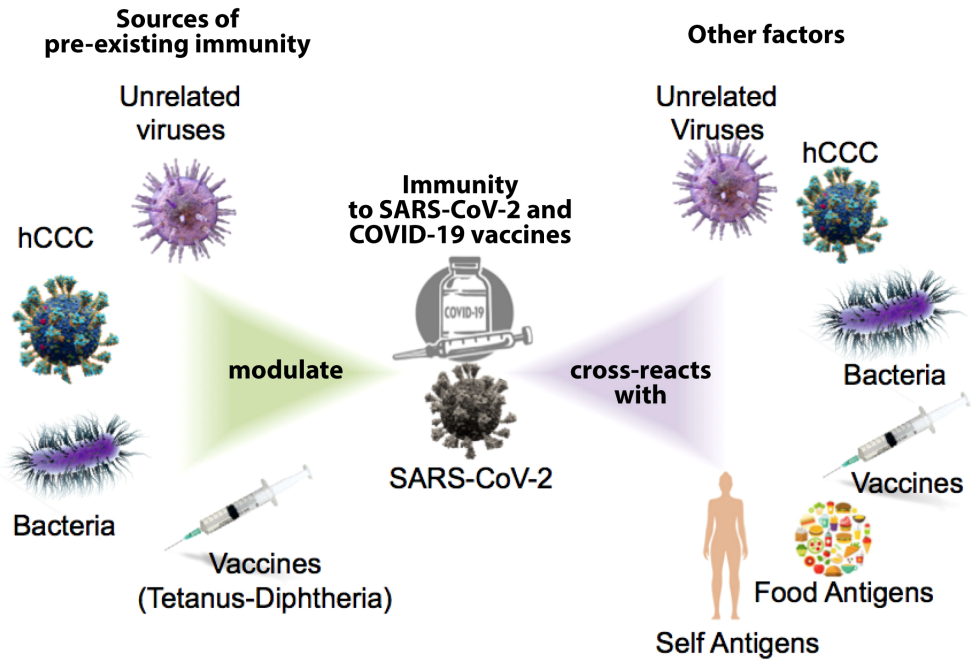

FIGURE 1
Potential sources of present immunity shape the response to SARS-CoV-2 and the COVID-19 vaccine; the immune response to SARS-CoV-2 and COVID vaccines can also produce cross-reactive immune responses to other factors.

Immunity and COVID-19," editors Aristo Vojdani, Pedro Reche, Alberto Beretta and Ahmed Yaqinuddin have gathered an impressive Research Topic of articles investigating sources of immune cross-reactivity with SARS-CoV-2, contribution to protection, COVID-19 course and its ancillary condition, long COVID.

On the face of it, it would seem that cross-reactive immunity would be a welcome weapon to wield against COVID-19. Pedro Reche, one of the editors of this Research Topic, published an article in 2020 (8) in which he concluded, "Overall, our results clearly support that cross-reactive immunity from DTP vaccines can be protecting children against SARS-CoV-2 and could protect the general population." In 2022, Fonte et al. looked at the lower susceptibility of children to SARS-CoV-2 infection and concluded that the lower incidence and severity of the disease in children could be due to nonspecific resistance to SARS-CoV-2 generated by the childhood vaccines received by the subjects (12).

The value of this general protection or immunity against SARS-CoV-2 and its variants is echoed by Chao et al.'s contribution to this Research Topic. These authors report that broadly neutralizing ability is critical for developing the next generation SARS-CoV-2 vaccine. They found that a specific homologous vaccine was insufficient for dealing with the Omicron virus variant, which had very different antigenic characteristics from the original. They also found that anti-ACE2 autoantibodies were significantly increased in all vaccinated test groups.

The Omicron variant also proved problematic for Li M. et al.'s study in this Research Topic. They found that vaccination contributes significantly in limiting the spread of SARS-CoV-2. However, they also found that this vaccine protection is not efficient against the Omicron variant. This was evidenced by the reduction in the binding of SARS-CoV-2 antibody-positive human sera to Omicron RBDs compared to its homogenous recombinant RBDs.

In their own article, Lunderberg et al. had a slightly different suggestion for dealing with the problem of SARS-CoV-2 variants escaping the host's immune response. Previously, researchers have identified IgG1 type pan-neutralizing antibodies (neutAbs) which can effectively neutralize several human coronaviruses, including SARS-CoV-2 and its variants, but with existing limitations and deficiencies in their efficiency and application. Lunderberg et al. proposed that using Reverse Technology 3.0 can help to further the use of this innate-like defense mechanism.

We have already mentioned that the emergence of SARS-CoV-2 variants prevents acquiring general immunity to the disease. Thompson et al. investigated the impact of cross-reactive immunity on the emergence of these variants. They found that if cross-reactivity immunity is complete, that the antigenically related novel variant must be more transmissible than the previous virus in order to invade the population. They highlighted that a fast assessment of the level of cross-reactive immunity conferred by related viruses against novel SAR-CoV-2 variants is essential to assessing the risk posed by those variants.

The more we know about SARS-CoV-2 variants, then, the better it is for understanding the virus, its diseases, and how to deal with them. Kuthning et al. monitored SARS-CoV-2 specific antibodies in children and adolescents to determine whether the S1-specific antibody response can identify the infecting variant of concern (VoC), estimate the prevalence of silent infections, and

test whether vaccination or infection with SARS-CoV-2 induces hCoV cross-reactive antibodies. They concluded that the antibody response to the S1 domain of the SARS-CoV-2 spike protein is highly specific, providing important information about the infecting VoC and revealing clinically silent infections.

The source and role of SARS-CoV-2 cross-reactive antibodies have received major attention in this Research Topic. In an article by Peng et al., the authors show that monoclonal antibodies constructed from COVID-19 convalescent memory B cells exhibited potent binding activity to the S2 spike subunit from MERS-CoV and other hCoVs. The authors did not investigate whether the cross-reactive antibodies resulted from the activation of pre-existing memory B cells or from the activation of naive B cells but, regardless, their results will be useful in the diagnosis of multiple coronaviruses. Although the S2 spike subunit SARS-CoV-2 can be the target of neutralizing antibodies, most of them target the receptor binding domain (RBD) in the spike S1 subunit, which is much less conserved that the S2 subunit (13).

Consistently, Adami et al. report that anti-RBD IgG antibodies from endemic hCoVs do not protect against the acquisition of SARS-CoV-2 infection among exposed uninfected individuals. In line with this result, Lin et al. reports that pre-existing humoral immunity to hCoVs negatively impacts the protective SARS-CoV-2 antibody response (14). Additionally, in one of the articles published in this Research Topic, Li N et al. looked at whether pre-existing antibodies induced by low pathogenic human coronaviruses (LPH-CoVs) in children can cross-react with SARS-CoV-2. They found that the seroprevalence of four analyzed LPH-CoVs reached 75.84%, and about 24.64% of the seropositive samples had cross-reactive IgG antibodies against the nucleocapsid S and against the receptor binding domain (RBD) antigens of SARS-CoV-2. These data suggest that children's pre-existing antibodies to LPH-CoVs have limited cross-reactive neutralizing antibodies against SARS-CoV-2.

In contrast, Cheng Y. et al. report antigenic cross-reactivity between the SARS-CoV-2 RBD and dengue virus, which in dengue patients can lead to anti-SARS-CoV-2 S1-RBD antibodies hindering pathogenicity. Likewise, SARS-CoV-2 and COVID-19 vaccines may in some occasions lead to pathological antibodies due to cross-reactivity. This possibility is illustrated by the case report presented by Shimizu et al., showing a new-onset dermatomyositis following COVID-19. The diagnosis was confirmed by the detection of anti-synthetase autoantibodies and other biochemical analyses. However, they did not provide evidence that this development of dermatomyositis may be due to cross-reactivity between SARS-CoV-2 antigens and tissue antigens involved in this disease. Zhong et al. present two case reports in which patients with bacterial pneumonia and high elevated immunoglobins did not get infected with SARS-CoV-2. This report provides experimental support onto the possibility that bacteria can elicit protective cross-reactive antibodies to SARS-CoV-2, as suggested by *in silico* works (15).

Unlike cross-reactive humoral immunity, which may enhance disease severity (16), there is mounting evidence of the protective role of SARS-CoV-2 cross-reactive T cells (17). The work by Coulon et al. support a protective role for alpha-hCoV-specific memory T cells cross-reactive with SARS-CoV-2. However, hCoV cannot account for all pre-existing SARS-CoV-2 cross-reactive T cells (18), and it is still unproven that hCoV can prime T cells cross-reactive with SARS-CoV-2. Interestingly, such a proof is provided in this Research Topic for tetanus-diphtheria vaccine. Thus, Fernandez et al. showed that antigen-inexperienced naive T cells primed with tetanus-diphtheria vaccine recognized SARS-CoV-2-specific CD8 T cell epitopes, as anticipated by Reche in a seminal in *silico* study (8). Given that children received several immunizations with vaccines containing tetanus-dihptheria antigens, the results by Fernandez et al. support that tetanus-diphtheria vaccine likely had a major contribution shaping exiting SARS-CoV-2 T cell responses. However, pre-existing cross-reative T cells may not always be protective. Thus, Ng'uni et al. report that pre-existing endemic NL63-coronavirus-specific T cells are associated with impaired SARS-CoV-2-specific T cell responses.

Continuing the thread of the protective or supportive role of T cells against SARS-CoV-2, in their article in this Research Topic, Ziehe et al. sought to study the human cytomegalovirus (HCMV) as a risk factor for the development of sepsis in COVID 19 patients. They found that although HCMV was significantly higher in COVID-19 patients compared to controls, the cross-reactivity of HCMV-specific CD8+ T cells with SARS-CoV-2 peptides might actually confer some protection to HCMV-seropositive patients.

On the other hand, Leung et al. found something interesting about B cells. We know that infection by SARS-CoV-2 can lead past COVID-19 to long COVID. Leung et al. examined different early immune factors in both hospitalized and non-hospitalized patients with COVID-19, and correlated the immune factors with the development of long COVID. They found that the predominant early immune indicator of long COVID was double-negative B cells, indicating a potentially important role for these cells in the development of the disease.

In another attempt to predict the progression and severity of COVID-19, You et al. measured serum levels of ACE2 and AXL in patients who were categorized into non-severe and severe cases. They compared these levels with SARS-CoV-2 IgG and IgM antibody titers at different time points in post-COVID infections. They found that in severe COVID-19 cases, a decrease in AXL level with an increase in SARS-CoV-2 IgG level predicts COVID-19 progression.

Pre-existing cross-reactive immunity have surely shaped the responses to COVID-19 vaccines. However, some COVID-19 vaccines may activate more than other cross-reactive immunity. This fact is exemplified in the report by Henze et al. These authors show that adenovirus-vector-based ChAdOx1 vaccine did not reactivate cross-reactive cellular and humoral immunity compared to mRNA-based BNT162b2.

One of this Research Topic's submissions had suggestions for treatment. Saito et al. observed that a significant percentage of SARS-CoV-2-infected individuals develop long COVID which overlaps with myalgic encephalomyelitis/chronic fatigue syndrome (ME/CFS). They identified alterations in metabolic

pathways, including the elevation of plasma pro-inflammatory cytokines with a reduction in ATP in long COVID patients. These metabolic abnormalities not only help in better understanding the pathophysiology of long COVID but also in finding supplements with potential therapeutic implications which were suggested by the researchers.

Taken all together, the 19 articles in this Research Topic examine cross-reactive immunity concerning SARS-CoV-2 and COVID-19. They highlight the intricate interplay between prior immune responses and the evolving viral landscape. The information obtained implies that response to antibodies and immune cells are likely to be critical in both the risk of infection and the response to vaccines. Although there are encouraging signs that pre-existing immunity may provide a degree of protection, the heterogeneity in responses—particularly against new variations such as Omicron—suggests that this phenomenon is not universally effective. As the pandemic evolved, it became evident that understanding of mechanisms involved in cross-reactive immunity will be essential for developing strategies to fight against COVID-19 and its variants.

Author contributions

AV: Project administration, Writing – original draft, Writing – review & editing. AY: Writing – original draft, Writing – review & editing. AB: Writing – original draft, Writing – review & editing. PR: Writing – original draft, Writing – review & editing.

Acknowledgments

We wish to thank all the reviewers who accepted and devoted their time and effort into guiding the authors into making their submissions the best they could be.

Conflict of interest

Author AV was employed by the company Immunosciences Lab., Inc. Author AV was employed by the company Cyrex Labs, LLC.

The remaining authors declare that the research was conducted in the absence of any commercial or financial relationships that could be construed as a potential conflict of interest.

The author(s) declared that they were an editorial board member of Frontiers, at the time of submission. This had no impact on the peer review process and the final decision.

Publisher's note

References

1. Agrawal B. Heterologous immunity: role in natural and vaccine-induced resistance to infections. *Front Immunol.* (2019) 10:2631. doi: 10.3389/fimmu.2019.02631

2. Sanchez-Trincado JL, Gomez-Perosanz M, Reche PA. Fundamentals and methods for T- and B-cell epitope prediction. *J Immunol Res.* (2017) 2017:2680160. doi: 10.1155/2017/2680160

3. Van Regenmortel MH. Specificity, polyspecificity, and heterospecificity of antibody-antigen recognition. *J Mol Recognit.* (2014) 27:627–39. doi: 10.1002/jmr.v27.11

4. Sewell AK. Why must T cells be cross-reactive? *Nat Rev Immunol.* (2012) 12:669–77. doi: 10.1038/nri3279

5. Ng KW, Faulkner N, Wrobel AG, Gamblin SJ and Kassiotis G. Heterologous humoral immunity to human and zoonotic coronaviruses: Aiming for the achilles heel. *Semin Immunol.* (2021) 55:101507. doi: 10.1016/j.smim.2021.101507

6. Murray SM, Ansari AM, Frater J, Klenerman P, Dunachie S, Barnes E, et al. The impact of pre-existing cross-reactive immunity on SARS-CoV-2 infection and vaccine responses. *Nat Rev Immunol.* (2023) 23:304–16. doi: 10.1038/s41577-41022-00809-x

7. Eggenhuizen PJ, Ng BH, Chang J, Cheong RMY, Yellapragada A, Wong WY, et al. Heterologous immunity between SARS-CoV-2 and pathogenic bacteria. *Front Immunol.* (2022) 13:821595. doi: 10.3389/fimmu.2022.821595

8. Reche PA. Potential cross-reactive immunity to SARS-CoV-2 from common human pathogens and vaccines. *Front Immunol.* (2020) 11:586984. doi: 10.3389/fimmu.2020.586984

9. Vojdani A, Vojdani E, Melgar AL and Redd J. Reaction of SARS-CoV-2 antibodies with other pathogens, vaccines, and food antigens. *Front Immunol.* (2022) 13:1003094. doi: 10.3389/fimmu.2022.1003094

10. Sharma S, Thomas PG. The two faces of heterologous immunity: protection or immunopathology. *J Leukoc Biol.* (2014) 95:405–16. doi: 10.1189/jlb.0713386

11. Vojdani A, Vojdani E and Kharrazian D. Reaction of human monoclonal antibodies to SARS-CoV-2 proteins with tissue antigens: Implications for autoimmune diseases. *Front Immunol.* (2021) 11:617089. doi: 10.3389/fimmu.2020.617089

12. Fonte L, Ginori M, Garcia G, Hernandez Y, de Armas Y, Calderon EJ. Nonspecific effects of infant vaccines make children more resistant to SARS-CoV-2 infection. *Children (Basel).* (2022) 9:1858. doi: 10.3390/children9121858

13. Ballesteros-Sanabria L, Pelaez-Prestel HF, Ras-Carmona A and Reche PA. Resilience of spike-specific immunity induced by COVID-19 vaccines against SARS-CoV-2 variants. *Biomedicines.* (2022) 10:996. doi: 10.3390/biomedicines10050996

14. Lin CY, Wolf J, Brice DC, Sun Y, Locke M, Cherry S, et al. Pre-existing humoral immunity to human common cold coronaviruses negatively impacts the protective SARS-CoV-2 antibody response. *Cell Host Microbe.* (2022) 30:83–96.e84. doi: 10.1016/j.chom.2021.1012.1005

15. Bodas-Pinedo A, Lafuente EM, Pelaez-Prestel HF, Ras-Carmona A, Subiza JL, Reche PA. Combining different bacteria in vaccine formulations enhances the chance for antiviral cross-reactive immunity: a detailed in silico analysis for influenza A virus. *Front Immunol.* (2023) 14:1235053. doi: 10.3389/fimmu.2023.1235053

16. Wratil PR, Schmacke NA, Karakoc B, Dulovic A, Junker D, Becker M, et al. Evidence for increased SARS-CoV-2 susceptibility and COVID-19 severity related to pre-existing immunity to seasonal coronaviruses. *Cell Rep.* (2021) 37:110169. doi: 10.111016/j.celrep.112021.110169

17. Kundu R, Narean JS, Wang L, Fenn J, Pillay T, Fernandez ND, et al. Cross-reactive memory T cells associate with protection against SARS-CoV-2 infection in COVID-19 contacts. *Nat Commun.* (2022) 13:80. doi: 10.1038/s41467-41021-27674-x

18. Tan CCS, Owen CJ, Tham CYL, Bertoletti A, van Dorp L, Balloux F. Pre-existing T cell-mediated cross-reactivity to SARS-CoV-2 cannot solely be explained by prior exposure to endemic human coronaviruses. *Infect Genet Evol.* (2021) 95:105075. doi: 10.1016/j.meegid.2021.105075

frontiers | Frontiers in Immunology

TYPE Perspective
PUBLISHED 28 July 2022
DOI 10.3389/fimmu.2022.960195

OPEN ACCESS

EDITED BY
Ahmed Yaqinuddin,
Alfaisal University, Saudi Arabia

REVIEWED BY
Junaid Kashir,
Alfaisal University, Saudi Arabia

*CORRESPONDENCE
Yu Wang
wangyu@jxau.edu.cn
Ting Wang
tingwang@jxau.edu.cn
Sha Li
lisha@jxau.edu.cn
Lingbao Kong
lingbaok@mail.jxau.edu.cn

†These authors have contributed equally to this work and share first authorship

SPECIALTY SECTION
This article was submitted to Viral Immunology, a section of the journal Frontiers in Immunology

RECEIVED 02 June 2022
ACCEPTED 28 June 2022
PUBLISHED 28 July 2022

CITATION
Li M, Weng S, Wang Q, Yang Z, Wang X, Yin Y, Zhou Q, Zhang L, Tao F, Li Y, Jia M, Yang L, Xin X, Li H, Kang L, Wang Y, Wang T, Li S and Kong L (2022) Reduced binding activity of vaccine serum to omicron receptor-binding domain. *Front. Immunol.* 13:960195. doi: 10.3389/fimmu.2022.960195

Reduced binding activity of vaccine serum to omicron receptor-binding domain

Mingzhi Li[1†], Shiqi Weng[1†], Quansheng Wang[1†], Zibing Yang[1], Xiaoling Wang[1,2], Yanjun Yin[3], Qiuxiang Zhou[4], Lirong Zhang[1], Feifei Tao[1], Yihan Li[1], Mengle Jia[1], Lingdi Yang[1], Xiu Xin[1], Hanguang Li[1], Lumei Kang[5,6], Yu Wang[1*], Ting Wang[1*], Sha Li[1*] and Lingbao Kong[1*]

[1]Nanchang City Key Laboratory of Animal Virus and Genetic Engineering, Institute of Pathogenic Microorganism, College of Bioscience and Engineering, Jiangxi Agricultural University, Nanchang, China, [2]GMU-GIBH Joint School of Life Sciences, Guangzhou Medical University, Guangzhou, China, [3]Department of Clinical Laboratory, Jiangxi Provincial Children's Hospital, Nanchang, China, [4]Department of Clinical Laboratory, The Affiliated Hospital of Jiangxi Agricultural University, Nanchang, China, [5]College of Animal Science and Technology, Jiangxi Agricultural University, Nanchang, China, [6]Center for Laboratory Animal Science, Nanchang University, Nanchang, China

Coronavirus disease 2019 (COVID-19) vaccination regimens contribute to limiting the spread of severe acute respiratory syndrome Coronavirus-2 (SARS-CoV-2). However, the emergence and rapid transmission of the SARS-CoV-2 variant Omicron raise a concern about the efficacy of the current vaccination strategy. Here, we expressed monomeric and dimeric receptor-binding domains (RBDs) of the spike protein of prototype SARS-CoV-2 and Omicron variant in *E. coli* and investigated the reactivity of anti-sera from Chinese subjects immunized with SARS-CoV-2 vaccines to these recombinant RBDs. In 106 human blood samples collected from 91 participants from Jiangxi, China, 26 sera were identified to be positive for SARS-CoV-2 spike protein antibodies by lateral flow dipstick (LFD) assays, which were enriched in the ones collected from day 7 to 1 month post-boost (87.0%) compared to those harvested within 1 week post-boost (23.8%) ($P < 0.0001$). A higher positive ratio was observed in the child group (40.8%) than adults (13.6%) ($P = 0.0073$). ELISA results showed that the binding activity of anti-SARS-CoV-2 antibody-positive sera to Omicron RBDs dropped by 1.48- to 2.07-fold compared to its

homogeneous recombinant RBDs. Thus, our data indicate that current SARS-CoV-2 vaccines provide restricted humoral protection against the Omicron variant.

KEYWORDS

COVID-19, omicron, spike protein, RBD, binding activity

Introduction

COVID-19 is a worldwide pandemic caused by SARS-CoV-2. Although multiple measures have been adopted, COVID-19 is still rife amid the world and poses a threat to social, mental, and economic wellbeing (1, 2). The newly evolved Omicron mutant spread quickly within highly vaccinated populations. Viral sequence analysis reveals that as the most heavily mutated variant, Omicron harbors 15 mutations in its spike RBD region. Considering that the RBD domain of the SARS-CoV-2 spike protein mediates the viral entry, thus contributing to viral infection and transmission, a primary concern arises about the effectiveness of the current vaccine regimen against this viral variant (3). To this end, we expressed the RBD monomer and dimer of Omicron spike protein and examined the cross-reactivity of anti-sera from subjects immunized with prototype SARS-CoV-2 vaccines (either inactivated vaccines or RBD dimer subunit vaccines) to Omicron RBDs. Our data showed that vaccine-immunized sera displayed reduced binding activity to Omicron RBDs, implying the low efficacy of the prototype SARS-CoV-2 vaccine to protect against the Omicron variant.

Methods

Materials

Ninety-three human serum samples from 78 individuals immunized with prototype SARS-CoV-2 vaccines including inactivated whole-virus vaccines Sinopharm BBIBP-CorV and Sinovac CoronaVac (n = 62), Sinopharm BBIBP-CorV (n = 16), Sinovac CoronaVac (n = 14), or RBD dimer-based subunit vaccine Zhifei ZF2001 (n = 1) were obtained from the Affiliated Hospital of Jiangxi Agricultural University and Jiangxi Children's Hospital (Supplementary Table 1). Thirteen unimmunized serum samples from Jiangxi Children's Hospital served as negative controls (Supplementary Table 1). All studies involving human sera were performed under the standard of the Jiangxi Agriculture University Ethical Committee. SARS-CoV-2 Antibody Detection Kits (Cat: W19501110, 2020340177, and Y5021010552A) were obtained from Wondfo, Innovita, and Vazyme of China, respectively. Antibodies against His-tag (RIID: AB_11,232,599), actin (RIID: AB_2,687,938), and HRP-labeled goat anti-human (Cat: SA00001-17) were purchased from Proteintech in USA. HEK293 cell-expressed RBDs of prototype SARS-CoV-2 (Cat: CSB-DP7031) and Omicron variant (Cat: 40592-V08H121) were obtained from CUSABIO and Sino Biological in China, respectively.

Protein expression and purification

The coding sequence for spike RBD of Omicron strain B.1.1.529 (GenBank: PRJNA784547) was used for prokaryotic expression. The Omicron RBD dimer was synthesized in a tandem repeat form of the RBD monomer separated by their own flexible terminal residues (2). The corresponding sequence of the Omicron spike RBD monomer was amplified with the synthetic dimer sequence as the template. A similar strategy was used to amplify the monomeric and dimeric RBDs of prototype SARS-CoV-2 (GenBank: YP_009724390). All RBD DNA segments were cloned into the pET-28a plasmid for expression in *E. coli*. After induction at 18°C for 8 h in the presence of IPTG (0.5 or 1 mM), cells were collected to examine the recombinant protein expressions. All RBDs were further purified by the NI-NTA column followed by renaturation using dialysis and then concentration with Amicon® Ultra-15 (10 or 30K) (4, 5).

Immunoblotting

Immunoblotting was performed as described previously (6). Briefly, after electrophoresis on an SDS-PAGE gel, separated proteins were transferred to polyvinylidene difluoride membranes (Millipore). The membranes were blocked with 10% skimmed milk and then incubated with an antibody specifically targeting His-tag at 4°. Finally, the proteins were visualized with Clarity ECL immunoblotting substrate (Bio-Rad).

LFD and ELISA

To detect SARS-CoV-2-specific antibodies in vaccine-immunized human sera, LFD assays were performed using SARS-CoV-2 Antibody Detection Kits according to the

manufacturer's instructions. ELISA was performed as described previously (4, 7). Briefly, plates were precoated with the recombinant RBDs (100 ng/well) at 4° overnight in 0.05 M carbonate-bicarbonate buffer. After blocking with 5% skim milk, human sera were diluted and added to each well. Goat anti-human IgG-HRP antibodies were then added. Plates were finally developed with TMB substrate. Commercial RBDs expressed in HEK293 cells were used to evaluate the quality of lab-made recombinant RBDs expressed in *E. coli*. To exclude the interference of His-tag reactivity, the anti-His antibody was also used in ELISA assays (Supplementary Figure 2). Optical density was measured at a wavelength of 450 nm using a plate reader (Tecan, Infinite M200 Pro).

Statistical analysis

Student's t-test and chi-square test were adopted to compare the intergroup differences using GraphPad Prism 8.0 software. $P < 0.05$ was considered statistical significance.

Results

Expression of monomeric and dimeric RBDs

Upon IPTG induction, the RBD monomer and dimer of the SARS-CoV-2 prototype and Omicron variant were expressed in *E. coli*, all of which dominated in the cellular inclusion bodies, accounting for 26%–55% of total protein mass (Figures 1A–D, top). After purification with Ni-NTA columns followed by the separation by electrophoresis on SDS-PAGE gel, intensive bands were detected for monomer and dimer RBD proteins in a buffer with 250 mM of imidazole. The purities of the recombinant RBD proteins were no less than 95% (Figures 1A–D, top). To confirm the identities of *E. coli*-derived recombinant proteins, we performed immunoblotting assays with an anti-His tag antibody. Expected bands were detected for all recombinant proteins in IPTG-induced lysate or purified samples, but not in un-induced ones, demonstrating the successful expression and purification of *E.coli*-expressed recombinant RBD proteins (Figures 1A–D, bottom).

Cross-reactivity of prototype SARS-CoV2 vaccine-immunized sera against Omicron RBDs

To assess the cross-reactivity of prototype SARS-CoV2 vaccine-immunized sera against Omicron RBDs, we first collected 106 blood samples based on availability. Among them, 44 samples were collected from 29 adults while the remains were from 62 children (Supplementary Table 1). LFD assays were conducted to identify vaccine sera with high-titer antibodies against prototype SARS-CoV-2 spike protein. Results revealed that 26 samples of 93 vaccine sera contained detectable antibodies specific to SARS-CoV-2 spike protein (Supplementary Figure 1). We next wondered the LFD-positive ratio of these samples by vaccine, age, sex, and post-immunization time. Therefore, a retrospective analysis was performed (Supplementary Table 2). The LFD-positive ratio for both BBIBP-CorV and CoronaVac immunization groups was 11 [17.7%] of 62 (adult: 6 [14.0%]/43, children: 5 [41.6%]/19). The LFD-positive ratio for the BBIBP-CorV immunization group was 7 [43.8%] of 16 (children). The LFD-positive ratio for the CoronaVac immunization group was 8 [57.1%] of 14 (children). The majority (20 [87.0%] of 23) of LFD-positive samples were the ones collected from day 7 to 1 month post-boost (BBIBP-CorV and CoronaVac immunization groups: (5 [83.3%] of 6); BBIBP-CorV immunization group: (7 [77.8%] of 9); CoronaVac immunization group: 8 [100%] of 8), different from those harvested within 1 week post-boost (5 [23.8%] of 21, BBIBP-CorV and CoronaVac immunization groups: 5 [23.8%] of 21; BBIBP-CorV immunization group: none; CoronaVac immunization group: none) ($P < 0.0001$, Figure 2A). A higher positive ratio was observed in the child group (20 [40.8%] of 49, BBIBP-CorV and CoronaVac immunization groups: 5 [26.3%] of 19; BBIBP-CorV immunization group: 7 [43.8%] of 16; CoronaVac immunization group: 8 [57.1%] of 14) than adult (6 [13.6%] of 44, BBIBP-CorV and CoronaVac immunization groups: 6 [13.6%] of 44; BBIBP-CorV immunization group: none; CoronaVac immunization group: none) ($P = 0.0073$, Figure 2B). The low LFD-positive ratio of vaccine sera is likely due to the limited sensitivity of the LFD assay. To test this possibility, we randomly chose three LFD-positive/-negative vaccine sera and three unimmunized sera to examine the quantities of antibodies targeting SARS-CoV-2 spike RBD. ELISA data showed that LFD-negative vaccine sera harbored small, but decent amounts of anti-SARS-CoV-2 spike RBD antibodies (Figure 2C).

To evaluate the binding activity of vaccine-immunized human sera to Omicron variants, LFD-positive sera were used. As shown in Figures 2D–F, although the tested sera cross-recognized Omicron spike RBDs, their reactivity magnitudes decreased by 1.48- to 2.07-fold compared to those of SARS-CoV-2 RBDs, which partially explained the rapid transmission of Omicron in the vaccinated regions. With the engagement of antibodies in human vaccine sera and RBDs as readout, general drops were observed for the *E.coli*-expressed prototype RBD monomer (1.53-fold, $P < 0.0001$), prototype RBD dimer (2.24-fold, $P < 0.0001$), Omicron monomer (1.26-fold, $P = 0.0006$), and dimer (1.62-fold, $P < 0.0001$) with the corresponding commercial ones as control (Figure 2G).

Of note, all recombinant RBD proteins carried a His-tag and recognized anti-His antibody with a reactivity corresponding to

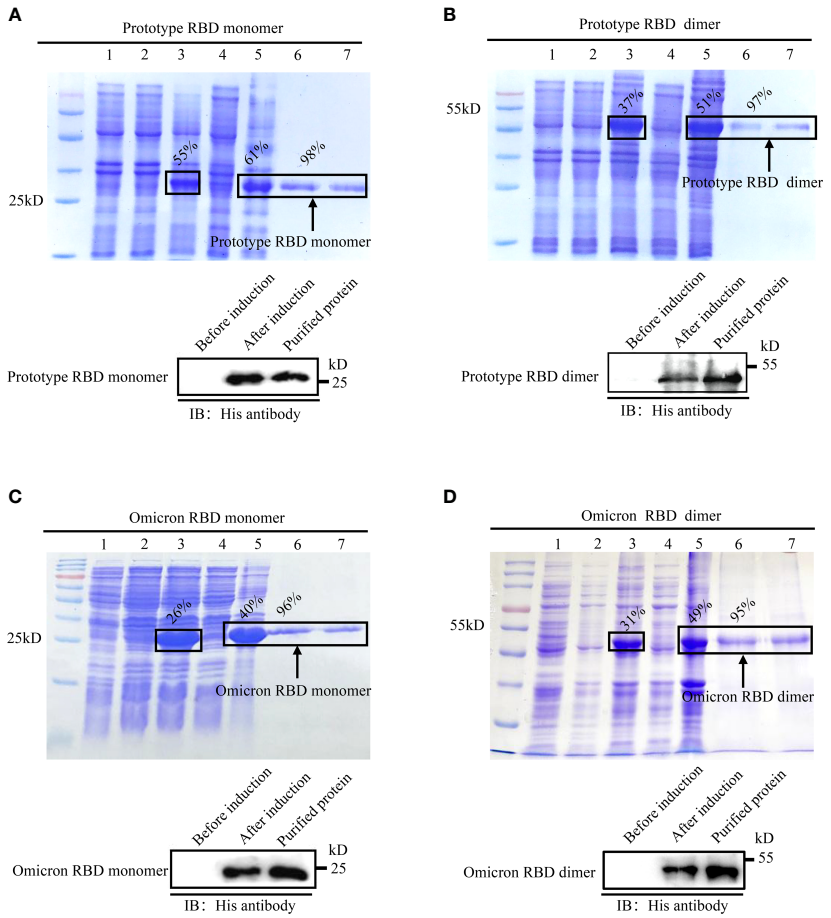

FIGURE 1
Expression, purification, and identification of recombinant spike RBDs. Recombinant pET-28a vectors expressing either monomeric or dimeric spike RBDs for prototype SARS-CoV-2 **(A, B)** and Omicron variant **(C, D)** were used to express the recombinant proteins in *E. coli*. The expressions and purities of RBDs were examined by SDS-PAGE (A-D, top) or immunoblotting (**A–D**, bottom). **(A-D)** Top: M: protein marker; lane 1: empty vector; lane 2: un-induced sample; lanes 3–5: IPTG induced whole-cell lysate (lane 3); cellular supernatant (lane 4); inclusion body (lane 5); lanes 6–7 (A-D): purified monomeric **(A, C)** or dimeric **(B, D)** RBDs in eluted buffer with 250 mM imidazole. **(A-D)** Bottom: identification of spike RBDs by immunoblotting with anti-His tag antibody.

the quantity of its His-tag. In addition, recombinant RBD proteins recognized vaccine sera, but not unimmunized control sera (Supplementary Figure 2; Figures 2C–F). These data together suggested that the difference in vaccine serum reactivity to recombinant RBD proteins was not due to the anti-His antibody which could exist in vaccine sera.

Discussion

Different from other SARS-CoV-2 variants, the Omicron strain occurs in the situation in which SARS-CoV2 vaccine immunization has been rolled out globally. Its fast spread in fully vaccinated countries such as the USA reveals that the existing vaccine provided limited protection. The World Health Organization (WHO) reported on February 15, 2022, that the Omicron variant had replaced the Delta variant as the main circulating strain worldwide. This study aimed to explore how the Omicron variant effectively evades the immune responses induced by heterogeneous SARS-CoV-2 vaccines. The CoV spike RBD is an attractive vaccine target. Its dimeric form fully exposes the dual receptor-binding motifs, thus significantly increasing neutralizing antibody (NAb) titers as compared to its conventional monomer (8). In this study, the Omicron spike RBD monomer and dimer were expressed and purified (Figure 1), serving as the antigens to evaluate the cross-protection of host immunity induced by prototype SARS-CoV-2 vaccines in the ELISA (Figure 2).

One hundred six blood samples from adults and children were collected and analyzed by LFD assays. The anti-SARS-

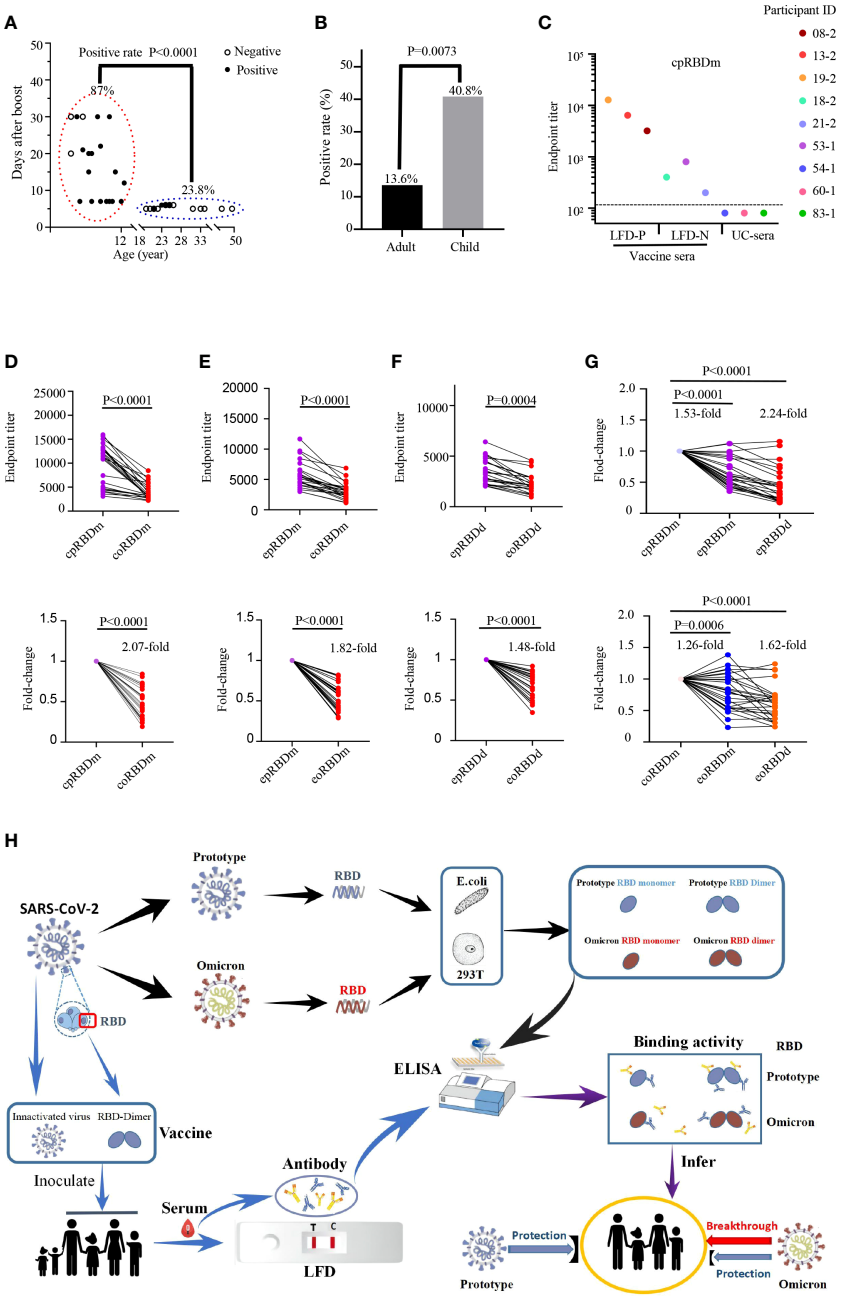

FIGURE 2
Reactivity of human sera with SARS-CoV-2 spike protein and recombinant RBDs. **(A, B)** Detection of anti-SARS-CoV-2 spike protein antibodies in human sera with LFD assays. **(A)** Examination of the contributions of age and sample collection time point to LFD-positive rates with the chi-square test. Children LFD-positive rate: (20 of 23, 86.9%); adult LFD-positive rate: (5 of 21, 23.8%). Child sera were collected at 7 days to 1 month after boost. Adult vaccine sera were collected within 1 week after boost. **(B)** Comparison of the LFD-positive rate of vaccine sera between adults (6 of 44, 13.6%) and children (20 of 49, 40.8%) with chi-square test. **(C)** Titration of SARS-CoV-2 RBD-specific antibodies in LFD-positive vaccine sera (participant IDs: 08-2, 13-2 and 19-2; LFD-P), LFD-negative vaccine sera (participant IDs: 18-2, 21-2 and 53-1; LFD-N), and unimmunized sera (participant IDs: 54-1, 60-1 and 83-1; UC-sera) by ELISA using the recombinant RBD monomer as coating proteins. The dashed line indicates the cutoff value. **(D-F)** Reactivity of 26 LFD-positive vaccine sera (further details in Supplemental Figure 1A and Supplemental Table 1) to commercial prototype and omicron RBD monomer **(D)**, *E. coli*-expressed prototype and omicron RBD monomer **(E)**, and *E. coli*-expressed prototype and omicron RBD dimer **(F)**. Top panels: absolute titers; bottom panels: fold change. cpRBDm/coRBDm: commercial prototype/omicron RBD monomer; epRBDm/eoRBDm: *E. coli*-expressed prototype/omicron RBD monomer; epRBDd/eoRBDd: *E. coli*-expressed prototype/omicron RBD dimer. **(G)** Fold change for comparison between commercial and lab-made RBDs. Prototype SARS-CoV-2 RBDs (top panel) and Omicron RBDs (bottom panel). Fold change is defined as mean fold change. Each dot represents a biological replicate, and the assays were performed three times **(A, C-G)**. **(H)** Schematic diagram showing reduced binding activity of vaccine serum to Omicron RBD.

CoV-2 spike protein antibody in vaccine sera collected at 5–6 months after the first boost dropped to below the detectable threshold, highlighting the necessity of the second boost (Supplementary Figure 1). Interestingly, vaccine sera at 7 days to 1 month after boost had a higher SARS-CoV-2 spike protein antibody titer than those within 1 week after boost ($P < 0.0001$, Figure 2A). Consistent with the finding, a recent report indicated that RBD antibody titers reached a plateau in 2 weeks or so after a boost, then dropped about fivefold within the following 2 weeks (9). These data suggest that boosted time affects the antibody titer of vaccine sera. Interestingly, a higher positive ratio was observed in the child group than in adults ($P = 0.0073$, Figure 2B), which could attribute to age besides the collection time points. Similarly, recent reports showed that immunity of CoronaVac for children seems better than that for adults (10, 11). It should be noted that LFD exhibited low sensitivity in detecting SARS-CoV-2 spike protein antibody of vaccine serum than ELISA (Figure 2C). Thus, the development of a more convenient and accurate CoV-2 antibody detection kit is warranted.

Coronavirus spike RBD is the key domain mediating the engagement between coronavirus and host. The majority of antibodies targeting spike RBDs bear neutralization function which in part determines the spread of CoV viruses. The positive sample in LFD assays displayed decent responses to SARS-CoV-2 and reduced binding to Omicron (Figures 2D–F), aligning with recent reports (8). Carreno et al. found that the eukaryotic expressed monomeric RBD of Omicron reduced binding activity to convalescent and vaccine (mRNA-1273 and BNT162b2) serum with a more than 1.5-fold drop (8). Cameroni et al. demonstrated that most receptor-binding motif (RBM)-directed monoclonal antibodies (mAbs) lost *in vitro* neutralizing activity against Omicron (8). High-throughput yeast display screening assays from Cao et al. revealed that over 85% of the RBD-neutralizing antibodies were escaped by Omicron (8). Neutralizing assays using authentic and pseudotype viruses indicated that the Omicron variant showed lower neutralizing sensitivity than other SARS-CoV-2 variants to convalescent and vaccine (mRNA1273, BNT162b2, BBIBP-CorV, and ZF2001) serum (8). All these data suggest that omicron can penetrate the vaccine-induced immune barrier, which explained at least in part the quick spread of Omicron. One thing that needs to be emphasized is that even in the vaccinated hosts who are negative in Omicron RBD-specific antibodies, the preexisting SARS-CoV-2-specific memory B cells and T cells can provide protection in the following Omicron infection, although they may contribute less to inhibit the entry of Omicron into host cells (8). This is possibly the reason why Omicron spreads rapidly but does not induce more severe symptoms.

Collectively, our study demonstrates that Omicron RBD displays a lower reactivity to prototype SARS-CoV-2 vaccine-immunized human sera as compared to homogeneous SARS-CoV-2 RBD, implying the insufficient protection of the prototype SARS-CoV-2 vaccine against the Omicron variant (Figure 2H). The booster of the prototype SARS-CoV-2 vaccine enhances the level of antibodies against both the SARS-CoV-2 prototype and the Omicron variant, which can help defend against the COVID-19 pandemic. Omicron RBD reactivity to SARS-CoV-2 vaccine-immunized human sera requires to be assessed on a large scale.

Data availability statement

The original contributions presented in the study are included in the article/supplementary material. Further inquiries can be directed to the corresponding authors.

Ethics statement

The animal study was reviewed and approved by the Jiangxi Agricultural University Ethics Committee with the protocol number JXAU20220007.

Author contributions

ML, SW, and QW contributed equally to this work. TW, ML, SW, and QW performed the majority of experiments, interpreted the data, and prepared the figures and tables. ZY, LZ, and FT performed the protein expression and denaturation. YY, QZ, MJ, and LY collected the samples and prepared the relevant information. XX, HL, and LK conducted the data analysis. XW and YL polished the draft. YW, SL, and LK developed the research plan and experimental strategy, analyzed the data, and wrote the paper. All authors contributed to the article and approved the submitted version.

Funding

This study was funded by research grants from the National Natural Science Foundation of China (grants 31460667, 31860038, and 31960699), Jiangxi Province (grants 20161BBF60084, GJJ180239, and GJJ200405), and Jiangxi Agriculture University (9232307726).

Conflict of interest

The authors declare that the research was conducted in the absence of any commercial or financial relationships that could be construed as a potential conflict of interest.

Publisher's note

Supplementary material

The Supplementary Material for this article can be found online at: https://www.frontiersin.org/articles/10.3389/fimmu.2022.960195/full#supplementary-material

SUPPLEMENTARY FIGURE 1
Examination of anti-SARS-CoV-2 spike protein antibodies in human immunized sera using LFD assays. **(A)** The intensity of LFD bands in was quantified using Image J. (B-C) Adult sera collected at month 1, 5, or 6 post the second round of vaccination were examined with SARS-CoV-2 Antibody Detection Kit from Vazyme **(B)** or Innovita **(C)**. **(D)** Adult sera collected at month 1 or day 5 post the third round of vaccination were examined with SARS-CoV-2 Antibody Detection Kit from Wondfo. **(E-F)** Children's sera collected at different time points after vaccination and unimmunized children's sera were examined with SARS-CoV-2 Antibody Detection Kit from Wondfo. Further details were provided in Supplementary Table 1.

SUPPLEMENTARY FIGURE 2
Identification of pre-coated recombinant RBDs by anti-His tag antibody. Recombinant RBDs were examined by ELISA assays with anti-His tag antibody, vaccine serum (participant ID: 31-1), and unimmunized sera (UC-sera, participant ID: 62-1), or PBS.

References

1. Carreno JM, Alshammary H, Tcheou J, Singh G, Raskin AJ, Kawabata H, et al. Activity of convalescent and vaccine serum against SARS-CoV-2 omicron. *Nature* (2022) 602(7898):682–88. doi: 10.1038/s41586-022-04399-5

2. Dai L, Zheng T, Xu K, Han Y, Xu L, Huang E, et al. A universal design of betacoronavirus vaccines against COVID-19, MERS, and SARS. *Cell* (2020) 182 (3):722–733.e11. doi: 10.1016/j.cell.2020.06.035

3. Ai J, Zhang H, Zhang Y, Lin K, Zhang Y, Wu J, et al. Omicron variant showed lower neutralizing sensitivity than other SARS-CoV-2 variants to immune sera elicited by vaccines after boost. *Emerg Microbes Infect* (2022) 11(1):337–43. doi: 10.1080/22221751.2021.2022440

4. Wan J, Wang T, Xu J, Ouyang T, Wang Q, Zhang Y, et al. Novel Japanese encephalitis virus NS1-based vaccine: Truncated NS1 fused with e. coli heat labile enterotoxin b subunit. *EBioMedicine* (2021) 67:103353. doi: 10.1016/j.ebiom.2021.103353

5. Wang X., Wang Y., Wu X., Wang J., Wang Y., Qiu Z, et al. Unbiased detection of off-target cleavage by CRISPR-Cas9 and TALENs using integrase-defective lentiviral vectors. *Nat Biotechnol* (2015) 33(2):175–8. doi: 10.1038/nbt.3127

6. Yang Z, Ouyang T, Aoyagi H, Wang T, Xing X, Zhang Y, et al. Cellular OCIAD2 protein is a proviral factor for hepatitis c virus replication. *Int J Biol Macromol* (2021) 188:147–59. doi: 10.1016/j.ijbiomac.2021.08.032

7. Li S, Choi HJ, Felio K, Wang CR. Autoreactive CD1b-restricted T cells: a new innate-like T-cell population that contributes to immunity against infection. *Blood* (2011) 118(14):3870–8. doi: 10.1182/blood-2011-03-341941

8. Krishnan K. Chapter 1 - Introduction to big data. In: K Krishnan, K Krishnan, editor. *Data warehousing in the age of big data*. Boston: Morgan Kaufmann (2013). p. 3–14.

9. Xue JB, Lai DY, Jiang HW, Qi H, Guo SJ, Zhu YS, et al. Landscape of the RBD-specific IgG, IgM, and IgA responses triggered by the inactivated virus vaccine against the omicron variant. *Cell Discov* (2022) 8(1):15. doi: 10.1038/s41421-022-00380-8

10. Han B, Song Y, Li C, Yang W, Ma Q, Jiang Z, et al. Safety, tolerability, and immunogenicity of an inactivated SARS-CoV-2 vaccine (CoronaVac) in healthy children and adolescents: a double-blind, randomised, controlled, phase 1/2 clinical trial. *Lancet Infect Dis* (2021) 21(12):1645–53. doi: 10.1016/S1473-3099(21)00319-4

11. Wu Z, Hu Y, Xu M, Chen Z, Yang W, Jiang Z, et al. Safety, tolerability, and immunogenicity of an inactivated SARS-CoV-2 vaccine (CoronaVac) in healthy adults aged 60 years and older: a randomised, double-blind, placebo-controlled, phase 1/2 clinical trial. *Lancet Infect Dis* (2021) 21(6):803–12. doi: 10.1016/S1473-3099(20)30987-7

frontiers | Frontiers in Immunology

TYPE Original Research
PUBLISHED 15 August 2022
DOI 10.3389/fimmu.2022.941923

OPEN ACCESS

EDITED BY
Aristo Vojdani
Immunosciences Lab., Inc.,
United States

REVIEWED BY
Subhajit Biswas,
Indian Institute of Chemical Biology (CSIR), India
Gregor Ebert,
Technical University of Munich, Germany

*CORRESPONDENCE
Trai-Ming Yeh
today@mail.ncku.edu.tw

†These authors have contributed equally to this work and share first authorship

SPECIALTY SECTION
This article was submitted to Viral Immunology, a section of the journal Frontiers in Immunology

RECEIVED 12 May 2022
ACCEPTED 28 July 2022
PUBLISHED 15 August 2022

CITATION
Cheng Y-L, Chao C-H, Lai Y-C, Hsieh K-H, Wang J-R, Wan S-W, Huang H-J, Chuang Y-C, Chuang W-J and Yeh T-M (2022) Antibodies against the SARS-CoV-2 S1-RBD cross-react with dengue virus and hinder dengue pathogenesis. *Front. Immunol.* 13:941923. doi: 10.3389/fimmu.2022.941923

Antibodies against the SARS-CoV-2 S1-RBD cross-react with dengue virus and hinder dengue pathogenesis

Yi-Ling Cheng[1†], Chiao-Hsuan Chao[1†], Yen-Chung Lai[1], Kun-Han Hsieh[1], Jen-Ren Wang[1], Shu-Wen Wan[2], Hong-Jyun Huang[2], Yung-Chun Chuang[1,3], Woei-Jer Chuang[4] and Trai-Ming Yeh[1*]

[1]Department of Medical Laboratory Science and Biotechnology, College of Medicine, National Cheng Kung University, Tainan, Taiwan, [2]Department of Microbiology and Immunology, College of Medicine, National Cheng Kung University, Tainan, Taiwan, [3]Leadgene Biomedical, Inc., Tainan, Taiwan, [4]Department of Biochemistry and Molecular Biology, College of Medicine, National Cheng Kung University, Tainan, Taiwan

Severe acute respiratory syndrome coronavirus 2 (SARS-CoV-2) has spread globally since December 2019. Several studies reported that SARS-CoV-2 infections may produce false-positive reactions in dengue virus (DENV) serology tests and vice versa. However, it remains unclear whether SARS-CoV-2 and DENV cross-reactive antibodies provide cross-protection against each disease or promote disease severity. In this study, we confirmed that antibodies against the SARS-CoV-2 spike protein and its receptor-binding domain (S1-RBD) were significantly increased in dengue patients compared to normal controls. In addition, anti-S1-RBD IgG purified from S1-RBD hyperimmune rabbit sera could cross-react with both DENV envelope protein (E) and nonstructural protein 1 (NS1). The potential epitopes of DENV E and NS1 recognized by these antibodies were identified by a phage-displayed random peptide library. In addition, DENV infection and DENV NS1-induced endothelial hyperpermeability *in vitro* were inhibited in the presence of anti-S1-RBD IgG. Passive transfer anti-S1-RBD IgG into mice also reduced prolonged bleeding time and decreased NS1 seral level in DENV-infected mice. Lastly, COVID-19 patients' sera showed neutralizing ability against dengue infection *in vitro*. Thus, our results suggest that the antigenic cross-reactivity between the SARS-CoV-2 S1-RBD and DENV can induce the production of anti-SARS-CoV-2 S1-RBD antibodies that cross-react with DENV which may hinder dengue pathogenesis.

KEYWORDS

COVID-19, dengue virus, SARS-CoV-2, diagnosis, antibody-dependent enhancement

Introduction

In late December 2019, a novel coronavirus designated severe acute respiratory syndrome coronavirus 2 (SARS-CoV-2) spread rapidly worldwide, resulting in a global coronavirus disease 2019 (COVID-19) pandemic (1). SARS-CoV-2 is a positive-sense single-stranded RNA enveloped virus which is composed of at least four structural proteins: spike (S), envelope, membrane, and nucleocapsid (2). SARS-CoV-2 binds to the cell surface receptor angiotensin-converting enzyme 2 (ACE2) through trimeric S glycoprotein expressed on the viral envelope (2). Each monomer of the S protein is approximately 180 kDa and contains two subunits, S1 and S2. The receptor-binding domain (RBD) in the S1 subunit (S1-RBD) is an immunodominant region that is the main target of neutralizing antibodies (3–5). Symptoms of COVID-19 can be nonspecific, such as fever, cough, and tiredness, which may appear 2 to 14 days after exposure. Other symptoms can include shortness of breath or difficulty breathing, muscle aches, sore throat, headache, chest pain, and rash. However, in some patients, these symptoms can progress to life-threatening respiratory insufficiency and affect multiple organs, such as the heart, liver, and kidney (6). While the gold standard in COVID-19 diagnosis is reverse transcriptase polymerase chain reaction (RT–PCR), it requires complex sample manipulation and expensive machinery. To control the spread of SARS-CoV-2 and strengthen countries' testing capacity, antigen and antibody rapid diagnostic kits are increasingly being used by many countries. However, several studies have reported that SARS-CoV-2 infections may produce false-positive antibody reactions in dengue virus (DENV) serology tests and vice versa, leading to misdiagnosis between COVID-19 and DENV infection based on rapid serological test results (7–10). Potential antigenic cross-reactivity between SARS-CoV-2 and DENV has been proposed to explain the false-positive serological test results among COVID-19 and dengue patients (11).

DENV infection, which is transmitted by Aedes mosquitoes, is prevalent in tropical and subtropical areas where the vector resides. However, it has dramatically increased in incidence within the last twenty years due to climate change and the convenient transportation system (12). It is estimated that greater than 2.5 billion people live in endemic areas, and the number of individuals infected by DENV is thought to exceed 50 million globally per year. DENV infection can cause mild dengue fever or more severe dengue hemorrhage fever (DHF) or dengue shock syndrome (DSS). DHF is a severe febrile disease characterized by abnormalities in homeostasis and increased capillary leakage that can progress to blood pressure decrease and hypovolemic shock (DSS) (13). However, most dengue patients show only flu-like illness, which is very similar to COVID-19. Therefore, the concurrence of SARS-CoV-2 and DENV infections has become a serious challenge for public health and medical management in dengue-endemic areas (14).

DENV is a positive-stranded RNA enveloped virus (15). It is composed of three structural proteins, namely, core protein (C), membrane-associated protein (M) produced as a precursor protein (prM), and envelope protein (E), and 7 nonstructural proteins (NSs). Based on the antigenic difference of the E protein, DENV can be divided into four different serotypes, DENV 1-4. Dengue NS1 is a glycosylated 48-kDa protein that can be secreted as a hexamer into the blood circulation during DENV infection. Circulating soluble NS1 can disrupt endothelial cell integrity and increase endothelial permeability (16–19). In addition, antibody-dependent enhancement (ADE) has been proposed to explain why many of the cases of DHF/DSS occur following secondary infection with a serotype of DENV different from that causing previous infection. Based on ADE, preexisting antibodies generated from previous infection or vaccination do not neutralize secondary infection of different serotypes, but enhance it, possibly by triggering Fc receptor-mediated virus uptake. Consequently, more severe disease may occur (20–22). ADE has been documented not only in DENV but also other respiratory virus infections, including SARS-CoV (20–22). Anti-SARS-CoV-2 antibodies could exacerbate COVID-19 through ADE has been suggested as well (23).

Previously, a computational simulation study revealed that a monoclonal antibody (mAb) against DENV E could bind to the SARS-CoV-2 S1-RBD and potentially block human ACE2 receptor binding (24). However, it remains unclear whether SARS-CoV-2 and DENV cross-reactive antibodies provide cross-protection against each disease or promote ADE and increase the risk of disease severity (14). To address this question, we first demonstrated that antibodies that cross-reacted with SARS-CoV-2 spike protein and the S1-RBD were increased in dengue patients' sera. Furthermore, we purified anti-S1-RBD IgG from SARS-CoV-2 S1-RBD hyperimmune rabbit (Rbt) sera and found that it could cross-react with dengue E and NS1. In addition, anti-S1-RBD IgG could inhibit DENV infection and block NS1-induced endothelial hyperpermeability *in vitro* and prevent DENV-induced prolonged bleeding time and decreased NS1seral level in mice. Last, an increase in antibody binding to DENV-related antigens was also found in some individuals after SARS-CoV-2 infection. Furthermore, DENV infection *in vitro* was inhibited in the presence of COVID-19 patients' but not healthy controls' sera. Thus, our results suggest anti-SARS-CoV-2 antibodies induced during SARS-CoV-2 infection may interfere with DENV infection, which should be further evaluated in clinical study.

Materials and methods

Recombinant proteins and peptides

DENV serotype 2 E, prM and NS4B recombinant proteins were expressed and purified from *Escherichia coli* (Leadgene

Biomedical Inc., Tainan, Taiwan). SARS-CoV-2 trimeric spike and nucleocapsid protein purified from HEK293 cells and human ACE2-Fc recombinant protein purified from CHO cells were provided by Leadgene company (Cat. No. 63233, 61633 and 63333). The synthetic peptides were customized, purified and synthesized by Leadgene company. DENV serotype 2 (strain Thailand/16681/84) NS1 recombinant protein produced in mammalian HEK293 cells was purchased from The Native Antigen Company (Oxfordshire, UK).

Human serum

Dengue patient sera were collected from National Cheng Kung University Hospital (NCKUH) at the acute stage of the disease during a DENV outbreak in Tainan, Taiwan, in 2015 (25). In addition, sera from 29 healthy donors were included as negative controls. All serum collections were performed in accordance with the relevant guidelines and regulations approved by the institutional review board of NCKUH (IRB #A-BR-101–140). SARS-CoV-2 antibody positive sera were purchased from Access Biologicals (Vista, CA), and the detailed information was shown in the supplementary table of our previous study (26). According to the manufacturer's documentation, the samples were collected in the U.S. in June 2020 from 30 COVID-19 patients (19 belong to the race of Caucasian, 10 African American, and one unknown) who were confirmed of infection during March to April 2020. The commercial COVID-19 patient sera were dispensed in a Biosafety Level-2 Plus (BSL-2+) laboratory by fully trained individuals according to the compliance policies of NCKUH. Dispensed patient sera were inactivated at 56°C for 30 min before being used in this study.

Cell lines

The *Aedes albopictus* cell line (C6/36) and baby hamster kidney cell line (BHK-21), maintained in Dulbecco's modified Eagle's medium (DMEM) supplemented with 10% fetal bovine serum (FBS, HyClone, Logan, UT), were purchased from the American Type Culture Collection (ATCC, Manassas, VA) and Japanese Collection of Research Bioresources (Japan), respectively. The *Drosophila melanogaster* cell line (S2) purchased from ATCC was maintained in Schneider's Drosophila Medium (SERVA Electrophoresis GmbH, Heidelberg, Germany) supplemented with 10% FBS. The human microvascular endothelial cell line (HMEC-1) was obtained from the Center for Disease Control and Prevention (CDC, Taiwan) and was cultured in Medium 200 (Thermo Fisher Scientific, Waltham, MA) supplemented with 10% FBS. Human monocytic cell line (THP-1) was grown in RPMI 1640 medium with 10% FBS. Except for S2 cells and C6/36 cells, which were cultured at 27 °C without CO_2 incubation and at 27 ° C in a 5% CO_2 atmosphere, respectively, the other cells were cultured at 37 °C in a 5% CO2 atmosphere.

Viral stocks

The DENV serotype 2 strain 16681 or 454009A was propagated in C6/36 cells as previously described (27). To obtain high titers of DENV, we used a Macrosep Advance Centrifugal Device (MW cutoff of 30 kDa; Pall Corp., Port Washington, NY) to concentrate the DENV-containing medium *via* centrifugation at 6000×g at 4°C, and the concentrated DENV was stored below −70°C until use.

Expression and purification of SARS-CoV-2 S1-RBD recombinant protein

For the expression and purification of SARS-CoV-2 S1-RBD recombinant protein, SARS-CoV-2 S1-RBD from a.a. 319 to 541 (YP_009724390) was cloned into pMT/BiP/V5-His B plasmid for the expression in S2 cells (Supplementary Figure 1). In brief, pMT-S1-RBD, containing 2x strep and 6x histidine, was transfected into S2 cells and induced with 500 μM $CuSO_4$. After four days of induction, S1-RBD protein in the supernatant was purified by Strep-Tactin Superflow Plus (QIAGEN GmbH, Hilden, Germany). 2.6 mg of S1-RBD protein were purified from a 500 mL induction medium. The purity of SARS-CoV-2 S1-RBD from S2 cell was checked using SDS-PAGE and western blotting with anti-His antibody (Cat. No. 10411, Leadgene Biomedical Inc.). Human ACE2 binding ability of the purified SARS-CoV-2 S1-RBD was further confirmed by its binding to human ACE2-Fc recombinant protein by ELISA and colocalization with ACE2 in human ACE2 expressing Caco-2 cells using immunofluorescence confocal microscopy (data not shown).

Immunization and antibody purification

For the preparation of anti-S1-RBD hyperimmune sera, two Rbt were primed and challenged on days 0, 14, and 28 with SARS-CoV-2 S1-RBD recombinant protein (250 μg for each Rbt) emulsified with incomplete Freund's adjuvant (Sigma-Aldrich, St. Louis, MO). Sera were collected 7 days after the final immunization and stored at -20°C until use. The above immunization procedures were performed by Leadgene company. For the purification of Rbt IgG, the collected Rbt sera (50 mL) were heat inactivated at 56°C for 30 min. After fivefold dilution with PBS and filtering with a 0.45 μm syringe filter, IgG in the Rbt immune sera was purified by Pierce Protein G Plus Agarose (Thermo Fisher Scientific) and eluted with 0.1 M glycine-HCl (pH 2.7) and immediately neutralized with neutralizing buffer (1 M Tris-HCl, pH 9.0). The purified Rbt

IgG was dialyzed against PBS at 4°C using SnakeSkin Dialysis Tubing with a 10 kDa molecular weight (MW) cutoff (Thermo Fisher Scientific). To obtain anti-S1-RBD IgG, S1-RBD affinity column was prepared by conjugation SARS-CoV-2 S1-RBD recombinant protein (5 mg) with 2 mL of NHS-activated Sepharose beads (Cytiva, Marlborough, MA) and blocked by ethanolamine followed the instruction provided by the manufacture. Purified Rbt IgG was incubated with S1-RBD-conjugated affinity column and eluted as described above to obtain anti-S1-RBD IgG. Those did not bind to SARS-CoV-2 S1-RBD affinity column after three rounds of incubation were also collected as flow-through Rbt IgG. In 50 mL of S1-RBD immunized rabbit serum, approximately 400 mg Rbt IgG could be purified from Protein G Plus Agarose. In addition, about 5.8 mg of anti-S1-RBD IgG, could be purified from 400 mg of these Rbt IgG by SARS-CoV-2 S1-RBD affinity column.

Enzyme-linked immunosorbent assay

To investigate whether the antibodies could bind to the targeted proteins, indirect ELISA was performed. Briefly, 2 μg/mL proteins were coated onto a high-binding 96-well ELISA plate (50 μL/well) overnight at 4°C. After blocking with 1% BSA in PBS (200 μL/well), the samples (anti-S1-RBD IgG, anti-DENV NS1 mAb/pAb, or patient/healthy donor anti-sera) were serially diluted with 1% BSA and incubated in wells for 1 h at 37°C. The bound antibodies were detected with anti-Rbt/mouse IgG-horseradish peroxidase (HRP) antibodies (1:10,000) (Leadgene Biomedical Inc.) or anti-human IgG-HRP antibody (1:4000) (Thermo Fisher Scientific) (50 μL/well) for 1 h at 37°C. Wells were washed three times with PBST (PBS containing 0.01% Tween 20, 250 μL/well) between each step. For color development, TMB (50 μL/well) was added, the plates were incubated for 10-15 min, and the reaction was stopped by addition of 2N H_2SO_4 (50 μL/well). The absorbance was read at OD 450 nm by a VersaMax microplate reader (Molecular Devices, Sunnyvale, CA). To investigate whether a peptide could inhibit antibody binding to the targeted proteins, competitive ELISA was performed. Briefly, antibodies with the indicated concentration were preincubated with the serially diluted peptide in PBS with 1% BSA before incubating with protein-coated ELISA plate. The bound antibodies were detected with an anti-Rbt or ant-mouse IgG-HRP antibody. The color development was performed as described above.

Western blotting

Trimeric spike protein and pseudovirus or concentrated supernatant of DENV were prepared under reducing condition prior to loading onto 10% SDS–PAGE gels for separation. The separated proteins were transferred onto a PVDF membrane (Pall, Ann Arbor, MI). The membrane was blocked with 5% skim milk in TBST (0.05% Tween 20 in Tris-buffered saline) and incubated with anti-S1-RBD IgG, anti-E poly IgG (Genetex), or anti-NS1 monoclonal IgG (33D2) overnight. To detect the bound IgG, the membrane was washed with TBST, followed by addition of a 1:10,000 dilution of HRP-conjugated anti-Rbt or anti-mouse immunoglobulin antibody (Leadgene). The bound HRP-conjugated antibodies were detected using WesternBright ECL (Advansta, San Jose, CA). The chemiluminescent signals were detected using an Image Quant LASS 4000 (GE Healthcare, Pittsburgh, PA).

SARS-CoV-2 pseudovirus neutralization test

ACE2-overexpressing HEK293 cells (HEK293-$ACE_{O/E}$) provided by Leadgene company were seeded on 96-well plates (3×10^4cells/well) 18-24 h before infection. Antibodies with the indicated concentration were preincubated with 50 $TCID_{50}$ of SARS-CoV-2 spike-expressing pseudovirus (lenti package with a nano luciferase reporter gene, which was kindly provided by Prof. Jen-Ren Wang's laboratory) (28) for 1 h and added to the HEK293-$ACE_{O/E}$ seeding plate. After 18-24 h, the infection rate was evaluated using a Nano-Glo Luciferase Assay System (Promega, Madison, WI), and the luciferase signal was detected by a SpectraMax iD5 (Molecular Devices).

Immunofluorescence assay

C6/36 cells or DENV (strain 454009A)-infected C6/36 cells were seeded for 16-18 h and fixed with 4% paraformaldehyde for 15 min. Later, the cells were washed with PBS and blocked with SuperBlock™ Blocking Buffer (Thermo Fisher Scientific) for 1 h. Anti-S1-RBD IgG (1 μg/mL) and different anti-DENV mAbs such as anti-E mAb (50-2), anti-prM mAb (70-21), and anti-NS1 mAb (33D2) (1 μg/mL) were diluted with PBS and incubated with the cells overnight at 4°C. After being washed with PBS, the cells were incubated with Alexa 488-conjugated goat anti-mouse IgG (1:1000) and Alexa 594-conjugated goat anti-Rbt IgG (1:1000) (Invitrogen, Carlsbad, CA) in PBS for 1 h. Finally, the secondary antibodies were washed away, and the cells were mounted on the slide with DAPI Fluoromount-G mounting medium (Thermo Fisher Scientific). The prepared slides were visualized by inverted fluorescence microscope and FV3000-Confocal laser scanning microscope (Olympus, Japan).

Epitope mapping using a phage-display random peptide library

To determine the epitopes recognized by anti-S1-RBD IgG, we used a phage-display random peptide library kit (PhD 12-mer; New England Biolabs, Ipswich, MA). Following the

manufacturer's suggestions, antibody (10 nM) was captured by protein A/G magnetic beads (Dynabeads; Invitrogen) for 30 min, followed by washing with 1 mL of Tris-buffered saline containing 0.5% Tween 20 (TBST). Phages (1×10^{11}, 10 μL) from the original library were incubated with antibody complexes for 20 min, followed by washing 10 times with 1 mL of TBST. Negative selection with control Rbt IgG was performed at every round of panning. Unbound phages from negative selection were further incubated with anti-S1-RBD IgG complexes and washed as described above. Bound phages were eluted with glycine buffer (pH 2.2) and immediately neutralized using 1 M Tris-HCl (pH 9.0), followed by the amplification for subsequent rounds of panning. After three rounds of panning, the specific binding of positive single phage clones against anti-S1-RBD IgG was confirmed by sandwich ELISA using anti-S1-RBD IgG coated ELISA plates and an HRP-conjugated anti-M13 mouse mAb (Zymed Laboratories, South San Francisco, CA). The DNA sequences of isolated phages were analyzed using extracted single-stranded DNA (ssDNA) according to the manufacturer's instructions.

Fluorescent focus assay and focus reduction neutralization test

To determine DENV titer, BHK (1×10^4/well) cells were seeded on 96 well plate for 16-18 h. Ten-fold serial dilutions of the virus stock or the sample containing DENV were added and incubated for 2 h at 37 °C (100 μL/well). For the FRNT, the antibodies (anti-S1-RBD IgG, control Rbt IgG, diluted COVID-19 patients' or healthy donors' sera) were preincubated with DENV serotype 2 strain 16681 (MOI=0.001) for 1 h before incubation. Later, the monolayers were overlaid with DMEM containing 2% FBS and 1% methylcellulose (100 μL/well), and the plates were incubated at 37 °C for another 4 days. The BHK cells were then fixed with 4% paraformaldehyde for 15 min at room temperature (RT). Later, the cells were washed with PBS. Virus foci were stained with an anti-NS1 antibody (mAb 33D2) (5 μg/mL) overnight at 4°C. After being washed with PBS, the cells were incubated with Alexa 488-conjugated goat anti-mouse IgG (Invitrogen) (1:1000) in PBS for 1 h. Finally, the secondary antibodies were washed away, and plaques were visualized using a DP72 fluorescence microscope (Olympus, Tokyo, Japan). The number of focus counted in the entire well was converted into the virus titer or infection rate (%).

Antibody-dependent enhancement

To investigate whether anti-S1-RBD IgG could cause ADE during DENV infection, THP-1 cells were infected with DENV serotype 2 strain 16681 (MOI=10) with or without the indicated antibody. After 72 h, the supernatants were collected and viral titers were further calculated using FFA in BHK cells, as mentioned above.

Transwell permeability assay

HMEC-1 cells (1×10^5) were seeded on the upper chambers of Transwell plates (0.4 μm; Corning, The Netherlands) to form a monolayer. NS1 (2 μg/mL) was preincubated with the indicated concentrations of different antibodies for 1 h at 37°C before incubation with the HMEC-1 monolayer for another 24 h. To determine the permeability of the HMEC-1 monolayer, the upper chamber was reconstituted with 300 μL of serum-free medium, which contained 3 μL of streptavidin-HRP (R&D Systems, Minneapolis, MN). After 15 min, 50 μL of the medium in the lower chamber was transferred into a 96-well plate, and 50 μL of TMB substrate (R&D Systems) was added to the wells for color development. The reaction was stopped by addition of 50 μL of 2N H_2SO_4. The absorbance at 450 nm was measured by a VersaMax microplate reader.

Mouse model of DENV infection

The animal study was performed in compliance with the Guide for the Care and Use of Laboratory Animals (The Chinese-Taipei Society of Laboratory Animal Sciences, 2010) and were approved by the Institutional Animal Care and Use Committee (IACUC) of NCKU under the number IACUC 109309. Six- to seven-week-old STAT1-deficient C57BL/6 (*STAT1-/-* B6) mice was used to infect DENV as previously described (29). The mice were maintained on standard laboratory food and water. To evaluate the protective effect provided by anti-S1-RBD IgG *in vivo*, *STAT1-/-* mice were intraperitoneally (i.p.) injected with mAb 33D2, control Rbt IgG, anti-S1-RBD IgG (150 μg/mouse) or PBS as a control 1 day before infection. Later, the mice were intravenously (i.v.) injected with concentrated DENV strain 16681 (1×10^7 PFU/mouse) or concentrated C6/36 medium as a control. In addition, mAb 33D2, control Rbt IgG or anti-S1-RBD IgG (150 μg/mouse) was i.p. administered 24 h after DENV inoculation. Three days after DENV infection, the tail bleeding time was tested, and mice were sacrificed to determine NS1 level in the blood by quantitative NS1 ELISA.

Bleeding time

Bleeding time was measured by cutting off 3–5 mm from the tip of the tail of the mouse. The duration of bleeding was recorded by monitoring the blood dripping onto filter paper every 30 s until the diameter of the blood droplet was smaller than 0.5 mm.

NS1 quantitative ELISA

To quantify the NS1 levels, an in-house NS1 sandwich ELISA was performed. Briefly, 5 μg/mL anti-NS1 mAb 31B2 was coated onto 96-well plates at 4°C overnight. After blocking with 1% BSA in PBS for 1 h, mouse sera (1:4 dilutions) were

coincubated with 2.5 μg/mL biotin-conjugated anti-NS1 mAb 33D2 at 37°C for 1 h. An HRP-labeled streptavidin solution (1:40) (R&D Systems) was added to the wells, which were incubated at RT for 40 min. After washing the wells three times with PBST (0.05% Tween 20 in PBS), TMB was added to the wells for color visualization. Following the addition of stop solution (2N H2SO4), the absorbance at 450 nm was read by a VersaMax microplate reader.

Statistical analysis

All data were analyzed by GraphPad Prism version 5.0 (GraphPad Software Inc., CA). The *in vitro* and *in vivo* data are expressed as the means ± standard deviations (SDs) from three independent experiments. Student's t test was used to analyze the differences between two groups One-way ANOVA with a Kruskal–Wallis comparison test was used to analyze the differences among multiple groups. P values <0.05 were considered statistically significant.

Results

Antibodies against the SARS-CoV-2 spike protein in archived dengue patient sera

A Previous study revealed that the anti-DENV E mAb could bind to the SARS-CoV-2 S1-RBD in a computational simulation (24). Here, to investigate whether antibodies in dengue patient sera could cross-react with SARS-CoV-2 spike proteins, SARS-CoV-2 recombinant proteins (trimeric spike and S1-RBD) were coated on ELISA plates and bound IgG was detected. The results showed that dengue patient sera contain more antibodies that could cross-react with SARS-CoV-2 proteins than healthy donor sera. Furthermore, the binding of antibodies to SARS-CoV-2 S1-RBD was much significant increase than to the trimeric spike protein in dengue patients as compared with healthy donors (P=0.0005 vs. P=0.0483) (Figure 1).

Anti-S1-RBD IgG purification and characterization

To further understand the antigenic cross-reactivity between the SARS-CoV-S1 RBD and DENV antigens, two Rbts were immunized with S1-RBD recombinant protein. Anti-S1-RBD IgG in the Rbt immune sera was purified by protein G agarose followed by S1-RBD-conjugated sepharose beads (Figure 2A). The binding ability of antibodies, including anti-S1-RBD IgG, IgG of S1-RBD-immunized Rbt serum, flow-through Rbt IgG, and normal Rbt IgG to the S1-RBD was compared using an indirect ELISA. The results showed that at the same concentration, the binding ability of anti-S1-RBD IgG was the highest, followed by IgG of S1-RBD-immunized Rbt serum, flow-through Rbt IgG, and normal rabbit IgG which showed no binding activity to the S1-RBD at all (Figure 2B). Since flow-through Rbt IgG was purified from the same immune Rbt sera, it was used as a control Rbt IgG (cRbt IgG) to compare with anti-S1-RBD IgG for later experiments. Next, to evaluate whether anti-S1-RBD IgG could recognized the RBD in native spike proteins, the binding ability of anti-S1-RBD IgG to the trimeric

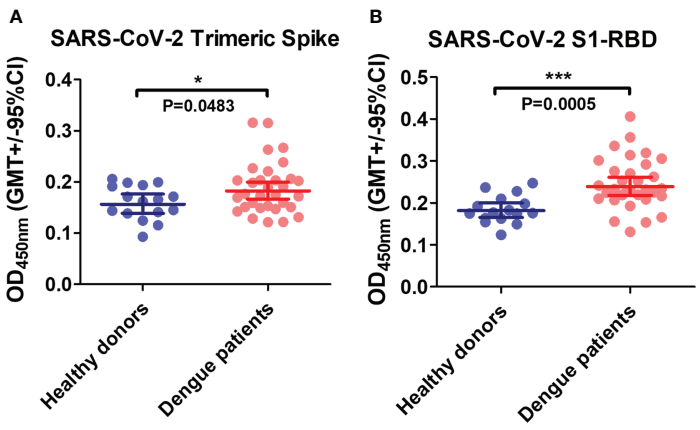

FIGURE 1
The presence of anti-SARS-CoV-2 antibodies in dengue patients' sera. Recombinant SARS-CoV-2 proteins **(A)** trimeric spike and **(B)** S1-RBD were coated on ELISA plates. The bound antibodies were detected using an indirect ELISA. *P < 0.05, ***P < 0.001. (n = 32 for dengue patient; n=16 for healthy donor).

spike protein and a SARS-CoV-2 pseudovirus was evaluated using Western blotting analysis (Figure 2C) and indirect ELISA (Figure 2D, E). The results showed that anti-S1-RBD IgG could recognize both the trimeric spike proteins and the SARS-CoV-2 pseudoviruses in both denatured and native forms. In addition, anti-S1-RBD IgG also showed neutralization activity against SARS-CoV-2 pseudovirus infection in a dose-dependent manner with an IC50 (the half maximal inhibitory concentration) value of 50 μg/mL (Supplementary Figure 2).

Anti-S1-RBD IgG cross-reacts with DENV proteins

Next, to investigate whether anti-S1-RBD IgG could cross-react with DENV proteins, the cross-reactivity of IgG from S1-RBD-immunized Rbt serum and anti-S1-RBD IgG to different DENV proteins, including E, PrM, NS1, and NS4B was tested. We found that 1 μg/mL of anti-S1-RBD IgG could cross-react with DENV E, prM, and NS1, particularly DENV E, which had the strongest cross-reaction compared to that of the others (Figure 3A). However, no cross-reactivity to DENV NS4 was observed. Since all these recombinant proteins contained 6X His-tag, these results ruled out that the bindings of anti-S1-RBD IgG to DENV E, PrM, and NS1 were due to His-tag. Purified IgG from S1-RBD-immunized Rbt sera could also bind to DENV E, prM, and NS1, however, much higher doses were required as compared with what we found in anti-S1-RBD IgG (25 vs. 1 μg/mL) (Figure 3A; Supplementary Figure 3). In addition, the cross-reactions of anti-S1-RBD IgG to native DENV proteins were also confirmed in DENV-infected C6/36 cells. As shown in Figure 3B, anti-S1-RBD IgG could cross-react with DENV-infected C6/36 cells but not the C6/36 mock infection control cells. Similar staining patterns of anti-S1-RBD IgG and anti-DENV E was noticed. We, therefore, used immunofluorescence confocal microscopy to further visualize the colocalization of anti-S1-RBD IgG and DENV E as shown in Figure 3C. Moreover, the cross-reactions of anti-S1-RBD IgG to DENV antigens were also confirmed in the concentrated supernatant of DENV by western blotting (Supplementary Figure 4). The results showed that both E and NS1 proteins of DENV were recognized by anti-S1-RBD IgG and the band of E protein recognized by anti-S1-RBD IgG was much stronger than the

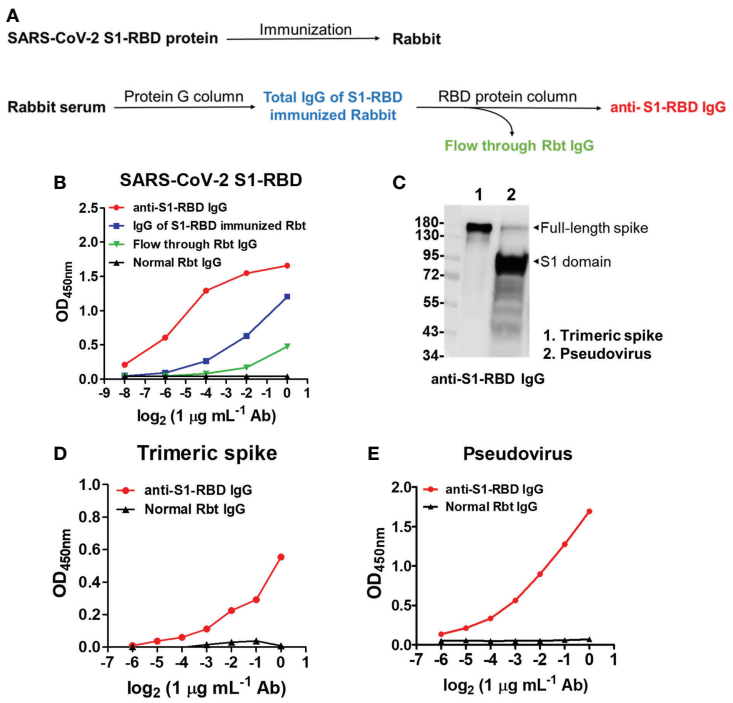

FIGURE 2
SARS-CoV-2 S1-RBD immunization and anti-S1-RBD IgG purification. **(A)** The flow chart of anti-S1-RBD IgG purification from anti-S1-RBD hyperimmune rabbit sera by protein G and RBD-conjugated affinity columns. **(B)** The binding ability of anti-S1-RBD IgG to the S1-RBD was detected by an indirect ELISA using an anti-Rbt IgG-HRP antibody. **(C)** The binding ability of anti-S1-RBD IgG to trimeric spike protein (lane 1) and SARS-CoV-2 pseudovirus (lane 2) was detected by Western blotting and by indirect ELISA **(D, E)**. The experiments were repeated two or three times with similar results, data from a single representative experiment was shown.

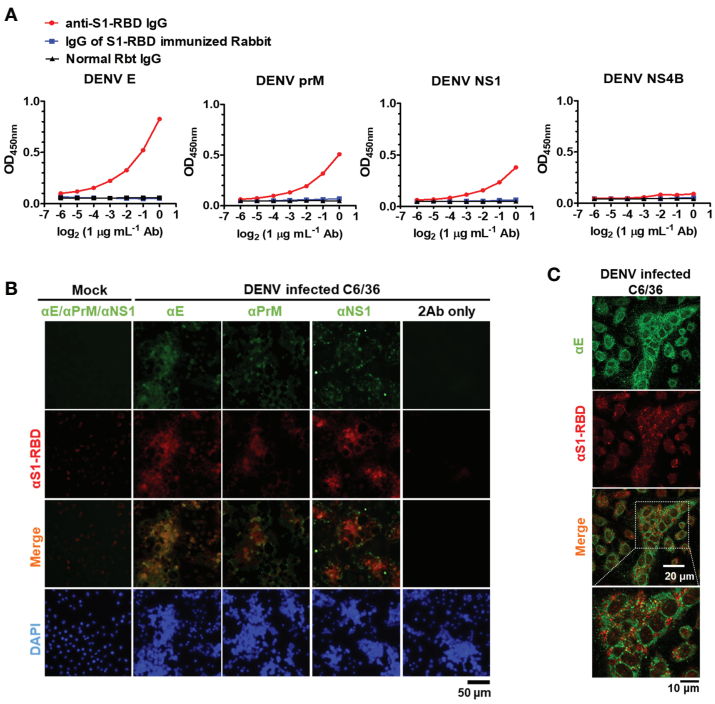

FIGURE 3
Anti-S1-RBD IgG cross-reacts with DENV proteins. **(A)** Recombinant DENV proteins, including envelope (E), precursor membrane (prM), and nonstructural proteins (NS1, NS4B), were coated in an ELISA plate. The cross-reactivity of anti-S1-RBD IgG to different DENV antigens was tested by an indirect ELISA. **(B)** The colocalization of anti-S1-RBD IgG (detected by goat-anti-Rbt-594) and different anti-DENV mAbs (detected by goat anti-mouse Alexa 488-conjugated antibodies) in DENV-infected C6/36 cells was determined by an immunofluorescent assay and visualized by Flourescence microscope DP72 (Olympus, Japan). **(C)** The colocalization of anti-S1-RBD IgG and anti-DENV E mAb were visualized by an FV3000-confocal laser scanning microscope (Olympus, Japan). The experiments were repeated two or three times with similar results, data from a single representative experiment was shown.

band of NS1 protein. These results suggest that most of the anti-S1-RBD IgG recognized E protein.

Identification of the sequences/epitopes recognized by Anti-S1-RBD IgG using a phage-displayed 12-mer random peptide library kit

To further identify the epitopes recognized by anti-S1-RBD IgG and investigate the antigenic similarity between the SARS-CoV-2 S1-RBD and DENV E, a phage-displayed 12-mer library kit was used. The detailed procedure was described in the materials and methods, and the workflow was presented in Supplementary Figure 5A. In brief, 10^{11} pfu of phages were negatively selected by flow-through Rbt IgG, followed by positive selection using anti-S1-RBD IgG. After three rounds of panning, fourteen single phage colonies were selected and the binding ability of these phages to anti-S1-RBD IgG were confirmed by a sandwich ELISA (Supplementary Figure 5B). The DNA of the selected phage was analyzed by Sanger sequencing and the nucleotide sequence encoding the displayed 12-mer peptide was further converted into the amino acid sequence. Twelve of fourteen (85.7%) phages showed an amino acid sequence of TQFEKASVNTTR (phage epitope 1), and two of fourteen (14.3%) showed an amino acid sequence of RDISIVPWNIRT (phage epitope 2) (Supplementary Figure 5C). This result suggested that most of the anti-S1-RBD IgG recognized the sequence of TQFEKASVNTTR (phage epitope 1).

The peptide TQFEKASVNTTR competitively reduces Anti-S1-RBD IgG binding to the SARS-CoV-2 S1-RBD and DENV E protein

Since the peptide TQFEKASVNTTR was recognized by most of the anti-S1-RBD IgG, we further confirmed whether the peptide TQFEKASVNTTR contributed to the cross-reaction of anti-S1-RBD IgG to DENV E by the competitive ELISA (Figure 4). The results showed that the binding ability of

anti-S1-RBD IgG to the SARS-CoV-2 S1-RBD and DENV E protein but not prM nor NS1 was significantly decreased by the TQFEKASVNTTR peptide in a dose-dependent manner (Figure 4A). On the other hand, the RDISIVPWNIRT peptide showed no inhibition on the binding of anti-S1-RBD IgG to the SARS-CoV-2 S1-RBD, DENV E, prM, or NS1 proteins. In addition, we also aligned the phage epitope (TQFEKASVNTTR) and SARS-CoV-2 S1-RBD protein sequence using BioEdit. The result showed that the sequence of amino acids (a.a.) 343-347 (FNATR) in the S1-RBD protein is similar to part of the sequence of phage epitope 1 (VNTTR) (Figure 4B). The amino acid positions 343-347 in the S1-RBD protein structure (PDB ID: 6M0J) was found to be located on the surface of the S1-RBD protein structure using PyMOL (Figure 4C). We further analyzed the epitope of DENV E protein recognized by anti-S1-RBD IgG using PyMOL visualization (DENV E protein structure, PDB ID: 1OAN) and sequence alignment by BioEdit (Figure 4B). The result suggested that anti-S1-RBD IgG might cross-react to DENV E protein a.a. 64-69, which are also located on the E protein surface (Figures 4B, C).

Anti-S1-RBD IgG inhibits DENV infection and NS1-induced endothelial hyperpermeability without causing ADE *in vitro*

To investigate whether anti-S1-RBD IgG could inhibit DENV infection, FRNT assay was used. The results showed that anti-S1-RBD IgG could decrease DENV infection *in vitro* in a dose-dependent manner. Significant inhibition of DENV infection was found when the concentration of anti-S1-RBD IgG reached to 20 μg/mL, while 20 μg/mL cRbt IgG did not (Figure 5A). In addition, since anti-S1-RBD IgG could bind to DENV NS1 (Figure 3A), a critical viral protein which could directly induce vascular leak (30–32), we investigated whether anti-S1-RBD IgG could block NS1-induced hyperpermeability in endothelial cells (HMEC-1) using Transwell assay. Surprisingly, the endothelial hyperpermeability induced by 2 μg/mL DENV NS1 could be blocked by 10 μg/mL anti-S1-RBD IgG, while 20 μg/mL cRbt IgG could not (Figure 5B). Anti-NS1 mAb 33D2, a homemade mAb (5 μg/mL) which can block NS1-induced hyperpermeability as previously described (33) was

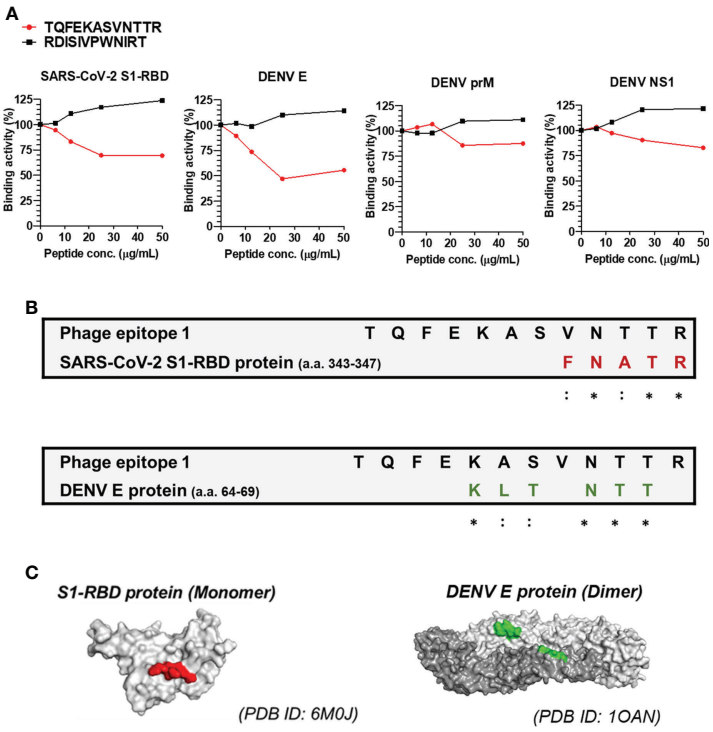

FIGURE 4
Epitope mapping of anti-S1-RBD IgG binding to DENV E protein. **(A)** Anti-S1-RBD IgG (0.125 μg/ml) was preincubated with a 2-fold dilution of synthetic free peptide of phage epitope 1 (TQFEKASVNTTR), and the binding ability to DENV proteins was detected by a competitive ELISA. **(B)** Alignment of the phage epitope 1 (TQFEKASVNTTR) with the SARS-CoV-2 S1-RBD and DENV envelope protein. *: identical,::conservative amino acid. **(C)** The positions of the consensus protein sequence in the structures of SARS-CoV-2 S1-RBD or DENV envelope protein are shown in red or green, respectively.

used as the positive control in this experiment. On the other hand, since ADE is a general concern in dengue infection, we further confirmed whether anti-S1-RBD IgG might cause ADE in DENV infection using human monocytic cell line THP-1 cells which express Fc receptor on their surface. Anti-prM mAb (clone 70-21) was used as a positive control for ADE (34). The result showed that DENV (MOI=10) could infect THP-1 cells only in the presence of anti-prM mAb (0.15-2.5 μg/mL). Twofold serial dilutions of anti-S1-RBD IgG, control mouse (cm) IgG, or cRbt IgG from 10 μg/mL were tested for their ability to enhance DENV infection of THP-1 cells. However, no enhancement of DENV infection in THP-1 cells was found in any concentrations of these antibodies we tested (Figure 5C).

Possible epitope of DENV NS1 recognized by anti-S1-RBD IgG

Since anti-S1-RBD IgG, like anti-NS1 mAb 33D2, can block NS1-induced endothelial hyperpermeability and the epitope recognized by the mAb 33D2 is known (33). We compared the sequences recognized by the mAb 33D2 and the S1-RBD and found sequence homology between NS1 (a.a. 115-119) and the S1-RBD (a.a. 376-380) (Figure 6A). It was further observed that only the mAb 33D2 but not other anti-NS1 mAb (2E8, 19-5. DN5C6) (30) and anti-NS1 polyclonal antibodies (pAb) could cross-react with the SARS-CoV-2 S1-RBD (Figure 6B). Furthermore, the results from competitive ELISA showed that mAb 33D2 binding to the SARS-CoV-2 S1-RBD was blocked in the presence of 33D2 recognized NS1 peptide (a.a. 109-122 of NS1, TELKYSWKTWGKAK) or RBD peptide (a.a. 367-381 of the SARS-CoV-2 S1-RBD, VLYNSASFSTFKCYG) but not phage epitope 1 (TQFEKASVNTTR) in a dose-dependent manner (Figure 6C), indicating there is a potential antigenic similarity between DENV NS1 and SARS-CoV-2 S1-RBD which can be recognized by anti-S1-RBD IgG.

Anti-S1-RBD IgG protects mice from DENV infection-induced prolonged bleeding time and decreases NS1 level in mouse sera

To evaluate the protective effect provided by anti-S1-RBD IgG against DENV infection *in vivo*, we evaluated DENV infection-induced hemorrhage in *STAT1*-/- mice (Figure 7A)

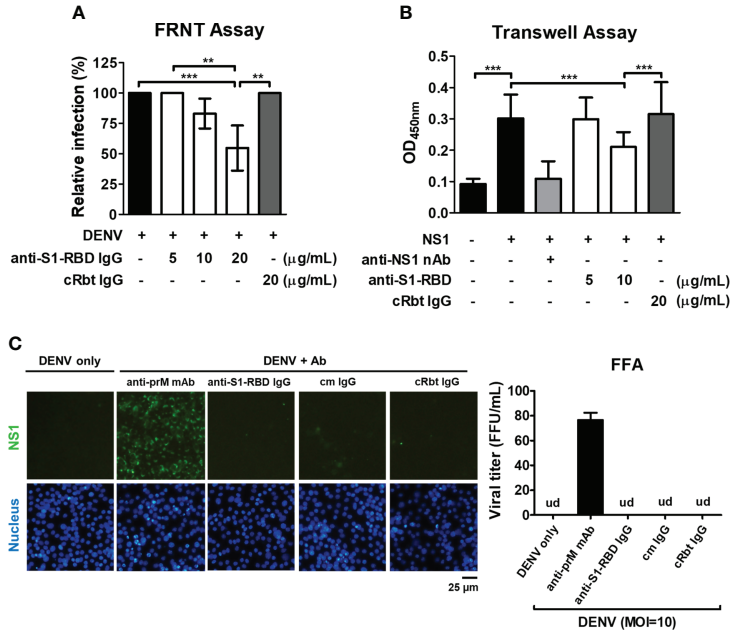

FIGURE 5
Influence of anti-S1-RBD IgG on DENV infection *in vitro*. **(A)** The neutralizing ability of different concentrations of anti-S1-RBD IgG or cRbt IgG against DENV infection was tested by a FRNT assay. **(B)** The permeability of HMEC-1 cells was measured by a Transwell assay. Different concentrations of antibodies as indicated were preincubated with DENV recombinant NS1 (2 μg/mL). The anti-NS1 mAb 33D2 (5 μg/mL) was used as a positive control. **(C)** ADE assay was performed in DENV infection (MOI=10) of THP-1 cells. Anti-S1-RBD IgG, an anti-prM mAb, control mouse (cm) IgG or control rabbit (cRbt) IgG (0.15 μg/mL) were incubated with DENV before infection. The infection of the cells was observed by immunofluorescent microscopy (left) and measured by FFA to determine viral titer (right). An anti-prM mAb (clone 70-21) was used as a positive control. Viral titer was un-detectable (ud) in all groups except in anti-prM mAb-treated group. $^{**}P < 0.01$, $^{***}P < 0.001$.

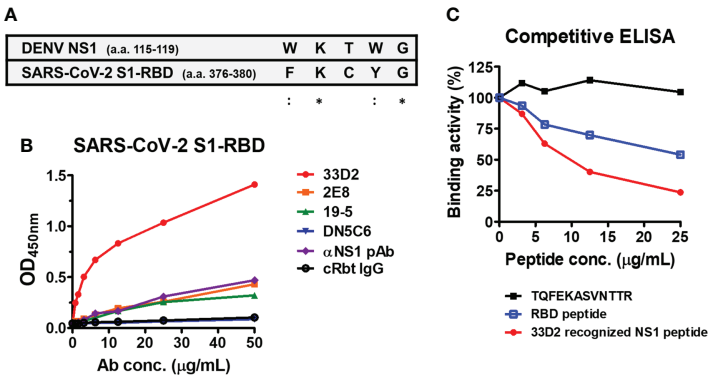

FIGURE 6
Monoclonal antibody against NS1 (33D2) cross-reacts with the SARS-CoV-2 S1-RBD. **(A)** Alignment between the epitope of DENV NS1 recognized by mAb 33D2 and SARS-CoV-2 S1-RBD protein sequence. *: identical;::conservative amino acid. **(B)** The binding of different NS1 antibodies to SARS-CoV-2 S1-RBD was measured by an indirect ELISA. **(C)** Competitive ELISA of mAb 33D2 binding to SARS-CoV-2 S1-RBD in the presence of different peptides. Anti-DENV NS1 mAb 33D2 (0.625 μg/ml) was preincubated with 2-fold dilutions of synthetic peptide (TQFEKASVNTTR), RBD peptide (VLYNSASFSTFKCYG), and 33D2-recognized NS1 peptide. The binding ability of the mAb 33D2 against the SARS-CoV-2 S1-RBD was detected by anti-mouse IgG-HRP antibodies. The experiments were repeated two or three times with similar results, data from a single experiment was presented.

(35). Mouse injected with the mAb 33D2, which can protect mice from DENV infection, was used as a positive control (34). In addition, mice injected with PBS or cRbt IgG were used as a negative control. The results showed that injection of mice with cRbt IgG 1 day before and 1 day after DENV infection induced bleeding time prolong and increased NS1 level in mouse sera as compared to those in mice injected with PBS without DENV infection. However, injection of mice with anti-S1-RBD IgG 1 day before and 1 day after DENV infection protected mice from DENV-induced prolonged bleeding time (Figure 7B) and reduced NS1 level in mouse sera as good as mouse injected with mAb 33D2 (Figure 7C). DENV titers in the sera of these mice after 3 days of infection were also evaluated by FFA using BHK cells; however, the DENV titers in these mice sera were too low to be detected.

Antibodies against DENV in COVID-19 patients' sera

Lastly, the COVID-19 patients' sera were used to investigate whether the cross-reaction of anti-S1-RBD IgG to DENV E protein can hinder DENV infection *in vitro*. As shown in (Figure 8A), the levels of antibodies against the SARS-CoV-2 S1-RBD recombinant protein were significantly increased in COVID-19 patients' sera. The levels of antibodies binding to DENV E and the synthetic peptide of phage epitope 1 in COVID patients' sera were also higher than those in healthy donors' sera, even though, no statistical difference was found in COVID patients as compared to that in healthy donors (Figure 8B, C). To further investigate whether antibodies in COVID-19 patients' sera could interfere with DENV infection, the neutralizing ability of sera from COVID-19 patient against DENV infection was tested by an FRNT assay. Surprisingly, the diluted (1:80) COVID-19 patients' sera could significantly reduce DENV infection with a MOI of 0.001 in the FRNT system (Figure 8D). In fact, COVID patients' sera with different dilution factors, from 1:20 to 1:160, showed neutralizing ability against dengue infection (data not shown). Furthermore, the neutralizing ability of sera from COVID-19 patients against DENV infection could be blocked in the presence of S1-RBD protein, but not SARS-CoV-2 nucleocapsid protein (Supplementary Figure 6). These results suggested that antibodies recognized S1-RBD may involve in the inhibition of DENV infection by COVID-19 patients' sera.

Discussion

In this study, we found a significant increase in antibody binding to SARS-CoV-2 trimeric spike and S1-RBD proteins from archived dengue sera collected from the 2015 dengue outbreak in Tainan city compared to that in healthy donor sera. Because these sera were collected predating the COVID-19 outbreak, we concluded that DENV infection may induce the production of SARS-CoV-2 cross-reactive antibodies and that most of these antibodies recognized the S1-RBD of spike protein. To further understand the antigenic cross-reactivity between the SARS-CoV-S1 RBD and DENV antigens, SARS-CoV-2 S1-RBD recombinant protein was used to immunize rabbits. Anti-S1-RBD IgG was purified from SARS-CoV-2 S1-RBD hyperimmune rabbit sera by both protein G and S1-RBD-

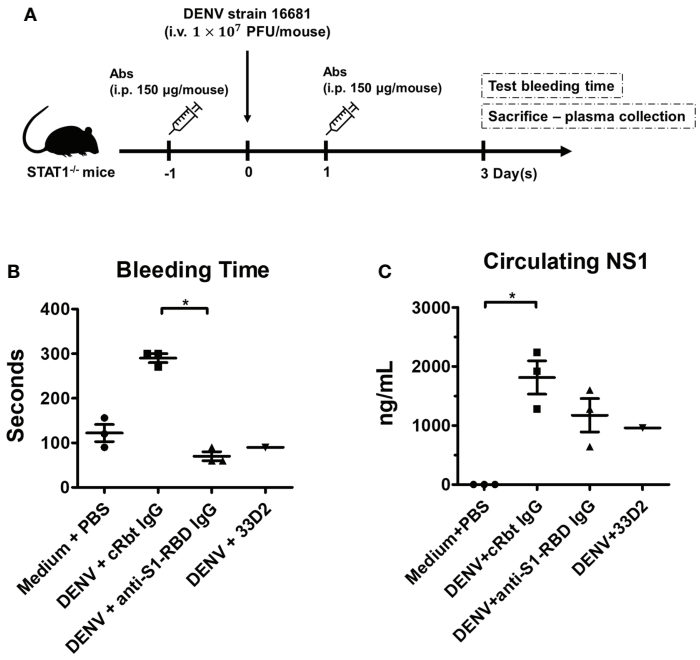

FIGURE 7
Anti-S1-RBD IgG protects mice from DENV infection-induced pathogenesis. **(A)** Anti-DENV NS1 (33D2), control Rbt IgG, and anti-S1-RBD IgG antibodies (150 μg/mouse) were intraperitoneally (i.p.) injected into STAT1-deficient C57BL/6 (STAT1-/- B6) mice, and one day later, 1×10^7 pfu/mouse DENV was intravenously (i.v.) injected into the mice. On day one post-infection, the mice were i.p. injected with 150 μg of antibodies. **(B)** The tail bleeding time was tested on day 3 postinfection. **(C)** The NS1 level in the sera was determined by an NS1 quantitative ELISA [n = 3 for medium control, control Rbt IgG, and anti-S1-RBD IgG, n = 1 for anti-DENV NS1 antibody (33D2)]. *P < 0.05; Kruskal–Wallis ANOVA.

conjugated affinity columns. These affinity-purified anti-S1-RBD IgG could recognize not only S1-RBD recombinant protein but also the trimeric spike protein and SARS-CoV-2 pseudovirus by ELISA and Western blotting analysis, indicating it could recognize S1-RBD in different native and denatured forms. In addition, anti-S1-RBD IgG could neutralize SARS-CoV-2 pseudovirus infection, even though the maximum inhibition was only about 50% at concentration of 50 μg/mL. Most importantly, these anti-S1-RBD IgG could cross-react with DENV recombinant proteins (including E, NS1, and PrM), concentrated dengue viral supernatant, and DENV-infected cells using different experimental approaches (including ELISA, western blotting, and IFA). Previously, antibodies in COVID-19 patient sera that can cross-react with DENV E and NS1 proteins have been reported (8, 11). In addition, possible similarities between SARS-CoV-2 epitopes in the HR2 domain of the S2 subunit of spike protein and the dengue E protein have been revealed by *in-silico* analysis (11). However, no experiment has been performed to prove that antigenic similarity between SARS-CoV-2 and DENV indeed can induce antibodies cross-react with each other. In this study, we are the first to demonstrate that immunization with SARS-CoV-2 S1-RBD indeed could induce DENV cross-reactive SARS-CoV-2 S1-RBD specific antibodies.

The results of dengue patients' sera from this study also confirmed previous reports that archived dengue patient sera prior to the pandemic of 2019 SARS-CoV-2 contain antibodies which can cross-react with SARS-CoV-2. These SARS-CoV-2 cross-reactive antibodies in dengue patients can cause false-positive SARS-CoV-2 serology results (7, 36). Since the clinical and laboratory features of COVID-19 and dengue can be very similar, potential misdiagnosis between COVID-19 and dengue may arise if only rapid serological tests are used in dengue endemic regions (10, 37, 38). The misdiagnosis of both diseases will have serious consequences for both patient treatment and public health control. Therefore, in addition to antibody detection, antigen detection and RT–PCR to detect the viral genome should be performed to confirm the diagnosis.

Currently, the impact of antibody cross-reactivity with SARS-CoV-2 and DENV on the severity of both diseases in patients is still controversial. It is unclear whether antibodies induced by the antigenic cross-reactivity between DENV and SARS-CoV-2 can provide protective immunity overlap between these two diseases or worsen the disease through ADE. A recent study showed that previous SARS-CoV-2 infection may increase the risk of severe dengue (39). However, dengue fever might follow a less severe course, has also been found in children with recent SARS-CoV-2 infection (40). In these children, a trend

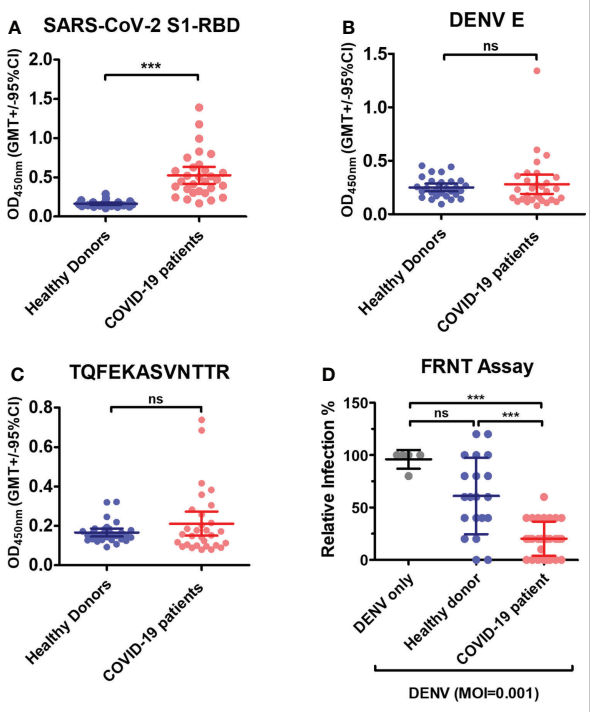

FIGURE 8
Antibodies in COVID-19 patients' sera cross-react with DENV E and inhibit DENV infection *in vitro*. **(A)** Recombinant SARS-CoV-2 S1-RBD, **(B)** DENV E or **(C)** synthetic peptide of phage epitope 1 (2 μg/mL) was coated on ELISA plates. The binding of antibodies in COVID patient sera (1:100 diluted) to these plates was detected by an indirect ELISA. ***P < 0.001, ns indicates no significant difference between two groups as determined by t test. **(D)** The neutralizing ability of sera from COVID-19 patient (1:80 diluted) against DENV infection was tested by an FRNT assay. ***P < 0.001; Kruskal–Wallis ANOVA. (n = 30 for COVID-19 patient; n = 21 for healthy donor).

toward a lower incidence of acute kidney injury and fewer organ dysfunctions has been reported. On the other hand, previous dengue infection may also increase the risk of severe COVID-19 due to cross-reactive non-neutralizing antibodies (41). To make the situation more complex, coinfection of SARS-CoV-2 and DENV is a significant public health problem, especially in dengue endemic areas. Therefore, the bidirectional impact of protection or ADE in COVID-19 and dengue is a growing concern (42, 43). In this study, we found that anti-S1-RBD IgG could inhibit DENV infection in BHK cells and DENV NS1-induced endothelial hyperpermeability in HMEC-1 cells. No ADE of DENV infection in THP-1 cells was found. Furthermore, these antibodies could reduce prolonged bleeding time and decrease NS1 seral level in DENV-infected mice. Therefore, our results suggest that SARS-CoV-2 S1-RBD-induced DENV cross-reactive antibodies may hinder dengue pathogenesis.

Four mAbs against DENV E that can neutralize DENV infection are predicted to bind to the S1-RBD, which is crucial for interaction with ACE2, based on *in silico* simulation (24). It is known that antibodies bound to E domain III (EDIII) are the most potent blockers of DENV (44). Another study also concluded that human mAbs recognizing EDIII, the EDI/EDII hinge, the E-dimer epitope, or a quaternary epitope involving EDI/EDII/EDIII are more potently neutralizing than antibodies recognizing the fusion loop (FL, 98–109 residues) of EDII (45). In this study, we used a phage-displayed random peptide library and identified that DENV E amino acid residues 64-69 were probably recognized by anti-S1-RBD IgG. Since anti-S1-RBD IgG could neutralize DENV infection only at low MOIs, residues 64-69 may represent a weak neutralizing epitope. It is known that N-linked glycans at Asn67 of DENV E dimer can bind to the carbohydrate recognition domain of DC-SIGN (46)., which are crucial for DENV binding and infection of cells (47). Therefore, we suspected that anti-S1-RBD IgG may interfere with the interaction between DENV E dimer and DC-SIGN, leading to the inhibition of DENV infection.

Based on the results of a competitive ELISA, the peptide TQFEKASVNTTR could inhibit only anti-S1-RBD IgG binding to the E protein, whereas it could not inhibit anti-S1-RBD IgG cross-reacting with prM or NS1. It is possible that the majority of the anti-S1-RBD IgG cross-reacted with DENV E. Therefore, the peptide (TQFEKASVNTTR) was identified by the phage-displayed random peptide library. Due to that, the epitope recognized by NS1 or prM cross-reactive anti-S1-RBD IgG could not be identified by this method. Since NS1 plays important roles in dengue pathogenesis (48, 49) and anti-S1-RBD IgG could also inhibit NS1-induced endothelial hyperpermeability, we tested the cross-reactivity of a few anti-NS1 mAbs with a SARS-CoV-2 S1-RBD protein-coated ELISA. Surprisingly, we found that only mAb 33D2 but not other anti-NS1 antibodies could cross-react with the SARS-CoV-2 S1-RBD. Since the epitope recognized by mAb 33D2 is known, we compared the NS1 a.a. 115-119 (WKTWG) sequence which was recognized by mAb 33D2 with SARS-CoV-2 S1-RBD protein and found a similar sequence FKCYG, which is located at a.a. 376-380 of SARS-CoV-2 S1-RBD. Thus, in addition to potential antigenic similarity between SARS-CoV-2 S1-RBD and DENV E protein, these results suggested that SARS-CoV-2 S1-RBD also contain potential antigenic similarity to DENV NS1 protein, which can induce antibodies that cross-react with NS1 and inhibit NS1-induced hyperpermeability.

In this study, even though we found significant increase of SARS-CoV-2 S1-RBD cross-reactive antibodies in the sera of dengue patients, the increase of DENV cross-reactive antibodies in the sera of COVID-19 patients was not significantly different from healthy controls. It is possible that the structural and conformational difference between SARS-CoV-2 S1-RBD and DENV (E and NS1) as well as the genetic background and immune status of different individuals may influence the generation of SARS-CoV-2 and DENV cross-reactive antibodies during DENV or SARS-CoV-2 infection. Nonetheless, we found DENV infection *in vitro* was inhibited in the presence of COVID-19 patients' sera. This is consistent

with a recent publication (50), in which the authors demonstrated that most of the sera of COVID-19 patients contain antibodies cross-react with DENV, which can neutralize dengue infection *in vitro*. Therefore, it is possible that DENV E protein cross-reactive anti-SARS-CoV-2 antibodies in COVID-19 patients' sera may play a role in the inhibition of DENV infection. To further confirm this possibility, we pre-incubated the sera of COVID-19 patients with S1-RBD or nucleocapsid recombinant proteins in this study, and found that the effect of inhibiting dengue infection by COVID-19 patients' sera could be reduced after preincubation with S1-RBD but not nucleocapsid protein. These results supported the phenomenon we observed in the experiments conducted with anti-S1-RBD IgG from rabbit serum and the hypothesis we proposed: anti-S1-RBD antibodies may inhibit dengue infection by cross-reacting with dengue antigens. However, we could not completely rule out the possibility of these COVID-19 patients having been infected by dengue previously or currently. Therefore, further investigation is needed to confirm the role of anti-S1RBD antibodies in inhibiting dengue infection. In summary, we demonstrated in this study that the antigenic similarity between the SARS-CoV-2 S1-RBD and DENV (E and NS1) has the potential to induce DENV cross-reactive antibodies after SARS-CoV-2 S1-RBD immunization or SARS-CoV-2 infection. These DENV cross-reactive antibodies may not only cause false-positive result in dengue serological test but also hinder dengue infection which should be further validated in clinical study.

Data availability statement

The datasets presented in this study can be found in online repositories. The names of the repository/repositories and accession number(s) can be found in the article/Supplementary Material.

Ethics statement

The studies involving human participants were reviewed and approved by the institutional review board (IRB). Dengue patient sera were collected from National Cheng Kung University Hospital (NCKUH) under the number IRB #A-BR-101–140. COVID-19-positive sera were purchased from Access Biologicals LLC. According to the manufacturer's documentation, the samples were collected under IRB-approved protocols (SDP-001-FDA Licensed Plasmapheresis Center; SDP-002- U.S. Physician Network; SDP-003 Reference Laboratory Network). Written informed consent for participation was not required for this study in accordance with the national legislation and the institutional requirements. The animal study was reviewed and approved by the Institutional Animal Care and Use Committee (IACUC) of National Cheng Kung University (NCKU) under the number IACUC-109309.

Author contributions

Y-LC, C-HC and T-MY conceived and designed the experiments. Y-LC, C-HC, K-HH and H-JH performed the experiments and analyzed the data. Y-LC, Y-CL, C-HC and T-MY wrote and edited the paper. J-RW, S-WW, Y-CC and W-JC provided comments and suggestions during the preparation of the manuscript. All authors contributed to the article and approved the submitted version.

Funding

This study was supported by the Ministry of Science and Technology of Taiwan (MOST 110-2320-B-006-033, MOST 111-2321-B-006-009) and the National Health Research Institute (NHRI-110A1-MRCO-02212102).

Acknowledgments

We appreciate the technical services provided by the "Bio-imaging Core Facility of the National Core Facility Program for Biotechnology, Ministry of Science and Technology, Taiwan, as well as the technical service provided by the Instrument Development Center of NCKU".

Conflict of interest

YC-C is employed by Leadgene Biomedical, Inc.

The remaining authors declare that the research was conducted in the absence of any commercial or financial relationship that could be considered a potential conflict of interest.

Publisher's note

Supplementary material

The Supplementary Material for this article can be found online at: https://www.frontiersin.org/articles/10.3389/fimmu.2022.941923/full#supplementary-material

References

1. Vabret N, Britton GJ, Gruber C, Hegde S, Kim J, Kuksin M, et al. Immunology of COVID-19: Current state of the science. *Immunity* (2020) 52 (6):910–41. doi: 10.1016/j.immuni.2020.05.002

2. Synowiec A, Szczepanski A, Barreto-Duran E, Lie LK, Pyrc K. Severe acute respiratory syndrome coronavirus 2 (SARS-CoV-2): A systemic infection. *Clin Microbiol Rev* (2021) 34(2):e00133–20. doi: 10.1128/CMR.00133-20

3. Huang Y, Yang C, Xu XF, Xu W, Liu SW. Structural and functional properties of SARS-CoV-2 spike protein: Potential antivirus drug development for COVID-19. *Acta Pharmacol Sin* (2020) 41(9):1141–9. doi: 10.1038/s41401-020-0485-4

4. Premkumar L, Segovia-Chumbez B, Jadi R, Martinez DR, Raut R, Markmann A, et al. The receptor binding domain of the viral spike protein is an immunodominant and highly specific target of antibodies in SARS-CoV-2 patients. *Sci Immunol* (2020) 5(48):eabc8413. doi: 10.1126/sciimmunol.abc841

5. Walls AC, Park YJ, Tortorici MA, Wall A, McGuire AT, Veesler D. Structure, function, and antigenicity of the SARS-CoV-2 spike glycoprotein. *Cell* (2020) 181 (2):281–92. doi: 10.1016/j.cell.2020.02.058

6. Cao X. COVID-19: immunopathology and its implications for therapy. *Nat Rev Immunol* (2020) 20(5):269–70. doi: 10.1038/s41577-020-0308-3

7. Nath H, Mallick A, Roy S, Sukla S, Basu K, De A, et al. Archived dengue serum samples produced false-positive results in SARS-CoV-2 lateral flow-based rapid antibody tests. *J Med Microbiol* (2021) 70(6):1369. doi: 10.1099/jmm.0.001369

8. Yan G, Lee CK, Lam LTM, Yan B, Chua YX, Lim AYN, et al. Covert COVID-19 and false-positive dengue serology in Singapore. *Lancet Infect Dis* (2020) 20 (5):536. doi: 10.1016/S1473-3099(20)30158-4

9. Santoso MS, Masyeni S, Haryanto S, Yohan B, Hibberd ML, Sasmono RT. Assessment of dengue and COVID-19 antibody rapid diagnostic tests cross-reactivity in Indonesia. *Virol J* (2021) 18(1):54. doi: 10.1186/s12985-021-01522-2

10. Khairunisa SQ, Amarullah IH, Churrotin S, Fitria AL, Amin M, Lusida MI, et al. Potential misdiagnosis between COVID-19 and dengue infection using rapid serological test. *Infect Dis Rep* (2021) 13(2):540–51. doi: 10.3390/idr13020050

11. Lustig Y, Keler S, Kolodny R, Ben-Tal N, Atias-Varon D, Shlush E, et al. Potential antigenic cross-reactivity between SARS-CoV-2 and dengue viruses. *Clin Infect Dis* (2020) 73(7):e2444–9. doi: 10.1093/cid/ciaa1207

12. Messina JP, Brady OJ, Golding N, Kraemer MUG, Wint GRW, Ray SE, et al. The current and future global distribution and population at risk of dengue. *Nat Microbiol* (2019) 4(9):1508–15. doi: 10.1038/s41564-019-0476-8

13. Halstead SB. Antibody, macrophages, dengue virus infection, shock, and hemorrhage: A pathogenetic cascade. *Rev Infect Dis* (1989) 11(Suppl 4):S830–9. doi: 10.1093/clinids/11.supplement_4.s830

14. Ulrich H, Pillat MM, Tarnok A. Dengue fever, COVID-19 (SARS-CoV-2), and antibody-dependent enhancement (ADE): A perspective. *Cytometry A* (2020) 97(7):662–7. doi: 10.1002/cyto.a.24047

15. Henchal EA, Putnak JR. The dengue viruses. *Clin Microbiol Rev* (1990) 3 (41):376–96. doi: 10.1128/CMR.3.4.376

16. Avirutnan P, Punyadee N, Noisakran S, Komoltri C, Thiemmeca S, Auethavornanan K, et al. Vascular leakage in severe dengue virus infections: A potential role for the nonstructural viral protein NS1 and complement. *J Infect Dis* (2006) 193(8):1078–88. doi: 10.1086/500949

17. Beatty PR, Puerta-Guardo H, Killingbeck SS, Glasner DR, Hopkins K, Harris E. Dengue virus NS1 triggers endothelial permeability and vascular leak that is prevented by NS1 vaccination. *Sci Transl Med* (2015) 7(304):304ra141–304ra141. doi: 10.1126/scitranslmed.aaa3787

18. Modhiran N, Watterson D, Muller DA, Panetta AK, Sester DP, Liu L, et al. Dengue virus NS1 protein activates cells *via* toll-like receptor 4 and disrupts endothelial cell monolayer integrity. *Sci Transl Med* (2015) 7(304):304ra142. doi: 10.1126/scitranslmed.aaa3863

19. Thomas SJ. NS1: A corner piece in the dengue pathogenesis puzzle? *Sci Transl Med* (2015) 7(304):304fs37. doi: 10.1126/scitranslmed.aad1255

20. Martina BE, Koraka P, Osterhaus AD. Dengue virus pathogenesis: An integrated view. *Clin Microbiol Rev* (2009) 22(4):564–81. doi: 10.1128/CMR.00035-09

21. Rothman AL. Dengue: defining protective versus pathologic immunity. *J Clin Invest* (2004) 113(7):946–51. doi: 10.1172/JCI21512

22. Lei HY, Yeh TM, Liu HS, Lin YS, Chen SH, Liu CC. Immunopathogenesis of dengue virus infection. *J BioMed Sci* (2001) 8(51):377–88. doi: 10.1007/BF02255946

23. Lee WS, Wheatley AK, Kent SJ, DeKosky BJ. Antibody-dependent enhancement and SARS-CoV-2 vaccines and therapies. *Nat Microbiol* (2020) 5 (10):1185–91. doi: 10.1038/s41564-020-00789-5

24. Nath H, Mallick A, Roy S, Sukla S, Biswas S. Computational modelling supports that dengue virus envelope antibodies can bind to SARS-CoV-2 receptor binding sites: Is pre-exposure to dengue virus protective against COVID-19 severity? *Comput Struct Biotechnol J* (2021) 19:459–66. doi: 10.1016/j.csbj.2020.12.037

25. Chen HR, Chao CH, Liu CC, Ho TS, Tsai HP, Perng GC, et al. Macrophage migration inhibitory factor is critical for dengue NS1-induced endothelial glycocalyx degradation and hyperpermeability. *PloS Pathog* (2018) 14(4): e1007033. doi: 10.1371/journal.ppat.1007033

26. Lai YC, Cheng YW, Chao CH, Chang YY, Chen CD, Tsai WJ, et al. Antigenic cross-reactivity between SARS-CoV-2 S1-RBD and its receptor ACE2. *Front Immunol* (2022) 13:868724. doi: 10.3389/fimmu.2022.868724

27. Chen LC, Shyu HW, Lin HM, Lei HY, Lin YS, Liu HS, et al. Dengue virus induces thrombomodulin expression in human endothelial cells and monocytes *in vitro*. *J Infect* (2009) 58(5):368–74. doi: 10.1016/j.jinf.2009.02.018

28. Huang SW, Tai CH, Hsu YM, Cheng D, Hung SJ, Chai KM, et al. Assessing the application of a pseudovirus system for emerging SARS-CoV-2 and re-emerging avian influenza virus H5 subtypes in vaccine development. *BioMed J* (2020) 43(4):375–87. doi: 10.1016/j.bj.2020.06.003

29. Tien SM, Chang PC, Lai YC, Chuang YC, Tseng CK, Kao YS, et al. Therapeutic efficacy of humanized monoclonal antibodies targeting dengue virus nonstructural protein 1 in the mouse model. *PLoS Pathog* (2022) 18(4):e1010469. doi: 10.1371/journal.ppat.1010469

30. Chen HR, Chuang YC, Lin YS, Liu HS, Liu CC, Perng GC, et al. Dengue virus nonstructural protein 1 induces vascular leakage through macrophage migration inhibitory factor and autophagy. *PLoS Negl Trop Dis* (2016) 10(7): e0004828. doi: 10.1371/journal.pntd.0004828

31. Puerta-Guardo H, Glasner DR, Harris E. Dengue virus NS1 disrupts the endothelial glycocalyx, leading to hyperpermeability. *PLoS Pathog* (2016) 12(7): e1005738. doi: 10.1371/journal.ppat.1005738

32. Glasner DR, Ratnasiri K, Puerta-Guardo H, Espinosa DA, Beatty PR, Harris E. Dengue virus NS1 cytokine-independent vascular leak is dependent on endothelial glycocalyx components. *PLoS Pathog* (2017) 13(11):e1006673. doi: 10.1371/journal.ppat.1006673

33. Lai YC, Chuang YC, Liu CC, Ho TS, Lin YS, Anderson R, et al. Antibodies against modified NS1 wing domain peptide protect against dengue virus infection. *Sci Rep* (2017) 7(1):6975. doi: 10.1038/s41598-017-07308-3.Huang

34. Huang KJ, Yang YC, Lin YS, Huang JH, Liu HS, Yeh TM, et al. The dual-specific binding of dengue virus and target cells for the antibody-dependent enhancement of dengue virus infection. *J Immunol* (2006) 176(5):2825–32. doi: 10.4049/jimmunol.176.5.2825

35. Wan SW, Chen PW, Chen CY, Lai YC, Chu YT, Hung CY, et al. Therapeutic effects of monoclonal antibody against dengue virus NS1 in a STAT1 knockout mouse model of dengue infection. *J Immunol* (2017) 199(8):2834–44. doi: 10.4049/jimmunol.1601523

36. Vanroye F, Bossche DVD, Brosius I, Tack B, Esbroeck MV, Jacobs J. COVID-19 antibody detecting rapid diagnostic tests show high cross-reactivity when challenged with pre-pandemic malaria, schistosomiasis and dengue samples. *Diagn. (Basel)* (2021) 11(7):1163. doi: 10.3390/diagnostics11071163

37. Bokhari S, Mahmood F, Bokhari S. Case report: Diagnosis of COVID-19 versus tropical diseases in Pakistan. *Am J Trop Med Hyg* (2020) 103(1):77–8. doi: 10.4269/ajtmh.20-0356

38. Nunthavichitra S, Prapaso S, Luvira V, Muangnoicharoen S, Leaungwutiwong P, Piyaphanee W. Case report: COVID-19 presenting as acute undifferentiated febrile illness-a tropical world threat. *Am J Trop Med Hyg* (2020) 103(1):83–5. doi: 10.4269/ajtmh.20-0440

39. Rana MS, Usman M, Alam MM, Ikram A, Salman M, Umair M. Impact of previous SARS-CoV-2 infection on the rate of mortality in dengue. a preliminary report from Pakistan. *J Infect* (2022) 84(5):722–46. doi: 10.1016/j.jinf.2022.01.027

40. Ravikumar N, Randhawa MS, Nallasamy K, Angurana SK, Kumar M, Mohi GK, et al. Impact of recent SARS-CoV-2 infection on the course and severity of dengue in children: A prospective observational study from north India. *Am J Trop Med Hyg* (2021) 105(3):751–5. doi: 10.4269/ajtmh.21-0586

41. Nicolete VC, Rodrigues PT, Johansen IC, Corder RM, Tonini J, Cardoso MA, et al. Interacting epidemics in Amazonian Brazil: Prior dengue infection associated with increased coronavirus disease 2019 (COVID-19) risk in a population-based cohort study. *Clin Infect Dis* (2021) 73(11):2045–54. doi: 10.1093/cid/ciab410

42. El-Qushayri AE, Kamel AMA, Reda A, Ghozy S. Does dengue and COVID-19 co-infection have worse outcomes? A systematic review of current evidence. *Rev Med Virol* (2022) 1–7:e2339. doi: 10.1002/rmv.2339

43. Prapty C, Rahmat R, Araf Y, Shounak SK, Noor AA, Rahaman TI, et al. SARS-CoV-2 and dengue virus co-infection: Epidemiology, pathogenesis, diagnosis, treatment, and management. *Rev Med Virol* (2022) 1–11:e2340. doi: 10.1002/rmv.2340

44. Crill WD, Roehrig JT. Monoclonal antibodies that bind to domain III of dengue virus e glycoprotein are the most efficient blockers of virus adsorption to vero cells. *J Virol* (2001) 75(16):7769–73. doi: 10.1128/JVI.75.16.7769-7773.2001

45. Costin JM, Zaitseva E, Kahle KM, Nicholson CO, Rowe DK, Graham AS, et al. Mechanistic study of broadly neutralizing human monoclonal antibodies against dengue virus that target the fusion loop. *J Virol* (2013) 87(1):52–66. doi: 10.1128/JVI.02273-12

46. Pokidysheva E, Zhang Y, Battisti AJ, Bator-Kelly CM, Chipman PR, Xiao C, et al. Cryo-EM reconstruction of dengue virus in complex with the carbohydrate recognition domain of DC-SIGN. *Cell* (2006) 124(3):485–93. doi: 10.1016/j.cell.2005.11.042

47. Alen MM, Dallmeier K, Balzarini J, Neyts J, Schols D. Crucial role of the n-glycans on the viral e-envelope glycoprotein in DC-SIGN-mediated dengue virus infection. *Antiviral Res* (2012) 96(3):280–7. doi: 10.1016/j.antiviral.2012.10.007

48. Chen HR, Lai YC, Yeh TM. Dengue virus non-structural protein 1: a pathogenic factor, therapeutic target, and vaccine candidate. *J BioMed Sci* (2018) 25 (1):58. doi: 10.1186/s12929-018-0462-0

49. Glasner DR, Puerta-Guardo H, Beatty PR, Harris E. The good, the bad, and the shocking: The multiple roles of dengue virus nonstructural protein 1 in protection and pathogenesis. *Annu Rev Virol* (2018) 5(1):227–53. doi: 10.1146/annurev-virology-101416-041848

50. Nath H, Mallick A, Roy S, Kayal T, Ranjan S, Sengupta S, et al. COVID-19 serum can be cross-reactive and neutralizing against the dengue virus, as observed by the dengue virus neutralization test. *Int J Infect Dis* (2022) 122:576–84. doi: 10.1016/j.ijid.2022.07.013

frontiers | Frontiers in Immunology

TYPE Original Research
PUBLISHED 19 October 2022
DOI 10.3389/fimmu.2022.1042406

OPEN ACCESS

EDITED BY
Pedro A. Reche,
Complutense University of Madrid, Spain

REVIEWED BY
Daniel Smrz,
Charles University, Czechia
Stephanie Longet,
University of Oxford, United Kingdom

*CORRESPONDENCE
Huanle Luo
luohle@mail.sysu.edu.cn
Yuelong Shu
shuylong@mail.sysu.edu.cn

†These authors have contributed equally to this work

SPECIALTY SECTION
This article was submitted to Viral Immunology, a section of the journal Frontiers in Immunology

RECEIVED 12 September 2022
ACCEPTED 03 October 2022
PUBLISHED 19 October 2022

CITATION
Li N, Li X, Wu J, Zhang S, Zhu L, Chen Q, Fan Y, Wu Z, Xie S, Chen Q, Wang N, Wu N, Luo C, Shu Y and Luo H (2022) Pre-existing humoral immunity to low pathogenic human coronaviruses exhibits limited cross-reactive antibodies response against SARS-CoV-2 in children. *Front. Immunol.* 13:1042406. doi: 10.3389/fimmu.2022.1042406

Pre-existing humoral immunity to low pathogenic human coronaviruses exhibits limited cross-reactive antibodies response against SARS-CoV-2 in children

Nina Li[1,2†], XueYun Li[1,2†], Jiani Wu[1,2], Shengze Zhang[1,2], Lin Zhu[1,2], Qiqi Chen[1,2], Ying Fan[1,2], Zhengyu Wu[1,2], Sidian Xie[1,2], Qi Chen[1,2], Ning Wang[3], Nan Wu[4], Chuming Luo[1,2], Yuelong Shu[1,2,5,6*] and Huanle Luo[1,2,6*]

[1]School of Public Health (Shenzhen), Shenzhen Campus of Sun Yat-sen University, Shenzhen, China, [2]School of Public Health (Shenzhen), Sun Yat-sen University, Guangzhou, China, [3]Shenzhen Institute of Advanced Technology, Chinese Academy of Sciences, Shenzhen, China, [4]Department of Epidemiology, Shenzhen Nanshan Center for Disease Control and Prevention, Shenzhen, China, [5]Institute of Pathogen Biology, Chinese Academy of Medical Sciences and Peking Union Medical College, Beijing, China, [6]Key Laboratory of Tropical Disease Control, Sun Yat-sen University, Ministry of Education, Guangzhou, China

Severe acute respiratory syndrome coronavirus 2 (SARS-CoV-2) infection causes asymptomatic or mild symptoms, even rare hospitalization in children. A major concern is whether the pre-existing antibodies induced by low pathogenic human coronaviruses (LPH-CoVs) in children can cross-react with SARS-CoV-2. To address this unresolved question, we analyzed the pre-existing spike (S)-specific immunoglobin (Ig) G antibodies against LPH-CoVs and the cross-reactive antibodies against SARS-CoV-2 in 658 serum samples collected from children prior to SARS-CoV-2 outbreak. We found that the seroprevalence of these four LPH-CoVs reached 75.84%, and about 24.64% of the seropositive samples had cross-reactive IgG antibodies against the nucleocapsid, S, and receptor binding domain antigens of SARS-CoV-2. Additionally, the re-infections with different LPH-CoVs occurred frequently in children and tended to increase the cross-reactive antibodies against SARS-CoV-2. From the forty-nine serum samples with cross-reactive anti-S IgG antibodies against SARS-CoV-2, we found that seven samples with a median age of 1.4 years old had detected neutralizing activity for the wild-type or mutant SARS-CoV-2 S pseudotypes. Interestingly, all of the seven samples contained anti-S IgG antibodies against HCoV-OC43. Together, these data suggest that children's pre-existing antibodies to LPH-CoVs have limited cross-reactive neutralizing antibodies against SRAS-CoV-2.

KEYWORDS

low pathogenic human coronaviruses, SARS-CoV-2, cross-reactive antibody, neutralizing activity, antigen specific antibody

Introduction

Coronaviruses (CoVs) refer to a large family of viruses that cause illnesses ranging from the common cold to more severe diseases. There are seven identified coronaviruses causing human infections. The highly pathogenic human coronaviruses (HPH-CoVs) including severe acute respiratory syndrome coronavirus (SARS-CoV), middle east respiratory syndrome coronavirus (MERS-CoV), and SARS-CoV-2 belong to the betacoronaviruses, while two alphacoronaviruses (HCoV-229E, HCoV-NL63) and two betacoronaviruses (HCoV-HKU1, HCoV-OC43) are identified as low pathogenic human coronaviruses (LPH-CoVs). Prior to the huge morbidity and mortality caused by HPH-CoVs, the LPH-CoVs have long been circulating in humans and cause common cold with mild respiratory syndromes (1–5). The serological assays by detecting antibodies induced by LPH-CoVs are used to define the population's herd immunity, and ≥90% of adults have antibody evidence against these four LPH-CoVs (6, 7). It is believed that the primary infection of LPH-CoVs commonly occurs in childhood, with repeated infection within 1-3 years and a higher infection frequency in children under 5 years old (8–11).

Though the LPH-CoVs induced antibody response is short-lasting and has limited protection from hosts infected by the same or different common cold coronaviruses (8), it is hypothesized that the cross-reactive antibodies response from prior LPH-CoVs exposure could have reduced the susceptibility and possibility of developing severe clinical syndrome on SARS-CoV-2 infection in children (12, 13). However, studies exploring whether the pre-existing antibodies induced by LPH-CoVs can cross-react with SARS-CoV-2 generate conflicting results. Some data showed that the pre-existing antibodies response in un-infected populations, especially in children and teenagers exhibited specific neutralizing activity against SARS-CoV-2 (14), and high levels of pre-existing immune responses against LPH-CoVs were associated with mitigating the disease severity of coronavirus disease 2019 (COVID-19) (15–17) or reduced the duration of symptom (18). Yet, other studies suggested a lack of SARS-CoV-2 cross-neutralization activity although antigen-specific antibodies response was detected from pre-pandemic serum samples of SARS-CoV-2 (11, 19, 20). These conclusions vary greatly in different cohorts which commonly include adults, and the cross-reactive antibodies against SRAS-CoV-2 in children with pre-existing LPH-CoVs humoral immunity need to be elucidated.

Here, we investigated the seroprevalence of LPH-CoVs in 658 serum samples obtained from hospitalized children prior to the SARS-CoV-2 pandemic and measured the cross-reactive antibodies against SARS-CoV-2. We observed that 40% to 60% of the serum samples contained spike (S)-specific immunoglobin (Ig) G antibodies for the different LPH-CoVs. Higher levels of the nucleocapsid (N)-, S-, and receptor binding domain (RBD)-specific IgG antibodies against SARS-CoV-2 were found in the LPH-CoVs exposed group, and re-infections with different LPH-CoVs appeared to increase the antigen-specific cross-reactive antibodies. However, limited neutralizing activity existed even for the samples with cross-reactive S-specific IgG antibodies against SARS-CoV-2.

Materials methods

Samples

A total of 658 pre-COVID-19 serum samples of children with respiratory infection symptoms (aged 0-15 years) collected between May 27 and December 15, 2019 were obtained from Guangzhou Women and Children's Medical Center. 28 serum samples from SARS-CoV-2 patients with strongly neutralization activity against SARS-CoV-2 WT spike in micro-neutralization assay were obtained from Shenzhen Center for Disease Control and Prevention (21). All the experiments were performed in compliance with and under the approval of the biomedical research ethics committee, the public health school (Shenzhen) of Sun Yat-Sen University (2020–034).

Plasmid and proteins

The env-deficient HIV-1 (pnl4-3.luc.R.-E-) plasmid expressing the luciferase reporter was constructed in our laboratory. The pcDNA3.1.SARS-CoV-2 WT spike plasmid was kindly provided by Dr. Yaoqing Chen of Sun Yat-sen University. cDNA of SARS-CoV-2 B.1.351(Delta) spike and SARS-CoV-2 P.1(Gamma) spike were synthesized and cloned into pcDNA3.1 vector. The proteins used in this study were purchased from Sino Biological (Beijing, China).

Enzyme-linked immunosorbent assay

Antigen-specific IgG antibodies to SARS-CoV-2 N/S/RBD and HCoV-229E S/HCoV-NL63 S/HCoV-HKU1 S/HCoV-OC43 S were detected using a standard enzyme-linked immunosorbent assay (ELISA) (21). The optimal coating concentration of antigen and serum were 250 ng/well of SARS-CoV-2 N and S, 150 ng/well of SARS-CoV-2 RBD, 50 ng/well of HCoV-OC43 S, 30 ng/well of HCoV-229E S, HCoV-NL63 S and HCoV-HKU1 S and 1:500. A positive control (serum sample FS B26 with strongly neutralization activity in micro-neutralization assay is kindly provided by Guangdong Provincial Center for Disease Control and Prevention) diluted in ten-fold dilutions was set on every ELISA plate to normalize all

the detected values. Besides, one serum from mice was used as a negative control on each plate to check the consistency of each plate.

SARS-CoV-2 pseudovirus neutralization assay

HEK 293T cells were co-transfected with SARS-CoV-2 Spike plasmid and HIV-1 plasmid (pnl4-3.luc.R.-E-). Cell supernatant was collected at 48 hours post-transfection and virus titers were determined as described in detail previously (22). Serially diluted sera were added to a 96-well plate and incubated for 1 hour at 37°C. HEK 293T-ACE2 cells were added and plates were incubated for 48 hours. The luciferase activity level was assessed by Bright-Glo Luciferase Assay System (cat# E2620) purchased from Promega (USA), and 50% inhibitory concentration (IC_{50}) was determined as the last serum dilution at which the titration curve matches inhibition equal to or above 50% of the 100% assay (21).

Statistics

The finite mixture model was used to define the positive value of antibodies against the S antigen of LPH-CoVs. The individuals with a positive value of cross-reactive antibody against SARS-CoV-2 were defined by an OD value greater than the mean OD values minus two times the standard deviation of COVID-19 patients. The student's *t* test was used to compare the differences between the two groups. A two-tailed *P* value<0.05 was considered statistically significant. The differences between male group and female group for each LPH-CoVs were compared by the $\chi 2$ test. Pearson's correlation was used to test the association between the S-specific antibodies against LPH-CoVs with the cross-reactive N, S, and RBD antigen-specific antibodies against SARS-CoV-2. Statistical analysis of the clinical data was performed using SPSS Statistics version 25 software (IBM, Armonk, NY, USA). All the experimental data were analyzed in GraphPad Prism software (version 8) and R Studio software.

Results

Pre-existing antibodies response against LPH-CoVs in the children cohort

In this retrospective study, 658 serum samples collected from hospitalized children with a median age of 3 years (IQR 0.8-4.2) including 402 boys and 256 girls in 2019 before the SARS-CoV-2 outbreak were enrolled. The cohort's pathological clinical features were summarized in Supplementary Table 1. To evaluate the pre-existing antibodies against LPH-CoVs in this cohort, we analyzed IgG antibodies response against the S antigen of HCoV-229E, HCoV-NL63, HCoV-HKU1, and HCoV-OC43 *via* ELISA (Figure 1A). Besides, 28 serum samples with neutralizing antibodies against SARS-CoV-2 from convalescent COVID-19 patients were used as an independent group. By utilizing the finite mixture model (Supplementary Figures 1A-D), we have observed that 40.73%, 38.30%, 39.67%, and 61.55% of the children's serum samples were classified as positive individuals with antibodies against the S antigen of HCoV-229E, HCoV-NL63, HCoV-HKU1, and HCoV-OC43 respectively, suggesting a higher prevalence of HCoV-OC43 in hospitalized children than the other three LPH-CoVs in our cohort (Figure 1B). Interestingly, the COVID-19 patients boosted comparable S-specific IgG antibodies against these four LPH-CoVs (Figure 1B). Overall, 499 samples (75.84%) from the cohort exhibited S-specific IgG antibodies response against at least one of the four LPH-CoVs. Importantly, re-infections with different LPH-CoVs occurred commonly, we have found that 140/113/107 cases (21.28%, 17.17%, 16.26%) contained S-specific IgG antibodies against two/three/four of the LPH-CoVs respectively (Figure 1C). Among the 139 serum samples showing S-specific IgG antibodies only to one of the four LPH-CoVs, we observed positive rates of 8.05% for HCoV-229E (24 cases), 5.37% for HCoV-NL63 (16 cases), 4.03% for HCoV-HKU1 (12 cases), and 29.19% for HCoV-OC43 (87 cases) (Figure 1D). Besides, we have found a higher seroprevalence rate (20.36%) for beta LPH-CoVs compared to alpha LPH-CoVs (7.60%) in this cohort (Figure 1E). These results indicate that a high prevalence of LPH-CoVs exists in the early phase of human life, however, the pre-existing antibodies response is short-lasting to protect host from the same or other LPH-CoVs infection.

Pre-existing antibodies response against LPH-CoVs in different age groups of the children cohort

We next compared the seroprevalence in different age groups for positively classified serum samples with antibodies against LPH-CoVs. As shown in Figure 2A, we observed that the majority of infants less than 3 months old had S-specific IgG antibodies against HCoV-229E (66.67%), HCoV-HKU1 (52.94%), and HCoV-OC43 (70.59%), while 23.53% of the samples were seropositive individuals for HCoV-NL63, indicating a maternal transient S-specific IgG antibody in infants. Without maternal antibody, the numbers of seropositive individuals in the age category of 3 to 9 months old decreased sharply for all the four types of LPH-CoVs, then started to keep a whole upward trend following the age increase (Figure 2A; Supplementary Figures 2A-D). In the 9-15 years old group, we have found a reduced seropositive rate for HCoV-

10.3389/fimmu.2022.1042406

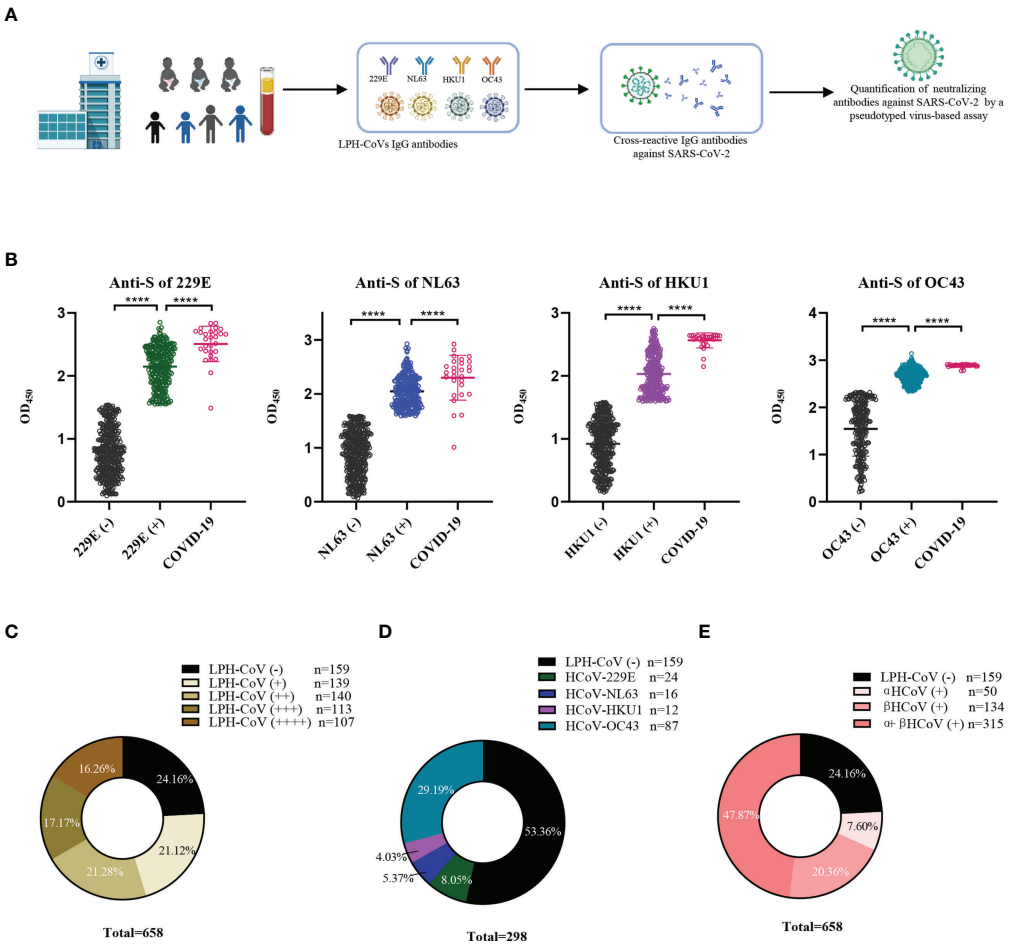

FIGURE 1
Identification of the pre-existing antibodies against LPH-CoVs in children's serum samples **(A)** The schematic diagram of studying pre-existing antibodies against human coronavirus for the children cohort. **(B)** IgG antibodies response against the S protein of HCoV-229E, HCoV-NL63, HCoV-HKU1, and HCoV-OC43 was analyzed in 658 serum samples from hospitalized children prior to SARS-CoV-2 outbreak. The finite mixture model was used to define the individuals with positive values. 28 serum samples from convalescent COVID-19 patients were used as control. Student's *t* test was used to compare the differences of medium values between groups, a two-tailed *P* value <0.05 was considered to be statistically significant, (****$P \leq 0.0001$). **(C-E)** The percentage of individuals with exposure to different LPH-CoVs (n=658) **(C, E)** or only one of the four LPH-CoVs (n=298) **(D)**.

NL63, HCoV-OC43 and HCoV-HKU1, but a raised trend for HCoV-229E compared to the 6-9 years old group (Figure 2A). As expected, we have observed that re-infections of different coronaviruses increased with age under five years old and became stable afterward (Figure 2B).

Next, the effect of biological sex on antibody levels of S-specific IgG against LPH-CoVs was analyzed. Due to the number difference of serum samples between boys and girls, we calculated the seropositive rates for boys and girls, respectively. Interestingly, boys had a higher positive rate compared with girls for HCoV-229E infection. However, no obvious gender-related pattern was found for the other three coronaviruses (Figures 3A–D; Supplementary Table 2).

Identification of the cross-reactive antibodies against SARS-CoV-2 in the children cohort

To understand the cross-reactive antibody responses against SARS-CoV-2 induced by LPH-CoVs, we evaluated the IgG antibodies response against the N, S, and RBD antigens of SARS-CoV-2 in the serum samples using ELISA method. For the classified samples with only one of the four LPH-CoVs exposure, both HCoV-229E and HCoV-OC43 seropositive samples stimulated significantly higher levels of IgG antibodies response against the N, S, and RBD antigens of SARS-CoV-2 compared to the negative samples. The HCoV-NL63

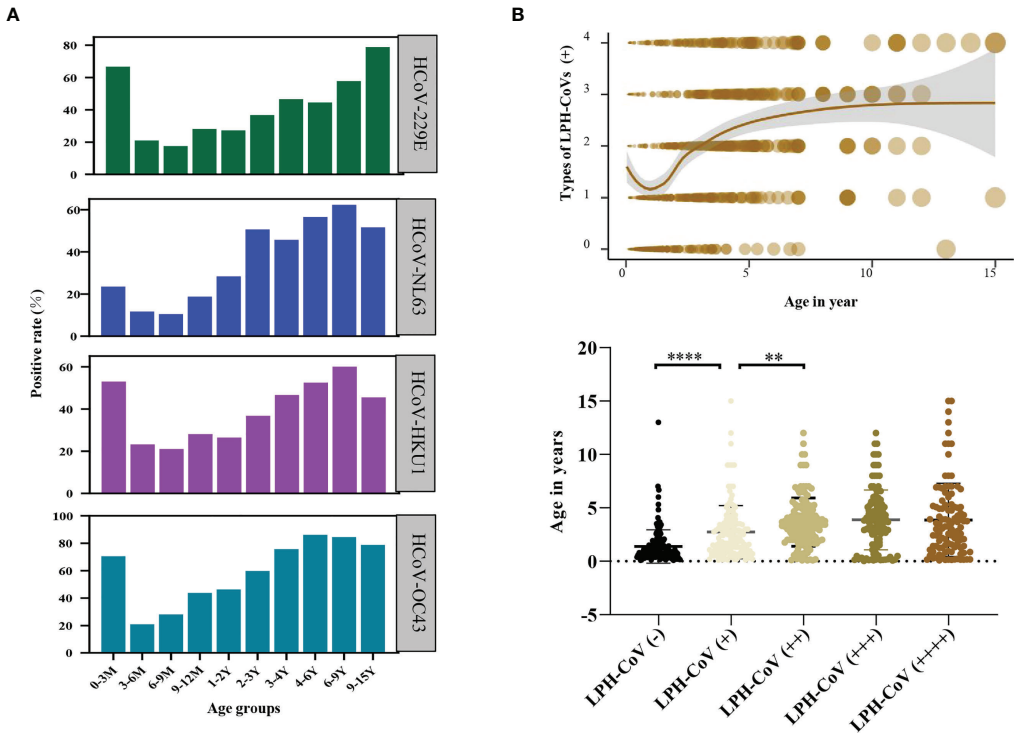

FIGURE 2
Analysis of the pre-existing antibodies response against LPH-CoVs in different age groups **(A)** The seropositive rates of HCoV-229E, HCoV-NL63, HCoV-HKU1, and HCoV-OC43 in different age groups. **(B)** The relation between age and re-infections of LPH-CoVs. The curve was fitted by Locally Weighted Regression (**B**, upper figure). A two-tailed *P* value <0.05 was considered to be statistically significant (**B**, lower figure), (***P* values of ≤0.01, ****P* ≤0.0001).

seropositive samples contained elevated levels of IgG antibody response against the S and RBD proteins of SARS-CoV-2 rather than the N protein. Interestingly, no significant difference for the IgG antibodies response against the N, S, and RBD proteins of SARS-CoV-2 was found between the HCoV-HKU1 seropositive samples and the seronegative samples (Figure 4A). However, both alpha and beta coronaviruses seropositive samples did show enhanced IgG antibodies response against the N, S, and RBD proteins of SARS-CoV-2 compared with the negative samples (Figure 4B). As expected, we have found that the levels of IgG antibodies against the N, S, and RBD proteins of SARS-CoV-2 tended to increase with re-infections, and patients with all the four types of LPH-CoVs exposure had the highest levels of cross-reactive antigen-specific IgG antibodies against SARS-CoV-2 (Figure 4C). These results suggest that the repeated infections with LPH-CoVs may facilitate the host generating high levels of antigen-specific antibodies with cross-reactivity to SARS-CoV-2. We further determined the correlation between the S-specific IgG antibodies against LPH-CoVs and the cross-reactive antigen-specific IgG antibodies against SARS-CoV-2. For the serum samples with only one of the LPH-CoVs exposure, the positive correlations were noted between the cross-reactive antigens-specific IgG antibodies against SARS-CoV-2 with the S-specific IgG antibodies against each of the LPH-CoVs, especially with HCoV-OC43. (Figures 5A–D).

Interestingly, the cross-reactive IgG antibodies against the N and S antigens of SARS-CoV-2 peaked mostly in the individuals with an age category of 9-12 months old, while the cross-reactive IgG antibody against the RBD antigen of SARS-CoV-2 peaked mostly in children of 6-9 months old (Figures 6A–C).

LPH-CoVs stimulate limited cross-reactive neutralizing antibodies against SARS-CoV-2

Forty-nine individuals with a positive cross-reactive S-specific IgG antibodies response against LPH-CoVs were determined by an OD value higher than two times the average of the COVID-19 patients. To examine whether the antibodies boosted by LPH-CoVs in these samples have neutralizing activity for SARS-CoV-2, we measured the neutralizing activity utilizing wild-type (WT) and two variants of concern (VOC) including Gamma and Delta SARS-CoV-2 S pseudotypes. As shown in Figures 7A, C, we have found

10.3389/fimmu.2022.1042406

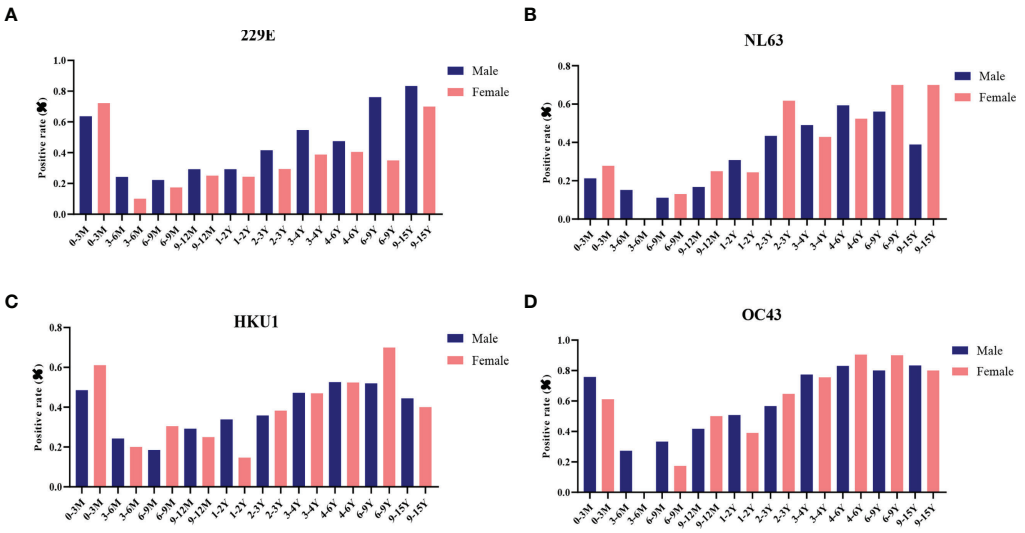

FIGURE 3
The effect of biological sex on pre-existing antibodies against LPH-CoVs in different age groups **(A-D)** The seropositive rates of HCoV-229E **(A)**, HCoV-NL63 **(B)**, HCoV-HKU1 **(C)** and HCoV-OC43 **(D)** in male and female individuals with different ages.

that five serum samples could neutralize WT SARS-CoV-2 though the majority of selected samples lack neutralizing activity. Out of the five serum samples, two samples could neutralize Delta SARS-CoV-2 and one contained the neutralizing activity against Gamma SARS-CoV-2, indicating an immune escape of the variants. Interestingly, only one serum sample was found having the ability of neutralizing Delta or Gamma SARS-CoV-2 respectively, but without neutralizing activity against WT SARS-CoV-2. Notably, all of the serum samples with neutralizing activity against SARS-CoV-2 were collected from individuals under 4 years old, with of median age of median age of 1.4 years old (Figures 7B, C), indicating the individuals with younger age may be beneficial to the cross-reactive neutralizing activity against SARS-CoV-2.

Next, we found all of the seven serum samples with cross-reactive neutralization activity against SARS-CoV-2 were HCoV-OC43 seropositive (Figure 7C), suggesting the pre-existing antibody against HCoV-OC43 may play a role in reducing SARS-CoV-2 infection.

Discussion

The impact of pre-existing LPH-CoV-specific antibodies with cross-reactivity against SARS-CoV-2 has been investigated since the beginning of SARS-CoV-2 pandemic. It is critical if the antibodies boosted by LPH-CoVs can neutralize SARS-CoV-2 due to the 90% herd immunity of humans against LPH-CoVs (23, 24), which usually occur repeatedly in early life. In this study, we detected a generally moderate level of seroprevalence in 658 children under 15 years old for the three human coronaviruses (HCoV-229E, HCoV-NL63, HCoV-HKU1) and a high positive rate for HCoV-OC43. Although the seroprevalence of LPH-CoVs varies greatly by reason of different antigens used, methodologies adopted, population with distinct ages, and other demographic characteristics (25–27), the seroprevalence acquired from this cohort is somewhat in line with the normal range within children (28–30). Besides, the obvious maternal transient passive IgG antibodies response against LPH-CoVs was observed for infants within 3-months, which is consistent with the previous stratified studies (29, 31).

Limited studies have investigated whether biological sex affects LPH-CoVs infection although several reports have indicated that male COVID-19 patients appeared to be more susceptible to SARS-CoV-2 and generated a higher level of antibodies (21, 32). In this study, we found that HCoV-229E boosted higher S-specific IgG antibodies in boys than girls after 3 months old while no obvious sex-based antibody trend was observed for the other three LPH-CoVs. A recent study has found a higher level of IgG antibody against HCoV-229E other than the other three coronaviruses in men compared with women in an adult cohort (older than 20 years of age) (33). These data indicate that sex may be a factor affecting the prevalence of HCoV-229E.

Most adults commonly contain antibodies against all the four LPH-CoVs since re-infections occur initially in children, causing the difficulty of evaluating the cross-reactive antibody response to every specific coronavirus. In this study, we selected samples which are positive with only one type of IgG antibody against LPH-CoVs to investigate the cross-reactive antibody response against SARS-CoV-2, HCoV-HKU1 seropositive

10.3389/fimmu.2022.1042406

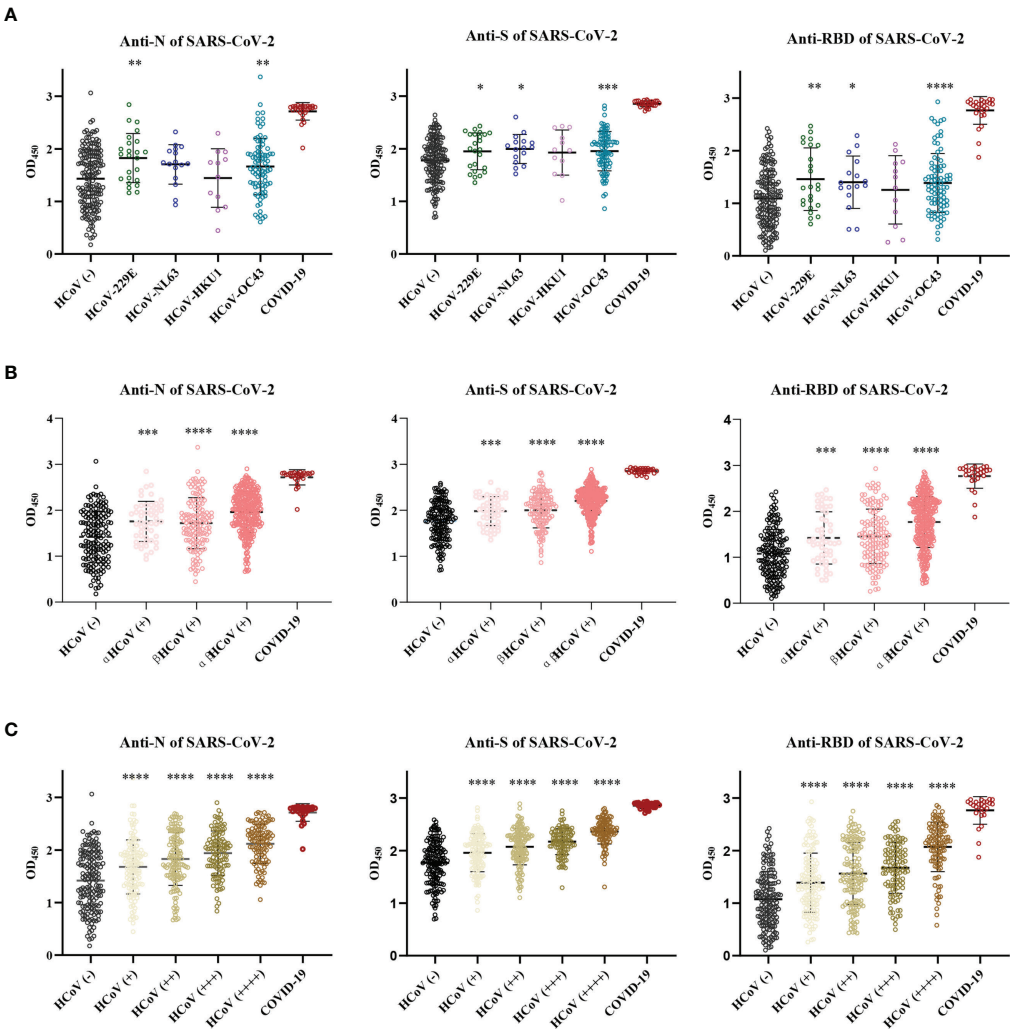

FIGURE 4
The pre-existing antibodies against LPH-CoVs contained cross-reactive antibodies against SARS-CoV-2 **(A-C)** The cross-reactive IgG antibodies against the N, S, and RBD proteins of SARS-CoV-2 in individuals with exposure to only one of the four LPH-CoVs, (n=298) **(A)** or re-exposed with different LPH-CoVs (n=658) **(B, C)**. The individuals with positive values were determined by an OD value greater than the mean OD values of COVID-19 patients minus two times the standard deviation of COVID-19 patients. A two-tailed *P* value<0.05 was considered statistically significant, (*P values of ≤ 0.05, **P values of ≤0.01, ***P values of ≤ 0.001, ****P ≤0.0001).

samples appeared to have no cross-reactive antibodies against the N, S, and RBD antigens of SARS-CoV-2. However, HCoV-OC43 seropositive samples showed significantly higher levels of, even comparable antigen-specific antibodies response against SARS-CoV-2 with the COVID-19 patients. Previous studies investigating whether the pre-existing anti-HCoV-OC43 antibodies affect SARS-CoV-2 infection yielded contradictory results. Several investigations have indicated high levels of N-specific antibodies against HCoV-OC43 in COVID-19 adult patients were associated with mild disease (34, 35), indicating a potential protective role of the pre-existing antibodies against HCoV-OC43 for SARS-CoV-2. On the other hand, Guo et al. have found significantly higher anti-S of HCoV-OC43 IgG antibody titers in patients with severe disease than those in mild patients, indicating the cross-reactive antibody may enhance the severity of COVID-19 patients (36). Unluckily, we were not able to track these patients in our cohort to assess the susceptibility or disease severity for SARS-CoV-2 infection. However, it is notable that all of the seven serum samples from children ≤ 4 years old with neutralizing activity against SARS-CoV-2 contained S-specific IgG against HCoV-OC43, indicating there may be a role for antibodies boosted by HCoV-OC43 in the earlier age during SARS-CoV-2 infection.

It is valuable that the serum samples of young individuals under 1-year-old were enrolled in this study. A prior study has reported that about 44% (21 cases in 48 samples in total) of the

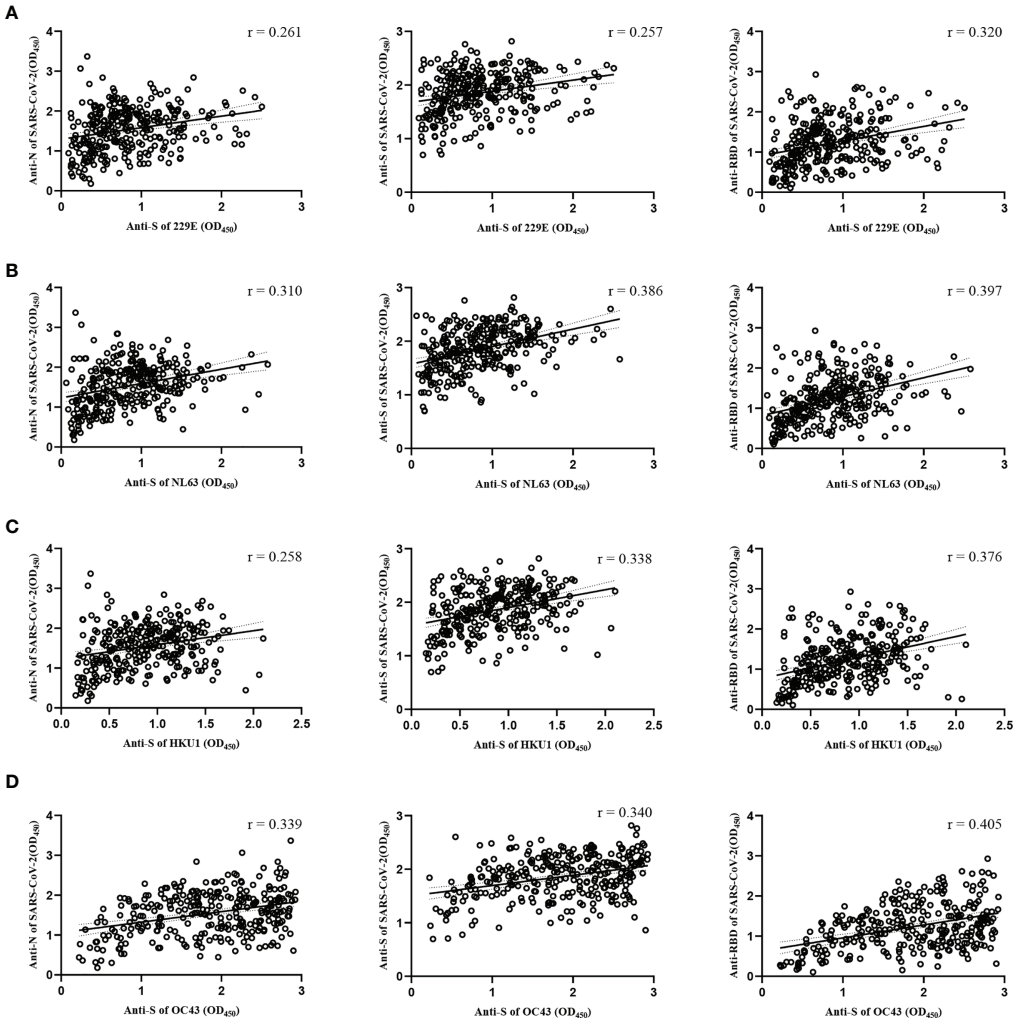

FIGURE 5
Correlations between the S-specific IgG antibodies against LPH-CoVs and the cross-reactive antigens-specific IgG antibodies against SARS-CoV-2 for the serum samples with only one of the LPH-CoVs exposure (n=298) **(A-D)** The correlations between the S-specific IgG antibodies against HCoV-229E **(A)**, HCoV-NL63 **(B)**, HCoV-HKU1 **(C)**, HCoV-OC43 **(D)** and the cross-reactive IgG antibodies against the N, S, RBD antigens of SARS-CoV-2 were assessed by Pearson correlation test. The *r* values were exhibited for the correlation. A two-tailed *P* value<0.05 was considered statistically significant.

individuals had detectable S-specific IgG antibodies against SARS-CoV-2 in children ranging from 1-16 years *via* a flow cytometry-based method, most of which could neutralize SARS-CoV-2 (14). Another study has observed that 20% of SARS-CoV-2-free individuals contained antibodies against the N, S RBD antigens of SARS-CoV-2, but with very low or undetectable neutralizing antibodies in a cohort ranging from 1-90 years. Besides, they also found age did not affect the cross-reactive antibodies (11). Consistent with this report, we have found about 24.64% of individuals with pre-existing LPH-CoVs antibodies contained the cross-reactive antigen-specific antibodies against SARS-CoV-2, most of which contained undetectable neutralizing antibodies. However, all the seven samples with neutralizing activity against SARS-CoV-2 were collected from children under 4 years old in our cohort. Notably, four samples were acquired from infants born within 1 year old in a total of eleven samples with positive S-specific antibodies against SARS-CoV-2 in this age group, indicating the cross-reactive antibodies against SARS-CoV-2 may be higher in the earlier life with LPH-CoVs exposure. Consistently, several studies have reported that the pre-existing antibodies boosted at a very early life can bind the S protein of SARS-CoV-2, which might be an explanation for mild or no symptoms following SARS-CoV-2 in children (14, 37, 38). Interestingly, the re-infections with age did not influence the neutralizing activity although it appeared to increase the cross-reactivity antigen-specific antibodies levels. Nevertheless, other

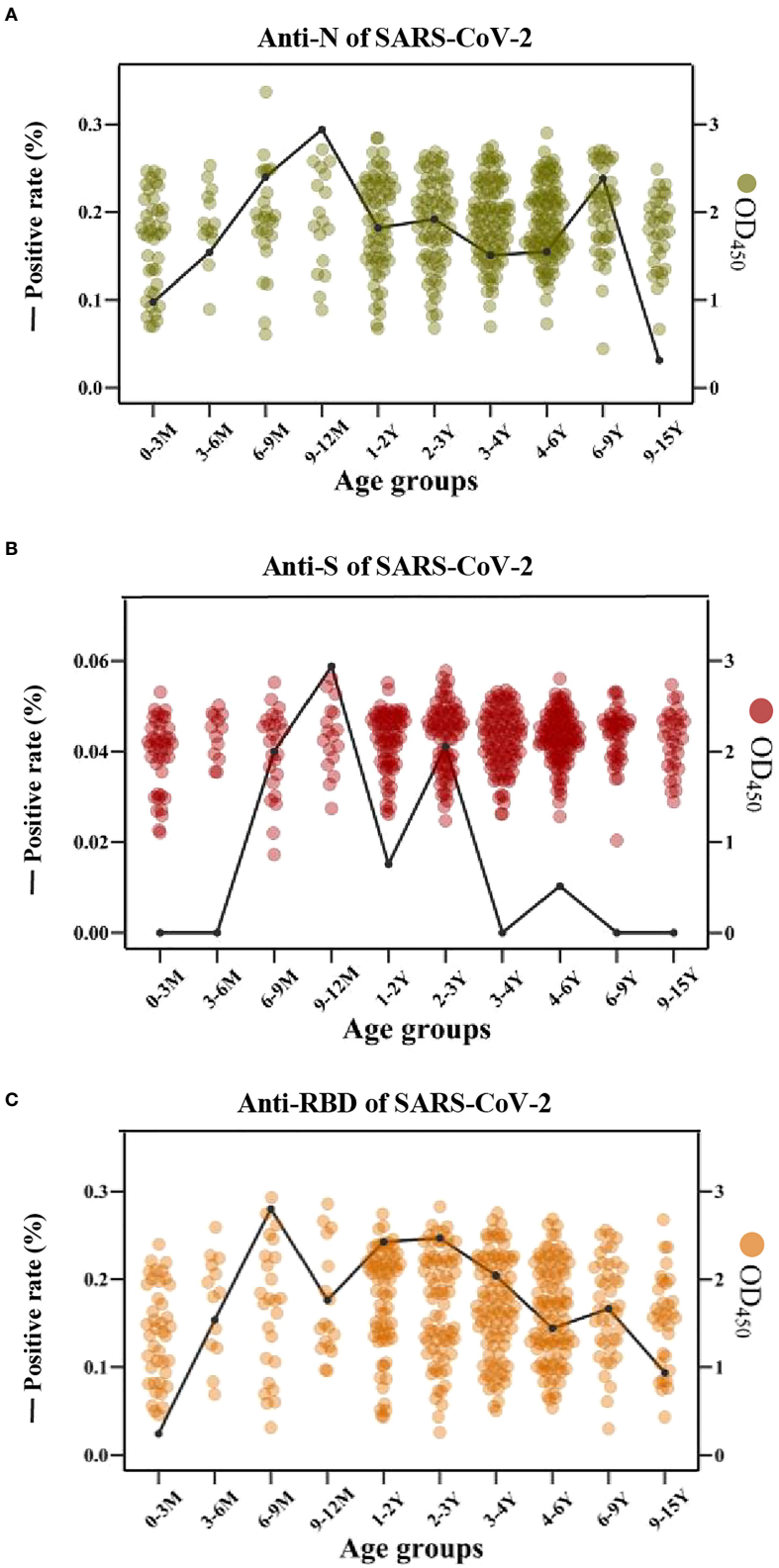

FIGURE 6
The cross-reactive IgG antibodies against SARS-CoV-2 in different age groups with pre-existing antibodies against LPH-CoVs **(A-C)** The prevalence (line) and OD values (dots) of cross-reactive IgG antibodies against the N **(A)**, S **(B)**, and RBD **(C)** of SARS-CoV-2 in different age groups.

10.3389/fimmu.2022.1042406

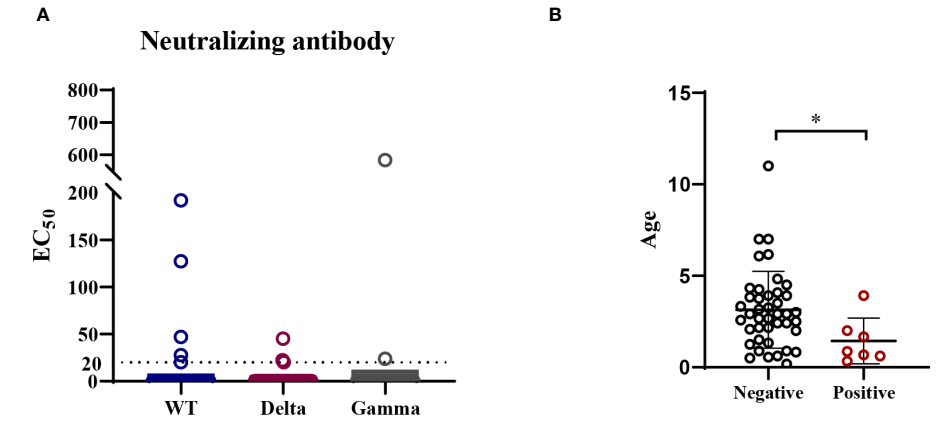

C

Sample	Sex（1=male, 0=female）	Age in years	LPH-CoVs				SARS-CoV-2 S pseudotypes		
			NL63	229E	HKU1	OC43	WT	DELTA	GAMMA
6	1	0.6	-	-	-	+	-	45.08	-
30	0	0.7	-	+	+	+	191.85	-	-
34	1	0.3	+	+	+	+	47.03	-	583.70
37	0	3.9	-	-	-	+	127.37	-	-
38	1	2.0	+	+	+	+	20.18	20.18	-
44	1	1.7	-	-	-	+	27.68	22.39	-
48	1	0.9	+	+	+	+	-	-	23.69

FIGURE 7
Low or undetectable neutralizing antibodies against WT or mutant SARS-CoV-2 S pseudotypes were found in the individuals with cross-reactive S-specific IgG antibodies against SARS-CoV-2 **(A)** The measurement of neutralization activity for the forty-nine serum samples with S-specific antibodies against SARS-CoV-2 *via* SARS-CoV-2 S pseudotypes neutralization assay. The dashed line represents a threshold set (EC_{50}>20). **(B)** The age range for the serum samples with neutralizing antibodies against SARS-CoV-2 or variants. A two-tailed *P* value <0.05 was considered to be statistically significant, (*P values of ≤ 0.05). **(C)** The list of serum samples with neutralizing antibodies against SARS-CoV-2 S pseudotypes.

studies have found that vaccination of measles-mumps-rubella or tetanus-diphtheria-pertussis provided a protective role against the severe COVID-19 by activating the cross-reactive T cell response, which is a possible explanation for children with reduced susceptibility and severe clinical syndrome in SARS-CoV-2 infection (39–41). Thus, the cross-reactive T cell response should be an important point for future study since poor cross-reactive neutralizing antibodies are stimulated by LPH-CoVs. Due to the lack of COVID-19 children, the SARS-CoV-2 positive samples used here as control were collected from adult COVID-19 patients. Although comparable S-specific IgG antibodies against all the four LPH-CoVs were boosted in SARS-CoV-2 patients, we could not get a solid conclusion about the memory antibodies since the baseline of antibodies against LPH-CoVs has not been measured before they were infected with SARS-CoV-2.

Overall, our data demonstrate that the pre-existing antibody response boosted by LPH-CoVs has a moderate to high seroprevalence in children under 15 years old. However, the majority of pre-existing antibodies lack the neutralizing activity against SARS-CoV-2. Besides, HCoV-OC43 has a higher prevalence and may boost the cross-reactive neutralizing antibody in children under four years old against SARS-CoV-2, providing an insight into immunogen design and vaccine development.

Data availability statement

The original contributions presented in the study are included in the article/Supplementary Material. Further inquiries can be directed to the corresponding authors.

Ethics statement

All the experiments were performed in compliance with and under the approval of the biomedical research ethics committee, the public health school (Shenzhen) of Sun Yat-Sen University (2020-034).

Author contributions

HL and YS conceived and designed the study. NL and XL performed experiments, analyzed data, and wrote the manuscript. JW, SZ, and LZ assisted in laboratory experiments. LZ and QiqC contributed to the data collection, formal analysis, and data interpretation. YF and SX collected clinical samples and data. QiC and NiW prepared experimental review materials. ZW, NaW, and CL provided experimental technical guidance. HL and YS approved the final version of the manuscript. All authors contributed to the article and approved the submitted version.

Funding

This work was supported by the National Key Research and Development Program of China (2021YFC2300100, 2021YFC086300), Shenzhen Science and Technology Program (KQTD20200820145822023, KQTD20180411143323605), National Natural Science Foundation of China (32000116, 32270147), Shenzhen Science and Technology Program (JSGG20200225152008136, GXWD20201231165807008, and 20200825113322001, JCYJ20190807155407443, KCXFZ 20211020172545006), High Level Project of Medicine in Nanshan, Shenzhen; Sanming Project of Medicine in Shenzhen (SZSM202103008).

Acknowledgments

We would like to thank Director Bing Zhu and fellows in the Central laboratory of Guangzhou Women and Children's Medical Center for their support in the collection of children samples in this study.

Conflict of interest

The authors declare that the research was conducted in the absence of any commercial or financial relationships that could be construed as a potential conflict of interest.

Publisher's note

All claims expressed in this article are solely those of the authors and do not necessarily represent those of their affiliated organizations, or those of the publisher, the editors and the reviewers. Any product that may be evaluated in this article, or claim that may be made by its manufacturer, is not guaranteed or endorsed by the publisher.

Supplementary material

The Supplementary Material for this article can be found online at: https://www.frontiersin.org/articles/10.3389/fimmu.2022.1042406/full#supplementary-material

References

1. Jiang S, Du L. Effect of low-pathogenic human coronavirus-specific antibodies on SARS-CoV-2. *Trends Immunol* (2020) 41:853–4. doi: 10.1016/j.it.2020.08.003

2. Zhu Z, Lian X, Su X, Wu W, Marraro GA, Zeng Y. From SARS and MERS to COVID-19: a brief summary and comparison of severe acute respiratory infections caused by three highly pathogenic human coronaviruses. *Respir Res* (2020) 21:224. doi: 10.1186/s12931-020-01479-w

3. Vabret A, Mourez T, Gouarin S, Petitjean J, Freymuth F. An outbreak of coronavirus OC43 respiratory infection in Normandy, France. *Clin Infect Dis* (2003) 36:985–9. doi: 10.1086/374222

4. Chiu SS, Chan KH, Chu KW, Kwan SW, Guan Y, Poon LL, et al. Human coronavirus NL63 infection and other coronavirus infections in children hospitalized with acute respiratory disease in Hong Kong, China. *Clin Infect Dis* (2005) 40:1721–9. doi: 10.1086/430301

5. Uddin SMI, Englund JA, Kuypers JY, Chu HY, Steinhoff MC, Khatry SK, et al. Burden and risk factors for coronavirus infections in infants in rural Nepal. *Clin Infect Dis* (2018) 67:1507–14. doi: 10.1093/cid/ciy317

6. Gorse GJ, Patel GB, Vitale JN, O'Connor TZ. Prevalence of antibodies to four human coronaviruses is lower in nasal secretions than in serum. *Clin Vaccine Immunol* (2010) 17:1875–80. doi: 10.1128/CVI.00278-10

7. Sariol A, Perlman S. Lessons for COVID-19 immunity from other coronavirus infections. *Immunity* (2020) 53:248–63. doi: 10.1016/j.immuni.2020.07.005

8. Edridge AWD, Kaczorowska J, Hoste ACR, Bakker M, Klein M, Loens K, et al. Seasonal coronavirus protective immunity is short-lasting. *Nat Med* (2020) 26:1691–3. doi: 10.1038/s41591-020-1083-1

9. Galanti M, Shaman J. Direct observation of repeated infections with endemic coronaviruses. *J Infect Dis* (2020) 223:409–15. doi: 10.1093/infdis/jiaa392

10. Aldridge RW, Lewer D, Beale S, Johnson AM, Zambon M, Hayward AC, et al. Seasonality and immunity to laboratory-confirmed seasonal coronaviruses (HCoV-NL63, HCoV-OC43, and HCoV-229E): results from the flu watch cohort study. *Wellcome Open Res* (2020) 5:52. doi: 10.12688/wellcomeopenres.15812.2

11. Anderson EM, Goodwin EC, Verma A, Arevalo CP, Bolton MJ, Weirick ME, et al. Seasonal human coronavirus antibodies are boosted upon SARS-CoV-2 infection but not associated with protection. *Cell* (2021) 184:1858–64. doi: 10.1016/j.cell.2021.02.010

12. Davies NG, Klepac P, Liu Y, Prem K, Jit M, Pearson CAB, et al. Age-dependent effects in the transmission and control of COVID-19 epidemics. *Nat Med* (2020) 26:1205–11. doi: 10.1038/s41591-020-0962-9

13. Waterlow NR, van Leeuwen E, Davies NG, Group CC-W, Flasche S, Eggo RM. How immunity from and interaction with seasonal coronaviruses can shape

SARS-CoV-2 epidemiology. *Proc Natl Acad Sci USA* (2021) 118:e2108395118. doi: 10.1073/pnas.2108395118

14. Monto AS, DeJonge PM, Callear AP, Bazzi LA, Capriola SB, Malosh RE, et al. Coronavirus occurrence and transmission over 8 years in the HIVE cohort of households in Michigan. *J Infect Dis* (2020) 222:9–16. doi: 10.1093/infdis/jiaa161

15. Cugno M, Meroni PL, Consonni D, Griffini S, Grovetti E, Novembrino C, et al. Effects of antibody responses to pre-existing coronaviruses on disease severity and complement activation in COVID-19 patients. *Microorganisms* (2022) 10 (6):1191. doi: 10.3390/microorganisms10061191

16. Sagar M, Reifler K, Rossi M, Miller NS, Sinha P, White LF, et al. Recent endemic coronavirus infection is associated with less-severe COVID-19. *J Clin Invest* (2021) 131(1):e145540. doi: 10.1172/JCI143380

17. Ortega N, Ribes M, Vidal M, Rubio R, Aguilar R, Williams S, et al. Seven-month kinetics of SARS-CoV-2 antibodies and role of pre-existing antibodies to human coronaviruses. *Nat Commun* (2021) 12:4740. doi: 10.1038/s41467-021-24979-9

18. Gouma S, Weirick ME, Bolton MJ, Arevalo CP, Goodwin EC, Anderson EM, et al. Health care worker seromonitoring reveals complex relationships between common coronavirus antibodies and COVID-19 symptom duration. *JCI Insight* (2021) 6(16):e150449. doi: 10.1172/jci.insight.150449

19. Poston D, Weisblum Y, Wise H, Templeton K, Jenks S, Hatziioannou T, et al. Absence of severe acute respiratory syndrome coronavirus 2 neutralizing activity in prepandemic sera from individuals with recent seasonal coronavirus infection. *Clin Infect Dis* (2021) 73:1208–11. doi: 10.1093/cid/ciaa1803

20. Miyara M, Saichi M, Sterlin D, Anna F, Marot S, Mathian A, et al. Pre-COVID-19 immunity to common cold human coronaviruses induces a recall-type IgG response to SARS-CoV-2 antigens without cross-neutralisation. *Front Immunol* (2022) 13:790334. doi: 10.3389/fimmu.2022.790334

21. Luo H, Jia T, Chen J, Zeng S, Qiu Z, Wu S, et al. The characterization of disease severity associated IgG subclasses response in COVID-19 patients. *Front Immunol* (2021) 12:632814. doi: 10.3389/fimmu.2021.632814

22. Nie J, Li Q, Wu J, Zhao C, Hao H, Liu H, et al. Quantification of SARS-CoV-2 neutralizing antibody by a pseudotyped virus-based assay. *Nat Protoc* (2020) 15:3699–715. doi: 10.1038/s41596-020-0394-5

23. Ma Z, Li P, Ikram A, Pan Q. Does cross-neutralization of SARS-CoV-2 only relate to high pathogenic coronaviruses? *Trends Immunol* (2020) 41:851–3. doi: 10.1016/j.it.2020.08.002

24. Abbasi J. COVID-19 and the common cold–preexisting coronavirus antibodies may hinder SARS-CoV-2 immunity. *JAMA* (2022) 327:609–10. doi: 10.1001/jama.2022.0326

25. Severance EG, Bossis I, Dickerson FB, Stallings CR, Origoni AE, Sullens A, et al. Development of a nucleocapsid-based human coronavirus immunoassay and estimates of individuals exposed to coronavirus in a U.S. metropolitan population. *Clin Vaccine Immunol* (2008) 15:1805–10. doi: 10.1128/CVI.00124-08

26. Mulabbi EN, Tweyongyere R, Wabwire-Mangen F, Mworozi E, Koehlerb J, Kibuuka H, et al. Seroprevalence of human coronaviruses among patients visiting hospital-based sentinel sites in Uganda. *BMC Infect Dis* (2021) 21:585. doi: 10.1186/s12879-021-06258-6

27. Owusu M, Sylverken AA, El-Duah P, Acheampong G, Mutocheluh M, Adu-Sarkodie Y. Sero-epidemiology of human coronaviruses in three rural communities in Ghana. *Pan Afr Med J* (2021) 38:244. doi: 10.11604/pamj.2021.38.244.26110

28. Dijkman R, Jebbink MF, El Idrissi NB, Pyrc K, Müller MA, Kuijpers TW, et al. Human coronavirus NL63 and 229E seroconversion in children. *J Clin Microbiol* (2008) 46:2368–73. doi: 10.1128/JCM.00533-08

29. Shao X, Guo X, Esper F, Weibel C, Kahn JS. Seroepidemiology of group I human coronaviruses in children. *J Clin Virol* (2007) 40:207–13. doi: 10.1016/j.jcv.2007.08.007

30. Zhou W, Wang W, Wang H, Lu R, Tan W. First infection by all four non-severe acute respiratory syndrome human coronaviruses takes place during childhood. *BMC Infect Dis* (2013) 13:433. doi: 10.1186/1471-2334-13-433

31. Woudenberg T, Pelleau S, Anna F, Attia M, Donnadieu F, Gravet A, et al. Humoral immunity to SARS-CoV-2 and seasonal coronaviruses in children and adults in north-eastern France. *eBioMedicine* (2021) 70:103495. doi: 10.1016/j.ebiom.2021.103495

32. Meng Y, Wu P, Lu W, Liu K, Ma K, Huang L, et al. Sex-specific clinical characteristics and prognosis of coronavirus disease-19 infection in wuhan, China: A retrospective study of 168 severe patients. *PloS Pathog* (2020) 16(4):e1008520. doi: 10.1371/journal.ppat.1008520

33. Lin C-Y, Wolf J, Brice DC, Sun Y, Locke M, Cherry S, et al. Pre-existing humoral immunity to human common cold coronaviruses negatively impacts the protective SARS-CoV-2 antibody response. *Cell Host Microbe* (2022) 30:83–96.e4. doi: 10.1016/j.chom.2021.12.005

34. Dugas M, Grote-Westrick T, Merle U, Fontenay M, Kremer AE, Hanses F, et al. Lack of antibodies against seasonal coronavirus OC43 nucleocapsid protein identifies patients at risk of critical COVID-19. *J Clin Virol* (2021) 139:104847. doi: 10.1016/j.jcv.2021.104847

35. Dugas M, Grote-Westrick T, Vollenberg R, Lorentzen E, Brix T, Schmidt H, et al. Less severe course of COVID-19 is associated with elevated levels of antibodies against seasonal human coronaviruses OC43 and HKU1 (HCoV OC43, HCoV HKU1). *Int J Infect Dis* (2021) 105:304–6. doi: 10.1016/j.ijid.2021.02.085

36. Guo L, Wang Y, Kang L, Hu Y, Wang L, Zhong J, et al. Cross-reactive antibody against human coronavirus OC43 spike protein correlates with disease severity in COVID-19 patients: a retrospective study. *Emerg Microbes Infect* (2021) 10:664–76. doi: 10.1080/22221751.2021.1905488

37. Shrwani K, Sharma R, Krishnan M, Jones T, Mayora-Neto M, Cantoni D, et al. Detection of serum cross-reactive antibodies and memory response to SARS-CoV-2 in prepandemic and post-COVID-19 convalescent samples. *J Infect Dis* (2021) 224:1305–15. doi: 10.1093/infdis/jiab333

38. Ma Z, Li P, Ji Y, Ikram A, Pan Q. Cross-reactivity towards SARS-CoV-2: the potential role of low-pathogenic human coronaviruses. *Lancet Microbe* (2020) 1: e151. doi: 10.1016/S2666-5247(20)30098-7

39. Monereo-Sánchez J, Luykx JJ, Pinzón-Espinosa J, Richard G, Motazedi E, Westlye LT, et al. Diphtheria and tetanus vaccination history is associated with lower odds of COVID-19 hospitalization. *Front Immunol* (2021) 12:749264. doi: 10.3389/fimmu.2021.749264

40. Reche PA. Potential cross-reactive immunity to SARS-CoV-2 from common human pathogens and vaccines. *Front Immunol* (2020) 11:586984. doi: 10.3389/fimmu.2020.586984

41. Mysore V, Cullere X, Settles ML, Ji X, Kattan MW, Desjardins M, et al. Protective heterologous T cell immunity in COVID-19 induced by the trivalent MMR and tdap vaccine antigens. *Med (N Y)* (2021) 2:1050–71.e7. doi: 10.1016/j.medj.2021.08.004

frontiers | Frontiers in Immunology

TYPE Case Report
PUBLISHED 24 October 2022
DOI 10.3389/fimmu.2022.1002329

OPEN ACCESS

EDITED BY
Ahmed Yaqinuddin,
Alfaisal University, Saudi Arabia

REVIEWED BY
Ming-Wei Lin,
The University of Sydney, Australia
Junaid Kashir,
Khalifa University,
United Arab Emirates

*CORRESPONDENCE
Kiyoshi Migita
migita@fmu.ac.jp

SPECIALTY SECTION
This article was submitted to Viral Immunology, a section of the journal Frontiers in Immunology

RECEIVED 25 July 2022
ACCEPTED 06 October 2022
PUBLISHED 24 October 2022

CITATION
Shimizu H, Matsumoto H, Sasajima T, Suzuki T, Okubo Y, Fujita Y, Temmoku J, Yoshida S, Asano T, Ohira H, Ejiri Y and Migita K (2022) New-onset dermatomyositis following COVID-19: A case report. *Front. Immunol.* 13:1002329. doi: 10.3389/fimmu.2022.1002329

New-onset dermatomyositis following COVID-19: A case report

Hiroshi Shimizu[1], Haruki Matsumoto[2], Tomomi Sasajima[3], Tomohiro Suzuki[1], Yoshinori Okubo[1], Yuya Fujita[2], Jumpei Temmoku[2], Shuhei Yoshida[2], Tomoyuki Asano[2], Hiromasa Ohira[4], Yutaka Ejiri[1] and Kiyoshi Migita[2]*

[1]Department of Gastroenterology, Fukushima Rosai Hospital, Iwaki, Japan, [2]Department of Rheumatology, Fukushima Medical University School of Medicine, Fukushima, Japan, [3]Department of Rheumatology, Fukushima Rosai Hospital, Iwaki, Japan, [4]Department of Gastroenterology, Fukushima Medical University School of Medicine, Fukushima, Japan

Coronavirus disease 2019 (COVID-19) is an infectious disease caused by severe acute respiratory syndrome coronavirus 2 (SARS-CoV-2). Most of the infected individuals have recovered without complications, but a few patients develop multiple organ involvements. Previous reports suggest an association between COVID-19 and various inflammatory myopathies, in addition to autoimmune diseases. COVID-19 has been known to exacerbate preexisting autoimmune diseases and trigger various autoantibodies and autoimmune disease occurrence. Here we report a case of complicated COVID-19 with anti-synthetase autoantibodies (ASSs) presenting with skin rash, muscle weakness, and interstitial lung disease (ILD) and subsequently diagnosed with dermatomyositis (DM). A 47-year-old Japanese male patient without any previous history of illness, including autoimmune diseases, presented with a high fever, sore throat, and cough. Oropharyngeal swab for SARS-Cov-2 polymerase chain reaction tested positive. He was isolated at home and did not require hospitalization. However, his respiratory symptoms continued, and he was treated with prednisolone (20 mg/day) for 14 days due to the newly developing interstitial shadows over the lower lobes of both lungs. These pulmonary manifestations remitted within a week. He presented with face edema and myalgia 4 weeks later when he was off corticosteroids. Subsequently, he presented with face erythema, V-neck skin rash, low-grade fever, and exertional dyspnea. High-resolution computed tomography of the chest showed ILD. Biochemical analysis revealed creatine kinase and aldolase elevations, in addition to transaminases. Anti-aminoacyl tRNA synthetase (ARS) was detected using an enzyme-linked immunosorbent assay (170.9 U/mL) (MESACUP™ (Medical & Biological Laboratories, Japan), and the tRNA component was identified as anti-PL-7 and anti-Ro-52 antibodies using an immunoblot assay [EUROLINE Myositis Antigens Profile 3 (IgG), Euroimmun, Lübeck,Germany]. The patient was diagnosed with DM, especially anti-synthase antibody syndrome based on the presence of myositis-specific antibodies, clinical features, and pathological findings. The present case suggests that COVID-19 may have contributed to the production of anti-

synthetase antibodies (ASAs) and the development of *de novo* DM. Our case highlights the importance of the assessment of patients who present with inflammatory myopathy post-COVID-19 and appropriate diagnostic work-up, including ASAs, against the clinical features that mimic DM after post-COVID-19.

KEYWORDS

anti-synthetase antibodies, anti-aminoacyl tRNA synthetase (ARS) antibodies, autoimmune diseases, dermatomyositis, COVID-19

Introduction

Coronavirus disease 2019 (COVID-19), which is caused by the severe acute respiratory syndrome coronavirus 2 (SARS-CoV-2), is a life-threatening respiratory illness (1). COVID-19 is a heterogeneous disease ranging from asymptomatic course to multi-organ failure during the inflammatory processes (2). In addition, COVID-19 shares clinical similarities with autoimmune diseases, and some patients have been reported to develop these autoimmune diseases (3). Moreover, clinical similarities had been suggested between COVID-19 and anti-melanoma differentiation-associated protein 5 (MDA5)-positive dermatomyositis (DM) (4). Robust activations of immune systems participate in the pathophysiological mechanisms of both disease conditions (5). The main pathophysiological mechanisms for severe inflammation and organ damage seen in patients with COVID-19 are thought to be immune activation and proinflammatory cytokine induction (6). Indeed, elevated serum levels of proinflammatory cytokines, including interleukin (IL)-1β, IL-16, IL-8, and IL-18, were demonstrated in patients with COVID-19 (7). Other clinical features of COVID-19 infection were reported as these viral infections are postulated to induce autoimmunity (8). Various autoantibodies have been detected in the serum of patients with COVID-19, including anti-nuclear antibodies (ANA) and anti-phospholipid antibodies (9). DM is an autoimmune disease in which the skin and muscles are the targets for immune-mediated destruction (10). This inflammatory myopathy can be complicated by vasculopathy and interstitial lung disease (ILD) (11). Autoantibodies, as a hallmark of autoimmune diseases, can also be detected transiently in patients with COVID-19 (12). Antibodies that recognize different amino tRNA synthase serve as the serological hallmark of the anti- synthase antibody syndrome (ASS) that consists of myositis, ILD, mechanic's hands and fever (13). A higher prevalence and increased severity of ILD were found in patients with ASS than those with DM and polymyositis (14). Here, we report a Japanese patient who presented with DM with skin rash, proximal limb weakness, and seropositivity of ASSs after COVID-19 infection. We focused on the new-onset anti- synthase antibody (ASA)-related DM and COVID-19 with a recent literature review.

Case description

A 47-year-old Japanese male patient presented with persistent low-grade fever, malaise, and cough after the once disappearance of the COVID-19-related symptoms 28 days from SARS-CoV-2 RNA detection by polymerase chain reaction. The patient had received the second dose of mRNA-1273 SARS-CoV-2 vaccination (Moderna), 5 months before the detection of SARS-CoV-2 RNA without any acute side effects. He received only symptomatic treatment, and these manifestations lasted for 10 days. Three weeks later from the SARS-CoV-2 RNA, the erythematous skin macules appeared on the patient's eyelid, which became more intense and extended to the anterior chest. He was referred to our Respiratory Medicine Department due to the sustained respiratory sympotoms. On first visit in our hosipital, he presented eyelid edema and skin rash on both upper extremities, chest, and back (Figures 1A–C). Chest computed tomography (CT) was performed since he had a history of nontuberculous mycobacterial disease. A CT scan revealed interstitial pneumonia (Figure 2A), and he was treated with antimicrobial agents. Concurrently, he visited our outpatient dermatology clinic for eyelid edema treatment and was transiently treated with prednisolone (PSL) at 20 mg for 14 days. Respiratory symptoms and eyelid edema improved with oral PSL administration; thereafter, PSL was discontinued. However, he presented with more severe dyspnea, cough, dysarthria, dysphagia, odynophagia, and severe generalized weakness with inability to ambulate, elevated transaminases, and relapsing interstitial pneumonia 3 weeks later. He was started on PSL at 10 mg and admitted to the hospital for further examinations for elevated transaminases, high immunoglobulin (Ig)G levels, and interstitial pneumonia.

Physical examination was significant for tachycardia to 110 beats per minute and oxygen saturation of 94% on room air. On examination, eyelid edema had resolved; however, mechanic's

10.3389/fimmu.2022.1002329

FIGURE 1
Skin findings on admission. Physical examination revealed skin manifestation of dermatomyositis. **(A)** Mechanic's hand, **(B)** V-neck sign on the chest, and **(C)** whiplash-like erythema on the back.

hands, V-neck skin rash, and whiplash-like erythema on the back were noted.

His proximal muscle power was 4/5 bilateral on the upper and lower limbs. Laboratory data showed positive ANA (speckled and cytoplasmic patterns at a serum dilution of 1:1280 and nucleolar pattenr at a serum dilution of 1:320 by indirect immunofluorescence) and were associated with significantly increased muscle enzymes [creatinine phosphokinase of 3,380 U/L (62-287 U/L)]. He was positive with high titers for anti-Ro/SSA Ab(>240 U/mL; normal range: <6.7) and anti-La/SSB (>240 U/mL; normal range: <6.7); however, negative results for the Saxon and Schirmer tests were observed. Anti-ARS antibodies were positive with high titers [170.9 U/mL (<24.9 U/mL)] according to the findings of an enzyme-linked immunosorbent assay (MESACUP^{TM} (Medical & Biological Laboratories, Japan). We further investigated the autoantigen of anti-ARS antibody by immunoblot assay [EUROLINE Myositis Antigens Profile 3 (IgG), Euroimmun, Lübeck,Germany], which thus revealed positivity (3+) for anti-PL-7 antibody. In HLA-DRB1 gene analysis, he had DR4 (DRB1*0405)) and HLA-DR15 (DRB1*15:01). (Supplemental Table 1). Magnetic resonance imaging (MRI) presented diffuse edema and inflammatory changes in the bilateral thigh muscles (Figure 2B). On pathologic examination, there was moderate size variation of the myofibers, and CD8-positive lymphocytes infiltration in atrophy of the myofibers, mainly at the periphery of the fascicles (Figures 2C–E). He was diagnosed with ASS according to criteria proposed by Lega JC, et al. (15). Treatment was started with 60 mg of PSL and 3 mg of tacrolimus per day. Fatigue, fever, and myalgia quickly improved post-treatment, whereas serum creatine kinase (CK) levels were not completely normalized during the PSL tapering phase; thus, a high dose of intravenous immunoglobulin (IVIG) was added. The patient's muscle strength improved with muscle enzyme level normalization after these combined treatments. Blood analysis revealed sustaining normal levels of muscle enzymes, and the patient remains in close medical observation at our out-patient clinic. The clinical course is summarized in Figure 3.

Discussion

ASS is an inflammatory myopathy caused by ASAs. Its clinical presentations are characterized by ILD, myositis, polyarthritis, fever, and "mechanic's hands" (16). Immuno-genetic study of HLA-DRB1 associations performed in cohort of Caucasian patients with ASS. In this study, HLA-DRB1*03:01 allele was identified as predisposition markers of ASS and HLA-DRB1*07:01 had a protective effect in the susceptibility to ASS. Our case showed both HLA-DR15 (DRB1*15:01) and DR4 (DRB1*0405), which may not affect the susceptibility for ASS in the present case (17). COVID-19 infection may present with a multitude of pulmonary findings, including diffuse ground-glass opacities (18). Similarly, the pulmonary manifestations of an ASS may present with patchy ground-glass opacities, similar to the interstitial shadows commonly seen in COVID-19-related pneumonia (19). The inflammatory process caused by SARS-CoV-2 infection involves cytokine storm and macrophage

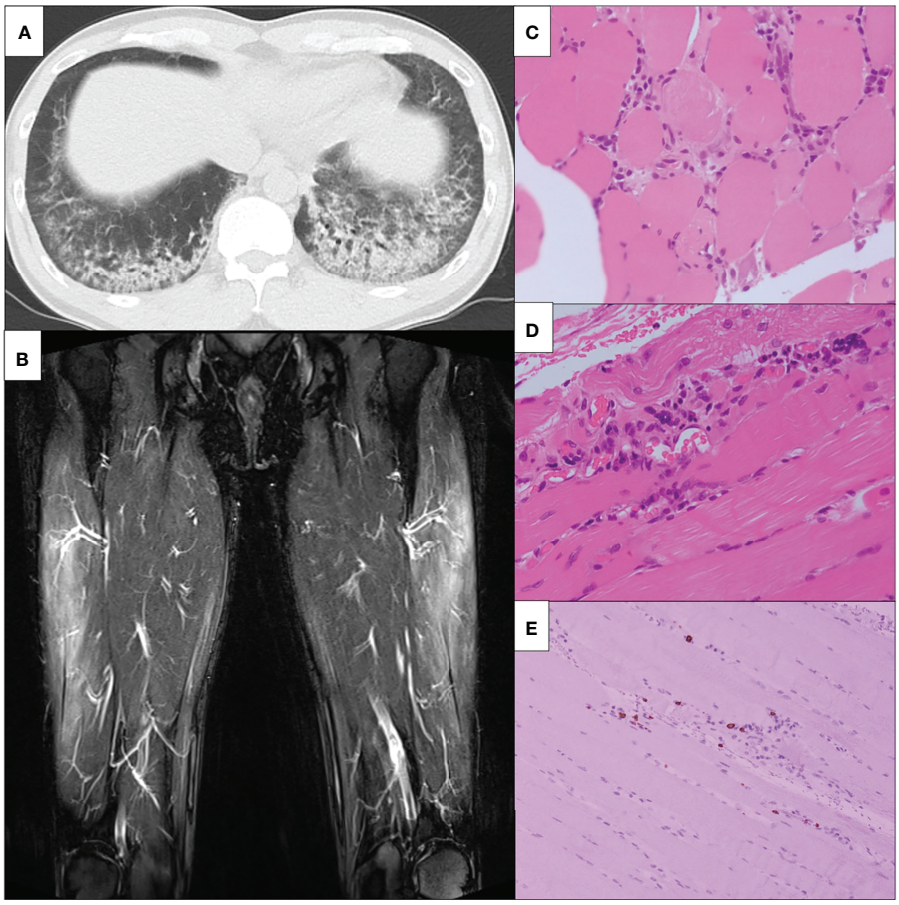

FIGURE 2
Clinical imagings. **(A)** Chest non-contrast CT findings. Chest non-contrast CT revealed bilateral ground-glass opacity. **(B)** MRI findings of bilateral lower limbs. MRI shows high signals on STIR in the bilateral vastus lateralis, suggesting muscular inflammation. MRI, magnetic resonance imaging; STIR, short T1 inversion recovery. **(C-E)** The slide showed **(C)** inflammatory cell infiltration around the myofiber bundles, **(D)** perivascular inflammatory cell infiltration, and **(E)** CD8-positive lymphocytes infiltration in atrophy of the myofibers. CT, computed tomography; HE, hematoxylin-eosin; MRI, magnetic resonance imagin; STIR, short T1 inversion recovery; CD, cluster of differentiation.

activation (20). Therefore, COVID-19 shared clinical features with rheumatic diseases characterized by elevated inflammatory cytokine levels. Here, we report a patient with COVID-19 who was later associated with DM that involves the proximal limb muscles and typical cutaneous manifestations, including V-neck skin ra. Our case describes a newly diagnosed anti-PL-7-positive DM complicated by ILD with a recent COVID-19 diagnosis. Some cases are reported to develop autoimmune diseases after COVID-19 (21). The overall incidence of COVID-19 associated with DM remains rare. COVID-19 had resulted in flares of preexisting rheumatic diseases (22); however, this is unlikely since no clinical symptoms were suggesting rheumatic manifestation before the onset of COVID-19 in the present case. Whether COVID-19-induced viral myositis mimics DM-like clinical manifestations or DM itself can be argued. The time interval between the onset of erythematous skin rash and the COVID-19 RNA detection is 3 weeks; thus, it can be presumed to be new-onset DM and not COVID-19-related myositis. In addition, the seroconversion of ASSs supports this idea; however, whether autoantibody positivity is persistent or transient should be evaluated. The newly appearing radiographic finding of nonspecific interstitial pneumonia (NSIP)-like bilateral ground-glass opacities also supports ASA-positive DM-associated ILD. Proinflammatory clinical manifestation seen as COVID-19 complications mimics the symptoms of DM (23). However, we should discriminate between real DM and post-viral myositis following SARS-CoV-2 infection.

SARS-CoV-2 may cause postinfectious myositis, which may range from direct virus-induced myositis to virus-triggered autoimmunity-related myositis (24). Whether COVID-19 contributes to the occurrence of typical DM that carries the myositis-specific autoantibodies remained unclear. As postulated, autoimmune mechanisms can be developed as a

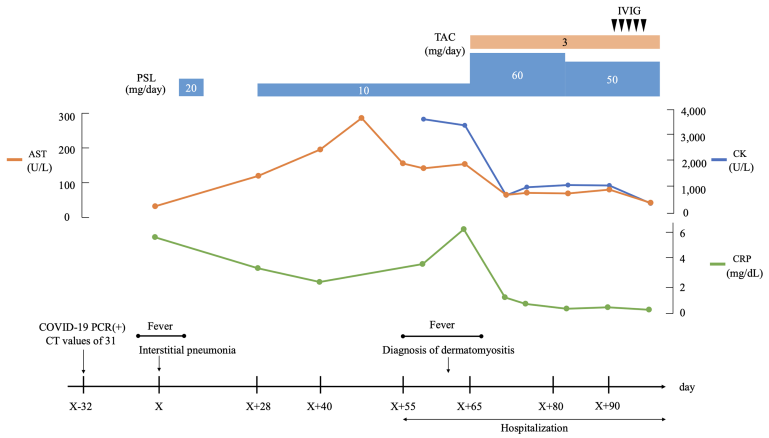

FIGURE 3
Clinical course. AST, aspartate aminotransferase; CK, creaine kinase; COVID-19, coronavirus disease 2019; CRP, C-reactive protein; CT, cycle threshold; IVIG, intravenous immunoglobulin; PCR, polymerase chain reaction; PSL, prednisolone; TAC, tacrolimus.

consequence of the molecular autoantigen transformation or modifications due to the influence of the SARS-CoV-2 infection (25). However, a limited number of case reports demonstrated the occurrence of myositis with specific autoantibodies as a consequence of the clinical course of COVID-19 (23). Idiopathic inflammatory myopathy is one of the potential autoimmune diseases that could be triggered by COVID-19 (23). These patients have both DM and COVID-19 presented with various cutaneous manifestations, elevated CK, and partly associated with seropositivity for myositis-specific antibodies (MSAs).

Viral infections may serve as a trigger although the association between COVID-19 and DM development remains unclear. A recent epidemiological survey suggests that the increasing number of patients with autoimmune diseases coincides with the COVID-19 pandemic (21). SARS-CoV-2 has been speculated to break the self-tolerance and trigger autoimmune responses through inflammatory cytokine induction (21). Dysregulation of neutrophil extracellular trap (NET) formation has been shown to mediate disease pathology in multiple viral infections (26), including SARS-CoV-2. Indeed, dysregulation of NET formation has been demonstrated in SARS-CoV-2 infection (27). Therefore, the complexity of COVID-19 and of NET formation may relate to the autoantibodies production through following an adaptive immune response. The clinical features of severe COVID-19 are postulated to be similar to those of anti-MDA-5-positive DM (28), which may suggest the immune-mediated mechanisms for these disorders. Type 1 interferon (IFN) signature has been implicated in the pathogenesis of autoimmune diseases, including rheumatic diseases (29). COVID-19 pathogenesis may include the induction of a hyper-inflammatory state with elevated inflammatory cytokines, including type 1 IFN, which leads to autoantibody induction (30). Another mechanism includes the molecular mimicry between viral antigen and damaged muscle antigen leading to the adaptive immune system producing autoantibodies (31). Therefore, determining the coexistent COVID-19 and DM with definitely diagnosed patients with DM with myositis-specific autoantibodies and typical histological manifestations is important to elucidate the immunopathology for COVID-19-related DM.

Myositis-specific autoantibodies are an important clue for DM diagnosis (32). Recent studies identified three immunogenic linear epitopes with coronavirus 2 (SARS-CoV-2) proteins in anti-TIF1-γ DM, which suggest the possibility of overlapping COVID-19 and DM (33). Newly diagnosed anti-MDA-5-positive DM following the recent COVID-19 diagnosis was reported (28). Furthermore, anti-MDA-5-Ab is frequently detected in patients with COVID-19, and its titers correlate with severe disease and poor COVID-19 outcomes (34). However, the coincidence between COVID-19 and the ASS is rarely reported. Blake T et al. reported a case of a patient with COVID-19-like pneumonia who was positive for anti-PL-7 antibody, but without virological evidence of COVID-19 (35). Table 1 shows cases with virologically proven COVID-19 infection complicated with dermatomyositis with MSAs excluding Anti-MDA5-Ab, suggesting a fair prognosis for these coexisting patients (32–36). In contrast to the other MSAs, such as an anti-MDA5 antibody, the associations between the other MSAs-positive DM and COVID-19 were limited, which may indicate the necessity to further evaluate MSAs in patients with COVID-19-related myopathy to elucidate their true relationships.

COVID-19 is a novel pandemic that has significant concern on the occurrence of various inflammatory disorders and subsequent organ damage. A possible linkage was found between COVID-19 and autoimmune diseases through the

TABLE 1 Complicated cases of COVID-19 and myositis with MSAs excluding anti-MDA5 Ab.

Authors	Year	Sex	Age of onset	Antibody of PM/DM	ILD	Symptoms of myositis	Skin rash	Outcomes
Zhang et al. (36)	2020	F	58	Anti-SAE, Ku Ab	NA	Bilateral ptosis, facial weakness, hypernasal dysarthria, and proximal limb weakness	NA	Recovered
Sacchi et al. (37)	2020	F	77	Anti-Ku, Mi-2 Ab	YES	Aprexia	NA	Recovered
Borges et al. (38)	2021	F	36	Anti-Mi-2 Ab	NA	Proximal limb weakness	Gottron's papules	Recovered
Okada et al. (39)	2021	F	64	Anti-NXP2 Ab	No	Neck and proximal limb weakness	Itchy erythematous lesions on forehead, bilateral ears, scalp, and neck, lacking typical heliotrope rash or Gottron's sign Periungual telangiectasias	Recovered
Faria et al. (40)	2022	F	59	Anti-Mi-2, SAE Ab	YES	Limb weakness	Heliotrope rash, Gottron's sign with ulcerations, and cuticular hypertrophy	Recovered

COVID-19, coronavirus disease 2019; MSA, myositis specific antibodies; PM, polymyositis; DM, dermatomyositis; ILD, interstitial lung disease; F, female; Ab, antibody; NA, not applicable.

immune-mediated inflammatory pathways. The present case report suggests that COVID-19 infection may trigger the SSA-related DM. More data are needed to elucidate the relationship between COVID-19 and the risk of the induction of MSAs and the occurrence of DM, and these patients possess a particular genetic susceptibility.

In conclusion, SARS-CoV-2 can induce myopathy in certain high risk hosts, which mimics the symptoms of DM. We reported a case of PL-7-positive DM in a patient with COVID-19, who responded to steroid plus immunosuppressive treatments. The link between COVID-19 and the development of ASS-related DM needs further investigation, and clinicians should remain vigilant about potential muscle involvement post-COVID-19. The natural history and prognosis or these patients compared to their *de novo* DM counterparts remain unclear.

Data availability statement

The original contributions presented in the study are included in the article/Supplementary Material. Further inquiries can be directed to the corresponding author.

Ethics statement

Written informed consent was obtained from the individual (s) for the publication of any potentially identifiable images or data included in this article.

Author contributions

HS, HM, YF, JT, SY, TA, HO and KM were involved with the conception of the work. HS, TSa, TSu, YO, and YE contributed to the treatment and collection of data. HS, HM and KM wrote the first draft of the manuscript. All authors contributed to the article and approved the submitted version.

Acknowledgments

We would like to thank Enago (www.enago.jp) for English language review.

Conflict of interest

The authors declare that the research was conducted in the absence of any commercial or financial relationships that could be construed as a potential conflict of interest.

Publisher's note

All claims expressed in this article are solely those of the authors and do not necessarily represent those of their affiliated organizations, or those of the publisher, the editors and the reviewers. Any product that may be evaluated in this article, or claim that may be made by its manufacturer, is not guaranteed or endorsed by the publisher.

Supplementary material

The Supplementary Material for this article can be found online at: https://www.frontiersin.org/articles/10.3389/fimmu.2022.1002329/full#supplementary-material

References

1. Wiersinga WJ, Rhodes A, Cheng AC, Peacock SJ, Prescott HC. Pathophysiology, transmission, diagnosis, and treatment of coronavirus disease 2019 (Covid-19): A review. *JAMA* (2020) 324(8):782–93. doi: 10.1001/jama.2020.12839

2. Osuchowski MF, Winkler MS, Skirecki T, Cajander S, Shankar-Hari M, Lachmann G, et al. The covid-19 puzzle: Deciphering pathophysiology and phenotypes of a new disease entity. *Lancet Respir Med* (2021) 9(6):622–42. doi: 10.1016/S2213-2600(21)00218-6

3. Liu Y, Sawalha AH, Lu Q. Covid-19 and autoimmune diseases. *Curr Opin Rheumatol* (2021) 33(2):155–62. doi: 10.1097/BOR.0000000000000776

4. Mehta P, Machado PM, Gupta L. Understanding and managing anti-mda 5 dermatomyositis, including potential covid-19 mimicry. *Rheumatol Int* (2021) 41 (6):1021–36. doi: 10.1007/s00296-021-04819-1

5. Thorne LG, Reuschl AK, Zuliani-Alvarez L, Whelan MVX, Turner J, Noursadeghi M, et al. Sars-Cov-2 sensing by rig-I and Mda5 links epithelial infection to macrophage inflammation. *EMBO J* (2021) 40(15):e107826. doi: 10.15252/embj.2021107826

6. Mangalmurti N, Hunter CA. Cytokine storms: Understanding covid-19. *Immunity* (2020) 53(1):19–25. doi: 10.1016/j.immuni.2020.06.017

7. Alosaimi B, Mubarak A, Hamed ME, Almutairi AZ, Alrashed AA, AlJuryyan A, et al. Complement anaphylatoxins and inflammatory cytokines as prognostic markers for covid-19 severity and in-hospital mortality. *Front Immunol* (2021) 12:668725. doi: 10.3389/fimmu.2021.668725

8. Dotan A, Muller S, Kanduc D, David P, Halpert G, Shoenfeld Y. The sars-Cov-2 as an instrumental trigger of autoimmunity. *Autoimmun Rev* (2021) 20 (4):102792. doi: 10.1016/j.autrev.2021.102792

9. Wang EY, Mao T, Klein J, Dai Y, Huck JD, Jaycox JR, et al. Diverse functional autoantibodies in patients with covid-19. *Nature* (2021) 595(7866):283–8. doi: 10.1038/s41586-021-03631-y

10. Callen JP. Dermatomyositis. *Lancet* (2000) 355(9197):53–7. doi: 10.1016/S0140-6736(99)05157-0

11. Long K, Danoff SK. Interstitial lung disease in polymyositis and dermatomyositis. *Clin Chest Med* (2019) 40(3):561–72. doi: 10.1016/j.ccm.2019.05.004

12. De Santis M, Isailovic N, Motta F, Ricordi C, Ceribelli A, Lanza E, et al. Environmental triggers for connective tissue disease: The case of covid-19 associated with dermatomyositis-specific autoantibodies. *Curr Opin Rheumatol* (2021) 33(6):514–21. doi: 10.1097/BOR.0000000000000844

13. Mahler M, Miller FW, Fritzler MJ. Idiopathic inflammatory myopathies and the anti-synthetase syndrome: A comprehensive review. *Autoimmun Rev* (2014) 13 (4-5):367–71. doi: 10.1016/j.autrev.2014.01.022

14. Satoh M, Tanaka S, Ceribelli A, Calise SJ, Chan EK. A comprehensive overview on myositis-specific antibodies: New and old biomarkers in idiopathic inflammatory myopathy. *Clin Rev Allergy Immunol* (2017) 52(1):1–19. doi: 10.1007/s12016-015-8510-y

15. Lega JC, Reynaud Q, Belot A, Fabien N, Durieu I, Cottin V. Idiopathic inflammatory myopathies and the lung. *Eur Respir Rev* (2015) 24(136):216–38. doi: 10.1183/16000617.00002015

16. Katzap E, Barilla-LaBarca ML, Marder G. Antisynthetase syndrome. *Curr Rheumatol Rep* (2011) 13(3):175–81. doi: 10.1007/s11926-011-0176-8

17. Remuzgo-Martinez S, Atienza-Mateo B, Ocejo-Vinyals JG, Pulito-Cueto V, Prieto-Pena D, Genre F, et al. Hla association with the susceptibility to anti-synthetase syndrome. *Joint Bone Spine* (2021) 88(3):105115. doi: 10.1016/j.jbspin.2020.105115

18. Pan F, Ye T, Sun P, Gui S, Liang B, Li L, et al. Time course of lung changes at chest ct during recovery from coronavirus disease 2019 (Covid-19). *Radiology* (2020) 295(3):715–21. doi: 10.1148/radiol.2020200370

19. Alfraji N, Mazahir U, Chaudhri M, Miskoff J. Anti-synthetase syndrome: A rare and challenging diagnosis for bilateral ground-glass opacities-a case report with literature review. *BMC Pulm Med* (2021) 21(1):11. doi: 10.1186/s12890-020-01388-0

20. Huang C, Wang Y, Li X, Ren L, Zhao J, Hu Y, et al. Clinical features of patients infected with 2019 novel coronavirus in wuhan, China. *Lancet* (2020) 395 (10223):497–506. doi: 10.1016/S0140-6736(20)30183-5

21. Gracia-Ramos AE, Martin-Nares E, Hernandez-Molina G. New onset of autoimmune diseases following covid-19 diagnosis. *Cells* (2021) 10(12):3592. doi: 10.3390/cells10123592

22. Ahmed S, Zimba O, Gasparyan AY. Covid-19 and the clinical course of rheumatic manifestations. *Clin Rheumatol* (2021) 40(7):2611–9. doi: 10.1007/s10067-021-05691-x

23. Qian J, Xu H. Covid-19 disease and dermatomyositis: A mini-review. *Front Immunol* (2021) 12:747116. doi: 10.3389/fimmu.2021.747116

24. Saud A, Naveen R, Aggarwal R, Gupta L. Covid-19 and myositis: What we know so far. *Curr Rheumatol Rep* (2021) 23(8):63. doi: 10.1007/s11926-021-01023-9

25. Chang SE, Feng A, Meng W, Apostolidis SA, Mack E, Artandi M, et al. New-onset igg autoantibodies in hospitalized patients with covid-19. *Nat Commun* (2021) 12(1):5417. doi: 10.1038/s41467-021-25509-3

26. Papayannopoulos V. Neutrophil extracellular traps in immunity and disease. *Nat Rev Immunol* (2018) 18(2):134–47. doi: 10.1038/nri.2017.105

27. Barnes BJ, Adrover JM, Baxter-Stoltzfus A, Borczuk A, Cools-Lartigue J, Crawford JM, et al. Targeting potential drivers of covid-19: Neutrophil extracellular traps. *J Exp Med* (2020) 217(6):e20200652. doi: 10.1084/jem.20200652

28. Giannini M, Ohana M, Nespola B, Zanframundo G, Geny B, Meyer A. Similarities between covid-19 and anti-Mda5 syndrome: What can we learn for better care? *Eur Respir J* (2020) 56(3):2001618. doi: 10.1183/13993003.01618-2020

29. Muskardin TLW, Niewold TB. Type I interferon in rheumatic diseases. *Nat Rev Rheumatol* (2018) 14(4):214–28. doi: 10.1038/nrrheum.2018.31

30. Darif D, Hammi I, Kihel A, El Idrissi Saik I, Guessous F, Akarid K. The pro-inflammatory cytokines in covid-19 pathogenesis: What goes wrong? *Microb Pathog* (2021) 153:104799. doi: 10.1016/j.micpath.2021.104799

31. Cusick MF, Libbey JE, Fujinami RS. Molecular mimicry as a mechanism of autoimmune disease. *Clin Rev Allergy Immunol* (2012) 42(1):102–11. doi: 10.1007/s12016-011-8294-7

32. Betteridge Z, McHugh N. Myositis-specific autoantibodies: An important tool to support diagnosis of myositis. *J Intern Med* (2016) 280(1):8–23. doi: 10.1111/joim.12451

33. Megremis S, Walker TDJ, He X, Ollier WER, Chinoy H, Hampson L, et al. Antibodies against immunogenic epitopes with high sequence identity to sars-Cov-2 in patients with autoimmune dermatomyositis. *Ann Rheum Dis* (2020) 79 (10):1383–6. doi: 10.1136/annrheumdis-2020-217522

34. Wang G, Wang Q, Wang Y, Liu C, Wang L, Chen H, et al. Presence of anti-Mda5 antibody and its value for the clinical assessment in patients with covid-19: A retrospective cohort study. *Front Immunol* (2021) 12:791348. doi: 10.3389/fimmu.2021.791348

35. Blake T, Noureldin B. Anti-Pl-7 antisynthetase syndrome presenting as covid-19. *Rheumatol (Oxford)* (2021) 60(7):e252–e4. doi: 10.1093/rheumatology/keab129

36. Zhang H, Charmchi Z, Seidman RJ, Anziska Y, Velayudhan V, Perk J. Covid-19-Associated myositis with severe proximal and bulbar weakness. *Muscle Nerve* (2020) 62(3):E57–60. doi: 10.1002/mus.27003

37. Sacchi MC, Tamiazzo S, Lauritano EC, Bonometti R. Case report of covid-19 in an elderly patient: Could sars-Cov2 trigger myositis? *Eur Rev Med Pharmacol Sci* (2020) 24(22):11960–3. doi: 10.26355/eurrev_202011_23857

38. Borges NH, Godoy TM, Kahlow BS. Onset of dermatomyositis in close association with covid-19-a first case reported. *Rheumatol (Oxford)* (2021) 60(SI): SI96. doi: 10.1093/rheumatology/keab290

39. Okada Y, Izumi R, Hosaka T, Watanabe S, Shijo T, Hatchome N, et al. Anti-Nxp2 antibody-positive dermatomyositis developed after covid-19 manifesting as type I interferonopathy. *Rheumatol (Oxford)* (2022) 61(4):e90–e2. doi: 10.1093/rheumatology/keab872

40. Faria M, Shinjo SK. Covid-19 as potential aggravating factor for the natural course of new onset-dermatomyositis. *Reumatismo* (2022) 74(1):41–3. doi: 10.4081/reumatismo.2022.1440

frontiers | Frontiers in Immunology

TYPE Perspective
PUBLISHED 28 October 2022
DOI 10.3389/fimmu.2022.1032574

OPEN ACCESS

EDITED BY
Alberto Beretta,
Independent researcher, Milano, Italy

REVIEWED BY
Jen-Ren Wang,
National Cheng Kung University, Taiwan

*CORRESPONDENCE
Wenda Gao
wgao@antagendiagnostics.com
Stefan Riedel
sriedel@bidmc.harvard.edu

†These authors share senior authorship

SPECIALTY SECTION
This article was submitted to Viral Immunology, a section of the journal Frontiers in Immunology

RECEIVED 31 August 2022
ACCEPTED 14 October 2022
PUBLISHED 28 October 2022

CITATION
Lunderberg JM, Dutta S, Collier A-RY, Lee J-S, Hsu Y-M, Wang Q, Zheng W, Hao S, Zhang H, Feng L, Robson SC, Gao W and Riedel S (2022) Pan-neutralizing, germline-encoded antibodies against SARS-CoV-2: Addressing the long-term problem of escape variants.
Front. Immunol. 13:1032574.
doi: 10.3389/fimmu.2022.1032574

Pan-neutralizing, germline-encoded antibodies against SARS-CoV-2: Addressing the long-term problem of escape variants

Justin Mark Lunderberg[1], Sanjucta Dutta[2], Ai-Ris Y. Collier[3], Jeng-Shin Lee[4], Yen-Ming Hsu[4], Qiao Wang[5], Weina Zheng[5], Shushun Hao[5], Haohai Zhang[1], Lili Feng[6], Simon C. Robson[1], Wenda Gao[7,8*†] and Stefan Riedel[2*†]

[1]Center for Inflammation Research, Department of Anesthesia, Critical Care and Pain Medicine, Beth Israel Deaconess Medical Center, Harvard Medical School, Boston, MA, United States, [2]Department of Pathology, Beth Israel Deaconess Medical Center, Harvard Medical School, Boston, MA, United States, [3]Center for Virology and Vaccine Research, Beth Israel Deaconess Medical Center, Harvard Medical School, Boston, MA, United States, [4]AB Biosciences, Inc., Concord, MA, United States, [5]Shijiazhuang Hipro Biotechnology Co., Ltd., Hebei, China, [6]Department of Hematology, Shandong Provincial Hospital Affiliated to Shandong First Medical University, Jinan, China, [7]Antagen Diagnostics, Inc., Canton, MA, United States, [8]Antagen Pharmaceuticals, Inc., Canton, MA, United States

Despite the initially reported high efficacy of vaccines directed against ancestral SARS-CoV-2, repeated infections in both unvaccinated and vaccinated populations remain a major global health challenge. Because of mutation-mediated immune escape by variants-of-concern (VOC), approved neutralizing antibodies (neutAbs) effective against the original strains have been rendered non-protective. Identification and characterization of mutation-independent pan-neutralizing antibody responses are therefore essential for controlling the pandemic. Here, we characterize and discuss the origins of SARS-CoV-2 neutAbs, arising from either natural infection or following vaccination. In our study, neutAbs in COVID-19 patients were detected using the combination of two lateral flow immunoassay (LFIA) tests, corroborated by plaque reduction neutralization testing (PRNT). A point-of-care neutAb LFIA, NeutraXpress™, was validated using serum samples from historical pre-COVID-19 negative controls, patients infected with other respiratory pathogens, and PCR-confirmed COVID-19 patients. Surprisingly, potent neutAb activity was mainly noted in patients generating both IgM and IgG against the Spike receptor-binding domain (RBD), in contrast to samples possessing anti-RBD IgG alone. We propose that low-affinity, high-avidity, germline-encoded natural IgM and subsequent generation of class-switched IgG may have an underappreciated role in cross-protection, potentially offsetting immune escape by SARS-CoV-2 variants. We suggest Reverse Vaccinology 3.0 to further exploit this innate-like defense mechanism. Our

proposition has potential implications for immunogen design, and provides strategies to elicit pan-neutAbs from natural B1-like cells. Refinements in future immunization protocols might further boost long-term cross-protection, even at the mucosal level, against clinical manifestations of COVID-19.

KEYWORDS

SARS-CoV-2, neutralizing antibodies, somatic hypermutation, B cell memory, vaccines, IgM, B-1 B cells, Reverse Vaccinology

Introduction

As of mid-2022, more than 560 million people globally have been infected with severe acute respiratory syndrome coronavirus 2 (SARS-CoV-2), the causative agent for coronavirus disease 2019 (COVID-19). Over 6.3 million people have died of infection-mediated complications. The extraordinarily rapid development of several vaccines in the first year of field deployment has saved close to 20 million lives that would otherwise have been lost to COVID-19 (1). However, as waves of variants-of-concern (VOC) emerge, breakthrough infections by the variants in fully vaccinated individuals have become increasingly common (2–7), and may still cause substantial morbidity and mortality. Particularly, SARS-CoV-2 Omicron strains have accumulated unprecedented numbers of mutations in the Spike protein with ~40 residue changes versus 10 on average in all the previous dominant variants (8, 9) that evade neutralizing antibody (neutAb) binding. As a result, individuals who received two doses of the BNT162b2 mRNA vaccine have over 22-fold decreases in neutralizing activity against the Omicron strain, when compared to the ancestral Wuhan-Hu-1 strain (10). Efficacies of the other current vaccines against Delta and Omicron VOCs have also declined (11).

Likewise, passive transfer of therapeutic neutralizing monoclonal antibodies (mAb) was initially successful in treating COVID-19 before the arrival of the variants (12), but many neutAbs previously approved for emergency use by the FDA do not retain efficacy against Delta and Omicron strains (13, 14). In separate studies, the neutralizing activity of the majority of tested SARS-CoV-2 mAbs were either abolished or impaired against Omicron (15, 16).

Therefore, for neutAb developers, active questions are: 1) Whether it is possible to identify, characterize and isolate pan-neutAbs against the majority of current and future SARS-CoV-2 variants and 2) if this venture is successful, whether developing recombinant pan-neutAbs as prophylactic and therapeutic modalities can stay ahead of evolving variants? These questions also apply to vaccine development to stimulate durable pan-neutralizing antibody responses.

The answer to the first question is in the affirmative. By adopting high throughput single cell sequencing of thousands of Spike-enriched memory B cells (MBCs) from the PBMCs of convalescent patients (17), researchers have identified IgG1 type pan-neutAbs, for example, DXP-604 (16) and 76E1 (18). Like VIR-7831 (Sotrovimab), DXP-604 effectively neutralizes SARS-CoV-2 D614G, Alpha, Beta, Gamma, Delta as well as Omicron (16). Unlike DXP-604, 76E1 binds to a unique S2 epitope partially buried in the pre-fusion state of the Spike trimer, which is only exposed when the Spike protein binds to ACE2. As a result, while all the other RBD-binding neutAbs bind to the pre-fusion state of Spike trimer, 76E1 does not.

Nevertheless, as the S2 regions are conserved among multiple human coronaviruses, blocking the interaction of the highly conserved S2' site and the fusion peptide by 76E1 can effectively block virus-cell fusion and broadly neutralize seven human coronaviruses, including two α-coronaviruses (HCoV-229E and HCoV-NL63) and five β-coronaviruses (SARS-CoV-2 and all its VOCs, SARS-CoV, MERS-CoV, HCoV-OC43 and HCoV-HKU1) (18). Thus, although very rare, pan-neutAbs with unique mechanisms of action can be isolated with extensive screening efforts. These studies indicate that MBCs exhibit repertoires with various specificities to Spike glycoprotein that are enhanced by somatic hypermutation and could avoid the SARS-CoV-2 immune escape.

The answer to the second question is more complex. Large-scale manufacturing, clinical trials and regulatory approval of the recombinant neutAbs typically take a long time and are hugely expensive. In light of certain neutAbs being "highly unlikely to be active against the Omicron variant, which is circulating at a very high frequency throughout the United States", on January 24th, 2022, the FDA restricted the emergency use of Bamlanivimab and Etesevimab (co-administered) and REGEN-COV (Casirivimab and Imdevimab) to "patients that are likely to have been infected with or exposed to a variant that is susceptible to these treatments".

To avoid such restrictions in future therapeutic mAbs, researchers need to reassess if there are fundamental immunological elements missing in our current understanding of such pan-neutAbs and of the durability of vaccine-induced

protection. The following sections are devoted to such mechanistic discussions, albeit with a focus on mRNA vaccination.

NeutAbs in natural infection have greater breadth than after vaccination

Using single B cell sequencing, ELISA, biolayer interferometry and pseudovirus neutralization assays, Cho et al. compared cloned antibodies from MBCs at 1.3 and 6.2 months after natural infection in a cohort of convalescent patients, with similarly cloned antibodies from MBCs at 1.3 and 5 months after the 2nd dose of either Moderna (mRNA-1273) or Pfizer-BioNTech (BNT162b2) mRNA vaccines in subjects having no prior history of SARS-CoV-2 infection (19). They found that at 1.3 and 5 months after the 2nd vaccine dose, mRNA vaccines induced 4.9- and 3.6-fold higher plasma neutAb titers than natural infection at 1.3 and 6.2 months following infection. Between the 1st and 2nd doses, MBCs continue to evolve antibodies with increased neutralizing activity, yet there is no further increase in potency or breadth thereafter. In contrast, individual MBC-derived antibodies selected over time by natural infection have greater potency and breadth than antibodies elicited by vaccination (19). Here, the key element is the breadth of MBCs, which directly determines the effectiveness of their secreted neutAbs against rising variants (20).

Antibody-secreting plasma cells and peripheral MBCs are independently regulated cell populations, playing different roles in the maintenance of protective humoral immunity. The initial burst of short-lived plasmablasts (21, 22) produces sufficient concentrations of neutAbs in the circulation to protect an individual at high risk of exposure to SARS-CoV-2. However, populations of plasmablasts and circulating plasma cells contract quickly and, as a result, the serum neutAb titers wane significantly over a period of months following antigen stimulation. Our own work with an LFIA test NeutraXpress™ has further confirmed this rapid waning of mRNA vaccine-induced neutAb titers, at 3-6 months after the 2nd dose (23). The kinetics of decreasing neutAb titers correlates with reports of reinfection in convalescent individuals and breakthrough infection by variants in fully vaccinated individuals (7, 24).

On the other hand, MBCs are responsible for swift recall responses to previously experienced epitopes. The number of quiescent MBCs is relatively stable over the first 5–6 months after mRNA vaccination or natural infection (25); during this period the cells undergo somatic hypermutation for increased antibody affinity (19, 26). At the molecular level, while 19% and 21% of the cloned antibodies recovered from single MBCs of vaccinated individuals have shown improved potency and greater breadth, respectively, these numbers for similarly cloned antibodies from convalescent patients are 59% and 69% (19). At the population level, SARS-CoV-2-naïve individuals who received two doses of the BNT162b2 mRNA vaccine exhibited a 13.06-fold increased risk for breakthrough infection with the Delta variant, when compared with previously-infected individuals who have not been vaccinated (24). Thus, natural infection-elicited neutAbs from MBCs show greater neutralizing potency and breadth than those induced by vaccination over a similar period of time (19, 24).

As broad antigen recognition is crucial for potential induction of pan-neutAbs to prevent both infection and disease caused by VOCs, it is important to understand the immunological processes that shape the breadth of neutAbs.

Low-affinity cross-reactive MBCs provide rapid and potent recall responses towards antigenic variants

Primary germinal center (GC) responses drive the development of two distinct but equally important B cell populations: the high-affinity long-lived plasma cells (LLPCs) (27, 28) generated by activation-induced cytidine deaminase (AID)-driven somatic hypermutation and the diverse pool of largely AID-independent rarely-mutated MBCs. LLPCs provide protective immunity by producing high-affinity circulating antibodies against the same re-encountered (homologous) pathogen, whereas MBCs induce a rapid, first-line antibody response to infections by secreting a diverse pool of cross-reactive antibodies that can recognize classes of related (heterologous) pathogens or recognize rapidly and continuously mutating pathogen variants (29, 30).

For example, upon infection or immunization with one flavivirus (West Nile virus, WNV), the low-affinity cross-reactive MBCs generated had a very limited capacity to re-enter secondary GCs, and were excluded from GC-somatic hypermutation. However, these MBCs developed enhanced affinities towards a heterologous flavivirus (Japanese Encephalitis virus, JEV) by forming extrafollicular plasmablasts (31). Lineage tracing and antibody cloning from single B cells also showed that a large fraction of the GC B cells express high-affinity B cell receptors, whereas the vast majority of simultaneously selected MBCs express receptors with very low-affinity for the antigen (32). In B cell receptor (BCR) transgenic mice, more MBCs were produced when mice were challenged with lower affinity antigens (33). It was also found that nascent MBCs require high valency interactions between their BCR and multimerized antigen; this increases the apparent affinity through avidity effects, resulting in a MBC population with much lower overall affinities than the contemporaneous GC B cells (32), the latter of which are the major source for the bone marrow (BM)-residing LLPCs.

Taken together, these studies address a critical question of how MBCs respond to heterologous challenges, *i.e.*, whether responses are through creating fundamentally new specificities through secondary GCs or through the selection of pre-existing clones without further affinity maturation. Unlike antigen-specific LLPCs derived from high-affinity naïve B cells, precursors of MBCs encoding low-affinity antibodies with germline sequences largely bypass secondary GCs in recall responses (34). Similarly, recall of MBCs with germline sequences, rather than activation of naïve, mature B cells, has been the primary component of the response to influenza strains exhibiting antigenic drift (35). Thus, the recall responses are restricted by clonal selection from the panel of pre-existing MBC specificities with limited contributions (25) from further affinity maturation (29, 30). Therefore, such low-affinity cross-reactive MBCs may contribute to the protection against future variants.

Early neutAbs against SARS-CoV-2 are enriched with germline sequences, and may have an IgM+ innate-like B-1 cell origin

In a relatively short longitudinal analysis (8-69 days after diagnosis) of SARS-CoV-2-infected subjects, Kreer and colleagues found highly potent neutAbs developed early after infection and exhibited limited ongoing somatic hypermutation (36). From sorted single B cells, 31 of 79 binding and 10 of 27 neutralizing antibodies exhibited 99%–100% germline identities, with no correlation between neutralizing activity and the level of somatic mutation. The potential precursor sequences of the SARS-CoV-2 binding and neutralizing antibodies were even identified as near-germline sequences (preference for IGHV3-30) in naïve B cell repertoires from healthy individuals, before the COVID-19 pandemic (36). The usage of near-germline sequences (*e.g.*, IGHV3-53 and IGHV3-66) by SARS-CoV-2 specific antibodies in the early response has also been confirmed by other studies (34, 37–45). Some potent therapeutic neutAbs are found to utilize germline sequences as well, including one which obtained emergency use authorization (CB6/LY-CoV016) (40) and several currently under clinical investigation (P2C-1F11/BRII-196 and BD-604/DXP-604) (46, 47). These studies suggest that neutAbs can be readily generated from existing germline antibody sequences found in the general population (48), a feature reminiscent of natural IgM-expressing B-1 cells in mice.

The B cell compartment can be divided into two developmentally and functionally distinct populations, B-1 and B-2 B cells (49). B-1 cells are primarily derived from the fetal liver, whereas the conventional B-2 cells originate from the BM and can be further characterized into follicular B (FOB) and marginal zone B (MZB) cells (50, 51). B-1 cells are found in the body cavities and in mucosal tissues as well, including the lamina propria of the gut and the respiratory tract. During respiratory infections, B-1 cells in the pleural cavity (accounting for 35% - 70% of total B cells found in this site) can produce large amounts of IgM and IgA natural antibodies as a first-line defense against pathogens (52). Innate natural antibodies are primarily encoded by germline sequences with minimal N-region addition and without somatic hypermutation; they are functionally important for early pathogen clearance (53). Recently, an elusive human B-1 cell population, equivalent to the well-studied mouse counterpart, has been proposed to have the unique surface phenotype CD20+CD27+CD43+, distinguishing it from other B cell subsets (54, 55). While controversy on precise phenotyping is still present, it is anticipated that, when compared to murine B-1 cells, the human analogue will possess a similar lineage and function.

It is important to understand the origin of neutAbs for SARS-CoV-2. B-1 cell antibodies are selected for function (*e.g.*, defense against microbial pathogens in innate immunity), and B-2 cell antibodies are selected for affinity to a pathogen (55). NeutAbs of B-1 ontogeny may initially have lower affinity and elevated cross-reactivity due to their origin of germline natural IgM (56). Indeed, of the 27 early-stage SARS-CoV-2 neutAbs isolated by Kreer et al., 4 showed low-to-moderate levels of autoreactivity and 2 showed cross-reactivity towards heterologous envelope proteins (Ebola glycoprotein and HIV-1 gp140) (36). This feature may allow such B cells to be preferentially recruited to the extrafollicular MBC compartment and subsequently evolve their neutAbs (*via* class-switching and low-degree somatic hypermutation) into antibodies with greater breadth and affinity to rising variants. To the contrary, because of the BCR sequence use, the malleability of neutAbs of B-2 ontogeny may be limited and these might be funneled towards high affinity with a LLPC host cell fate, targeting only the original strain. These neutAbs are highly specific to the homologous immunogen and yet are not flexible in their response and are eventually outpaced by a rapidly-mutating pathogen.

To test this hypothesis, we proposed these studies: 1) Whether neutAb activities can be detected in the early phase of SARS-CoV-2 infection (<40 days post onset of symptoms); and 2) Whether RBD-specific IgM contributes to the serum neutralizing activity. First, we stratified PCR-confirmed COVID-19 patients based on days following symptom onset and IgM/IgG profiles of anti-RBD antibodies in their serum samples. For that, we used an LFIA rapid test DISCOVID™ to detect the presence of RBD-specific IgM and/or IgG in their preserved serum samples. The specificity (96.6%) and sensitivity (92.7%) of DISCOVID™ have been previously determined with historical samples collected prior to the pandemic and in PCR-confirmed COVID-19 patients (Supplementary Tables 1 and 2). Therefore, patients were stratified into 4 subgroups of RBD reactivity: IgM+IgG-, IgM+IgG+, IgM-IgG+, and IgM-IgG-. Then, we used the second LFIA rapid test NeutraXpress™ to detect the presence of

neutAbs in each subgroup, and to correlate with the time following symptom onset or PCR positivity in asymptomatic patients. The rapid test NeutraXpress™ with a double-lane design for simultaneous side-by-side comparison of neutAb activity in patient samples with buffer control has been described in field testing of healthy individuals following mRNA vaccination (23). NeutraXpress™ was also validated with $PRNT_{90}$ assay of PCR-confirmed COVID-19 samples with a high sensitivity (88%) to detect $PRNT_{90} \geq 80$ neutAb activity (Supplementary Figures 1 and 2, Supplementary Tables 3 and 4).

Intriguingly, samples in IgM-IgG+ subgroup fulfill two requirements for neutAb generation: 1) adequate time post symptom onset; and 2) IgG isotype RBD reactivity, indicative of post-GC events. However, in direct comparison to IgM +IgG+ subgroup (66.7% samples neutAb positive), there appears to be much lower neutralization activity in IgM-IgG+ subgroup (30% samples positive) ($P<0.05$) (Figure 1). Our observation that neutAbs maybe encoded by innate IgM during early SARS-CoV-2 infection (detectable in patients with symptom onset time of less than 40 days) is in line with a previous report demonstrating that neutAbs isolated on days 8–17 and days 34–42 after COVID-19 diagnosis showed 97.2% and 97.0% VH gene germline identities, respectively (36). Such innate IgM-expressing B cells, possibly B-1 cells enriched at the infection site (pleural cavity), might be preferentially engaged in the development of SARS-CoV-2 neutAbs.

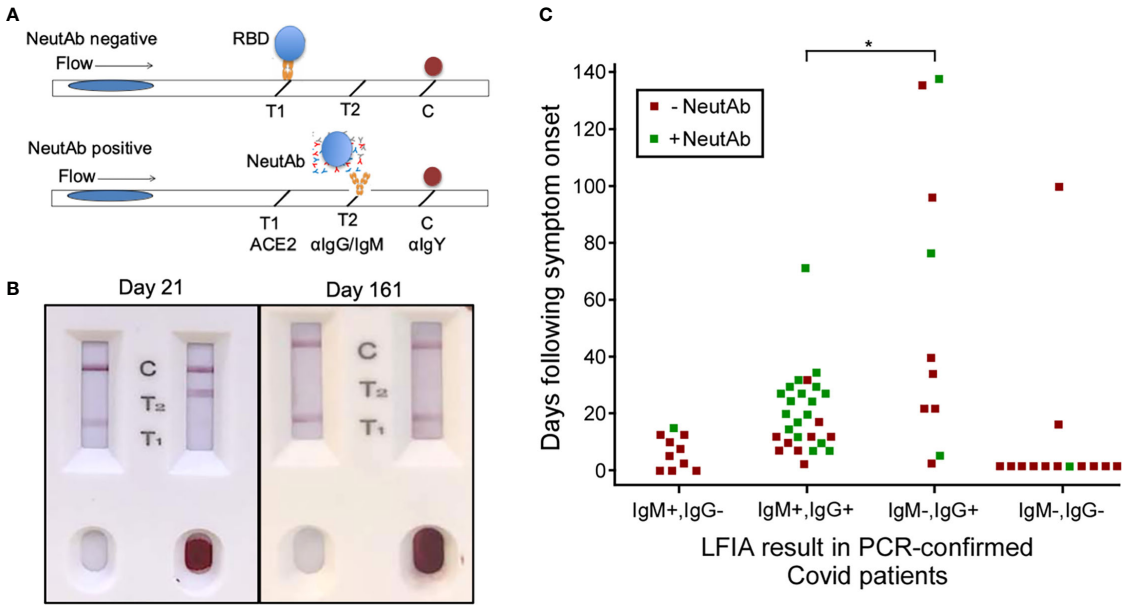

FIGURE 1
NeutAbs against SARS-CoV-2 detected with NeutraXpress™ in the early phase of natural infection are enriched in COVID-19 patients possessing the IgM+ signature. **(A)** Illustration of NeutraXpress™ design (23). T1 is striped with recombinant His-tagged human ACE2 protein. T2 is striped with anti-human IgM + IgG Abs. The conjugate pad is impregnated with colloidal gold nanoparticles (GNP)-labeled recombinant RBD from Spike protein of SARS-CoV-2, as well as GNP-labeled chicken IgY used as a tracer to indicate the completion of the lateral flow when it is captured by goat anti-chicken antibody at the C line. If there is no neutAb or binding antibody in the specimen, GNP-RBD is captured by ACE2 at T1 line and the T2 line should not appear. If the specimen contains neutAbs, the interaction between GNP-RBD with ACE2 at the T1 line is blocked and T1 disappears or shows reduced intensity, in comparison with T1 from the control well with added diluent only. The appearance of the T2 line indicates the presence of IgM and/or IgG Abs specific for RBD, *i.e.*, T2 shows the totality of both neutralizing and non-neutralizing RBD-binding IgM and IgG Abs. T2 intensity correlates with higher titers for RBD-binding IgM + IgG Abs, but T2 does not provide information on neutAbs. **(B)** Examples of NeutraXpress™ showing blood samples from healthy subjects at 21 days (left) and 161 days (right) after receiving the 2nd dose of mRNA vaccine. Note that the left sample wells were added with diluent only, whereas the right sample wells were added with 1 drop of whole blood. **(C)** PCR-confirmed COVID-19 patients were sub grouped based on their serum IgM/IgG profiles of anti-RBD reactivity, using an LFIA rapid test DISCOVID™ and graphed according to the number of days following symptom onset or PCR positivity (in asymptomatic patients) that the sample was taken. Each square symbol represents one patient. Each data point was further differentiated to show the presence of neutAbs in the serum samples as determined by a second LFIA rapid test NeutraXpress™. Green coloration indicates the presence of neutAbs and red coloration indicates the absence of neutAbs. Samples positive for SARS-CoV-2 neutAbs were concentrated in patients having an IgM+IgG+ anti-RBD profile, compared with patients that were anti-RBD IgG+ only (*P <0.05, two-sided two proportion z test).

Different B cell subsets are engaged by particulate antigen *vs.* soluble antigen

There are three distinct features that may precipitate the different immunologic outcomes of natural infection and mRNA vaccination: 1) route of antigen exposure (respiratory track *vs.* intramuscular inoculation); 2) antigen dose and persistence (weeks *vs.* days); and 3) antigen form [particulate intact virus *vs.* cell-surface displayed Spike trimer locked in a stabilized pre-fusion state (57)]. Notably, antigens in particulate form and soluble form can trigger distinct immunological responses (58). Upon injection of an mRNA vaccine, leukocytes are attracted to the injection site and take up the vaccine formulation. The mRNA-mediated *de novo* expression of the vaccine antigen is similar to the presentation of engulfed soluble antigens by antigen-presenting cells (APCs); following vaccination, full length Spike protein expressed by monocytes, macrophages and dendritic cells (DCs) stimulates conventional B-2 cells in the axillary lymph nodes *via* the classical MHC class I and class II antigen presentation pathways (57). In support of this notion, it has been reported that soluble Spike protein can be detected in the plasma of 96% of subjects 1-2 days following receipt of their first mRNA vaccine (median Spike concentration of 47 pg/mL) and in 63% of subjects 7 days post vaccination (median Spike concentration of 1.7 pg/mL) (59). Nevertheless, when encountering repetitive antigens on intact viruses or on particulate virus-like particles (VLPs), antigen-specific B cells but not DCs are the dominant APCs, and are sufficient to stimulate T follicular helper (Tfh) cells (60). While DCs are required to present soluble antigens for CD4+ T cell development, DCs are dispensable but B cells are engaged for the initial CD4+ T cell activation when particulate antigens are presented (60). Thus, human B-1-like cells with low-affinity and potentially cross-reactive BCR enriched in the pleural cavity and lung mucosa are likely to be differentially activated by the high valency Spike proteins displayed on virus particles during natural infection. These B-1-like cells meet the requirements for affinity restriction and have the repertoire diversity to develop into MBCs, and are likely the endogenous resource for pan-neutAbs against future mutated pathogen variants.

Perspective on the design of broadly protective vaccines for COVID-19

Widespread danger from SARS-CoV-2 still lingers, due to the evolution of new escape variants impervious to current vaccination strategies. A broader sobering outlook includes the estimation that 58% (218 out of 375) of infectious diseases currently confronted by humanity worldwide may be aggravated by the effects of climate change in the near future (61). There is a long and ever-growing list of desired vaccines, and yet fewer than 30 pathogens have vaccines licensed for human use (www.who.int/immunization/diseases/en). For pathogens with strong immune-evasion potential, what could be the ideal strategy to aid the development of pan-protective vaccines against the circulating strains and emerging variants?

Reverse vaccinology 3.0

More than half of the currently licensed vaccines were developed with the classical vaccinology tenants of three "I"s: Isolate, Inactivate and Inject (62). In recent years, more advanced technologies in sequencing pathogen genomes and single B cells, aided with highly sophisticated means for protein structural analysis, have been used in identifying vaccine candidates by "Reverse Vaccinology". In Reverse Vaccinology 1.0, vaccine antigens are selected *in silico* using the genomic sequence information of the pathogen without the need for growing the specific microorganism. This strategy directly led to the successful development of the meningococcal B vaccine (63).

In Reverse Vaccinology 2.0, neutAbs are used to identify protective antigens/epitopes, and to derive structural information to guide the immunogen design (64, 65). For example, the metastability of the surface F glycoprotein of respiratory syncytial virus (RSV) causes its pre-fusion form to readily decay to the post-fusion form. Antibodies against the post-fusion form bind poorly to the pre-fusion form and do not neutralize the virus effectively. When the quaternary epitope at the apex of F trimer was revealed to be bound by a pre-fusion locking neutAb, disulfide linkages and cavity-filling mutations were introduced to generate a stabilized F protein as an immunogen, which induced excellent RSV-neutralizing titers in animal models and showed great promise as a potential human vaccine (66, 67). A similar strategy of studying the structural interactions between neutAbs and immunogen for more rational design has been adopted to derive the uncleaved prefusion-optimized (UFO) envelope protein of HIV-1 as a highly promising vaccine candidate for HIV (68).

Based on the aforementioned discussion and work by others on neutAb sequence usage and B cell ontogeny, we propose that the era of Reverse Vaccinology 3.0 is being ushered in with the inclusion of B cell ontogeny as a major consideration (69, 70) (Figure 2). In this strategy, rational immunogen design for broad neutAbs relies on not only the tertiary/quaternary structural information of the pathogen antigen that is relevant to the induction of neutAbs, but also on the preferential usage of germline sequences in the elicited neutAbs. To achieve the preferential usage of germline sequences, immunogen should be displayed in a multimeric form, such as on liposomes (76, 77), synthetic protein nanoparticles (78–80), or VLPs (81) to trigger the low-affinity high-avidity germline BCRs from B-1 cells. Once

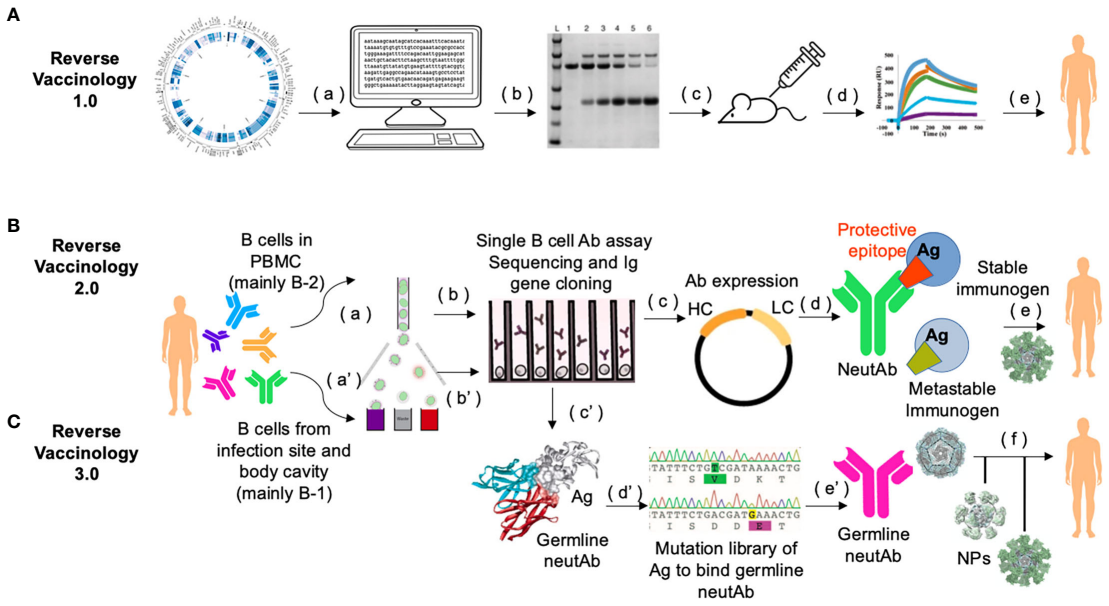

FIGURE 2
Workflow of Reverse Vaccinology 3.0. **(A)** In Reverse Vaccinology 1.0, complete genome sequences of pathogens are analyzed and genes coding for surface exposed proteins are identified (a). Potential surface-exposed proteins are expressed (b), and used to immunize the mice (c). Immunogens that can most efficiently elicit protective responses are screened (d), and further optimized as clinical trial leads for human vaccines (e). This process obviates the need to directly culture the pathogen. **(B)** In Reverse Vaccinology 2.0, structural data are utilized to guide immunogen design. First, MBCs or plasmablasts from PBMCs of subjects seropositive through infection are enriched and sorted (a). Then sorted single B cells are cultured and stimulated to screen for antigen-specific B cell clones in neutralization assays and their paired VH and VL genes are PCR amplified and sequenced (b). Recombinant neutAbs are expressed in mammalian cells, *e.g.*, HEK293 cells or CHO cells (c), to obtain sufficient materials for function confirmation in animal models (not shown), and for structural characterization of such neutAbs bound to their target antigen (Ag). Co-crystallization analysis of neutAb (usually Fab) and antigen provides detailed structural information of the protective epitope or the conformation of the antigen in general, which is different from the one in the metastable form of the antigen that often can fail to induce neutAbs (d). Protein engineering is guided by 3D modeling to stabilize the monomer immunogen and present it in a multimeric nanoparticle format as a potential candidate for human vaccine (e). **(C)** In Reverse Vaccinology 3.0, the goal is to design a germline-antibody-binding immunogen and gradually evolve germline neutAbs into ones with sufficient breadth to neutralize the current pathogen and its future variants. This process starts by enriching of B cells from the first-line of defense, *i.e.*, fluids in the body cavity and mucosa [*e.g.*, from sputum, ref (71)], where natural antibody-secreting B-1 B cells are predominantly present (a'). Antigen-binding single B cells are functionally screened and their Ig sequences are scrutinized with software [*e.g.*, IgSCUEAL, ref (72)] to identify the germline sequences (b'). Next generation sequencing of enriched B-1 B cells from a cohort of infected patients at early stages of the disease (*e.g.*, stratified by our method in Figure 1), may help identify convergent germline sequences induced by infection (38). Modeling with software such as Rosetta allows for the calculation of the interacting area between the Fab of germline neutAbs and the antigen (c'). Since the native antigen usually does not bind the germline antibody sequences (73, 74), it is necessary to generate a yeast surface displayed random mutational library of the antigen to select for variants that bind germline neutAbs as the initial immunogen (d'). Such immunogens would be presented in multimeric form on self-assembled nanoparticles during primary vaccination (e'), followed by sequential boosting with homologous and/or heterologous immunogens to facilitate somatic hypermutation and nurture broad neutAbs that also protect against future variants (f). This strategy relies heavily on computational bioinformatics, and has a species restriction on Ig repertoire, hence humanized mice with knock in human Ig locus would be the preferred preclinical animal model (75).

germline antibodies are activated, further immunogens modeled on related variants and presented on multimeric nanoparticles could then be applied in sequential or cocktail immunizations to shepherd the antibody response towards greater breadth.

Implications for COVID-19 vaccine enhancement

Breakthrough infections are indicative of vaccine failure. Intramuscular injections generate systemic immunity but little or no mucosal immunity in the respiratory tract, where SARS-CoV-2 enters the body. Hence, intramuscular injections are unlikely, on their own, to completely stop viral transmission, abolish community spread, and prevent the emergence of new variants. Repeated boosting with the same mRNA-based vaccines, not only isn't the solution for this conundrum, but also could generate more complications by restricting the repertoire against SARS-CoV-2, particularly when considering the natural immune repertoire of the young. It has been demonstrated, *e.g.*, in the HIV vaccine field, that repeated immunization with the same immunogen

is not effective in inducing broad neutAbs (82). For a pathogen that is prone to immune-evasion, like SARS-CoV-2, the most effective vaccination strategies should be aimed for breadth over depth.

As breadth is intrinsically associated with activating the germline-bearing natural antibodies of the B-1 B cell origin, the most relevant immunization route for COVID-19 should be to target local B-1 cells within the pleural cavity and lung mucosa, rather than using intramuscular inoculation that primarily targets B-2 B cells. For this to be successful, immunogen would need to be presented in a high valency multimeric form, *e.g.*, Spike protein displayed on nanoparticles, which can stimulate potent neutAbs at a faster rate with minute doses (78). To reduce the possibility of inducing non-protective antibodies, RBD alone or in conjunction with the 76E1 epitope (18) can be displayed. In addition, including certain T cell epitopes as a peptide linker of the immunogen may also be necessary for the development of long-term T cell immunity to COVID-19 disease (83, 84). Moreover, immunogen delivery would likely need to be through a more physiologically relevant route, *i.e.*, nasal spraying or bronchial inhalation. More than a dozen nasal sprays or drops are actively being tested against COVID-19 in humans, either as a primary immunization or as a booster (85). Among them, some utilize HBV VLPs or attenuated RSV/Adenovirus (86) to display the Spike protein of SARS-CoV-2. Notably, an inhaled Adenoviral COVID-19 booster can effectively induce high titers of neutAbs against Omicron BA.5, and IgA in blood (most likely in respiratory mucosa as well) (86). Strategies which present a multimeric immunogen to harness B-1 germline antibody sequences are the first steps towards nurturing a broadly protective vaccine that not only prevents severe disease, but also may block symptomatic infection on exposure and thwart future variants if they arise.

Conclusions

Mammalian hosts can never fully "outrun" pathogens, given the pathogen's replication speed and mutation rates. Thus, chasing recombinant pan-neutralizing antibodies as prophylactic and therapeutic modalities is, at most, a temporary fix to the long-term problem of escape variants. Strategies laid out by Reverse Vaccinology 3.0 exploit the diversity and plasticity of the natural B cell repertoire pre-existing within our own body, and may help the host change the rules in the arms race between host and pathogen (30).

Data availability statement

The original contributions presented in the study are included in the article/Supplementary Material. Further inquiries can be directed to the corresponding authors.

Ethics statement

The studies involving discarded clinical samples were reviewed and approved by an IRB of Beth Israel Deaconess Medical Center, Harvard Medical School.

Author contributions

JL, SD, A-RC, J-SL, Y-MH, HZ and LF collected data in testing the clinical samples with DISCOVID™ and NeutraXpress™, QW, WZ and SH optimized and produced the LFIA tests, WG, SCR and SR designed research conceptually and secured funding. JL, SCR and WG wrote and edited the manuscript. All authors contributed to the article and approved the submitted version.

Funding

This research was funded by Massachusetts Life Science Center's Accelerating Coronavirus Testing Solutions (ACTS), and SBIR 75N93019C00014, 75N93020C00042, and 75N93022C00011.

Acknowledgment

We thank Dr. Xuemei Zhong for the insightful discussion on the basic immunological mechanisms involved in this topic.

Conflict of interest

WG is employed by Antagen Diagnostics, Inc., which is the developer of DISCOVID™ and NeutraXpress™. WG is also employed by company Antagen Pharmaceuticals, Inc. SCR is a scientific founder of Purinomia Biotech Inc and consults for eGenesis, AbbVie and SynLogic Inc; his interests are reviewed and managed by HMFP at Beth Israel Deaconess Medical Center in accordance with the conflict-of-interest policies. Authors J-SL and Y-MH are employed by AB Biosciences,

Inc. Authors WZ and SH are employed by Shijiazhuang Hipro Biotechnology Co.

The remaining authors declare that the research was conducted in the absence of any commercial or financial relationships that could be construed as a potential conflict of interest.

Publisher's note

All claims expressed in this article are solely those of the authors and do not necessarily represent those of their affiliated organizations, or those of the publisher, the editors and the reviewers. Any product that may be evaluated in this article, or claim that may be made by its manufacturer, is not guaranteed or endorsed by the publisher.

Supplementary material

The Supplementary Material for this article can be found online at: https://www.frontiersin.org/articles/10.3389/fimmu.2022.1032574/full#supplementary-material

References

1. Watson OJ, Barnsley G, Toor J, Hogan AB, Winskill P, Ghani AC. Global impact of the first year of COVID-19 vaccination: A mathematical modelling study. *Lancet Infect Dis* (2022) 22(9):1293–302. doi: 10.1016/S1473-3099(22)00320-6

2. Abu-Raddad LJ, Chemaitelly H, Butt AA. Effectiveness of the BNT162b2 covid-19 vaccine against the B.1.1.7 and B.1.351 variants. *N Engl J Med* (2021) 385:187–9. doi: 10.1056/NEJMc2104974

3. Cohn BA, Cirillo PM, Murphy CC, Krigbaum NY, Wallace AW. Breakthrough SARS-CoV-2 infections in 620,000 U. *S. Veterans February 1 2021 to August* (2021) 13:2021. doi: 10.1101/2021.10.13.21264966

4. Goga A, Bekker L-G, Garrett N, Reddy T, Yende-Zuma N, Fairall L, et al. Breakthrough SARS-CoV-2 infections during periods of delta and omicron predominance, south Africa. *Lancet* (2022) 400:269–71. doi: 10.1016/S0140-6736(22)01190-4

5. Juthani PV, Gupta A, Borges KA, Price CC, Lee AI, Won CH, et al. Hospitalisation among vaccine breakthrough COVID-19 infections. *Lancet Infect Dis* (2021) 21:1485–6. doi: 10.1016/S1473-3099(21)00558-2

6. Klompas M. Understanding breakthrough infections following mRNA SARS-CoV-2 vaccination. *JAMA* (2021) 326(20):2018–20. doi: 10.1001/jama.2021.19063

7. Mizrahi B, Lotan R, Kalkstein N, Peretz A, Perez G, Ben-Tov A, et al. Correlation of SARS-CoV-2-breakthrough infections to time-from-vaccine. *Nat Commun* (2021) 12:6379. doi: 10.1038/s41467-021-26672-3

8. Harvey WT, Carabelli AM, Jackson B, Gupta RK, Thomson EC, Harrison EM, et al. SARS-CoV-2 variants, spike mutations and immune escape. *Nat Rev Microbiol* (2021) 19:409–24. doi: 10.1038/s41579-021-00573-0

9. Wei C, Shan K-J, Wang W, Zhang S, Huan Q, Qian W. Evidence for a mouse origin of the SARS-CoV-2 omicron variant. *J Genet Genomics* (2021) 48:1111–21. doi: 10.1016/j.jgg.2021.12.003

10. Muik A, Lui BG, Wallisch A-K, Bacher M, Mühl J, Reinholz J, et al. Neutralization of SARS-CoV-2 omicron by BNT162b2 mRNA vaccine-elicited human sera. *Science* (2022) 375:678–80. doi: 10.1126/science.abn7591

11. Bian L, Liu J, Gao F, Gao Q, He Q, Mao Q, et al. Research progress on vaccine efficacy against SARS-CoV-2 variants of concern. *Hum Vaccin Immunother* (2022) 18:2057161. doi: 10.1080/21645515.2022.2057161

12. Corti D, Purcell LA, Snell G, Veesler D. Tackling COVID-19 with neutralizing monoclonal antibodies. *Cell* (2021) 184:4593–5. doi: 10.1016/j.cell.2021.07.027

13. Takashita E, Kinoshita N, Yamayoshi S, Sakai-Tagawa Y, Fujisaki S, Ito M, et al. Efficacy of antibodies and antiviral drugs against covid-19 omicron variant. *N Engl J Med* (2022) 386:995–8. doi: 10.1056/NEJMc2119407

14. Takashita E, Kinoshita N, Yamayoshi S, Sakai-Tagawa Y, Fujisaki S, Ito M, et al. Efficacy of antiviral agents against the SARS-CoV-2 omicron subvariant BA.2. *New Engl J Med* (2022) 386:1475–7. doi: 10.1056/NEJMc2201933

15. Liu L, Iketani S, Guo Y, Chan JF-W, Wang M, Liu L, et al. Striking antibody evasion manifested by the omicron variant of SARS-CoV-2. *Nature* (2022) 602:676–81. doi: 10.1038/s41586-021-04388-0

16. Cao Y, Wang J, Jian F, Xiao T, Song W, Yisimayi A, et al. Omicron escapes the majority of existing SARS-CoV-2 neutralizing antibodies. *Nature* (2022) 602:657–63. doi: 10.1038/s41586-021-04385-3

17. Cao Y, Su B, Guo X, Sun W, Deng Y, Bao L, et al. Potent neutralizing antibodies against SARS-CoV-2 identified by high-throughput single-cell sequencing of convalescent patients' b cells. *Cell* (2020) 182:73–84.e16. doi: 10.1016/j.cell.2020.05.025

18. Sun X, Yi C, Zhu Y, Ding L, Xia S, Chen X, et al. Neutralization mechanism of a human antibody with pan-coronavirus reactivity including SARS-CoV-2. *Nat Microbiol* (2022) 7:1063–74. doi: 10.1038/s41564-022-01155-3

19. Cho A, Muecksch F, Schaefer-Babajew D, Wang Z, Finkin S, Gaebler C, et al. Anti-SARS-CoV-2 receptor-binding domain antibody evolution after mRNA vaccination. *Nature* (2021) 600:517–22. doi: 10.1038/s41586-021-04060-7

20. Sokal A, Barba-Spaeth G, Fernández I, Broketa M, Azzaoui I, de la Selle A, et al. mRNA vaccination of naive and COVID-19-recovered individuals elicits potent memory b cells that recognize SARS-CoV-2 variants. *Immunity* (2021) 54:2893–907.e5. doi: 10.1016/j.immuni.2021.09.011

21. Li G-M, Chiu C, Wrammert J, McCausland M, Andrews SF, Zheng N-Y, et al. Pandemic H1N1 influenza vaccine induces a recall response in humans that favors broadly cross-reactive memory b cells. *Proc Natl Acad Sci U.S.A.* (2012) 109:9047–52. doi: 10.1073/pnas.1118979109

22. Wrammert J, Smith K, Miller J, Langley WA, Kokko K, Larsen C, et al. Rapid cloning of high-affinity human monoclonal antibodies against influenza virus. *Nature* (2008) 453:667–71. doi: 10.1038/nature06890

23. Wang Q, Feng L, Zhang H, Gao J, Mao C, Landesman-Bollag E, et al. Longitudinal waning of mRNA vaccine-induced neutralizing antibodies against SARS-CoV-2 detected by an LFIA rapid test. *Antibody Ther* (2022) 5:55–62. doi: 10.1093/abt/tbac004

24. Gazit S, Shlezinger R, Perez G, Lotan R, Peretz A, Ben-Tov A, et al. SARS-CoV-2 naturally acquired immunity vs. vaccine-induced immunity, reinfections versus breakthrough infections: A retrospective cohort study. *Clin Infect Dis* (2022) 75(1):e545–e551. doi: 10.1093/cid/ciac262

25. Sokal A, Chappert P, Barba-Spaeth G, Roeser A, Fourati S, Azzaoui I, et al. Maturation and persistence of the anti-SARS-CoV-2 memory b cell response. *Cell* (2021) 184:1201–13.e14. doi: 10.1016/j.cell.2021.01.050

26. Gaebler C, Wang Z, Lorenzi JCC, Muecksch F, Finkin S, Tokuyama M, et al. Evolution of antibody immunity to SARS-CoV-2. *Nature* (2021) 591:639–44. doi: 10.1038/s41586-021-03207-w

27. Amanna IJ, Carlson NE, Slifka MK. Duration of humoral immunity to common viral and vaccine antigens. *N Engl J Med* (2007) 357:1903–15. doi: 10.1056/NEJMoa066092

28. Halliley JL, Tipton CM, Liesveld J, Rosenberg AF, Darce J, Gregoretti IV, et al. Long-lived plasma cells are contained within the CD19(-)CD38(hi)CD138(+) subset in human bone marrow. *Immunity* (2015) 43:132–45. doi: 10.1016/j.immuni.2015.06.016

29. Baumgarth N. How specific is too specific? b-cell responses to viral infections reveal the importance of breadth over depth. *Immunol Rev* (2013) 255:82–94. doi: 10.1111/imr.12094

30. Baumgarth N. Memory lapses-winning the slow race. *Immunity* (2020) 53:902–4. doi: 10.1016/j.immuni.2020.10.017

31. Wong R, Belk JA, Govero J, Uhrlaub JL, Reinartz D, Zhao H, et al. Affinity-restricted memory b cells dominate recall responses to heterologous flaviviruses. *Immunity* (2020) 53:1078–94.e7. doi: 10.1016/j.immuni.2020.09.001

32. Viant C, Weymar GHJ, Escolano A, Chen S, Hartweger H, Cipolla M, et al. Antibody affinity shapes the choice between memory and germinal center b cell fates. *Cell* (2020) 183:1298–311.e11. doi: 10.1016/j.cell.2020.09.063

33. Taylor JJ, Pape KA, Steach HR, Jenkins MK. Humoral immunity. apoptosis and antigen affinity limit effector cell differentiation of a single naïve b cell. *Science* (2015) 347:784–7. doi: 10.1126/science.aaa1342

34. Mesin L, Schiepers A, Ersching J, Barbulescu A, Cavazzoni CB, Angelini A, et al. Restricted clonality and limited germinal center reentry characterize memory b cell reactivation by boosting. *Cell* (2020) 180:92–106.e11. doi: 10.1016/j.cell.2019.11.032

35. Schmidt AG, Do KT, McCarthy KR, Kepler TB, Liao H-X, Moody MA, et al. Immunogenic stimulus for germline precursors of antibodies that engage the influenza hemagglutinin receptor-binding site. *Cell Rep* (2015) 13:2842–50. doi: 10.1016/j.celrep.2015.11.063

36. Kreer C, Zehner M, Weber T, Ercanoglu MS, Gieselmann L, Rohde C, et al. Longitudinal isolation of potent near-germline SARS-CoV-2-Neutralizing antibodies from COVID-19 patients. *Cell* (2020) 182:843–54.e12. doi: 10.1016/j.cell.2020.06.044

37. Brouwer PJM, Caniels TG, van der Straten K, Snitselaar JL, Aldon Y, Bangaru S, et al. Potent neutralizing antibodies from COVID-19 patients define multiple targets of vulnerability. *Science* (2020) 369:643–50. doi: 10.1126/science.abc5902

38. Robbiani DF, Gaebler C, Muecksch F, Lorenzi JCC, Wang Z, Cho A, et al. Convergent antibody responses to SARS-CoV-2 in convalescent individuals. *Nature* (2020) 584:437–42. doi: 10.1038/s41586-020-2456-9

39. Seydoux E, Homad LJ, MacCamy AJ, Parks KR, Hurlburt NK, Jennewein MF, et al. Analysis of a SARS-CoV-2-Infected individual reveals development of potent neutralizing antibodies with limited somatic mutation. *Immunity* (2020) 53:98–105.e5. doi: 10.1016/j.immuni.2020.06.001

40. Shi R, Shan C, Duan X, Chen Z, Liu P, Song J, et al. A human neutralizing antibody targets the receptor binding site of SARS-CoV-2. *Nature* (2020) 584 (7819):120–124. doi: 10.1038/s41586-020-2381-y

41. Zost SJ, Gilchuk P, Chen RE, Case JB, Reidy JX, Trivette A, et al. Rapid isolation and profiling of a diverse panel of human monoclonal antibodies targeting the SARS-CoV-2 spike protein. *Nat Med* (2020) 26:1422–7. doi: 10.1038/s41591-020-0998-x

42. Yuan M, Liu H, Wu NC, Lee C-CD, Zhu X, Zhao F, et al. Structural basis of a shared antibody response to SARS-CoV-2. *Science* (2020) 369:1119–23. doi: 10.1126/science.abd2321

43. Rogers TF, Zhao F, Huang D, Beutler N, Burns A, He W, et al. Isolation of potent SARS-CoV-2 neutralizing antibodies and protection from disease in a small animal model. *Science* (2020) 369:956–63. doi: 10.1126/science.abc7520

44. Barnes CO, West AP, Huey-Tubman KE, Hoffmann MAG, Sharaf NG, Hoffman PR, et al. Structures of human antibodies bound to SARS-CoV-2 spike reveal common epitopes and recurrent features of antibodies. *Cell* (2020) 182:828–42.e16. doi: 10.1016/j.cell.2020.06.025

45. Kim SI, Noh J, Kim S, Choi Y, Yoo DK, Lee Y, et al. Stereotypic neutralizing VH antibodies against SARS-CoV-2 spike protein receptor binding domain in patients with COVID-19 and healthy individuals. *Sci Transl Med* (2021) 13: eabd6990. doi: 10.1126/scitranslmed.abd6990

46. Ju B, Zhang Q, Ge J, Wang R, Sun J, Ge X, et al. Human neutralizing antibodies elicited by SARS-CoV-2 infection. *Nature* (2020) 584:115–9. doi: 10.1038/s41586-020-2380-z

47. Du S, Cao Y, Zhu Q, Yu P, Qi F, Wang G, et al. Structurally resolved SARS-CoV-2 antibody shows high efficacy in severely infected hamsters and provides a potent cocktail pairing strategy. *Cell* (2020) 183:1013–23.e13. doi: 10.1016/j.cell.2020.09.035

48. Windsor IW, Tong P, Lavidor O, Moghaddam AS, McKay LGA, Gautam A, et al. Antibodies induced by an ancestral SARS-CoV-2 strain that cross-neutralize variants from alpha to omicron BA.1. *Sci Immunol* (2022) 7:eabo3425. doi: 10.1126/sciimmunol.abo3425

49. Wang Y, Liu J, Burrows PD, Wang J-Y. B cell development and maturation. *Adv Exp Med Biol* (2020) 1254:1–22. doi: 10.1007/978-981-15-3532-1_1

50. Hayakawa K, Hardy RR, Parks DR, Herzenberg LA. The "Ly-1 b" cell subpopulation in normal immunodefective, and autoimmune mice. *J Exp Med* (1983) 157:202–18. doi: 10.1084/jem.157.1.202

51. Ansel KM, Harris RBS, Cyster JG. CXCL13 is required for B1 cell homing, natural antibody production, and body cavity immunity. *Immunity* (2002) 16:67–76. doi: 10.1016/s1074-7613(01)00257-6

52. Kato A, Hulse KE, Tan BK, Schleimer RP. B lymphocyte lineage cells and the respiratory system. *J Allergy Clin Immunol* (2013) 131:933–57. doi: 10.1016/j.jaci.2013.02.023

53. Baumgarth N. The double life of a b-1 cell: self-reactivity selects for protective effector functions. *Nat Rev Immunol* (2011) 11:34–46. doi: 10.1038/nri2901

54. Rothstein TL, Quach TD. The human counterpart of mouse b-1 cells. *Ann N Y Acad Sci* (2015) 1362:143–52. doi: 10.1111/nyas.12790

55. Rothstein TL, Griffin DO, Holodick NE, Quach TD, Kaku H. Human b-1 cells take the stage. *Ann N Y Acad Sci* (2013) 1285:97–114. doi: 10.1111/nyas.12137

56. Baumgarth N. A hard(y) look at b-1 cell development and function. *J Immunol* (2017) 199:3387–94. doi: 10.4049/jimmunol.1700943

57. Rijkers GT, Weterings N, Obregon-Henao A, Lepolder M, Dutt TS, van Overveld FJ, et al. Antigen presentation of mRNA-based and virus-vectored SARS-CoV-2 vaccines. *Vaccines (Basel)* (2021) 9:848. doi: 10.3390/vaccines9080848

58. Snapper CM. Distinct immunologic properties of soluble versus particulate antigens. *Front Immunol* (2018) 9:598. doi: 10.3389/fimmu.2018.00598

59. Röltgen K, Nielsen SCA, Silva O, Younes SF, Zaslavsky M, Costales C, et al. Immune imprinting, breadth of variant recognition, and germinal center response in human SARS-CoV-2 infection and vaccination. *Cell* (2022) 185:1025–40.e14. doi: 10.1016/j.cell.2022.01.018

60. Hong S, Zhang Z, Liu H, Tian M, Zhu X, Zhang Z, et al. B cells are the dominant antigen-presenting cells that activate naive CD4+ T cells upon immunization with a virus-derived nanoparticle antigen. *Immunity* (2018) 49:695–708.e4. doi: 10.1016/j.immuni.2018.08.012

61. Mora C, McKenzie T, Gaw IM, Dean JM, von Hammerstein H, Knudson TA, et al. Over half of known human pathogenic diseases can be aggravated by climate change. *Nat Clim Chang* (2022) 12(9):869–75. doi: 10.1038/s41558-022-01426-1

62. Hilleman MR. Six decades of vaccine development–a personal history. *Nat Med* (1998) 4:507–14. doi: 10.1038/nm0598supp-507

63. Pizza M, Scarlato V, Masignani V, Giuliani MM, Aricò B, Comanducci M, et al. Identification of vaccine candidates against serogroup b meningococcus by whole-genome sequencing. *Science* (2000) 287:1816–20. doi: 10.1126/science.287.5459.1816

64. Burton DR. Antibodies, viruses and vaccines. *Nat Rev Immunol* (2002) 2:706–13. doi: 10.1038/nri891

65. Rappuoli R, Bottomley MJ, D'Oro U, Finco O, De Gregorio E. Reverse vaccinology 2.0: Human immunology instructs vaccine antigen design. *J Exp Med* (2016) 213:469–81. doi: 10.1084/jem.20151960

66. McLellan JS, Chen M, Leung S, Graepel KW, Du X, Yang Y, et al. Structure of RSV fusion glycoprotein trimer bound to a prefusion-specific neutralizing antibody. *Science* (2013) 340:1113–7. doi: 10.1126/science.1234914

67. McLellan JS, Chen M, Joyce MG, Sastry M, Stewart-Jones GBE, Yang Y, et al. Structure-based design of a fusion glycoprotein vaccine for respiratory syncytial virus. *Science* (2013) 342:592–8. doi: 10.1126/science.1243283

68. He L, Kumar S, Allen JD, Huang D, Lin X, Mann CJ, et al. HIV-1 vaccine design through minimizing envelope metastability. *Sci Adv* (2018) 4:eaau6769. doi: 10.1126/sciadv.aau6769

69. Kwong PD, Mascola JR. Human antibodies that neutralize HIV-1: identification, structures, and b cell ontogenies. *Immunity* (2012) 37:412–25. doi: 10.1016/j.immuni.2012.08.012

70. Kwong PD. What are the most powerful immunogen design vaccine strategies? a structural biologist's perspective. *Cold Spring Harb Perspect Biol* (2017) 9:a029470. doi: 10.1101/cshperspect.a029470

71. Lay JC, Peden DB, Alexis NE. Flow cytometry of sputum: assessing inflammation and immune response elements in the bronchial airways. *Inhal Toxicol* (2011) 23:392–406. doi: 10.3109/08958378.2011.575568

72. Frost SDW, Murrell B, ASMdM H, GJ S, Pond SLK. Assigning and visualizing germline genes in antibody repertoires. *Philos Trans R Soc Lond B Biol Sci* (2015) 370:20140240. doi: 10.1098/rstb.2014.0240

73. Xiao X, Chen W, Feng Y, Zhu Z, Prabakaran P, Wang Y, et al. Germline-like predecessors of broadly neutralizing antibodies lack measurable binding to HIV-1 envelope glycoproteins: implications for evasion of immune responses and design of vaccine immunogens. *Biochem Biophys Res Commun* (2009) 390:404–9. doi: 10.1016/j.bbrc.2009.09.029

74. Jardine J, Julien J-P, Menis S, Ota T, Kalyuzhniy O, McGuire A, et al. Rational HIV immunogen design to target specific germline b cell receptors. *Science* (2013) 340:711–6. doi: 10.1126/science.1234150

75. Jardine JG, Ota T, Sok D, Pauthner M, Kulp DW, Kalyuzhniy O, et al. HIV-1 VACCINES. priming a broadly neutralizing antibody response to HIV-1 using a germline-targeting immunogen. *Science* (2015) 349:156–61. doi: 10.1126/science.aac5894

76. Ingale J, Stano A, Guenaga J, Sharma SK, Nemazee D, Zwick MB, et al. High-density array of well-ordered HIV-1 spikes on synthetic liposomal nanoparticles efficiently activate b cells. *Cell Rep* (2016) 15:1986–99. doi: 10.1016/j.celrep.2016.04.078

77. Martinez-Murillo P, Tran K, Guenaga J, Lindgren G, Àdori M, Feng Y, et al. Particulate array of well-ordered HIV clade c env trimers elicits neutralizing

antibodies that display a unique V2 cap approach. *Immunity* (2017) 46:804–17.e7. doi: 10.1016/j.immuni.2017.04.021

78. Zhang B, Chao CW, Tsybovsky Y, Abiona OM, Hutchinson GB, Moliva JI, et al. A platform incorporating trimeric antigens into self-assembling nanoparticles reveals SARS-CoV-2-spike nanoparticles to elicit substantially higher neutralizing responses than spike alone. *Sci Rep* (2020) 10:18149. doi: 10.1038/s41598-020-74949-2

79. Ueda G, Antanasijevic A, Fallas JA, Sheffler W, Copps J, Ellis D, et al. Tailored design of protein nanoparticle scaffolds for multivalent presentation of viral glycoprotein antigens. *eLife* (2020) 9:e57659. doi: 10.7554/eLife.57659

80. Fallas JA, Ueda G, Sheffler W, Nguyen V, McNamara DE, Sankaran B, et al. Computational design of self-assembling cyclic protein homo-oligomers. *Nat Chem* (2017) 9:353–60. doi: 10.1038/nchem.2673

81. Hennrich AA, Sawatsky B, Santos-Mandujano R, Banda DH, Oberhuber M, Schopf A, et al. Safe and effective two-in-one replicon-and-VLP minispike vaccine for COVID-19: Protection of mice after a single immunization. *PLoS Pathog* (2021) 17:e1009064. doi: 10.1371/journal.ppat.1009064

82. Burton DR. What are the most powerful immunogen design vaccine strategies? reverse vaccinology 2.0 shows great promise. *Cold Spring Harb Perspect Biol* (2017) 9:a030262. doi: 10.1101/cshperspect.a030262

83. Wherry EJ, Barouch DH. T Cell immunity to COVID-19 vaccines. *Science* (2022) 377:821–2. doi: 10.1126/science.add2897

84. Seyran M. Artificial intelligence and clinical data suggest the T cell-mediated SARS-CoV-2 nonstructural protein intranasal vaccines for global COVID-19 immunity. *Vaccine* (2022) 40:4296–300. doi: 10.1016/j.vaccine.2022.06.052

85. Nasal vaccines are commercially high risk, perhaps high reward, in: *The scientist magazine* . Available at: https://www.the-scientist.com/bio-business/nasal-vaccines-are-commercially-high-risk-perhaps-high-reward-70068 (Accessed August 16, 2022).

86. Zhong J, Liu S, Cui T, Li J, Zhu F, Zhong N, et al. Heterologous booster with inhaled adenovirus vector COVID-19 vaccine generated more neutralizing antibodies against different SARS-CoV-2 variants. *Emerg Microbes Infect* (2022) 1–18. doi: 10.1080/22221751.2022.2132881

frontiers | Frontiers in Immunology

TYPE Original Research
PUBLISHED 15 November 2022
DOI 10.3389/fimmu.2022.1023943

OPEN ACCESS

EDITED BY
Ahmed Yaqinuddin,
Alfaisal University, Saudi Arabia

REVIEWED BY
David Forgacs,
Lerner Research Institute,
United States
Bharat Madan,
University of Kansas, United States

*CORRESPONDENCE
Jen-Ren Wang
jrwang@mail.ncku.edu.tw

SPECIALTY SECTION
This article was submitted to Viral Immunology, a section of the journal Frontiers in Immunology

RECEIVED 20 August 2022
ACCEPTED 31 October 2022
PUBLISHED 15 November 2022

CITATION
Chao C-H, Cheng D, Huang S-W, Chuang Y-C, Yeh T-M and Wang J-R (2022) Serological responses triggered by different SARS-CoV-2 vaccines against SARS-CoV-2 variants in Taiwan. *Front. Immunol.* 13:1023943. doi: 10.3389/fimmu.2022.1023943

Serological responses triggered by different SARS-CoV-2 vaccines against SARS-CoV-2 variants in Taiwan

Chiao-Hsuan Chao[1], Dayna Cheng[2], Sheng-Wen Huang[3], Yung-Chun Chuang[4], Trai-Ming Yeh[1,5] and Jen-Ren Wang[1,2,5,6]*

[1]Department of Medical Laboratory Science and Biotechnology, College of Medicine, National Cheng Kung University, Tainan, Taiwan, [2]Institute of Basic Medical Sciences, College of Medicine, National Cheng Kung University, Tainan, Taiwan, [3]National Mosquito-Borne Diseases Control Research Center, National Health Research Institutes, Tainan, Taiwan, [4]Leadgene Biomedical, Inc., Tainan, Taiwan, [5]Center of Infectious Disease and Signaling Research, National Cheng Kung University, Tainan, Taiwan, [6]National Institute of Infectious Diseases and Vaccinology, National Health Research Institutes, Tainan, Taiwan

Broadly neutralizing ability is critical for developing the next-generation SARS-CoV-2 vaccine. We collected sera samples between December 2021-January 2022 from 113 Taiwan naïve participants after their second dose of homologous vaccine (AZD1222, mRNA-1273, BNT162-b2, and MVC-COV1901) and compared the differences in serological responses of various SARS-CoV-2 vaccines. Compared to AZD1222, the two mRNA vaccines could elicit a higher level of anti-S1-RBD binding antibodies with higher broadly neutralizing ability evaluated using pseudoviruses of various SARS-CoV-2 lineages. The antigenic maps produced from the neutralization data implied that Omicron represents very different antigenic characteristics from the ancestral lineage. These results suggested that constantly administering the vaccine with ancestral Wuhan spike is insufficient for the Omicron outbreak. In addition, we found that anti-ACE2 autoantibodies were significantly increased in all four vaccinated groups compared to the unvaccinated pre-pandemic group, which needed to be investigated in the future.

KEYWORDS

COVID-19, vaccine, binding antibodies, neutralizing antibodies, anti-ACE2 antibodies

Introduction

COVID-19 pandemic occurred at the end of 2019 and has caused 624 million infections and 6.5 million deaths as of 25 October 2022, according to the statistics of World Health Organization (WHO) (1). In addition to the serious health problems, the COVID-19 pandemic has caused a negative impact on the global economy (2). Scientists

worldwide were dedicated to investigating the SARS-CoV-2-related research, especially in vaccines and antiviral drug developments to combat coronavirus. To date, there are eleven COVID-19 vaccines based on different platforms that have been granted emergency use listing (EUL) by the World Health Organization (WHO) (https://covid19.trackvaccines.org/agency/who/). The platforms of these granted vaccines include inactivated virus (Covaxin from Bharat Biotech, Covilo from Sinopharm (Beijing), and CoronaVac from Sinovac), non-replicating viral vector (Convidcia from CanSino, Ad26.COV2.S from Janssen, Vaxzevria (AZD1222, ChAdOx1 nCoV-19) from Oxford/AstraZeneca, and Covishield (Oxford/AstraZeneca formulation) from Serum Institute of India), RNA (Spikevax (mRNA-1273) from Moderna and Comirnaty (BNT162-b2) from Pfizer/BioNTech), and protein subunit (Nuvaxovid (NVX-CoV2373) from Novavax and COVOVAX (Novavax formulation) from Serum Institute of India) (3, 4). The strategy of all these vaccine platforms except inactivated virus vaccines is based on the SARS-CoV-2 spike protein. Among these vaccines, Pfizer/BioNTech was the first COVID-19 vaccine that has been approved by the U.S. Food and Drug Administration (FDA) in 2021. Subsequently, Moderna, Johnson & Johnson, and Novavax have also been approved by the FDA in 2022 (5, 6).

SARS-CoV-2 spike protein is a ~180 kDa glycoprotein that can form a trimeric structure that protrudes from the surface of the viral particle and play a key role in host cell entry (7–9). The total length of the SARS-CoV-2 spike protein contains 1273 amino acids (a.a) consisting of a signal peptide (a.a. 1–13 residues), S1 subunit (a.a. 14-685), and S2 subunit (a.a. 686-1273). The S1 subunit contains a N-terminal domain (a.a. 14–305), a receptor-binding domain (S1-RBD, a.a. 319-541), and a receptor-binding motif (RBM, a.a. 437–508). The S2 subunit includes the fusion peptide (a.a. 788–806), heptapeptide repeat sequence 1 (HR1, a.a. 912–984), heptapeptide repeat sequence 2 (HR2, a.a. 1163–1213), transmembrane domain (a.a. 1213–1237), and cytoplasm domain (a.a. 1237–1273) (10). The RBM is a portion of the S1-RBD that makes direct contact with the human cell surface receptor angiotensin-converting enzyme 2 (ACE2), whereas the S2 subunit mediates subsequent membrane fusion with the host cell membrane by forming a six-helical bundle *via* the two HR domain (7, 11). Within the S1 and S2 subunits, the S1-RBD has been considered an immunodominant region and the main target of neutralizing antibodies (12–14).

In Taiwan, four COVID-19 vaccines have been granted emergency use authorization (EUA) by Taiwan Food and Drug Administration (TFDA), including AZD1222 (Vaxzevria, Oxford/AstraZeneca), mRNA-1273 (Spikevax, Moderna), BNT162-b2 (Comirnaty, Pfizer/BioNTech), and MVC-COV1901 (Taiwan-based Medigen Vaccine Biologics Corporation) at the study time. With similar strategies to NVX-CoV2373 (Novavax), MVC-COV1901 is a protein subunit vaccine adjuvanted with CpG 1018 and aluminum hydroxide. To stabilize the prefusion form spike protein for preserving neutralizing epitopes, a GSAS replacement at the S1/S2 furin cleavage sites to confer protease resistance and two proline substitutions at residues 986 and 987 (K986P, V987P) in the sequence of the wild-type spike from the Wuhan strain were incorporated (15). Additionally, a trimerization domain (IZN4) is added to the C-terminus for improving the conformational homogeneity (16). According to the statistical data from the TFDA website (https://www.cdc.gov.tw/En/File/Get/BlkBAw7kMxwGx–DsPEvtg), a total of 63.17 million doses have been administered in Taiwan (mRNA-1273: 23.89 million doses, BNT162-b2: 19.3 million doses, AZD1222: 15.3 million doses, MVC-COV1901: 3.06 million doses) as of October 24th, 2022.

Vaccination reduces not only COVID-19 transmission, but also severe illness and deaths from COVID-19 infection (17). However, vaccines could not provide full protection from COVID-19 infection, especially when SARS-CoV-2 has an extremely high mutation rate (around 8×10^{-4} nucleotides/genome annually) compared to other viruses (18, 19). Indeed, the surveillance data showed that SARS-CoV-2 had generated a lot of mutations since 2019 (20, 21). According to the WHO classification, there were at least five variants of concerns (VOCs) that caused large outbreak waves in different countries in different periods, including B.1.1.7 (Alpha), B.1.351 (Beta), P.1 (Gamma), B.1.617.2 (Delta), and B.1.1.529 (Omicron). The possible attributes of VOCs include the evidence of higher transmissibility, increased virulence, and reduced effectiveness of vaccines, therapeutics, or diagnostics (22, 23). Currently, Omicron is the dominant variant circulating globally and accounting for nearly all sequences reported to GISAID (24). Omicron and its sublineages (BA.1, BA.2, BA.3, BA.4, BA.5, and descendent lineages) have significantly more mutations than previous SARS-CoV-2 variants particularly in the spike gene (25–27). Compared to the original strain, thirty amino acid changes (among which fifteen are in the RBD region), three deletions, and one insertion occur in the Omicron spike protein (27). Not only breakthrough infection, but the number of people reinfected with the coronavirus has increased since the Omicron variant spread globally (28–30).

As a part of the global value chain, Taiwan would surely loosen the broad restrictions (or lockdown restrictions). Therefore, evaluating the neutralizing activity especially against the SARS-CoV-2 variant of concerns is very important. Many factors affect immune responses to the SARS-CoV-2 vaccines, including age, gender, nutritional status, body mass index, host genetic polymorphism, chronic disease, and immune history (31, 32). More and more studies indicate that SARS-CoV-2 infection could cause immune disturbance and trigger autoantibodies production (33, 34). Several studies have shown that anti-ACE2 autoantibodies increase in COVID-19 patient serum and significantly positively correlate with disease severity

(35, 36). However, whether COVID-19 vaccines would trigger anti-ACE2 autoantibodies or by which vaccine platform is unclear.

This study focused on the serological responses of various COVID-19 vaccines used in Taiwan by analyzing the production of anti-spike, anti-S1-RBD, and anti-ACE2 autoantibodies. In addition, the breadth of neutralizing antibody response was evaluated using a lentiviral pseudovirus system encoding the spike protein of ancestral SARS-CoV-2 and other six SARS-CoV-2 variants. Furthermore, the antigenic maps were generated by using the neutralizing titer and were rendered separately or combined with various vaccines.

Materials and methods

Cohort information

This study recruited Taiwanese who received two homologous doses of a COVID vaccine. The serum samples were collected four weeks after the second dose of vaccination. Four different COVID-19 vaccine brands were included, including AZD1222 (Vaxzevria, Oxford/AstraZeneca), mRNA-1273 (Spikevax, Moderna), BNT162-b2 (Comirnaty, Pfizer/BioNTech), and MVC-COV1901 (Taiwan-based Medigen Vaccine Biologics Corporation). The pre-pandemic serum samples from the healthy donors were collected before 2019 and used as the negative control sera.

Serum collection and storage

All blood samples were processed on the collection day in a single-step standardized method. Briefly, whole blood was collected in red-topped vacutainers, plastic vacutainers containing clot activators but no anticoagulants (BD Biosciences, Franklin Lakes, New Jersey). The blood was allowed to clot by leaving it undisturbed at room temperature for 30 minutes. Sera were collected after centrifuging whole blood at 1500 ×g for 15 min at room temperature without brake. The undiluted sera were transferred and stored in polypropylene conical tubes at −80 °C for subsequent analysis. Before conducting the micro-neutralization assay, the serum was aliquoted and heat-inactivated at 56 °C for 30 min for complement inactivation.

Recombinant proteins

C-terminal His-tag SARS-CoV-2 trimeric spike (extracellular domain, ECD) recombinant protein and N-terminal 6×His-SUMO tag SARS-CoV-2 nucleocapsid protein expressed from HEK293 were purchased from Leadgene Biomedical, Inc. Tainan, Taiwan. C-terminal 6×His and Avi-tagged human ACE2 (ECD) protein from HEK293 were purchased from GeneTex, Inc. Irvine, CA. C-terminal His-tagged SARS-CoV-2 S1-RBD recombinant proteins (YP_009724390) purified from S2 cells (37).

Indirect enzyme-linked immunosorbent assay

An indirect ELISA was performed to quantify the levels of anti-nucleocapsid/spike/S1-RBD binding antibodies and anti-ACE2 autoantibodies in COVID post-vaccination sera. Briefly, the indicated proteins (2 μg/mL) were coated onto a high-binding 96-well ELISA plate overnight at 4°C. After blocking with 1% BSA in PBS, diluted sera (1:100 for anti-nucleocapsid/spike/S1-RBD binding antibodies, 1:50 for anti-ACE2 autoantibodies) were added and incubated in wells for 1 h at 37°C. The primary antibodies were allowed to bind to the anti-human IgG-HRP detection antibody (1:4000) (Thermo Fisher Scientific, Waltham, MA) for 1 h at 37°C. Wells were washed three times with PBST (PBS containing 0.01% Tween 20) between each step. For color visualization, the tetramethylbenzidine (TMB) reagent (Clinical Science Products, Mansfield, MA) was added to the wells for 10-15 min, and the reaction was stopped by the addition of 2N H_2SO_4. The absorbance at OD 450 nm was read by a VersaMax microplate reader (Molecular Devices, Sunnyvale, CA).

Production of SARS-CoV-2 lenti-pseudovirus

We applied the lentiviral vector system provided by the National RNAi Core of Academia Sinica Taiwan to generate SARS-CoV-2 pseudovirus as mentioned previously (38). The sequences of SARS-CoV-2 full-length spike protein, including Wuhan (YP_009724390.1), B.1.1.7 (alpha), B.1.351 (beta), B.1.617.2 (delta), and B.1.1.529 (omicron) were optimized synthesized and cloned into a pcDNA3.1+ vector for expression (Leadgene, Tainan, Taiwan). The P. 1 (gamma) and C. 37 (lambda) were purchased from Sino Biological (Beijing, China). Several silent mutations were introduced into the full-length DNA sequence of SARS-CoV-2 Spike (S gene) to increase the protein expression level in mammalian cell system. HEK293T cells were co-transfected with pCMVdeltaR8.9, pLVX-NanoLuc-Puro (Leadgene, Tainan, Taiwan), and the plasmids expressing S gene for different SARS-CoV-2 variants were transfected into 293T cells using a TransIT-X2 transfection reagent (Mirus Bio LLC, Madison, Wisconsin). After 24 h transfection, the culture medium was displaced by FreeStyle™ 293 expression medium (Thermo Fisher Scientific, Waltham, MA) and then cultured for an additional 24 h. The lentiviral

supernatant was further 30-fold concentrated using Lenti-X concentrator (Takara Bio, San Jose, CA), and the infectivity of SARS-CoV-2 lenti-pseudoviruses were determined by using the median tissue culture infectious dose ($TCID_{50}$) in a HEK293-human ACE2 overexpression stable cell line (HEK293-$ACE_{O/E}$) (Leadgene, Tainan, Taiwan).

Commutability assessment

To convert the binding OD values and NT50 into binding antibodies units (BAU) and international units (IU), the COVID-19 patients standard sera calibrated by WHO international standard (IS) sera (20/130, 20/136, and 20/268) were kindly provided by Prof. Shin-Ru Shih (Chang Gung University). The 50% neutralization titer (NT50) values for standard patients sera were determined by pseudovirus micro-neutralization assay. To confirm the test accuracy of our pseudovirus micro-neutralization assay, another standard serum (COV 110-09) co-calibrated by five different labs in Taiwan, provided by Taiwan Food and Drug Administration (TFDA), was used. Each standard serum sample was tested in duplicate or triplicate independently.

Pseudovirus micro-neutralization assay

The neutralizing antibody titer of each vaccinee against different SARS-CoV-2 variants of concern were tested using a lenti-pseudovirus system. HEK293-$ACE_{O/E}$ cells were seeded on 96-well plates 18-24 h before infection. Complement-inactivated sera with the indicated dilution factors were preincubated with 100 $TCID_{50}$ of SARS-CoV-2 spike-expressing pseudovirus for 1 h and added to the HEK293-$ACE_{O/E}$ seeding plate. After 18-24 h incubation, the infection rate of SARS-CoV-2 lenti-pseudoviruses was evaluated using a Nano-Glo Luciferase Assay System (Promega, Madison, WI), and the luciferase signal was detected by a SpectraMax iD5 (Molecular Devices). The titers were determined using curve-fitting functions statistical packages (GraphPad Prism). The tabular neutralization data were analyzed manually and also using antigenic cartography.

Antigenic cartography

Antigenic cartography is a method to visualize neutralization data by reflecting the antigenic properties of a pathogen. In an antigenic map, the positions and distances of antigens and sera represent their antigenic relationship. The difference between the $\log_2$ of the maximum titer observed and the $\log_2$ of the titer for the serum and antigen coincides with the distance between the serum and antigen. Thus, each titer in a neutralization assay can be thought of as specifying a target distance for the points in an antigenic map. In this study, the antigenic maps were generated using a web-based tool (Acmacs Web Cherry, an open resource available from https://acmacs-web.antigenic-cartography.org/).

Statistical analysis

All data were analyzed by GraphPad Prism version 6.0 (GraphPad Software Inc., CA). The results were presented as geometric mean titers (GMT) with 95% confidence interval (CI). Student's unpaired t-test was used to analyze the differences between two groups. One-way ANOVA with a Kruskal–Wallis comparison test was used to analyze the differences among multiple groups. The correlation between the neutralizing titers and the serological response against the proteins (trimeric spike, S1-RBD, and human ACE2) was calculated through Spearman's correlation. P values <0.05 were considered statistically significant.

Results

Participants (Cohort information)

We enrolled 113 SARS-CoV-2-naïve participants and collected their sera samples within days 30 to 120 after the second dose of homologous COVID vaccination (Figure S1A) between December 2021-January 2022. To confirm the serological activity was only triggered by the vaccination but not by infection, the binding antibodies against SARS-CoV-2 nucleocapsid and trimeric spike proteins of all sera samples were tested. The pre-pandemic serum samples from the healthy donors were collected before 2019 and used as the negative control sera. As shown in Figure S1B, the mean optical densities (OD) of antibodies against nucleocapsid in the vaccinated sera has no significant difference from that in the pre-pandemic sera, suggesting all the participants had not been infected by COVID-19 before. The anti-SARS-CoV-2 spike binding antibody in the post-vaccination sera was significantly higher than in the pre-pandemic sera, indicating the robust antibodies response was triggered by the vaccination (Figure S1C).

To compare the serological response induced by different vaccine brands, the participants were further classified into four groups according to the received vaccine brands (including AZD1222 (n=42), mRNA-1273 (n=19), MVC-COV1901 (n=27), and BNT162-b2 (n=25)). Median age, gender ratio, average sample collection days after the second dose vaccination, and the detailed age/gender distribution of the participants in each group were shown in Table 1 and Figure S2. The average sample collection days after the second dose vaccination of the MVC-COV1901 group (69.46 days) was

10.3389/fimmu.2022.1023943

TABLE 1 Demographic characteristics of vaccinated individuals.

Sample group	Case Number	Average Age	Gender	Average Collection time (days)
ChAdOx1 nCoV-19 (AZD1222, AZ)	42	35.26	M: 40.5% F: 59.5%	42.1
mRNA-1273 (Moderna)	19	33.37	M: 26.4% F: 73.6%	46.74
MVC-COV1901 (Medigen)	27	31.00	M: 51.8% F: 48.2%	69.46
BNT162b2 (Pfizer- BioNTech, BNT)	25	33.71	M: 36.0% F: 64.0%	45.08

28-120 days after homologous 2nd vaccine dose.

significantly higher than the other three groups (42.1 days in the AZD1222 group, 46.74 days in the mRNA-1273 group, and 45.08 days in the BNT162-b2 group) (Figure S1D), while there was no significant difference in the mean ages between each group (Figure S1E).

The serological response triggered by different vaccine brands

Anti-spike and anti-S1-RBD antibodies response

The serological response triggered by different vaccine brands was evaluated by the anti-spike and anti-S1-RBD binding antibodies quantification using ELISA, and the neutralizing (NT) antibody titers were determined by NT50 value in a lenti-pseudovirus neutralization assay. The binding OD values and NT50 values were converted into binding antibodies units (BAU) and international units (IU), respectively, using WHO standard calibrated sera that were kindly provided by Prof. Shin-Ru Shih (Figure S3).

The geometric mean end-point titers (GMTs) of the anti-spike binding antibodies in the mRNA-1273 sera group were 3214 BAU/mL (95% confidence interval [CI], 1626 to 6353 BAU/mL), which were significantly higher than in AZD1222 (GMTs, 245.4 BAU/mL, 95% CI, 194.9 to 308.9 BAU/mL), MVC-COV1901 (GMTs, 442.8 BAU/mL, 95% CI, 226.3 to 753.3 BAU/mL), and BNT162-b2 (GMTs, 944.3 BAU/mL, 95% CI, 758.6 to 1176 BAU/mL) vaccinees (Figure 1A). Notably, we observed that mRNA-1273 recipients show a bimodal distribution in anti-spike binding antibodies (Figure 1A and S4A). However, there were no significant difference in the neutralizing activity (Figure S4B). We therefore separated the mRNA-1273 recipients into two groups: high- and low-anti-spike antibody production groups (Figure S4A), and further investigated the factors involved in the bimodal distribution (Figure S4). As shown in Figure S4, age might be responsible for the differences in anti-spike binding antibody production, but not sample collection time (Figure S4C, 4D, 4E, and 4F). The GMTs of the anti-S1-RBD binding antibodies in the mRNA-1273 and BNT162-b2 vaccinees were 950 BAU/mL (95% CI, 550.8 to 1639 BAU/mL) and 441.8 BAU/mL (95% CI, 321.2 to 607.6 BAU/mL), that were significantly higher than in AZD1222 (GMTs, 145.8 BAU/mL, 95% CI, 125.4 to 169.5 BAU/mL) and MVC-COV1901 (GMTs, 188.6 BAU/mL, 95% CI, 134 to 265.3 BAU/mL) vaccinees (Figure 1B). Since the S1-RBD has been considered an immunodominant region and the main target of neutralizing antibodies. We further compared the ratios of antibodies targeting S1-RBD to total anti-spike binding antibodies in the different vaccine sera groups. We found no significant difference in the ratios of anti-S1-RBD to anti-spike binding antibodies between each vaccine sera group (Figure 1C). In the pseudovirus neutralization test, the neutralizing activity of the AZD1222 antisera group (GMTs, 107.8 IU/mL, 95% CI, 68.52 to 169.7 IU/mL) was significantly lower than the other three groups (Figure 1D). There was no significant difference in the neutralizing activity between the mRNA-1273 (GMTs, 478.3 IU/mL, 95% CI, 255.3 to 896.1 IU/mL), BNT162-b2 (GMTs, 515.9 IU/mL, 95% CI, 297.3 to 895.3 IU/mL) and MVC-COV1901 (GMTs, 411.4 IU/mL, 95% CI, 224.5 to 754 IU/mL) vaccinees (Figure 1D). These results indicated that mRNA vaccines (mRNA-1273 and BNT162-b2) could elicit a more robust serological response, including anti-spike/S1-RBD binding and neutralizing antibodies, than adenovirus-based vaccine (AZD1222). In addition, the S-2P spike protein subunit vaccine, MVC-COV1901, was not inferior to mRNA vaccines in the ability to induce neutralizing antibodies production. ()

Anti-ACE2 antibodies triggered by SARS-CoV-2 vaccination

To compare the levels of anti-ACE2 antibodies in the sera of pre-pandemic and vaccinated subjects, we detected the binding antibodies (IgG) against human ACE2 using indirect ELISA. The mean OD of antibodies against human ACE2 in the sera of COVID-19 vaccinees was significantly higher than that in pre-pandemic cohorts (Figure 2A). In addition, four vaccinated groups showed a higher anti-ACE2 antibody level when compared with the pre-pandemic group (Figure 2B). However, there were no significant correlations between the levels of spike/S1-RBD binding antibodies and the levels of ACE2 antibodies in all vaccine types (Figure S5).

Moreover, we also compared the levels of anti-ACE2 antibodies in the sera of individuals after the first dose and the second dose of COVID-19 vaccination. As shown in Figure 2C, D, the levels of anti-ACE2 antibodies were significantly

10.3389/fimmu.2022.1023943

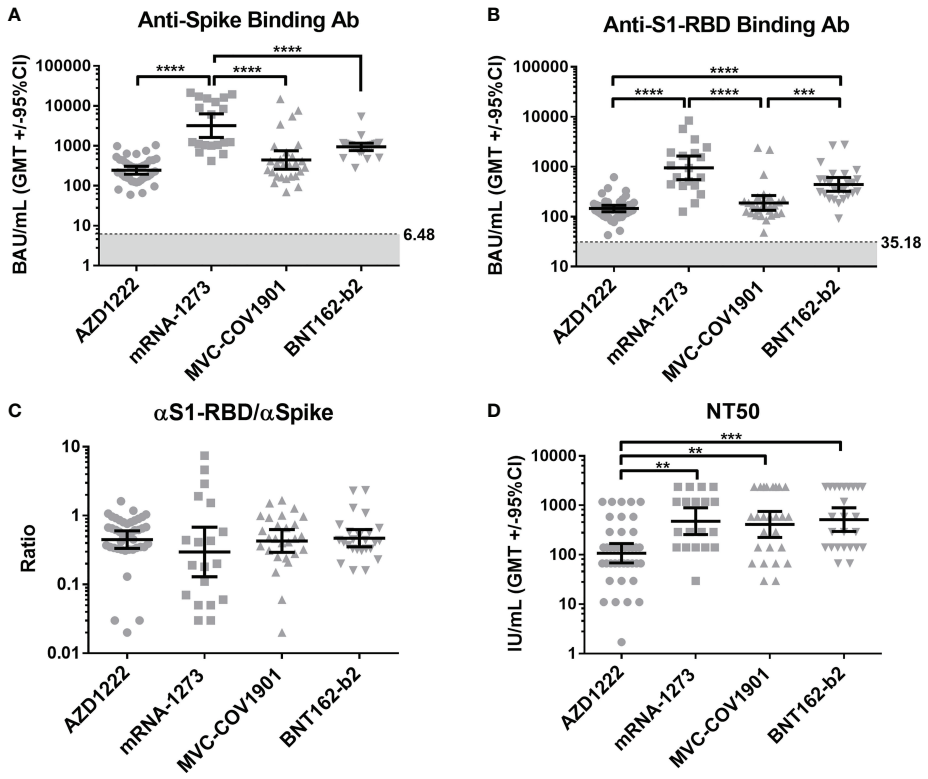

FIGURE 1
Compare the serological response triggered by different vaccine brands. **(A)** The levels of anti-spike binding antibody and **(B)** anti-S1-RBD binding antibody in the sera of four vaccinee groups (AZD1222, mRNA-1273, MVC-COV1901, and BNT162-b2) were evaluated by indirect ELISA. The mean value from the pre-pandemic serum group was determined as the cutoff value (grey). **(C)** The ratio of anti-S1-RBD to anti-spike binding antibody was shown. **(D)** Comparison of sera's neutralizing antibodies titers (NT50) in different COVID-19 vaccine groups. **P < 0.01, ***P < 0.001, ****P < 0.0001,.

increased after the second dose of vaccination in the vaccinees. Overall, these results indicated that vaccination could induce the production of anti-ACE2 antibodies in individuals.

Factors correlated to neutralizing titers

Several studies have reported that anti-spike and anti-S1-RBD IgG levels in human serum/plasma positively correlate with neutralizing titer and represent the neutralization potency (39, 40). Here, we investigated the correlation between the neutralizing titers and the serological response against trimeric spike, S1-RBD, and ACE2 in different vaccinated groups. In the Spearman rank-order correlation results, anti-spike binding antibodies levels were not significantly correlated with NT titers in AZD1222 (r= 0.181; p=0.26), mRNA-1273 (r= 0.003; p=0.9), and MVC-COV1901 (r= 0.06; p=0.76) (Figure 3A). Moderate or weak correlation between neutralizing titers and anti-spike binding antibodies levels were observed in the BNT162-b2 vaccinee group (r= 0.475; p=0.029) and in total sera of post-vaccination groups (r= 0.307; p=0.001) (Figures 3A, S6A). On the other hand, anti-S1-RBD binding antibodies levels and NT titers were strongly correlated in mRNA-1273 vaccinee group (r= 0.874; p<0.0001), moderately correlated in BNT162-b2 (r= 0.465; p<0.03) and weakly correlated in total sera groups (r=0.373; p<0.03) (Figure 3B and S6B). However, no significant correlation between anti-S1-RBD binding antibodies levels and NT titers was observed in AZD1222 (r=0.221; p=0.1) and MVC-COV1901 (r=0.089; p=0.67) sera groups (Figure 3B). Interestingly, anti-ACE2 antibodies level was negatively correlated with the NT titers in the BNT162-b2 sera group (r=-0.54; p=0.008), but not in the other sera group (Figure 3C and S6C).

Cross neutralizing activity to different SARS-CoV-2 variants

Next, we evaluated the neutralizing activity against different SARS-CoV-2 variants of different vaccinated groups using lenti-pseudovirus that encodes the spike protein of ancestral SARS-

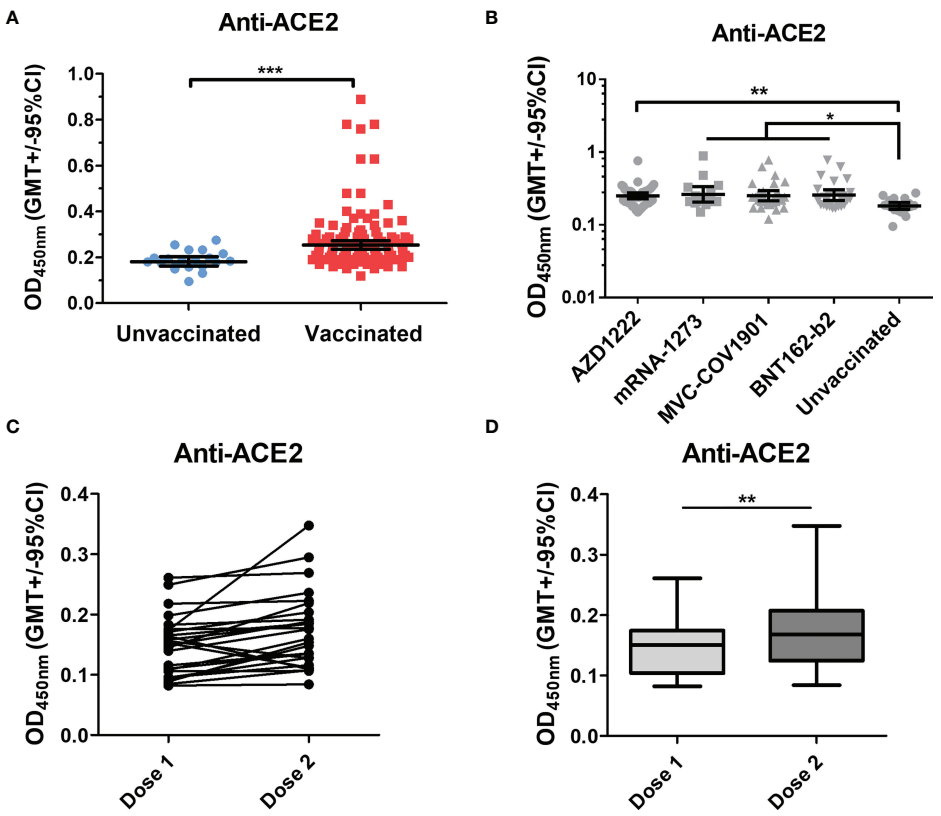

FIGURE 2
Anti-ACE2 Abs significantly increased in the COVID post-vaccination group. **(A)** Anti-ACE2 antibodies in the sera of pre-pandemic and vaccinated groups were tested. **(B)** The vaccinated group was separated into four groups (AZD1222, mRNA-1273, MVC-COV1901, and BNT162-b2), and the anti-ACE2 antibodies in the sera of these groups were compared with the pre-pandemic group. **(C, D)** Anti-ACE2 antibodies in the vaccinated sera after the first dose (dose 1) and the second dose (dose 2) were detected by an indirect ELISA. *P < 0.05, **P < 0.01, ***P < 0.001.

CoV-2 and other six SARS-CoV-2 variants (Table 2), including B.1.1.7 (alpha), B.1.351 (beta), C.37 (lambda), P.1 (gamma), B.1.617.2 (delta), and B.1.1.529 (omicron). According to a previous study, the antibody neutralization level of protection from symptomatic infection and protection from severe infection is 20.2% and 3.0% of the mean convalescent level, which correspond to approximately 54 IU/mL and 8.02 IU/mL, respectively (41). We, therefore, used the 54 and 8.02 IU/mL as the cut-off values to present the neutralizing levels. The neutralizing antibody mean titers higher than 54 IU/mL (blue), in the range of 8.02-54 IU/mL (orange), or lower than 8.02 IU/mL (red). In the AZD1222 sera group, the neutralizing activity exceeded 54 IU/mL was only for the ancestral Wuhan lineage (GMTs, 107.8 IU/mL, 95% CI, 68.52 to 169.7 IU/mL). The GMTs of NT50 against Alpha (35.44, 95% CI, 22.84 to 754.99), Lambda (29.18, 95% CI, 15.86 to 53.68), Gamma (20.08, 95% CI, 10.45 to 38.61), and Delta (13.77, 95% CI 8.68 to 21.87) were in the range of 8.02-54 IU/mL. The neutralizing titers against Beta (4.15, 95% CI 2.78 to 6.19) and Omicron (3.01, 95% CI 2.06 to 4.39) were decreased by a factor of 25.96 and 35.79, respectively (Figure 4A, E). In the MVC-COV1901 sera group, the GMTs of NT50 against ancestral lineage and Alpha reached 411.4 (95% CI 224.5 to 754) and 153.4 (95% CI 88.26 to 266.7). The GMTs of NT50 against Beta (15.94, 95% CI, 8.25 to 30.81), Lambda (33.49, 95% CI, 21.54 to 52.06), Gamma (18.38, 95% CI, 11.71 to 28.86), Delta (31.62, 95% CI 16.89 to 59.2) and Omicron (14.03, 95% CI 7.37 to 26.69) were in the range of 8.02-54 IU/mL (Figure 4C). As shown in Figure 4B, D, similar cross-neutralizing patterns with higher titers in the mRNA-1273 and BNT162-b2 vaccinee groups were observed. In detail, the GMTs of NT50 were 478.3 (95% CI 255.3 to 896.1), 171.5 (95% CI 78.18 to 376.2), 13.09 (95% CI 6.32 to 27.12), 54.25 (95% CI 30.66 to 95.99), 26.52 (95% CI 13.57 to 51.81), 68.7 (95% CI 28.95 to 163.0) and 7.09 (95% CI 3.68 to 13.69) for ancestral lineage, Alpha, Beta, Lambda, Gamma, Delta, and Omicron, respectively, in the mRNA-1273 vaccinee group (Figure 4B). The GMTs of NT50 were 515.9 (95% CI 297.3 to 895.3), 332.8 (95% CI 185.2 to 598.3), 17.41 (95% CI 9.26 to 32.72), 55.23 (95% CI 29.25 to

10.3389/fimmu.2022.1023943

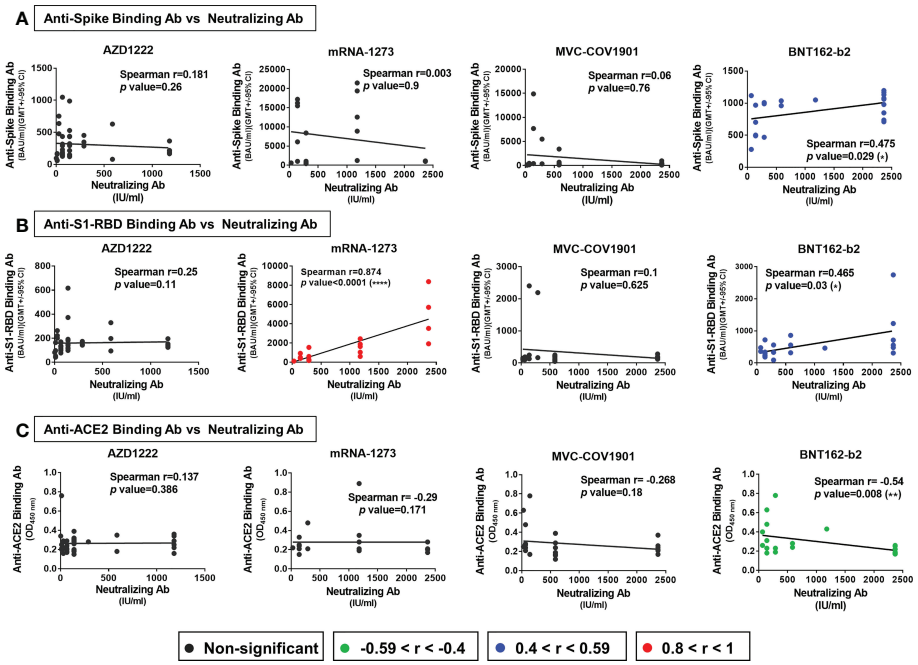

FIGURE 3
Factors correlated with neutralizing titers in different vaccine groups. The correlation of **(A)** anti-spike binding antibody levels **(B)** anti-S1-RBD antibody levels **(C)** anti-ACE2 antibody levels and neutralizing antibodies titers (NT50) of the AZD1222, mRNA-1273, MVC-COV1901, and BNT162-b2 vaccinees' sera were evaluated. The levels of correlation coefficients are presented with different colors and the statistical significance in the correlations between each factor and neutralizing titers was shown. *P < 0.05, **P < 0.01, ****P < 0.0001.

TABLE 2 Spike substitutions of all VOCs relative to ancestral Wuhan lineage in this study.

Variants of Concern	Spike mutation profile
B.1.1.7 (α)	69-70 del, 144Y del, N501Y, A570D, D614G, P681H, T716I, S982A, D1118H
B.1.351 (β)	L18F, D80A, D215G, 242-244 del, R246I, k417N, E484K, N501Y, D614G, A701V
C.37 (λ)	G75V, T76I, 246-252 del, D253N, L452Q, F490S, D614G, T859N
P.1 (γ)	L18F, T20N, P26S D138Y, R190S, K417N, E484K, N501Y, D614G, H655Y, T10271, V1176F
B.1.617.2(δ)	T19R, T95I, G142D, 156-157 del, R158G, L452R, T478K, D614G, P681R, D950N
B.1.1.529(o)	A67V, 69-70 del, T95I, 142-144 del, Y145D, 211 del, L212I, ins214EPE, G339D, S371L, S373P, S375F, K417N, N440K, G446S, 477N, T478K, E484A, Q493R, Q496S, Q498R, N501Y, Y505H, T547K, D614G, H655Y, N679K, P681H, N764K, D796Y, N856K, Q954H, N959K, L981F

104.3), 17.38 (95% CI 9.84 to 30.71), 109.1 (95% CI 59.57 to 199.8), and 8.07 (95% CI 4.54 to 14.35) for ancestral Wuhan lineage, Alpha, Beta, Lambda, Gamma, Delta, and Omicron, respectively, in the BNT162-b2 vaccinee group (Figure 4D). Notably, none of the neutralizing titers against various variants was lower than 8.02 IU/mL in the MVC-COV1901, mRNA-1273, and BNT162-b2 sera group (Figure 4C). In addition, our results suggested that mRNA vaccines, including mRNA-1273 and BNT162-b2, elicit higher breadth of neutralizing antibody titers than MVC-COV1901, followed by AZD1222. The reduction neutralizing titers folds of each variant to the ancestral Wuhan were presented in Figure 4E. Compared with Wuhan, the reductions in neutralization against Omicron were the greatest in each vaccine group (about 65-fold in mRNA-1273 and BNT162-b2, 35.79-fold in AZD1222 and 29.32-fold in MVC-COV1901), followed by Beta (25.96-fold in AZD1222, 36.54-fold in mRNA-1273, 25.81-fold in MVC-COV1901 and 29.63-fold in BNT162-b2) and Gamma (5.37-fold in AZD1222, 18.04-fold in mRNA-1273, 22.38-fold in MVC-COV1901 and 29.63-fold in BNT162-b2). The reductions in neutralization against the other variants in each vaccine group were from 1.55-fold to 13.01-fold.

10.3389/fimmu.2022.1023943

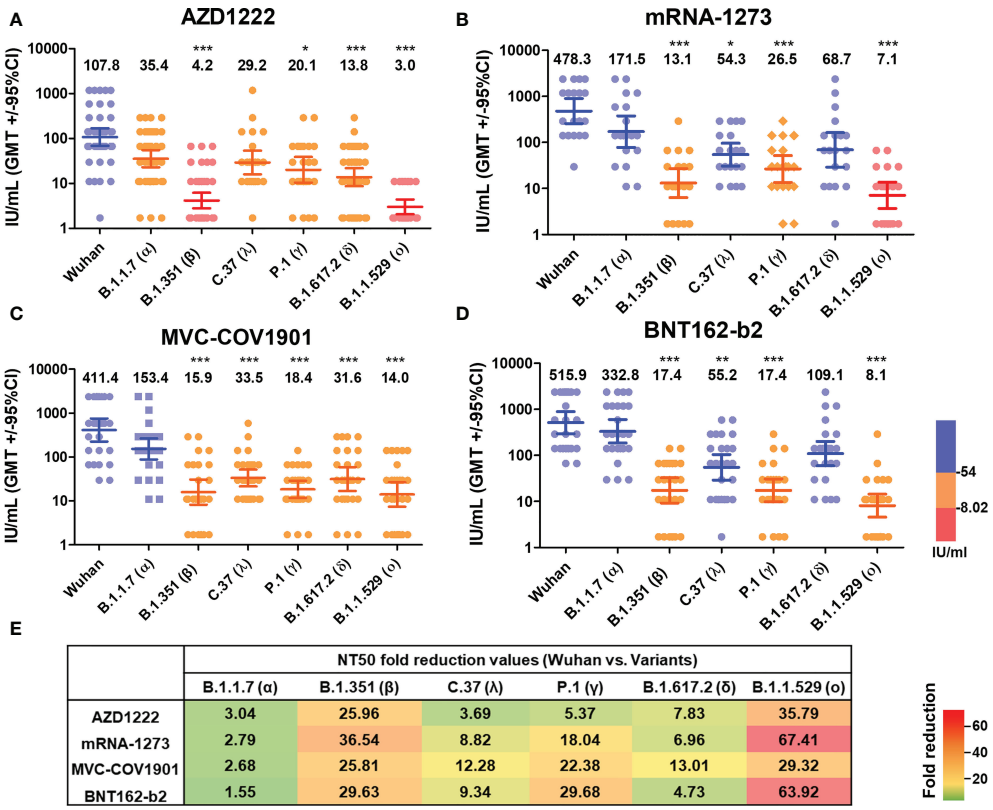

E

	NT50 fold reduction values (Wuhan vs. Variants)					
	B.1.1.7 (α)	B.1.351 (β)	C.37 (λ)	P.1 (γ)	B.1.617.2 (δ)	B.1.1.529 (ο)
AZD1222	3.04	25.96	3.69	5.37	7.83	35.79
mRNA-1273	2.79	36.54	8.82	18.04	6.96	67.41
MVC-COV1901	2.68	25.81	12.28	22.38	13.01	29.32
BNT162-b2	1.55	29.63	9.34	29.68	4.73	63.92

Fold reduction 60 40 20

FIGURE 4
Neutralizing Ab response against different SARS-CoV-2 VOCs of different vaccine brands. **(A)** AZD1222, **(B)** mRNA-1273, **(C)** MVC-COV1901, and **(D)** BNT162-b2 vaccinees' sera were tested by pseudovirus micro-neutralization assay. Each sample's neutralizing antibodies titer (NT50) against different SARS-CoV-2 VOCs was shown. Low neutralizing antibody response was red, medium neutralizing antibody response was orange, and high neutralizing antibody response was blue. **(E)** Values of fold-reduction in the neutralization of Alpha, Beta, Lambda, Gamma, Delta, and Omicron are presented as heat maps with colors. The statistical difference compared to the Wuhan strain was shown. *P < 0.05, **P < 0.01, ***P < 0.001.

Antigenic cartography generated from homologous vaccinated sera with pseudovirus neutralizing assay

Next, we constructed two-dimensional antigenic maps using neutralizing antibody titers from the sera of naïve vaccinees as described previously and were presented separately or combined with various vaccines (38, 42). Since the strategies of all four vaccine brands are based on the ancestral spike sequence, the sera tend to cluster around the ancestral Wuhan strain, reflecting that homologous neutralization is dominant. As shown in Figure 5, the maps generated from the neutralizing titers of mRNA-1273, MVC-COV1901, BNT162-b2, and total vaccinee groups were more similar than which generated from the neutralizing titers of AZD1222 group (Figure 5A). In the mRNA-1273 (Figure 5B), MVC-COV1901 (Figure 5C), BNT162-b2 (Figure 5D), and the total vaccinee maps (Figure 5E), the ancestral Wuhan and Alpha viruses cluster tightly together in the center of the map within 2 antigenic unit (1 unit = 2-fold change in neutralization titer). However, the distances between ancestral Wuhan and Lambda/Delta, Beta/Gamma, or Omicron were 2.48-3.83, 4.07-4.65, or more than 5 antigenic units, respectively (Figure S7). On the other hand, the lower neutralization titer to the ancestral Wuhan strain in AZ vaccinated group might result in a slight difference in the calculated distance between Wuhan to each variant. Indeed, all the antigenic distances between Wuhan to each variant below 4 in the map generated from the AZD1222 vaccine group (Figure S7).

Discussion

In this study, we compared the serological response of naïve individuals with various homologous SARS-CoV-2 vaccine platforms. Consistent with the previous studies, mRNA vaccines (mRNA-1273 and BNT162-b2) could elicit more robust serological responses (anti-spike and anti-S1-RBD binding

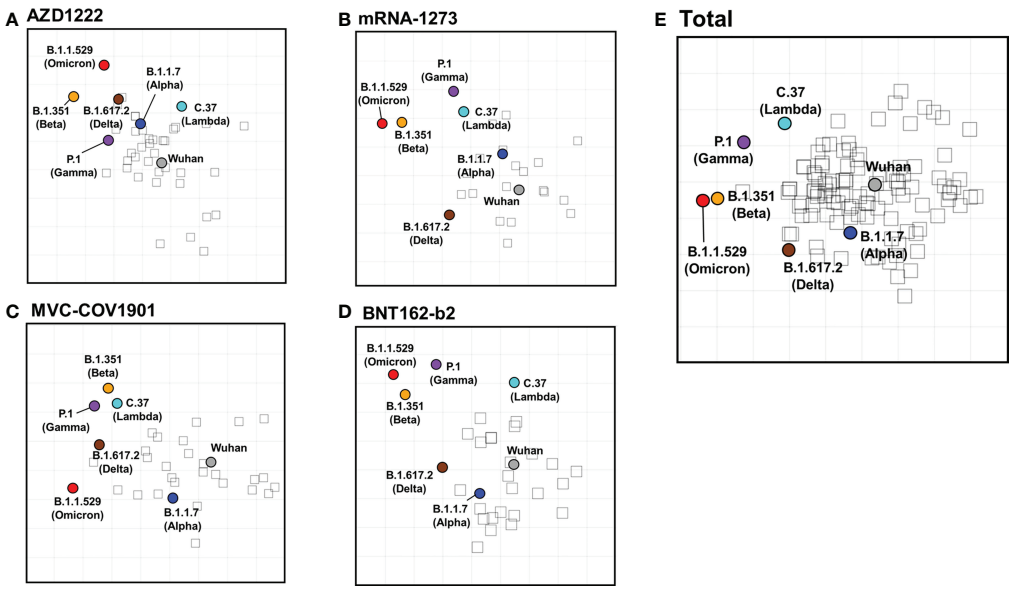

FIGURE 5
SARS-CoV-2 antigenic cartography generated from neutralizing antibodies response of different vaccine brands. Antigenic maps of SARS-CoV-2 VOCs were generated using neutralizing antibody titers from **(A)** AZD1222, **(B)** mRNA-1273, **(C)** MVC-COV1901, **(D)** BNT162-b2, and **(E)** total vaccinees' sera. SARS-CoV-2 VOCs are shown as colored circles and sera are indicated as hollow squares. Both the x and y-axes of the map are antigenic distance, and each grid square (1 antigenic unit) represents a 2-fold change in neutralization titer.

antibodies production and broadly neutralizing antibodies titer) than other platforms (AZD1222 and MVC-COV1901) (43–45). Notably, although the MVC-COV1901 vaccinee group had a lower amount of anti-spike and anti-S1-RBD binding antibodies than mRNA-1273 and BNT162-b2 groups, no significant difference in neutralizing antibody titers of them was found. In addition to vaccine platform, the strategies for SARS-CoV-2 spike protein sequence design might affect the vaccine efficacy (4, 46). There are several different strategies to stabilize the prefusion form spike protein. One is adding mutations at the S1/S2 furin cleavage sites to confer protease resistance; another is incorporating two proline substitutions at residues 986 and 987 (K986P, V987P) in the sequence of the wild-type spike from the Wuhan strain (47). Moreover, MVC-COV1901 adds a trimerization domain to the C-terminal for improving the conformational homogeneity (16). The mRNA-1273, BNT162-b2, and MVC-COV1901 use similar strategies to stabilize the prefusion form spike protein for preserving neutralizing epitopes; however, AZD1222 does not. This could be the possible reason for AZD1222 showing a lower neutralizing activity, compared with mRNA-1273, BNT162-b2, and MVC-COV1901 in this study.

Several limitations that should be taken into consideration in this study include the sample collection time period, sample sizes, and the use of a SARS-CoV-2 pseudovirus system for determining the neutralizing antibodies titers. In this study, only the MVC-COV1901 group had a significantly higher average sample collection days compared to the other groups. In addition, we found that there was no significant correlation between the neutralizing antibody titers and the time of sample collection (Figure S8). However, the influence of different sample collection times on neutralizing titers cannot be ignored. On the other hand, pseudoviruses can only replicate for a single round and the conformation/distribution of the spike protein on the pseudotyped virus may not exactly reflect the natural state of spike proteins on real SARS-CoV-2 (48). The neutralizing antibodies titers might be overestimated in the SARS-CoV-2 pseudovirus system. Indeed, inflating titers for the particular SARS-CoV-2 gamma (P.1) variant was observed in other studies using lentiviral pseudotype virus (49).

According to the statistical data from the TFDA website (https://www.cdc.gov.tw/En/File/Get/YTqTkmtAHH7fmKY6JF3l_A), 93.8% of the population has received at least one dose of a COVID-19 vaccine, 88.2% of the Taiwanese population have received two doses of the COVID-19 vaccines, and 73.8% of persons have received the booster dose as of October 24th, 2022. A total of 63.18 million doses have been administered in Taiwan (mRNA-1273: 23.89 million doses, BNT162-b2: 19.3 million doses, AZD1222: 15.3 million doses, MVC-COV1901: 3.06 million doses) and 20,172 cases of vaccine adverse reactions have been reported (AZD1222: 8,541; mRNA-1273: 5,513; MVC-COV1901: 826; BNT162-b2: 5,731). Although the proportion is very low, vaccine adverse reaction still causes concern to the public. One of the known causes of adverse vaccine reactions is autoimmune disease (50, 51). Indeed, many

autoimmune phenomena, including vaccine-induced immune thrombotic thrombocytopenia, immune thrombocytopenic purpura, and rheumatoid arthritis, could be associated with COVID-19 vaccines (52–55). Several studies have reported that SARS-CoV-2 infection could induce the production of autoantibodies (33, 34, 56). Previous studies have shown that SARS-CoV-2 infection could induce the production of antibodies against ACE2 in the serum (35, 36, 57, 58), which might cause angiotensin II levels to increase and finally lead to a pro-inflammatory state (59). Thus, investigating whether COVID-19 vaccination induces the production of ACE2 autoantibodies is needed. In this study, we compared the levels of ACE2 cross-reactive antibodies in the sera of individuals after the first dose and the second dose of vaccination. We found a significant increase in the levels of ACE2 cross-reactive antibodies in COVID-19 vaccinees. Some subjects showed an elevation in the levels of ACE2 cross-reactive antibodies after the second dose of vaccination. This indicated that the SARS-CoV-2 spike antigen induces the production of antibodies that can cross-react with ACE2.

With the increasing cases of re-infection and breakthrough, developing the next-generation SARS-CoV-2 vaccines is necessary. At this time, the public's willingness to vaccinate seasonally is a big challenge. Since the durability of responses from different vaccine platform were comparable: the reduction folds at 180 days from the peak seen at 14 days after the second dose of neutralizing antibody titers were 4.5-7.1 in the mRNA platform (60, 61), 6.2 in the MVC-COV1901 (62), and 4.5 in AZD1222 (63). Increasing the breadth of neutralizing antibodies and reducing the vaccine adverse reaction will be the main goals for next-generation vaccines. In this study, we found that the mRNA vaccine platform could trigger robust serological response and the protein-subunit vaccine (MVC-COV1901) was able to induce neutralizing antibodies production as well as the mRNA vaccine. Therefore, we suggested that the design of spike with S-2P, furin-cleavage resistant and trimerization could be a mix strategy to the various vaccine platforms to produce the anti-spike/S1-RBD antibodies with neutralizing ability.

Another key point for the next-generation vaccine strategies would be to find a strain more suitable considering the new strains and outbreaks. Consistent with the antigenic maps have published by other groups, Omicron showed the farthest antigenic distance to Wuhan, implying Omicron represents very different antigenic characteristics from the ancestral lineage (64, 65). As autoimmune disease in COVID-19 has received attention, several studies have begun to examine whether SARS-CoV-2 vaccination can lead to autoantibodies production. However, the anti-ACE2 antibody was not commonly involved in the autoantibodies testing array (66). Here, we raised the issue that SARS-CoV-2 vaccines might trigger the anti-ACE2 antibodies production. Therefore, whether SARS-CoV-2 vaccines-induced anti-ACE2 autoantibody plays any biological function and the mechanisms of how SARS-CoV-2 vaccines lead to ACE2 autoantibodies production needs further investigation.

Data availability statement

The datasets presented in this study can be found in online repositories. The names of the repository/repositories and accession number(s) can be found in the article/Supplementary Material.

Ethics statement

The studies involving human participants were reviewed and approved by The Institutional Review Board of National Cheng Kung University Hospital (NCKUH) (IRB #A-BR-101–140, IRB #A-ER-110-423). The patients/participants provided their written informed consent to participate in this study.

Author contributions

J-RW conceived the experiments. C-HC designed and performed the experiments and analyzed the data. C-HC and J-RW wrote and edited the paper. DC provided English editing and comments/suggestions for the manuscript. S-WH provided comments and suggestions during the preparation of the manuscript. Y-CC and T-MY shared the materials used in this study. All authors contributed to the article and approved the submitted version.

Funding

This study was supported by the Ministry of Science and Technology of Taiwan (MOST 109-2327-B-006-005, MOST 111-2321-B-006-009); and National Health Research Institutes (NHRI IV-111-PP-06).

Acknowledgments

We thank Prof. Shin-Ru Shih and Dr. Yu-An Kung (Research Center for Emerging Viral Infections, College of Medicine, Chang Gung University, Taoyuan City, Taiwan) provided the sera calibrated by WHO standard sera for the commutability assessment. We thank TFDA who provided the sera calibrated by five independent labs in Taiwan. We also thank the study participants who donated specimens for this study.

Conflict of interest

Author Y-CC is employed by Leadgene Biomedical, Inc.

The remaining authors declare that the research was conducted in the absence of any commercial or financial relationship that could be considered a potential conflict of interest.

Publisher's note

All claims expressed in this article are solely those of the authors and do not necessarily represent those of their affiliated organizations, or those of the publisher, the editors and the reviewers. Any product that may be evaluated in this article, or claim that may be made by its manufacturer, is not guaranteed or endorsed by the publisher.

Supplementary material

The Supplementary Material for this article can be found online at: https://www.frontiersin.org/articles/10.3389/fimmu.2022.1023943/full#supplementary-material

References

1. World Health Organization. *Coronavirus disease (COVID-19)* (2022). Available at: https://www.who.int/emergencies/diseases/novel-coronavirus-2019.

2. Pak A, Adegboye OA, Adekunle AI, Rahman KM, McBryde ES, Eisen DP. Economic consequences of the COVID-19 outbreak: the need for epidemic preparedness. *Front Public Health* (2020) 8:241. doi: 10.3389/fpubh.2020.00241

3. Forni G, Mantovani A. COVID-19 vaccines: where we stand and challenges ahead. *Cell Death Differ* (2021) 28:626–39. doi: 10.1038/s41418-020-00720-9

4. Kyriakidis NC, López-Cortés A, González EV, Grimaldos AB, Prado EO. SARS-CoV-2 vaccines strategies: a comprehensive review of phase 3 candidates. *NPJ Vaccines* (2021) 6:28. doi: 10.1038/s41541-021-00292-w

5. Hogan MJ, Pardi N. mRNA vaccines in the COVID-19 pandemic and beyond. *Annu Rev Med* (2022) 73:17–39. doi: 10.1146/annurev-med-042420-112725

6. Pardi N, Hogan MJ, Porter FW, Weissman D. mRNA vaccines - a new era in vaccinology. *Nat Rev Drug Discovery* (2018) 17:261–79. doi: 10.1038/nrd.2017.243

7. Shang J, Wan Y, Luo C, Ye G, Geng Q, Auerbach A, et al. Cell entry mechanisms of SARS-CoV-2. *Proc Natl Acad Sci U.S.A.* (2020) 117:11727–34. doi: 10.1073/pnas.2003138117

8. Hoffmann M, Kleine-Weber H, Schroeder S, Krüger N, Herrler T, Erichsen S, et al. SARS-CoV-2 cell entry depends on ACE2 and TMPRSS2 and is blocked by a clinically proven protease inhibitor. *Cell* (2020) 181:271–280.e278. doi: 10.1016/j.cell.2020.02.052

9. Shang J, Ye G, Shi K, Wan Y, Luo C, Aihara H, et al. Structural basis of receptor recognition by SARS-CoV-2. *Nature* (2020) 581:221–4. doi: 10.1038/s41586-020-2179-y

10. Huang Y, Yang C, Xu XF, Xu W, Liu SW. Structural and functional properties of SARS-CoV-2 spike protein: potential antivirus drug development for COVID-19. *Acta Pharmacol Sin* (2020) 41:1141–9. doi: 10.1038/s41401-020-0485-4

11. Jackson CB, Farzan M, Chen B, Choe H. Mechanisms of SARS-CoV-2 entry into cells. *Nat Rev Mol Cell Biol* (2022) 23:3–20. doi: 10.1038/s41580-021-00418-x

12. Premkumar L, Segovia-Chumbez B, Jadi R, Martinez DR, Raut R, Markmann A, et al. The receptor binding domain of the viral spike protein is an immunodominant and highly specific target of antibodies in SARS-CoV-2 patients. *Sci Immunol* (2020) 5:eabc8413. doi: 10.1126/sciimmunol.abc8413

13. Dai L, Gao GF. Viral targets for vaccines against COVID-19. *Nat Rev Immunol* (2021) 21:73–82. doi: 10.1038/s41577-020-00480-0

14. Polyiam K, Phoolcharoen W, Butkhot N, Srisaowakarn C, Thitithanyanont A, Auewarakul P, et al. Immunodominant linear b cell epitopes in the spike and membrane proteins of SARS-CoV-2 identified by immunoinformatics prediction and immunoassay. *Sci Rep* (2021) 11:20383. doi: 10.1038/s41598-021-99642-w

15. Tian JH, Patel N, Haupt R, Zhou H, Weston S, Hammond H, et al. SARS-CoV-2 spike glycoprotein vaccine candidate NVX-CoV2373 immunogenicity in baboons and protection in mice. *Nat Commun* (2021) 12:372. doi: 10.1038/s41467-020-20653-8

16. Hsieh SM, Liu MC, Chen YH, Lee WS, Hwang SJ, Cheng SH, et al. Safety and immunogenicity of CpG 1018 and aluminium hydroxide-adjuvanted SARS-CoV-2 s-2P protein vaccine MVC-COV1901: interim results of a large-scale, double-blind, randomised, placebo-controlled phase 2 trial in Taiwan. *Lancet Respir Med* (2021) 9:1396–406. doi: 10.1016/S2213-2600(21)00402-1

17. Suthar AB, Wang J, Seffren V, Wiegand RE, Griffing S, Zell E. Public health impact of covid-19 vaccines in the US: observational study. *Bmj* (2022) 377:e069317. doi: 10.1136/bmj-2021-069317

18. Bano I, Sharif M, Alam S. Genetic drift in the genome of SARS COV-2 and its global health concern. *J Med Virol* (2022) 94:88–98. doi: 10.1002/jmv.27337

19. Wang S, Xu X, Wei C, Li S, Zhao J, Zheng Y, et al. Molecular evolutionary characteristics of SARS-CoV-2 emerging in the united states. *J Med Virol* (2022) 94:310–7. doi: 10.1002/jmv.27331

20. Oude Munnink BB, Worp N, Nieuwenhuijse DF, Sikkema RS, Haagmans B, Fouchier RAM, et al. The next phase of SARS-CoV-2 surveillance: real-time molecular epidemiology. *Nat Med* (2021) 27:1518–24. doi: 10.1038/s41591-021-01472-w

21. Cascella M, Rajnik M, Aleem A, Dulebohn SC, Di Napoli R. *Features, evaluation, and treatment of coronavirus (COVID-19)*. Treasure Island (FL: StatPearls (StatPearls Publishing Copyright © 2022, StatPearls Publishing LLC. (2022).

22. Otto SP, Day T, Arino J, Colijn C, Dushoff J, Li M, et al. The origins and potential future of SARS-CoV-2 variants of concern in the evolving COVID-19 pandemic. *Curr Biol* (2021) 31:R918–929. doi: 10.1016/j.cub.2021.06.049

23. Aleem A, Akbar Samad AB, Slenker AK. *Emerging variants of SARS-CoV-2 and novel therapeutics against coronavirus (COVID-19)*. Treasure Island (FL: StatPearls (StatPearls Publishing Copyright © 2022, StatPearls Publishing LLC. (2022).

24. Karim SSA, Karim QA. Omicron SARS-CoV-2 variant: a new chapter in the COVID-19 pandemic. *Lancet* (2021) 398:2126–8. doi: 10.1016/S0140-6736(21)02758-6

25. Viana R, Moyo S, Amoako DG, Tegally H, Scheepers C, Althaus CL, et al. Rapid epidemic expansion of the SARS-CoV-2 omicron variant in southern Africa. *Nature* (2022) 603:679–86. doi: 10.1038/s41586-022-04411-y

26. Ou J, Lan W, Wu X, Zhao T, Duan B, Yang P, et al. Tracking SARS-CoV-2 omicron diverse spike gene mutations identifies multiple inter-variant recombination events. *Signal Transduct Target Ther* (2022) 7:138. doi: 10.1038/s41392-022-00992-2

27. Cao Y, Yisimayi A, Jian F, Song W, Xiao T, Wang L, et al. BA.2.12.1, BA.4 and BA.5 escape antibodies elicited by omicron infection. *Nature* (2022) 608:593–602. doi: 10.1038/s41586-022-04980-y

28. Pulliam JRC, van Schalkwyk C, Govender N, von Gottberg A, Cohen C, Groome MJ, et al. Increased risk of SARS-CoV-2 reinfection associated with emergence of omicron in south Africa. *Science* (2022) 376:eabn4947. doi: 10.1126/science.abn4947

29. Kuhlmann C, Mayer CK, Claassen M, Maponga T, Burgers WA, Keeton R, et al. Breakthrough infections with SARS-CoV-2 omicron despite mRNA vaccine booster dose. *Lancet* (2022) 399:625–6. doi: 10.1016/S0140-6736(22)00090-3

30. Blom K, Marking U, Havervall S, Norin NG, Gordon M, García M, et al. Immune responses after omicron infection in triple-vaccinated health-care workers with and without previous SARS-CoV-2 infection. *Lancet Infect Dis* (2022) 22:943–5. doi: 10.1016/S1473-3099(22)00362-0

31. Zimmermann P, Curtis N. Factors that influence the immune response to vaccination. *Clin Microbiol Rev* (2019) 32:e00084–18. doi: 10.1128/CMR.00084-18

32. Falahi S, Kenarkoohi A. Host factors and vaccine efficacy: Implications for COVID-19 vaccines. *J Med Virol* (2022) 94:1330–5. doi: 10.1002/jmv.27485

33. Liu Y, Sawalha AH, Lu Q. COVID-19 and autoimmune diseases. *Curr Opin Rheumatol* (2021) 33:155–62. doi: 10.1097/BOR.0000000000000776

34. Dotan A, Muller S, Kanduc D, David P, Halpert G, Shoenfeld Y. The SARS-CoV-2 as an instrumental trigger of autoimmunity. *Autoimmun Rev* (2021) 20:102792. doi: 10.1016/j.autrev.2021.102792

35. Arthur JM, Forrest JC, Boehme KW, Kennedy JL, Owens S, Herzog C, et al. Development of ACE2 autoantibodies after SARS-CoV-2 infection. *PloS One* (2021) 16:e0257016. doi: 10.1371/journal.pone.0257016

36. Casciola-Rosen L, Thiemann DR, Andrade F, Trejo Zambrano MI, Hooper JE, Leonard E, et al. IgM autoantibodies recognizing ACE2 are associated with severe COVID-19. *medRxiv [preprint]* (2020). doi: 10.1101/2020.10.13.20211664v1

37. Lai YC, Cheng YW, Chao CH, Chang YY, Chen CD, Tsai WJ, et al. Antigenic cross-reactivity between SARS-CoV-2 S1-RBD and its receptor ACE2. *Front Immunol* (2022) 13:868724. doi: 10.3389/fimmu.2022.868724

38. Huang SW, Tai CH, Hsu YM, Cheng D, Hung SJ, Chai KM, et al. Assessing the application of a pseudovirus system for emerging SARS-CoV-2 and re-emerging avian influenza virus H5 subtypes in vaccine development. *BioMed J* (2020) 43:375–87. doi: 10.1016/j.bj.2020.06.003

39. Han Y, Liu P, Qiu Y, Zhou J, Liu Y, Hu X, et al. Effective virus-neutralizing activities in antisera from the first wave of survivors of severe COVID-19. *JCI Insight* (2021) 6:e146267. doi: 10.1172/jci.insight.146267

40. Perkmann T, Koller T, Perkmann-Nagele N, Klausberger M, Duerkop M, Holzer B, et al. Spike protein antibodies mediate the apparent correlation between SARS-CoV-2 nucleocapsid antibodies and neutralization test results. *Microbiol Spectr* (2021) 9:e0021821. doi: 10.1128/Spectrum.00218-21

41. Khoury DS, Cromer D, Reynaldi A, Schlub TE, Wheatley AK, Juno JA, et al. Neutralizing antibody levels are highly predictive of immune protection from symptomatic SARS-CoV-2 infection. *Nat Med* (2021) 27:1205–11. doi: 10.1038/s41591-021-01377-8

42. Huang SW, Tai CH, Fonville JM, Lin CH, Wang SM, Liu CC, et al. Mapping enterovirus A71 antigenic determinants from viral evolution. *J Virol* (2015) 89:11500–6. doi: 10.1128/JVI.02035-15

43. Shrotri M, Navaratnam AMD, Nguyen V, Byrne T, Geismar C, Fragaszy E, et al. Spike-antibody waning after second dose of BNT162b2 or ChAdOx1. *Lancet* (2021) 398:385–7. doi: 10.1016/S0140-6736(21)01642-1

44. Dashdorj NJ, Wirz OF, Röltgen K, Haraguchi E, Buzzanco AS 3rd, Sibai M, et al. Direct comparison of antibody responses to four SARS-CoV-2 vaccines in Mongolia. *Cell Host Microbe* (2021) 29:1738–1743.e1734. doi: 10.1016/j.chom.2021.11.004

45. Cheng SMS, Mok CKP, Leung YWY, Ng SS, Chan KCK, Ko FW, et al. Neutralizing antibodies against the SARS-CoV-2 omicron variant BA.1 following homologous and heterologous CoronaVac or BNT162b2 vaccination. *Nat Med* (2022) 28:486–9. doi: 10.1038/s41591-022-01704-7

46. Dong Y, Dai T, Wei Y, Zhang L, Zheng M, Zhou F. A systematic review of SARS-CoV-2 vaccine candidates. *Signal Transduct Target Ther* (2020) 5:237. doi: 10.1038/s41392-020-00352-y

47. Dagotto G, Yu J, Barouch DH. Approaches and challenges in SARS-CoV-2 vaccine development. *Cell Host Microbe* (2020) 28:364–70. doi: 10.1016/j.chom.2020.08.002

48. Wilks SH, Mühlemann B, Shen X, Türeli S, LeGresley EB, Netzl A, et al. Mapping SARS-CoV-2 antigenic relationships and serological responses. *bioRxiv [preprint]* (2022). doi: 10.1101/2022.01.28.477987v2.abstract

49. Dupont L, Snell LB, Graham C, Seow J, Merrick B, Lechmere T, et al. Neutralizing antibody activity in convalescent sera from infection in humans with SARS-CoV-2 and variants of concern. *Nat Microbiol* (2021) 6:1433–42. doi: 10.1038/s41564-021-00974-0

50. Greinacher A, Selleng K, Palankar R, Wesche J, Handtke S, Wolff M, et al. Insights in ChAdOx1 nCoV-19 vaccine-induced immune thrombotic thrombocytopenia. *Blood* (2021) 138:2256–68. doi: 10.1182/blood.2021013231

51. Buchhorn R, Meyer C, Schulze-Forster K, Junker J, Heidecke H. Autoantibody release in children after corona virus mRNA vaccination: A risk factor of multisystem inflammatory syndrome? *Vaccines (Basel)* (2021) 9:1353. doi: 10.3390/vaccines9111353

52. Mingot-Castellano ME, Butta N, Canaro M, Gómez Del Castillo Solano MDC, Sánchez-González B, Jiménez-Bárcenas R, et al. COVID-19 vaccines and autoimmune hematologic disorders. *Vaccines (Basel)* (2022) 10:961. doi: 10.3390/vaccines10060961

53. Jara LJ, Vera-Lastra O, Mahroum N, Pineda C, Shoenfeld Y. Autoimmune post-COVID vaccine syndromes: does the spectrum of autoimmune/inflammatory syndrome expand? *Clin Rheumatol* (2022) 41:1603–9. doi: 10.1007/s10067-022-06149-4

54. Greinacher A, Thiele T, Warkentin TE, Weisser K, Kyrle PA, Eichinger S. Thrombotic thrombocytopenia after ChAdOx1 nCov-19 vaccination. *N Engl J Med* (2021) 384:2092–101. doi: 10.1056/NEJMoa2104840

55. Chen Y, Xu Z, Wang P, Li XM, Shuai ZW, Ye DQ, et al. New-onset autoimmune phenomena post-COVID-19 vaccination. *Immunology* (2022) 165:386–401. doi: 10.1111/imm.13443

56. Wang EY, Mao T, Klein J, Dai Y, Huck JD, Jaycox JR, et al. Diverse functional autoantibodies in patients with COVID-19. *Nature* (2021) 595:283–8. doi: 10.1038/s41586-021-03631-y

57. Murphy WJ. & longo, D.L. a possible role for anti-idiotype antibodies in SARS-CoV-2 infection and vaccination. *N Engl J Med* (2022) 386:394–6. doi: 10.1056/NEJMcibr2113694

58. McMillan P, Dexhiemer T, Neubig RR, Uhal BD. COVID-19-A theory of autoimmunity against ACE-2 explained. *Front Immunol* (2021) 12:582166. doi: 10.3389/fimmu.2021.582166

59. Takahashi Y, Haga S, Ishizaka Y, Mimori A. Autoantibodies to angiotensin-converting enzyme 2 in patients with connective tissue diseases. *Arthritis Res Ther* (2010) 12:R85. doi: 10.1186/ar3012

60. Doria-Rose N, Suthar MS, Makowski M, O'Connell S, McDermott AB, Flach B, et al. Antibody persistence through 6 months after the second dose of mRNA-1273 vaccine for covid-19. *N Engl J Med* (2021) 384:2259–61. doi: 10.1056/NEJMc2103916

61. Widge AT, Rouphael NG, Jackson LA, Anderson EJ, Roberts PC, Makhene M, et al. Durability of responses after SARS-CoV-2 mRNA-1273 vaccination. *N Engl J Med* (2021) 384:80–2. doi: 10.1056/NEJMc2032195

62. Hsieh SM, Chang SC, Cheng HY, Shih SR, Lien CE. Durability and immunogenicity of neutralizing antibodies response against omicron variants after three doses of subunit SARS-CoV-2 vaccine MVC-COV1901: An extension to an open-label, dose-escalation phase 1 study. *Infect Dis Ther* (2022) 11:1493–504. doi: 10.1007/s40121-022-00652-6

63. Madhi SA, Kwatra G, Richardson SI, Koen AL, Baillie V, Cutland CL, et al. Durability of ChAdOx1 nCoV-19 (AZD1222) vaccine and hybrid humoral immunity against variants including omicron BA.1 and BA.4 6 months after vaccination (COV005): a post-hoc analysis of a randomised, phase 1b-2a trial. *Lancet Infect Dis* (2022). doi: 10.1016/S1473-3099(22)00596-5

64. Mykytyn AZ, Rissmann M, Kok A, Rosu ME, Schipper D, Breugem TI, et al. Antigenic cartography of SARS-CoV-2 reveals that omicron BA.1 and BA.2 are antigenically distinct. *Sci Immunol* (2022) 7:eabq4450. doi: 10.1126/sciimmunol.abq4450

65. Bekliz M, Adea K, Vetter P, Eberhardt CS, Hosszu-Fellous K, Vu DL, et al. Neutralization capacity of antibodies elicited through homologous or heterologous infection or vaccination against SARS-CoV-2 VOCs. *Nat Commun* (2022) 13:3840. doi: 10.1038/s41467-022-31556-1

66. Arunachalam PS, Scott MKD, Hagan T, Li C, Feng Y, Wimmers F, et al. Systems vaccinology of the BNT162b2 mRNA vaccine in humans. *Nature* (2021) 596:410–6. doi: 10.1038/s41586-021-03791-x

frontiers | Frontiers in Immunology

TYPE Original Research
PUBLISHED 22 December 2022
DOI 10.3389/fimmu.2022.1056272

OPEN ACCESS

EDITED BY
Pedro A. Reche,
Complutense University of Madrid, Spain

REVIEWED BY
Matthew Zirui Tay,
A*STAR Infectious Disease Labs, Singapore
Hongqi Liu,
Chinese Academy of Medical Sciences and Peking Union Medical College, China
Zhengkun Tu,
First Affiliated Hospital of Jilin University, China

*CORRESPONDENCE
Yi-Ping Li
lyiping@mail.sysu.edu.cn
Xiaowang Qu
quxiaowang@163.com

†These authors have contributed equally to this work

SPECIALTY SECTION
This article was submitted to Viral Immunology, a section of the journal Frontiers in Immunology

RECEIVED 28 September 2022
ACCEPTED 29 November 2022
PUBLISHED 22 December 2022

CITATION
Peng Y, Liu Y, Hu Y, Chang F, Wu Q, Yang J, Chen J, Teng S, Zhang J, He R, Wei Y, Bostina M, Luo T, Liu W, Qu X and Li Y-P (2022) Monoclonal antibodies constructed from COVID-19 convalescent memory B cells exhibit potent binding activity to MERS-CoV spike S2 subunit and other human coronaviruses. *Front. Immunol.* 13:1056272. doi: 10.3389/fimmu.2022.1056272

Monoclonal antibodies constructed from COVID-19 convalescent memory B cells exhibit potent binding activity to MERS-CoV spike S2 subunit and other human coronaviruses

Yuan Peng[1,2†], Yongcheng Liu[3†], Yabin Hu[2†], Fangfang Chang[3], Qian Wu[2,3], Jing Yang[4], Jun Chen[5], Shishan Teng[2], Jian Zhang[2], Rongzhang He[2], Youchuan Wei[1], Mihnea Bostina[6], Tingrong Luo[1], Wenpei Liu[2], Xiaowang Qu[2*] and Yi-Ping Li[3,7*]

[1]College of Animal Sciences and Veterinary Medicine, Guangxi University, Nanning, Guangxi, China, [2]Translational Medicine Institute, The First People's Hospital of Chenzhou, Hengyang Medical School, University of South China, Chenzhou, China, [3]Institute of Human Virology, Department of Pathogen Biology and Biosecurity, and Key Laboratory of Tropical Disease Control of Ministry of Education, Zhongshan School of Medicine, Sun Yat-sen University, Guangzhou, China, [4]School of Laboratory Medicine and Biotechnology, Southern Medical University, Guangzhou, China, [5]School of Public Health, Southern Medical University, Guangzhou, China, [6]Department of Microbiology and Immunology, University of Otago, Dunedin, New Zealand, [7]Department of Infectious Diseases, The Third Affiliated Hospital of Sun Yat-Sen University, Guangzhou, China

Introduction: The Middle East respiratory syndrome coronavirus (MERS-CoV) and the severe acute respiratory syndrome coronavirus 2 (SARS-CoV-2) are two highly contagious coronaviruses causing MERS and COVID-19, respectively, without an effective antiviral drug and a long-lasting vaccine. Approaches for diagnosis, therapeutics, prevention, etc., particularly for SARS-CoV-2 that is continually spreading and evolving, are urgently needed. Our previous study discovered that >60% of sera from convalescent COVID-19 individuals, but <8% from general population, showed binding activity against the MERS-CoV spike protein, indicating that SARS-CoV-2 infection boosted antibodies cross-reactive with MERS-CoV.

Methods: To generate antibodies specific to both SARS-CoV-2 and MERS-CoV, here we screened 60 COVID-19 convalescent sera against MERS-CoV spike extracellular domain and S1 and S2 subunits. We constructed and characterized monoclonal antibodies (mAbs) from COVID-19 convalescent memory B cells and examined their binding and neutralizing activities against human coronaviruses.

Results and Discussion: Of 60 convalescent serum samples, 34 showed binding activity against MERS-CoV S2, with endpoint titers positively correlated with the titers to SARS-CoV-2 S2. By sorting single memory B cells from COVID-19 convalescents, we constructed 38 mAbs and found that

11 mAbs showed binding activity with MERS-CoV S2, of which 9 mAbs showed potent cross-reactivity with all or a proportion of spike proteins of alphacoronaviruses (229E and NL63) and betacoronaviruses (SARS-CoV-1, SARS-CoV-2, OC43, and HKU1). Moreover, 5 mAbs also showed weak neutralization efficiency against MERS-CoV spike pseudovirus. Epitope analysis revealed that 3 and 8 mAbs bound to linear and conformational epitopes in MERS-CoV S2, respectively. In summary, we have constructed a panel of antibodies with broad-spectrum reactivity against all seven human coronaviruses, thus facilitating the development of diagnosis methods and vaccine design for multiple coronaviruses.

KEYWORDS

COVID-19, convalescents, monoclonal antibody, coronavirus, middle eastern respiratory syndrome coronavirus, spike protein

1 Introduction

Coronaviruses are enveloped, single-stranded positive-sense RNA viruses belonging to the genus *Coronavirus* of the family *Coronaviridae* in the order *Nidovirales*. Animal coronaviruses cause respiratory, enteric, and neurological system diseases in a wide range of wildlife and domestic animals (1, 2). Human coronaviruses (hCoVs) mainly infect the respiratory tract causing respiratory symptoms ranging from mild to lethal. However, due to the changing habitat of host animals and the high plasticity of the viral receptor, animal coronaviruses have spread across species and caused infections in humans (3).

To date, seven coronaviruses have proven to transmit from animals to humans, including three highly pathogenic coronaviruses: the severe acute respiratory syndrome coronavirus 1 (SARS-CoV-1), SARS-CoV-2, and Middle East respiratory syndrome coronavirus (MERS-CoV), and four mild coronaviruses: 229E and NL63 (alpha [α] coronavirus) and OC43 and HKU1 (beta [β] coronavirus). The intermediate hosts of MERS-CoV and SARS-CoV-2 are dromedary camels and bats, respectively (1). Since first reported in Saudi Arabia and Jordan in 2012, MERS cases have been reported in 27 countries with a infection fatality rate of ~35% (4). SARS-CoV-2 infection caused coronavirus disease 2019 (COVID-19), first identified in 2019, which has spread globally, resulted in ~600 million infections and approximately 6.5 million deaths recorded by October 2022 (5). The fatality of COVID-19 varies substantially within the range of 0.0%-1.6%, much lower than estimations made earlier in the pandemic (6). Age, gender, co-infection with other pathogens, initial diseases, etc. relate to the severity of COVID-19 symptoms (7, 8). Infection of mild hCoVs often leads to common cold symptoms, however, individuals with severe combined immunodeficiency (SCID) may develop serious clinical symptoms and even death (9). While resolving the pandemics and therapy are important, probing and diagnosis of existing or emerging coronaviruses with potential outbreak as well as identifying the origin and intermediate hosts of coronaviruses could significantly prevent a pandemic to occur or restrict the spreading. Therefore, approaches for early diagnosis, prevention of cross transmission, and treatment of infections by multiple coronaviruses are urgently needed.

Coronavirus spike (S) protein extracellular domain (ECD) ectodomain comprises two functional subunits, S1 and S2. The S1 domain is responsible for recognition and binding to the receptor, while S2 determines the membrane fusion for viral entry into the cell (10). Different receptors recognize the S protein and mediate cell entry, such as human aminopeptidase N (APN) for HCoV-229E, angiotensin-converting enzyme 2 (ACE2) for HCoV-NL63, SARS-CoV-1, and SARS-CoV-2, and dipeptidyl peptidase 4 (DPP4) for MERS-CoV (10–14). The spike protein was shown to have multiple epitopes essential for eliciting immune responses (15), thus spike is main target of antibodies generated prophylactic and therapeutic purposes. The S2 subunit is also a potential target for neutralizing antibodies interfering with the rearrangement of the S protein and the insertion of fusion peptide, and it can be a vaccine targeted to elicit cross-immunity (16, 17). Considering that S2 is more conserved than S1, the fusion site of S2 could be an ideal target for epitope-focused vaccine development raising broadly neutralizing antibodies (nAbs) against multiple coronaviruses (10, 18).

Recently, we demonstrated that a small proportion (<8%) of the general population elicited antibodies against MERS-CoV S protein, while most of sera from COVID-19 convalescent individuals (>60%) showed binding to MERS-CoV S protein, indicating that SARS-CoV-2 infection boosted antibody response with cross-reactivity against MERS-CoV (19). Other

studies also showed that plasma IgG from COVID-19 convalescents reacted with MERS-CoV S protein (20), and the mAbs targeting S2 subunit blocked MERS-CoV infection and showed cross-reactivity with betacoronaviruses (21). A MERS-CoV S2-targeting antibody isolated from immunized mice had cross-reaction with S proteins of eight betacoronaviruses (22). In addition, blood samples from Sierra Leoneans exposed to seasonal coronavirus contained antibodies cross-reactive to both SARS-CoV-2 and MERS-CoV (23). These observations suggest that there is a possibility of isolating antibodies with broad-spectrum reactivity against multiple coronaviruses from COVID-19 convalescent individuals.

In this study, we demonstrated that the majority of serum antibodies from 60 COVID-19 convalescents reacted with MERS-CoV S2 subunit and neutralized MERS-CoV pseudovirus. We constructed and identified 11 mAbs specific to MERS-CoV S2 subunit from single memory B cells from COVID-19 convalescents, of which 9 mAbs had cross-reactivity with other seven hCoVs S proteins. This study provides a panel of antibodies with broad-spectrum reactivity, thus facilitating the development of accurate diagnosis for multiple coronavirus infections.

2 Materials and methods

2.1 Human subjects

The study protocol was approved by the Institutional Review Board of Shaoyang Central Hospital, Hunan Province, China (V.1.0, 203200301), and all subjects or their legal guardians who participated in this study provided written informed consents. All patients were identified as SARS-CoV-2 infected according to the Guidelines for the Diagnosis and Treatment of COVID-19 (v.5) published by the National Health Commission of China, combined with clinical symptoms and quantitative PCR by the local health authorities. We collected information from 60 patients discharged from Shaoyang Central Hospital from January 23, 2020 to March 2, 2020, and the peripheral blood mononuclear cells (PBMCs) were drawn from the convalescents on the 28th day after discharge (equivalent to 44-52 days after COVID-19 symptom onset) and used for antibody construction. PBMCs and sera were isolated with lymphocyte separation solution and stored in liquid nitrogen and -80°C, respectively. For serum antibody binding assays, blood from the 2nd, 5th, 8th, and 12th months after recovery were taken.

2.2 ELISA analysis of serum antibodies binding to MERS-CoV spike protein

To determine the binding of serum antibody to MERS-CoV S protein, indirect ELISA was performed using spike (S) and subunits S1 and S2 were used as coating antigens. Briefly, 96-well plates were coated with MERS-CoV S, S1, and S2 (200 ng/well; S ECD, 40069-V08B; S1, 40069-V08H; S2, 40070-V08B; Sino Biological, China) in PBS at 4°C overnight. The plates were washed five times with PBS-T (0.05% Tween-20 in PBS) and then blocked with blocking buffer (2% FBS and 2% BSA in PBS-T) at room temperature for 2 h. The serum (1:1000 dilution, 100 µl/well) was added to the well and incubated at 37°C for 1 h, followed by addition of HRP-conjugated goat anti-human IgG (1:5000 dilution, 100 µl/well; D110150-0100, Sangon Biotech, China) and incubation at 37°C for 1 h. After washing five times with PBS-T, 3,3′,5,5′-tetramethylbenzidine (TMB, 100µl/well; 34029, Thermo Fisher Scientific, USA) was added and incubated at room temperature for 5 min. The reaction was stopped with 2M H_2SO_4. The absorbance (OD_{450} nm) was measured using a microplate reader (Thermo Fisher Scientific). The ratio of OD_{450} nm for each sample relative to the negative control was calculated and the value of positive/negative >3 was defined as a positive reaction.

To determine the endpoint titer of the serum antibody, 96-well plates were coated with 200 ng/well of MERS-CoV S2 at room temperature for 2 h. After washing five times with PBS-T, the wells were incubated with blocking buffer at 4°C overnight. A 4-fold serial dilution of serum (starting from 1:800) was added to the 96-well plate and incubated at 37°C for 1 h. The 96-well plate was washed five times and detected for antibody binding to MERS-CoV S2 using a microplate reader (Thermo Fisher Scientific), as described above. All experiments were performed using human healthy control (HC) sera as negative controls.

2.3 Avidity assay of serum antibodies

The avidity of serum IgG antibody to MERS-CoV-2 S2 was measured using a modified two-step method. In the first step, the serum dilutions were optimized to obtain OD_{450} nm values in the range of 0.5-1.5, which ensures a linear measurement of antibody avidity. The second step was the ELISA procedure described above, but with or without, as required, treating the plates with 1 M sodium thiocyanate (NaSCN) for 15 min after 1 h of antibody incubation (100 µl/well). The avidity index of the antibody was calculated by equation of OD NaSCN $_{1\ M}$/OD NaSCN $_{0\ M} \times 100\%$.

2.4 Neutralization assay of serum antibodies

The neutralizing activity of the serum was determined by a reduction in luciferase expression after infection of ACE2-expressing 293T cells (ACE2-293T), developed in our lab, by the spike pseudovirus as described in a previous neutralization assay with SARS-CoV-2 pseudovirus (19). MERS-CoV-2 pseudovirus was cultured at 37°C with serial dilutions of serum samples for 1 h (dilutions, 1:30, 1:90, 1:270, 1:810, 1:2430, and 1:7290). The reaction mix was incubated with fresh ACE2-293T

cells at 5% CO_2 and 37°C for 24 h, and then the cells were lysed using 1× luciferase cell culture lysis buffer (E1510, Promega, USA), and luciferase activity was assessed using a Luciferase Assay System (E1510, Promega). The control wells containing only virus or cells were included in six replicates in parallel. Background relative light unit (RLU) values (cells only) were subtracted from each assay. Healthy control sera were used as negative controls, and guinea pig serum immunized with MERS-CoV spike protein were used as positive controls. ID_{50} was defined as a serum dilution with a 50% reduction in RLU values compared to the RLU of control solution wells (virus + cells). The cut-off value was defined as ID_{50} = 40, and ID_{50}>40 was considered a neutralization effect. Neutralization titers were log_{10}-transformed.

2.5 Neutralization of pseudovirus with mAbs

The ACE2-293T cells were plated in a 96-well plate (2×10^4 cells/well) and cultured at 37°C with 5% CO_2 for 24 h. The antibody and pseudovirus were treated before the experiment: mAbs were diluted with DMEM containing 50 μg/ml of streptomycin (strepDMEM), of which 165 μl was added to a 96-well plate in triplicate. The pseudovirus was diluted to 10000 $TCID_{50}$/ml, and 75 μl of virus was added to each well that contained antibody and then cultured at 37°C for 1 h. Virus control contained 150 μl of strepDMEM and 75 μl of pseudovirus. Cell control contained 225 μl of strepDMEM. After cell incubation, the supernatant was discarded, 70 μl of virus-antibody mixture was added and incubated at 37°C for 24 h, and then replenished with 100 μl/well and incubated for 24 h. The cell supernatant was discarded and 50 μl of cell lysate was added into a shaking table at room temperature for 30 min, of which 30 μl was added to an optical white bottom plate. Fifty microliters of luciferase reagent were added to each well to measure luciferase activity by measuring RLU. Neutralization was calculated by an equation of [1- (average RLU of test antibody sample - average RLU of cell control)/(average RLU of virus control - average RLU of cell control)] × 100% (24).

2.6 Flow cytometry isolation of single B cells

To sort out MERS-CoV S2-specific single B cell, PBMCs stored in liquid nitrogen were thawed in a 37°C water bath and immediately cultured in RPMI 1640 medium supplemented with 10% FBS in an incubator with 5% CO_2 at 37°C. To prepare fluorescent MERS-CoV S2 probes, the MERS-CoV S2 protein was conjugated to fluorescein isothiocyanate (FITC) and labeled with Alexa Fluor® 647 or Alexa Fluor® 488. For cell surface staining, 1×10^6 PBMCs were first labeled using the LIVE/DEAD Fixed Blue DEAD cell staining kit (L34962, Thermo Fisher Scientific) to distinguish live and dead cells. The treated PBMCs were immunostained with antibodies that have been diluted to the optimum concentration and incubated at 4°C for 30 min. The fluorescently labeled antibodies used were as the followings: IgG PE (G18-145, BD Biosciences, USA), IgD PE/Dazzle™ 594 (IA6-2, BioLegend, USA), CD19 percp 5.5 (HIB19, BioLegend), CD27 PE-cy7 (M-T271, BioLegend), and CD3 BUV737 (SK7, BD Bioscience). Immediately after antibody staining, samples were loaded to MoFlo XDP flow cytometer (Beckman Coulter, USA) and single B cells (S2+AF647+ and S2+AF488+) was sorted into each well of 96-well plates containing 7 μl lysis buffer (10% IGEPAL, 100 mM DTT, 40 U/μl RNAase) and placed on dry ice to freeze quickly. The antibody heavy chain and light chain mRNA were reverse transcribed and nested PCR amplified (below). The frequency of sorted S2+ B cells was analyzed using FlowJo, version 10.8.1.

2.7 Expression and purification of antibodies

The VH and VL sequences of the IgG antibodies were amplified by RT-PCR and cloned into the vector plasmids AbVec2.0-hIgG1 (80795, Adgene, USA) for expressing the heavy chain, MapAbVec1.1-IGKC (80796, Adgene) for expressing the kappa light chain, and AbVec1.1-IGLC2 (99575, Adgene) for expressing the lambda light chain. Antibody expression plasmids (0.5 μg/ml) were co-transfected into 293F cells (1×10^6 cells/ml) in SMM 293-TII expression medium (M293TII, SinoBiological) using PEI transfection reagent (23996-2, Polysciences, Pennsylvania, USA) and cultured for 6-7 days, and the cells and cell debris were removed by centrifugation at 4500 ×g and filtration (0.22 mm). The supernatant containing recombinant antibodies were purified using an ÄKTA express FPLC device using Protein A columns, washed with 20 ml of PBS, and eluted with glycine elution buffer (pH=2.0) into a collection tube containing Tris HCl (pH = 8.0). The purified antibody was dialyzed three times in PBS and stored at -40°C for later use. The purity of the antibodies were checked by running a polyacrylamide gel electrophoresis (PAGE) and visualized with Coomassie staining.

2.8 Determination of antibody binding epitopes

To distinguish whether antibodies recognize linear or discontinuous epitopes of S protein, we adopted the method previously described (21). Ninety-six-well plates were coated with MERS-CoV S2 (200 ng/well) in PBS at 4°C overnight. The plates were washed five times, and the coated-S2 was treated with or without denaturing buffer (50 μl/well; 200 mM DTT and 4% SDS in PBS) for 1 h at 37°C. After washing five times with

PBS-T, the plates were blocked with blocking buffer at RT for 2 h. The mAbs (1 μg/ml) were added to the plate (100 μl/well) and incubated at 37°C for 1 h. The plates were washed five times and then analyzed for antibody binding to MERS-CoV S2 using a microplate reader (Thermo Fisher Scientific).

2.9 mAbs binding of synthetic MERS-CoV S2 stem peptides

To determine the regions of MERS-CoV S2 potentially bound by mAbs, peptides covering the S2 region were used as coating antigen in the indirect ELISA. Briefly, peptides 15-25 amino acids (aa) were synthesized, coated to 96-well ELISA plates (20 ng/μl, 100 μl/well), and incubated at 37°C for 2 h. The plate was then washed three times with PBS-T and blocked with a blocking buffer at room temperature for 3 h. The mAb (1 μg/ml) was added to the well at 100 μl/well and incubated at 37°C for 1 h. After washing five times, the plate was incubated with the HRP-conjugated goat anti-human IgG at 37°C for 1 h. The OD_{450} nm was measured using the microplate reader. MERS-CoV S2 (2 ng/μl) was used as a positive control, and BSA protein was used as a negative control.

2.10 Data analysis

The data were processed and figures were plotted using GraphPad Prism (version 8.0).

3 Results

3.1 Serum IgG antibodies from COVID-19 convalescents reacted with MERS-CoV S2 subunit

To examine whether SARS-CoV-2 infection elicit antibodies reactive to MERS-CoV, we assessed COVID-19 convalescent sera (n=60, the 2nd month after discharge) using IgG-specific ELISAs against MERS-CoV spike (S) protein extracellular domain (ECD). Healthy donor control blood (HC, n=165) were collected before the COVID-19 pandemic (Supplementary Table S1). We found that 6.06% (10/165) of healthy sera showed binding activity to the MERS-CoV S ECD, while 66.67% (40/60) of COVID-19 convalescent sera had binding activity (Figure 1A). The binding activity of HC sera may result from previous exposures to seasonal coronavirus, eliciting cross immunity with other coronaviruses. Following SARS-CoV-2 infection, cross-reactive memory B cells were activated and secreted antibodies responsive to MERS CoV S ECD (25). Further, 20% (2/10) of the S ECD-binding healthy sera reacted with S1 subunit, but none bound with S2 (Figure 1B). In contrast, 85% (34/40) of S ECD-binding convalescent sera had binding activity to S2, and only 2.5% (1/40) had binding with S1 (Figure 1B). We also determined the endpoint titers of 34 IgG antibodies targeting MERS-CoV S2 (median, 1:12800 dilution; [$\log_{10}$ = 4.11; interquartile range [IQR], 3.81–4.71]) (Figure 1C) and found that they positively correlated with the titers of SARS-CoV-2 S2-targeting antibodies (r=0.4616, p=0.006) (Figure 1D). All 34 IgG antibodies had avidity values similarly for MERS-CoV S2 (median, 64.30; IQR, 55.59-77.18) and SARS-CoV-2 S2 SARS-CoV-2 (median, 55.04; IQR, 46.91-65.76) (Figure 1E).

To evaluate the dynamics of COVID-19 serum IgGs, we examined the binding activity and endpoint titers of the sera against MERS-CoV S2 at the 5th month (n=36), 8th month (n=39), and 12th month (n=43) after discharge. The number of MERS-CoV S2 reactive sera decreased sharply from the 2nd month to the 5th month, and only 25.64% (10/39) of sera remained reactive with S2 at the 5th month (Figure 1F). The number of S2-binding sera continually decreased to 13.95% (6/43) from the 5th to the 12th month (Figure 1F). The endpoint titers of reactive sera were 4.11, 3.98, 3.70, and 4.88 for the 2nd, 5th, 8th, and 12th months, respectively ($\log_{10}$ transformed; Figure 1G).

Next, we evaluated the neutralization of COVID-19 convalescent sera against MERS-CoV spike pseudovirus and found that 21.67% (13/60) of sera neutralized MERS-CoV pseudovirus (defined by 50% inhibitory dilution [ID_{50}] of 1.71, namely 1:51.26 dilution without $\log_{10}$ transformed; IQR, 1.69-1.75, namely 1:48.55-1:56.71 dilution) (Figure 1H and Supplementary Table S2), with ID_{50} ranging from 42 to 108 (Figure 1I). In contrast, 45% (27/60) of sera showed neutralization with SARS-CoV-2 (Figure 1H), with ID50 ranging from 113 to 3457 (Figure 1I). Taken together, these data suggest that a small proportion of the general population elicited antibodies with binding activity to MERS-CoV S ECD, of which 80% did not bind to S1 and S2 fragments; 85% of COVID-19 convalescent serum antibodies reacted with MERS-CoV S2. Few of COVID-19 convalescent IgG antibody could neutralize MERS-CoV spike pseudovirus.

3.2 mAbs constructed from COVID-19 convalescent memory B cells showed binding activity with MERS-CoV spike

The binding and neutralizing activity of COVID-19 convalescent sera with MERS-CoV urged us to construct mAbs with dual-reactivity from the convalescent memory B cells. We isolated PBMCs from 16 COVID-19 convalescents using MERS-CoV S2 probes and sorted single memory B cells (CD19+/CD3-/CD27+/IgD-/IgG+) (Figure 2A and Supplementary Table S3). Flow cytometry analysis revealed that 0.18% of COVID-19 PBMCs were memory B cells specific to MERS-CoV S2, while only 0.02% was found in healthy control PBMCs (p = 0.017) (Figure 2B and Figure S1). The variable

10.3389/fimmu.2022.1056272

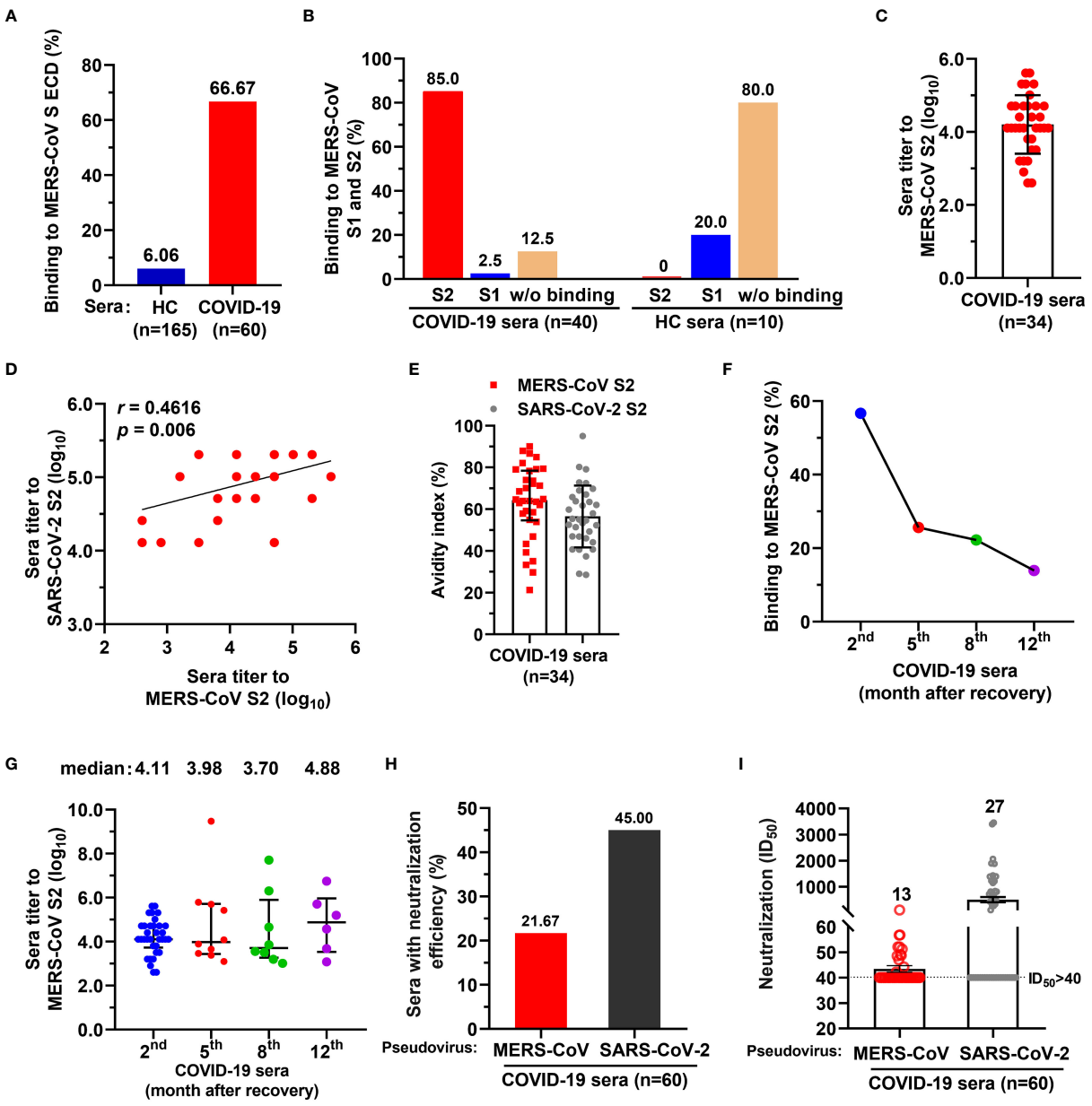

FIGURE 1
A proportion of serum antibodies from COVID-19 convalescents had binding activity to MERS-CoV spike S2 subunit and neutralized spike pseudoviruses. **(A)** A proportion of COVID-19 sera showed binding activity to MERS-CoV spike (S) extracellular domain (ECD). Sera from COVID-19 convalescents (n=60) and healthy control (HC) blood donors (n=165) (both at 1:1000 dilution) were tested for binding to MERS-CoV S ECD by ELISA. The percentage of sera binding to MERS-CoV S ECD are shown. Data are the average values from two independent experiments. **(B)** The percentage of sera from COVID-19 convalescents or HC reacted with MERS-CoV S1 and/or S2. **(C)** Endpoint titer of serum IgGs from COVID-19 convalescents against MERS-CoV S2. **(D)** Correlation coefficient of endpoint titers for antibodies reactive with MERS-CoV S2 and SARS-CoV-2 S2. Pearson's correlation, $p<0.05$ was considered statistically significant. **(E)** Avidity of COVID-19 convalescent serum antibody to MERS-CoV S2 and SARS-CoV-2 S2. **(F)** Dynamics of COVID-19 convalescent serum antibody after discharge. Binding activity of COVID-19 serum antibody against MERS-CoV S2 subunit was examined after discharge, at the 2^{nd} month (n=60), the 5^{th} month (n=39), the 8^{th} month (n=36), and 12^{th} month (n=43). **(G)** Endpoint titers of COVID-19 convalescent serum antibody for MERS-CoV S2 after discharge from hospital. The convalescent sera were tested at the 2^{nd} month (n=34), the 5^{th} month (n=10), the 8^{th} month (n=8), and 12^{th} month (n=6). One-way ANOVA with Tukey's *post hoc* test was used. **(H)** The percentage of COVID-19 convalescent serum IgG antibody with neutralizing activity for MERS-CoV and SARS-CoV-2 spike pseudoviruses. $ID_{50}>40$ was considered positive for neutralization (21.67% [13/60] and 45% [27/60], respectively). **(I)** Neutralization titers of 13 COVID-19 convalescent serum antibodies for MERS-CoV and SARS-CoV-2 spike pseudoviruses. $ID_{50}>40$ was considered positive for neutralization. For panels *C*, *D*, and *G*, endpoint titers were log_{10}-transformed; for panels *C*, *E*, *G* and *I*, data are median ± IQR (25–75%) and the error bars indicate median with interquartile range (IQR).

heavy (VH) and variable light (VL) chains of antibodies were amplified by RT-PCR, cloned, and expressed in 293F cells. A total of 38 mAbs were purified and tested for reactivity with MERS-CoV S2 proteins by single concentration qualitative ELISA (Figure 2A and Figure S2). The results showed that 11 mAbs showed binding activity to MERS-CoV S2, of which 2 mAbs also bound to S1 (Figures 2C, D).

To further determine the binding efficiency, the 11 mAbs were made into 3-fold serial dilutions and quantitatively detected by a MERS-CoV S2-coated ELISA. The results showed that 4 mAbs had potent binding activity (MSP2-34, MSP2-36, MSP5-44, and MSP6-31; EC_{50}, 0.003–0.014 μg/ml), 5 mAbs showed strong binding (MSP2-3, MSP4-33, MSP6-10, MSP6-19, and MSP6-25; EC_{50}, 0.135 - 0.516 μg/ml), and 1 mAb had moderate binding (MSP6-40; EC_{50}, 2.453 μg/ml), and 1 mAb showed weak binding activity (MSP5-45; EC_{50}, 8.810 μg/ml) to MERS-CoV S2 (Figure 2E). In addition, we also tested the binding activity to MERS-CoV S1 and found that 2 of the 11

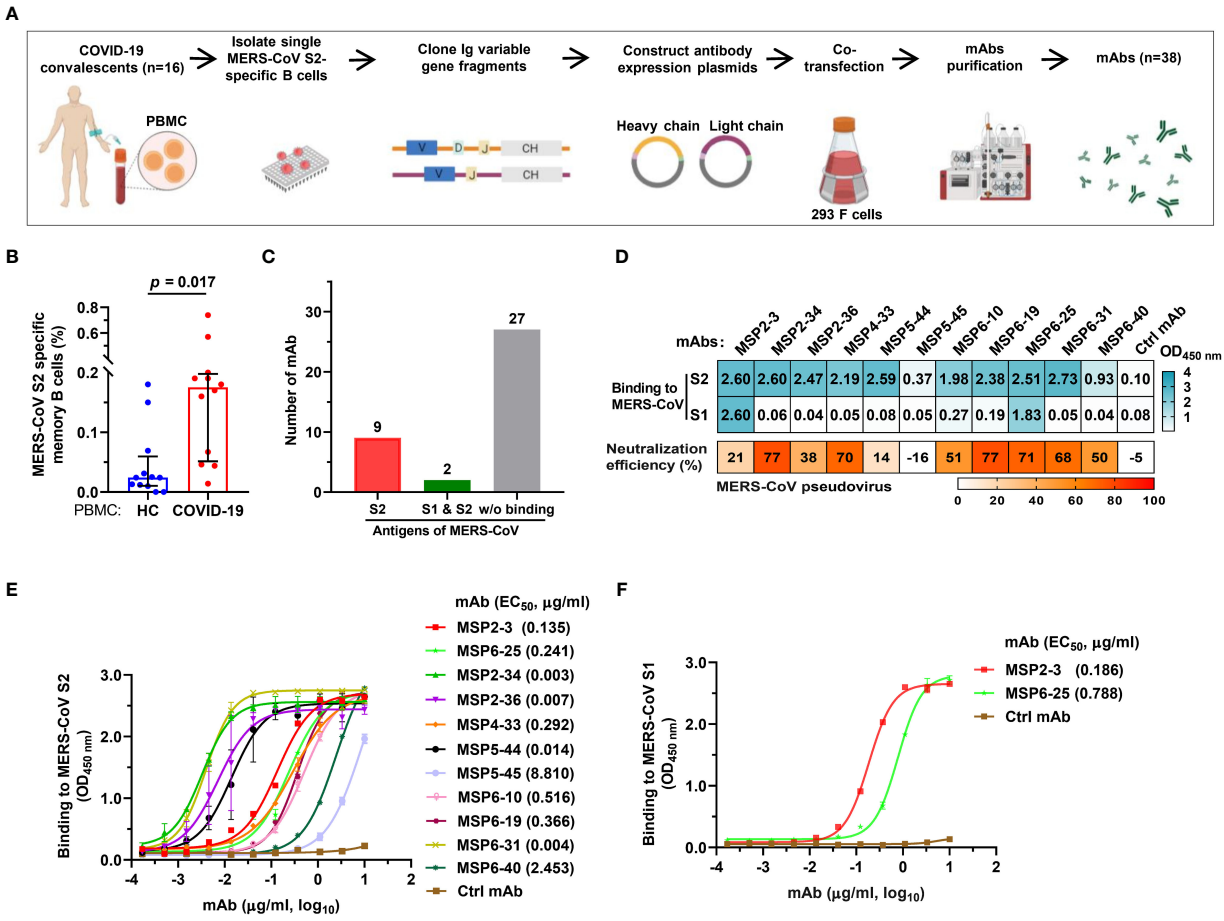

FIGURE 2
Isolation of MERS-CoV S2-specific antibodies from COVID-19 convalescent memory B cells. **(A)** The workflow of producing human monoclonal antibodies (mAbs) by cloning antibody genes from memory B cells. The memory B cells were isolated from PBMCs of 16 COVID-19 convalescents, and the variable regions of the heavy and light chains of antibodies (VH, VL/VK) were amplified from single B cells by RT-PCR and cloned into antibody expression vector plasmids. The selected VH and VL/VK clones were sequenced and co-transfected into 293F cells. The supernatants were taken after 6-7 days of culture, and the monoclonal antibodies were purified by ÄKTA Purifier. **(B)** The frequency of MERS-CoV spike S2-specific memory B cells in healthy blood donors and COVID-19 convalescents. Twelve experiments of cell screening were performed, and one healthy sample (negative control) was included in each experiment. Unpaired *t*-test was used to compare the difference between two groups, $p<0.05$ was considered for statistical significance (GraphPad Prism, version 8.0). **(C)** mAbs binding to MERS-CoV S1 and/or S2. A total of 38 mAbs constructed in this study were tested. **(D)** The binding of mAbs (1 μg/ml) to MERS-CoV S1 or S2 (cyan). The OD_{450nm}>0.3 was defined as positive. Neutralization of mAbs (50 μg/ml) against MERS-COV pseudovirus was defined as >50% infection reduction. **(E, F)** ELISA curves of antibodies binding to MERS-CoV S1 and S2. An unrelated anti-HCV mAb, 2HCV5, was used as negative control (Ctrl mAb). Error bars indicate the mean ± standard error of mean (SEM), and the data represent technical replicates of at least two independent experiments. Data were analyzed and plotted by GraphPad Prism (version 8.0).

mAbs were capable of binding with S1 (MSP2-3, EC_{50}, 0.186 μg/ml; MSP6-25, EC_{50}, 0.788 μg/ml) (Figure 2F).

Next, we tested neutralization effect on MERS-CoV pseudovirus and found that seven mAbs, MSP2-34, MSP4-33, MSP6-10, MSP6-19, MSP6-25, MSP6-31 and MSP6-40 could neutralize MERS-CoV spike pseudovirus, with infection reduction by ~50%-77% when mAbs were used up to 50 μg/mL (Figure 2D). Thus, 11 mAbs had weak neutralization effect against MERS-CoV pseudovirus.

To further characterize these antibodies, we analyzed the coding sequences of 11 mAbs using IgBLAST tool (http://www.ncbi.nlm.nih.gov/igblast/) (Table 1). The VH sequences of mAbs were from four gene classes, VH1, VH2, VH3, and VH4, and most antibodies were composed of VH3 heavy chain subgroup and kappa (κ) light chains. The average length of the antibody complementarity-determining region 3 of the heavy chain (H-CDR3) and light chains (L-CDR3) were 15 and 10 amino acids, respectively. The frequency of somatic mutations in VH and VL nucleotide sequences was within the normal range, from 5% to 14% for VH and from 5% to 13% for VL, with exception of MSP6-25 and MSP6-40, whose mutation frequency of VH and VL was from 2% to 5% (Table 1). Collectively, we have constructed a panel of mAbs from COVID-19 convalescent single B cell, of which most had reactivity with MERS-CoV S2 subunit.

3.3 Cross-reactivity of mAbs with all seven human coronaviruses

To assess whether these mAbs react with other human coronaviruses, we screened the binding of the 11 mAbs (1 μg/ml) with spike trimers of six coronaviruses by ELISA. The results showed that MSP2-3, MSP6-25, and MSP6-31 efficiently bound to all six spike proteins (OD_{450} nm >1.7), MSP2-34, MSP2-36, and MSP5-44 bound to each of SARS-CoV-1, SARS-CoV-2, OC43, and HKU1, while other mAbs showed weak or no binding to these viruses (Figure 3A). Moreover, dose-dependent ELISA revealed that MSP2-3, MSP6-25, and MSP6-31 showed broad and potent cross-reactivity with all 6 spike ECDs and MERS-CoV S2 (EC_{50}, 0.003-0.540 μg/ml) (Figures 3B–H). MSP6-10 bound potently MERS-CoV S2 and weakly with 4 spike ECDs (EC_{50} >0.55 μg/ml), and had no binding with SARS-COV-2 and NL63 (EC_{50}>10 μg/ml) (Figures 3B–G). MSP2-34, MSP2-36, and MSP5-44 displayed cross-reactivity with the spike ECDs of SARS-CoV-1, SARS-CoV-2, OC43, and HKU1 (Figures 3B–E, H). MSP4-33 and MSP6-19 did not react with other coronaviruses but MERS-CoV S2 (Figure 3A and 3H). MSP6-40 and MSP5-45 had weak cross-reaction with MERS-CoV S2, SARS-CoV-1, SARS-CoV-2, and OC43 (Figures 3A–E, H).

3.4 Binding epitope analysis of mAbs for MERS-CoV S2

Further, we proceeded to determine the antibody binding epitopes. We analyzed the binding activity of 11 mAbs against heat-denatured and untreated natural MERS-CoV S2 antigens in the presence of SDS and DTT by ELISA. The results showed that MSP2-34, MSP6-25, and MSP6-31 had good binding to both denatured and natural antigens, while other antibodies reacted with the non-denatured S2 only. These results suggest that MSP2-34, MSP6-25, and MSP6-31 recognized a continuous linear epitope in MERS-CoV S2, while the other mAbs may bind to conformational epitopes (Figure 4A). Since MSP6-25 showed binding to both MERS-CoV S1 and S2 (Figures 2D–F), we analyzed the binding epitope of MSP6-25 in the S1 and found

TABLE 1 Genetic characteristics of mAbs with reactivity against MERS-COV S1 and/or S2.

mAbs	MERS-CoV, EC_{50}(μg/mL)		Binding domain	Heavy chain			Light chain		
	S1	S2		VH gene	H-CDR3 (bp)	VH identify (%)	VL gene	L-CDR3 (bp)	VL identify (%)
MSP2-3	0.186	0.135	S1 and S2	IGHV3-74	8	89.2	IGLV2-14	10	92.9
MSP2-34	–	0.003	S2	IGHV1-46	13	91.1	IGKV1-27	11	94.1
MSP2-36	–	0.007	S2	IGHV4-59	19	86.4	IGLV2-8	10	96.9
MSP4-33	–	0.292	S2	IGHV2-5	15	90	IGKV4-1	9	86.7
MSP5-44	–	0.014	S2	IGHV3-11	20	92.5	IGKV3-11	11	90.9
MSP5-45	–	8.810	S2	IGHV3-7	16	91.6	IGKV2-30	9	95.7
MSP6-10	–	0.516	S2	IGHV3-7	16	89.2	IGKV3-20	9	89.8
MSP6-19	–	0.366	S2	IGHV3-48	12	88.2	IGLV1-44	11	92.8
MSP6-25	0.788	0.241	S1 and S2	IGHV3-11	19	97.6	IGLV2-23	13	96.2
MSP6-31	–	0.004	S2	IGHV3-30	12	94.6	IGKV1-9	9	95.1
MSP6-40	–	2.453	S2	IGHV3-7	16	95.6	IGKV2-30	9	95.3

ELISA-based half-maximal effective concentrations (EC_{50}) and genetic characterization of mAbs. Heavy and light chain genes, % difference relative to germline sequence and CDR3 length were analyzed using the IgBlast website (http://www.ncbi.nlm.nih.gov/igblast/).

10.3389/fimmu.2022.1056272

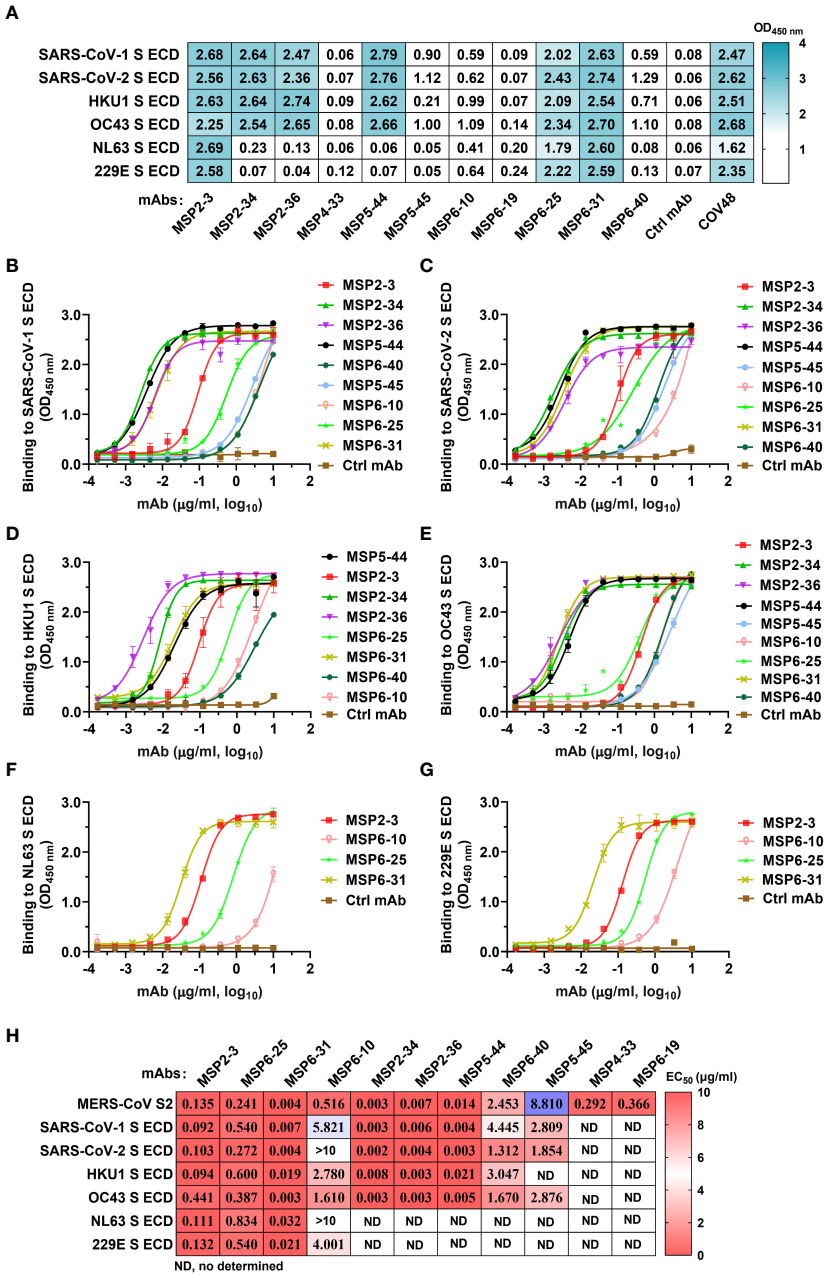

FIGURE 3
Cross-reactivity of mAbs isolated from COVID-19 convalescents with other hCoVs. **(A)** Cross-reactivity of mAbs with seven human coronaviruses (hCoVs) at a concentration of 1 μg/ml. The positive control COVID-19 serum COV48 (1:1000 dilution) and unrelated anti-HCV mAb 2HCV5 (Ctrl mAb) were used as positive and negative controls, respectively. $OD_{450\ nm}$ >0.3 was defined as a positive reaction. **(B–G)** ELISA binding curves of mAbs reactive to hCoVs S ECD (panel A). The S ECDs of SARS-CoV-1, SARS-CoV-2, HKU1, OC43, NL3, and 229E were coated at 2 μg/ml. An unrelated anti-HCV mAb 2HCV5 (Ctrl mAb) was used as a negative control. Data represent the mean ± SEM of two replicates. **(H)** The EC_{50} of mAbs binding to various spike ECD proteins. Data are calculated from panes **(B–G)**. ND, no or low reaction in single dose screening **(A)**, thus it was not determined by dose-dependent ELISA. Data were analyzed and plotted by GraphPad Prism (version 8.0).

that MSP6-25 recognizes a linear sequence of MERS-CoV S1 (Figure 4B).

Next, we attempted to analyze which regions of MERS-CoV S2 were recognized by mAbs MSP2-34, MSP6-25, and MSP6-31. We synthesized seven peptides covering the conserved regions in the S2 subunits of seven hCoVs (Figures 5A, B) and performed ELISA with three mAbs (Figure 5C and Figure S3). The results showed that only MSP2-34 had weak binding to peptide P/1229-

1243 (OD_{450} = 0.61) (Figure 5C), located in the stem helix region of MERS-CoV S2 upstream of heptapeptide repeat 2 (HR2) region (Figure 5A). MSP6-25 and MSP6-31 had no binding to peptides (Figure 5C).

4 Discussion

In recent years, sporadic cases of MERS-CoV were recorded in the Middle East, increasing the risk of spreading to other countries and regions. To date, there are not any MERS-CoV vaccine or antiviral drugs available for the prevention and treatment of MERS (26). SARS-CoV-2 is rampant around the world, with rapid emergence of various variants, causing tremendous losses to global socio-economies and public health. Therefore, there is an urgent need to develop approaches for therapy, control, and prevention of MERS-CoV and SARS-CoV-2, as well as other coronaviruses. In this study, we identified 11 out of 38 mAbs from COVID-19 convalescent individuals had binding activity to MERS-CoV S2, and 5 mAbs showed neutralizing activity for MERS-CoV spike pseudovirus. Moreover, 9 of the 11 mAbs also showed binding with SARS-CoV-2 spike ECD, as well as the other three or five hCoVs. The mAbs with broad-spectrum binding activity for CoVs contribute to the diagnosis and research for MERS-CoV and SARS-CoV-2, as well as other coronaviruses.

Coronaviruses enter the host cells through the binding of spike protein to cellular receptors. Therefore, targeting the spike protein represents the main mechanism for antibody neutralization of coronaviruses. The coronavirus S protein consist of S1 and S2 subunits; S1 subunit includes the receptor binding domain important for receptor recognition (DPP4 in the case of MERS-CoV, also known as CD26), while S2 subunit contains the fusion peptide, heptad repeats (HR) 1 and 2, and a transmembrane structural domain. These S2 domains are required for membrane fusion of the virus and host cells (27). Theoretically, antibodies targeting the conserved epitopes of coronavirus S protein have a high chance to exhibit broad neutralizing activity against multiple coronaviruses, and such antibodies are attractive for treatment and for pan-coronavirus vaccine design (28). Here, we first analyzed the serological responses of COVID-19 convalescent individuals and found that SARS-CoV-2 infection enhanced the cross-reactivity of serum antibodies to MERS-CoV spike, mainly targeting S2 subunit. This notion is supported by the positive correlation of the serum antibody titers to MERS-CoV S2 and SARS-COV-2 S2 (Figure 1D). However, it should be noted that such correlation may be partially due to the similarities in structure and sequence between SARS-CoV-2 S2 and MERS-CoV S2 that share a 45% sequence homology in the conserved S2 region. Of serum antibodies, only 21.67% (13/60) showed neutralization effect against MERS-CoV spike pseudovirus, suggesting that antibodies binding to S2 may not necessarily interfere with the binding of the DPP4 receptor (Figure 1H). Together, these data showed that COVID-19 convalescent sera could serve as better candidates for construction of mAbs neutralizing or binding to other coronaviruses.

We constructed 38 mAbs from memory B cells and found 11 mAbs with binding activity to MERS-CoV S2. Three of them, MSP2-3, MSP6-25, and MSP6-31 showed broad and potent binding activity to all other hCoVs, while MSP2-34, MSP2-36, and MSP5-44 bound only to beta-coronaviruses (Figure 3H). In addition, 5 mAbs (MSP2-34, MSP4-33, MSP6-19, MSP6-25, and MSP6-31) showed weak neutralization effect to MERS-CoV pseudovirus. Given the reactivity to multiple coronaviruses, these mAbs, singly or in combination, could be useful in the development of diagnosis methods distinguishing MERS-CoV and other coronaviruses.

Antibody binding epitopes could be linear and conformational, with about 10% of antibodies recognizing linear epitopes (29). Three mAbs recognized linear epitopes, and 8 mAbs bound to conformational epitopes (Figure 4A). It has been reported that

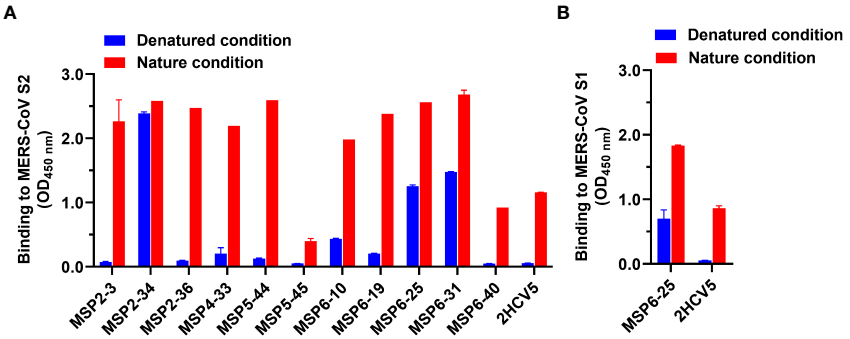

FIGURE 4
Analysis of binding epitopes of mAbs. **(A)** Binding of mAbs (1 μg/ml) to MERS-CoV S2 in non-treated nature condition and heat-denatured condition (37°C, 1 h, in the presence of SDS and DTT, blue). An unrelated conformational anti-HCV mAb 2HCV5 was used as a control, to which the coating antigen was HCV E2 protein. **(B)** Binding of antibody MSP6-25 (1 μg/ml) to MERS-CoV S1 in nature condition and in heat-denatured condition in the presence of SDS and DTT (blue). Data were analyzed and plotted by GraphPad Prism (version 8.0).

10.3389/fimmu.2022.1056272

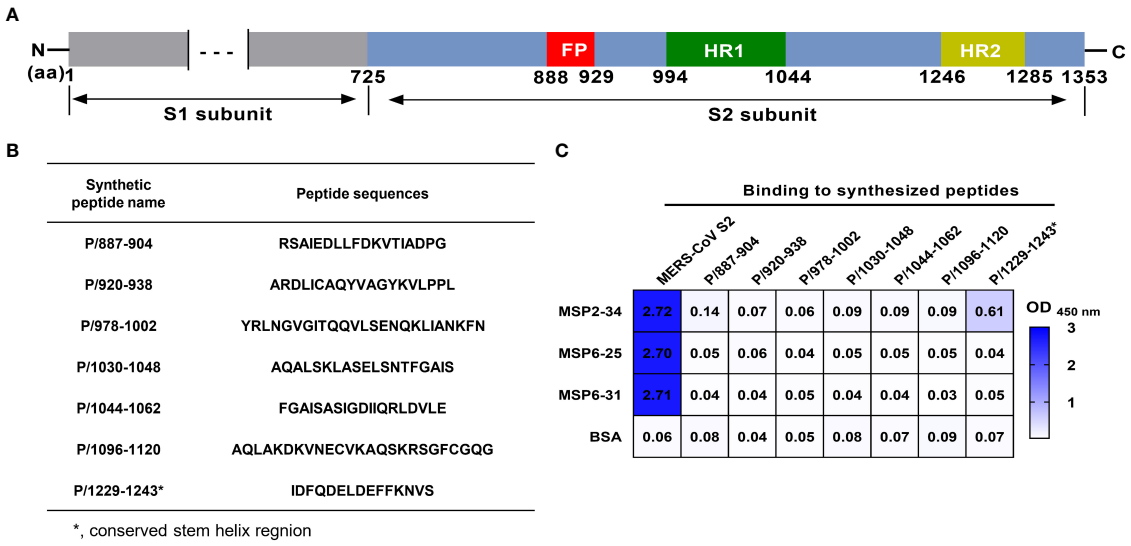

FIGURE 5
Binding of mAbs to different synthetic MERS-CoV S2 peptides. **(A)** Diagram of MERS-CoV S protein. Amino acid (aa) positions are referred to the sequence of strain HCoV-EMC (GenBank: AFS88936.1). **(B)** Amino acid sequence of peptides. **(C)** Binding of mAbs MSP2-34, MSP6-25, and MSP6-31 (1 μg/ml) to synthetic peptides (20 ng/μl) by ELISA. MERS-CoV S2 subunit (2 μg/ml) was positive control. BSA was used as negative control.

antibodies targeting the S2 stem region could neutralize MERS-CoV pseudovirus, as the antibody binding obstructed the formation of the hexa-helix bundle of spike proteins during fusion step of virus entry (21, 22). The other antibody 76E1 was reported to target the conserved S2' site of SARS-CoV-2 spike protein and inhibits S2' cleavage, thus blocking membrane fusion and virus entry (30). However, antibodies MSP2-34, MSP6-25, and MSP6-31, targeting linear epitopes, bound efficiently to multiple coronaviruses (Figures 2–4), though they had a low neutralization efficiency to MERS-CoV spike pseudovirus (Figure 2D). Several key residues have been reported to be involved in antibody-antigen interactions; they are imbedded fully or partially in pre-fusion S trimers and go through conformational changes from pre-fusion to post-fusion states of the viral S-trimers, thus leading to epitope exposure and binding of neutralizing antibodies (30–32). The weaker neutralization of MSP2-34, MSP6-25, and MSP6-31 may result from a limited epitope exposure of the S protein. However, further analysis of these S2-specific antibodies is needed.

Although mechanism of action of non-neutralizing antibodies is complex or unknown, nine broadly reactive antibodies constructed here are of great value in the diagnosis and prevention of early viral infections. Binding of antibody Fab fragments to viral antigens forms antigen-antibody immune complexes, and the antibody Fc fragment mediates antiviral function by binding to the Fc receptor (FcγRs) on natural immune cells through antibody-dependent cellular cytotoxicity (ADCC), complement-dependent cytotoxicity (CDC), or antibody-dependent cell phagocytosis (ADCP) (33, 34). It has been shown that non-neutralizing antibodies that target Ebola virus and respiratory syncytial virus could mediate ADCC effects and lead to a promising outcome in virus-infected mice (35, 36). In addition, non-neutralizing antibodies binding to conserved viral epitopes could trigger ADCC and thus result in a broad cross-protective response (37, 38). Due to the antiviral pressure, viruses tend to evade neutralizing antibody responses. Thus, the cross-protective immune responses that non-neutralizing antibodies may have would be particularly important.

In summary, we generated mAbs with specific binding activity to all seven human coronaviruses. These antibodies will facilitate future studies on neutralizing and binding antibodies against multiple coronaviruses, as well as vaccine design for pan-coronaviruses. Given broad-reactivity of these antibodies, more mAbs from COVID-19 convalescents, epitope analysis, and structure-guided antibody engineering will be of great interest.

Data availability statement

The original contributions presented in the study are included in the article/Supplementary Material. Further inquiries can be directed to the corresponding authors.

Author contributions

YP, YL, YH, XQ, and Y-PL contributed to the study design and data interpretation. YP, YL, YH, FC, QW, JY, JC, ST JZ, RH,

XQ, and Y-PL contributed to clinical management, patient recruitment and data collection. YP,YL, YH, FC, JZ, RH, YW, MB, TL, and WL contributed to statistical analysis and data visualization. YP, YL, Y-PL drafted the manuscript. MB, XQ and Y-PL contributed to revision of the manuscript for important intellectual content. All authors contributed to the article and approved the submitted version.

Funding

This work was supported by the SC1-PHE-CORONAVIRUS-2020: Advancing Knowledge for the Clinical and Public Health Response to the 2019-nCoV Epidemic' from the European Commission (CORONADX, no. 101003562, to Y-PL), National Natural Science Foundation of China (82061138020, 32270996, 82102365), The Science and Technology Innovation Program of Hunan Province of China (2022RC3079), Natural Science Foundation of Hunan Province of China (2021JJ40006, 2022JJ30095), Educational Commission of Hunan Province of China (21A0529), Clinical Medical Innovation Technology Guide Project of Hunan Province (2021SK50304, 2021SK50306 and 2021SK50312).

Acknowledgments

We thank all the donors enrolled in this study.

Conflict of interest

The authors declare that the research was conducted in the absence of any commercial or financial relationships that could be construed as a potential conflict of interest.

Publisher's note

Supplementary material

The Supplementary Material for this article can be found online at: https://www.frontiersin.org/articles/10.3389/fimmu.2022.1056272/full#supplementary-material

SUPPLEMENTARY FIGURE 1
Gating strategy for isolating MERS-CoV spike S2-specific memory B cells from COVID-19 convalescents. PBMC of COVID-19 convalescents were first stained with LIVE/DEAD and CD3/CD19 -specific antibodies to exclude T cells and monocytes. Then, CD27/IgD/IgG antibodies were used to select mature B cells. Two probes MRES-CoV S2-AF488 and S2-AF647 were used to select MERS-CoV S2-specific memory B cells. Single B cell position for $S2^+/AF647^+$ and $S2^+/AF488^+$ was sorted into 96-well plates for construction of mAbs.

SUPPLEMENTARY FIGURE 2
The purity of mAbs by using PAGE. The mAbs constructed in this study were purified by AKTA and PFLC approaches. The purity of mAbs was checked by PAGE with Coomassie staining. The evelen mAbs with binding to MERS-CoV S2 are showen.

SUPPLEMENTARY FIGURE 3
Amino acid sequence alignment of the stem region of spike proteins of seven hCoVs. The alignment was performed using spike protein sequences: MERS-CoV (GenBank accession number: AFS88936.1), SARS-CoV-2 (NCBI Reference Sequence: YP_009724390.1), SARS-CoV (NCBI Reference Sequence: NP_828851.1), OC43 (GenBank: AVR40344.1), HKU1 (UniProtKB/Swiss-Prot: Q0ZME7.1), NL63 (GenBank: APF29071.1), and 229E (GenBank: APT69883.1). Sequence alignment was performed using CLUSTALW (Clustal Omega < Multiple Sequence Alignment < EMBL-EBI) and visualized using ESPript 3.0 (ESPript 3.x/ENDscript 2.x).

References

1. de Wit E, van Doremalen N, Falzarano D, Munster VJ. Sars and mers: Recent insights into emerging coronaviruses. *Nat Rev Microbiol* (2016) 14(8):523–34. doi: 10.1038/nrmicro.2016.81

2. Cui J, Li F, Shi ZL. Origin and evolution of pathogenic coronaviruses. *Nat Rev Microbiol* (2019) 17(3):181–92. doi: 10.1038/s41579-018-0118-9

3. Colina SE, Serena MS, Echeverría MG, Metz GE. Clinical and molecular aspects of veterinary coronaviruses. *Virus Res* (2021) 297:198382. doi: 10.1016/j.virusres.2021.198382

4. World Health Organization. *Mers situation update (August 2022)*. Available at: http://www.emro.who.int/health-topics/MERS-CoV/mers-outbreaks.html.

5. World Health Organization. *Covid-19 outbreaks (2022, august 30)*. Available at: http://www.emro.who.int/pandemic-epidemic-diseases/outbreaks/index.html.

6. Guan WJ, Zhong NS. Clinical characteristics of covid-19 in China. *Reply N Engl J Med* (2020) 382(19):1861–2. doi: 10.1056/NEJMc2005203

7. O'Driscoll M, Ribeiro Dos Santos G, Wang L, Cummings DAT, Azman AS, Paireau J, et al. Age-specific mortality and immunity patterns of sars-Cov-2. *Nature* (2021) 590(7844):140–5. doi: 10.1038/s41586-020-2918-0

8. Oishi K, Horiuchi S, Minkoff JM, tenOever BR. The host response to influenza a virus interferes with sars-Cov-2 replication during coinfection. *J Virol* (2022) 96(15):e0076522. doi: 10.1128/jvi.00765-22

9. Morfopoulou S, Brown JR, Davies EG, Anderson G, Virasami A, Qasim W, et al. Human coronavirus Oc43 associated with fatal encephalitis. *N Engl J Med* (2016) 375(5):497–8. doi: 10.1056/NEJMc1509458

10. Walls AC, Park YJ, Tortorici MA, Wall A, McGuire AT, Veesler D. Structure, function, and antigenicity of the sars-Cov-2 spike glycoprotein. *Cell* (2020) 181(2):281–92.e6. doi: 10.1016/j.cell.2020.02.058

11. V'Kovski P, Kratzel A, Steiner S, Stalder H, Thiel V. Coronavirus biology and replication: Implications for sars-Cov-2. *Nat Rev Microbiol* (2021) 19(3):155–70. doi: 10.1038/s41579-020-00468-6

12. Wang N, Shi X, Jiang L, Zhang S, Wang D, Tong P, et al. Structure of mers-cov spike receptor-binding domain complexed with human receptor Dpp4. *Cell Res* (2013) 23(8):986–93. doi: 10.1038/cr.2013.92

13. Yeager CL, Ashmun RA, Williams RK, Cardellichio CB, Shapiro LH, Look AT, et al. Human aminopeptidase n is a receptor for human coronavirus 229e. *Nature* (1992) 357(6377):420–2. doi: 10.1038/357420a0

14. Wu K, Li W, Peng G, Li F. Crystal structure of Nl63 respiratory coronavirus receptor-binding domain complexed with its human receptor. *Proc Natl Acad Sci USA* (2009) 106(47):19970–4. doi: 10.1073/pnas.0908837106

15. Arashkia A, Jalilvand S, Mohajel N, Afchangi A, Azadmanesh K, Salehi-Vaziri M, et al. Severe acute respiratory syndrome-Coronavirus-2 spike (S) protein based vaccine candidates: State of the art and future prospects. *Rev Med Virol* (2021) 31(3):e2183. doi: 10.1002/rmv.2183

16. Dai L, Gao GF. Viral targets for vaccines against covid-19. *Nat Rev Immunol* (2021) 21(2):73–82. doi: 10.1038/s41577-020-00480-0

17. Ng KW, Faulkner N, Cornish GH, Rosa A, Harvey R, Hussain S, et al. Preexisting and *De novo* humoral immunity to sars-Cov-2 in humans. *Science* (2020) 370(6522):1339–43. doi: 10.1126/science.abe1107

18. Walls AC, Tortorici MA, Bosch BJ, Frenz B, Rottier PJM, DiMaio F, et al. Cryo-electron microscopy structure of a coronavirus spike glycoprotein trimer. *Nature* (2016) 531(7592):114–7. doi: 10.1038/nature16988

19. Zhang J, Wu Q, Liu Z, Wang Q, Wu J, Hu Y, et al. Spike-specific circulating T follicular helper cell and cross-neutralizing antibody responses in covid-19-Convalescent individuals. *Nat Microbiol* (2021) 6(1):51–8. doi: 10.1038/s41564-020-00824-5

20. Barnes CO, West APJr., Huey-Tubman KE, Hoffmann MAG, Sharaf NG, Hoffman PR, et al. Structures of human antibodies bound to sars-Cov-2 spike reveal common epitopes and recurrent features of antibodies. *Cell* (2020) 182 (4):828–42.e16. doi: 10.1016/j.cell.2020.06.025

21. Wang C, van Haperen R, Gutiérrez-Álvarez J, Li W, Okba NMA, Albulescu I, et al. A conserved immunogenic and vulnerable site on the coronavirus spike protein delineated by cross-reactive monoclonal antibodies. *Nat Commun* (2021) 12(1):1715. doi: 10.1038/s41467-021-21968-w

22. Sauer MM, Tortorici MA, Park YJ, Walls AC, Homad L, Acton OJ, et al. Structural basis for broad coronavirus neutralization. *Nat Struct Mol Biol* (2021) 28 (6):478–86. doi: 10.1038/s41594-021-00596-4

23. Borrega R, Nelson DKS, Koval AP, Bond NG, Heinrich ML, Rowland MM, et al. Cross-reactive antibodies to sars-Cov-2 and mers-cov in pre-Covid-19 blood samples from Sierra leoneans. *Viruses* (2021) 13(11):2325. doi: 10.3390/v13112325

24. Nie J, Li Q, Wu J, Zhao C, Hao H, Liu H, et al. Quantification of sars-Cov-2 neutralizing antibody by a pseudotyped virus-based assay. *Nat Protoc* (2020) 15 (11):3699–715. doi: 10.1038/s41596-020-0394-5

25. Song G, He WT, Callaghan S, Anzanello F, Huang D, Ricketts J, et al. Cross-reactive serum and memory b-cell responses to spike protein in sars-Cov-2 and endemic coronavirus infection. *Nat Commun* (2021) 12(1):2938. doi: 10.1038/s41467-021-23074-3

26. World Health Organization. *Middle East respiratory syndrome (August 2022)*. Available at: https://www.emro.who.int/health-topics/mers-cov/mers-cov.html.

27. Wec AZ, Wrapp D, Herbert AS, Maurer DP, Haslwanter D, Sakharkar M, et al. Broad neutralization of sars-related viruses by human monoclonal antibodies. *Science* (2020) 369(6504):731–6. doi: 10.1126/science.abc7424

28. Burton DR, Walker LM. Rational vaccine design in the time of covid-19. *Cell Host Microbe* (2020) 27(5):695–8. doi: 10.1016/j.chom.2020.04.022

29. Van Regenmortel MHV. Mapping epitope structure and activity: From one-dimensional prediction to four-dimensional description of antigenic specificity. *Methods* (1996) 9(3):465–72. doi: 10.1006/meth.1996.0054

30. Sun X, Yi C, Zhu Y, Ding L, Xia S, Chen X, et al. Neutralization mechanism of a human antibody with pan-coronavirus reactivity including sars-Cov-2. *Nat Microbiol* (2022) 7(7):1063–74. doi: 10.1038/s41564-022-01155-3

31. Fan X, Cao D, Kong L, Zhang X. Cryo-em analysis of the post-fusion structure of the sars-cov spike glycoprotein. *Nat Commun* (2020) 11(1):3618. doi: 10.1038/s41467-020-17371-6

32. Benton DJ, Wrobel AG, Xu P, Roustan C, Martin SR, Rosenthal PB, et al. Receptor binding and priming of the spike protein of sars-Cov-2 for membrane fusion. *Nature* (2020) 588(7837):327–30. doi: 10.1038/s41586-020-2772-0

33. Ali MG, Zhang Z, Gao Q, Pan M, Rowan EG, Zhang J. Recent advances in therapeutic applications of neutralizing antibodies for virus infections: An overview. *Immunol Res* (2020) 68(6):325–39. doi: 10.1007/s12026-020-09159-z

34. Yassine HM, Boyington JC, McTamney PM, Wei CJ, Kanekiyo M, Kong WP, et al. Hemagglutinin-stem nanoparticles generate heterosubtypic influenza protection. *Nat Med* (2015) 21(9):1065–70. doi: 10.1038/nm.3927

35. Hiatt A, Bohorova N, Bohorov O, Goodman C, Kim D, Pauly MH, et al. Glycan variants of a respiratory syncytial virus antibody with enhanced effector function and in vivo efficacy. *Proc Natl Acad Sci U S A* (2014) 111(16):5992–7. doi: 10.1073/pnas.1402458111

36. Zeitlin L, Pettitt J, Scully C, Bohorova N, Kim D, Pauly M, et al. Enhanced potency of a fucose-free monoclonal antibody being developed as an Ebola virus immunoprotectant. *Proc Natl Acad Sci U S A* (2011) 108(51):20690–4. doi: 10.1073/pnas.1108360108

37. Jegaskanda S, Job ER, Kramski M, Laurie K, Isitman G, de Rose R, et al. Cross-reactive influenza-specific antibody-dependent cellular cytotoxicity antibodies in the absence of neutralizing antibodies. *J Immunol* (2013) 190 (4):1837–48. doi: 10.4049/jimmunol.1201574

38. Manicassamy B, Medina RA, Hai R, Tsibane T, Stertz S, Nistal-Villan E, et al. Protection of mice against lethal challenge with 2009 H1n1 influenza a virus by 1918-like and classical swine H1n1 based vaccines. *PLoS Pathog* (2010) 6(1): e1000745. doi: 10.1371/journal.ppat.1000745

frontiers | Frontiers in Immunology

TYPE Original Research
PUBLISHED 11 January 2023
DOI 10.3389/fimmu.2022.1049458

OPEN ACCESS

EDITED BY
Aristo Vojdani
Immunosciences Lab., Inc.
United States

REVIEWED BY
Amruta Naik,
University of Pennsylvania,
United States
Alexander Chen,
California State University, Dominguez Hills, United States
Mark Forest,
University of North Carolina at Chapel Hill, United States

*CORRESPONDENCE
Robin N. Thompson
robin.n.thompson@warwick.ac.uk

†These authors have contributed equally to this work

SPECIALTY SECTION
This article was submitted to Viral Immunology, a section of the journal Frontiers in Immunology

RECEIVED 20 September 2022
ACCEPTED 05 December 2022
PUBLISHED 11 January 2023

CITATION
Thompson RN, Southall E, Daon Y, Lovell-Read FA, Iwami S, Thompson CP and Obolski U (2023) The impact of cross-reactive immunity on the emergence of SARS-CoV-2 variants. *Front. Immunol.* 13:1049458. doi: 10.3389/fimmu.2022.1049458

The impact of cross-reactive immunity on the emergence of SARS-CoV-2 variants

Robin N. Thompson[1,2*], Emma Southall[1,2], Yair Daon[3,4], Francesca A. Lovell-Read[5], Shingo Iwami[6], Craig P. Thompson[7†] and Uri Obolski[3,4†]

[1]Mathematics Institute, University of Warwick, Coventry, United Kingdom, [2]Zeeman Institute for Systems Biology and Infectious Disease Epidemiology Research, University of Warwick, Coventry, United Kingdom, [3]School of Public Health, Faculty of Medicine, Tel Aviv University, Tel Aviv, Israel, [4]Porter School of the Environment and Earth Sciences, Faculty of Exact Sciences, Tel Aviv University, Tel Aviv, Israel, [5]Mathematical Institute, University of Oxford, Oxford, United Kingdom, [6]Division of Natural Science, Graduate School of Science, Nagoya University, Nagoya, Japan, [7]Division of Biomedical Sciences, Warwick Medical School, University of Warwick, Coventry, United Kingdom

Introduction: A key feature of the COVID-19 pandemic has been the emergence of SARS-CoV-2 variants with different transmission characteristics. However, when a novel variant arrives in a host population, it will not necessarily lead to many cases. Instead, it may fade out, due to stochastic effects and the level of immunity in the population. Immunity against novel SARS-CoV-2 variants may be influenced by prior exposures to related viruses, such as other SARS-CoV-2 variants and seasonal coronaviruses, and the level of cross-reactive immunity conferred by those exposures.

Methods: Here, we investigate the impact of cross-reactive immunity on the emergence of SARS-CoV-2 variants in a simplified scenario in which a novel SARS-CoV-2 variant is introduced after an antigenically related virus has spread in the population. We use mathematical modelling to explore the risk that the novel variant invades the population and causes a large number of cases, as opposed to fading out with few cases.

Results: We find that, if cross-reactive immunity is complete (i.e. someone infected by the previously circulating virus is not susceptible to the novel variant), the novel variant must be more transmissible than the previous virus to invade the population. However, in a more realistic scenario in which cross-reactive immunity is partial, we show that it is possible for novel variants to invade, even if they are less transmissible than previously circulating viruses. This is because partial cross-reactive immunity effectively increases the pool of susceptible hosts that are available to the novel variant compared to complete cross-reactive immunity. Furthermore, if previous infection with the antigenically related virus assists the establishment of infection with the novel variant, as has

been proposed following some experimental studies, then even variants with very limited transmissibility are able to invade the host population.

Discussion: Our results highlight that fast assessment of the level of cross-reactive immunity conferred by related viruses against novel SARS-CoV-2 variants is an essential component of novel variant risk assessments.

KEYWORDS

cross-reactive immunity, mathematical modelling, infectious disease epidemiology, SARS-CoV-2, COVID-19, variants, emergence

1 Introduction

When a new SARS-CoV-2 variant first arrives in a host population, a key question for policy makers is whether or not it will become widespread. For this to occur, two steps are required: introduction and invasion. First, the variant must arrive in the host population, either through *de novo* mutation or importation from elsewhere (introduction). Second, the variant must then spread from person to person and cause a large number of cases, as opposed to fading out with few cases (invasion). Following introduction, a range of factors affect the risk that a novel variant will invade, including its inherent transmissibility and the connectivity of the location in which it is introduced (1, 2). An additional crucial factor in this process is the background level of immunity to the new variant in the host population. For example, a feature of the Omicron (B.1.1.529) variant that allowed it to become widespread is its ability to evade immunity from past infection or vaccination, at least partially, meaning that the background immunity level was low (3–5).

Mathematical modelling has often been used to explore the impact of cross-reactive immunity between pathogen strains on the dynamics of infectious disease outbreaks (6–11). During the COVID-19 pandemic, models have provided real-time insights into the risk posed by novel variants. For example, Bhatia et al. (12) extended existing methods for estimating pathogen transmissibility (13–15) to enable the transmissibility of novel variants to be assessed, including estimating the infectiousness of the Alpha (B.1.1.7), Beta (B.1.351) and Gamma (P.1) variants relative to the wild type virus (the SARS-CoV-2 virus that first emerged in Wuhan, China). Dyson et al. (16) analysed epidemiological data from England, and projected the course of the outbreak in that country if a variant emerged with different transmission characteristics. They warned that a variant with high transmissibility or substantial immune escape properties had the potential to generate large numbers of infections and hospitalisations.

Meanwhile, experimental and statistical studies have explored the effects of prior infections with related viruses on infections with different SARS-CoV-2 variants. Some studies have found previous infections with other SARS-CoV-2 variants to have a protective effect. For example, Wratil et al. (17) demonstrated that a combination of infection and vaccination induced hybrid immunity is protective against SARS-CoV-2 variants including the Omicron variant. A recent analysis of infection data from Portugal found that previous SARS-CoV-2 infections were protective against infection with the BA.5 Omicron subvariant, with the level of protection particularly high in individuals who were previously infected by the BA.1 or BA.2 Omicron subvariants (18). However, some studies have indicated that prior infection with other SARS-CoV-2 variants may instead have a detrimental effect on subsequent infections with novel SARS-CoV-2 variants. For example, earlier infection with the SARS-CoV-2 wild type was found to inhibit the immune response to infections with the Omicron variant among triple-vaccinated healthcare workers (5).

Similarly to the cross-reactive immunity conferred by other SARS-CoV-2 variants, the impact of prior infections with seasonal coronaviruses on subsequent infections by SARS-CoV-2 is also unclear. Some analyses have found that previous infections with seasonal coronaviruses are likely to be protective against SARS-CoV-2 infection. The SARS-CoV-2 spike protein can be divided into the S1 and S2 subunits. The S1 subunit contains an antigenically variable receptor binding domain, while the S2 subunit is more conserved between coronaviruses. Kaplonek et al. (19) showed that SARS-CoV-2 S2 antibody responses are associated with milder COVID-19 symptoms, suggesting that previous infection with seasonal coronaviruses may lead to COVID-19 infections being less severe. Furthermore, strong and multispecific cross-reactive T-cell responses induced by seasonal coronavirus infection prior to SARS-CoV-2 infection have been associated with protection against SARS-CoV-2 infection in seronegative healthcare workers (5, 20).

In contrast, there is also evidence that previous infections with seasonal coronaviruses can have detrimental effects on susceptibility to and outcomes of infection with SARS-CoV-2. With respect to disease outcomes, McNaughton et al. (21) showed that prior immunity to seasonal coronaviruses was positively associated with fatal outcomes in individuals with severe COVID-19. Similar results were found by Smit et al. (22) in an independent cohort. Conflicting results to Kaplonek et al. (19) were found by Garrido et al. (23), who found that S2 antibody responses were associated with greater disease severity. With respect to susceptibility, Wratil et al. (24) demonstrated that cross-reactive immunity imparted by seasonal coronaviruses may increase susceptibility to SARS-CoV-2. Additionally, a modelling analysis by Pinotti et al. (25) has suggested that the general trend of increased severity of SARS-CoV-2 infections in older individuals may be explained by an increased chance that older individuals have been exposed to seasonal coronaviruses.

Given this conflicting evidence in the literature, and to help understand the possible effects of prior infections on the risk of emergence of SARS-CoV-2 variants, in this study we develop a mathematical model considering two viruses: a novel SARS-CoV-2 variant and an antigenically related virus that has previously spread in the population. We investigate the factors affecting the risk that the novel variant invades the host population. We assume that infection with the previously circulating virus affects the chance of successful infection with, and subsequent transmission of, the novel variant, considering scenarios in which prior infection is either protective (partially or completely) or detrimental. We show that the level of cross-reactive immunity between novel SARS-CoV-2 variants and antigenically related viruses is a key factor determining whether or not a novel variant will invade the host population. This highlights the need to conduct a rapid assessment of the level of cross-reactive immunity between previously circulating viruses and newly emerged SARS-CoV-2 variants whenever a novel SARS-CoV-2 variant is introduced into a new host population.

2 Methods

2.1 Epidemiological model

We consider the introduction of a novel variant to a population consisting of N hosts. We assume that prior immunity has been conferred by infections with a related virus that has already spread within the host population. Assuming that this previously circulating virus follows dynamics that are characterised by the standard (deterministic) SEIR model, the number of individuals in the population who have been previously infected by that virus is given by the solution, N_p, to the final size equation (8),

$$N_p = N - Ne^{\frac{-R_{0p}N_p}{N}} \quad (1)$$

In this expression, R_{0p} is the reproduction number of the previously circulating virus, which we assume accounts for any interventions that were introduced (prior to, or immediately after, its arrival in the host population) to limit its spread. We assume that N_p individuals were previously infected by that virus (we round N_p to the nearest integer value), and the remaining $N–N_p$ individuals in the population are immunologically naïve (i.e. they do not carry any immunity against the novel variant). The dependence of N_p on R_{0p} is shown in Figure S1.

We then model the emergence of the novel variant. If an individual has previously been infected by the related virus, their susceptibility to the novel variant is assumed to be modified by a multiplicative factor $1–\alpha$ (relative to the susceptibility of a host who has not previously been infected by the related virus). Consequently, if $\alpha > 0$, prior infection with the related virus is protective against infection with the novel variant. If instead $\alpha = 0$, then earlier infection with the related virus does not affect the risk of infection with the novel variant. If $\alpha < 0$, earlier infection with the related virus promotes infection with the novel variant. Similarly, the infectiousness of a host infected with the novel variant who has previously been infected by the related virus is modified by a multiplicative factor $1–\epsilon$ (relative to the infectiousness of a host who has not previously been infected by the related virus). Again, positive (negative) values of ϵ reflect scenarios in which prior infection with the related virus reduces (increases) the infectiousness of an individual who is infected with the novel variant.

Transmission dynamics for the novel variant are also modelled using an SEIR model, but with two main differences compared to the dynamics of the previously circulating virus. First, the SEIR model for the novel variant is extended to account for cross-reactive immunity conferred by the related virus. Second, since we are modelling invasion, we use a stochastic model in which, in each simulation of the model, the novel variant may either invade the host population or fade out with few infections. The analogous deterministic model to the stochastic model that we consider for the novel variant is given by:

$$\frac{dS_n}{dt} = -\beta I_n S_n - \beta(1-\epsilon) I_p S_n,$$

$$\frac{dE_n}{dt} = \beta I_n S_n + \beta(1-\epsilon) I_p S_n - \gamma E_n,$$

$$\frac{dI_n}{dt} = \gamma E_n - \mu I_n,$$

$$\frac{dR_n}{dt} = \mu I_n,$$

10.3389/fimmu.2022.1049458

$$\frac{dS_p}{dt} = -\beta(1-\alpha)I_nS_p - \beta(1-\epsilon)(1-\alpha)I_pS_p,$$

$$\frac{dE_p}{dt} = \beta(1-\alpha)I_nS_p + \beta(1-\epsilon)(1-\alpha)I_pS_p - \gamma E_p,$$

$$\frac{dI_p}{dt} = \gamma E_p - \mu I_p,$$

$$\frac{dR_p}{dt} = \mu I_p. \quad (2)$$

In these equations, the variables S_n, E_n, I_n and R_n refer to the infection status (with the novel variant) of individuals who have not been infected previously by the related virus, and S_p, E_p, I_p and R_p refer to the infection status of individuals who have previously been infected by the related virus. A schematic illustrating the transitions of individuals between these states, and the rates at which those transitions occur, is shown in Figure 1A. The parameter β is the infection rate parameter, and the mean latent period and infectious period are $1/\gamma$ days and $1/\mu$ days, respectively. We define the reproduction number of the novel variant to be $R_{0n} = \frac{\beta N}{\mu}$, reflecting the transmission potential of the novel variant if the host population is entirely immunologically naïve. For a full description of the stochastic model, see Text S1.

2.2 Risk of invasion

As noted above, since we are interested in the risk of invasion of the novel variant, we use the analogous stochastic

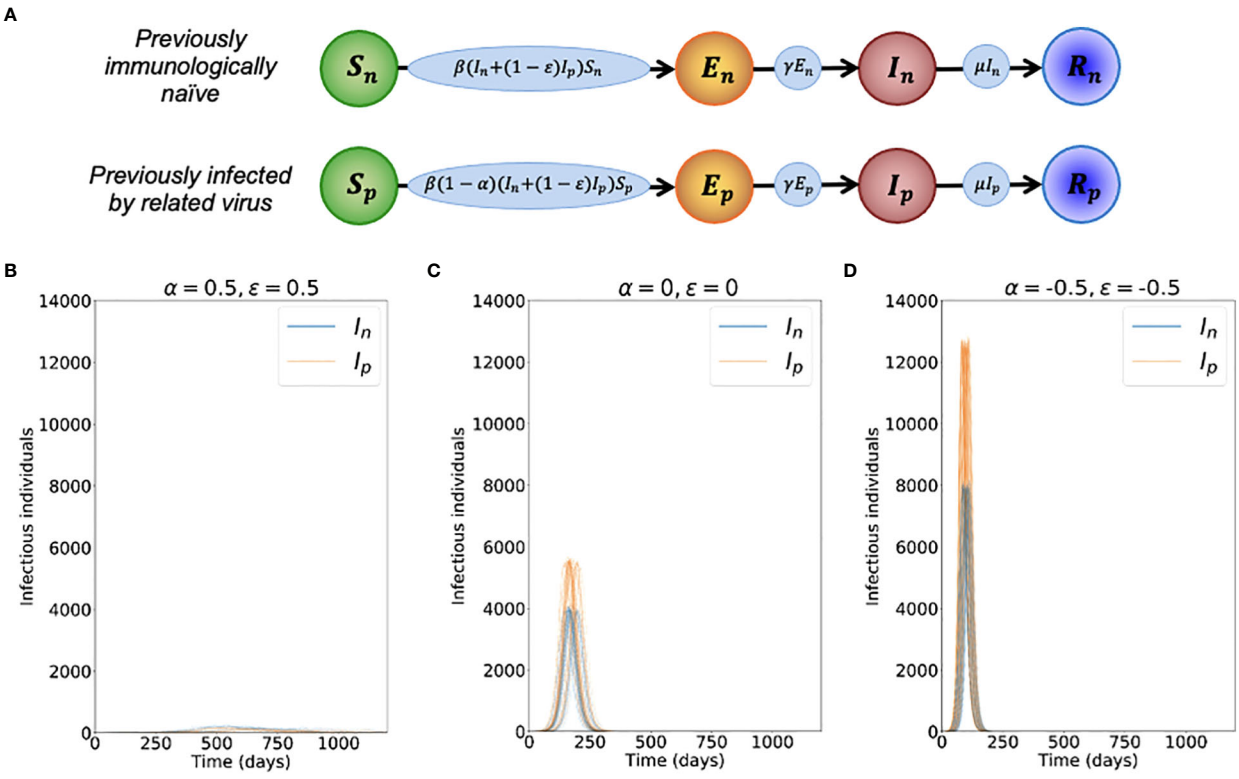

FIGURE 1
Dynamics of the novel variant invading a population in which a related virus has previously spread. **(A)** Schematic showing the transitions (and their rates) in the stochastic model of novel variant invasion (the analogous stochastic model to system of equations (2)). **(B)** Realisations of 50 stochastic simulations of the model, for $R_{0n} = 2$ and with protective cross-reactive immunity ($\alpha = \epsilon = 0.5$; other parameter values are as stated in Table 1). Orange lines represent the number of individuals infected by the novel variant who were previously infected by the related virus (I_p), and blue lines represent the number of individuals infected by the novel variant who were previously immunologically naïve (I_n). **(C)** Analogous to panel B, but with no cross-reactive immunity ($\alpha = \epsilon = 0$). **(D)** Analogous to panel B, but with cross-reactive immunity instead promoting infection with the novel variant ($\alpha = \epsilon = -0.5$). Simulations were initiated with a single infected, previously immunologically naïve individual ($I_n = 1$), with all other individuals susceptible ($S_n = N\text{-}N_p\text{-}1$ and $S_p = N_p$, where N_p is the solution of the final size equation for the previously circulating virus, equation (1), rounded to the nearest integer value).

10.3389/fimmu.2022.1049458

model to system of equations (2) rather than solving the differential equations numerically. When we compute the risk of invasion by simulation, we run model simulations using the direct method version of the Gillespie stochastic simulation algorithm [(26; see Text S1)] until the novel variant fades out (i.e. $E_n+I_n+E_p+I_p$ reaches zero). The parameter values used in our main analyses are given in Table 1.

When the novel variant is introduced, we also approximate the probability that it invades the population analytically. To do this, we assume that infections occur according to a branching process (32–35). Specifically, we denote by q_{ij} the probability that the novel variant fails to invade the host population, starting from i currently infected individuals who are immunologically naïve and j currently infected individuals who were previously infected by the related virus. In this analysis, "currently infected" individuals refer to those who are either exposed or infectious, since exposed and infectious individuals are each expected to infect the same number of other hosts in future. This is because exposed individuals are not yet infectious, and only start generating infections when they move into the infectious states in the model.

We then consider the probability of the novel variant failing to invade the host population starting from a single currently infected individual who was previously immunologically naïve, q_{10}. As in similar previous branching process analyses (36–39), we consider the various possibilities for what happens next: either that individual infects another individual who was also previously immunologically naïve (with probability $\frac{\beta(N-N_p)}{\beta(N-N_p)+\beta(1-\alpha)N_p+\mu}$); or, that individual infects someone who was previously infected with the related virus (with probability $\frac{\beta(1-\alpha)N_p}{\beta(N-N_p)+\beta(1-\alpha)N_p+\mu}$); or, that individual recovers without infecting anyone else (with probability $\frac{\mu}{\beta(N-N_p)+\beta(1-\alpha)N_p+\mu}$). Applying the law of total probability therefore gives $q_{10} = \frac{\beta(N-N_p)}{\beta(N-N_p)+\beta(1-\alpha)N_p+\mu} q_{20} + \frac{\beta(1-\alpha)N_p}{\beta(N-N_p)+\beta(1-\alpha)N_p+\mu} q_{11} + \frac{\mu}{\beta(N-N_p)+\beta(1-\alpha)N_p+\mu} q_{00}$.

Instead starting from a single currently infected individual who was previously infected by the related virus gives $q_{01} = \frac{\beta(1-\varepsilon)(N-N_p)}{\beta(1-\varepsilon)(N-N_p)+\beta(1-\varepsilon)(1-\alpha)N_p+\mu} q_{11} + \frac{\beta(1-\varepsilon)(1-\alpha)N_p}{\beta(1-\varepsilon)(N-N_p)+\beta(1-\varepsilon)(1-\alpha)N_p+\mu} q_{02} + \frac{\mu}{\beta(1-\varepsilon)(N-N_p)+\beta(1-\varepsilon)(1-\alpha)N_p+\mu} q_{00}$.

We then assume that infections occur according to a branching process (so that $q_{20} = q_{10}^2$; as infection lineages failing to establish starting from two currently infected hosts requires the infection lineages from both currently infected hosts to fail independently (36–38)). Making similar approximations throughout the equations above, and noting that $q_{00} = 1$ (since the novel variant will not invade if there are no currently infected individuals) gives

$$q_{10} = \frac{\beta(N-N_p)}{\beta(N-N_p)+\beta(1-\alpha)N_p+\mu} q_{10}^2 + \frac{\beta(1-\alpha)N_p}{\beta(N-N_p)+\beta(1-\alpha)N_p+\mu} q_{10}q_{01} + \frac{\mu}{\beta(N-N_p)+\beta(1-\alpha)N_p+\mu},$$

$$q_{01} = \frac{\beta(1-\epsilon)(N-N_p)}{\beta(1-\epsilon)(N-N_p)+\beta(1-\epsilon)(1-\alpha)N_p+\mu} q_{10}q_{01} + \frac{\beta(1-\epsilon)(1-\alpha)N_p}{\beta(1-\epsilon)(N-N_p)+\beta(1-\epsilon)(1-\alpha)N_p+\mu} q_{01}^2 + \frac{\mu}{\beta(1-\epsilon)(N-N_p)+\beta(1-\epsilon)(1-\alpha)N_p+\mu}. \quad (3)$$

The probability of invasion starting from one currently infected individual who was previously immunologically naïve, p_{10}, and the probability of invasion starting from one currently infected individual who was previously infected by the related virus, p_{01}, are then given by $p_{10} = 1-q_{10}$ and $p_{01} = 1-q_{01}$, where q_{10} and q_{01} are the minimal non-negative solutions of system of equations (3) (40).

TABLE 1 Illustrative parameter values used in model simulations.

Parameter	Meaning	Value used
N	Size of local host population	100,000
$1/\gamma$	Mean latent period of novel variant	5 days (27, 28)
$1/\mu$	Mean infectious period of novel variant	8 days (29–31)
R_{0p}	Reproduction number of previously circulating virus (accounting for interventions)	1.5, so that N_p = 58,281 individuals are assumed to have been infected by the previously circulating virus (approximately 58% of the population)
R_{0n}	Reproduction number of novel variant (accounting for interventions)	Varies (see figures)
β	Transmission rate of novel variant	Set so that $R_{0n} = \frac{\beta N}{\mu}$
α	Reduction (positive) or increase (negative) in susceptibility due to cross-reactive immunity	Varies (see figures)
ϵ	Reduction (positive) or increase (negative) in infectiousness due to cross-reactive immunity	Varies (see figures)

2.3 Special cases

In general, we solve system of equations (3) numerically. However, an analytic solution can be obtained straightforwardly in some special cases.

For example, in a scenario in which previous infection with the related virus is entirely protective against infection with the novel variant, then $\alpha = 1$. In that case, since a previously infected individual cannot be infected with the novel variant, then p_{01} does not apply. However, in that scenario, $p_{10} = 1 - \frac{\mu}{\beta(N-N_p)}$ (whenever $\frac{\beta(N-N_p)}{\mu} > 1$; otherwise, the novel variant will never invade the host population). This can be seen by substituting $\alpha = 1$ into the first equation of system of equations (3), solving the resulting quadratic equation for q_{10} (taking the minimal non-negative solution (40)), and then calculating $p_{10} = 1 - q_{10}$. In a scenario in which the related virus has not previously spread in the host population, then this solution for p_{10} is identical to the classic branching process estimate for the probability of a major outbreak, $p_{10} = 1 - \frac{1}{R_{0n}}$ (33, 41, 42).

Alternatively, we can consider a scenario in which prior infection with the related virus eliminates the infectiousness of a host infected by the novel variant (i.e. the individual can become infected, but the virus cannot then establish, so onwards transmission cannot occur). In that case, $\epsilon = 1$ and so, in a similar fashion to above, we obtain $p_{10} = 1 - \frac{\mu}{\beta(N-N_p)}$ (whenever $\frac{\beta(N-N_p)}{\mu} > 1$) and $p_{01} = 0$. Again, in a scenario in which a related virus has not previously spread in the population, this is the classic estimate for the probability of a major outbreak, $p_{10} = 1 - \frac{1}{R_{0n}}$ (33, 41, 42).

Finally, in a scenario in which previous infection by the related virus does not affect the dynamics of the novel variant (so that $\alpha = \epsilon = 0$), we expect the risk of novel variant invasion to be independent of whether or not the initial infected individual has previously been infected by the related virus. In other words, we expect $q_{10} = q_{01}$. In this case, system of equations (3) reduces to a single quadratic equation for q_{10}. Taking the minimal non-negative solution of that equation (40) indicates that $p_{10} = p_{01} = 1 - q_{10} = 1 - \frac{1}{R_{0n}}$ (whenever $R_{0n} > 1$; otherwise the novel variant will never invade the host population).

3 Results

To investigate the effects of prior infection by an antigenically related virus on the epidemiological dynamics of a newly emerged variant, we first ran stochastic simulations of the analogous stochastic model to system of equations (2). Representative time series of the dynamics illustrate that, if the novel variant successfully spreads in the host population, outbreaks tend to have a lower peak number of infections and have a longer duration when cross-reactive immunity has a protective effect (Figure 1B), compared to when prior infection by the related virus has no effect (Figure 1C). In contrast, if prior infection by the related virus instead promotes infection by the novel variant, outbreaks tend to have a higher peak number of infections and a shorter duration (Figure 1D).

However, rather than focusing on the dynamics of outbreaks once the novel variant has invaded the host population, our main goal was to quantify the risk of the novel variant successfully invading in the first place (as opposed to fading out with few cases). We therefore calculated the risk of the novel variant invading the population, starting from the introduction of a single case to the population (Figure 2). We not only calculated this quantity by numerically solving system of equations (3) (Figure 2 - red solid and dashed lines), but also confirmed that these numerical approximations matched estimates of the invasion probability obtained using large numbers of simulations of the stochastic model (Figure 2 - black dots and crosses).

We found that, when previous infection with the related virus is completely protective against the novel variant (i.e. $\alpha = \epsilon = 1$), then the reproduction number of the novel variant must be higher than the reproduction number of the antigenically related virus in order for the novel variant to invade. Specifically, in Figure 2A (in which $R_{0p} = 1.5$, as marked by the vertical blue dotted line), the probability of the novel variant invading the host population is zero unless $R_{0n} > R_{0p}$, and indeed remains zero whenever R_{0n} is only slightly larger than R_{0p}. This can be explained analytically as follows. The previously circulating virus will spread around the population until sufficiently many individuals have been infected that herd immunity (to the previous virus) is reached. This occurs when $N(1 - \frac{1}{R_{0p}})$ individuals have become infected (43). However, at this point, infections do not stop immediately: there is an "overshoot" in infections while transmission slows and the previously circulating virus fades out. As a result, a lower bound on the final size of the outbreak caused by the previously circulating virus is $N_p > N(1 - \frac{1}{R_{0p}})$. As noted in the Methods (Special cases), in a scenario involving complete cross-reactive immunity, the novel variant can only invade the population if $\frac{\beta(N-N_p)}{\mu} > 1$, or equivalently $R_{0n} > \frac{N}{N-N_p}$. Substituting the lower bound for N_p into this expression shows that invasion of the novel variant requires $R_{0n} > R_{0p}$. In contrast, if cross-reactive immunity is only partial, then the novel variant may invade for lower values of R_{0n} than when cross-reactive immunity is complete (Figure 2B). This can include scenarios in which $R_{0n} < R_{0p}$ (in some cases lying between those shown in Figures 2B, C). As noted in the Methods, when previous infection by the antigenically related virus does not affect the epidemiological dynamics of the novel variant, then the novel variant can only invade if $R_{0n} > 1$ (Figure 2C), mirroring the classical result for models in which cross-reactive immunity is not accounted for (41). Finally, in scenarios in which prior infection

10.3389/fimmu.2022.1049458

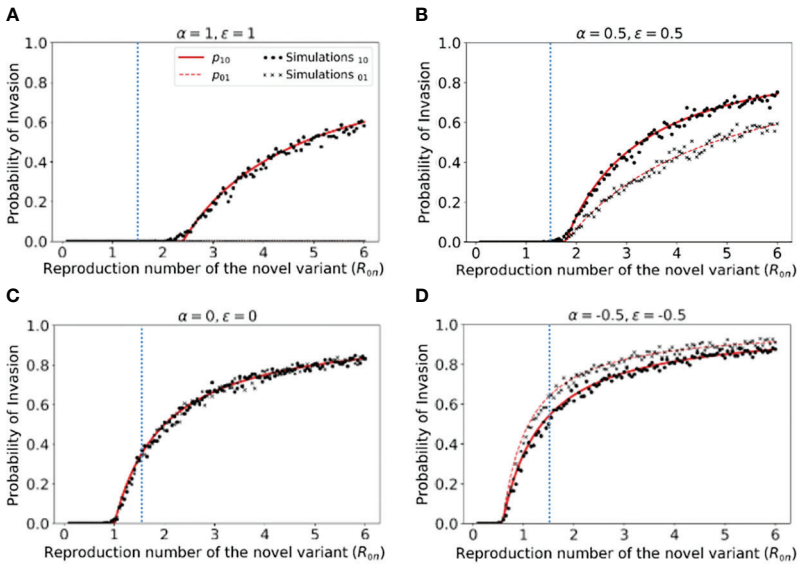

FIGURE 2
Probability of the novel variant invading the host population, starting from the introduction of a single infectious individual. **(A)** The probability of the novel variant invading under an assumption of perfectly protective cross-reactive immunity ($\alpha = \epsilon = 1$). Results are shown both for analytic approximations of the invasion probability calculated using system of equations (3) (either starting from a single infected individual who was previously immunologically naïve (red solid) or starting from a single infected individual who was previously infected by the related virus (red dashed)) and for the invasion probability calculated using stochastic simulations (either starting from a single infected individual who was previously immunologically naïve (black dots) or starting from a single infected individual who was previously infected by the related virus (black crosses)). The vertical blue dotted line represents the reproduction number of the previously circulating virus ($R_{0p} = 1.5$). **(B)** Analogous results to panel A, but with partial protective cross-reactive immunity ($\alpha = \epsilon = 0.5$). **(C)** Analogous results to panel A, but with no cross-reactive immunity ($\alpha = \epsilon = 0$). **(D)** Analogous to panel A, but with cross-reactive immunity instead promoting infection with the novel variant ($\alpha = \epsilon = -0.5$). In the simulations, the probability of invasion was calculated as the proportion of simulations in which the number of simultaneously infected individuals (I_n+I_p) exceeded 15 at any time (analyses for different values of this threshold are shown in Figures S2, S3, with similar results). As in Figure 1, the division of the host population between individuals who were previously immunologically naïve and those who were previously infected by the related virus was calculated based on the final size equation for the previously circulating virus (equation (1)). Other parameter values used are shown in Table 1.

by the related virus promotes infection with the novel variant, the novel variant can invade even if R_{0n} is small. This includes scenarios in which $R_{0n} < 1$ (Figure 2D).

In Figure 2, we note that the immune status of the initial infected individual affects the risk that the novel variant will invade the host population. In particular, when cross-reactive immunity is protective, we found that the probability of invasion is higher if the initially infected host had not previously been infected by the related virus (Figure 2B). In contrast, if cross-reactive immunity promotes infection with the novel variant, then the probability of the novel variant invading is higher if the initial infection arose in an individual who had previously been infected with the related virus (Figure 2D).

We then explored how the probability of invasion of the novel variant depends on the susceptibility- and infectiousness-modifying effects of cross-reactive immunity individually (Figure 3). We found that the values of α and ϵ affect the probability of a major outbreak differently. This is because, starting from a single infected individual, the number of infections generated by that individual is crucial in determining whether or not a novel variant will invade. If the first infected host infects multiple others, then all of those individuals' transmission lineages must fade out in order for invasion to fail to occur. Hence, invasion is more likely if the first infected individual infects many individuals. Starting from a single infected individual who was not previously infected by the related virus, only susceptibility-modifying immunity (characterised by α) affects the number of infections generated by the first infected individual. As such, the probability of invasion in this case is more sensitive to α than to ϵ (Figure 3A).

In contrast, if the first infected individual was previously infected by the related virus, then infectiousness-modifying immunity (characterised by ϵ) also affects the probability of this individual infecting any other member of the population. In fact, ϵ then affects all potential transmissions generated by the first infected individual, whereas α only affects potential transmissions to part of the population (those individuals who were previously infected by the related virus). In that scenario, the probability of a major outbreak is therefore slightly more sensitive to ϵ than α (Figure 3B). The different effects of

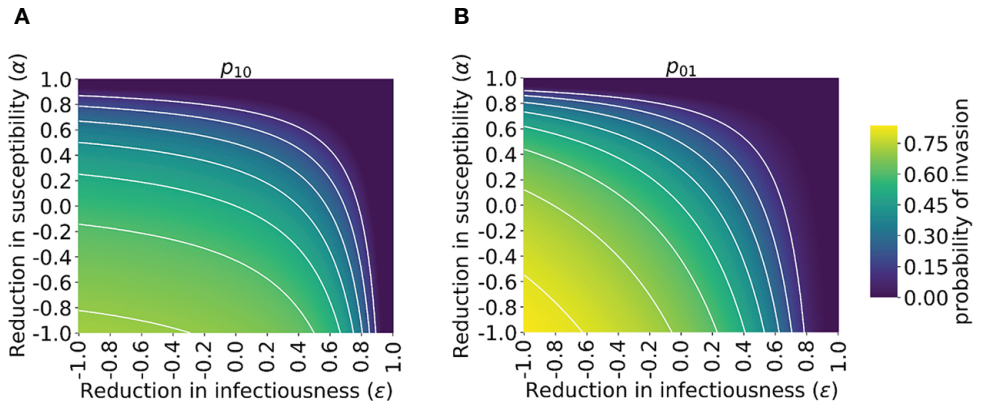

FIGURE 3
Probability of the novel variant invading the host population, starting from the introduction of a single infectious individual, for different levels of cross-reactive immunity affecting susceptibility and infectiousness individually. The invasion probability is approximated analytically by solving system of equations (3) numerically. **(A)** The probability of the novel variant invading, starting from a single infected individual who was previously immunologically naïve. **(B)** Analogous to panel A, but starting from a single infected individual who was previously infected by the related virus. White lines represent contours of constant probability of invasion of the novel variant. As in Figure 1, the division of the host population between individuals who were previously immunologically naïve and those who were previously infected by the related virus was calculated based on the final size equation for the previously circulating virus (equation (1)). In this figure, R_{0p} = 1.5 and R_{0n} = 2 (analyses for other values of R_{0p} and R_{0n} are shown in Figure S4). Other parameter values used are shown in Table 1.

susceptibility-modifying and infectiousness-modifying cross-reactive immunity therefore explain the asymmetric nature of the contours about the diagonal $\epsilon = \alpha$ in Figure 3.

4 Discussion

The epidemiological dynamics of the COVID-19 pandemic have been shaped by the emergence of different SARS-CoV-2 variants. However, not all variants that have appeared have spread widely and caused a large number of cases. Most novel variants have faded out, with relatively few variants being responsible for the vast majority of SARS-CoV-2 infections.

Here, we have developed a mathematical model to investigate the impact of cross-reactive immunity (generated by previous infections by related viruses) on the probability that a newly introduced variant will invade the host population. We found that, if prior infection with a related virus has a strong protective effect, then the novel variant must be more infectious than the related virus to be able to invade the host population (Figure 2A). If instead, however, the previously circulating virus has a very weak protective effect or no protective effect on infection with the novel variant, then the risk of invasion of the novel variant is unaffected by the outbreak of the related virus, and so the invasion probability matches the well-known estimate for the "probability of a major outbreak" (Figure 2C) (33, 41, 42). If prior infection with the related virus promotes infection by the novel variant, as has been indicated as possible in some studies exploring the impact of prior infections by SARS-CoV-2 or seasonal coronaviruses on infections with SARS-CoV-2 variants, then even novel variants with limited transmissibility are able to invade (Figure 2D).

We further showed that the immune status of the first individual in the population infected by the novel variant affects the probability that the novel variant invades (Figures 2, 3). This is in turn influenced by the pathway by which the novel variant is introduced into the host population. If the variant is introduced from elsewhere, for example by an incoming traveller (1, 15), then it may be introduced by someone who was not previously infected by the related virus. If instead it appears as a result of mutation from a related virus within the local population (as was likely the case for the emergence of the Alpha variant in Kent, England (44)), then the initial infected case would be an individual who was previously infected by the related virus.

Previous modelling studies have explored the risk of a novel virus invading when it is introduced to a host population, including scenarios in which the pathogen evolves to facilitate emergence (45–49). Of significant relevance to our study, Hartfield and Alizon (50) applied a branching process model to investigate the invasion probability in a scenario in which a resident pathogen strain that confers cross-reactive immunity is spreading in the host population, and considered Chikungunya virus as a case study. Those authors demonstrated that the standard estimate for the probability of a major outbreak overestimates the invasion probability in that scenario, due to the potential for depletion of susceptible individuals by the

resident strain over the timescale of invasion of the novel virus. Echoing this result in a single strain setting, Sachak-Patwa et al. (51) showed that simple estimates for the probability of a major outbreak are overestimates if the pathogen enters the host population during a vaccination campaign, again due to depletion of susceptible individuals occurring within the period of the pathogen either invading or fading out. Other researchers have investigated the emergence of a novel pathogen strain that is introduced to the population when a resident strain is endemic (52). In contrast to previous studies, we focussed on a scenario in which a related virus has already spread widely around the host population and caused a completed outbreak, rather than being resident in the host population. An additional novel aspect of the current study is that we conducted a thorough investigation of the effects of different levels of cross-reactive immunity, including scenarios in which prior infection with an antigenically related virus can promote infection with the novel variant. Although such scenarios may seem counterintuitive, recent evidence suggests that there is a clear possibility that infection-promoting cross-reactivity may occur, as described in the Introduction.

To understand general principles governing the relationship between cross-reactive immunity and the risk of invasion of a novel variant, we constructed the simplest possible model in this study. Further developments could involve including additional epidemiological and evolutionary detail in our transmission model, particularly if it is to be used to predict emergence of specific variants rather than to understand general principles. For example, in the model considered here, the infectious period of individuals infected by the novel variant is assumed to follow an exponential distribution. However, gamma distributions have been found to represent observed epidemiological periods more accurately than exponential distributions (53–55), and gamma-distributed infectious periods can be incorporated into calculations of invasion probabilities (56, 57). We also assumed a fixed level of cross-reactive immunity for all individuals who were previously infected by the related virus. In reality, immunity is heterogeneous between previously infected hosts, and is likely to wane over time (58, 59). The level of cross-reactive immunity in any individual may depend on a range of factors, including whether or not the individual is immunocompromised or has underlying comorbidities (60), and the characteristics of their previous infection (61). Waning immunity has been included previously in a range of epidemiological models (62, 63), and is a target for future addition to the modelling framework presented here, along with consideration of heterogeneity in immunity between previously infected hosts. Additionally, similar investigations to those conducted here could be undertaken for scenarios in which multiple viruses are co-circulating (potentially allowing for superinfection (64)). This could include analyses of epidemiological dynamics beyond the early phase of the outbreak of the novel variant, after it has invaded the host population.

A key challenge going forwards is to develop reliable approaches for inferring the level of cross-reactive immunity between previously circulating viruses and newly emerged SARS-CoV-2 variants (i.e. the values of the parameters α and ϵ in our model). Serological studies measuring correlates of immune responses in infected patients (e.g. ELISA analyses of cross-reactive antibody responses (21)) have the potential to determine broadly whether previous infections might be protective or detrimental. This may be sufficient to approximate the risk that a new variant will invade host populations in which it is not yet widespread (in Figure 3A, for example, if the values of α and ϵ are both negative, then the probability of the novel variant invading if it is introduced to new host populations is high). More precise estimates of the level of cross-reactive immunity may require substantial epidemiological investigations. As an example, Altarawneh et al. (65) used data from national databases in Qatar to estimate the effect of previous SARS-CoV-2 infection on the risk of symptomatic reinfection by specific SARS-CoV-2 variants. If similar analyses can be carried out in locations in which novel variants first emerge, then estimates of the probability of those variants invading other locations can be refined. We note, however, that there is currently substantial uncertainty in estimates of the level of cross-reactive immunity between different viruses. Altarawneh et al. estimated that previous infection with other SARS-CoV-2 variants has around 56% effectiveness at preventing symptomatic reinfection by the Omicron variant (65), whereas other analyses have suggested that previous infections by other variants have only a limited effect on reinfection rates by the Omicron variant (3). This uncertainty needs to be resolved before the modelling approach described here can be used to make precise quantitative predictions rather than demonstrating qualitative principles about the general impacts of cross-reactive immunity.

In summary, understanding the risk posed by a novel variant requires the degree of cross-reactive immunity between previously circulating viruses and the new variant to be assessed. In scenarios in which previous infections by antigenically related viruses have a limited effect, or promote infection with the novel variant, then the risk of the variant invading the host population is substantially higher than in scenarios in which previous infections by related viruses are protective. Given the impact that different variants have had on transmission and control during the COVID-19 pandemic, fast detection and analyses of novel variants is essential for both national and global public health.

Data availability statement

The datasets presented in this study can be recreated using code in online repositories. The names of the repository/

repositories can be found below: https://github.com/yairdaon/waning.

Author contributions

Conceptualisation: RT, CT, SI, UO. Methodology: RT, UO, ES, FL-R. Formal analysis: RT, ES, YD, UO. Supervision: RT, UO. Writing – Original draft: RT, CT, UO. Writing – Review and editing: All authors. All authors contributed to the article and approved the submitted version.

Funding

RT was funded by the EPSRC through the Mathematics for Real-World Systems CDT (grant number EP/S022244/1). The collaboration between RT and SI was supported by an International Exchange grant from the Royal Society (grant number IES\R3\193037) and a Computer Science Small Grant from the London Mathematical Society. SI was funded by Moonshot Research and Development programme grants from JST (grant numbers JPMJMS2021 and JPMJMS2025). YD and UO were supported by a grant from Tel Aviv University Center for AI and Data Science in collaboration with Google, as part of the AI and Data Science for social good initiative. FL-R was funded by the BBSRC through the Oxford Interdisciplinary Bioscience DTP (grant number BB/M011224/1).

Acknowledgments

Thanks to members of the Zeeman Institute for Systems Biology and Infectious Disease Epidemiology Research at the University of Warwick for useful discussions about this work.

Conflict of interest

The authors declare that the research was conducted in the absence of any commercial or financial relationships that could be construed as a potential conflict of interest.

Publisher's note

Supplementary material

The Supplementary Material for this article can be found online at: https://www.frontiersin.org/articles/10.3389/fimmu.2022.1049458/full#supplementary-material

References

1. Daon Y, Thompson RN, Obolski U. Estimating COVID-19 outbreak risk through air travel. *J Trav Med* (2020) 27:taaa093. doi: 10.1093/jtm/taaa093

2. Davies N, Abbott S, Barnard R, Jarvis C, Kucharski A, Munday J, et al. Estimated transmissibility and impact of SARS-CoV-2 lineage B.1.1.7 in England. *Science* (2021) 372:149. doi: 10.1126/science.abg3055

3. Ferguson N, Ghani A, Cori A, Hogan A, Hinsley W, Volz E, et al. *Report 49 - growth, population distribution and immune escape of omicron in England* (2021). Available at: https://www.imperial.ac.uk/mrc-global-infectious-disease-analysis/covid-19/report-49-omicron/

4. Viana R, Moyo S, Amoako DG, Tegally H, Scheepers C, Althaus CL, et al. Rapid epidemic expansion of the SARS-CoV-2 omicron variant in southern Africa. *Nature* (2022) 603:679–86. doi: 10.1038/s41586-022-04411-y

5. Reynolds CJ, Pade C, Gibbons JM, Otter AD, Lin K-M, Muñoz Sandoval D, et al. Immune boosting by B.1.1.529 (Omicron) depends on previous SARS-CoV-2 exposure. *Science* (2022) 377:eabq1841. doi: 10.1126/science.abq1841

6. Saunders IW. Epidemics in competition. *J Math Biol* (1981) 11:311–8. doi: 10.1007/BF00276899

7. Allen L, Ackleh A. Competitive exclusion in SIS and SIR epidemic models with total cross immunity and density-dependent host mortality. *DCDS-B* (2005) 5:175–88. doi: 10.3934/dcdsb.2005.5.175

8. Thompson RN, Thompson CP, Pelerman O, Gupta S, Obolski U. Increased frequency of travel in the presence of cross-immunity may act to decrease the chance of a global pandemic. *Phil Trans Roy Soc B* (2019) 374:20180274. doi: 10.1098/rstb.2018.0274

9. Amador J, Armesto D, Gómez-Corral A. Extreme values in SIR epidemic models with two strains and cross-immunity. *Math Biosci Eng* (2019) 16:1992–2022. doi: 10.3934/mbe.2019098

10. Opatowski L, Baguelin M, Eggo RM. Influenza interaction with cocirculating pathogens and its impact on surveillance, pathogenesis, and epidemic profile: A key role for mathematical modelling. *PloS Pathog* (2018) 14: e1006770. doi: 10.1371/journal.ppat.1006770

11. Bhattacharyya S, Gesteland PH, Korgenski K, Bjørnstad ON, Adler FR. Cross-immunity between strains explains the dynamical pattern of paramyxoviruses. *Proc Natl Acad Sci* (2015) 112:13396–400. doi: 10.1073/pnas.1516698112

12. Bhatia S, Wardle J, Nash RK, Nouvellet P, Cori A. *Report 47 - a generic method and software to estimate the transmission advantage of pathogen variants in real-time: SARS-CoV-2 as a case-study* (2021). Available at: https://www.imperial.ac.uk/mrc-global-infectious-disease-analysis/covid-19/report-47-mvepiestim/

13. Cori A, Ferguson NM, Fraser C, Cauchemez S. A new framework and software to estimate time-varying reproduction numbers during epidemics. *Am J Epi* (2013) 178:1505–12. doi: 10.1093/aje/kwt133

14. Thompson RN, Stockwin JE, van Gaalen RD, Polonsky JA, Kamvar ZN, Demarsh PA, et al. Improved inference of time-varying reproduction numbers during infectious disease outbreaks. *Epidemics* (2019) 29:100356–6. doi: 10.1016/j.epidem.2019.100356

15. Creswell R, Augustin D, Bouros I, Farm HJ, Miao S, Ahern A, et al. Heterogeneity in the onwards transmission risk between local and imported cases affects practical estimates of the time-dependent reproduction number. *Phil Trans R Soc A.* (2022) 380:20210308. doi: 10.1098/rsta.2021.0308

16. Dyson L, Hill EM, Moore S, Curran-Sebastian J, Tildesley MJ, Lythgoe KA, et al. Possible future waves of SARS-CoV-2 infection generated by variants of concern with a range of characteristics. *Nat Commun* (2021) 12:5730. doi: 10.1038/s41467-021-25915-7

17. Wratil PR, Stern M, Priller A, Willmann A, Almanzar G, Vogel E, et al. Three exposures to the spike protein of SARS-CoV-2 by either infection or vaccination elicit superior neutralizing immunity to all variants of concern. *Nat Med* (2022) 28:496–503. doi: 10.1038/s41591-022-01715-4

18. Malato J, Ribeiro RM, Leite PP, Casaca P, Fernandes E, Antunes C, et al. Risk of BA.5 infection among persons exposed to previous SARS-CoV-2 variants. *N Engl J Med* (2022) 387:953–4. doi: 10.1056/NEJMc2209479

19. Kaplonek P, Wang C, Bartsch Y, Fischinger S, Gorman MJ, Bowman K, et al. Early cross-coronavirus reactive signatures of humoral immunity against COVID-19. *Sci Immunol* (2021) 6:eabj2901. doi: 10.1126/sciimmunol.abj2901

20. Swadling L, Diniz MO, Schmidt NM, Amin OE, Chandran A, Shaw E, et al. Pre-existing polymerase-specific T cells expand in abortive seronegative SARS-CoV-2. *Nature* (2022) 601:110–7. doi: 10.1038/s41586-021-04186-8

21. McNaughton AL, Paton RS, Edmans M, Youngs J, Wellens J, Phalora P, et al. Fatal COVID-19 outcomes are associated with an antibody response targeting epitopes shared with endemic coronaviruses. *JCI Insight* (2022) 7:e156372. doi: 10.1172/jci.insight.156372

22. Smit WL, van Tol S, van der WS, van Vulpen F, la Grouw S, van Lelyveld L, et al. Heterologous immune responses of serum IgG and secretory IgA against the spike protein of endemic coronaviruses during severe COVID-19. *Front Immunol* (2022) 13:839367. doi: 10.3389/fimmu.2022.839367

23. Garrido JL, Medina MA, Bravo F, McGee S, Fuentes-Villalobos F, Calvo M, et al. IgG targeting distinct seasonal coronavirus-conserved SARS-CoV-2 spike subdomains correlates with differential COVID-19 disease outcomes. *Cell Rep* (2022) 39:110904. doi: 10.1016/j.celrep.2022.110904

24. Wratil PR, Schmacke NA, Karakoc B, Dulovic A, Junker D, Becker M, et al. Evidence for increased SARS-CoV-2 susceptibility and COVID-19 severity related to pre-existing immunity to seasonal coronaviruses. *Cell Rep* (2021) 37:110169. doi: 10.1016/j.celrep.2021.110169

25. Pinotti F, Wikramaratna PS, Obolski U, Paton RS, Damineli DSC, Alcantara LCJ, et al. Potential impact of individual exposure histories to endemic human coronaviruses on age-dependent severity of COVID-19. *BMC Med* (2021) 19:19. doi: 10.1186/s12916-020-01887-1

26. Gillespie DT. Exact stochastic simulation of coupled chemical reactions. *J Phys Chem* (1977) 8:2340–61. doi: 10.1021/j100540a008

27. Xin H, Li Y, Wu P, Li Z, Lau EHY, Qin Y, et al. Estimating the latent period of coronavirus disease 2019 (COVID-19). *Clin Infect Dis* (2022) 74:1678–81. doi: 10.1093/cid/ciab746

28. Davies NG, Kucharski AJ, Eggo RM, Gimma A, Edmunds WJ, Jombart T, et al. Effects of non-pharmaceutical interventions on COVID-19 cases, deaths, and demand for hospital services in the UK: a modelling study. *Lancet Pub Health* (2020) 5:e375–85. doi: 10.1016/S2468-2667(20)30133-X

29. Arons MM, Hatfield KM, Reddy SC, Kimball A, James A, Jacobs JR, et al. Presymptomatic SARS-CoV-2 infections and transmission in a skilled nursing facility. *N Engl J Med* (2020) 382:2081–90. doi: 10.1056/NEJMoa2008457

30. Bullard J, Dust K, Funk D, Strong JE, Alexander D, Garnett L, et al. Predicting infectious severe acute respiratory syndrome coronavirus 2 from diagnostic samples. *Clin Infect Dis* (2020) 71:2663–6. doi: 10.1093/cid/ciaa638

31. Wölfel R, Corman VM, Guggemos W, Seilmaier M, Zange S, Müller MA, et al. Virological assessment of hospitalized patients with COVID-2019. *Nature* (2020) 581:465–9. doi: 10.1038/s41586-020-2196-x

32. Ball F, Donnelly P. Strong approximations for epidemic models. *Stoch Proc Appl* (1995) 55:1–21. doi: 10.1016/0304-4149(94)00034-Q

33. Britton T. Stochastic epidemic models: A survey. *Math Biosci* (2010) 225:24–35. doi: 10.1016/j.mbs.2010.01.006

34. Allen LJS, van den Driessche P. Relations between deterministic and stochastic thresholds for disease extinction in continuous- and discrete-time infectious disease models. *Math Biosci* (2013) 243:99–108. doi: 10.1016/j.mbs.2013.02.006

35. Kaye AR, Hart WS, Bromiley J, Iwami S, Thompson RN. A direct comparison of methods for assessing the threat from emerging infectious diseases in seasonally varying environments. *J Theor Biol* (2022) 548:111195. doi: 10.1016/j.jtbi.2022.111195

36. Lovell-Read FA, Funk S, Obolski U, Donnelly CA, Thompson RN. Interventions targeting non-symptomatic cases can be important to prevent local outbreaks: SARS-CoV-2 as a case study. *J R Soc Interface* (2021) 18:20201014. doi: 10.1098/rsif.2020.1014

37. Lovell-Read FA, Shen S, Thompson RN. Estimating local outbreak risks and the effects of non-pharmaceutical interventions in age-structured populations: SARS-CoV-2 as a case study. *J Theor Biol* (2022) 535:110983. doi: 10.1016/j.jtbi.2021.110983

38. Thompson RN, Gilligan CA, Cunniffe NJ. Will an outbreak exceed available resources for control? estimating the risk from invading pathogens using practical definitions of a severe epidemic. *J R Soc Interface* (2020) 17:20200690. doi: 10.1098/rsif.2020.0690

39. Thompson RN. Novel coronavirus outbreak in wuhan, China, 2020: Intense surveillance is vital for preventing sustained transmission in new locations. *J Clin Med* (2020) 9:498. doi: 10.3390/jcm9020498

40. Norris JR. *Markov Chains*. Cambridge, UK: Cambridge University Press (1998).

41. Keeling MJ, Rohani P. *Modeling infectious diseases in humans and animals*. Princeton, USA: Princeton University Press (2008).

42. Thompson RN, Gilligan CA, Cunniffe NJ. Detecting presymptomatic infection is necessary to forecast major epidemics in the earliest stages of infectious disease outbreaks. *PloS Comp Biol* (2016) 12:e1004836. doi: 10.1371/journal.pcbi.1004836

43. Britton T, Ball F, Trapman P. A mathematical model reveals the influence of population heterogeneity on herd immunity to SARS-CoV-2. *Science* (2020) 369:846–9. doi: 10.1126/science.abc6810

44. Kraemer MUG, Hill V, Ruis C, Dellicour S, Bajaj S, McCrone JT, et al. Spatiotemporal invasion dynamics of SARS-CoV-2 lineage B.1.1.7 emergence. *Science* (2021) 373:889–95. doi: 10.1126/science.abj0113

45. Chabas H, Lion S, Nicot A, Meaden S, van Houte S, Moineau S, et al. Evolutionary emergence of infectious diseases in heterogeneous host populations. *PloS Biol* (2018) 16:e2006738–e2006738. doi: 10.1371/journal.pbio.2006738

46. Antia R, Regoes RR, Koella JC, Bergstrom CT. The role of evolution in the emergence of infectious diseases. *Nature* (2003) 426:658–61. doi: 10.1038/nature02104

47. Arinaminpathy N, McLean AR. Evolution and emergence of novel human infections. *Proc Roy Soc B* (2009) 276:3937–43. doi: 10.1098/rspb.2009.1059

48. Kubiak RJ, Arinaminpathy N, McLean AR. Insights into the evolution and emergence of a novel infectious disease. *PloS Comp Biol* (2010) 6:e1000947. doi: 10.1371/journal.pcbi.1000947

49. Leventhal GE, Hill AL, Nowak MA, Bonhoeffer S. Evolution and emergence of infectious diseases in theoretical and real-world networks. *Nat Commun* (2015) 6:6101. doi: 10.1038/ncomms7101

50. Hartfield M, Alizon S. Epidemiological feedbacks affect evolutionary emergence of pathogens. *Am Nat* (2014) 183:E105–17. doi: 10.1086/674795

51. Sachak-Patwa R, Byrne HM, Dyson L, Thompson RN. The risk of SARS-CoV-2 outbreaks in low prevalence settings following the removal of travel restrictions. *Comms Med* (2021) 1:39. doi: 10.1038/s43856-021-00038-8

52. Meehan MT, Cope RC, McBryde ES. On the probability of strain invasion in endemic settings: Accounting for individual heterogeneity and control in multi-strain dynamics. *J Theor Biol* (2020) 487:110109. doi: 10.1016/j.jtbi.2019.110109

53. Lloyd AL. Destabilization of epidemic models with the inclusion of realistic distributions of infectious periods. *Proc Roy Soc B* (2001) 268:985–93. doi: 10.1098/rspb.2001.1599

54. Wearing HJ, Rohani P, Keeling MJ. Appropriate models for the management of infectious diseases. *PloS Med* (2005) 2:0621–7. doi: 10.1371/journal.pmed.0020174

55. Hart WS, Maini PK, Yates CA, Thompson RN. A theoretical framework for transitioning from patient-level to population-scale epidemiological dynamics: influenza a as a case study. *J R Soc Interface* (2020) 17:20200230. doi: 10.1098/rsif.2020.0230

56. Anderson D, Watson R. On the spread of a disease with gamma distributed latent and infectious periods. *Biometrika* (1980) 67:191–8. doi: 10.1093/biomet/67.1.191

57. Thompson RN, Jalava K, Obolski U. Sustained transmission of Ebola in new locations: more likely than previously thought. *Lancet Inf Dis* (2019) 19:1058–59. doi: 10.1016/S1473-3099(19)30483-9

58. Goldberg Y, Mandel M, Bar-On YM, Bodenheimer O, Freedman LS, Ash N, et al. Protection and waning of natural and hybrid immunity to SARS-CoV-2. *N Engl J Med* (2022) 386:2201–12. doi: 10.1056/NEJMoa2118946

59. Townsend JP, Hassler HB, Sah P, Galvani AP, Dornburg A. The durability of natural infection and vaccine-induced immunity against future infection by SARS-CoV-2. *Proc Natl Acad Sci USA* (2022) 119:e2204336119. doi: 10.1073/pnas.2204336119

60. DeWolf S, Laracy JC, Perales M-A, Kamboj M, van den Brink MRM, Vardhana S. SARS-CoV-2 in immunocompromised individuals. *Immunity* (2022) 55:1779–98. doi: 10.1016/j.immuni.2022.09.006

61. Boyton RJ, Altmann DM. The immunology of asymptomatic SARS-CoV-2 infection: what are the key questions? *Nat Rev Immunol* (2021) 21:762–8. doi: 10.1038/s41577-021-00631-x

62. Carlsson R-M, Childs LM, Feng Z, Glasser JW, Heffernan JM, Li J, et al. Modeling the waning and boosting of immunity from infection or vaccination. *J Theor Biol* (2020) 497:110265. doi: 10.1016/j.jtbi.2020.110265

63. Le A, King AA, Magpantay FMG, Mesbahi A, Rohani P. The impact of infection-derived immunity on disease dynamics. *J Math Biol* (2021) 83:61. doi: 10.1007/s00285-021-01681-4

64. Hunter M, Fusco D. Superinfection exclusion: A viral strategy with short-term benefits and long-term drawbacks. *PloS Comput Biol* (2022) 18:e1010125. doi: 10.1371/journal.pcbi.1010125

65. Altarawneh HN, Chemaitelly H, Hasan MR, Ayoub HH, Qassim S, AlMukdad S, et al. Protection against the omicron variant from previous SARS-CoV-2 infection. *N Engl J Med* (2022) 386:1288–90. doi: 10.1056/NEJMc2200133

frontiers | Frontiers in Immunology

TYPE Original Research
PUBLISHED 31 January 2023
DOI 10.3389/fimmu.2023.1056525

OPEN ACCESS

EDITED BY
Pedro A. Reche,
Complutense University of Madrid, Spain

REVIEWED BY
Tesfaye Gelanew,
Armauer Hansen Research Institute, Ethiopia
Shengtao Fan,
Chinese Academy of Medical Sciences and Peking Union Medical College, China

*CORRESPONDENCE
Andreas Thiel
andreas.thiel@charite.de

†These authors share last authorship

SPECIALTY SECTION
This article was submitted to Viral Immunology, a section of the journal Frontiers in Immunology

RECEIVED 28 September 2022
ACCEPTED 10 January 2023
PUBLISHED 31 January 2023

CITATION
Henze L, Braun J, Meyer-Arndt L, Jürchott K, Schlotz M, Michel J, Grossegesse M, Mangold M, Dingeldey M, Kruse B, Holenya P, Mages N, Reimer U, Eckey M, Schnatbaum K, Wenschuh H, Timmermann B, Klein F, Nitsche A, Giesecke-Thiel C, Loyal L and Thiel A (2023) Primary ChAdOx1 vaccination does not reactivate pre-existing, cross-reactive immunity.
Front. Immunol. 14:1056525.
doi: 10.3389/fimmu.2023.1056525

Primary ChAdOx1 vaccination does not reactivate pre-existing, cross-reactive immunity

Larissa Henze[1,2], Julian Braun[1,2], Lil Meyer-Arndt[1,2,3,4], Karsten Jürchott[1,2], Maike Schlotz[5], Janine Michel[6], Marica Grossegesse[6], Maike Mangold[1,2], Manuela Dingeldey[1,2], Beate Kruse[1,2], Pavlo Holenya[7], Norbert Mages[1,2,8], Ulf Reimer[7], Maren Eckey[7], Karsten Schnatbaum[7], Holger Wenschuh[7], Bernd Timmermann[8], Florian Klein[5,9,10], Andreas Nitsche[6], Claudia Giesecke-Thiel[8], Lucie Loyal[1,2†] and Andreas Thiel[1,2*†]

[1]Si-M/"Der Simulierte Mensch" a science framework of Technische Universität Berlin and Charité - Universitätsmedizin Berlin, corporate member of Freie Universität Berlin, Humboldt-Universität zu Berlin, Berlin, Germany, [2]Regenerative Immunology and Aging, BIH Immunomics, Berlin Institute of Health, Berlin, Germany, [3]NeuroCure Clinical Research Center, Charité – Universitätsmedizin Berlin, corporate member of Freie Universität Berlin, Humboldt-Universität zu Berlin, and Berlin Institute of Health, Berlin, Germany, [4]Department of Neurology with Experimental Neurology, Charité – Universitätsmedizin Berlin, corporate member of Freie Universität Berlin, Humboldt-Universität zu Berlin, and Berlin Institute of Health, Berlin, Germany, [5]Laboratory of Experimental Immunology, Institute of Virology, Faculty of Medicine and University Hospital Cologne, University of Cologne, Cologne, Germany, [6]Highly Pathogenic Viruses, Centre for Biological Threats and Special Pathogens, WHO Reference Laboratory for SARS-CoV-2 and WHO Collaborating Centre for Emerging Infections and Biological Threats, Robert Koch Institute, Berlin, Germany, [7]JPT Peptide Technologies GmbH, Berlin, Germany, [8]Max Planck Institute for Molecular Genetics, Berlin, Germany, [9]German Center for Infection Research (DZIF), Partner site Bonn-Cologne, Cologne, Germany, [10]Center for Molecular Medicine Cologne (CMMC), University of Cologne, Cologne, Germany

Currently available COVID-19 vaccines include inactivated virus, live attenuated virus, mRNA-based, viral vectored and adjuvanted protein-subunit-based vaccines. All of them contain the spike glycoprotein as the main immunogen and result in reduced disease severity upon SARS-CoV-2 infection. While we and others have shown that mRNA-based vaccination reactivates pre-existing, cross-reactive immunity, the effect of vector vaccines in this regard is unknown. Here, we studied cellular and humoral responses in heterologous adenovirus-vector-based ChAdOx1 nCOV-19 (AZ; Vaxzeria, AstraZeneca) and mRNA-based BNT162b2 (BNT; Comirnaty, BioNTech/Pfizer) vaccination and compared it to a homologous BNT vaccination regimen. AZ primary vaccination did not lead to measurable reactivation of cross-reactive cellular and humoral immunity compared to BNT primary vaccination. Moreover, humoral immunity induced by primary vaccination with AZ displayed differences in linear spike peptide epitope coverage and a lack of anti-S2 IgG antibodies. Contrary to primary AZ vaccination, secondary vaccination with BNT reactivated pre-existing, cross-reactive immunity, comparable to homologous primary and secondary mRNA vaccination. While induced anti-S1 IgG antibody titers were higher after heterologous vaccination, induced $CD4^+$ T cell responses were highest in homologous vaccinated. However, the overall TCR repertoire breadth was comparable between heterologous AZ-BNT-vaccinated and homologous BNT-BNT-vaccinated individuals, matching TCR repertoire breadths after SARS-CoV-2 infection, too. The reasons why AZ and BNT primary vaccination elicits different immune response patterns to

essentially the same antigen, and the associated benefits and risks, need further investigation to inform vaccine and vaccination schedule development.

KEYWORDS

SARS-CoV-2, antigen-specific T-cells, cross-reactivity, heterologous vaccination, humoral response

Introduction

The COVID-19 pandemic caused by severe acute respiratory syndrome coronavirus 2 (SARS-CoV-2) still challenges health care systems and the economy globally. SARS-CoV-2 vaccines were developed and approved at unprecedented speed. However, contrary to initial hopes, they failed to induce sterile immunity (1, 2). These first-generation vaccines included lipid nanoparticle-formulated, nucleoside-modified mRNA vaccines BNT162b2 (Comirnaty, BioNTech/Pfizer, in the following abbreviated as BNT) and m-1273 (Moderna) as well as the adenovirus-vector-based ChAdOx1 nCOV-19 vaccine (Vaxzeria, AstraZeneca, in the following abbreviated as AZ), all encoding for the spike glycoprotein (spike) (3, 4). The BNT vaccine was initially approved for a 21-days interval, 2 dose regimen, whereas for the AZ vaccine, three months between the first and the second dose were approved (5). At first, Germany's authorities recommended AZ only for the younger adults (<60 years) due to lacking data on efficacy in the elderly (6). Following reports of rare cases of vaccine-induced immune thrombotic thrombocytopenia in young individuals in relation to vaccination with AZ, recommendations for the younger were changed to BNT at the end of March 2021, and resulted in a small cohort of young, heterologous vector-mRNA-vaccinated individuals (7–9). This cohort revealed not only good tolerance of heterologous vaccination but also reported both higher antibody titers and higher neutralization capacity against novel variants of concern (VOCs) (10–13). Vaccination-induced cellular immune responses were comparable between heterologous AZ-BNT vaccination and homologous vector-based vaccination, and higher than following homologous AZ-AZ vaccination (13–16). Accordingly, vector vaccines later were recommended to be combined with mRNA also for third and fourth doses (17, 18). Although the efficacy of mRNA-based vaccines remained unmet, their need for deep cooling and challenging production limits their global usage (5, 19). Additional obstacles of both mRNA- and vector-based vaccines are the administration by injection and especially the reduced effectiveness of neutralizing and blocking antibodies against arising VOCs (20). Some of these hurdles may get solved with the development of second-generation nasal vaccines targeting mucosal immunity and shifting the focus from RBD-specific antibodies to strengthening a broader, pan-coronavirus immunity including optimized T cell responses (21–24). Coronaviruses are widespread in the animal kingdom and further spillover to humans can be expected in the future (25). Prior to SARS-CoV-2, four other common cold coronavirus (hCoV) strains (HKU1, OC43, NL63, 229E) circulated with a seasonal pattern among humans. These are responsible for normal colds and, accordingly, ubiquitous cellular immunity to endemic coronaviruses (26–28). We and others could demonstrate that hCoV induced pre-existing pan-coronavirus-reactive immunity provides rapidly responding $CD4^+$ and $CD8^+$ T cells in blood and mucosa upon SARS-CoV-2 infection or COVID-19 vaccination (29–34). Within spike, due to homology, cross-reactivity focuses on the S2 subunit. Here, a conserved epitope (iCope) within the fusion domain (aa 816–830) accounts for the majority of responsive $CD4^+$ T cells and cross-reactive neutralizing antibodies (28, 29, 35, 36). While infection and homologous BNT vaccination has been shown to boost this cross-reactive immunity (29, 37), the capacity of heterologous vaccination to engage cross-reactive pre-existing immunity is unknown. Therefore, here we comprehensively assessed the quantity and quality of immune responses induced in AZ-BNT vaccination and compare it to that induced by homologous BNT vaccination regimen.

Results

Kinetics of cellular and humoral responses in heterologous AZ-BNT vaccination

At first, we examined cellular and humoral response kinetics of 17 donors during heterologous vaccination with a primary dose of AZ and, three months later, a secondary dose of BNT in a 3–4-day sampling interval for the first two weeks and thereafter weekly until day 28 (Figure S1). We stimulated PBMCs with a S1 spike peptide pool (S-I) covering the N-terminal amino acid residues 1–643 and a S2 peptide pool (S-II) covering the C-terminal amino acid residues 633–1273. In line with our previous findings (29), antigen-specific $CD40L^+4\text{-}1BB^+$ cross-reactive $CD4^+$ T cells with high TCR avidity characterized by downregulated CD3 cell surface expression ($CD3^{lo}$) could be observed in response to S-II but not S-I stimulation prior to vaccination (d0) (Figures 1A, B). After the second vaccination, both S-I- and S-II-specific $CD4^+$ T cells displayed a secondary response kinetics peaking already at d10 with comparable frequencies and TCR avidity which remained stable until week 12 after the third dose of vaccine with BNT (Figures 1A, B, D). Utilizing HLA-DR and CD38, we also monitored the proportion of recent *in vivo* activation among S-I- and S-II-specific $CD4^+$ T cells in the periphery (Figure 1C). The frequencies of $HLA\text{-}DR^+CD38^+$ S-I- or S-II-specific $CD4^+$ T cells were highest upon the first dose of vaccine and displayed lower frequencies after the second, and particularly following the third dose of vaccine even though the overall frequency of $CD40L^+4\text{-}1BB^+$ $CD4^+$ T cells were comparable at each peak between S-I and S-II

10.3389/fimmu.2023.1056525

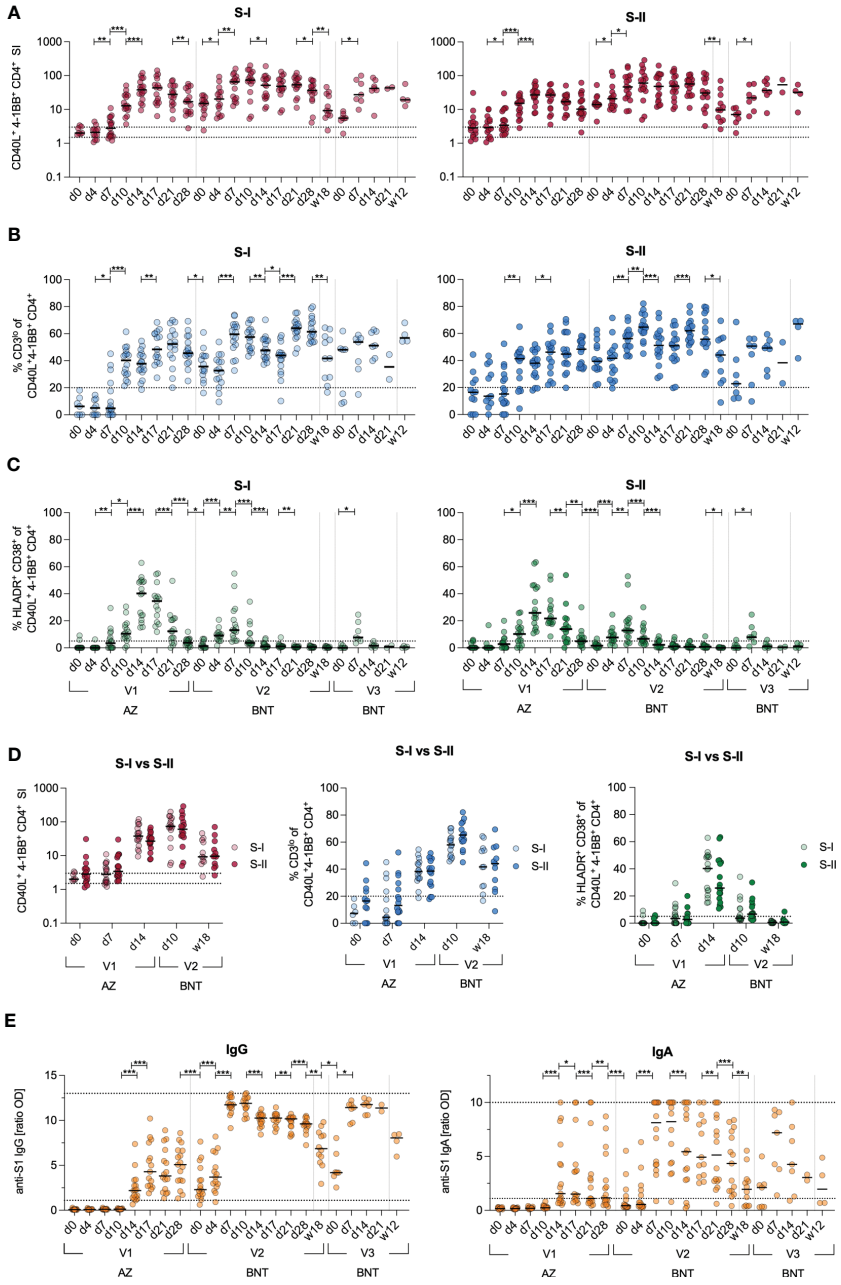

FIGURE 1
Kinetics of adaptive immune responses upon heterologous vaccination. Immune response kinetics following heterologous SARS-CoV-2 vaccination of unexposed young healthy donors (n=17) vaccinated with AZ at d0, then BNT 85(+/-3) days after first dose and 142(+/-7) days after second dose. **(A)** Ex vivo stimulation of PBMCs with S-I and S-II peptide pools. The percentage of CD40L+4-1BB+ within CD4+ T cells among stimulated PBMCs was divided by the percentage of these cells in the unstimulated control, resulting in the stimulation index (SI). Dotted lines indicate a SI of 1.5 and 3, separating non-responders from responders with uncertainty and definite responders. **(B)** Frequencies of CD3lo cells among S-I- or S-II-reactive CD40L+4-1BB+ CD4+ T cells of T cell responses with a SI ≥ 1.5. **(C)** Frequencies of HLA-DR+CD38+ among CD40L+4-1BB+ CD4+ T cells. **(D)** Direct comparison of the SI, frequencies of CD3lo and HLA-DR+CD38+ cells of CD40L+4-1BB+ CD4+ T cells at indicated time points upon stimulation with S-I or S-II peptide pools. **(E)** Serum anti-SARS-CoV-2 S1 IgA and IgG titer ratios. Only significant differences are shown with *p < 0.05, **p<0.01, ***p<0.001 (A-C, E-F: Wilcoxon matched-pairs signed-rank test between consecutive days, D: Mann-Whitney test). SI below 1 were excluded from further analysis, as they are below the lower limit of detection. Black line indicates the median.

stimulations. (Figure 1D). Primary AZ vaccination induced anti-S1 IgG titers in all donors at day 17, but only 66 % (10 of 15) displayed detectable IgA titers above threshold (Figure 1E). The second and third vaccine dose increased IgG titers, which however decreased significantly over the observation period of three months. IgA responses were highly heterologous across donors and displayed faster reduction than IgG, already within weeks after the second dose.

Heterologous vaccination results in slower induction of CD4$^+$ T cell responses, but higher IgG responses compared to homologous vaccination

Next, we investigated quantitative and qualitative differences in the adaptive responses upon heterologous vaccination and compared them

to these of 16 age- and gender-matched donors from a previously published cohort of homologous BNT-vaccinated individuals (29). Note, while the heterologous AZ-BNT vaccination involved a three-month interval between first and second vaccination, the second vaccination in the BNT-BNT cohort was administered three weeks after the first dose. We weekly assessed the response to the first dose, the peak of response after the second dose (d7, d14) and the long-term response at 12 weeks after the third dose of BNT vaccine, administered to both cohorts 6-10 months after the second dose (Figure S1). Primary BNT vaccination resulted in a more rapid T cell response, inducing higher frequencies of S-I- and S-II-reactive T cells early at day 7 post primary and after secondary vaccination. This difference, however, vanished three months after the third dose of vaccine (Figure 2A). In contrast to BNT-vaccinated, AZ-primed individuals did not display higher frequencies of S-II-specific than S-I-specific T cells early (d7) after primary vaccination (Figure 2B). The population's TCR avidity increased faster following first BNT vaccination in both cohorts, but remained comparable thereafter (Figures 2C, D). Upon secondary BNT vaccination, AZ-primed individuals displayed higher IgG levels, but lower IgA levels compared to homologous vaccinated (Figure 2E). These differences leveled out three months after the third dose of vaccine. Neutralization against the Alpha variant was achieved as early as 14 days following primary vaccination with AZ or BNT and remained comparable following secondary and tertiary vaccination with BNT (Figure 2F). However, neutralization of the Omicron variant was largely absent following primary vaccination and significantly higher following homologous BNT vaccination (Figure 2F).

Lack of evidence for reactivation of cross-reactive CD4$^+$ T cells after primary AZ vaccination

To investigate the recruitment of cross-reactive T cells in the immune response following heterologous vaccination, we longitudinally compared the S-II-specific CD4$^+$ T cell response from donors with cross-reactive (SI>3 at baseline) CD4$^+$ T cells to donors without cross-reactive CD4$^+$ T cells (SI<3 at baseline) (Figure 3A). Overall, S-II-specific CD4$^+$ T cell frequencies remained higher in the cross-reactive cohort and more stable over time. Next, we evaluated CD4$^+$ T cell responses against the dominant cross-reactive epitope (iCope) within the fusion domain of spike (aa 816–830). Primary AZ vaccination induced a quantitatively and qualitatively weak response, that was boosted significantly by the second dose with BNT (Figure 3B). Compared to the homologous BNT vaccination regimen, heterologous vaccinated individuals exhibited a lower increase of iCope-specific T cells early in the immune response at day 7 and peaked at lower levels following primary immunization (Figure 3C). In line, comparison of SI

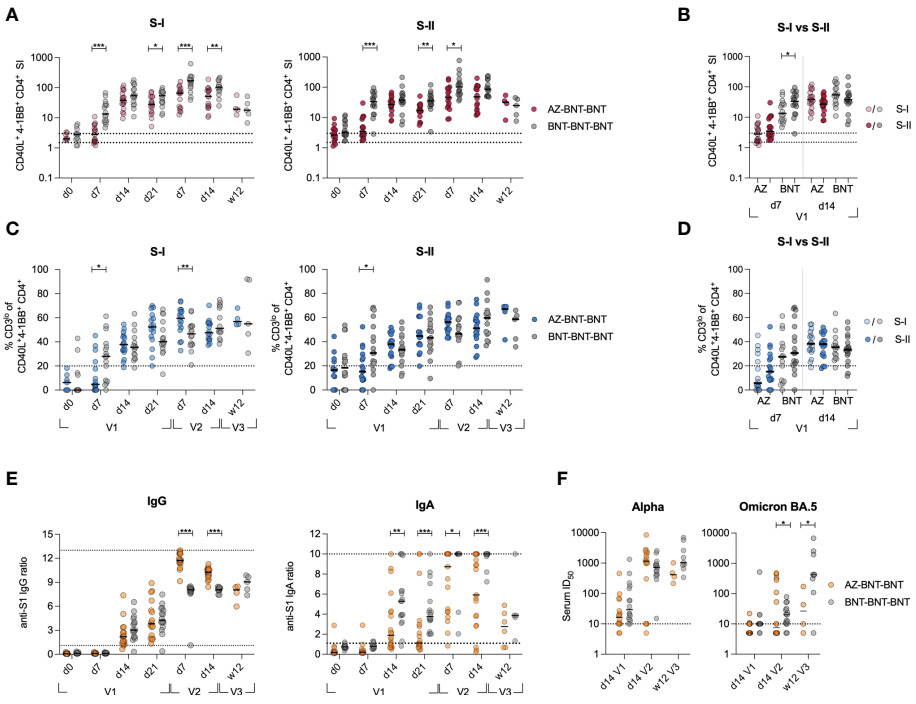

FIGURE 2
Heterologous vaccination results in slower induction of CD4+ T cell responses, but higher IgG responses compared to homologous vaccination. **(A)** *Ex vivo* stimulation of PBMCs from donors receiving heterologous AZ-BNT and homologous BNT-BNT vaccination with S-I and S-II peptide pools at indicated time points. SI of antigen-specific CD40L+4-1BB+ CD4+ T cells is shown. **(B)** *Ex vivo* stimulation of PBMCs from AZ or BNT primary vaccinated donors with S-I and S-II peptide pools early and at peak of immune response. SI of antigen-specific CD40L+4-1BB+ CD4+ T cells is shown. **(C)** Frequencies of CD3lo cells among S-I- or S-II-reactive CD40L+4-1BB+ CD4+ T cells of T cell responses with a SI $\geq$ 1.5. **(D)** *Ex vivo* stimulation of PBMCs from AZ or BNT primary vaccinated donors with S-I and S-II peptide pools early and at peak of immune response. Frequencies of CD3lo antigen-specific CD40L+4-1BB+ CD4+ T cells are shown. **(E)** Serum anti-SARS-CoV-2 S-1 IgG and IgA antibody levels (OD) were determined at indicated time points. Upper and lower levels of detection were set at 1 and 13 (IgG)/ 10 (IgA), respectively, indicated by dotted lines. **(F)** Anti-SARS-CoV-2 B.1.1.7 (Alpha) and B1.1.529 (Omicron) subtype BA.5 variant spike neutralizing capacity at d14 post primary, d14 post secondary and 12 weeks post booster vaccination. Positivity thresholds: >10 ID50 for spike neutralization. Serum ID50 values less than the lowest serum dilution tested (1:10) were assigned a value of 5 for plotting the graph and for statistical analysis. Only significant differences are shown with *P < 0.05, **P < 0.01, ***P < 0.001, Mann-Whitney test. SI below 1 were excluded from further analysis, as they are below the lower limit of detection. Black line indicates the median.

10.3389/fimmu.2023.1056525

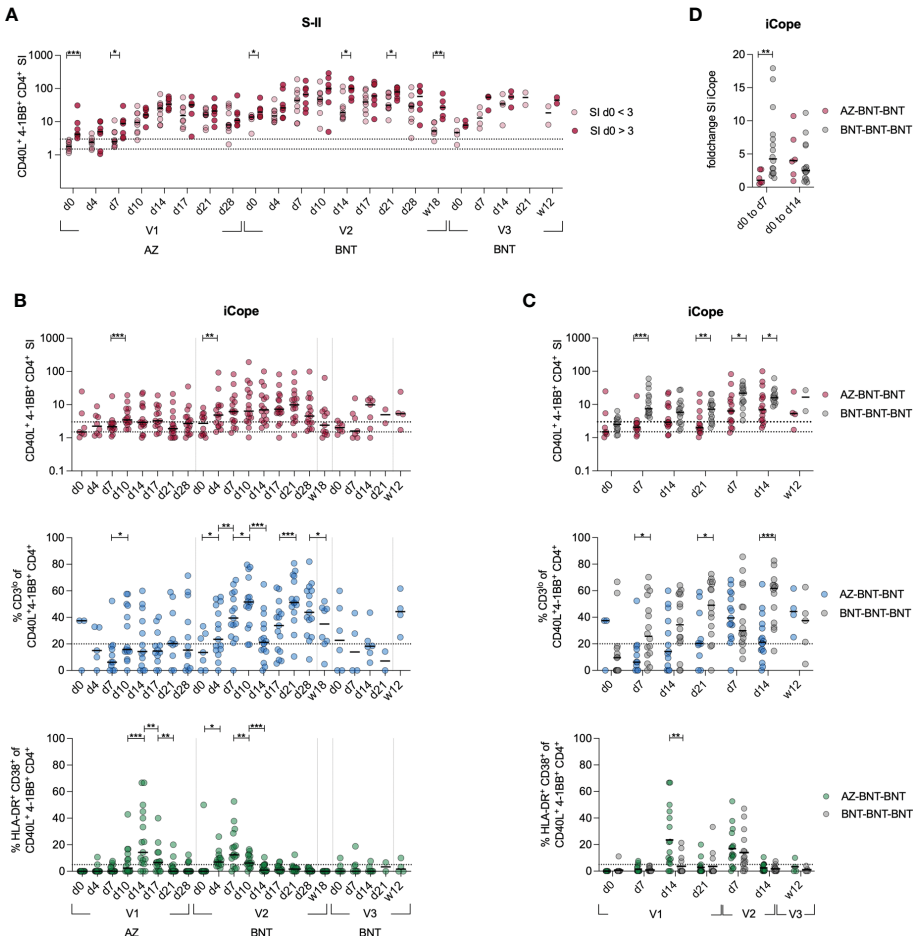

FIGURE 3
Cross-reactive cellular responses are not effectively induced by AZ primary vaccination. **(A)** *Ex vivo* stimulation of PBMCs with S-II peptide pool. Donors were separated into cross-reactive responders according to an SI of >3 at d0 and non-cross-reactive responders (baseline SI <3). **(B)** Stimulation index of antigen specific $CD40L^+4\text{-}1BB^+$ $CD4^+$ T cells, frequencies of $CD3^{lo}$ cells among iCope-reactive $CD40L^+4\text{-}1BB^+$ $CD4^+$ T cells of T cell responses with a SI ≥ 1.5, and $HLA\text{-}DR^+CD38^+$ among iCope-reactive $CD4^+$ T cells are shown. **(C)** Comparison of SI, $CD3^{lo}$ and $HLA\text{-}DR^+CD38^+$ between heterologous (AZ-BNT-BNT) and homologous (BNT-BNT-BNT) vaccinated donors.**(D)** Foldchange of the SI of iCope-specific T cells from d0 to d7 and d0 to d14. Only significant differences are shown with $^*P < 0.05$, $^{**}P < 0.01$, $^{***}P < 0.001$. A, C-D: Mann-Whitney test B: Wilcoxon matched-pairs signed-rank test. SI below 1 were excluded from further analysis, as they are below the lower limit of detection. Black line indicates the median.

changes between d0 and d7 or d14 revealed an early response of cross-reactive clones upon priming with the BNT vaccine whereas donors vaccinated with AZ responded rather late around d14, indicative of recruitment and expansion of only naïve T cell clones rather than recruitment from a pre-existing cross-reactive repertoire (Figure 3D). Compared to primary AZ vaccination, primary BNT vaccination also elicited T cell responses of higher TCR avidity, indicated by higher frequencies of CD3 surface downregulation ($CD3^{lo}$) in activated $CD4^+$ T cells. Among the few detectable iCope-reactive T cells in AZ-primed individuals, a larger proportion displayed an *in vivo* activation phenotype ($HLA\text{-}DR^+CD38^+$) at d14 compared to BNT-vaccinated donors (Figure 3C). In the homologous BNT vaccination regimen, early responses of cross-reactive $CD4^+$ T cell clones correlated with higher and more robust antibody titers, as already shown in Loyal et al., 2021 (29). However, we could not identify any correlation between early S-I, S-II or iCope responses (d4, d7) with early and late IgG and IgA titers upon vaccination (first dose d14, second dose d0 or second dose d28) in heterologous vaccinated donors (Figure S2A). This lack of measurable early reactivation of cross-reactive $CD4^+$ T cells in primary AZ vaccination suggests that this immunization cannot leverage pre-existing T cells to augment the primary response, which was facilitated by BNT primary vaccination and is associated with advantages for both cellular (higher TCR avidity) as well as the humoral (earlier onset) immune response (Figure S2A, (29). However, an overall robust IgG and IgA humoral response correlates with a general good S-I but not S-II T cell reactivity later in the response (Figure S2B).

Heterologous AZ-BNT vaccination recruits a distinct antibody repertoire compared to homologous BNT-BNT vaccination

Next, we compared *de novo* and cross-reactive humoral immune responses in homologous BNT-BNT versus heterologous AZ-BNT vaccination. We screened for linear epitope hot spots of humoral immunity within spike by utilizing a peptide microarray displaying a scan through the spike protein with linear 15mers (overlapping by

10.3389/fimmu.2023.1056525

11 amino acids (aa)) and calculated the responsiveness per amino acid. In both homo- and heterologous vaccinated cohorts we observed three dominant immunogenic regions: aa 537–609, aa 624–676, and aa 1144–1200 (Figures 4A; S2A, B). By contrast, convalescents (CS) only responded weakly to a region at aa 19–43 located within the NTD and strongest to two distinct regions between aa 777–829, containing iCope and the fusion domain.

Homologous BNT vaccination induced antibodies only towards the segment of aa809–829, whereas heterologous vaccination resulted in a humoral response linear epitope pattern comparable with natural infection but lower (Figures 4A; S3A, B). Longitudinal linear peptide-specific antibody analysis revealed poor induction of cross-reactive humoral immunity against the conserved regions aa 813–827 and 1145–1159 by primary AZ vaccination, however, antibodies to the latter were induced by secondary BNT vaccination (Figures 4A, S2B). Strikingly, AZ-primed donors predominantly reacted against linear epitopes in the S1 part of spike that is less conserved among coronaviruses (Figures 4A, S2A, B). We also assessed whether the differences in linear epitope recognition was reflected in binding full spike S1 or S2 protein subunits. S1 binding was comparable after infection or primary vaccination with either AZ or BNT. However, S2 binding was comparable only between naturally infected and BNT-primed individuals, while primary AZ vaccination resulted in low levels of anti-S2 antibodies in 8 out of 16 donors (Figure 4B).

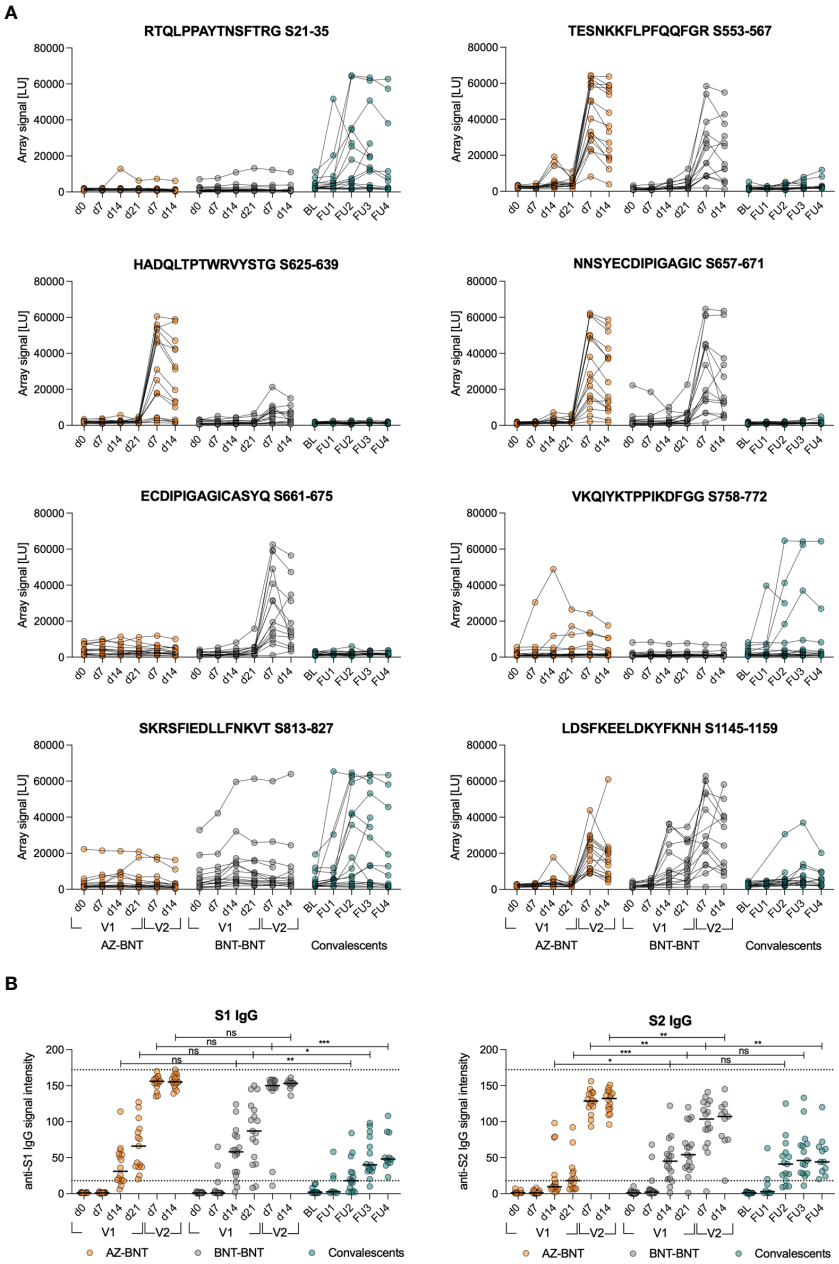

FIGURE 4
Cross-reactive humoral responses are not effectively induced by AZ primary vaccination. **(A)** Signal from sample incubation on peptide microarrays for selected peptides following AZ-BNT (n=16), BNT-BNT (n=15) vaccination or infection (convalescents (CS), n=17). **(B)** Levels of anti-S1 or anti-S2 IgG binding antibody intensity units in indicated cohorts. Dotted lines indicate lower cut-off at 18 for values classified as positive and upper cut-off at 172. BL=baseline, FU=follow-up. ns=not significant, *P < 0.05, **P < 0.01, ***P < 0.001. Mann-Whitney test. Black line indicates the median.

10.3389/fimmu.2023.1056525

T cell clonotype repertoire breadth and depth are comparable in heterologous and homologous vaccination

To assess the capacity of *de novo* recruitment of naive T cells (excluding cross-reactive clones targeting the S-II part) we compared S-I-specific $CD40L^{+}4\text{-}1BB^{+}$ $CD4^{+}$ T cells of donors undergoing heterologous AZ-BNT-BNT with homologous BNT-BNT-BNT vaccination and additionally to natural infection after BNT-BNT vaccination (BNT-BNT-INF) by droplet scRNA-seq three months post last antigen encounter. Diversity 50 (D50, i.e. the number of dominant clones occupying 50 % of the total repertoire) and inverse Simpson index (38) indicated higher TCR breadth in the heterologous vaccinated, but diversity was overall comparable between groups (Figures 5A, B). None of the conditions resulted in a strong enrichment of clonotypes (Figure 5C). Despite high diversity between samples, some overlapping TCR clones could be found both between donors of the same group and in-between groups. Here, clonal overlap between BNT-BNT-BNT-vaccinated and BNT-BNT-INF individuals was more than threefold higher than between AZ-BNT-BNT-vaccinated and BNT-BNT-INF individuals (Figure 5D). All donors demonstrated overlapping clones, both in absolute and relative (normalized to the sample size) numbers (Figures 5E, S4A). We also found no difference in the phenotypic

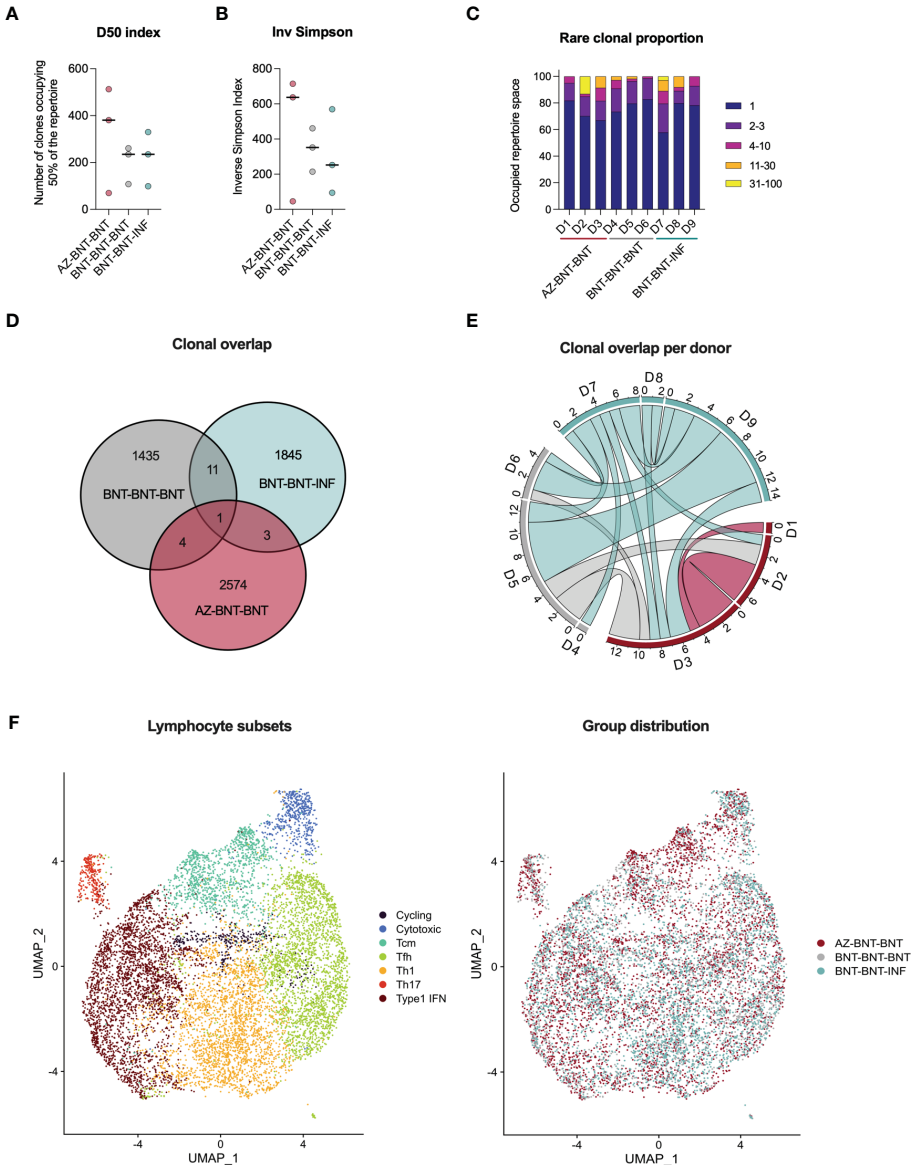

FIGURE 5
Three months post last antigen contact, single cell RNA sequencing of S-I-reactive CD4+ T cells reveals comparable TCR repertoire in heterologous (AZ-BNT-BNT) vaccinated, homologous (BNT-BNT-BNT) vaccinated and homologous vaccinated and infected (BNT-BNT-INF) individuals. **(A)** D50 index indicates the number of clones occupying 50 % of the repertoire. **(B)** Inverse Simpson Index indicates the TCRαβ repertoire diversity. High values represent a more even distribution of clonotypes, whereas low values indicate enrichment of certain clonotypes. **(C)** Rare clonal proportion shows the summary proportion of clonotypes with specific counts. **(D)** Venn diagram displaying the repertoire overlap between groups. **(E)** Circos plot giving the numbers of shared clones between samples of the different cohort. **(F)** UMAP clustering of seven lymphocyte subsets based on marker genes and distributions of groups across them. **(A, B)** Mann-Whitney test revealed no significant differences between groups ($P > 0.05$). Black line indicates the median.

distribution of S-I-specific clones across homo- and heterologous vaccinated and vaccination-breakthrough-infection groups indicating a comparable breadth and quality of antigen-specific $CD4^+$ T cells in all three groups (Figures 5F, S4B).

Discussion

Cross-reactive immunity, resulting from previous exposure to common cold coronaviruses, has been shown to benefit early immune responses during SARS-CoV-2 infection (29–32, 37, 39). We have also shown that primary BNT vaccination engages these pre-existing cross-reactive T cells within the first week following immunization resulting in a more rapid response and higher frequencies of high-quality $CD4^+$ T cells compared with donors in whom such pre-existing, cross-reactive T cells were not detectable (29, 40). However, the capacity of vector-based AZ vaccines to elicit cross-reactive immunity was unknown. By comprehensively characterizing a young, healthy cohort of volunteers receiving an AZ-BNT vaccination regimen, we here found slower onset of spike-specific $CD4^+$ T cell responses suggesting that pre-existing cross-reactive cellular immunity was not activated when primed with AZ. Moreover, $CD4^+$ T cell immunity towards the universal, immunodominant coronavirus-specific epitope iCope (S816-830) was only weakly induced by primary vector-based AZ vaccination compared to primary mRNA-based BNT vaccination, and AZ induced significantly fewer $CD4^+$ T cells with high functional TCR avidity. However, following a secondary BNT vaccination, iCope-responsiveness was readily detectable in heterologous immunized individuals. Notably, humoral immunity towards the S1 subunit was comparable between both vaccination regimens, whereas humoral immunity towards the conserved S2 subunit was reduced in AZ-primed individuals. This suggests an altered B cell immune response upon priming with AZ, which was rectified with the secondary BNT vaccination increasing anti-S2 IgG titers to higher levels than homologous BNT-BNT vaccination. Interestingly, spike peptide array analysis revealed distinct areas of humoral epitope recognition, with different profiles depending on the priming vaccine. Our findings are validated by Ng et al., who found AZ vaccination to result in reduced B cell responses targeting distinct S2 regions of spike, especially those against iCope (S816-830) and S1145–1159 (41). It has been shown that iCope-specific antibodies account for 20% of overall neutralization capacity in blood of convalescents, potentially by altering the fusion peptide accessibility (41). S1144–1159 is located in the stem helix and antibodies targeting this area were previously shown to inhibit spike-mediated membrane fusion for beta coronaviruses (42, 43). Both epitopes are immunodominant and highly conserved across human coronaviruses (44, 45) which suggests that the respective areas of spike are probably indispensable for membrane fusion. In addition, antibodies targeting the S2-located, highly conserved HR1 domain were shown to act as pan-coronavirus fusion inhibitor (46, 47). Accordingly, antibodies directed against these regions could play a critical role in protecting against SARS-CoV-2 and other coronavirus infections and hence in disease control. The search for vaccination regimens that could specifically boost these antibodies might be important for future pandemics involving novel coronavirus VOCs.

The significantly higher antibody titers observed following heterologous vaccination may be attributed to the three-month time window between first and second vaccine dose (AZ-BNT), allowing for prolonged germinal center maturation, resulting in high affinity maturation of previously low to non-binding antibodies (48, 49). AZ-AZ vaccination with a three month interval was reported to mount lower titers than observed here and BNT-BNT vaccination with a three week interval induced comparable titers in relation to heterologous vaccination (13, 14, 50). This suggests that other mechanisms may be responsible for the lower titers in homologous AZ prime-boost vaccination regimens, such as vector immunity (48, 49). Additionally, secondary BNT-immunization containing a slightly different spike protein variant than the AZ vaccine exposed the B cells to new epitopes not yet covered by AZ-induced antibodies. However, while mutations in neutralizing epitopes comparatively affect neutralization capacity in homo- and heterologous vaccinated donors, homologous BNT vaccination shows higher neutralization capacity against immune escape variant Omicron BA.5 after the third dose. This finding highlights the importance of in-depth understanding of the underlying immune maturation mechanisms to design long-term protective vaccines and vaccination schedules.

The observed differences in linear spike epitope antibody coverage between AZ and BNT vaccination may originate from structural differences of the spike protein expressed during the distinct vaccination regimens. Underlying mechanisms could be sequence modifications, different processing in target cells (receptor mediated uptake in vector vaccines, random uptake in lipid nanoparticle encapsulated mRNA vaccines), different glycosylation patterns and protein stability. The transmembrane protein consists of three S2 subunits with three non-covalently attached S1 subunits (51). The N-terminal S1 subunit harbors the N-terminal domain (NTD) and receptor binding domain (RBD) and is relevant for ACE2 recognition on the host cell. Upon binding of ACE2, proteolytic cleavage at the S2' site results in the dissociation of S1 and a conformation change of S2 into post-fusion conformation which facilitates the membrane fusion (51–54). The fusion peptide region harboring iCope is concealed by S1 in the pre-fusion status but becomes exposed upon S2' cleavage and S1 dissociation until it penetrates the host membrane in the post-fusion conformation (55). Spontaneous S1 shedding has been described to occur in non-stabilized spike, whereas two Prolines introduced in S2 at K986P and V987P in BNT162b2 as well as Moderna's mRNA-1273 vaccine prevent a conformational switch into an elongated alpha helix of the post-fusion form (56, 57). For both mRNA vaccines, the recruitment of pre-existing, cross-reactive immunity into the immune response was previously shown (29, 37). Therefore, lack of stabilizing mutations in AZ might result in an altered accessibility to the fusion-peptide-derived epitopes. Whether and how this changed conformation then translates into an apparently less efficient priming of cross-reactive B and T cells remains to be elucidated. We also observed delayed induction of cellular immune responses in AZ vaccinees relative to primary BNT vaccination. This may be due to the fact that the lipid nanoparticle-formulated, nucleoside-modified delivered mRNA could be rapidly available to the immune system, whereas vector-based antigen delivery additionally requires infection of the host cell and transcription of the adenoviral DNA (58). At day 14, the differences became smaller.

Our findings are limited by the lack of further cohorts, particularly a homologous AZ vaccination and a homologous BNT vaccination group with a three-month interval as control group, as well as

relatively small cohorts for the kinetics and the single cell RNA-sequencing. Additionally, it would be interesting to check for differences in the TCR repertoire following only primary vaccination and against the whole spike protein. Finally, comparison of other pre-fusion stabilized versus non-stabilized vaccines would prove the concept of optimal pan-coronavirus immunity induction by stabilized variants independently of their mRNA versus vector basis. To address the constant challenges of newly arising VOCs, second generation vaccines should target pan-coronavirus immunity, focusing on conserved regions and ideally activating mutation-resilient immunity. We here demonstrate that the AZ vector vaccine induces robust adaptive immune responses however does not engage cross-reactive pan-coronavirus immunity targeting the conserved S2 subunit of spike.

Materials and methods

Study participants

This study was approved by the Institutional Review board of the Charité (EA/152/20). Written informed consent was obtained from all included participants and the study was conducted in agreement with the declaration of Helsinki. All vaccinated donors were assessed for age and gender as indicated in Supplementary Table 1. The timepoints week 18 (w18) after second and week 12 (w12) after the third dose of vaccine spans the days 131-165 and 85-126 respectively. Previous infection was excluded by a questionnaire asking for SARS-CoV-2 related symptoms and nucleocapsid IgG ELISA. Detailed specifications of the convalescent cohort including the time points of the follow-up measurements (FU) and symptoms are given in Loyal et al., Science, 2021 (29).

Coronavirus RT-qPCR

For all visits and donors, RNA was extracted from 140 µl of wet nasopharyngeal swabs (Copan mini UTM) using the QIAamp Viral RNA Mini Kit and QIAcube Connect with the manual lysis protocol. SARS-CoV-2 RNA detection was performed using a simultaneous two duplex one-step real-time RT-PCR assay with primers and probes (in-house protocol, primers and probes ordered at Metabion and Thermo Fischer Scientific (MGB probe)) for SARS-CoV-2 E Gene and SARS-CoV-2 ORF1ab according to the RKI/ZBS1 SARS-CoV-2 protocol as described before (59). Each one is duplexed with a control that either indicates potential PCR inhibition or proves the successful extraction of nucleic acid from the clinical specimen. As positive controls genomic SARS-CoV-2 RNA and genomic SARS-CoV RNA were used for the ORF1ab and the E-Gene assay, respectively, adjusted to the Ct values 28 and 32. PCR was conducted with the AgPath-ID™ One-Step RT-PCR Reagents kit (Applied Biosystems) using a Bio-Rad CFX96 or Bio-Rad Opus real-time PCR cycler.

SARS-CoV-2 IgG and IgA S1 ELISA

Anti-SARS-CoV-2 IgG and IgA ELISA specific for the S subunit 1 (S1) was performed using the commercial kits (QuantiVac for IgG), EUROIMMUN Medizinische Labordiagnostika AG) according to the manufacturer's instructions. Upper and lower cut-off were set at a ratio of 1 and 13 for IgG, respectively, and at 1 and 10 for IgA, respectively.

Epitope-specific antibody ELISA

400nM of biotinylated peptide S809-826 (Biotin-Ttds-PSKPSKRS*FIEDLLFNKV*-OH, Ttds linker: N-(3-{2-[2-(3-Amino-propoxy)-ethoxy]-ethoxy}-propyl)-succinamic acid, JPT Peptide Technologies) was immobilized on a 96-well Streptavidin plate (Steffens Biotechnische Analysen GmbH) for 1 hour at RT. After blocking (1 hour, 30°C) serum samples were diluted 1:100 and incubated for 1 hour at 30°C. HRP-coupled, anti-human-IgG secondary antibody (Jackson Immunoresearch) was diluted 1:5000 (Jackson Immunoresearch) and added to the serum samples for 1 hour at 30°C, then HRP substrate was added (TMB, Kem-En-Tec). The reaction was stopped by adding sulfuric acid and absorption was measured at 450 nm using a FlexStation 3.

SARS-CoV-2 spike epitope-specific peptide microarray

The peptides were synthesized using SPOT synthesis, cleaved from the solid support and chemoselectively immobilized on functionalized glass slides. Each peptide was deposited on the microarray in triplicates. The peptide microarrays were incubated with human sera (applied dilution 1:200) in a 96-well microarray incubation chamber for one hour at 30°C, followed by incubation with 0.1 µg/ml fluorescently labeled anti human IgG detection antibody (Jackson Immunoresearch). Washing steps were performed after each incubation step with 0.1 % Tween-20 in 1x TBS. After the final incubation step the microarrays were washed and dried. Each microarray slide was scanned using a GenePix Scanner 4300 SL50 (Molecular Devices). Signal intensities were evaluated using GenePix Pro 7.0 analysis software (Molecular Devices). For each peptide, the MMC2 value of the three triplicates was calculated. The MMC2 value was equal to the mean value of all three instances on the microarray except when the coefficient of variation (CV) – standard-deviation divided by the mean value – was larger than 0.5. In this case the mean of the two values closest to each other (MC2) was assigned to MMC2. Further data analysis and generation of the bar plots was performed using the statistical computing and graphics software R (Version 4.1.1, (60)).

SARS-CoV-2 pseudovirus neutralization assay

The SARS-CoV-2 pseudovirus neutralization assay was conducted as previously described in (61). Shortly, SARS-CoV-2 pseudoviruses were generated by co-transfection of plasmids encoding HIV Tat, HIV Gag/Pol, HIV Rev, luciferase followed by an IRES and ZsGreen, and the alpha and omicron BA.5 SARS-CoV-2 spike protein into HEK 293T cells using FuGENE 6 Transfection

Reagent (Promega). Virus culture supernatant was harvested at 48 h and 72 h post transfection and stored at -80°C till use. Harvested virus was titrated by infecting 293T expressing ACE242 and after a 48-hour incubation at 37°C and 5 % CO_2, luciferase activity was determined after addition of luciferin/lysis buffer (10 mM MgCl2, 0.3 mM ATP, 0.5mM Coenzyme A, 17 mM IGEPAL (all Sigma-Aldrich), and 1 mM D-Luciferin (GoldBio) in Tris-HCL) using the Tristar microplate reader (Berthold). Neutralization assays were performed as described before. Briefly, 3-fold serial dilutions of serum (1:10 starting dilution) were co-incubated with pseudovirus supernatants for 1 h at 37°C, following which 293T-ACE-2 cells were added. After 48 h at 37°C and 5% CO_2, luciferase activity was determined using the luciferin/lysis buffer. Background relative light units (RLUs) of non-infected cells was subtracted and 50% inhibitory dilution (ID_{50}) were calculated as the serum dilution resulting in a 50% reduction in RLU compared to the untreated virus control wells. ID_{50} values were calculated by plotting a non-linear fit dose response curve in GraphPad Prism 7.0.

Blood and serum sampling and PBMC isolation

Whole blood was collected in lithium heparin tubes for peripheral blood mononuclear cells (PBMC) isolation and SST™II advance (Vacuette®, Greiner Bio One and Vacutainer BD) tubes for serology. SST™II advance tubes were centrifuged for 10 min at 1000 g prior to removing serum. Serum aliquots were frozen at -20°C until further use. PBMCs were isolated by gradient density centrifugation according to the manufacturer's instructions (Leucosep tubes, Greiner; Biocoll, Bio&SELL).

Ex vivo T cell stimulation

Freshly isolated PBMC were cultivated at a concentration of $5*10^6$ PBMC/ml in AB-medium containing RPMI 1640 medium (Gibco) supplemented with 10 % heat inactivated AB serum (Pan Biotech), 100 U/ml of penicillin (Biochrom), and 0.1 mg/ml of streptomycin (Biochrom). Stimulations were conducted with PepMix™ overlapping peptide pools (15 aa length with 11 aa overlaps, JPT Peptide Technologies) covering the proteins of interest (all JPT Peptide Technologies). iCope single peptide stimulation was conducted with iCope (N'-SFIEDLLFNKVTLAD-C' (all JPT Peptide Technologies)). All stimulations (peptide pools and single peptides) were performed at final concentrations of 1 µg/ml per peptide. For negative control the stimulation peptide solvent DMSO diluted 1:1 in PBS was used at the same concentration as in peptide-stimulated tubes. The CEFX Ultra SuperStim pool (1 µg/ml per peptide) (JPT Peptide Technologies) was used as positive stimulation control. For optimized costimulation, purified anti-CD28 (clone CD28.2, BD Biosciences) was added to each stimulation at a final concentration of 1 µg/ml. Incubation was performed at 37°C, 5% CO_2 for 16 hours in the presence of 10 µg/ml Brefeldin A (Sigma-Aldrich) during the last 14 hours. $CD4^+$ T cell activation was calculated as a stimulation index (SI). Stimulation index is the ratio of $CD40L^+4\text{-}1BB^+$ $CD4^+$ T cells in the stimulation to the percentage of $CD40L^+4\text{-}1BB^+$ $CD4^+$ T cells in the unstimulated control. Stimulation index between 1.5 and 3 indicate a response with uncertainty, an index of 3 and higher a definite response. Both limits are indicated by dotted lines in the respective figures.

Flow cytometry

Stimulations were stopped by incubation in 2mM EDTA for 5 min. Surface staining was performed for 15 min in the presence of 1 mg/ml of Beriglobin (CSL Behring) with the following fluorochrome-conjugated antibodies titrated to their optimal concentrations as specified in Supplementary Table 2: anti-CD3-FITC (Miltenyi), anti-CD4-VioGreen (Miltenyi), anti-CD8-VioBlue (Miltenyi), anti-CD38-APC (Miltenyi), and anti-HLA-DR-PerCpVio700 (Miltenyi). During the last 10 min of incubation, Zombie Yellow fixable viability staining (Biolegend) was added. Fixation and permeabilization were performed with eBioscience™ FoxP3 fixation and PermBuffer (Invitrogen) according to the manufacturer's protocol. Intracellular staining was carried out for 30 min in the dark at room temperature with anti-4-1BB-PE (Miltenyi), anti-CD40L-PEVio770 (Miltenyi) and anti-CD40L-PECy7 (Biolegend), anti-IFN-γ-A700 (Biolegend) and anti-TNF-α-BV605 (Biolegend). All samples were measured on a MACSQuant®Analyzer 16 (Miltenyi). Instrument performance was monitored prior to every measurement with Rainbow Calibration Particles (BD Biosciences).

Single-cell RNA sequencing

For single-cell RNA sequencing, PBMC of three BNT-BNT-BNT-vaccinated, three AZ-BNT-BNT vaccinated, and three BNT-BNT-infected donors were stimulated with 1 µg/ml S-I peptide pool in the presence of purified anti-CD28 (clone CD28.2, BD Biosciences) and anti-CD40 (clone HB14, Miltenyi Biotec). $CD4^+$ T cells were enriched by MACS (Miltenyi Biotec) and $CD40L^+4\text{-}1BB^+$ $CD4^+$ T cells FACS sorted using an FACS Melody (BD). The cells were loaded with a maximum concentration of 1000 cells/µl and a maximum cell number of 17.000 cells on a Chromium Chip G (10x Genomics). Gene expression and TCR libraries were generated according to the manufacturer's instruction using the Chromium Next GEM single cell 5'Library and Gel bead Kit V1.1 and Chromium Single Cell V(D)J Enrichment Kit for human T cells (10x Genomics). Sequencing was conducted with a NovaSeq 6000 cartridge (Illumina) with 20.000 reads per cell for GEX libraries and 5.000 reads per cell for TCR libraries.

Single-cell transcriptome analysis

Single cell RNA expression data were mapped to reference genome GRCh38-2020-A and preprocessed using the Cell Ranger Software v6.1.2 (10x Genomics). Quality control and analysis of data was done in R 4.0.5 (R Core Team (2021). R: A language and environment for statistical computing. R Foundation for Statistical Computing, Vienna, Austria. URL https://www.R-project.org/) using the "Seurat" package (62). To remove low quality cells, doublets and empty cells thresholds were set to 840–4000 RNA features and less than 5 % mitochondrial RNA per cell. Data were normalized by using the LogNormalize function of the Seurat package and genes detected in less than 0.1% of the cells were excluded. For gene expression

analysis the TCR genes were excluded from the data set to avoid TCR biased clustering. A heatmap with the scaled expression values of selected genes was generated using the DoHeatmap() function of the Seurat package. Furthermore, the expression values of these genes were aggregated according to the experimental groups and shown in a heatmap generated with GraphPad Prism.

Single cell TCR analysis

Single cell TCR data were preprocessed using the Cell Ranger Software v6.1.2 (10x Genomics) and the GRCh38-2020-A reference genome. Data was further processed in R using the "immunarch" package (63). Only cells which passed the quality controls in the gene expression analysis and containing exactly one TCR alpha and one TCR beta chain were used for further analysis. D50 Index, Inverse Simpson Diversity index and rare clonal proportions were calculated using the corresponding functions of the immunarch package. Overlaps of clonotypes between experimental groups were determined using the repOverlap function and visualized as heatmap and with the vis_circos functions of the immunarch package. Numbers for the Venn diagram were calculated using the calculate.overlap function of the VennDiagram package Version 1.7.3 (64).

Data analysis and statistics

Study data were collected and managed using REDCap electronic data capture tools hosted at Charité (65, 66). Flow cytometry data were analyzed with FlowJo 10.6 (FlowJo LLC), and statistical analysis conducted with GraphPad Prism 9. If not stated otherwise, data are plotted as median. *N* indicates the number of donors. *P*-values were set as follows: $*P < 0.05$, $**P < 0.01$, and $***P < 0.001$.

Data availability statement

Raw single-cell sequencing data is available in the GEO repository, accession number GSE222872.

Ethics statement

The studies involving human participants were reviewed and approved by Institutional Review board of the Charité (EA/152/20). The patients/participants provided their written informed consent to participate in this study.

Author contributions

Conceptualization: LH, LL, and AT; Data curation: LH and JB; Formal Analysis: LH; Funding acquisition: AT; Investigation: LH, JB, and LL; Resources: LM-A, KJ, MS, JM, MG, MM, MD, BK, PH, NM, UR, ME, KS, HW, BT, FK and AN; Visualization: LH, JB, KJ, PH and LL; Writing: LH, CG-T, LL and AT. All authors contributed to the article and approved the submitted version.

Funding

This work was funded by the Federal Ministry of Health through a resolution of the German Bundestag (Charité Corona Cross (CCC) 2.0 and 2.1 and Charité Corona Protect (CCP)).

Acknowledgments

The authors thank the CCC associates Zehra Uyar-Aydin, Kübrah Gürcan, Luzie Bartsch, Janna Schmitz, Ilias Katsianas, Antonia Brendler, Ahmed Farghaly, Jessica Felk, Neval Avinc, Benedict Bohnen, Maxim Girod, Louis Löser, Florent Fauchere, Rebecca Kleminci, Clara Unger, Lea Hintze, Andre Braginets, Nickolai Matuschewski, Philipp Resch, Andreas Grimm, Jasmin Berger, Arthur Bilinsky, Ana V. Estrada Ortega, Nona-Ana Ghiroltean, Parniyan Haji Babaei, Doga Ikizogullari, Melanie J. Mindach, Mohammed Naneh, Ming-Yuen Ng, Huyen Nguyen, Clara M. Petersohn, Marwan Radwan, Merlin F. Thieme, Alexandra Völkner, Barbro Wilcke and Thao Nguyen for their contributions to donor recruitment, sample processing and measurement. The authors want to thank Franz B. Gutsch for IT support.

Conflict of interest

The authors UR, PH, ME, KS are employees, HW is the CEO of JPT. LL, LH, JB and AT are named on a filed patent application regarding the usage of CD3 downregulation as method for direct analysis of functional avidity of T cells and a patent application regarding the usage of iCope as method for the direct analysis of SARS-CoV-2 immune responses.

The remaining authors declare that the research was conducted in the absence of any commercial or financial relationships that could be construed as a potential conflict of interest.

Publisher's note

Supplementary material

The Supplementary Material for this article can be found online at: https://www.frontiersin.org/articles/10.3389/fimmu.2023.1056525/full#supplementary-material

References

1. Ball P. The lightning-fast quest for COVID vaccines — and what it means for other diseases. *Nature* (2020) 589(7840):16–8. doi: 0.1038/d41586-020-03626-1

2. Yewdell JW. Individuals cannot rely on COVID-19 herd immunity: Durable immunity to viral disease is limited to viruses with obligate viremic spread. *PloS Pathog* (2021) 17(4):e1009509. doi: 10.1371/journal.ppat.1009509

3. Folegatti PM, Ewer KJ, Aley PK, Angus B, Becker S, Belij-Rammerstorfer S, et al. Safety and immunogenicity of the ChAdOx1 nCoV-19 vaccine against SARS-CoV-2: a preliminary report of a phase 1/2, single-blind, randomised controlled trial. *Lancet Lond Engl* (2020) 396(10249):467–78. doi: 10.1016/S0140-6736(20)31604-4

4. Sahin U, Muik A, Vogler I, Derhovanessian E, Kranz LM, Vormehr M, et al. BNT162b2 vaccine induces neutralizing antibodies and poly-specific T cells in humans. *Nature* (2021) 595(7868):572–7. doi: 10.1038/s41586-021-03653-6

5. Voysey M, Costa Clemens SA, Madhi SA, Weckx LY, Folegatti PM, Aley PK, et al. Single-dose administration and the influence of the timing of the booster dose on immunogenicity and efficacy of ChAdOx1 nCoV-19 (AZD1222) vaccine: A pooled analysis of four randomised trials. *Lancet Lond Engl* (2021) 397(10277):881–91. doi: 10.1016/S0140-6736(21)00432-3

6. Beschluss der STIKO zur 2. *Aktualisierung der COVID-19-Impfempfehlung*. (2021) (Berlin: Robert Koch-Institut, Nordufer), 5:84. Available at: https://www.rki.de/DE/Content/Infekt/EpidBull/Archiv/2021/Ausgaben/05_21.pdf?__blob=publicationFile.

7. Greinacher A, Thiele T, Warkentin TE, Weisser K, Kyrle PA, Eichinger S. Thrombotic thrombocytopenia after ChAdOx1 nCov-19 vaccination. *N Engl J Med* (2021) 384(22):2092–101. doi: 10.1056/NEJMoa2104840

8. Schultz NH, Sørvoll IH, Michelsen AE, Munthe LA, Lund-Johansen F, Ahlen MT, et al. Thrombosis and thrombocytopenia after ChAdOx1 nCoV-19 vaccination. *N Engl J Med* (2021) 384(22):2124–30. doi: 10.1056/NEJMoa2104882

9. Vygen-Bonnet S, Koch J, Bogdan C, Harder T, Heininger U, Kling K, et al. *Beschlussentwurf der STIKO zur 4. aktualisierung der COVID-19-Impfempfehlung und die dazugehörige wissenschaftliche begründung* (2021). Available at: https://edoc.rki.de/handle/176904/8071.

10. Lee HK, Go J, Sung H, Kim SW, Walter M, Knabl L, et al. Heterologous ChAdOx1-BNT162b2 vaccination in Korean cohort induces robust immune and antibody responses that includes omicron. *iScience* (2022) 25(6). doi: 10.1016/j.isci.2022.104473

11. Liu X, Shaw RH, Stuart ASV, Greenland M, Aley PK, Andrews NJ, et al. Safety and immunogenicity of heterologous versus homologous prime-boost schedules with an adenoviral vectored and mRNA COVID-19 vaccine (Com-COV): a single-blind, randomised, non-inferiority trial. *Lancet Lond Engl* (2021) 398(10303):856–69. doi: 10.1016/S0140-6736(21)01694-9

12. Hillus D, Schwarz T, Tober-Lau P, Vanshylla K, Hastor H, Thibeault C, et al. Safety, reactogenicity, and immunogenicity of homologous and heterologous prime-boost immunisation with ChAdOx1 nCoV-19 and BNT162b2: a prospective cohort study. *Lancet Respir Med* (2021) 9(11):1255–65. doi: 10.1016/S2213-2600(21)00357-X

13. Barros-Martins J, Hammerschmidt SI, Cossmann A, Odak I, Stankov MV, Morillas Ramos G, et al. Immune responses against SARS-CoV-2 variants after heterologous and homologous ChAdOx1 nCoV-19/BNT162b2 vaccination. *Nat Med* (2021) 27(9):1525–9. doi: 10.1038/s41591-021-01449-9

14. Schmidt T, Klemis V, Schub D, Mihm J, Hielscher F, Marx S, et al. Immunogenicity and reactogenicity of heterologous ChAdOx1 nCoV-19/mRNA vaccination. *Nat Med* (2021) 27(9):1530–5. doi: 10.1038/s41591-021-01464-w

15. Bánki Z, Mateus J, Rössler A, Schäfer H, Bante D, Riepler L, et al. Heterologous ChAdOx1/BNT162b2 vaccination induces stronger immune response than homologous ChAdOx1 vaccination: The pragmatic, multi-center, three-arm, partially randomized HEVACC trial. *eBioMedicine* (2022) 80. doi: 10.1016/j.ebiom.2022.104073

16. Vogel E, Kocher K, Priller A, Cheng CC, Steininger P, Liao BH, et al. Dynamics of humoral and cellular immune responses after homologous and heterologous SARS-CoV-2 vaccination with ChAdOx1 nCoV-19 and BNT162b2. *eBioMedicine* (2022) 85. doi: 10.1016/j.ebiom.2022.104294

17. Behrens GMN, Barros-Martins J, Cossmann A, Ramos GM, Stankov MV, Odak I, et al. BNT162b2-boosted immune responses six months after heterologous or homologous ChAdOx1nCoV-19/BNT162b2 vaccination against COVID-19. *Nat Commun* (2022) 13:4872. doi: 10.1038/s41467-022-32527-2

18. EMA. EMA and ECDC recommendations on heterologous vaccination courses against COVID-19: 'mix-and-match' approach can be used for both initial boosters [Internet]. *Eur Medicines Agency* (2021).

19. Polack FP, Thomas SJ, Kitchin N, Absalon J, Gurtman A, Lockhart S, et al. Safety and efficacy of the BNT162b2 mRNA covid-19 vaccine. *N Engl J Med* (2020) 383 (27):2603–15. doi: 10.1056/NEJMoa2034577

20. Zhang GF, Meng W, Chen L, Ding L, Feng J, Perez J, et al. Neutralizing antibodies to SARS-CoV-2 variants of concern including delta and omicron in subjects receiving mRNA-1273, BNT162b2, and Ad26.COV2.S vaccines. *J Med Virol* 94(12):5678–90. doi: 10.1002/jmv.28032

21. Alu A, Chen L, Lei H, Wei Y, Tian X, Wei X. Intranasal COVID-19 vaccines: From bench to bed. *eBioMedicine* (2022) 76. doi: 10.1016/j.ebiom.2022.103841

22. Tang J, Zeng C, Cox TM, Li C, Son YM, Cheon IS, et al. Respiratory mucosal immunity against SARS-CoV-2 following mRNA vaccination. *Sci Immunol* (2022) 0(0): eadd4853. doi: 10.1126/sciimmunol.add4853

23. Tarke A, Coelho CH, Zhang Z, Dan JM, Yu ED, Methot N, et al. SARS-CoV-2 vaccination induces immunological T cell memory able to cross-recognize variants from alpha to omicron. *Cell* (2022) 185(5):847–859.e11. doi: 10.1016/j.cell.2022.01.015

24. Chen J, Wang P, Yuan L, Zhang L, Zhang L, Zhao H, et al. A live attenuated virus-based intranasal COVID-19 vaccine provides rapid, prolonged, and broad protection against SARS-CoV-2. *Sci Bull* (2022) 67(13):1372–87. doi: 10.1016/j.scib.2022.05.018

25. Gorbalenya AE, Baker SC, Baric RS, de Groot RJ, Drosten C, Gulyaeva AA, et al. The species severe acute respiratory syndrome-related coronavirus: classifying 2019-nCoV and naming it SARS-CoV-2. *Nat Microbiol* (2020) 5(4):536–44. doi: 10.1038/s41564-020-0695-z

26. Monto AS, DeJonge PM, Callear AP, Bazzi LA, Capriola SB, Malosh RE, et al. Coronavirus occurrence and transmission over 8 years in the HIVE cohort of households in Michigan. *J Infect Dis* (2020) 222(1):9–16. doi: 10.1093/infdis/jiaa161

27. Song G, He Wt, Callaghan S, Anzanello F, Huang D, Ricketts J, et al. Cross-reactive serum and memory b-cell responses to spike protein in SARS-CoV-2 and endemic coronavirus infection. *Nat Commun* (2021) 12(1):2938. doi: 10.1038/s41467-021-23074-3

28. Braun J, Loyal L, Frentsch M, Wendisch D, Georg P, Kurth F, et al. SARS-CoV-2-reactive T cells in healthy donors and patients with COVID-19. *Nature* (2020) 587 (7833):270–4. doi: 10.1038/s41586-020-2598-9

29. Loyal L, Braun J, Henze L, Kruse B, Dingeldey M, Reimer U, et al. Cross-reactive CD4+ T cells enhance SARS-CoV-2 immune responses upon infection and vaccination. *Science* (2021) 374(6564):eabh1823. doi: 10.1126/science.abh1823

30. Kundu R, Narean JS, Wang L, Fenn J, Pillay T, Fernandez ND, et al. Cross-reactive memory T cells associate with protection against SARS-CoV-2 infection in COVID-19 contacts. *Nat Commun* (2022) 13(1):80. doi: 10.1038/s41467-021-27674-x

31. Swadling L, Diniz MO, Schmidt NM, Amin OE, Chandran A, Shaw E, et al. Pre-existing polymerase-specific T cells expand in abortive seronegative SARS-CoV-2. *Nature* (2022) 601(7891):110–7. doi: 10.1038/s41586-021-04186-8

32. Mallajosyula V, Ganjavi C, Chakraborty S, McSween AM, Pavlovitch-Bedzyk AJ, Wilhelmy J, et al. CD8+ T cells specific for conserved coronavirus epitopes correlate with milder disease in COVID-19 patients. *Sci Immunol* (2021) 6(61):eabg5669. doi: 10.1126/sciimmunol.abg5669

33. Niessl J, Sekine T, Lange J, Konya V, Forkel M, Maric J, et al. Identification of resident memory CD8+ T cells with functional specificity for SARS-CoV-2 in unexposed oropharyngeal lymphoid tissue. *Sci Immunol* (2021) 6(64):eabk0894. doi: 10.1126/sciimmunol.abk0894

34. Diniz MO, Mitsi E, Swadling L, Rylance J, Johnson M, Goldblatt D, et al. Airway-resident T cells from unexposed individuals cross-recognize SARS-CoV-2. *Nat Immunol* (2022) 23(9):1324–9. doi: 10.1038/s41590-022-01292-1

35. Low JS, Vaqueirinho D, Mele F, Foglierini M, Jerak J, Perotti M, et al. Clonal analysis of immunodominance and cross-reactivity of the CD4 T cell response to SARS-CoV-2. *Science* (2021) 372(6548):1336–41. doi: 10.1126/science.abg8985

36. Low JS, Jerak J, Tortorici MA, McCallum M, Pinto D, Cassotta A, et al. ACE2-binding exposes the SARS-CoV-2 fusion peptide to broadly neutralizing coronavirus antibodies. *Science* (2022) 377(6607):735–42. doi: 10.1126/science.abq2679

37. Mateus J, Dan JM, Zhang Z, Rydyznski Moderbacher C, Lammers M, Goodwin B, et al. Low-dose mRNA-1273 COVID-19 vaccine generates durable memory enhanced by cross-reactive T cells. *Science* (2021) 374(6566):eabj9853. doi: 10.1126/science.abj9853

38. Chaudhary N, Wesemann DR. Analyzing immunoglobulin repertoires. *Front Immunol* (2018) 9:462. doi: 10.3389/fimmu.2018.00462

39. Ng KW, Faulkner N, Cornish GH, Rosa A, Harvey R, Hussain S, et al. Preexisting and *de novo* humoral immunity to SARS-CoV-2 in humans. *Science* (2020) 370 (6522):1339–43. doi: 10.1126/science.abe1107

40. Meyer-Arndt L, Schwarz T, Loyal L, Henze L, Kruse B, Dingeldey M, et al. Cutting edge: Serum but not mucosal antibody responses are associated with pre-existing SARS-CoV-2 spike cross-reactive CD4+ T cells following BNT162b2 vaccination in the elderly. *J Immunol* (2022). doi: 10.1101/2021.10.05.21264545

41. Ng KW, Faulkner N, Finsterbusch K, Wu M, Harvey R, Hussain S, et al. SARS-CoV-2 S2–targeted vaccination elicits broadly neutralizing antibodies. *Sci Transl Med* (2022) 14(655):eabn3715. doi: 10.1126/scitranslmed.abn3715

42. Pinto D, Sauer MM, Czudnochowski N, Low JS, Tortorici MA, Housley MP, et al. Broad betacoronavirus neutralization by a stem helix–specific human antibody. *Science* (2021) 373(6559):1109–16. doi: 10.1126/science.abj3321

43. Sauer MM, Tortorici MA, Park YJ, Walls AC, Homad L, Acton OJ, et al. Structural basis for broad coronavirus neutralization. *Nat Struct Mol Biol* (2021) 28(6):478–86. doi: 10.1038/s41594-021-00596-4

44. Shrock E, Fujimura E, Kula T, Timms RT, Lee IH, Leng Y, et al. Viral epitope profiling of COVID-19 patients reveals cross-reactivity and correlates of severity. *Science* (2020) 370(6520):eabd4250. doi: 10.1126/science.abd4250

45. Holenya P, Lange PJ, Reimer U, Woltersdorf W, Panterodt T, Glas M, et al. Peptide microarray-based analysis of antibody responses to SARS-CoV-2 identifies unique epitopes with potential for diagnostic test development. *Eur J Immunol* (2021) 51 (7):1839–49. doi: 10.1002/eji.202049101

46. Xia S, Zhu Y, Liu M, Lan Q, Xu W, Wu Y, et al. Fusion mechanism of 2019-nCoV and fusion inhibitors targeting HR1 domain in spike protein. *Cell Mol Immunol* (2020) 17 (7):765–7. doi: 10.1038/s41423-020-0374-2

47. Jiang S, Zhang X, Du L. Therapeutic antibodies and fusion inhibitors targeting the spike protein of SARS-CoV-2. *Expert Opin Ther Targets.* (2021) 25(6):415–21. doi: 10.1080/14728222.2020.1820482

48. Cho A, Muecksch F, Schaefer-Babajew D, Wang Z, Finkin S, Gaebler C, et al. Anti-SARS-CoV-2 receptor-binding domain antibody evolution after mRNA vaccination. *Nature* (2021) 600(7889):517–22. doi: 10.1038/s41586-021-04060-7

49. Goel RR, Painter MM, Apostolidis SA, Mathew D, Meng W, Rosenfeld AM, et al. mRNA vaccines induce durable immune memory to SARS-CoV-2 and variants of concern. *Science* (2021) 374(6572):abm0829. doi: 10.1126/science.abm0829

50. Borobia AM, Carcas AJ, Pérez-Olmeda M, Castaño L, Bertran MJ, García-Pérez J, et al. Immunogenicity and reactogenicity of BNT162b2 booster in ChAdOx1-s-primed participants (CombiVacS): a multicentre, open-label, randomised, controlled, phase 2 trial. *Lancet* (2021) 398(10295):121–30. doi: 10.1016/S0140-6736(21)01420-3

51. Wrapp D, Wang N, Corbett KS, Goldsmith JA, Hsieh CL, Abiona O, et al. Cryo-EM structure of the 2019-nCoV spike in the prefusion conformation. *Science* (2020) 367 (6483):1260–3. doi: 10.1126/science.abb2507

52. Madu IG, Roth SL, Belouzard S, Whittaker GR. Characterization of a highly conserved domain within the severe acute respiratory syndrome coronavirus spike protein S2 domain with characteristics of a viral fusion peptide. *J Virol* (2009) 83 (15):7411–21. doi: 10.1128/JVI.00079-09

53. Xu C, Wang Y, Liu C, Zhang C, Han W, Hong X, et al. Conformational dynamics of SARS-CoV-2 trimeric spike glycoprotein in complex with receptor ACE2 revealed by cryo-EM. *Sci Adv* (2021) 7(1):eabe5575. doi: 10.1126/sciadv.abe5575

54. Cai Y, Zhang J, Xiao T, Peng H, Sterling SM, Walsh RM, et al. Distinct conformational states of SARS-CoV-2 spike protein. *Science* (2020) 369(6511):1586–92. doi: 10.1126/science.abd4251

55. Jackson CB, Farzan M, Chen B, Choe H. Mechanisms of SARS-CoV-2 entry into cells. *Nat Rev Mol Cell Biol* (2022) 23(1):3–20. doi: 10.1038/s41580-021-00418-x

56. Kirchdoerfer RN, Wang N, Pallesen J, Wrapp D, Turner HL, Cottrell CA, et al. Stabilized coronavirus spikes are resistant to conformational changes induced by receptor recognition or proteolysis. *Sci Rep* (2018) 8(1):15701. doi: 10.1038/s41598-018-34171-7

57. Brun J, Vasiljevic S, Gangadharan B, Hensen M, V. Chandran A, Hill ML, et al. Assessing antigen structural integrity through glycosylation analysis of the SARS-CoV-2 viral spike. *ACS Cent Sci* (2021) 7(4):586–93. doi: 10.1021/acscentsci.1c00058

58. Heinz FX, Stiasny K. Distinguishing features of current COVID-19 vaccines: knowns and unknowns of antigen presentation and modes of action. *NPJ Vaccines* (2021) 6(1):1–13. doi: 10.1038/s41541-021-00369-6

59. Michel J, Neumann M, Krause E, Rinner T, Muzeniek T, Grossegesse M, et al. Resource-efficient internally controlled in-house real-time PCR detection of SARS-CoV-2. *Virol J* (2021) 18(1):110. doi: 10.1186/s12985-021-01559-3

60. *R: The r project for statistical computing* (2022). Available at: https://www.r-project.org/.

61. Vanshylla K, Di Cristanziano V, Kleipass F, Dewald F, Schommers P, Gieselmann L, et al. Kinetics and correlates of the neutralizing antibody response to SARS-CoV-2 infection in humans. *Cell Host Microbe* (2021) 29(6):917–929.e4. doi: 10.1016/j.chom.2021.04.015

62. Hao Y, Hao S, Andersen-Nissen E, Mauck WM, Zheng S, Butler A, et al. Integrated analysis of multimodal single-cell data. *Cell* (2021) 184(13):3573–3587.e29. doi: 10.1016/j.cell.2021.04.048

63. Popov A. *Immunomind/immunarch: Immunarch 0.7.0.* Zenodo (2022). Available at: https://zenodo.org/record/6984421.

64. Chen H, Boutros PC. VennDiagram: a package for the generation of highly-customizable Venn and Euler diagrams in r. *BMC Bioinf* (2011) 12:35. doi: 10.1186/1471-2105-12-35

65. Harris PA, Taylor R, Minor BL, Elliott V, Fernandez M, O'Neal L, et al. The REDCap consortium: Building an international community of software platform partners. *J BioMed Inform.* (2019) 95:103208. doi: 10.1016/j.jbi.2019.103208

66. Harris PA, Taylor R, Thielke R, Payne J, Gonzalez N, Conde JG. Research electronic data capture (REDCap)–a metadata-driven methodology and workflow process for providing translational research informatics support. *J BioMed Inform.* (2009) 42(2):377–81. doi: 10.1016/j.jbi.2008.08.010

frontiers | Frontiers in Immunology

TYPE Original Research
PUBLISHED 18 January 2024
DOI 10.3389/fimmu.2024.1341843

OPEN ACCESS

EDITED BY
Ahmed Yaqinuddin,
Alfaisal University, Saudi Arabia

REVIEWED BY
Suresh D. Sharma,
United States Department of Health and Human Services, United States
Cecilia Söderberg-Nauclér,
Karolinska Institutet (KI), Sweden

*CORRESPONDENCE
Shokrollah Elahi
elahi@ualberta.ca

RECEIVED 21 November 2023
ACCEPTED 04 January 2024
PUBLISHED 18 January 2024

CITATION
Saito S, Shahbaz S, Luo X, Osman M, Redmond D, Cohen Tervaert JW, Li L and Elahi S (2024) Metabolomic and immune alterations in long COVID patients with chronic fatigue syndrome.
Front. Immunol. 15:1341843.
doi: 10.3389/fimmu.2024.1341843

Metabolomic and immune alterations in long COVID patients with chronic fatigue syndrome

Suguru Saito[1], Shima Shahbaz[1], Xian Luo[2], Mohammed Osman[3], Desiree Redmond[3], Jan Willem Cohen Tervaert[3], Liang Li[2,4] and Shokrollah Elahi[1,5*]

[1]School of Dentistry, Division of Foundational Sciences, Edmonton, AB, Canada, [2]The Metabolomics Innovation Centre, University of Alberta, Edmonton, AB, Canada, [3]Department of Medicine, Division of Rheumatology, Edmonton, AB, Canada, [4]Department of Chemistry, University of Alberta, Edmonton, AB, Canada, [5]Li Ka Shing Institute of Virology, Faculty of Medicine and Dentistry, University of Alberta, Edmonton, AB, Canada

Introduction: A group of SARS-CoV-2 infected individuals present lingering symptoms, defined as long COVID (LC), that may last months or years post the onset of acute disease. A portion of LC patients have symptoms similar to myalgic encephalomyelitis or chronic fatigue syndrome (ME/CFS), which results in a substantial reduction in their quality of life. A better understanding of the pathophysiology of LC, in particular, ME/CFS is urgently needed.

Methods: We identified and studied metabolites and soluble biomarkers in plasma from LC individuals mainly exhibiting ME/CFS compared to age-sex-matched recovered individuals (R) without LC, acute COVID-19 patients (A), and to SARS-CoV-2 unexposed healthy individuals (HC).

Results: Through these analyses, we identified alterations in several metabolomic pathways in LC vs other groups. Plasma metabolomics analysis showed that LC differed from the R and HC groups. Of note, the R group also exhibited a different metabolomic profile than HC. Moreover, we observed a significant elevation in the plasma pro-inflammatory biomarkers (e.g. IL-1α, IL-6, TNF-α, Flt-1, and sCD14) but the reduction in ATP in LC patients. Our results demonstrate that LC patients exhibit persistent metabolomic abnormalities 12 months after the acute COVID-19 disease. Of note, such metabolomic alterations can be observed in the R group 12 months after the acute disease. Hence, the metabolomic recovery period for infected individuals with SARS-CoV-2 might be long-lasting. In particular, we found a significant reduction in sarcosine and serine concentrations in LC patients, which was inversely correlated with depression, anxiety, and cognitive dysfunction scores.

Conclusion: Our study findings provide a comprehensive metabolomic knowledge base and other soluble biomarkers for a better understanding of the pathophysiology of LC and suggests sarcosine and serine supplementations might have potential therapeutic implications in LC patients. Finally, our study reveals that LC disproportionally affects females more than males, as evidenced by nearly 70% of our LC patients being female.

KEYWORDS

sarcosine, serine, soluble CD14, depression, cognitive performance

Introduction

SARS-CoV-2 infection can result in asymptomatic or symptomatic presentations, ranging from mild to fatal coronavirus disease 2019 (COVID-19) (1). The coordinated action of the innate and adaptive immune systems provides adequate control of SARS-CoV-2 replication, resulting in the recovery of most immunocompetent individuals.

However, a substantial number of patients recovering from COVID-19 have reported a wide range of symptoms that last for many months or years after the onset of acute infection (2, 3). This syndrome is defined as post-acute COVID-19 syndrome (PACS), long-term COVID or "long hauler" patients (2, 4, 5). Multiple studies have evaluated LC symptoms in hospitalized patients, inevitably including only the more severe end of the spectrum (6–8). LC is not restricted to hospitalized patients and its estimated incidence is reported to lie between 10% and 60%, which depends on the definition of LC used and patient cohorts under study (9). LC is composed of heterogeneous sequelae that often affect multiple organ systems, with an impact on functional status and ability to work. The most prominent reported LC manifestations include breathlessness, headache, cough, chest pain, abdominal pain, muscle pain, fatigue, sleep disturbance, cognitive dysfunction (also termed "brain fog"), anxiety, and diarrhea (4, 9). Recent studies and surveys conducted by patient groups indicate that 50 to 80% of patients continue to have bothersome symptoms three months after the onset of COVID-19 disease even after tests no longer detect the virus in their body (7, 10, 11). In support of these observations, a recent study reported that 36% of COVID-19 patients experience several symptoms more than 3-6 months after the acute phase of the disease (3). Nevertheless, around 10% of individuals who have recovered may experience symptoms for over a year following the initial SARS-CoV-2 infection. These symptoms closely resemble those of myalgic encephalomyelitis or chronic fatigue syndrome (ME/CFS) (7, 12, 13), and/or exhibit other manifestations similar to systemic autoimmune rheumatic diseases (SARDs).

Any acute infection that damages multiple organs (e.g. cardiac, pulmonary, and/or renal involvement), like SARS-CoV-2, can be associated with lingering symptoms. In some individuals with persistent, debilitating fatigue following SRAS-CoV-2 infection, documented damage of vital organs may be a sufficient explanation for their fatigue. However, many cases of post-infectious fatigue follow acute infections that did not cause discernible organ damage or in those who had mild disease.

In people with lingering severe fatigue post-COVID-19 and without chronic cardiac, pulmonary, or renal dysfunction one likely explanation for the chronic fatigue is a state of chronic low-grade neuroinflammation (14). SARS-CoV-2 may form reservoirs resulting in viral-associated damage affecting the brain (15, 16), intestine, and liver, which can result in ongoing damage (17). It is known that SARS-CoV-2 enters the olfactory mucosa and can penetrate into the brain from the cribriform plate or via vagal pathways (18). Alternatively, the virus may also directly translocate across the blood-brain barrier (BBB) as a result of increased permeability stemming from inflammatory cytokines or inflammatory cells (e.g. monocytes) (19). Also, SARS-CoV-2 can reach neural tissue via circumventricular organs (CVOs) (20). Therefore, long-term neuropsychiatric symptoms may stem from chronic neuroinflammation and hypoxic injury (20). Indeed, recent studies have suggested that patients with LC may suffer from chronic hypoxic changes affecting the brain (21). Consistent with this, a vascular inflammation associated with hypoxia-inducible factor-1 is reported to contribute to neurological and cardiometabolic dysfunction in LC (22).

Another possible mechanism to explain LC may be that the initial infection triggers a broad immune response characterized by inflammation and immune dysregulation (1, 23). Furthermore, inflammation outside the brain can activate both immunological and somatic signals via both humoral and retrograde neuronal signals which largely involve the vagus nerve (24). These changes can culminate in symptoms of fatigue through the action of various cytokines which act on a "fatigue nucleus" or a collection of neurons dedicated to inhibiting energy-consuming activities that promote focusing on available energy stores for healing (25). Finally, impaired energy production associated with oxidative stress, glycolytic T cell metabolism, and immune alterations are suggested to play important roles in patients with idiopathic ME/CFS (26–29).

Given the global burden of LC and lack of understanding regarding its immunobiology, and pathophysiology, we aimed to systematically follow a cohort of individuals for > 12 months after the acute SARS-CoV-2 infection. This cohort was characterized by multiple clinical visits and laboratory analyses, and compared with a cohort of individuals who had been infected with SARS-CoV-2 but recovered without displaying any clinical symptoms. These individuals were recruited to the Long-COVID clinic at the University of Alberta hospital, with the recruitment was facilitated through patient community groups and the Alberta Long-COVID Facebook community. We also compared these two groups with a cohort of healthy controls (HCs, unexposed to SARS-CoV-2), and with patients suffering from a severe form of acute COVID-19 (A) who were admitted to the Intensive Care Unit (ICU). Collectively, these studies allowed us to analyze metabolomic profiles in these cohorts.

Results

Cohort characteristics

This is a single-centered cohort and consisted of 60 PCR-confirmed SARS-CoV-2 infected individuals (30 LC patients, 15 individuals without LC symptoms who were previously infected with SARS-CoV-2 but recovered without any symptoms per se (recovered group, denoted R), 15 acute hospitalized COVID-19 patients (A)) as well as 15 healthy controls (HCs) without acute symptoms and negative SARS-CoV-2 immunoassays (Figure 1A, Supplementary Table 1). Study participants were age -and sex-matched (Figure 1B) and all were infected with the Wuhan strain

10.3389/fimmu.2024.1341843

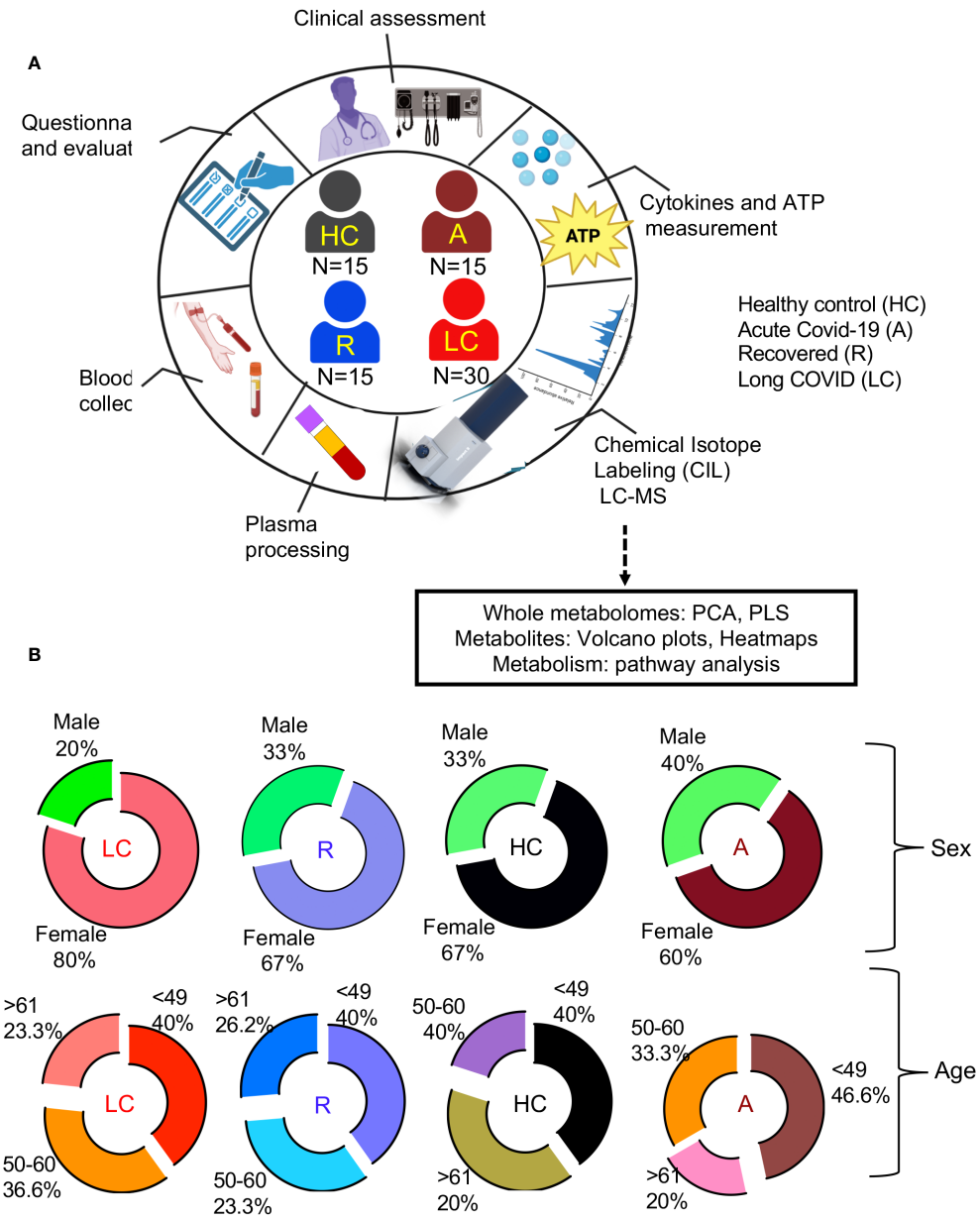

FIGURE 1
Demographic analysis of LC cohorts. **(A)** schematic of the study design. Numbers in center of diagram indicate participants in each study cohort (HC, healthy controls with no prior-SARS-CoV-2 exposure/vaccination; A, acute SARS-CoV-2 infected and ICU-admitted; LC, Long COVID; R, recovered). Outer ring indicates different studies/assays performed on patients/samples. **(B)** Demographic characteristics for each group displayed as ring charts for sex and age.

and recruited at ~12 months post the onset of acute infection (Supplementary Table 1). Considering that the majority of our LC and R participants had a mild acute infection, confounding health conditions were not common (Supplementary Table 1).

HCs were HIV, HCV, and HB seronegative, and mainly recruited pre-COVID-19 pandemic.

A key strength of this study was our unique focus on LC patients who met classification criteria for ME/CFS, which was not rigorously performed in any previous study. Those LC patients who did not fulfill ME/CFS criteria were excluded. Our LC patients were evaluated based on diagnostic criteria developed by CDC and WHO (30, 31) for ME/CFS. Moreover, we used a set of validated clinical questionnaires to capture the severity of symptoms for ME/CFS. This was conducted through in-person meetings using 7 different questionnaires including 1) De Paul Symptom Questionnaires (DSQ); 2) Functional Assessment of Chronic Illness Therapy (FACIT) Fatigue scale questionnaire; 3) FACIT-Dyspnea; 4) Fibromyalgia (FM) diagnostic criteria; 5) Cognitive Failure Questionnaire (CFQ); 6) The Pittsburgh Sleep Quality Index (PSQI): 7) The Hospital Anxiety and Depression Scale (HADS). We evaluated each patient based on different components of each questionnaire. For instance, the DSQ is used to assess symptoms related to ME/CFS (32). In this survey, patients were asked to rate 54 symptoms, and based on their responses we characterized them

into 6 groups: fatigue (I), malaise (II), sleep difficulties (III), pain (IV), cognitive/neurological manifestations (V), and other (VI) which included autonomic, neuroendocrine, and immune manifestations. At the same time, the frequency of symptoms was evaluated using a 5-point Likert scale with 0: none of the time, 1: a little of the time, 2: about half the time, 3: most of the time, and 4: all of the time. Similarly, the severity of the symptoms was also recorded with 0: no symptom, 1: mild, 2: moderate, 3: severe, and 4: very severe. Each patient was considered positive if scored frequency and severity of ≥2 on at least one symptom from each category. For neurologic/cognitive manifestations, patients were considered positive if they scored a frequency and severity of ≥2 on at least two symptoms. For other categories (category VI), patients were considered positive if they had a minimum of one symptom from two of the autonomic, neuroendocrine, and immune manifestations. The diagnosis of ME/CFS was made if the patients met the criteria for categories I, II, III, IV, V, and VI (32–34).

A similar evaluation approach was utilized for the other questionnaires mentioned above. Thus, based on the obtained information from these questionnaires and clinical analyses, we characterized our LC patients.

LC patients are presented with a distinct metabolomic profile compared to R, HC, and acute COVID-19 patients

A total of 2584 metabolites were detected from 75 plasma samples including LC n=30, acute n=15, R n=15, and HC n=15. First, we compared the whole metabolome in our four study groups. Partial least squares-discrimination analysis (PLS-DA) and the heatmap showed a clear classification of the metabolomes between four groups (Figures 2A, B). The acute COVID-19 group showed clearly a distinct metabolome profile from the other three groups. Once the acute group was excluded from analysis, the LC group displayed a more distinct metabolome profile compared to the HC and R groups (Figures 2C, D).

While the LC and HC groups were separated, it appeared that the R group was located between these two groups (Figure 2C). Next, we characterized the difference at the single metabolite level between groups. Volcano plots showed 478 metabolites were significantly reduced while 294 metabolites were significantly increased in acute (A) COVID-19 patients compared to HCs (Figure 2E). Compared to HCs, 103 metabolites were elevated but 123 were declined in the R group (Figure 2F). Interestingly, the number of altered metabolites were much lower between LC and HC groups, showing 61 and 76 decreased and increased, respectively (Figure 2G). The number of altered metabolites between acute patients and the R group were very similar to those of acute/HCs with 419 increased and 285 decreased metabolites (Figure 2H). Compared to acute patients, we noted 495 metabolites were significantly reduced but 167 metabolites were elevated in the plasma of LC patients (Figure 2I). Finally, compared to the R group, LC patients had 49 reduced but 111 increased metabolites (Figure 2J). When we compared the top 100 altered metabolites between groups, we found that acute COVID-19 patients had a distinct metabolomic profile from HCs and R groups (Supplementary Figures 1A, B, Supplementary Table 2). Even though in general R individuals were segregated from HCs, three R patients assimilated with HCs (Supplementary Figure 1C, Supplementary Table 2). Next, we compared the pattern of metabolomic profile in LC patients versus the R and HC groups. These analyses indicated that when the top 100 altered metabolites were compared the LC group was segregated from both the R and HC groups (Supplementary Figures 2A, B, Supplementary Table 2). Overall, these observations demonstrate that LC and even R individuals present an altered metabolomic profile even ~12 months post the acute disease onset.

Differential metabolic pathways in LC patients versus the R and HC groups

To obtain further insight into the differential metabolic characteristics of LC from R and HCs, we performed a metabolic pathway enrichment analysis (https://www.metaboanalyst.ca/) (35–37). Compared to HCs, these analyses revealed that 18 pathways were significantly altered in LC patients (Figure 3A). These alterations in metabolic pathways, resulted in a significant decline in the levels of aspartate, uracil, serine, sarcosine, arginine, dehydroalanine, thymine, and porphobilinogen in LC patients versus HCs (Figure 3B, Supplementary Figure 3A). However, the levels of other metabolites such as 5-Aminolevulinate, cysteate, putrescine, 4-Aminobutyraldehyde, kynurenine, serotonin, Formyl-5-hydroxykynurenamine, 5-Hydroxykynurenine, 2-Aminomuconate, xanthine, and 5-Aminolevulinate were significantly increased in LC patients (Figure 3C, Supplementary Figure 3A). Given the role of Metabolic pathway analyses between the LC and R group revealed also the alteration of 18 pathways, however, 15 out of these 18 pathways were similar to those observed between LC versus HCs (Figure 4A). The three differentially altered pathways between the LC vs HCs were glutamine, nitrogen, and butanoate mechanisms whereas cysteine and methionine, taurine, and glutathione metabolisms were altered between the LC and R groups (Figure 4A). Overall these alterations in metabolism pathways resulted in a substantial reduction in the levels of metabolites such as aspartate, asparagine, glutamine, histidine, N-formimino-glutamate, sarcosine, and ethanolamine phosphate in LC patients (Figure 4B, Supplementary Figure 3B). In contrast, metabolites such as 4-Aminobutanoate, 4-aminobutyraldehyde, 3-hydroxyanthranilate and porphobilinogen were elevated in the plasma of LC patients compared to the R group (Figure 4C, Supplementary Figure 3B).

Finally, we conducted a metabolic enrichment pathway analysis between the R and HCs. Although these individuals did not have any clinical symptoms and appeared to be healthy, they exhibited alterations in 15 metabolomics pathways compared with HCs (Figure 5A). Interestingly, 13 of these pathways were similar to those altered pathways between LC and HCs. Of note, the other two altered pathways in the R group were vitamin B and glutathione metabolisms (Figure 5A). These 15 altered metabolomics pathways resulted in increased levels of glutamate, 4-Aminobutanoate, carnosine, thymine, porphobilinogen, homogentisate and 4-

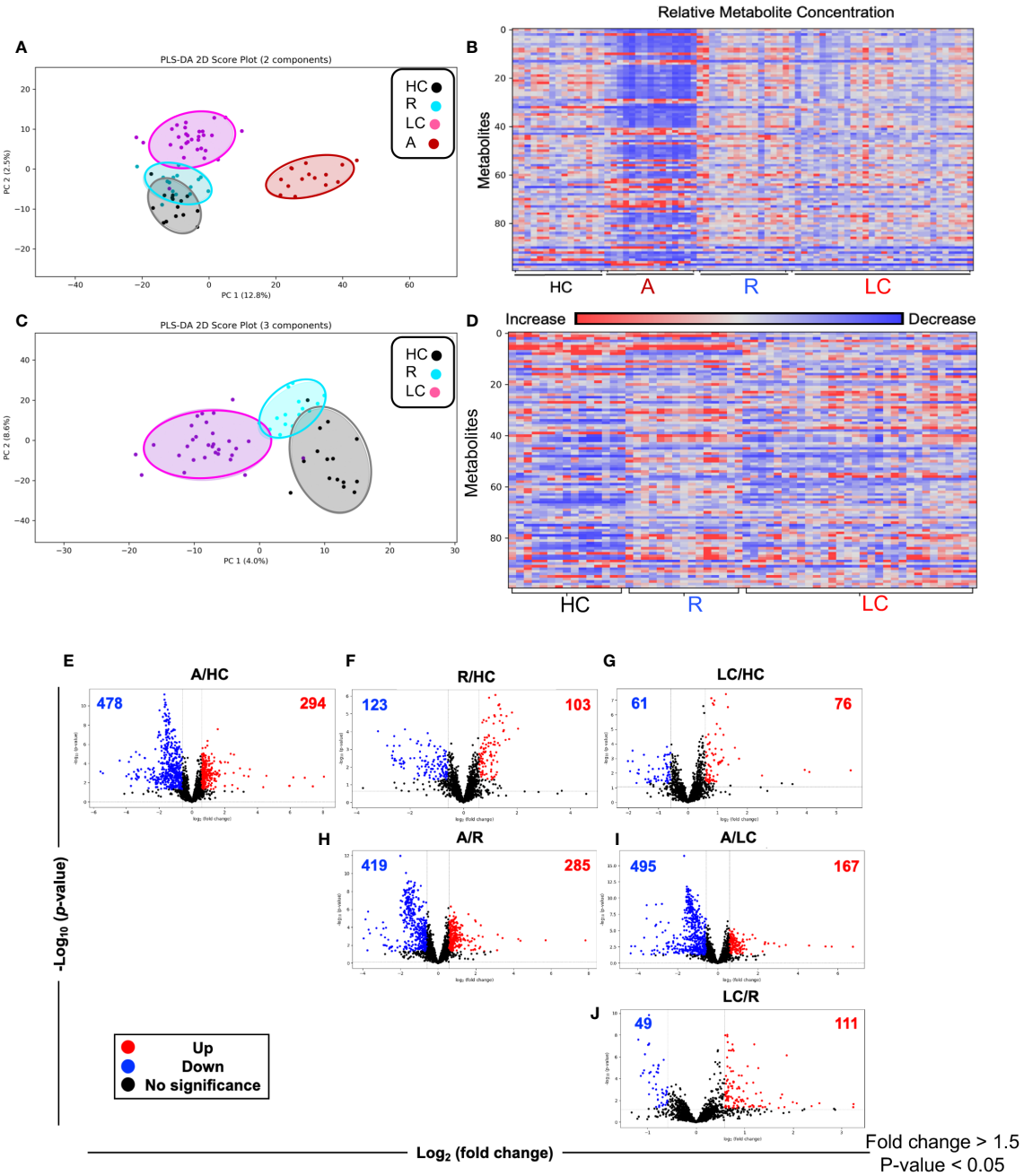

FIGURE 2
Altered metabolomic profile in SARS-CoV-2 infected individuals. **(A)** Partial least squares-discrimination analysis (PLS-DA) plot based on the metabolites in LC (n=30), acute COVID-19 (n=15), HC (n=15) and R (n=15). **(B)** Heatmap based on ANOVA using the top 100 significantly altered metabolites. The heatmap indicates the auto scaled levels of each metabolite in each sample, colored blue for decline and red for elevation as indicated on the horizontal bar. **(C)** Partial least squares-discrimination analysis (PLS-DA) plot based on the metabolites in LC (n=30), HC (n=15) and R (n=15). **(D)** Heatmap based on ANOVA using the 100 significantly altered metabolites. The heatmap indicates the auto scaled levels of each metabolite in each sample, colored blue for decline and red for elevation as indicated on the horizontal bar. **(E)** Volcano plots of significantly increased (red), decreased (blue) or unchanged (black) metabolites in acute A vs HCs. **(F)** Volcano plots of significantly increased, decreased or unchanged metabolites in R vs HC. **(G)** Volcano plots of significantly increased, decreased or unchanged metabolites in LC vs HC. **(H)** Volcano plots of significantly increased, decreased or unchanged metabolites in A vs R. **(I)** Volcano plots of significantly increased, decreased or unchanged metabolites in A vs LC. **(J)** Volcano plots of significantly increased, decreased or unchanged metabolites in LC vs R.

Guanidinobutanoate in the R group (Figure 5B, Supplementary Figure 4A). At the same time, compared to HCs, the levels of a wide range of metabolites such as glutamine, asparagine, N-Formimino-glutamate, putrescine, serotonin, kynurenine, 2-Aminomuconate, Cys-Gly, 5-Aminolevulinate, and pyridoxine were reduced in the plasma of R group (Figure 5C, Supplementary Figure 4A). Despite the lack of clinical symptoms, the R group also exhibited a differential metabolomics profile compared to HCs. Taken

10.3389/fimmu.2024.1341843

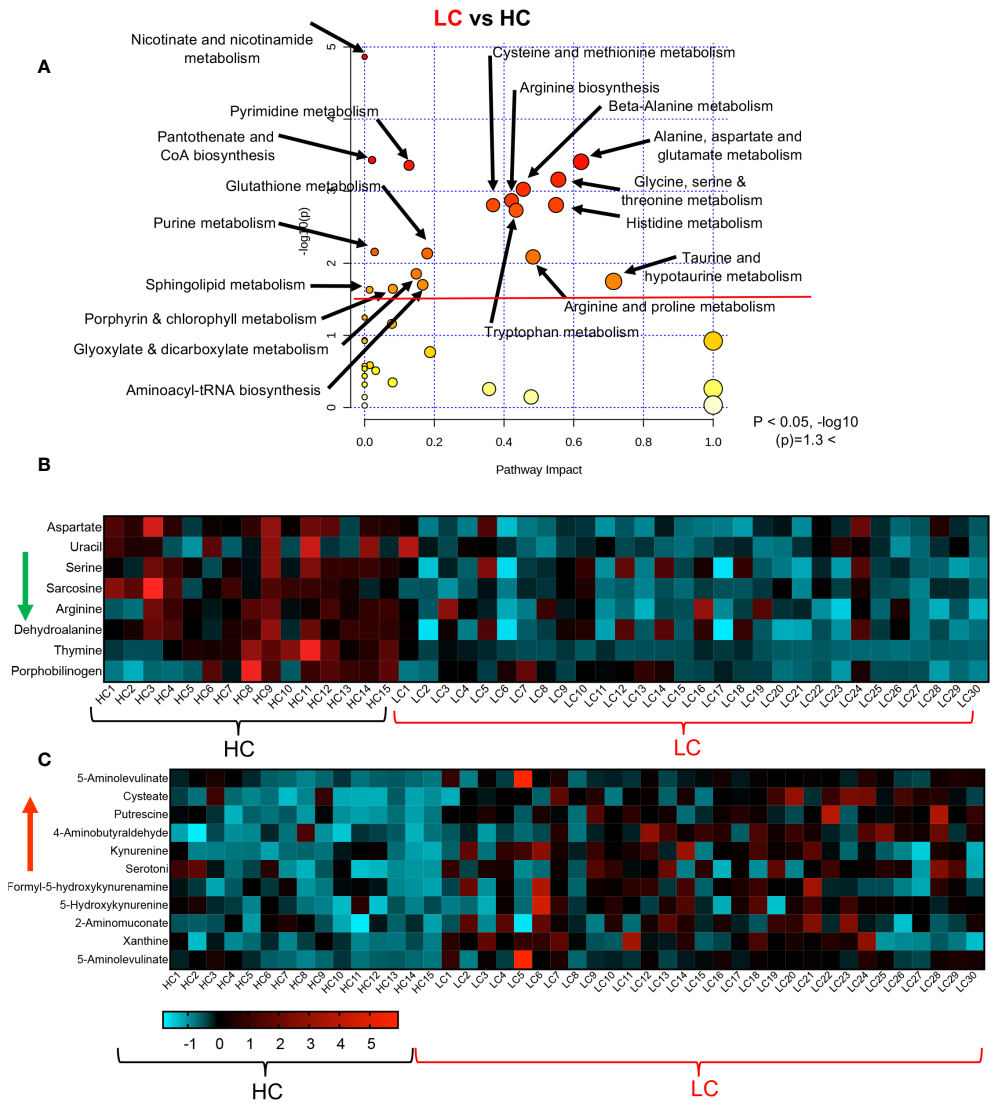

FIGURE 3
Altered metabolomic profile in LC vs HC. **(A)** Metabolic pathway enrichment analysis plot shows significantly altered pathways in LC vs HC. **(B)** The heatmap shows significantly decreased metabolites in different metabolic pathways in LC vs R. **(C)** The heatmap shows significantly elevated metabolites in different metabolomics pathways in LC vs R.

together, these observations imply substantial metabolic pathways alterations in LC patients.

Differential metabolomic profile of acute COVID-19 patients vs HCs

In agreement with previous reports (38), we observed alteration in plasma metabolite levels of acute patients vs HCs. Pathway analysis between acute and HCs revealed alteration in 29 pathways as indicated in Supplementary Figure 4B. These modifications in metabolism pathways resulted in a substantial increase in the levels of 48 metabolites such as Xanthine, ascorbate, Cys-Gly, kynurenine, phenylalanine, 5-hydroxykynurenine, and others as outlined in Supplementary Figures 5A, B. In contrast, we found that these metabolomic alterations led to a reduction in the plasma level of different metabolites including uridine, thymine, carnosine, theophylline, aspartate, taurine, serine, glutamate, tryptophan, arginine, and 53 other metabolites in the acute patients compared to HCs (Supplementary Figures 6A, B).

Differential metabolomic profile of acute COVID-19 patients vs R individuals

We also compared a metabolomic profile of those recovered from COVID-19 infection with the acute stage of the disease. Pathway analysis between acute and R indicated alteration in 36

10.3389/fimmu.2024.1341843

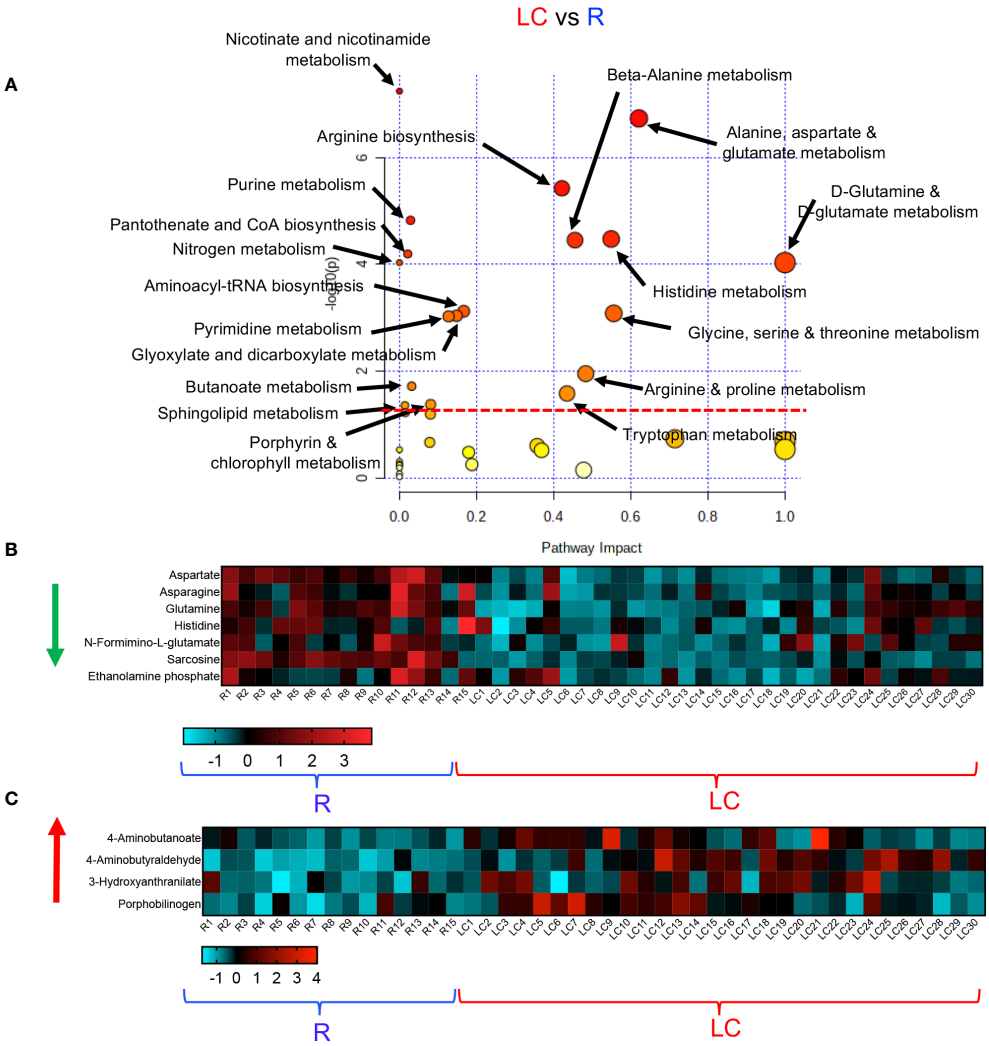

FIGURE 4
Altered metabolomic profile in LC vs R. **(A)** Metabolic pathway enrichment analysis plot shows significantly altered pathways in LC vs R. **(B)** The heatmap shows significantly decreased metabolites in different metabolic pathways in LC vs R. **(C)** The heatmap shows significantly elevated metabolites in different metabolomics pathways in LC vs R.

pathways as indicated in Supplementary Figure 7. These modifications in metabolism pathways resulted in a substantial increase in the levels of 39 metabolites in acute COVID 19 patients compared to the R group such as phenylaniline, pyrimidodiazepine, xanthine, ascorbate, kynurenine, 5-hydroxykynurenine and others as outlined in Supplementary Figures 8A, B. In contrast, we found that these metabolomic alterations led to a reduction in the plasma level of 66 different metabolites in acute patients versus the R group (Supplementary Figures 9A-C). Finally, we compared the metabolomic profile of LC vs acute COVID-19 patients. These analyses revealed alteration in 30 metabolism pathways (Supplementary Figure 10). These changes in metabolism pathways were associated with a significant increase in 29 metabolites as shown in Supplementary Figure 11. In contrast, we observed a significant reduction in 16 metabolites in LC patients compared to those with acute COVID-19 disease (Supplementary Figure 12).

Increased levels of pro-inflammatory cytokines and auto-antibody in LC

Considering the alteration in a variety of pathways such as tryptophan-kynurenine and Xanthine/hypoxanthine, we quantified the levels of inflammatory cytokines. We found a significant increase in the plasma IL-1α, IL-6, TNF-α, IP-10, and liver-associated active phase proteins (CRP and SAA) in LC patients versus R and HCs (Figures 6A-F). However, the plasma IL-13 and IL-1β concentrations remained unchanged between groups (Figures 6G, H). Although we did not find any significant difference between soluble Flt-1, also known as vascular endothelial growth factor receptor 1, levels in the plasma of R and LC patients, LC group exhibits a significant plasma elevation compared to the HC cohort (Figure 6I). We also quantified sCD14, a nonspecific monocyte activation marker, levels in the plasma of our study participants, which showed a significant elevation in LC patients compared to the HC and R groups (Figure 6J). In light of

10.3389/fimmu.2024.1341843

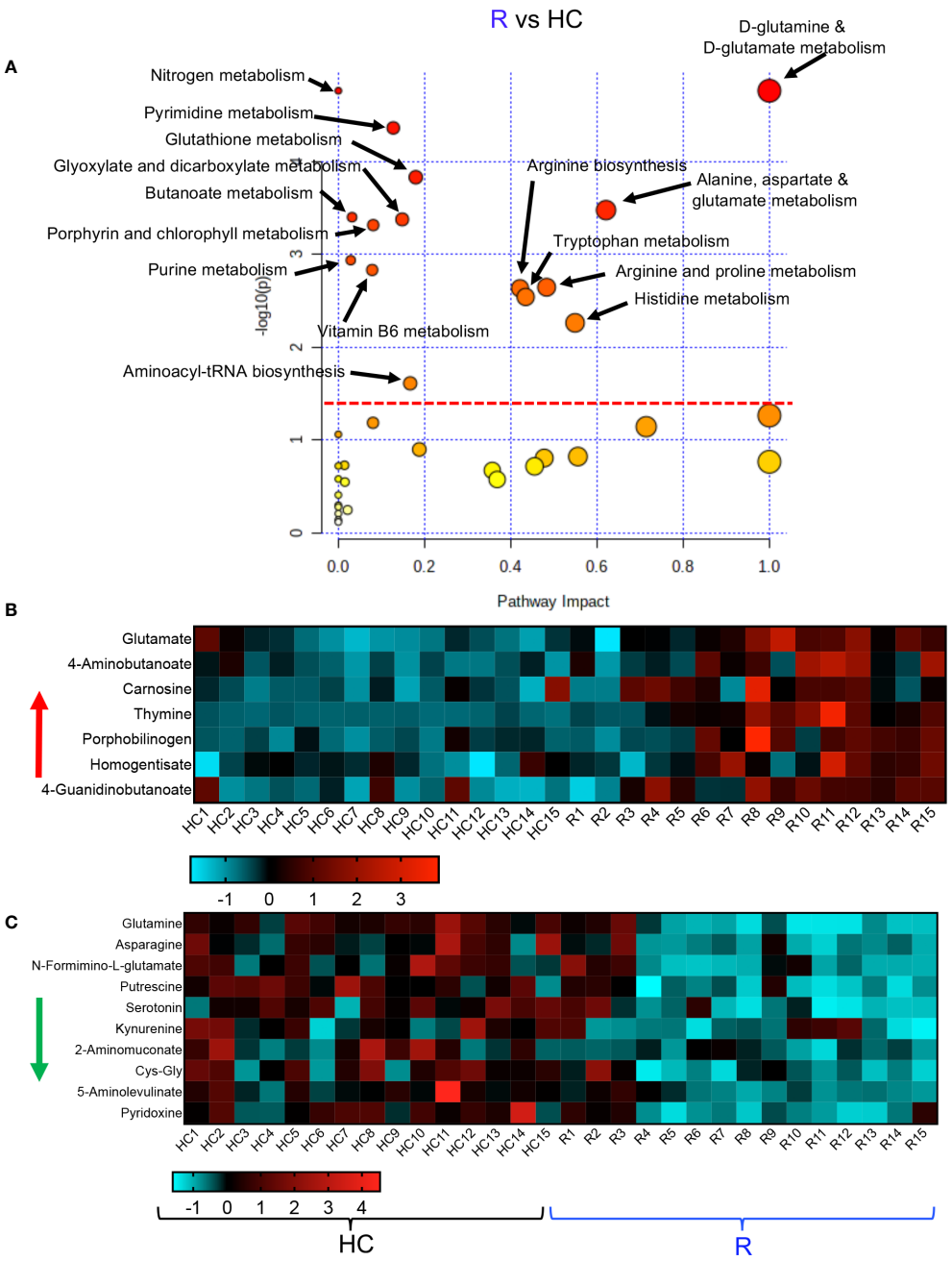

FIGURE 5
Altered metabolomic profile in R vs HC. **(A)** Metabolic pathway enrichment analysis plots of significantly altered pathways in the R vs HC group. **(B)** The heatmap shows significantly increased metabolites in different metabolic pathways in the R vs HC group. **(C)** The heatmap shows significantly decreased metabolites in different metabolic pathways in the R vs HC group.

hypocalcemia in COVID-19 patients and its association with hypoparathyroidism (39, 40), we detected significant levels of the anti-CaSR antibody (calcium receptor) in LC cohort (Figure 6K). This observation forced us to measure the soluble form of CaSR in our different cohorts. Interestingly, we observed the elevation of soluble/shed CaSR in the plasma of acute COVID-19 patients, which was not the case in LC patients (Figure 6L). Finally, considering the impact of COVID-19 infection on the purinergic system (41), we quantified the plasma levels of ATP in our different cohorts. We found a significant reduction in the plasma ATP levels in acute COVID-19 patients compared to HCs and R groups (Figure 6M). Notably, LC patients had a substantially reduced level of ATP in their plasmas compared to either R and HCs (Figure 6M). Intriguingly, the R groups exhibited a significant elevation in the plasma ATP compared to the HC and R groups (Figure 6M). Overall, these observations imply a dysregulated and inflammatory immune response in LC patients.

10.3389/fimmu.2024.1341843

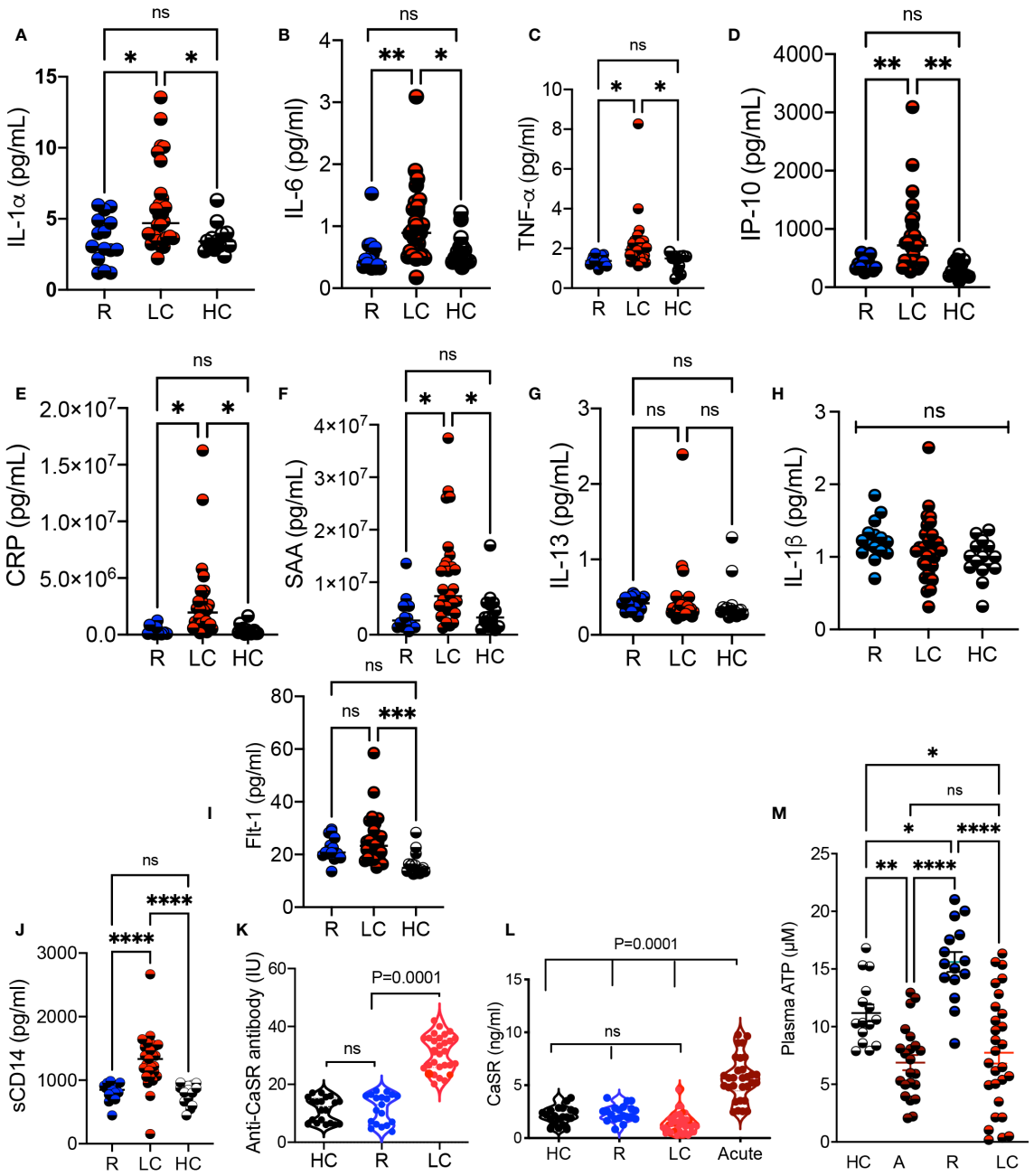

FIGURE 6
Elevated levels of proinflammatory biomarkers in LC patients. **(A)** Cumulative data comparing the plasma IL-1α, **(B)** IL-6, **(C)** TNF-α, **(D)** IP-10, **(E)** CRP, **(F)** SAA, **(G)** IL-13, and **(H)** IL-1β, **(I)** Flt-1, and **(J)** soluble CD14 measured by ELISA in the plasma of R, LC, and HC groups. **(K)** Comparing the Anti-CaSR antibody levels in plasma samples of HC, R, and LC group. **(L)** Soluble CaSR levels in plasma samples of HC, R, LC and acute COVID-19 patients. **(M)** Cumulative data of the plasma ATP in HC, acute, R, and LC groups. Kruskal–Wallis analysis with Dunn's multiple comparisons test. ns, not significant. Each dot represents a study subject. * $p < 0.5$, ** $p \leq 0.01$, *** $p \leq 0.001$, and **** $p \leq 0.0001$.

The association of sarcosine and serine with clinical manifestations in LC

In our investigations of metabolite levels associated with symptoms commonly seen in LC patients such as cognitive function, anxiety, chronic pain, and depression in LC patients, we conducted additional analyses. Despite finding no association between serotonin, tryptophan, aspartate, and kynurenine plasma levels with these symptoms, interestingly, we observed a subtle inverse correlation between sarcosine concentrations and both cognitive failure function scores (Figure 7A) and depression scores in LC patients (Figure 7B). Moreover, our observations revealed a similar association between the plasma serine levels and anxiety and depression scores in LC patients (Figures 7C, D). These initial findings suggest a potential link between reduced levels of sarcosine and serine metabolites and some of the clinical symptoms seen in LC patients.

10.3389/fimmu.2024.1341843

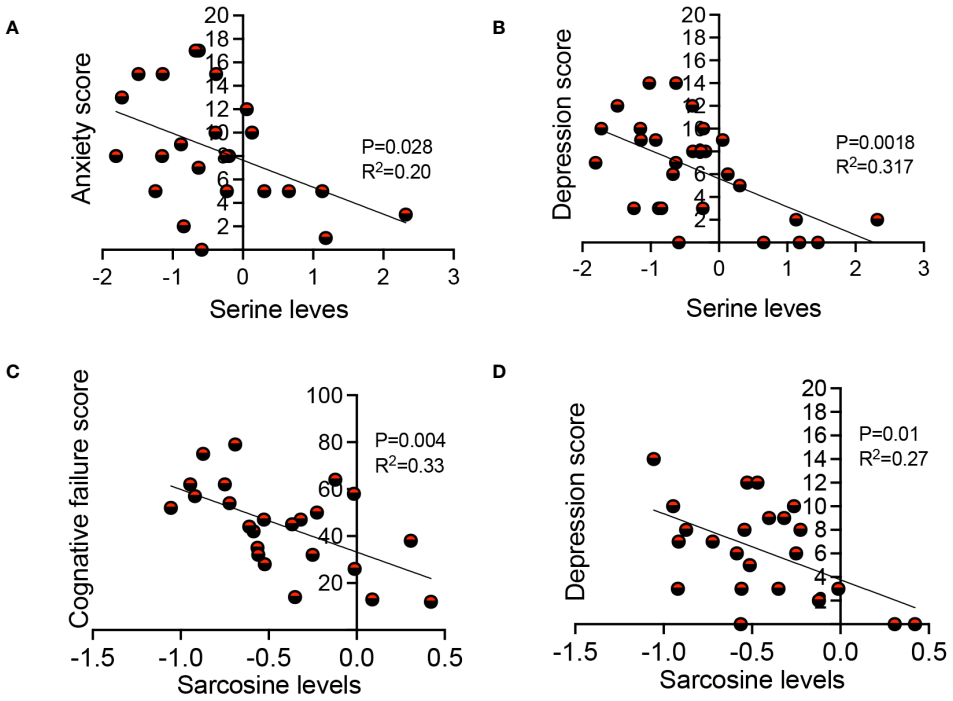

FIGURE 7
The association of sarcosine and serine with clinical symptoms in LC. **(A)** The correlation between serine levels with anxiety score, and **(B)** depression score in LC patients. **(C)** The correlation between sarcosine levels with cognitive failure score, and **(D)** depression score in LC patients. Each dot represents a study subject. P values and R^2 were obtained by Simple linear repression analysis.

Discussion

Diverse metabolomic alterations are reported in the acute phase of SARS-CoV-2 infection (42, 43). However, there have been limited studies to determine whether such metabolomic signature is transient or last for a while after the recovery from the acute disease. To elucidate potential mechanisms, the plasma metabolome of LC patients was investigated and compared to age-sex-matched acutely ill COVID-19, R, and HCs. Our metabolomic analysis revealed alterations in a variety of metabolic pathways in both LC and R individuals even 12 months after the onset of COVID-19 disease. Although our metabolomic analyses are descriptive, they provide insights into metabolomic changes following SARS-CoV-2 infection that lasts for months and possibly years in the absence of a detectable virus. Our results suggest that LC has the potential to severely impact the functionality of different organs. It is possible to speculate that the delay in the tissue repair process following acute COVID-19 disease and the inflammatory milieu result in metabolomic alterations in LC. For example, we noted a reduction in glutamine and ornithine plasma levels, which suggests a disturbance in amino acid and nitrogen metabolism as reported in CFS (44). This may also be consistent with impaired mitochondrial biogenesis as described in circulating lymphocytes in chronic inflammatory conditions (45) and in patients with idiopathic ME/CFS (29).

Also, we detected a reduction in serine concentration, which was inversely associated with depression and anxiety scores in LC patients. Considering that this amino acid is essential for central nervous system (CNS) function and development (46), its decline has been associated with severe neurological disorders (47, 48). Therefore, recognition of serine deficiency in LC is highly important because serine therapy has shown promising outcomes in neurological conditions (49) and in reducing depression and cognitive impairment (50).

We found a significant decline in plasma sarcosine levels in LC patients, which is also reported in critically ill COVID-19 patients (35). Sarcosine, a glycine transporter-I inhibitor, is reported to reduce depression-like symptoms in animal models and human subjects (51). Although, it is unclear whether sarcosine is the cause or the effect, our findings support a link between the low sarcosine levels with cognitive dysfunction and depression scores in LC patients. In support of this concept, sarcosine supplementation has shown promising outcomes in those with learning and memory deficits (52), Parkinson's disease (53), and depression (54). Ultimately, whether sarcosine supplementation can be harnessed to target some of the deleterious manifestations of LC through stimulation of autophagy (55) is an intriguing potential therapy to explore further.

Despite previous reports on the role of tryptophan/serotonin in anxiety and depression (56), our results did not support the idea that changes in these metabolites are associated with depression, anxiety, and cognitive function scores in our LC patients.

The lower arginine in LC patients as reported in acute COVID-19 (57) can be related to increased frequency of CD71+ erythroid cells (CECs) expressing arginase-I and II (58, 59) or the pathology associated with the effects of the virus on the endothelium (60).

Based on this, there is a possibility that arginine has beneficial effects on endothelium function in LC patients.

Other metabolites such as L/D-aspartate and serine amino acids are enriched in the brain and their reduction/dysfunction have been associated with neurological disorders (61). Considering the ability of D-aspartate to cross the BBB (62), D-aspartate supplementation may have therapeutic potential in LC patients. Similarly, arginine and aspartate intake has been associated with delayed muscle fatigue and increased exercise tolerance (63), which could be beneficial in LC with ME/CFS.

Notably, a lower ATP plasma level may imply the impact of LC on the glycolytic and mitochondria pathway for cellular energy production. Such alterations may result in dysfunction or symptoms involving high energy-consuming organs such as the brain, liver, heart, and skeletal muscles (64). While intermediate metabolites associated with TCA cycle (Tricarboxylic Acid Cycle) such as fumarate, succinate, and malate were not significantly different between the groups, we suggest a decrease in mitochondrial activity may result in lower ATP generation as reported in other inflammatory conditions (65, 66). Alternatively, the lingering low level of hypoxia (1) following the acute COVID-19 infection may also contribute to lower ATP levels. Overall, the elevation of pro-inflammatory cytokines may result in mitochondrial dysfunction and/or alteration in LC patients. In line with our observations, mitochondrial dysfunction has been reported in ME/CFS (67, 68). Although we were unable to quantify tissue-specific ATP levels, it is likely to suggest that a lower plasma ATP in LC may contribute to, at least in part, ME/CFS. Given the role of ATP in tissue repair, its low level in LC patients may delay the tissue repair process resulting in sustained inflammatory condition. Therefore, increased ATP levels by ATP regulators may provide a strategy for cell/tissue protection in LC as reported in neurological condition (69).

It has been shown that tryptophan metabolism is enhanced in COVID-19 infection, leading to a decrease in tryptophan and increased levels of kynurenine metabolites (43), which can have multiple deleterious effects on the musculoskeletal system (70). Therefore, increased plasma kynurenine could be linked to LC symptoms. Similarly, increased plasma serotonin levels may explain the mechanism associated with diarrhea in LC patients as reported in acute COVID-19 (71). Similarly, elevated Xanthine/hypoxanthine in LC patients can be associated with increased pro-inflammatory cytokine and acute phase proteins (e.g. IL-1, TNF- α, IL-6, CRP, and SAA) as reported elsewhere (72). While we did not specifically evaluate the M1/M2 macrophage phenotype in our study cohorts, the observed pro-inflammatory immune profile suggests an activation of M1-type macrophages in patients with LC. This finding contrasts with a recent study that proposed higher M2-type macrophage activity in LC (73). Several factors may account for the disparities in our results. Our LC and R groups were recruited 12 months post-acute SARS-CoV-2 infection, whereas Kovarik et al. conducted their study at a much shorter interval (3 months) (73). Additionally, our study cohorts were vaccine-naïve, while subjects in the other study had received 2 doses of SARS-CoV-2 vaccines. Lastly, our cohort represents a homogeneous subset of LC patients with ME/CFS. Other factors such as reduced thymine, increased Flt-1 and pro-inflammatory analytes may favor vascular inflammation in LC (22, 74). Moreover, elevated plasma levels of sCD14 (monocyte activation marker) support the residual general immune activation in LC.

Although we did not find any difference in glutathione and methionine pathways between LC and R groups, they were significantly altered in LC vs HCs. A recent study has reported the prevalence of the genotype CC of the methylenetetrahydrofolate reductase (*MTHFR*) gene in LC patients (75). Hence, this genetic polymorphism may explain differences in cysteine and methionine metabolism in LC patients.

Likewise, alteration in glutathione metabolism may promote oxidative stress and an inflammatory milieu in LC patients as reported in acute COVID-19 disease (76).

Taken together, our results demonstrate diverse metabolomic alterations in patients with LC syndrome. The existence of metabolomic alterations and chronic systemic inflammation even 12 months after acute SARS-CoV-2 infection suggests a dysregulated immune response. This has been supported by the presence of autoantibodies (77, 78). In light of hypocalcemia in COVID-19 patients and its association with hypoparathyroidism (39, 40), we detected significant levels of the anti-CaSR antibody in our LC cohort. Mechanistically, the consequences of SARS-CoV-2 infection-induced mediators (e.g. cytokines, chemokines, growth factors, and metabolites) can have a prominent impact on hematopoietic stem and progenitor cells (HSPCs)[1]. Lingering dysregulated hematopoiesis in LC patients suggests a potentially impaired antiviral response and/or increased innate immune response. Subsequently, an impaired antiviral response may increase antigen persistence and promote chronic inflammation which contributes to metabolomic alteration. Therefore, our studies add novel insights into a growing body of evidence implying that a combination of virus and host factors such as residual immune activation, hematopoietic dysregulation, and autoimmune phenomena could contribute to LC syndrome.

While a recent study has reported alterations in the taurine pathway in LC patients (79), our findings do not support this concept. We did not observe any changes in taurine and hypotaurine metabolism in LC compared to the R group. However, a slight alteration in this metabolic pathway was noted in LC when compared to HCs. In contrast, our results reveal a significant reduction in sarcosine and serine concentrations in LC patients compared to both HCs and the R group. Notably, the inverse correlation between sarcosine/serine levels and cognitive dysfunction/depression suggests that sarcosine/serine supplementations might have therapeutic applications in LC patients.

The substantial differences in our findings compared to the recent study (79) might be related to two main factors. Firstly, our study subjects were recruited 12 months post the onset of acute infection, as opposed to 6 months in the recent report. It is possible to speculate that alterations in the taurine pathway are transient and does not persist until 12 months post the acute disease onset. Secondly, our cohort comprised a homogenous subset of LC patients with ME/CFS, in contrast to the heterogenous cohort in the recent study. In summary, our study provides an insight into

lingering immune activation and altered/impaired mitochondrial bioenergetics in LC patients with ME/CFS. In particular, our global metabolomic analyses revealed important therapeutic targets in LC patients. Nevertheless, it's important to note that further research and clinical trials are needed to validate and establish the efficacy of sarcosine and serine supplementations for therapeutic purposes in LC.

We are aware of several study limitations. This is a single-centered study, therefore, similar studies in larger cohorts of LC patients with ME/CFS are needed. Also, we were unable to collect blood samples on multiple occasions to determine changes in metabolites over time. This study was done on patients infected with the Wuhan strain of SARS-CoV-2. In lights of differential immune response in those infected with other SARS-CoV-2 viral variants (e.g. Delta, Omicron, etc.) (80), further comparative studies are needed. Although sex is a crucial biological variable, the limited representation of males with LC compared to females in our cohort prevented us from observing any significant differences. Moreover, we encountered difficulties in recruiting an equal number of study subjects for each group due to participants availability. This imbalance in group sizes has implications for the statistical power of our study. Our metabolomic analyses did not include lipids; therefore, the lack of data on lipid metabolism in LC prevents our study from providing a comprehensive picture of metabolic alterations. This limitation highlights the importance of future studies incorporating lipid analysis in large prospective LC cohorts. Finally, further studies in animal models of Long-COVID may provide deeper insight into disease pathogenesis and validation of our observations for therapeutic purposes.

Materials and methods

Study population

Sixty PCR-confirmed SARS-CoV-2 infected individuals comprised of 30 LC patients, 15 individuals without LC symptoms who were previously infected with SARS-CoV-2 but recovered without any symptoms per se (recovered group, denoted R), 15 acute hospitalized COVID-19 patients) as well as 15 healthy controls (HCs) without acute symptoms and negative SARS-CoV-2 immunoassays (Figure 1A, Supplementary Table 1). All individuals were infected with SARS-CoV-2 Wuhan viral strain in 2020, which was confirmed by PCR at University of Alberta Hospital, Edmonton. Both LC and R groups were recruited ~12 months after the onset of SARS-CoV-2 infection (Supplementary Table 1).

Ethics statement

This study was approved by the Human Research Ethics Board (HREB) at the University of Alberta (protocol # Pro00099502). A written informed consent form was obtained from all participants but a waiver of consent was obtained for those admitted to the ICU.

Plasma collection

Plasma samples were collected following centrifugation of fresh blood samples and kept frozen at -80 until use.

Metabolomic profiling

Frozen plasma samples were thawed at RT, then were centrifuged at 600 g for 5 min. The 100 µl of soluble fraction was transferred into a new tube and mixed with 300 µl of LC-MS grade methanol. The samples were stored at -20°C for 30 min, then were centrifuged at 16,260 g to let precipitate proteins. The supernatants were transferred into new tubes and dried up completely. The dried samples were reconstituted by dissolving in 85 µl of water. The metabolomic analysis was performed by following the Chemical Isotope Labeling (CIL) LC-MS protocol described in our previous report (81). Briefly, each individual sample was labeled with $^{12}C_2$-dansyl chloride. The pooled sample was generated by mixing each of the individual samples, and labeled by $^{13}C_2$-dansyl chloride. After mixing each ^{12}C-labeled sample with an equal volume of the ^{13}C-labeled pool, the ^{12}C-/^{13}C- mixtures were injected onto LC-MS for analysis. The LC-MS system was Agilent 1290 LC linked to Brukler Impact II QTOF Mass spectrometer. The samples were injected into an Agilent Eclipse Plus reversed-phase C18 column (2.1 mm × 150 mm, 1.8 µm particle size, 95 Å pore size) for separation. Solvent A was 0.1% (v/v) formic acid in water, and solvent B was 0.1% (v/v) formic acid in acetonitrile. The chromatographic conditions were: t= 0 min, 25% B; t= 10 min, 99% B; t= 15 min, 99% B; t= 15.1 min, 25% B; t= 18 min, 25% B. The flow rate was 400 µL/min. All MS spectra were obtained in the positive ion mode. The MS conditions used for Q-TOF were as follows: nebulizer, 1.0 bar; dry temperature, 230°C; dry gas, 8 L/min; capillary voltage, 4500 V; end plate offset, 500 V; spectra rate, 1.0 Hz. The raw data were exported by Bruker Data Analysis 4.4. as.csv files, and the.csv files were processed by IsoMS Pro 1.2.15. The $^{12}C/^{13}C$- peak pairs were extracted, and missing values in the data matrix were filled. Metabolite identification was performed by searching against libraries with different confidence levels. Tier 1 library (DnsID library) contains accurate mass, MS/MS, and retention time information; Tier 2 library (Linked ID library) contains accurate mass and predicted retention time information; Tier 3 library (My Compound ID library, www.MycompoundID.org) contains accurate mass of predicted metabolites. IsoMS Pro was also used for performing the univariate analysis (volcano plot) and multivariate analysis (PCA and PLS-DA). The data file containing Tier 1 metabolites was uploaded to Metaboanalyst 5.0 (www.metaboanalyst.ca) for generating Heatmap. Pathway enrichment analysis was performed by using Metaboanalyst 5.0.

Cytokine and chemokine multiplex analysis

Frozen plasma samples at -80 °CC were thawed and centrifuged for 15 min at 1500g followed by dilution for quantifying cytokine

and chemokine profiles, respectively. The concentration of cytokines and chemokines was quantified using the V-PLEX from Meso Scale Discovery (MSD). Data were acquired on the V-plex® Sector Imager 2400 plate reader. Analyte concentrations were extrapolated from a standard curve calculated using a four-parameter logistic fit using MSD Workbench 3.0 software according to reported protocols (82–84).

The plasma concentration of ATP was quantified using the ATPlite luminescence assay system (PerkinElmer, MA) as we have reported elsewhere (85). The plasma was subjected to ELISA kit sCD14 (R&D, 383CD-050) (80) and Anti-CaSR (EAGLE Biosciences).

Statistical analysis

We initially determined the distribution of data using the Wilks-Shapiro test and then based on the distribution of data the appropriate test was used. When data were not normally distributed the non-parametric tests such as the Mann-Whitney U-test or Kruskal–Wallis analysis of variance were used. Depending on the data set different *post hoc* tests were used. The Dunn's multiple comparisons as the *post hoc* test for the Kruskal–Wallis analysis. The Tukey-Kramer test was used for one-way ANOVA with multiple comparisons. For nonparametric correlational studies tow-tailed Spearman correlation was used. *P*-values are shown in the graphs and measures are expressed as mean ± SEM and *P*-value < 0.05 was considered to be statistically significant. In violin plots, the middle line represents median, the bottom line 1st quartile, and to top line 3rd quartile. No randomization was performed and no data points were excluded.

Data availability statement

The original contributions presented in the study are included in the article/Supplementary Material. Further inquiries can be directed to the corresponding author.

Ethics statement

The studies involving humans were approved by Ethics Board of the University of Alberta. The studies were conducted in accordance with the local legislation and institutional requirements. The participants provided their written informed consent to participate in this study.

Author contributions

SSa: Conceptualization, Writing – review & editing, Data curation, Formal Analysis, Investigation, Methodology, Software, Validation. SSh: Data curation, Formal Analysis, Investigation, Methodology, Writing – review & editing, Visualization. XL: Data curation, Formal Analysis, Investigation, Writing – review & editing, Software. MO: Investigation, Conceptualization, Resources, Writing – review & editing. DR: Investigation, Writing – review & editing, Data curation. JC: Writing – review & editing, Resources. LL: Resources, Writing – review & editing, Software. SE: Resources, Writing – review & editing, Conceptualization, Funding acquisition, Project administration, Supervision, Writing – original draft.

Funding

The author(s) declare financial support was received for the research, authorship, and/or publication of this article. MO is supported by the Arthritis Society through a STAR/IMHA award (award 00049). DR and JC are supported by the Dutch Kidney Foundation. This work was primarily supported by a grant from the Canadian Institutes of Health Research (CIHR) and another grant from the Li Ka Shing Institute of Virology (both to SE).

Acknowledgments

We thank our study volunteers for providing samples and supporting this work and the clinical staff for their dedication to this research. We also acknowledge Biorender.com (Figure 1).

Conflict of interest

The authors declare that the research was conducted in the absence of any commercial or financial relationships that could be construed as a potential conflict of interest.

The author(s) declared that they were an editorial board member of Frontiers, at the time of submission. This had no impact on the peer review process and the final decision.

Publisher's note

Supplementary material

The Supplementary Material for this article can be found online at: https://www.frontiersin.org/articles/10.3389/fimmu.2024.1341843/full#supplementary-material

SUPPLEMENTARY FIGURE 1
(A) The heatmap of the top 100 altered metabolites in acute COVID-19 patients (A) vs HC. **(B)** A vs R, and **(C)** HC vs R.

SUPPLEMENTARY FIGURE 2
(A) The heatmap of the top 100 altered metabolites in R vs LC, and **(B)**, LC vs HC.

SUPPLEMENTARY FIGURE 3
(A) Cumulative data showing relative concentrations of increased and decreased metabolites in the LC vs R group. **(B)** Cumulative data showing relative concentrations of increased and decreased metabolites in LC vs R. Each dot represents a study subject. *P* values were calculated using one-way ANOVA.

SUPPLEMENTARY FIGURE 4
(A) Cumulative data showing relative concentrations of increased and decreased metabolites in R vs HC. **(B)** Metabolic pathway enrichment analysis plot shows significantly altered pathways in A vs HC. Each dot represents a study subject. Data are analyzed by one-way ANOVA.

SUPPLEMENTARY FIGURE 5
(A, B) Cumulative data showing relative concentrations of increased metabolites in the A vs HC group. Each dot represents a study subject. *P* values were calculated using one-way ANOVA.

SUPPLEMENTARY FIGURE 6
(A, B) Cumulative data showing relative concentrations of decreased metabolites in the A vs HC group. Each dot represents a study subject. *P* values were calculated using one-way ANOVA.

SUPPLEMENTARY FIGURE 7
Metabolic pathway enrichment analysis plot shows significantly altered pathways in A vs R.

SUPPLEMENTARY FIGURE 8
(A, B) Cumulative data showing relative concentrations of decreased metabolites in the R vs A group. Each dot represents a study subject. *P* values were calculated using one-way ANOVA.

SUPPLEMENTARY FIGURE 9
Cumulative data showing relative concentrations of elevated metabolites in the R vs A group. Each dot represents a study subject. *P* values were calculated using one-way ANOVA.

SUPPLEMENTARY FIGURE 10
Metabolic pathway enrichment analysis plot shows significantly altered pathways in A vs LC.

References

1. Elahi S. Hematopoietic responses to SARS-CoV-2 infection. *Cell Mol Life Sci CMLS.* (2022) 79(3):187. doi: 10.1007/s00018-022-04220-6

2. Desai AD, Lavelle M, Boursiquot BC, Wan EY. Long-term complications of COVID-19. *Am J Physiol Cell Physiol* (2022) 322(1):C1–C11. doi: 10.1152/ajpcell.00375.2021

3. Taquet M, Dercon Q, Luciano S, Geddes JR, Husain M, Harrison PJ. Incidence, co-occurrence, and evolution of long-COVID features: A 6-month retrospective cohort study of 273,618 survivors of COVID-19. *PloS Med* (2021) 18(9):e1003773. doi: 10.1371/journal.pmed.1003773

4. Gorna R, MacDermott N, Rayner C, O'Hara M, Evans S, Agyen L, et al. Long COVID guidelines need to reflect lived experience. *Lancet* (2021) 397(10273):455–7. doi: 10.1016/S0140-6736(20)32705-7

5. Mehandru S, Merad M. Pathological sequelae of long-haul COVID. *Nat Immunol* (2022) 23(2):194–202. doi: 10.1038/s41590-021-01104-y

6. Bakamutumaho B, Cummings MJ, Owor N, Kayiwa J, Namulondo J, Byaruhanga T, et al. Severe COVID-19 in Uganda across two epidemic phases: A prospective cohort study. *Am J Trop Med Hyg* (2021) 105(3):740–4. doi: 10.4269/ajtmh.21-0551

7. Couzin-Frankel J. The long haul. *Science* (2020) 369(6504):614–7. doi: 10.1126/science.369.6504.614

8. Parums DV. Editorial: long COVID, or post-COVID syndrome, and the global impact on health care. *Med Sci Monitor* (2021) 27:e933446. doi: 10.12659/MSM.933446

9. Sapkota HR, Nune A. Long COVID from rheumatology perspective - a narrative review. *Clin Rheumatol* (2022) 41(2):337–48. doi: 10.1007/s10067-021-06001-1

10. Carfi A, Bernabei R, Landi F, Gemelli Against C-P-ACSG. Persistent symptoms in patients after acute COVID-19. *Jama* (2020) 324(6):603–5. doi: 10.1001/jama.2020.12603

11. Nath A. Long-haul COVID. *Neurology* (2020) 95(13):559–60. doi: 10.1212/WNL.0000000000010640

12. Ferrari R, Russell AS. A questionnaire using the modified 2010 american college of rheumatology criteria for fibromyalgia: specificity and sensitivity in clinical practice. *J Rheumatol* (2013) 40(9):1590–5. doi: 10.3899/jrheum.130367

13. Komaroff AL, Lipkin WI. Insights from myalgic encephalomyelitis/chronic fatigue syndrome may help unravel the pathogenesis of postacute COVID-19 syndrome. *Trends Mol Med* (2021) 27(9):895–906. doi: 10.1016/j.molmed.2021.06.002

14. Mueller C, Lin JC, Sheriff S, Maudsley AA, Younger JW. Evidence of widespread metabolite abnormalities in Myalgic encephalomyelitis/chronic fatigue syndrome: assessment with whole-brain magnetic resonance spectroscopy. *Brain Imaging Behav* (2020) 14(2):562–72. doi: 10.1007/s11682-018-0029-4

15. Douaud G, Lee S, Alfaro-Almagro F, Arthofer C, Wang CY, McCarthy P, et al. SARS-CoV-2 is associated with changes in brain structure in UK Biobank. *Nature* (2022) 604(7907):697–+. doi: 10.1038/s41586-022-04569-5

16. Pan RG, Zhang QR, Anthony SM, Zhou Y, Zou XF, Cassell M, et al. Oligodendrocytes that survive acute coronavirus infection induce prolonged inflammatory responses in the CNS. *Proc Natl Acad Sci United States America.* (2020) 117(27):15902–10. doi: 10.1073/pnas.2003432117

17. Ledford H. Do vaccines protect against long COVID? What the data say. *Nature* (2021) 559(7886):546–8. doi: 10.1038/d41586-021-03495-2

18. Meinhardt J, Radke J, Dittmayer C, Franz J, Thomas C, Mothes R, et al. Olfactory transmucosal SARS-CoV-2 invasion as a port of central nervous system entry in individuals with COVID-19. *Nat Neurosci* (2021) 24(2):168–75. doi: 10.1038/s41593-020-00758-5

19. Daniels BP, Holman DW, Cruz-Orengo L, Jujjavarapu H, Durrant DM, Klein RS. Viral pathogen-associated molecular patterns regulate blood-brain barrier integrity *via* competing innate cytokine signals. *mBio* (2014) 5(5):e01476–14. doi: 10.1128/mBio.01476-14

20. Boldrini M, Canoll PD, Klein RS. How COVID-19 affects the brain. *JAMA Psychiat.* (2021) 78(6):682–3. doi: 10.1001/jamapsychiatry.2021.0500

21. Nalbandian A, Sehgal K, Gupta A, Madhavan MV, McGroder C, Stevens JS, et al. Post-acute COVID-19 syndrome. *Nat Med* (2021) 27(4):601–15. doi: 10.1038/s41591-021-01283-z

22. Iosef C, Knauer MJ, Nicholson M, Van Nynatten LR, Cepinskas G, Draghici S, et al. Plasma proteome of Long-COVID patients indicates HIF-mediated vasculo-proliferative disease with impact on brain and heart function. *J Trans Med* (2023) 21(1):377. doi: 10.1186/s12967-023-04149-9

23. Carvalho T, Krammer F, Iwasaki A. The first 12 months of COVID-19: a timeline of immunological insights. *Nat Rev Immunol* (2021) 21(4):245–56. doi: 10.1038/s41577-021-00522-1

24. Poon DC, Ho YS, Chiu K, Wong HL, Chang RC. Sickness: From the focus on cytokines, prostaglandins, and complement factors to the perspectives of neurons. *Neurosci Biobehav Rev* (2015) 57:30–45. doi: 10.1016/j.neubiorev.2015.07.015

25. Dantzer R, Heijnen CJ, Kavelaars A, Laye S, Capuron L. The neuroimmune basis of fatigue. *Trends Neurosci* (2014) 37(1):39–46. doi: 10.1016/j.tins.2013.10.003

26. Kennedy G, Spence VA, McLaren M, Hill A, Underwood C, Belch JJ. Oxidative stress levels are raised in chronic fatigue syndrome and are associated with clinical symptoms. *Free Radic Biol Med* (2005) 39(5):584–9. doi: 10.1016/j.freeradbiomed.2005.04.020

27. Mandarano AH, Maya J, Giloteaux L, Peterson DL, Maynard M, Gottschalk CG, et al. Myalgic encephalomyelitis/chronic fatigue syndrome patients exhibit altered T cell metabolism and cytokine associations. *J Clin Invest* (2020) 130(3):1491–505. doi: 10.1172/JCI132185

28. Naviaux RK, Naviaux JC, Li K, Bright AT, Alaynick WA, Wang L, et al. Metabolic features of chronic fatigue syndrome. *Proc Natl Acad Sci United States America.* (2016) 113(37):E5472–80. doi: 10.1073/pnas.1607571113

29. Vermeulen RCW, Kurk RM, Visser FC, Sluiter W, Scholte HR. Patients with chronic fatigue syndrome performed worse than controls in a controlled repeated exercise study despite a normal oxidative phosphorylation capacity. *J Trans Med* (2010) 8:93. doi: 10.1186/1479-5876-8-93

30. Jason LA, Sunnquist M, Brown A, Evans M, Vernon SD, Furst J, et al. Examining case definition criteria for chronic fatigue syndrome and myalgic encephalomyelitis. *Fatigue* (2014) 2(1):40–56. doi: 10.1080/21641846.2013.862993

31. Lim EJ, Ahn YC, Jang ES, Lee SW, Lee SH, Son CG. Systematic review and meta-analysis of the prevalence of chronic fatigue syndrome/myalgic encephalomyelitis (CFS/ME). *J Trans Med* (2020) 18(1):100. doi: 10.1186/s12967-020-02269-0

32. Bedree H, Sunnquist M, Jason LA. The dePaul symptom questionnaire-2: A validation study. *Fatigue* (2019) 7(3):166–79. doi: 10.1080/21641846.2019.1653471

33. Gandasegui IM, Laka LA, Gargiulo PA, Gomez-Esteban JC, Sanchez JVL. Myalgic encephalomyelitis/chronic fatigue syndrome: A neurological entity? *Medicina-Lithuania* (2021) 57(10):1030. doi: 10.3390/medicina57101030

34. Maes M, Twisk FNM. Why myalgic encephalomyelitis/chronic fatigue syndrome (ME/CFS) may kill you: disorders in the inflammatory and oxidative and nitrosative stress (IO&NS) pathways may explain cardiovascular disorders in ME/CFS. *Neuroendocrinol Lett* (2009) 30(6):677–93.

35. Fraser DD, Slessarev M, Martin CM, Daley M, Patel MA, Miller MR, et al. Metabolomics profiling of critically ill coronavirus disease 2019 patients: identification of diagnostic and prognostic biomarkers. *Crit Care Explor* (2020) 2(10):e0272. doi: 10.1097/CCE.0000000000000272

36. Meng X, Dunsmore G, Koleva P, Elloumi Y, Wu RY, Sutton RT, et al. The profile of human milk metabolome, cytokines, and antibodies in inflammatory bowel diseases versus healthy mothers, and potential impact on the newborn. *J Crohns Colitis.* (2019) 13(4):431–41. doi: 10.1093/ecco-jcc/jjy186

37. Pang ZQ, Chong J, Zhou GY, Morais DAD, Chang L, Barrette M, et al. MetaboAnalyst 5.0: narrowing the gap between raw spectra and functional insights. *Nucleic Acids Res* (2021) 49(W1):W388–W96. doi: 10.1093/nar/gkab382

38. Xu J, Zhou M, Luo P, Yin Z, Wang S, Liao T, et al. Plasma metabolomic profiling of patients recovered from coronavirus disease 2019 (COVID-19) with pulmonary sequelae 3 months after discharge. *Clin Infect Dis* (2021) 73(12):2228–39. doi: 10.1093/cid/ciab147

39. Elkattawy S, Alyacoub R, Ayad S, Pandya M, Eckman A. A novel case of hypoparathyroidism secondary to SARS-coV-2 infection. *Cureus* (2020) 12(8):e10097. doi: 10.7759/cureus.10097

40. Liu J, Han P, Wu J, Gong J, Tian D. Prevalence and predictive value of hypocalcemia in severe COVID-19 patients. *J Infect Public Health* (2020) 13 (9):1224–8. doi: 10.1016/j.jiph.2020.05.029

41. da Silva GB, Manica D, da Silva AP, Kosvoski GC, Hanauer M, Assmann CE, et al. High levels of extracellular ATP lead to different inflammatory responses in COVID-19 patients according to the severity. *J Mol Med (Berl).* (2022) 100(4):645–63. doi: 10.1007/s00109-022-02185-4

42. Shen B, Yi X, Sun Y, Bi X, Du J, Zhang C, et al. Proteomic and metabolomic characterization of COVID-19 patient sera. *Cell* (2020) 182(1):59–72 e15. doi: 10.1016/j.cell.2020.05.032

43. Thomas T, Stefanoni D, Reisz JA, Nemkov T, Bertolone L, Francis RO, et al. COVID-19 infection alters kynurenine and fatty acid metabolism, correlating with IL-6 levels and renal status. *JCI Insight* (2020) 5(14):e140327. doi: 10.1172/jci.insight.140327

44. Armstrong CW, McGregor NR, Sheedy JR, Buttfield I, Butt HL, Gooley PR. NMR metabolic profiling of serum identifies amino acid disturbances in chronic fatigue syndrome. *Clin Chim Acta* (2012) 413(19-20):1525–31. doi: 10.1016/j.cca.2012.06.022

45. Nagy G, Barcza M, Gonchoroff N, Phillips PE, Perl A. Nitric oxide-dependent mitochondrial biogenesis generates Ca2+ signaling profile of lupus T cells. *J Immunol* (2004) 173(6):3676–83. doi: 10.4049/jimmunol.173.6.3676

46. Yoshida K, Furuya S, Osuka S, Mitoma J, Shinoda Y, Watanabe M, et al. Targeted disruption of the mouse 3-phosphoglycerate dehydrogenase gene causes severe neurodevelopmental defects and results in embryonic lethality. *J Biol Chem* (2004) 279(5):3573–7. doi: 10.1074/jbc.C300507200

47. Tabatabaie L, Klomp LW, Rubio-Gozalbo ME, Spaapen LJ, Haagen AA, Dorland L, et al. Expanding the clinical spectrum of 3-phosphoglycerate dehydrogenase deficiency. *J Inherit Metab Dis* (2011) 34(1):181–4. doi: 10.1007/s10545-010-9249-5

48. Murtas G, Marcone GL, Sacchi S, Pollegioni L. L-serine synthesis *via* the phosphorylated pathway in humans. *Cell Mol Life Sci CMLS.* (2020) 77(24):5131–48. doi: 10.1007/s00018-020-03574-z

49. de Koning TJ. Amino acid synthesis deficiencies. *J Inherit Metab Dis* (2017) 40 (4):609–20. doi: 10.1007/s10545-017-0063-1

50. MacKay MB, Kravtsenyuk M, Thomas R, Mitchell ND, Dursun SM. Baker GB. *D-Serine: Potential Ther Agent and/or biomark Schizophr Depression? Front Psychiatry* (2019) 10:25. doi: 10.3389/fpsyt.2019.00025

51. Huang CC, Wei IH, Huang CL, Chen KT, Tsai MH, Tsai P, et al. Inhibition of glycine transporter-I as a novel mechanism for the treatment of depression. *Biol Psychiat.* (2013) 74(10):734–41. doi: 10.1016/j.biopsych.2013.02.020

52. Kumar V, Ahmad MA, Najmi AK, Akhtar M. Effect of sarcosine (a glycine transport 1 inhibitor) and risperidone (an atypical antipsychotic drug) on MK-801 induced learning and memory deficits in rats. *Drug Res (Stuttg).* (2016) 66(1):11–7. doi: 10.1055/s-0035-1545299

53. Tsai CH, Huang HC, Liu BL, Li CI, Lu MK, Chen X, et al. Activation of N-methyl-D-aspartate receptor glycine site temporally ameliorates neuropsychiatric symptoms of Parkinson's disease with dementia. *Psychiatry Clin Neurosci* (2014) 68 (9):692–700. doi: 10.1111/pcn.12175

54. Chen KT, Wu CH, Tsai MH, Wu YC, Jou MJ, Huang CC, et al. Antidepressant-like effects of long-term sarcosine treatment in rats with or without chronic unpredictable stress. *Behav Brain Res* (2017) 316:1–10. doi: 10.1016/j.bbr.2016.06.004

55. Walters RO, Arias E, Diaz A, Burgos ES, Guan FX, Tiano S, et al. Sarcosine is uniquely modulated by aging and dietary restriction in rodents and humans. *Cell Rep* (2018) 25(3):663–+. doi: 10.1016/j.celrep.2018.09.065

56. Lindseth G, Helland B, Caspers J. The effects of dietary tryptophan on affective disorders. *Arch Psychiat Nurs.* (2015) 29(2):102–7. doi: 10.1016/j.apnu.2014.11.008

57. Reizine F, LesouHaitier M, Gregoire M, Pinceaux K, Gacouin A, Maamar A, et al. SARS-coV-2-induced ARDS associates with MDSC expansion, lymphocyte dysfunction, and arginine shortage. *J Clin Immunol* (2021) 41(3):515–25. doi: 10.1007/s10875-020-00920-5

58. Shahbaz S, Xu L, Osman M, Sligl W, Shields J, Joyce M, et al. Erythroid precursors and progenitors suppress adaptive immunity and get invaded by SARS-CoV-2. *Stem Cell Rep* (2021) 16(5):1165–81. doi: 10.1016/j.stemcr.2021.04.001

59. Saito S, Shahbaz S, Sligl W, Osman M, Tyrrell DL, Elahi S. Differential impact of SARS-coV-2 isolates, namely, the wuhan strain, delta, and omicron variants on erythropoiesis. *Microbiol Spectr* 2022 10(4):e0173022. doi: 10.1128/spectrum.01730-22

60. Fiorentino G, Coppola A, Izzo R, Annunziata A, Bernardo M, Lombardi A, et al. Effects of adding L-arginine orally to standard therapy in patients with COVID-19: A randomized, double-blind, placebo-controlled, parallel-group trial. *Results first interim analysis. Eclinicalmedicine.* (2021) 40:101125. doi: 10.1016/j.eclinm.2021.101125

61. Errico F, Nuzzo T, Carella M, Bertolino A, Usiello A. The emerging role of altered d-aspartate metabolism in schizophrenia: new insights from preclinical models and human studies. *Front Psychiatry* (2018) 9:559. doi: 10.3389/fpsyt.2018.00559

62. Sacchi S, Novellis V, Paolone G, Nuzzo T, Iannotta M, Belardo C, et al. Olanzapine, but not clozapine, increases glutamate release in the prefrontal cortex of freely moving mice by inhibiting D-aspartate oxidase activity. *Sci Rep* (2017) 7:46288. doi: 10.1038/srep46288

63. Burtscher M, Brunner F, Faulhaber M, Hotter B, Likar R. The prolonged intake of L-arginine-L-aspartate reduces blood lactate accumulation and oxygen consumption during submaximal exercise. *J Sports Sci Med* (2005) 4(3):314–22.

64. Wang Z, Ying Z, Bosy-Westphal A, Zhang J, Schautz B, Later W, et al. Specific metabolic rates of major organs and tissues across adulthood: evaluation by mechanistic model of resting energy expenditure. *Am J Clin Nutr* (2010) 92(6):1369–77. doi: 10.3945/ajcn.2010.29885

65. Brealey D, Brand M, Hargreaves I, Heales S, Land J, Smolenski R, et al. Association between mitochondrial dysfunction and severity and outcome of septic shock. *Lancet* (2002) 360(9328):219–23. doi: 10.1016/S0140-6736(02)09459-X

66. Lee I, Huttemann M. Energy crisis: the role of oxidative phosphorylation in acute inflammation and sepsis. *Biochim Biophys Acta* (2014) 1842(9):1579–86. doi: 10.1016/j.bbadis.2014.05.031

67. Myhill S, Booth NE, McLaren-Howard J. Targeting mitochondrial dysfunction in the treatment of Myalgic Encephalomyelitis/Chronic Fatigue Syndrome (ME/CFS) - a clinical audit. *Int J Clin Exp Med* (2013) 6(1):1–15.

68. Castro-Marrero J, Cordero MD, Saez-Francas N, Jimenez-Gutierrez C, Aguilar-Montilla FJ, Aliste L, et al. Could mitochondrial dysfunction be a differentiating marker between chronic fatigue syndrome and fibromyalgia? *Antioxid Redox Sign* (2013) 19 (15):1855–60. doi: 10.1089/ars.2013.5346

69. Nakano M, Imamura H, Sasaoka N, Yamamoto M, Uemura N, Shudo T, et al. ATP maintenance *via* two types of ATP regulators mitigates pathological phenotypes in mouse models of parkinson's disease. *Ebiomedicine* (2017) 22:225–41. doi: 10.1016/j.ebiom.2017.07.024

70. Duan Z, Lu J. Involvement of aryl hydrocarbon receptor in L-kynurenine-mediated parathyroid hormone-related peptide expression. *Horm Cancer* (2019) 10(2-3):89–96. doi: 10.1007/s12672-019-0357-x

71. Ha S, Jin B, Clemmensen B, Park P, Mahboob S, Gladwill V, et al. Serotonin is elevated in COVID-19-associated diarrhoea. *Gut* (2021) 70(10):2015–+. doi: 10.1136/gutjnl-2020-323542

72. Fonseca W, Malinczak CA, Schuler CF, Best SKK, Rasky AJ, Morris SB, et al. Uric acid pathway activation during respiratory virus infection promotes Th2 immune response *via* innate cytokine production and ILC2 accumulation. *Mucosal Immunol* (2020) 13(4):691–701. doi: 10.1038/s41385-020-0264-z

73. Kovarik JJ, Bileck A, Hagn G, Meier-Menches SM, Frey T, Kaempf A, et al. A multi-omics based anti-inflammatory immune signature characterizes long COVID-19 syndrome. *iScience* (2023) 26(1):105717. doi: 10.1016/j.isci.2022.105717

74. Omori K, Katakami N, Yamamoto Y, Ninomiya H, Takahara M, Matsuoka TA, et al. Identification of metabolites associated with onset of CAD in diabetic patients using CE-MS analysis: A pilot study. *J Atheroscler Thromb* (2019) 26(3):233–45. doi: 10.5551/jat.42945

75. da Silva R, de Sarges KML, Cantanhede MHD, da Costa FP, Dos Santos EF, Rodrigues FBB, et al. Thrombophilia and immune-related genetic markers in long COVID. *Viruses* (2023) 15(4):885. doi: 10.3390/v15040885

76. Labarrere CA, Kassab GS. Glutathione: A Samsonian life-sustaining small molecule that protects against oxidative stress, ageing and damaging inflammation. *Front Nutr* (2022) 9. doi: 10.3389/fnut.2022.1007816

77. Rojas M, Rodriguez Y, Acosta-Ampudia Y, Monsalve DM, Zhu CS, Li QZ, et al. Autoimmun is hallmark post-COVID syndrome. *J Trans Med* (2022) 20(1):129. doi: 10.1186/s12967-022-03328-4

78. Su Y, Yuan D, Chen DG, Ng RH, Wang K, Choi J, et al. Multiple early factors anticipate post-acute COVID-19 sequelae. *Cell* (2022) 185(5):881–95 e20. doi: 10.1016/j.cell.2022.01.014

79. Wang K, Khoramjoo M, Srinivasan K, Gordon PMK, Mandal R, Jackson D, et al. Sequential multi-omics analysis identifies clinical phenotypes and predictive biomarkers for long COVID. *Cell Rep Med* (2023) 4(11):101254. doi: 10.1016/j.xcrm.2023.101254

80. Shahbaz S, Bozorgmehr N, Lu J, Osman M, Sligl W, Tyrrell DL, et al. Analysis of SARS-CoV-2 isolates, namely the Wuhan strain, Delta variant, and Omicron variant, identifies differential immune profiles. *Microbiol Spectr*. (2023) 11(5):e0125623. doi: 10.1128/spectrum.01256-23

81. Guo K, Li L. Differential 12C-/13C-isotope dansylation labeling and fast liquid chromatography/mass spectrometry for absolute and relative quantification of the metabolome. *Anal Chem* (2009) 81(10):3919–32. doi: 10.1021/ac900166a

82. Bozorgmehr N, Mashhouri S, Perez Rosero E, Xu L, Shahbaz S, Sligl W, et al. Galectin-9, a player in cytokine release syndrome and a surrogate diagnostic biomarker in SARS-coV-2 infection. *mBio* (2021) 12(3):e00384-21. doi: 10.1128/mBio.00384-21

83. Bozorgmehr N, Okoye I, Oyegbami O, Xu L, Fontaine A, Cox-Kennett N, et al. Expanded antigen-experienced CD160(+)CD8(+)effector T cells exhibit impaired effector functions in chronic lymphocytic leukemia. *J Immunother Cancer* (2021) 9 (4):e002189. doi: 10.1136/jitc-2020-002189

84. Bozorgmehr N, Syed H, Mashhouri S, Walker J, Elahi S. Transcriptomic profiling of peripheral blood cells in HPV-associated carcinoma patients receiving combined valproic acid and avelumab. *Mol Oncol* (2023). doi: 10.1002/1878-0261.13519

85. Shahbaz S, Okoye I, Blevins G, Elahi S. Elevated ATP *via* enhanced miRNA-30b, 30c, and 30e downregulates the expression of CD73 in CD8+ T cells of HIV-infected individuals. *PloS Pathog* (2022) 18(3):e1010378. doi: 10.1371/journal.ppat.1010378

frontiers | Frontiers in Immunology

TYPE Original Research
PUBLISHED 22 January 2024
DOI 10.3389/fimmu.2024.1348041

OPEN ACCESS

EDITED BY
Aristo Vojdani,
Immuno Sciences Lab Inc., United States

REVIEWED BY
James Lyons-Weiler,
Institute for Pure and Applied Knowledge, United States
Tinatin Chikovani,
Tbilisi State Medical University, Georgia
Modra Murovska,
Riga StradiņšUniversity, Latvia
Giorgi Kharebava,
Tbilisi State Medical University, Georgia

*CORRESPONDENCE
Charles C. Kim
charliekim@verily.com

†These authors share first authorship

RECEIVED 01 December 2023
ACCEPTED 02 January 2024
PUBLISHED 22 January 2024

CITATION
Leung JM, Wu MJ, Kheradpour P, Chen C, Drake KA, Tong G, Ridaura VK, Zisser HC, Conrad WA, Hudson N, Allen J, Welberry C, Parsy-Kowalska C, Macdonald I, Tapson VF, Moy JN, deFilippi CR, Rosas IO, Basit M, Krishnan JA, Parthasarathy S, Prabhakar BS, Salvatore M and Kim CC (2024) Early immune factors associated with the development of post-acute sequelae of SARS-CoV-2 infection in hospitalized and non-hospitalized individuals. *Front. Immunol.* 15:1348041. doi: 10.3389/fimmu.2024.1348041

Early immune factors associated with the development of post-acute sequelae of SARS-CoV-2 infection in hospitalized and non-hospitalized individuals

Jacqueline M. Leung[1†], Michelle J. Wu[1†], Pouya Kheradpour[1†], Chen Chen[1], Katherine A. Drake[1], Gary Tong[1], Vanessa K. Ridaura[1], Howard C. Zisser[1], William A. Conrad[2], Natalia Hudson[3], Jared Allen[3], Christopher Welberry[3], Celine Parsy-Kowalska[3], Isabel Macdonald[3], Victor F. Tapson[4], James N. Moy[5], Christopher R. deFilippi[6], Ivan O. Rosas[7], Mujeeb Basit[8], Jerry A. Krishnan[9], Sairam Parthasarathy[10], Bellur S. Prabhakar[11], Mirella Salvatore[12] and Charles C. Kim[1*]

[1]Verily Life Sciences, South San Francisco, CA, United States, [2]Providence Little Company of Mary Medical Center Torrance, Torrance, CA, United States, [3]Oncimmune Limited, Nottingham, United Kingdom, [4]Department of Medicine, Cedars-Sinai Medical Center, Los Angeles, CA, United States, [5]Department of Internal Medicine, Rush University Medical Center, Chicago, IL, United States, [6]Inova Schar Heart and Vascular, Falls Church, VA, United States, [7]Department of Medicine, Baylor College of Medicine, Houston, TX, United States, [8]Department of Internal Medicine, University of Texas Southwestern Medical Center, Dallas, TX, United States, [9]Breathe Chicago Center, University of Illinois Chicago, Chicago, IL, United States, [10]Division of Pulmonary, Allergy, Critical Care & Sleep Medicine, University of Arizona, Tucson, AZ, United States, [11]Department of Microbiology and Immunology, University of Illinois - College of Medicine, Chicago, IL, United States, [12]Department of Medicine and Department of Population Health Sciences, Weill Cornell Medicine, New York, NY, United States

Background: Infection by severe acute respiratory syndrome coronavirus 2 (SARS-CoV-2) can lead to post-acute sequelae of SARS-CoV-2 (PASC) that can persist for weeks to years following initial viral infection. Clinical manifestations of PASC are heterogeneous and often involve multiple organs. While many hypotheses have been made on the mechanisms of PASC and its associated symptoms, the acute biological drivers of PASC are still unknown.

Methods: We enrolled 494 patients with COVID-19 at their initial presentation to a hospital or clinic and followed them longitudinally to determine their development of PASC. From 341 patients, we conducted multi-omic profiling on peripheral blood samples collected shortly after study enrollment to investigate early immune signatures associated with the development of PASC.

Results: During the first week of COVID-19, we observed a large number of differences in the immune profile of individuals who were hospitalized for COVID-19 compared to those individuals with COVID-19 who were not hospitalized. Differences between individuals who did or did not later develop PASC were, in comparison, more limited, but included significant differences in autoantibodies and in epigenetic and transcriptional signatures in double-negative 1 B cells, in particular.

Conclusions: We found that early immune indicators of incident PASC were nuanced, with significant molecular signals manifesting predominantly in double-negative B cells, compared with the robust differences associated with hospitalization during acute COVID-19. The emerging acute differences in B cell phenotypes, especially in double-negative 1 B cells, in PASC patients highlight a potentially important role of these cells in the development of PASC.

KEYWORDS

COVID-19, PASC, long COVID, autoantibody, double-negative B cells

Introduction

Since 2019, the Coronavirus Disease 2019 (COVID-19) pandemic, caused by infection with severe acute respiratory syndrome coronavirus 2 (SARS-CoV-2), has caused significant morbidity and mortality around the world. Although rates of hospitalizations and deaths from COVID-19 have declined in recent years (1), COVID-19 remains a global public health challenge and was ranked as the fourth leading cause of death in the United States in 2022 (2). COVID-19 is characterized by a spectrum of illnesses ranging from asymptomatic infection to severe disease and mortality. While the majority of individuals recover from COVID-19, a subset of SARS-CoV-2-infected individuals experience persistent (or emerging) symptoms that can last for weeks to years following initial infection (3), a condition known as post-acute sequelae of SARS-CoV-2 infection (PASC) or long COVID. Individuals with PASC experience a wide range of symptoms affecting multiple organ systems, including symptoms such as loss of taste or smell, post-exertional malaise, fatigue, brain fog, gastrointestinal symptoms, chronic cough, and chest pain, among others (4). The biological driver(s) of the diverse manifestations of PASC are currently unknown (5), and it is still unclear why some individuals develop PASC while others do not. Emerging evidence suggests that PASC development is associated with long lasting dysregulation of the immune response that may be a consequence from various factors including excessive inflammatory responses due to viral activation, viral reservoirs persisting in infected tissues, gut dysbiosis, microvascular dysfunction, and autoimmunity to self-antigens (6, 7).

A number of studies have evaluated the immune response during acute COVID-19 and between individuals with and without established PASC (8–15). However, the early immune response during acute SARS-CoV-2 infection in individuals who eventually do and do not develop PASC remains relatively understudied. In this study, we collected peripheral blood samples from COVID-19 patients during their initial presentation to an ambulatory clinic or hospital in the early stages of the pandemic (May 2020 to June 2021) and followed them longitudinally to determine their development of PASC. We conducted multi-omic assays on samples collected at hospital and clinic presentation, with the aim of uncovering early immune mechanisms that differentiated individuals on different trajectories of PASC.

Materials and methods

Study design

The Predictors of Severe COVID-19 Outcomes (PRESCO) study (Trial Registration Number: NCT04388813) was a multi-center, prospective, cohort study aimed at identifying molecular and clinical features associated with the progression to severe COVID-19. Adults age 18 years and older with a confirmed, positive test for SARS-CoV-2 infection (via reverse transcription-polymerase chain reaction (RT-PCR) or antigen testing), who received care at one of eight sites across the United States (Baylor College of Medicine, Cedars-Sinai Medical Center, Inova Health Care Services, Rush University Medical Center, The University of Arizona, University of Illinois Chicago, University of Texas Southwestern Medical Center, and Weill Cornell Medical College) between May 2020 and June 2021 were invited to participate. Individuals who were pregnant were excluded from the study. Participants were followed for three months after enrollment. Enrollment for the PRESCO study was completed before the SARS-CoV-2 delta variant emerged as the predominant variant in the United States during the summer of 2021 and before the availability of the COVID-19 treatments, nirmatrelvir, ritonavir, and molnupiravir. The PRESCO study included up to five study visits: (1) at enrollment during a participants' initial presentation to an ambulatory clinic or hospital, and, in people who were hospitalized, (2) two days after hospitalization, (3) the day of admission to an intensive care unit (if this occurred), (4) the day of hospital discharge, and, for all participants, (5) a follow-up visit three months after enrollment. Participants were followed through visit 5 or study exit for other reasons (e.g., death or lost to follow-up), whichever occurred first.

As the COVID-19 pandemic evolved, information on PASC and any remaining symptoms at the 3-month follow-up visit were collected. Participants who developed PASC (termed the "PASC"

group) and participants who did not develop PASC (termed the "non-PASC" group) were grouped based on the definition of PASC from the Center for Disease Control and Prevention (16). Specifically, during the 3-month follow-up visit, participants were asked about the duration, in weeks, that it took for them, since their last study visit, to return to their usual state of health. Individuals with PASC were then defined as those individuals who did not recover to their usual state of health for four or more weeks since the start of COVID-19, which was determined by the earliest of several non-self-reported dates, including enrollment in the PRESCO study, first laboratory-confirmed positive SARS-CoV-2 test, date of hospital presentation, and hospitalization date (17).

Approval to conduct the PRESCO study was obtained by a central Western Institutional Review Board (IRB Protocol number: 20201016) and from each of the eight sites that enrolled participants. All participants or their legally authorized representatives provided written informed consent before any study-related procedures began. See the Supplementary Material for more details.

Multi-omic analysis

All comparisons were conducted on blood samples collected at either hospital or clinic presentation or two days after hospitalization for hospitalized patients. Given the close proximity in the timing of these sample collections, samples from these two visits were analyzed together for all downstream analyses. All comparisons were either between hospitalized and non-hospitalized participants or PASC and non-PASC participants.

Verily's Immune Profiler platform was used to conduct multi-omic analyses of collected blood samples. Briefly, 25 immune cell subsets, including a bulk peripheral blood mononuclear cell (PBMC) sample, 5 myeloid cell subsets, 7 B cell subsets, 10 T cell subsets, and 2 natural killer (NK) cell subsets, were isolated from approximately 10 million cryopreserved PBMCs per participant. The bulk PBMC subset was used for quality control measures only and was not analyzed further in the multi-omic comparisons. Assay for transposase-accessible chromatin using sequencing (ATAC-seq) and RNA sequencing (RNA-seq) were performed for all of the 25 subsets, and targeted protein estimation by sequencing (TaPE-seq) (18) was performed for the 12 immune cell subsets within the T and NK panel (Supplementary Table 1). Flow cytometry, ATAC-seq, RNA-seq, and TaPE-seq were performed as previously described (19).

Quantification of plasma cytokines

From plasma samples, 47 cytokines (EGF, Eotaxin, FGF-2, Flt-3 ligand, Fractalkine, G-CSF, GM-CSF, GROα, IFNα2, IFNγ, IL-1α, IL-1β, IL-1ra, IL-2, IL-3, IL-4, IL-5, IL-6, IL-7, IL-8, IL-9, IL-10, IL-12p40, IL-12p70, IL-13, IL-15, IL-17A, IL-17E/IL-25, IL-17F, IL-18, IL-22, IL-27, IP-10, LTA [TNFβ], MCP-1, MCP-3, M-CSF, MDC, MIG, MIP-1α, MIP-1β, PDGF-AA, PDGF-AB/BB, sCD40L, TGFα, TNF [TNFα], and VEGF-A) were quantified using the MILLIPLEX MAP Human Cytokine/Chemokine/Growth Factor Panel A on a Luminex FLEXMAP 3D instrument, according to the manufacturer's instructions. For each measured cytokine, concentration values that fell outside of the standard curve were imputed to the nearest standard concentration. The cytokine, GM-CSF, was excluded from further analysis because 98% of its measurements were outside of the kit's quantification range. Downstream cytokine analyses thus included a total of 46 cytokines. Additionally, individual cytokine measurements that did not have either a) bead counts ≥ 35 and technical coefficients of variation (CV) ≤ 30%, or b) bead counts ≥ 20 and technical CV ≤ 15%, were excluded from further analysis.

Quantification of autoantibodies and antibodies against viral antigens

Multiplexed bead-based arrays were assembled with a total of 744 antigens: 441 human proteins indicated in immune responses (and including 3 Ig controls), 114 viral proteins that included differing recombinant versions of proteins of SARS-CoV-2 as well as other viruses (MERS-CoV, SARS-CoV-1, SARS-CoV-2, HCoV-HKU1, HCoV-229E, HCoV-NL63, HCoV-OC43, Influenza A, and Influenza B), and 192 viral peptides, of which 178 originated from SARS-CoV-2 sequences and 14 were from other viruses. A full list of the human and viral proteins used in this study can be found in Supplementary Table 2, Supplementary Table 3, respectively, and is summarized in Supplementary Table 4. A full list of the viral peptides used can be found in Supplementary Table 5 and is summarized in Supplementary Table 6. See the Methods section in the Supplementary Material for more details.

Assay methodology for autoantibody and viral antibody detection has been described previously (20). Briefly, beads were analyzed on a FLEXMAP 3D instrument for fluorescent signal readout, as measured by median fluorescence intensity (MFI). Measurements were excluded when there were low numbers of bead events (< 10 beads) counted per bead region. Median inter- and intra-plate CV were calculated by measuring three reference samples: one COVID-19 positive, one Systemic Lupus Erythematosus (SLE) positive, and one SLE and COVID-19 negative.

Several fixed control criteria were defined to enforce high data quality. A data completeness threshold was set at > 98% of available instrument data. Additionally, bead count statistics were controlled to disallow more than 10% drop-outs. This criterion prevented the use of MFI values for plates, samples, and antigens with insufficient bead counts. The lower MFI range was monitored via median MFI of BSA-coupled beads and was set to be below 500. Upper median MFI range of the IgG-coupled beads was set to > 20,000. The antigen panel was divided into 4 bead-based arrays for ease of processing of up to 230 bead regions. Assays contained control reference samples as well as sample-antigen pairs measured in triplicate in each plate. This allowed for control of inter- and intra-plate variance, which were both set to < 30%. Additionally, for proteins raised in *E. coli*, background reactivity of sera to *E. coli* proteins was monitored. See the Supplementary Material for more details.

Differential analysis

Linear modeling methods were used for univariate differential analysis as previously described (19). Briefly, for these analyses, each molecular feature was regressed on the outcome group and appropriate clinical and technical covariates. For count-based data such as ATAC-seq, RNA-seq, and TaPE-seq, the voom-limma method was used (21). For non-count-based data such as cell subset frequencies, autoantibody/antibody concentrations, and cytokine levels, differential analysis was performed by fitting generalized linear models (GLMs). Where appropriate, data were transformed (e.g., log transformation) prior to fitting the GLMs.

Our models adjusted for a number of covariates, including demographic and clinical variables and assay-specific variables. The full model in the PASC versus non-PASC comparisons included covariates for age, sex, race, tobacco use, WHO score, and the time from COVID-19 start to sample collection. In comparing hospitalized and non-hospitalized participants, WHO score was removed as a covariate given its association with hospitalization. Association analyses with multi-omic data also adjusted for variables associated with sample quality, including neutrophil frequency (as a measure of neutrophil contamination during the isolation of PBMCs), cell viability, and the recovered subset cell counts.

Following linear modeling, the Benjamini-Hochberg procedure was used to correct for multiple hypothesis testing within each molecular data type. For the multi-omic data, comparisons were conducted per immune cell subset, and the resulting p-values across all tests within a cell subset were corrected. Significance was assessed at a false discovery rate (FDR) of 0.1, unless otherwise noted.

Pathway analysis

Gene sets from the Molecular Signatures Database (MSigDB) were used for pathway analysis through two independent methods. First, gene set enrichment of significant differential genes were tested using hypergeometric tests. Second, Gene Set Enrichment Analysis (GSEA) (22) was conducted using effect estimates from the univariate differential analysis, which enabled the identification of gene sets where the individual genes may not be significantly differentially expressed, but are nonetheless coordinated in their association with hospitalization or PASC development.

Results

Overview of the PRESCO cohort and molecular data generation

A total of 494 participants with COVID-19 were enrolled in the PRESCO study, of which 354 participants had follow-up symptom surveys collected approximately 3 months after the start of COVID-19 that could inform on their development of PASC. Demographic and clinical characteristics associated with PASC in this cohort were previously described (17). Briefly, in the PRESCO cohort, participants with PASC were significantly older in age, had greater proportions of tobacco use and obesity, and had a greater proportion of Non-Hispanic White people than non-PASC participants (17). The PASC group also had more severe COVID-19 based on their WHO score, had greater usage of dexamethasone and remdesivir for COVID-19, had a higher proportion of hospitalized patients, and, for those hospitalized, had a longer duration of hospitalization compared to non-PASC participants (17).

Peripheral blood from 476 PRESCO participants (381 hospitalized and 95 non-hospitalized participants), was available from the time of initial presentation to an ambulatory clinic or hospital for COVID-19 (Figure 1; Table 1). These samples were used to compare immune responses in hospitalized versus non-hospitalized COVID-19 patients. Of these, blood samples from 341 participants (132 PASC and 209 non-PASC) with information regarding their PASC status were also analyzed, with a focus on those that were hospitalized for COVID-19 (110 hospitalized PASC and 151 hospitalized non-PASC participants) (Figure 1; Table 1). Together, these PASC and non-PASC samples were used to investigate early molecular signatures associated with the development of PASC (Figure 1; Table 1; Supplementary Figure 1).

For all PASC and non-PASC participants, the blood samples used for multi-omic profiling, cytokine assessment, and autoantibody assays had a mean (standard deviation) time to collection of 3.02 (3.73) days, 3.05 (3.96) days, and 2.58 (3.72) days from the start of COVID-19, respectively. From the isolated PBMCs, 24 cell subsets, which included 5 myeloid cell subsets, 7 B cell subsets, 10 T cell subsets, and 2 NK cell subsets, were phenotyped by flow cytometry and further profiled by ATAC-seq, RNA-seq, and TaPE-seq (Figure 1; Supplementary Figure 2; Supplementary Table 1). Plasma samples collected during hospital or clinic presentation were also analyzed for concentrations of cytokines, autoantibodies, and antibodies against SARS-CoV-2 and other common viral antigens (Figure 1).

Widespread immunological differences are observed between hospitalized and non-hospitalized COVID-19 participants during acute SARS-CoV-2 infection

PASC occurs in individuals with mild to severe COVID-19, but it is more common in patients hospitalized for more severe disease (23, 24). We hypothesized that differences in disease severity would be the strongest molecular signal during acute COVID-19, so we started with a comparison of hospitalized and non-hospitalized participants to inform our PASC comparisons. Using multi-omic profiling and assays for cytokine, autoantibody, and viral antibody detection, we compared molecular signatures between 381 hospitalized participants and 95 non-hospitalized participants at their initial presentation to a hospital or ambulatory clinic for COVID-19 (Table 1). Blood samples were collected at a similar timeframe since the start of COVID-19 for both hospitalized and

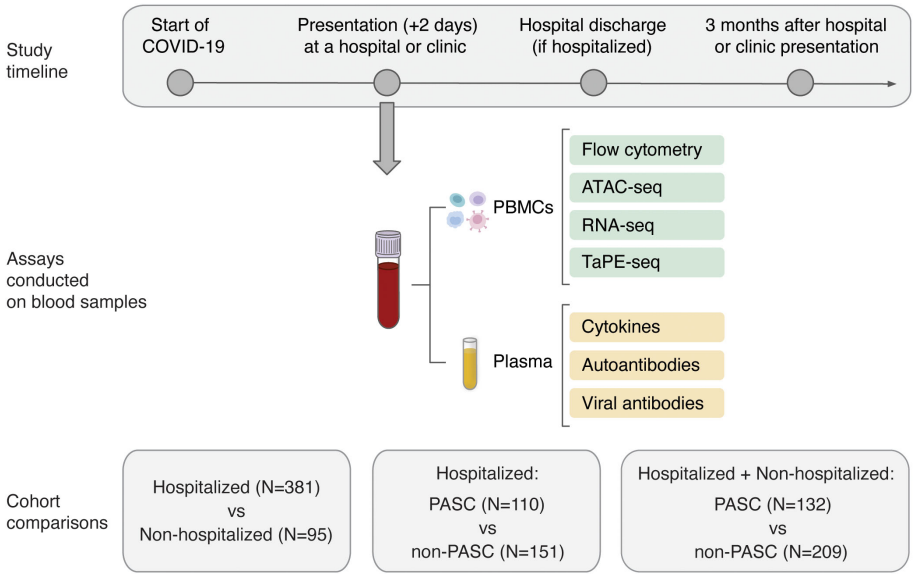

FIGURE 1
Overview of the study design and molecular assays conducted for the PRESCO study. Participants were classified based on their development of PASC over time, and samples collected during presentation at a hospital or ambulatory clinic were compared between individuals hospitalized and not hospitalized for COVID-19 and between individuals who did and did not develop PASC. The molecular assays conducted on isolated PBMCs and plasma are shown; PBMCs = peripheral blood mononuclear cells.

non-hospitalized patients (mean 2.9 (SD 2.1) days for hospitalized patients versus mean 3.1 (SD 4.2) days for non-hospitalized patients) (Supplementary Table 7). Demographics of hospitalized and non-hospitalized patients were also summarized (Supplementary Table 7). Approximately 4% of all patients had a prior autoimmune disease before contracting COVID-19.

At an FDR of 0.05, hospitalized participants exhibited increases in cell subset frequencies of unswitched naive B cells (BnUS) and decreases in a number of T cell subsets, including regulatory T cells (Treg), central and effector memory CD4+ T cells (T4cm, T4em), and central and effector memory CD8+ T cells (T8cm, T8em), in addition to decreased frequencies of certain myeloid cells, including conventional dendritic cells (coDC), plasmacytoid dendritic cells (plDC), and non-classical monocytes (MoNC) (Figure 2A). Additionally, numerous differentially accessible regions (DARs) and differentially expressed genes (DEGs) within innate and adaptive immune cells were associated with hospitalization status, highlighting diverse molecular changes early on in SARS-CoV-2 infection that can differentiate individuals on different disease severity trajectories (Figure 2B). At an FDR of 0.05, 46.9% of all DEGs had a proximally associated DAR in their respective cell subset, and of the differentially expressed proteins (DEPs) in the T and NK cell subsets (Figure 2B), nine of the 32 DEPs had coordinated changes in DARs and DEGs. These DEPs, all of which were increased in hospitalized participants, included CD127 (gene: *IL7R*) in T4em, naive CD8+ T cells, and CD56hi NK cells (NKhi), CD184 (*CXCR4*) in naive CD4+ T cells, CD38 (*CD38*) and CD366 (*HAVCR2*) in T8em, CD39 (*ENTPD1*) and CD314 (*KLRK1*) in NKhi, and CD279 (*PDCD1*) in Treg cells.

At an FDR of 0.05, numerous cytokines and chemokines in plasma were also upregulated in hospitalized participants, including key inflammatory cytokines such as IP-10, IL-6, IL-8, IL-18, TNF, and IFNα2 (Figure 2C). No significant differences in autoantibodies or antibodies against SARS-CoV-2 or other common viral pathogens, however, were found between hospitalized and non-hospitalized participants during acute SARS-CoV-2 infection. Given the large differences in immune status between hospitalized and non-hospitalized participants and the potential for this to be a

TABLE 1 Overview of sample sizes for each cohort comparison and molecular assay.

Cohort with available blood samples	Comparison groups	Total participants	Multi-omic profiling	Cytokines	Auto-antibodies
Hospitalized + non-hospitalized COVID-19 patients	Hospitalized	381	205	378	128
	Non-hospitalized	95	64	93	22
Hospitalized COVID-19 patients	PASC	110	72	109	54
	non-PASC	151	106	149	74
Hospitalized + non-hospitalized COVID-19 patients	PASC	132	85	131	60
	non-PASC	209	147	206	90

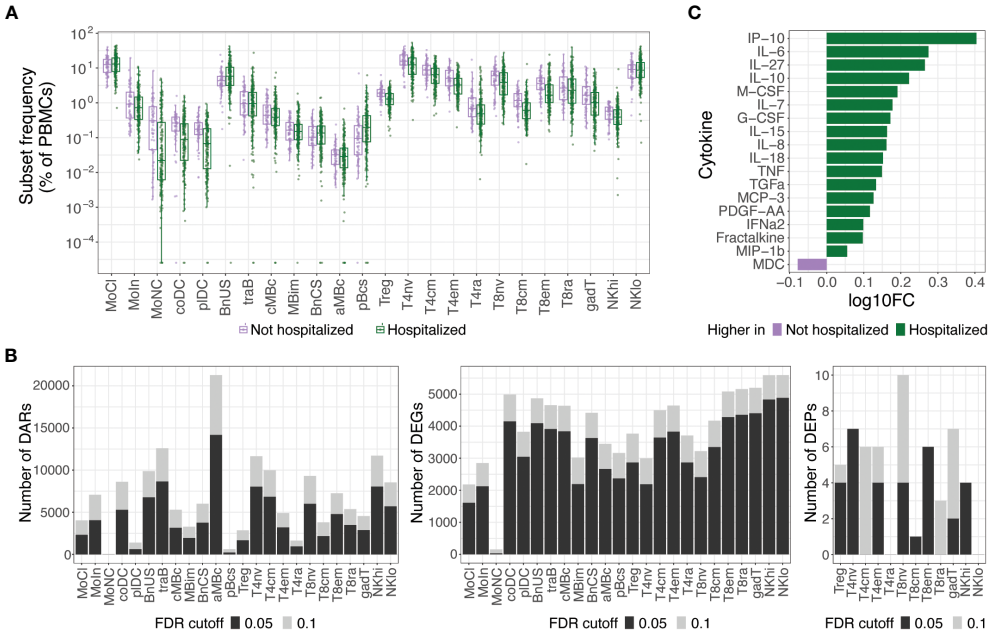

FIGURE 2
Molecular differences observed in hospitalized versus non-hospitalized participants. **(A)** Box plots of cell subset frequencies grouped by hospitalized participants and non-hospitalized participants at hospital/clinic presentation. **(B)** Identified number of significant differentially accessible regions (DARs) from ATAC-seq data, differentially expressed genes (DEGs) from RNA-seq data, and differentially expressed proteins (DEPs) from TaPE-seq data between hospitalized and non-hospitalized participants by cell subset at hospital/clinic presentation. **(C)** Cytokines and chemokines elevated in plasma of hospitalized versus non-hospitalized participants at a FDR of 0.05 as measured by Luminex assay. Comparative values are expressed as log10 fold change (log10FC); Abbreviations for immune cell subsets are defined in Supplementary Table 1.

source of variance for PASC, we further examined differences in PASC and non-PASC participants within those who were hospitalized for COVID-19.

Alterations in double-negative B cells and interferon signaling pathways are observed in hospitalized PASC participants at initial hospital presentation for COVID-19

Of the hospitalized participants with molecular samples analyzed, PASC status information was available for 261 individuals, of which 110 participants eventually developed PASC and 151 participants did not develop PASC (Table 1). Demographics of hospitalized PASC and non-PASC patients were summarized (Supplementary Table 8). There were no significant differences in cell subset frequencies or plasma cytokines between hospitalized PASC versus hospitalized non-PASC participants (Supplementary Figure 3; Supplementary Figure 4). However, during acute SARS-CoV-2 infection, we observed differences in autoantibodies and in epigenetic and transcriptional signatures in B cells between PASC and non-PASC participants that were hospitalized for COVID-19 (Figure 3).

We found a small number of IgG autoantibodies increased in hospitalized PASC compared to hospitalized non-PASC participants at the time of hospital presentation. Hospitalized PASC participants had relative increases in three autoantibodies with reactivity to the complement protein, Complement C1q Binding Protein (C1QBP), an adipokine, Dermatopontin (DPT), and a SARS-CoV-2 entry receptor, Neuropilin-2 (NRP2) (Figure 3A). However, no significant differences in antibodies against SARS-CoV-2 or other common viral pathogens were observed.

B cells are the major effector cells responsible for antibody production and also contribute to other effector functions such as cytokine production and immune regulation. At an FDR of 0.05, the predominant differences between hospitalized PASC and non-PASC participants during acute SARS-CoV-2 infection were found in B cell subsets for both DARs and DEGs (Figure 3B). Specifically, we found that the majority of DARs identified by ATAC-seq were observed in double-negative (DN; CD27-IgD-) B cells of the DN1 subset (BnCS) (Figure 3B). Double-negative B cells lack CD27 expression, making them similar to naive B cells, but they also lack IgD expression, suggesting that they have undergone immunoglobulin isotype switching similar to switched memory B cells (25, 26). Recently, subsets of DN B cells (DN1, DN2, DN3, and DN4) have been categorized using various markers such as CD21, CD11c, CXCR5, T-box expressed in T cells (T-bet), and Fc Receptor Like 5 (FcRL5) (25, 26), but to date, the phenotypic markers of DN B cells have not yet been standardized across studies. We classify DN1 B cells by cell surface expression of CD27- CD21+ IgM- IgD- (BnCS; Supplementary Table 1) and find this cell subset to exhibit the most epigenetic differences between hospitalized PASC and non-PASC participants at initial presentation to a hospital for COVID-19.

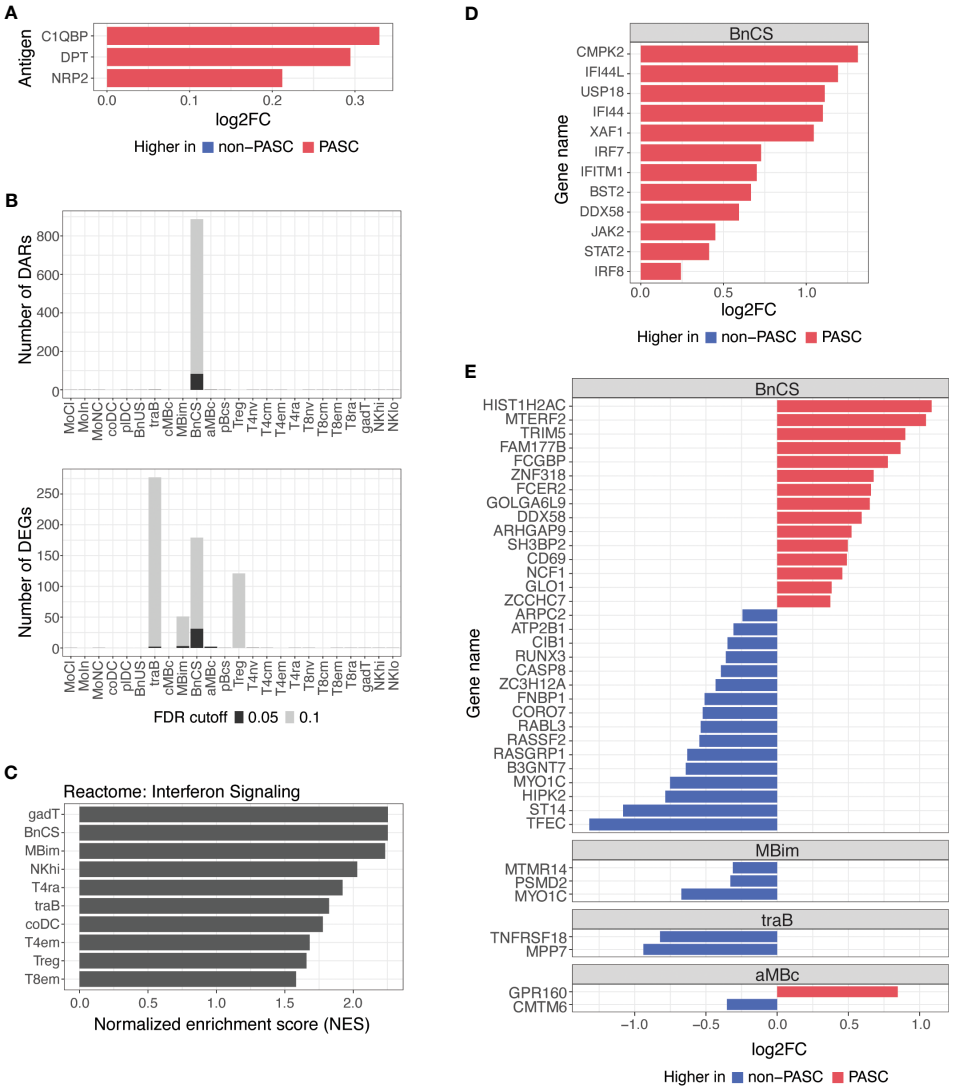

FIGURE 3
Differences in autoantibodies and in B cell epigenetic and transcriptional features in hospitalized PASC versus non-PASC participants at hospital presentation. **(A)** Log2 fold-change (log2FC) of plasma autoantibodies in hospitalized PASC versus non-PASC participants at hospital presentation at FDR of 0.1. **(B)** Identified number of significant differentially accessible regions (DARs) from ATAC-seq data and differentially expressed genes (DEGs) from RNA-seq data between hospitalized PASC and non-PASC participants by cell subset at hospital presentation. FDR cutoffs for each data type were set and graphed as FDR of 0.05 (black bar) or FDR of 0.1 (gray bar). **(C)** Pathway analysis of differentially expressed genes (DEGs) in PASC vs non-PASC participants that were hospitalized. Analysis was done for the Reactome pathway set (curated by the MsigDB collections) using a hypergeometric test of all DEGs in the 24 immune subsets. Shown are the subsets with significant enrichment of genes in the interferon signaling pathway at an FDR of 0.1. **(D)** Interferon stimulated genes that are differentially expressed in DN1 B cells at an FDR of 0.1 in PASC vs non-PASC participants that were hospitalized. **(E)** Log2FC of DEGs between hospitalized PASC and non-PASC participants at hospital presentation at an FDR of 0.05; Abbreviations for immune cell subsets are defined in Supplementary Table 1.

Severe COVID-19 has been associated with both impaired and overly robust type 1 interferon responses, which may either limit anti-viral immunity or exacerbate hyperinflammation, respectively (27–30), and thereby contribute to disease progression. Dysregulation of interferon responses have been observed as far as 8 months after initial SARS-CoV-2 infection (8) and may therefore be associated with the development of PASC. By conducting pathway analysis using GSEA on differentially expressed genes, we observed an enrichment of genes involved in interferon signaling in hospitalized PASC compared to non-PASC participants, particularly in effector B and T cell subsets (Figure 3C). Hospitalized PASC participants exhibited increased expression of numerous interferon stimulated genes (ISGs), including *CMPK2*, *IFI44L*, *USP18*, *IFI44*, *XAF1*, *IRF7*, *IFITM1*, *BST2*, *DDX58*, *JAK2*, *STAT2*, and *IRF8*, specifically in the DN1 B cell subset, during acute SARS-CoV-2 infection (Figure 3D). These ISGs are involved in both positive and negative regulation of the interferon signaling pathway. Interferon regulatory factor (IRF)7 and *IRF8*, for example, bind interferon-stimulated response elements and drive ISG expression in response to type I interferons (31), whereas ISGs such as *USP18*, *IFI44*, and *IFI44L* negatively regulate the type I interferon pathway and can promote viral production (32–34). As WHO score was

included as a covariate in our model, the increases observed in interferon pathways and ISGs in DN1 B cells in hospitalized PASC participants occur despite controlling for disease severity. Together, these results suggest that in the acute phase of SARS-CoV-2 infection, the regulation of interferons and their impacts on anti-viral immunity and inflammation may be influencing the development of PASC.

Thirty-eight genes were also differentially expressed between hospitalized PASC and non-PASC participants at an FDR of 0.05, all of which were found within a B cell subset (Figure 3E). Similar to the ATAC-seq data, most DEGs from RNA-seq were found in the DN1 B cell subset. In particular, in the DN1 subset, we observed increased expression of genes related to anti-viral immune responses, including *TRIM5* and *DDX58*. *TRIM5* promotes innate immune signaling and is a restriction factor that blocks the early stages of retrovirus infection (35). *DDX58*, which encodes RIG-I, is also an innate immune sensor that recognizes double stranded RNA viruses and drives type I interferon signaling (36). Genes related to B cell activation were also upregulated in the DN1 subset of hospitalized PASC participants, including *CD69*, an early lymphoid activation marker (37, 38), and *FCER2*, which encodes CD23 and can indicate an activated B cell state (39). Together, the DEGs upregulated in DN1 B cells of hospitalized PASC participants indicate cells that have adopted an activated state and are potentially primed for anti-viral immunity. Additionally, a number of genes downregulated in DN1 B cells of hospitalized PASC participants, are involved in the process of apoptosis via various mechanisms, including *RUNX3*, *CASP8*, *RASSF2*, and *HIPK2* (40–43), and may relate to potential dysregulation of apoptotic pathways in DN1 B cells of PASC participants during acute SARS-CoV-2 infection. A smaller number of significant gene differences were observed in IgM+ IgD- classical memory B cells, transitional B cells, and atypical memory B cells at an FDR of 0.05 (Figure 3E).

Minor alterations in autoantibodies and B cell epigenetic and transcriptional signatures are observed in hospitalized and non-hospitalized PASC participants during acute SARS-CoV-2 infection

To understand differences between individuals with and without PASC more broadly, we examined molecular signatures between PASC and non-PASC in the full cohort, which included both hospitalized and non-hospitalized participants (Figure 1; Table 1). At the time of a participants' initial presentation to a hospital or ambulatory clinic for COVID-19, we detected fewer molecular differences between PASC and non-PASC participants in the full cohort compared to the hospitalized group only, but similar overlapping signals between the two cohorts were observed. There were no significant differences in immune cell subset frequencies or plasma cytokines between PASC and non-PASC participants during acute COVID-19. Similar to the hospitalized cohort, we observed increased autoantibodies against the three antigens, C1QBP, DPT, and NRP2, in PASC compared to non-PASC participants, and these differences were significant at an FDR of 0.05 (Figure 4A). Additional autoantibodies against immune cell surface receptors (IL7R, CD69), SARS-CoV-2 entry receptors (ACE2), thrombosis proteins (APOH, TFPI), and an apoptosis factor (TNFRSF11B) were increased in PASC participants at an FDR of 0.1, while autoantibodies against the tumor protein, p53, was increased in non-PASC participants (Figure 4A). No differences in antibodies against SARS-CoV-2 or other common viruses were observed.

Additionally, epigenetic and transcriptional differences between PASC and non-PASC participants in the full cohort were predominantly in B cells, as was observed in the hospitalized cohort only, with most differences occurring in the DN1 B cell subset (Figure 4B). A similar profile in DN1 B cells was observed in PASC participants, with DEGs related to increased activation (e.g., *CD69* and *FCER2*) and anti-viral immunity (e.g., *CD9* and *TRIM5*) being upregulated in PASC participants. A DN1 DAR proximal to TRIM5 was also increased, indicating increased chromatin accessibility to this anti-viral gene in DN1 B cells of PASC participants. A smaller number of gene differences were observed in central and atypical memory B cells, transitional B cells, and CD56 low NK cells (Figure 4C).

Discussion

Infection with SARS-CoV-2 can lead to post-acute sequelae that persists for weeks, months, and even years following infection (3, 44–46). A combination of host and virus factors are thought to be associated with the pathogenesis of PASC, including the persistence of viral antigens, microvascular dysfunction, gut dysbiosis, chronic inflammation, and autoreactive immune responses (6, 7). A limited number of studies have investigated the molecular mechanisms of PASC as it relates to the acute phase of SARS-CoV-2 infection (6, 47, 48). Using multi-omic immune profiling, we sought to investigate early differences in immune responses to SARS-CoV-2 in individuals who eventually did and did not develop PASC.

Our study is unique in that we were able to collect blood samples from COVID-19 patients early in the pathogenesis of disease, with > 90% of samples collected less than a week from the start of COVID-19. Overall, we found a small set of early immune differences in PASC and non-PASC individuals within the first week of COVID-19 disease, with significant molecular signals occurring predominantly in double-negative B cells. The lack of a more robust signal may reflect the heterogeneity in mechanisms underlying PASC and the diverse manifestations of PASC symptoms (49), but our findings suggest that there may be some common immune-mediated mechanisms that begin to influence the ultimate development of PASC even during the acute stage of SARS-CoV-2 infection. We have not examined whether these same signatures continue to differentiate PASC and non-PASC individuals during recovery from acute infection and beyond, but our results suggest that longitudinal monitoring of B cell responses could have value in better understanding and managing PASC.

Previous studies have reported significant molecular differences between individuals hospitalized for COVID-19 compared to those

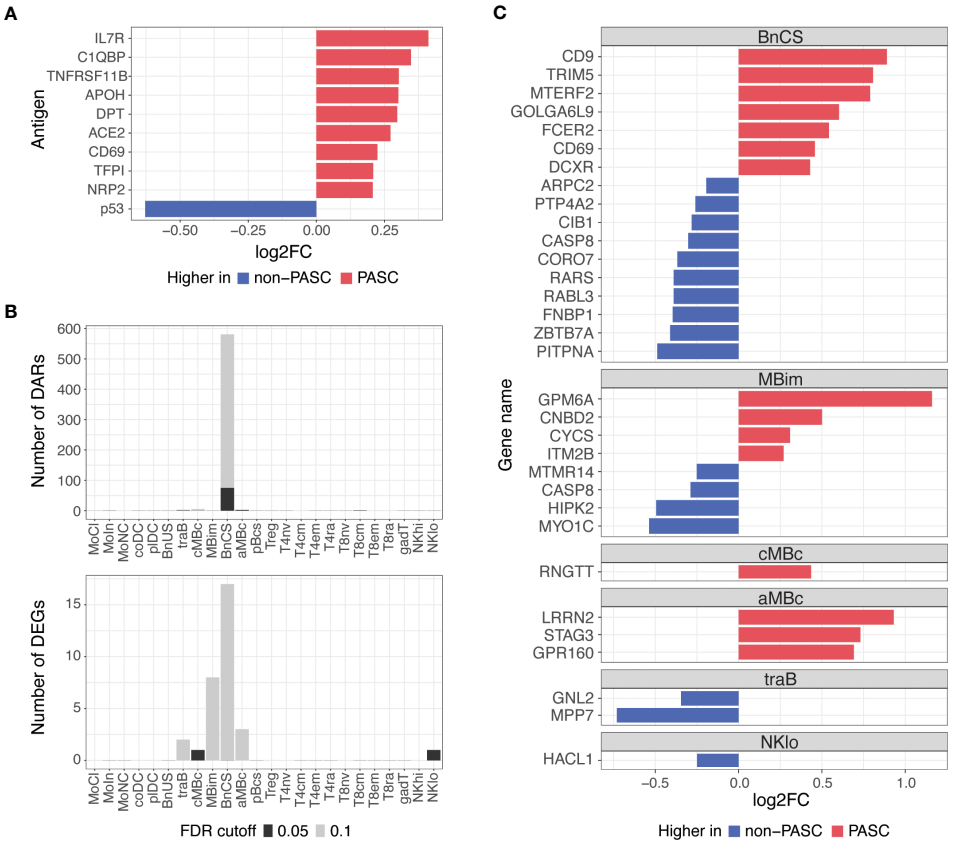

FIGURE 4
Differences in autoantibodies and in B cell epigenetic and transcriptional features in PASC versus non-PASC participants at hospital/clinic presentation. **(A)** Log2 fold-change (log2FC) of plasma autoantibodies in PASC versus non-PASC participants at hospital/clinic presentation at FDR of 0.1. **(B)** Identified number of significant differentially accessible regions (DARs) from ATAC-seq data and differentially expressed genes (DEGs) from RNA-seq data between PASC and non-PASC participants by cell subset at hospital/clinic presentation. FDR cutoffs for each data type were set and graphed as FDR of 0.05 (black bar) or FDR of 0.1 (gray bar). **(C)** Log2FC of DEGs between PASC and non-PASC participants at hospital/clinic presentation at FDR of 0.1; Abbreviations for immune cell subsets are defined in Supplementary Table 1.

who were not hospitalized, with early immune mechanisms being capable of differentiating trajectories of mild, moderate, and severe COVID-19 (50–53). We similarly observed large differences in the immune response between hospitalized and non-hospitalized COVID-19 patients in their epigenetic and transcriptional signatures, their frequency of cell subsets, and their production of inflammatory cytokines. These findings support previous literature and indicate that within the first week of SARS-CoV-2 pathogenesis, differences in immune responses can differentiate SARS-CoV-2 infected individuals on different disease trajectories.

To reduce the heterogeneity observed among participants, we thus stratified participants based on hospitalization to account for the different follow-up strategies for more severe COVID-19 that may influence the likelihood of developing PASC. As a majority (77%) of our analyzed participants were hospitalized, we did not analyze differences in PASC and non-PASC participants in non-hospitalized patients, given the small sample size for the comparisons in this group (N=13 PASC; N=41 non-PASC). We observed increases in a small number of autoantibodies in hospitalized PASC compared to hospitalized non-PASC participants. Previous studies have found increased autoantibodies to be associated with COVID-19 and PASC (6, 54–60), though the findings associating PASC and autoantibodies have been inconsistent (61). Additionally, prior autoimmunity and antibody cross-reactivity between tissue proteins and SARS-CoV-2 antigens could also be contributing to the pathophysiology of COVID-19, and hence, PASC (62, 63). We did not observe any significant differences in antibodies against SARS-CoV-2 or other common viral pathogens between hospitalized PASC and non-PASC participants, indicating that hospitalized PASC participants likely have a functional acute immune response against the SARS-CoV-2 virus, similar to that of hospitalized non-PASC participants. Similarly, other studies did not find an association between PASC and acute antibody titers against the spike surface protein of SARS-CoV-2 (47, 64), though decreased total acute antibody titers against SARS-CoV-2 were able to predict the development of PASC symptoms (47). We did not have samples collected prior to SARS-CoV-2 infection to assess whether the presence of prior autoantibodies or viral antibodies in our cohort are associated with the development of PASC, which would require further investigation.

We additionally observed an increased interferon signature in hospitalized PASC participants compared to hospitalized non-PASC participants. In particular, numerous ISGs were

upregulated in the DN1 B cell subset in PASC participants, and interferon signaling pathways were also increased in a number of effector B and T cell subsets. While interferon signaling plays a critical role in the defense against SARS-CoV-2 during acute infection (65, 66), persistent expression of interferons can lead to inflammatory damage to organ systems and may be linked to autoimmunity (29, 30, 54, 67), thereby contributing to the development of PASC (8, 68). While we have only analyzed the acute immune response to SARS-CoV-2 in PASC and non-PASC individuals, longer term monitoring of interferon responses in individuals with and without PASC could further elucidate whether sustained interferon signaling and pathways may be contributing to the development of PASC in hospitalized patients.

We also observed epigenetic and transcriptional differences in B cells emerging between hospitalized PASC and non-PASC participants early in infection, which may be linked to the increased autoantibodies that we observed in PASC participants. Previous studies have observed dysregulated B cells and new autoreactivity in patients with more severe acute COVID-19 (69–73), which could also be related to the observation that PASC is more common in individuals who experience more severe acute COVID-19 (23, 24). The epigenetic differences we observed in hospitalized PASC versus non-PASC participants were predominantly found in the DN1 subset of DN B cells. In recent years, DN B cells have been suggested to play important roles in cancers, infections, and autoimmune diseases (74), though their function in these contexts remain unclear. Double-negative B cells make up approximately 5% of PBMCs (75). They are matured, peripheral B cells that lack expression of CD27 and IgD and are thought to be precursors of memory B cells (25), with DN1 cells showing strong transcriptional similarity to class-switched memory B cells (76). Severe COVID-19 has been associated with a decreased frequency of DN1 cells and increased frequencies of DN2 and DN3 cells (70, 72, 77). These changes, however, may be transient, as studies have found that DN2 cells disappear soon after recovery from COVID-19 (70, 78, 79). Changes in DN B cells in the context of PASC, however, remain relatively understudied (15), and the exact function of DN B cells remains unclear. We observed no significant differences in DN1 cell or B cell frequencies between hospitalized PASC and non-PASC participants during their presentation to a hospital for COVID-19. However, it is intriguing that most of the epigenetic and transcriptional differences that we observe were found within DN1 B cells. Additionally, the increase in activation and anti-viral genes in the DN1 subset of hospitalized PASC participants indicate potential priming of this subset compared to non-PASC participants. Long term evaluation of this subset from acute infection to recovery could help elucidate the possible roles of DN1 B cells in the development of PASC.

We also examined molecular differences in PASC and non-PASC participants that were and were not hospitalized for COVID-19 to better understand the immune signals emerging from a broader population. We observed overlapping molecular differences in autoantibodies and DN1 B cells as with the hospitalized PASC and non-PASC cohort only, although a smaller number of significant differences emerged, possibly due to the increased heterogeneity within this group. The mechanisms of PASC may thereby vary according to the severity of acute SARS-CoV-2 infection, which may need to be considered when elucidating the role of the immune system in the development of PASC.

In summary, our analyses provide a detailed examination of the early immune response to COVID-19 and its ability to differentiate individuals on different severity and PASC trajectories. While individuals hospitalized for COVID-19 have significantly different immune responses compared to non-hospitalized individuals early on in SARS-CoV-2 infection, less differences are observed in individuals who do and do not develop PASC. The emerging differences in autoantibody responses and B cell phenotypes in PASC participants, however, are intriguing, in addition to the interferon signatures observed in PASC participants that were hospitalized. Future studies elucidating the function of DN B cells are needed to better understand the contribution and role of these cells in COVID-19, PASC, and other diseases. Together, our data ultimately provides a framework for guiding future research when monitoring longitudinal immune responses in the development of PASC.

Data availability statement

The datasets presented in this article are not readily available because of limitations protecting proprietary information. Requests to access the datasets should be directed to immuneprofiler@verily.com.

Ethics statement

The PRESCO study was approved by a central Western Institutional Review Board (Protocol number: 20201016) and at each of the eight sites. The studies were conducted in accordance with the local legislation and institutional requirements. The participants provided their written informed consent to participate in this study.

Author contributions

JL: Data curation, Formal Analysis, Writing – original draft, Writing – review & editing. MW: Data curation, Formal Analysis, Writing – original draft, Writing – review & editing. PK: Data curation, Formal Analysis, Writing – review & editing. CC: Conceptualization, Writing – review & editing. KD: Conceptualization, Writing – review & editing. GT: Data curation, Formal Analysis, Writing – review & editing. VR: Conceptualization, Writing – review & editing. HZ: Conceptualization, Writing – review & editing. WC: Conceptualization, Writing – review & editing. NH: Data curation, Formal Analysis, Writing – review & editing. JA: Data curation, Formal Analysis, Writing – review & editing. CW: Data curation, Formal Analysis, Writing – review & editing. CP: Data curation, Formal Analysis, Writing – review & editing. IM: Data curation, Formal Analysis, Writing – review & editing.

VT: Investigation, Writing – review & editing. JM: Investigation, Writing – review & editing. CD: Investigation, Writing – review & editing. IR: Investigation, Writing – review & editing. MB: Investigation, Writing – review & editing. JK: Investigation, Writing – review & editing. SP: Formal analysis, Investigation, Writing – review & editing. BP: Formal analysis, Writing – review & editing. MS: Formal analysis, Investigation, Writing – review & editing. CK: Conceptualization, Writing – original draft, Writing – review & editing.

Funding

The author(s) declare financial support was received for the research, authorship, and/or publication of this article. Funding for this study was provided by Verily Life Sciences. Verily Life Sciences was responsible for data collection. Authors were fully responsible for the data analysis and interpretation presented herein and the writing of this manuscript. Authors had access to the full dataset for the study, and reviewed and approved the final manuscript for submission.

Acknowledgments

We thank all the participants and study staff that were involved in this study during a challenging time when COVID-19 was first emerging. See the Supplementary Material for the list of personnel involved in the PRESCO study.

Conflict of interest

JL, MW, PK, CC, KD, GT, and CK maintain equity ownership and employment at Verily Life Sciences. NH, JA, CW, CP-K, and IM were employed at Oncimmune Limited. SP reports personal fees from Jazz Pharmaceuticals, Inc., and UpToDate, Inc., and grants from Philips, Inc., Sommetrics, Inc., and Regeneron. CD serves on advisory boards for Abbott Diagnostics, Ortho/Quidel Diagnostics, and Roche Diagnostics. JK receives research funding from Regeneron. JK has also provided consulting for GlaxoSmithKline, AstraZeneca, CereVu Medical, Propeller/ResMed, and BData, Inc.

The remaining authors declare that the research was conducted in the absence of any commercial or financial relationships that could be construed as a potential conflict of interest.

Publisher's note

Supplementary material

The Supplementary Material for this article can be found online at: https://www.frontiersin.org/articles/10.3389/fimmu.2024.1348041/full#supplementary-material

References

1. Silk BJ, Scobie HM, Duck WM, Palmer T, Ahmad FB, Binder AM, et al. COVID-19 surveillance after expiration of the public health emergency declaration - United States, May 11, 2023. *MMWR Morb Mortal Wkly Rep* (2023) 72:523–8. doi: 10.15585/mmwr.mm7219e1

2. Ahmad FB, Cisewski JA, Xu J, Anderson RN. Provisional mortality data - United States, 2022. *MMWR Morb Mortal Wkly Rep* (2023) 72:488–92. doi: 10.15585/mmwr.mm7218a3

3. Bowe B, Xie Y, Al-Aly Z. Postacute sequelae of COVID-19 at 2 years. *Nat Med* (2023) 29:2347–57. doi: 10.1038/s41591-023-02521-2

4. Thaweethai T, Jolley SE, Karlson EW, Levitan EB, Levy B, McComsey GA, et al. Development of a definition of postacute sequelae of SARS-CoV-2 infection. *JAMA* (2023) 329:1934–46. doi: 10.1001/jama.2023.8823

5. Davis HE, McCorkell L, Vogel JM, Topol EJ. Long COVID: major findings, mechanisms and recommendations. *Nat Rev Microbiol* (2023) 21:133–46. doi: 10.1038/s41579-022-00846-2

6. Su Y, Yuan D, Chen DG, Ng RH, Wang K, Choi J, et al. Multiple early factors anticipate post-acute COVID-19 sequelae. *Cell* (2022) 185:881–95.e20. doi: 10.1016/j.cell.2022.01.014

7. Peluso MJ, Deeks SG. Early clues regarding the pathogenesis of long-COVID. *Trends Immunol* (2022) 43:268–70. doi: 10.1016/j.it.2022.02.008

8. Phetsouphanh C, Darley DR, Wilson DB, Howe A, Munier CML, Patel SK, et al. Immunological dysfunction persists for 8 months following initial mild-to-moderate SARS-CoV-2 infection. *Nat Immunol* (2022) 23:210–6. doi: 10.1038/s41590-021-01113-x

9. Patterson BK, Francisco EB, Yogendra R, Long E, Pise A, Rodrigues H, et al. Persistence of SARS CoV-2 S1 protein in CD16+ Monocytes in post-acute sequelae of COVID-19 (PASC) up to 15 months post-infection. *Front Immunol* (2021) 12:746021. doi: 10.3389/fimmu.2021.746021

10. Peluso MJ, Deitchman AN, Torres L, Iyer NS, Munter SE, Nixon CC, et al. Long-term SARS-CoV-2-specific immune and inflammatory responses in individuals recovering from COVID-19 with and without post-acute symptoms. *Cell Rep* (2021) 36:109518. doi: 10.1016/j.celrep.2021.109518

11. Cheon IS, Li C, Son YM, Goplen NP, Wu Y, Cassmann T, et al. Immune signatures underlying post-acute COVID-19 lung sequelae. *Sci Immunol* (2021) 6:eabk1741. doi: 10.1126/sciimmunol.abk1741

12. Ong EZ, Chan YFZ, Leong WY, Lee NMY, Kalimuddin S, Haja Mohideen SM, et al. A dynamic immune response shapes COVID-19 progression. *Cell Host Microbe* (2020) 27:879–82.e2. doi: 10.1016/j.chom.2020.03.021

13. Wilk AJ, Rustagi A, Zhao NQ, Roque J, Martínez-Colón GJ, McKechnie JL, et al. A single-cell atlas of the peripheral immune response in patients with severe COVID-19. *Nat Med* (2020) 26:1070–6. doi: 10.1038/s41591-020-0944-y

14. Brodin P. Immune determinants of COVID-19 disease presentation and severity. *Nat Med* (2021) 27:28–33. doi: 10.1038/s41591-020-01202-8

15. Klein J, Wood J, Jaycox J, Dhodapkar RM, Lu P, Gehlhausen JR, et al. Distinguishing features of Long COVID identified through immune profiling. *Nature* (2023) 623:139–48. doi: 10.1038/s41586-023-06651-y

16. CDC. Long COVID or post-COVID conditions, in: *Centers for Disease Control and Prevention* (2023). Available at: https://www.cdc.gov/coronavirus/2019-ncov/long-term-effects/index.html (Accessed October 3, 2023).

17. Chen C, Parthasarathy S, Leung JM, Wu MJ, Drake KA, Ridaura VK, et al. Distinct temporal trajectories and risk factors for Post-acute sequelae of SARS-CoV-2 infection. *Front Med* (2023) 10:1227883. doi: 10.3389/fmed.2023.1227883

18. Peikon I, Tong G, Liu D, Chu C. *Quantitative massively parallel proteomics* (2021). US Patent. Available at: https://patentimages.storage.googleapis.com/c5/ad/a7/d0f4ff04f8712a/US20210132078A1.pdf (Accessed October 2, 2023).

19. Drake KA, Talantov D, Tong GJ, Lin JT, Verheijden S, Katz S, et al. Multi-omic profiling reveals early immunological indicators for identifying COVID-19 Progressors. *Clin Immunol* (2023) 256:109808. doi: 10.1016/j.clim.2023.109808

20. Liu Y, Ebinger JE, Mostafa R, Budde P, Gajewski J, Walker B, et al. Paradoxical sex-specific patterns of autoantibody response to SARS-CoV-2 infection. *J Transl Med* (2021) 19:524. doi: 10.1186/s12967-021-03184-8

21. Bursac Z, Gauss CH, Williams DK, Hosmer DW. Purposeful selection of variables in logistic regression. *Source Code Biol Med* (2008) 3:17. doi: 10.1186/1751-0473-3-17

22. Subramanian A, Tamayo P, Mootha VK, Mukherjee S, Ebert BL, Gillette MA, et al. Gene set enrichment analysis: a knowledge-based approach for interpreting genome-wide expression profiles. *Proc Natl Acad Sci U S A* (2005) 102:15545–50. doi: 10.1073/pnas.0506580102

23. Xie Y, Bowe B, Al-Aly Z. Burdens of post-acute sequelae of COVID-19 by severity of acute infection, demographics and health status. *Nat Commun* (2021) 12:6571. doi: 10.1038/s41467-021-26513-3

24. LaVergne SM, Stromberg S, Baxter BA, Webb TL, Dutt TS, Berry K, et al. A longitudinal SARS-CoV-2 biorepository for COVID-19 survivors with and without post-acute sequelae. *BMC Infect Dis* (2021) 21:677. doi: 10.1186/s12879-021-06359-2

25. Beckers L, Somers V, Fraussen J. IgDCD27 double negative (DN) B cells: Origins and functions in health and disease. *Immunol Lett* (2023) 255:67–76. doi: 10.1016/j.imlet.2023.03.003

26. Sanz I, Wei C, Jenks SA, Cashman KS, Tipton C, Woodruff MC, et al. Challenges and opportunities for consistent classification of human B cell and plasma cell populations. *Front Immunol* (2019) 10:2458. doi: 10.3389/fimmu.2019.02458

27. Hadjadj J, Yatim N, Barnabei L, Corneau A, Boussier J, Smith N, et al. Impaired type I interferon activity and inflammatory responses in severe COVID-19 patients. *Science* (2020) 369:718–24. doi: 10.1126/science.abc6027

28. Blanco-Melo D, Nilsson-Payant BE, Liu W-C, Uhl S, Hoagland D, Møller R, et al. Imbalanced host response to SARS-CoV-2 drives development of COVID-19. *Cell* (2020) 181:1036–45.e9. doi: 10.1016/j.cell.2020.04.026

29. Lee JS, Park S, Jeong HW, Ahn JY, Choi SJ, Lee H, et al. Immunophenotyping of COVID-19 and influenza highlights the role of type I interferons in development of severe COVID-19. *Sci Immunol* (2020) 5:eabd1554. doi: 10.1126/sciimmunol.abd1554

30. Lucas C, Wong P, Klein J, Castro TBR, Silva J, Sundaram M, et al. Longitudinal analyses reveal immunological misfiring in severe COVID-19. *Nature* (2020) 584:463–9. doi: 10.1038/s41586-020-2588-y

31. Jefferies CA. Regulating IRFs in IFN driven disease. *Front Immunol* (2019) 10:325. doi: 10.3389/fimmu.2019.00325

32. DeDiego ML, Nogales A, Martinez-Sobrido L, Topham DJ. Interferon-induced protein 44 interacts with cellular FK506-binding protein 5, negatively regulates host antiviral responses, and supports virus replication. *MBio* (2019) 10:e01839–19. doi: 10.1128/mBio.01839-19

33. DeDiego ML, Martinez-Sobrido L, Topham DJ. Novel functions of IFI44L as a feedback regulator of host antiviral responses. *J Virol* (2019) 93:e01159–19. doi: 10.1128/JVI.01159-19

34. Basters A, Knobeloch K-P, Fritz G. USP18 - a multifunctional component in the interferon response. *Biosci Rep* (2018) 38:BSR20180250. doi: 10.1042/BSR20180250

35. Stremlau M, Perron M, Lee M, Li Y, Song B, Javanbakht H, et al. Specific recognition and accelerated uncoating of retroviral capsids by the TRIM5alpha restriction factor. *Proc Natl Acad Sci U S A* (2006) 103:5514–9. doi: 10.1073/pnas.0509996103

36. Rehwinkel J, Gack MU. RIG-I-like receptors: their regulation and roles in RNA sensing. *Nat Rev Immunol* (2020) 20:537–51. doi: 10.1038/s41577-020-0288-3

37. Risso A, Smilovich D, Capra MC, Baldissarro I, Yan G, Bargellesi A, et al. CD69 in resting and activated T lymphocytes. Its association with a GTP binding protein and biochemical requirements for its expression. *J Immunol* (1991) 146:4105–14. doi: 10.4049/jimmunol.146.12.4105

38. Testi R, Phillips JH, Lanier LL. T cell activation via Leu-23 (CD69). *J Immunol* (1989) 143:1123–8. doi: 10.4049/jimmunol.143.4.1123

39. Pignarre A, Chatonnet F, Caron G, Haas M, Desmots F, Fest T. Plasmablasts derive from CD23- activated B cells after the extinction of IL-4/STAT6 signaling and IRF4 induction. *Blood* (2021) 137:1166–80. doi: 10.1182/blood.2020005083

40. Kim BR, Park SH, Jeong YA, Na YJ, Kim JL, Jo MJ, et al. RUNX3 enhances TRAIL-induced apoptosis by upregulating DR5 in colorectal cancer. *Oncogene* (2019) 38:3903–18. doi: 10.1038/s41388-019-0693-x

41. Fritsch M, Günther SD, Schwarzer R, Albert M-C, Schorn F, Werthenbach JP, et al. Caspase-8 is the molecular switch for apoptosis, necroptosis and pyroptosis. *Nature* (2019) 575:683–7. doi: 10.1038/s41586-019-1770-6

42. Vos MD, Ellis CA, Elam C, Ulku AS, Taylor BJ, Clark GJ. RASSF2 is a novel K-Ras-specific effector and potential tumor suppressor. *J Biol Chem* (2003) 278:28045–51. doi: 10.1074/jbc.M300554200

43. D'Orazi G, Cecchinelli B, Bruno T, Manni I, Higashimoto Y, Saito S'ichi, et al. Homeodomain-interacting protein kinase-2 phosphorylates p53 at Ser 46 and mediates apoptosis. *Nat Cell Biol* (2002) 4:11–9. doi: 10.1038/ncb714

44. Peter RS, Nieters A, Kräusslich H-G, Brockmann SO, Göpel S, Kindle G, et al. Post-acute sequelae of covid-19 six to 12 months after infection: population based study. *BMJ* (2022) 379:e071050. doi: 10.1136/bmj-2022-071050

45. Groff D, Sun A, Ssentongo AE, Ba DM, Parsons N, Poudel GR, et al. Short-term and long-term rates of postacute sequelae of SARS-CoV-2 infection: A systematic review. *JAMA Netw Open* (2021) 4:e2128568. doi: 10.1001/jamanetworkopen.2021.28568

46. Kelly JD, Curteis T, Rawal A, Murton M, Clark LJ, Jafry Z, et al. SARS-CoV-2 post-acute sequelae in previously hospitalised patients: systematic literature review and meta-analysis. *Eur Respir Rev* (2023) 32:220254. doi: 10.1183/16000617.0254-2022

47. Cervia C, Zurbuchen Y, Taeschler P, Ballouz T, Menges D, Hasler S, et al. Immunoglobulin signature predicts risk of post-acute COVID-19 syndrome. *Nat Commun* (2022) 13:446. doi: 10.1038/s41467-021-27797-1

48. Thompson RC, Simons NW, Wilkins L, Cheng E, Del Valle DM, Hoffman GE, et al. Molecular states during acute COVID-19 reveal distinct etiologies of long-term sequelae. *Nat Med* (2022) 29:236–46. doi: 10.1038/s41591-022-02107-4

49. Proal AD, VanElzakker MB. Long COVID or post-acute sequelae of COVID-19 (PASC): an overview of biological factors that may contribute to persistent symptoms. *Front Microbiol* (2021) 12:698169. doi: 10.3389/fmicb.2021.698169

50. Arunachalam PS, Wimmers F, Mok CKP, Perera RAPM, Scott M, Hagan T, et al. Systems biological assessment of immunity to mild versus severe COVID-19 infection in humans. *Science* (2020) 369:1210–20. doi: 10.1126/science.abc6261

51. Su Y, Chen D, Yuan D, Lausted C, Choi J, Dai CL, et al. Multi-omics resolves a sharp disease-state shift between mild and moderate COVID-19. *Cell* (2020) 183:1479–95.e20. doi: 10.1016/j.cell.2020.10.037

52. Bergamaschi L, Mescia F, Turner L, Hanson AL, Kotagiri P, Dunmore BJ, et al. Longitudinal analysis reveals that delayed bystander CD8+ T cell activation and early immune pathology distinguish severe COVID-19 from mild disease. *Immunity* (2021) 54:1257–75.e8. doi: 10.1016/j.immuni.2021.05.010

53. Carsetti R, Zaffina S, Piano Mortari E, Terreri S, Corrente F, Capponi C, et al. Different innate and adaptive immune responses to SARS-CoV-2 infection of asymptomatic, mild, and severe cases. *Front Immunol* (2020) 11:610300. doi: 10.3389/fimmu.2020.610300

54. Bastard P, Rosen LB, Zhang Q, Michailidis E, Hoffmann H-H, Zhang Y, et al. Autoantibodies against type I IFNs in patients with life-threatening COVID-19. *Science* (2020) 370:eabd4585. doi: 10.1126/science.abd4585

55. Bastard P, Gervais A, Le Voyer T, Rosain J, Philippot Q, Manry J, et al. Autoantibodies neutralizing type I IFNs are present in 4% of uninfected individuals over 70 years old and account for 20% of COVID-19 deaths. *Sci Immunol* (2021) 6:eabl4340. doi: 10.1126/sciimmunol.abl4340

56. Wang EY, Mao T, Klein J, Dai Y, Huck JD, Jaycox JR, et al. Diverse functional autoantibodies in patients with COVID-19. *Nature* (2021) 595:283–8. doi: 10.1038/s41586-021-03631-y

57. Damoiseaux J, Dotan A, Fritzler MJ, Bogdanos DP, Meroni PL, Roggenbuck D, et al. Autoantibodies and SARS-CoV2 infection: The spectrum from association to clinical implication: Report of the 15th Dresden Symposium on Autoantibodies. *Autoimmun Rev* (2022) 21:103012. doi: 10.1016/j.autrev.2021.103012

58. Fagyas M, Nagy B Jr, Ráduly AP, Mányiné IS, Mártha L, Erdősi G, et al. The majority of severe COVID-19 patients develop anti-cardiac autoantibodies. *Geroscience* (2022) 44:2347–60. doi: 10.1007/s11357-022-00649-6

59. Seeßle J, Waterboer T, Hippchen T, Simon J, Kirchner M, Lim A, et al. Persistent symptoms in adult patients 1 year after coronavirus disease 2019 (COVID-19): A prospective cohort study. *Clin Infect Dis* (2022) 74:1191–8. doi: 10.1093/cid/ciab611

60. Wallukat G, Hohberger B, Wenzel K, Fürst J, Schulze-Rothe S, Wallukat A, et al. Functional autoantibodies against G-protein coupled receptors in patients with persistent Long-COVID-19 symptoms. *J Transl Autoimmun* (2021) 4:100100. doi: 10.1016/j.jtauto.2021.100100

61. Mohandas S, Jagannathan P, Henrich TJ, Sherif ZA, Bime C, Quinlan E, et al. Immune mechanisms underlying COVID-19 pathology and post-acute sequelae of SARS-CoV-2 infection (PASC). *Elife* (2023) 12:e86014. doi: 10.7554/eLife.86014

62. Yadaw AS, Sahner DK, Sidky H, Afzali B, Hotaling N, Pfaff ER, et al. Preexisting autoimmunity is associated with increased severity of coronavirus disease 2019: A retrospective cohort study using data from the national COVID cohort collaborative (N3C). *Clin Infect Dis* (2023) 77:816–26. doi: 10.1093/cid/ciad294

63. Vojdani A, Vojdani E, Kharrazian D. Reaction of human monoclonal antibodies to SARS-CoV-2 proteins with tissue antigens: implications for autoimmune diseases. *Front Immunol* (2020) 11:617089. doi: 10.3389/fimmu.2020.617089

64. Pereira C, Harris BHL, Di Giovannantonio M, Rosadas C, Short C-E, Quinlan R, et al. The association between antibody response to severe acute respiratory syndrome Coronavirus 2 infection and post-COVID-19 syndrome in healthcare workers. *J Infect Dis* (2021) 223:1671–6. doi: 10.1093/infdis/jiab120

65. Kim Y-M, Shin E-C. Type I and III interferon responses in SARS-CoV-2 infection. *Exp Mol Med* (2021) 53:750–60. doi: 10.1038/s12276-021-00592-0

66. Kim M-H, Salloum S, Wang JY, Wong LP, Regan J, Lefteri K, et al. II, and III interferon signatures correspond to coronavirus disease 2019 severity. *J Infect Dis* (2021) 224:777–82. doi: 10.1093/infdis/jiab288

67. Manry J, Bastard P, Gervais A, Le Voyer T, Rosain J, Philippot Q, et al. The risk of COVID-19 death is much greater and age dependent with type I IFN autoantibodies. *Proc Natl Acad Sci U S A* (2022) 119:e2200413119. doi: 10.1073/pnas.2200413119

68. Espín E, Yang C, Shannon CP, Assadian S, He D, Tebbutt SJ. Cellular and molecular biomarkers of long COVID: a scoping review. *EBioMedicine* (2023) 91:104552. doi: 10.1016/j.ebiom.2023.104552

69. Woodruff MC, Ramonell RP, Haddad NS, Anam FA, Rudolph ME, Walker TA, et al. Dysregulated naive B cells and *de novo* autoreactivity in severe COVID-19. *Nature* (2022) 611:139–47. doi: 10.1038/s41586-022-05273-0

70. Woodruff MC, Ramonell RP, Nguyen DC, Cashman KS, Saini AS, Haddad NS, et al. Extrafollicular B cell responses correlate with neutralizing antibodies and morbidity in COVID-19. *Nat Immunol* (2020) 21:1506–16. doi: 10.1038/s41590-020-00814-z

71. Hoehn KB, Ramanathan P, Unterman A, Sumida TS, Asashima H, Hafler DA, et al. Cutting edge: distinct B cell repertoires characterize patients with mild and severe COVID-19. *J Immunol* (2021) 206:2785–90. doi: 10.4049/jimmunol.2100135

72. Sosa-Hernández VA, Torres-Ruíz J, Cervantes-Díaz R, Romero-Ramírez S, Páez-Franco JC, Meza-Sánchez DE, et al. B cell subsets as severity-associated signatures in COVID-19 patients. *Front Immunol* (2020) 11:611004. doi: 10.3389/fimmu.2020.611004

73. Nielsen SCA, Yang F, Jackson KJL, Hoh RA, Röltgen K, Jean GH, et al. Human B cell clonal expansion and convergent antibody responses to SARS-Cov-2. *Cell Host Microbe* (2020) 28:516–25.e5. doi: 10.1016/j.chom.2020.09.002

74. Chung MKY, Gong L, Kwong DL-W, Lee VH-F, Lee AW-M, Guan X-Y, et al. Functions of double-negative B cells in autoimmune diseases, infections, and cancers. *EMBO Mol Med* (2023) 15:e17341. doi: 10.15252/emmm.202217341

75. Li Y, Li Z, Hu F. Double-negative (DN) B cells: an under-recognized effector memory B cell subset in autoimmunity. *Clin Exp Immunol* (2021) 205:119–27. doi: 10.1111/cei.13615

76. Jenks SA, Cashman KS, Woodruff MC, Lee FE-H, Sanz I. Extrafollicular responses in humans and SLE. *Immunol Rev* (2019) 288:136–48. doi: 10.1111/imr.12741

77. Castleman MJ, Stumpf MM, Therrien NR, Smith MJ, Lesteberg KE, Palmer BE, et al. Autoantibodies elicited with SARS-CoV-2 infection are linked to alterations in double negative B cells. *Front Immunol* (2022) 13:988125. doi: 10.3389/fimmu.2022.988125

78. Reyes RA, Clarke K, Gonzales SJ, Cantwell AM, Garza R, Catano G, et al. SARS-CoV-2 spike-specific memory B cells express higher levels of T-bet and FcRL5 after non-severe COVID-19 as compared to severe disease. *PLoS ONE* (2021) 16(12): e0261656. doi: 10.1371/journal.pone.0261656

79. Oliviero B, Varchetta S, Mele D, Mantovani S, Cerino A, Perotti CG, et al. Expansion of atypical memory B cells is a prominent feature of COVID-19. *Cell Mol Immunol* (2020) 17:1101–3. doi: 10.1038/s41423-020-00542-2

frontiers | Frontiers in Immunology

TYPE Original Research
PUBLISHED 26 January 2024
DOI 10.3389/fimmu.2023.1291048

OPEN ACCESS

EDITED BY
Alberto Beretta,
Independent Researcher, Milano, Italy

REVIEWED BY
Alireza Haghparast,
Ferdowsi University of Mashhad, Iran
Laura Fantuzzi,
National Institute of Health (ISS), Italy

*CORRESPONDENCE
Zaza M. Ndhlovu
zaza.ndhlovu@ahri.org

RECEIVED 08 September 2023
ACCEPTED 18 December 2023
PUBLISHED 26 January 2024

CITATION
Ng'uni TL, Musale V, Nkosi T, Mandolo J, Mvula M, Michelo C, Karim F, Moosa MYS, Khan K, Jambo KC, Hanekom W, Sigal A, Kilembe W and Ndhlovu ZM (2024) Low pre-existing endemic human coronavirus (HCoV-NL63)-specific T cell frequencies are associated with impaired SARS-CoV-2-specific T cell responses in people living with HIV.
Front. Immunol. 14:1291048.
doi: 10.3389/fimmu.2023.1291048

Low pre-existing endemic human coronavirus (HCoV-NL63)-specific T cell frequencies are associated with impaired SARS-CoV-2-specific T cell responses in people living with HIV

Tiza L. Ng'uni[1], Vernon Musale[2,3], Thandeka Nkosi[1], Jonathan Mandolo[4], Memory Mvula[4], Clive Michelo[2,3], Farina Karim[1], Mohomed Yunus S. Moosa[5], Khadija Khan[1], Kondwani Charles Jambo[4,6], Willem Hanekom[1,7], Alex Sigal[1], William Kilembe[2,3] and Zaza M. Ndhlovu[1,5,8]*

[1]Africa Health Research Institute (AHRI), Nelson R. Mandela School of Medicine, Durban, South Africa, [2]Emory-University of Georgia, Center of Excellence of Influenza Research and Surveillance (CEIRS), Lusaka, Zambia, [3]Center for Family Health Research in Zambia (CFHRZ), formerly Zambia Emory HIV Research Project (ZEHRP), Lusaka, Zambia, [4]Infection and Immunity Research Group, Malawi-Liverpool-Wellcome Trust Clinical Research Programme, Blantyre, Malawi, [5]Human Immunodeficiency Virus (HIV) Pathogenesis Program, School of Laboratory Medicine and Medical Sciences, University of KwaZulu Natal, Durban, South Africa, [6]Department of Clinical Sciences, Liverpool School of Tropical Medicine, Liverpool, United Kingdom, [7]Division of Infection and Immunity, University College London, London, United Kingdom, [8]Ragon Institute of Massachusetts General Hospital (MGH), Massachusetts Institute of Technology (MIT) and Harvard University, Cambridge, MA, United States

Background: Understanding how HIV affects SARS-CoV-2 immunity is crucial for managing COVID-19 in sub-Saharan populations due to frequent coinfections. Our previous research showed that unsuppressed HIV is associated with weaker immune responses to SARS-CoV-2, but the underlying mechanisms are unclear. We investigated how pre-existing T cell immunity against an endemic human coronavirus HCoV-NL63 impacts SARS-CoV-2 T cell responses in people living with HIV (PLWH) compared to uninfected individuals, and how HIV-related T cell dysfunction influences responses to SARS-CoV-2 variants.

Methods: We used flow cytometry to measure T cell responses following PBMC stimulation with peptide pools representing beta, delta, wild-type, and HCoV-NL63 spike proteins. Luminex bead assay was used to measure circulating plasma chemokine and cytokine levels. ELISA and MSD V-PLEX COVID-19 Serology and ACE2 Neutralization assays were used to measure humoral responses.

Results: Regardless of HIV status, we found a strong positive correlation between responses to HCoV-NL63 and SARS-CoV-2. However, PLWH exhibited weaker $CD4^+$ T cell responses to both HCoV-NL63 and SARS-CoV-2 than HIV-uninfected individuals. PLWH also had higher proportions of functionally exhausted (PD-1high) $CD4^+$ T cells producing fewer proinflammatory

cytokines (IFNγ and TNFα) and had elevated plasma IL-2 and IL-12(p70) levels compared to HIV-uninfected individuals. HIV status didn't significantly affect IgG antibody levels against SARS-CoV-2 antigens or ACE2 binding inhibition activity.

Conclusion: Our results indicate that the decrease in SARS-CoV-2 specific T cell responses in PLWH may be attributable to reduced frequencies of pre-existing cross-reactive responses. However, HIV infection minimally affected the quality and magnitude of humoral responses, and this could explain why the risk of severe COVID-19 in PLWH is highly heterogeneous.

KEYWORDS

HIV, SARS-CoV-2, HCoV-NL63, COVID-19, T-cell response, antibody response

1 Introduction

The novel Severe Acute Respiratory Syndrome Coronavirus 2 (SARS-CoV-2), responsible for causing coronavirus disease 2019 (COVID-19), has emerged as a significant public health menace, leading to the unprecedented loss of millions of lives globally (1). The World Health Organization (WHO) designated it as a pandemic on March 11th, 2020 (2). It is hypothesized that the rapid increase in global cases primarily resulted from a lack of pre-existing immunity to the novel SARS-CoV-2 (3). While many countries have successfully curbed the COVID-19 pandemic through extraordinary preventive measures, the potential for a global resurgence still looms large, hence the need to better understand immune responses to SARS-CoV-2, particularly in regions with a high HIV burden like sub-Saharan Africa.

To design the next generation of COVID-19 vaccines, it is essential to better understand both individual and population-level immunity, encompassing both humoral and adaptive responses (3). While the role of antibodies in clearing the virus and influencing the severity of COVID-19 is relatively well understood, the understanding of T cell immunity to SARS-CoV-2 has been limited due to a lack of studies focusing on T cells (4).

Furthermore, understanding the potential susceptibility of People Living with HIV (PLWH) to SARS-CoV-2 infection and severe COVID-19 holds significant relevance for developing next generation vaccines and therapies. Although it is well known that HIV weakens the immune system, which could have a negative impact on SARS-CoV-2 immunity, the precise immune defects associated with reduced SARS-CoV-2 immune responses in PLWH are still unresolved (5–7). As the COVID-19 pandemic is still rapidly evolving, more studies are needed to understand the interplay between HIV and SARS-CoV-2 in PLWH to inform both clinical and public health guidelines on HIV and SARS-CoV-2 coinfection.

It has been shown that over 90% of the human population is seropositive for at least three of the endemic human coronaviruses (EHC), HCoV-OC43, HCoV-HKU1, HCoV-NL63 and HCoV-229E, which widely circulate in the human population (8, 9). The memory T cell responses to these EHCs commonly exhibit cross-reactivity with SARS-CoV-2 (10, 11). In fact, detectable SARS-CoV-2-specific T cells have been identified in some individuals who lack any prior history of COVID-19 or SARS-CoV-2 exposure from an infected person (9, 12, 13). However, the potential influence of HIV infection on these cross-reactive immune responses remains under explored.

In this study, we utilized cohorts comprising both HIV-infected and HIV-uninfected participants from South Africa and Zambia who had contracted COVID-19 to explore the mechanisms linked to impaired SARS-CoV-2-specific T cell responses in PLWH. We examined whether pre-existing immunity to EHCs, specifically HCoV-NL63, influence SARS-CoV-2-specific T cell immunity and humoral responses in PLWH. Our findings demonstrate that HIV infection HIV exerts a more pronounced impact on T cell responses to both HCoV-NL63 and SARS-CoV-2, but minimally impacted humoral immunity against SARS-CoV-2.

2 Materials and methods

2.1 Ethical statement

The study was approved by the University of KwaZulu-Natal Institutional Review Board (approval BREC/00001275/2020) and the National Health Research Authority and University of Zambia Biomedical Research Ethics Committee (REF. No. 1648-2021). Adult patients (18 years and older) presenting at King Edward VIII, Inkosi Albert Luthuli Central, Kwadabeka community healthcare center or Clairwood Hospitals in Durban, South Africa, and the Center for Family Health Research in Zambia, research clinics and collaborating GRZ health facilities in Lusaka and Ndola, between October 2020 to August 2021, diagnosed to be SARS-CoV-2 PCR positive were eligible for the study. All

participants enrolled into the study provided written informed consent.

2.2 Study participants and sample collection

A total of 68 adult participants were recruited in South Africa and Zambia (34 from each site). We also recruited 11 healthy controls who were HIV-uninfected and matched for sex and age to the South African cohort (Table 1). The groups are represented as HIV-uninfected and SARS-CoV-2-infected (HIV-/SARS-CoV-2+); HIV-infected and SARS-CoV-2-infected (HIV+/SARS-CoV-2+); and healthy controls (HIV-/SARS-CoV-2-). Peripheral blood mononuclear cells (PBMCs) and plasma samples collected from Zambia were shipped to Durban, South Africa and matched with samples collected from South Africa. The matching criteria included HIV status, age, sex, time point and the wave of infection (wild-type, beta, or delta infection). PBMCs and plasma samples used in this study were collected between 1- and 4-weeks post-SARS-CoV2 PCR-positive diagnosis. Peripheral blood mononuclear cells (PBMCs) from healthy donors collected for other studies before 2018, prior to the COVID-19 pandemic, were included as healthy controls.

2.3 Peptide pools

To detect virus-specific T-cell responses, PBMCs were stimulated with the following peptide pools: 1) PepMix™ SARS-CoV-2 (Spike B.1.351/Beta Variant): Pool of 315 peptides derived from a peptide scan (15mers with 11 aa overlap) through the entire Spike glycoprotein - containing mutations D0080A, D0215G, L0242-, A0243-, L0244-, K0417N, E0484K, N0501Y, D614G and A0701V (JPT Peptide Technologies). 2) PepMix™ SARS-CoV-2 (Spike B.1.617.2/Delta Variant): Pool of 315 peptides derived from a peptide scan (15mers with 11 aa overlap - 4x 13mer + last peptide = 17mer) through the Spike glycoprotein - containing mutations T0019R, G0142D, E0156-, F0157-, R0158G, L0452R, T0478K, D0614G, P0681R and D0950N (JPT Peptide Technologies). 3) PepMix™ HCoV-NL63 (Spike Glycoprotein): Pool of 337 peptides derived from a peptide scan (15mers with 11 aa overlap) through the Spike glycoprotein (Swiss-Prot ID: Q6Q1S2) of Human Coronavirus (HCoV) (JPT Peptide Technologies). 4) PepTivator SARS-CoV-2 Prot_S Complete: Pool of peptides consisting mainly of 15-mers overlapping by 11 amino acids residues covering the entire protein coding sequence of the spike glycoprotein (aa 5–1273) (Miltenyi Biotec). 5) PepTivator SARS-CoV-2 Prot_S1: Pool of peptides covering the N-terminal S1 domain of the spike glycoprotein (aa 1–692) (Miltenyi Biotec).

2.4 T cell phenotyping by flow cytometry

PBMCs were isolated from blood samples by density gradient method and cryopreserved in liquid nitrogen prior to being used for flow cytometry. Frozen PBMCs were thawed, rested, and stimulated for 18 h at 37°C, 5% CO2 with the following peptide pools: SARS-CoV-2 S and S1 (wild-type – WT, 2 µg/ml) (Miltenyi, Biotec), beta and delta variants (0.5 µg/ml) (JPT Peptide Technologies), or

TABLE 1 Cohort Demographics and Clinical Characteristics.

	All (N = 79)	HIV-uninfected (*n* = 48)	HIV-infected (*n* = 20)	Healthy controls (*n* = 11)	Statistics
Demographics					
Age years, median (IQR)	35 (27 – 44)	34.5 (28 - 43.75)	41.5 (32 - 49.75)	19.5 (18.75 – 21.50)	0.0002[a]
Male sex, n (%)	29 (36.71)	22 (45.83)	4 (20)	3 (27.27)	ns[b]
Female sex, n (%)	50 (63.29)	26 (54.17)	16 (80)	8 (72.73)	ns[b]
Days since diagnosis, median (range)	14 (1 – 28)	14 (6 – 28)	13.5 (7 – 28)	–	ns[c]
HIV-associated parameters					
HIV viral load copies/mL, median (IQR)		–	13,981 (352-65,386)	–	n/a
CD4 cells/µL median (IQR)	760.5 (580.5 - 874.3)	783 (633 -921.5)	197 (75.5 - 726)	840 (739 - 996.3)	ns[d]
Disease severity					
Asymptomatic, n (%)	11 (16.18)	10 (20.83)	1 (5)	–	ns[b]
Mild, n (%)	54 (79.4)	37 (77.1)	17 (85)	–	ns[b]
Severe/oxygen supplementation, n (%)	3 (4.41)	1 (2.08)	2 (10)	–	ns[b]

P values were calculated by one-way ANOVA, Fischer's exact test, Mann-Whitney test or Kruskal-Wallis test for unpaired three groups. Convalescent HIV-infected and HIV-uninfected individuals were infected with either the beta (second wave) or delta (third wave) variants.
[a]One-way ANOVA,
[b]Fisher's exact probability test.
[c]Mann-Whitney test.
[d]Kruskal-Wallis test.
'ns' not significant and 'n/a' not applicable.

HCoV-NL63 (0.5 μg/ml) (JPT Peptide Technologies). Staphylococcal enterotoxin B (SEB, 0.5 μg/ml) was used as a positive control. Unstimulated wells were also included as negative controls. Brefeldin A (BioLegend, CA) and CD28/CD49d (BD Biosciences, Franklin Lakes, NJ) were added ahead of the 18 h incubation at 5 and 1 μg, respectively. The cells were stained with an antibody cocktail containing: Live/Dead fixable aqua dead cell stain, anti-CD3 PE-CF594 (BD), anti-CD4 Brilliant Violet (BV) 650, anti-CD8 BV 786 (BD), anti-CD38 Alexa Fluor (AF) 700 (BD), anti-human leukocyte antigen (HLA) – DR Allophycocyanin (APC) Cy 7 (BD), and anti-programmed cell death protein 1 (PD) BV 421 (BD). After a 20-minute incubation at room temperature, the cells were washed, fixed, and permeabilized using the BD Cytofix/Cytoperm fixation permeabilization kit. Thereafter, the cells were stained for 40 minutes at room temperature with an intracellular antibody cocktail containing: anti-IFN-γ BV 711 (BD), anti-IL-2 PE (BD), anti-TNF-α PE-Cy 7 and anti-granzyme B PE-CF594 (BD). Finally, the cells were washed and acquired on an LSR Fortessa and analyzed on FlowJo v10.7.1. Differences between groups were significant at a $p< 0.05$. Statistical analyses were performed using GraphPad Prism 9.0 (GraphPad Software, Inc, San Diego, CA).

2.5 Cytokine and chemokine measurements

The following cytokines and chemokines, IL-1β, IL-1ra, IL-2, IL-4, IL-6, IL-7, IL-8, IL-9, IL-10, IL-12p70, IL-13, IL-15, IL-17, basic FGF, eotaxin, granulocyte-colony stimulating factor (G-CSF), granulocyte macrophage-colony stimulating factor (GM-CSF), IFN-γ, interferon gamma-induced protein-10 (IP-10), monocyte chemoattractant protein-1 (MCP-1), macrophage inflammatory protein 1 (MIP-1)α, MIP-1β, platelet-derived growth factor-(PDGF-) BB, regulated on activation, normal T cell expressed and secreted (RANTES), TNF-α, and vascular endothelial growth factor (VEGF), were simultaneously assessed in plasma samples from healthy controls and HIV-infected and HIV-uninfected COVID-19 participants via the Bio-Plex Pro Human Cytokine 27-plex Assay (Bio-Rad) as per manufacturer's instructions. Briefly 50 μL of plasma samples and various concentrations of the assay standards were added in duplicate to a 96-well plate containing magnetic beads. The plate was incubated for 30 minutes followed by a wash step. The plate was subsequently coated with biotinylated detection antibody solution and incubated for a further 30 minutes. After the 30-minute incubation, the plate was washed and streptavidin-conjugated phycoerythrin was added to the plate and incubated for 10 minutes. After this final incubation, the plate was washed, and assay buffer was added to each well. Data was acquired using the Bio-Plex Array Reader system 2200 (Bio-Rad). A standard curve was derived using the different concentrations of the assay standards. All plasma samples from participants were assayed on the same plate at the same time in duplicate. Intra-assay variability was represented as the coefficient of variation as per manufacturer's instructions.

2.6 V-PLEX COVID-19 serology assay

The MSD V-PLEX COVID-19 Serology platform was used to quantitatively measure antibodies to SARS-CoV-2 antigens including its variants. The kits comprise 96-well plates with antigens precoated to individual carbon spots. Each well on the 96-well plate contains eight SARS-CoV-2-related antigens coated at the bottom of the well. The assay was performed as previously described (14, 15) and per manufacturer's instructions. Briefly, to measure antigen-specific IgG antibodies, plates were blocked with MSD Blocker A (150 μL/well) after which reference standard, controls and samples diluted to 1:50000 in Diluent buffer were added. After incubation, detection antibody (MSD SULFO-TAG™ Anti-Human IgG Antibody) diluted to 2 μg/mL in Diluent 100 (MSD) was used to label bound antibodies at 50 μL/well. This was followed by the addition of 150 μL MSD GOLD™ Read Buffer B and plates were read using an MSD QuickPlex SQ120 instrument. Calibration curves were used to calculate antibody concentrations and were established by fitting the signals from the calibrators to a 4-parameter logistic (or sigmoidal dose-response) model. Best quantification of unknown samples was achieved by generating a calibration curve for each plate using a minimum of two replicates at each calibrator level. Antibody unit concentrations in controls and diluted samples were determined from their ECL signals by backfitting to the calibration curve. Quantification was reported in Arbitrary Units/mL (AU/mL).

2.7 V-PLEX COVID-19 ACE2 neutralization assay

The V-PLEX COVID-19 ACE2 Neutralization Kit was used to measure antibodies that block the binding of angiotensin-converting enzyme 2 (ACE2) to the SARS-CoV-2 Spike and RBD antigens, including variants of the SARS-CoV-2 virus. The assay serves as a high-throughput alternative to traditional neutralization assays. Plates are provided with antigens on spots in the wells of a 96-well plate. Blocking antibodies in the samples bind to antigens on the spots, and human ACE2 protein conjugated with MSD SULFO-TAG is used for detection. The assay was performed according to manufacturer's instructions. Briefly, 150 μL/well of Blocker A solution was added to the plates, sealed with an adhesive and incubated at RT with shaking (~700 rpm) for 30 minutes. The plates were washed three times with 150 μL/well of 1X MSD Wash buffer. Samples were prediluted (1:10 dilution) according to the manufacturer's instructions. Samples and calibrators were then added to the plate (25 μL/well), plates sealed with an adhesive plate seal and incubated at RT with shaking (~700 rpm) for 1h. After the incubation, 25 μL/well of 1X SULFO-TAG Human ACE2 Protein detection solution was added to the plate. The plates were sealed with an adhesive plate seal and incubated at RT with shaking (~700 rpm) for 1h. After the detection incubation step, the plates were washed three times with 150 μL/well of 1X MSD Wash buffer. MSD GOLD Read Buffer B was added (150 μL/well) and the plate

was immediately read on the MSD instrument. Results were reported as percent inhibition, calculated using the equation below. Percentage inhibition was calculated relative to the assay calibrator (maximum 100% inhibition). Highly positive samples show high percent inhibition whereas negative or low samples show low percent inhibition.

$$\% \text{ Inhibition} = 1 - \frac{\text{Average Sample ECL Signal}}{\text{Average ECL Signal of Calibrator 8 (Diluent only)}} \times 100$$

2.8 Enzyme-linked immunosorbent assay

This in-house developed indirect qualitative ELISA was used to measure human IgG specific for the SARS-CoV2 RBD antigen in human plasma. To set up our in-house quantitative ELISA for COVID-19 serology, standard techniques were applied. Briefly, 96-well plates were coated with 100 µL/well of 1ug/mL Recombinant RBD (diluted in 1x PBS) except for blank and the "No RBD" negative control wells. blank and the 'No RBD' negative control wells contained 100 µL 1x PBS only. Plates were covered and incubated overnight at 4°C. The coated ELISA plates were washed four times with Wash buffer (containing 1x PBS and 0.05% Tween-20). The plates were then blocked with 200 µL/well of ELISA buffer (containing 1x PBS, 1% BSA and 0.05% Tween-20), except for the blank wells which contained 200 µL/well of Wash buffer. The plates were covered and incubated for 2h. After incubation, 100 µL/well of diluted samples (1:200 dilution in ELISA buffer) and positive controls were added to appropriate wells. To the "No RBD", blank, and "No primary antibody" wells, 100 µL/well of 0.2 µg/mL standard, Wash buffer and ELISA buffer were added, respectively. The plates were covered and incubated for 90 minutes at RT. Following incubation, the plates were washed four times with Wash buffer and 100 µL/well of peroxidase-conjugated anti-human IgG (1:2000) was added to the wells except the blank wells to which 100 µL/well Wash buffer was added. The plates were then covered and incubated for 60 minutes at RT. The plates were washed four times with Wash buffer and once with 1x PBS. The plates were tapped to remove residual PBS and 100 µL of developing buffer added to all wells. The plates were incubated for 5 minutes at RT and the reaction was stopped by adding 100 µL of 1N HCl to each well. The plates were read immediately at an optical density (OD) of 490 using an ELISA reader. The ELISA controls and test sample result OD values were blank corrected before interpretation. The ELISA test was negative if the average OD value was less than or equal to 0.7 and positive if the average OD value was greater than 0.7.

2.9 Statistical analyses

Prism 9 (GraphPad Software) was used for statistical analysis as follows: the two-tailed Mann–Whitney U test was used for single comparisons of independent groups, the Wilcoxon-test paired t test was used to compare two paired groups. For multiple groups statistical significance was assessed using a one-way analysis of variance (ANOVA) with multiple comparisons. The non-parametric Spearman test was used for correlation analysis. The statistical significances are indicated in the figures (*p< 0.05, **p< 0.01, ***p< 0.001, and ****p< 0.0001) and all tests were two-tailed.

3 Results

3.1 PLWH have lower frequencies of HCoV-specific CD4$^+$ T cells compared to HIV-uninfected individuals

The impact of pre-existing immune responses against endemic human coronaviruses (EHC), particularly HCoV-NL63, on SARS-CoV-2 specific T cell responses has been a subject of interest. Previous studies have linked existing cross-reactive memory responses to EHC with milder COVID-19 outcomes and robust vaccine responses, but how these responses are affected in PLWH remains unclear (9, 10, 16). Thus, our investigation aimed to determine if HIV infection alters the influence of pre-existing EHC responses on SARS-CoV-2 specific T cell responses.

Initially, we assessed the frequency of T cells reactive to HCoV-NL63 in COVID-19 convalescent individuals, with and without HIV infection. For comparison, we included HIV-uninfected individuals sampled before the pandemic as healthy controls. To gauge pre-existing immune responses to the endemic human coronavirus, we employed peptide pools encompassing the entire Spike Glycoprotein of HCoV-NL63. This choice was informed by HCoV-NL63 being a prominent endemic human coronavirus circulating in the region (8). PBMCs were stimulated with HCoV-NL63 peptide pools and responding cytokine-producing cells enumerated as described in the methods. Our findings, illustrated through representative flow plots (Figure 1A) and collated data (Figure 1B), indicate that a considerable portion of the participants exhibited visible HCoV-NL63-specific CD4$^+$ T and CD8$^+$ T cell responses, as signified by the presence of IFN-γ or TNF-a producing cells. Notably, the aggregate data demonstrates that HIV-uninfected individuals with COVID-19 displayed elevated levels of HCoV-NL63 specific CD4$^+$ T cells compared to PLWH and healthy controls (Figure 1B). The stable and sustained HCoV-NL63 responses observed in HIV-uninfected individuals are likely due to a relatively stable pool of HCoV-NL63-specific memory CD4$^+$ T cells. Our findings also showed significantly higher frequencies of SARS-CoV-2-specific CD4$^+$ and CD8$^+$ T cells following stimulation with SARS-CoV-2 peptide pools shown in the representative flow plots and summary plots (Figures 1C, D). These observations underscore the potential of SARS-CoV-2 to activate HCoV-NL63 specific CD4$^+$ T cells and emphasize the attenuation of pre-existing memory responses due to the presence of HIV.

Next, we measured SARS-CoV-2 specific T cell responses. We found a correlation between HCoV-NL63 -specific and SARS-CoV-2-specific CD4$^+$T and CD8$^+$ T cell responses regardless of HIV status (Figures 1E, F). These results are consistent with a previous report (17) that showed pre-existing cross-reactive CD4$^+$ T cells enhance immune responses to SARS-CoV-2 infection and BNT162b2 vaccination (17).

10.3389/fimmu.2023.1291048

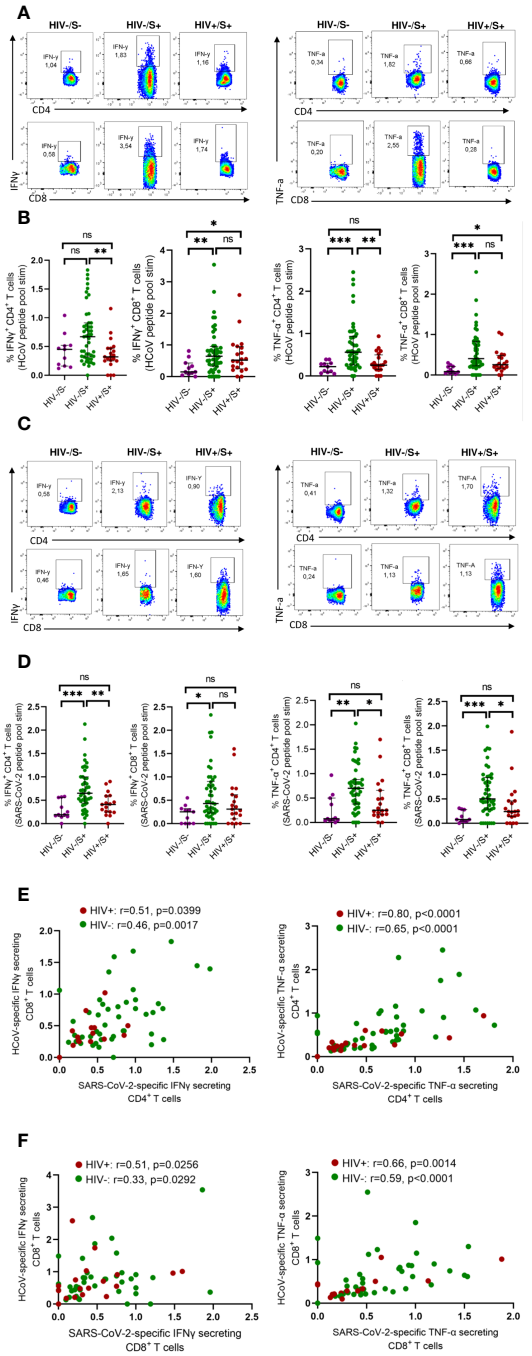

FIGURE 1
Comparison of HCoV-specific T cells in convalescent HIV-infected and HIV-uninfected individuals and healthy controls. Blood samples collected between 1- and 28-days post infection during the second (beta) and third (delta) waves were used. Intracellular cytokine staining (ICS) was performed to detect cytokine-producing T cells to HCoV overlapping peptide pools in HIV-uninfected (HIV-/SARS-CoV-2+, *n* = 47) and PLWH (HIV+/SARS-CoV-2+, *n* = 20) individuals and healthy controls (HIV-/SARS-CoV-2-; HC, *n* = 11). **(A)** Representative flow cytometry plots for the identification of antigen-specific $CD4^+$ and $CD8^+$ T cells based on expression IFNγ and TNF-α, following 18-h stimulation with HCoV peptides pools. **(B)** Summary plots showing the frequency of HCoV-specific $CD4^+$ and $CD8^+$ T cells ($IFN\gamma^+$ and $TNF\text{-}\alpha^+$). **(C)** Representative flow cytometry plots for the identification of antigen-specific $CD4^+$ and $CD8^+$ T cells based on expression of IFNγ and TNF-α, following 18-h stimulation with SARS-CoV-2 peptides pools. **(D)** Summary plots showing the frequency of SARS-CoV-2-specific $CD4^+$ and $CD8^+$ T cells ($IFN\gamma^+$ and $TNF\text{-}\alpha^+$). **(E)** Correlation of HCoV-specific and SARS-CoV-2-specific $CD4^+$ T cells in HIV-infected and HIV-uninfected individuals based on expression of IFNγ and TNF-α. **(F)** Correlation of HCoV-specific and SARS-CoV-2-specific $CD8^+$ T cells in HIV-infected and HIV-uninfected individuals based on expression of IFNγ and TNF-α. Significance was determined by two-tailed Mann-Whitney test and the two-tailed nonparametric Spearman test was used for correlation analysis, $p < 0.05$ was considered statistically significant. *$p < 0.05$, **$p < 0.01$, ***$p < 0.001$. 'ns' not significant.

3.2 Altered phenotypic characteristics of bulk CD4$^+$ T cells in PLWH

To investigate the mechanisms associated with impaired T cell response in PLWH, we first compared the activation profile of CD4$^+$ and CD8$^+$ T cells between PLWH and HIV-uninfected COVID-19 convalescent individuals as well as healthy controls. Here, T cell activation is defined as HLA-DR$^+$CD38$^+$ T cells. Representative flow plots (Figure 2A) and aggregate data (Figure 2B) show that PLWH had greater frequencies of activated (HLA-DR$^+$ CD38$^+$) CD8$^+$ T cells (p = 0.0006) and a trend towards more activated CD4$^+$ T cells compared to HIV-uninfected individuals and healthy controls (Figure 2B). Furthermore, we show that both the CD4$^+$ and CD8$^+$ T cells were more activated in the HIV-infected and HIV-uninfected COVID-19 participants compared to the healthy control group (Figure 2B).

Our investigation of the potential impact of T cell activation on the frequency of SARS-CoV-2 and HCoV-NL63 specific responses unveiled a significant correlation between the T cell activation and the frequency of SARS-CoV-2 CD4$^+$ T cell responses, irrespective of HIV status (PLWH: p=0.0076 and HIV-negative individuals: p=0.0059) (Figure 2C). These findings indicate that the SARS-CoV-2 specific CD4$^+$ T cells represented recent activated effector cells. Conversely, no discernible correlation was detected between the frequency of HCoV-NL63 responses and T cell activation (Figure 2C), which could be attributed to HCoV-NL63 responses being quiescent long-lived memory cells. Moreover, no correlation was observed for CD8$^+$T cell responses (Figure 2D).

Next, we examined T cell exhaustion, which we defined by the presence of the canonical T cell exhaustion marker PD-1 (18). Surprisingly, the healthy controls had significantly higher PD-1 expression in CD4$^+$ T cells compared to the HIV-infected and HIV-uninfected groups whereas the PD-1 expression in CD8 T cells was only significantly higher in the HIV-uninfected group (Figure 2D). This could probably be due to other underlying conditions or infections. However, our observations revealed that PLWH exhibited higher frequencies of exhausted CD4$^+$ and CD8$^+$ T cells (p = 0.0149 for CD4$^+$ T cells and p = 0.0105 for CD8$^+$ T cells, respectively) as depicted in representative plots and aggregate data (Figures 2E, F). These findings are line with previous reports (19–22). However, we did not find any significant correlation between either HCoV-NL63 or SARS-CoV-2 responses and T cell exhaustion (Supplementary Figure 1). Taken together, these results suggest a link between weakened SARS-CoV-2-specific responses and heightened T-cell activation.

3.3 Elevated plasma cytokine levels persist during recovering COVID-19 patients

Systemic inflammation has been shown to impair immune responses to SARS-CoV-2 infection (23, 24). To investigate whether systemic inflammation contributes to impaired T cell function observed in PLWH, we used the Bio-Plex Pro Human Cytokine Grp I Panel 27-Plex Assay to measure circulating chemokines and cytokines in COVID-19 convalescent patients and healthy controls. This multiplex analysis allowed us to measure 27 plasma cytokines produced in the convalescent phase of infection. The groups were denoted as HIV-uninfected and SARS-CoV-2-infected (HIV-/S+); HIV-infected and SARS-CoV-2-infected (HIV+/S+); and healthy controls being HIV-uninfected and SARS-CoV-2-uninfected (HIV-/S-). 21 participants comprising of 8 healthy controls (HIV-/S-); 5 HIV+/S+; 8 HIV-/S+ selected based on sample availability were used for these studies (Table 2). The plasma cytokine concentrations from the Luminex readout were normalized and presented as percentages, where 0% defined the smallest mean in each data set and 100% defined the largest mean in each data set shown as heatmap (Figure 3A). Our data show that the convalescent phase of SARS-CoV-2 infection is associated with persistent cytokine storm including IL-1b, IL-1ra, IL-2, IL-4, IL-5, IL-9, IL-10, IL-12(p70), IL-13, IL17, FGF basic, G-CSF, GM-CSF, IFN-g, MIP-1a and RANTES (Figures 3B–Q). Among COVID-19 donors, IL-2, and IL-12(p70) were significantly elevated in PLWH compared to HIV-uninfected participants (Figures 3D, I). Additionally, IL-10 trended toward higher levels in PLWH relative to HIV-uninfected individuals and healthy controls (Figure 3H). However, we did not find significant differences in the levels of IL-6, IL-8, Eotaxin, IP-10, MCP-1 (MCAF), PDGF-bb, MIP-1b and TNF-a in the three groups (Supplementary Figure 2). Overall, these data show that convalescent COVID-19 donors had elevated systemic inflammation as widely reported in the literature (25–27). Importantly, HIV infection was associated with significantly elevated cytokines such as IL-2, IL-12p70, and a trend towards more IL-10. These three cytokines have previously been associated with severe COVID-19 disease (28, 29). Overall, the plasma cytokine/chemokine levels in COVID-19 participants were much higher than in healthy donors in the convalescent phase of infection.

3.4 Anti-RBD IgG levels do not correlate with SARS-CoV-2-specific CD4$^+$T cell responses

Having demonstrated the negative effects of HIV infection on T cell immunity to EHC and SARS-CoV-2, we next investigated whether HIV has similar deleterious effects on humoral immunity to coronaviruses. Firstly, we used an in-house ELISA assay to measure antibodies targeting the receptor-binding domain (RBD) of the spike (S) protein of SARS-CoV-2 because of the potential of these antibodies to neutralize the virus and therefore desirable to induce by vaccination (30–32). We screened plasma samples from 10 HIV-infected and 24 HIV-uninfected subjects (PCR-confirmed SARS-CoV-2 infection) for antibodies against the RBD antigen. A sample was considered positive if the O.D value was greater than or equal to 0.7 and negative if the O.D value was less than 0.7, as previously described (33). The ELISA results are reported as optical densities with the limit of detection set at 0.7 shown by the dotted line on the graph (Figure 4A). Fifty four percent (13/24) of the HIV-uninfected individuals had measurable anti-RBD IgG antibodies, whereas 90% (9/10) of the PLWH had measurable anti-RBD

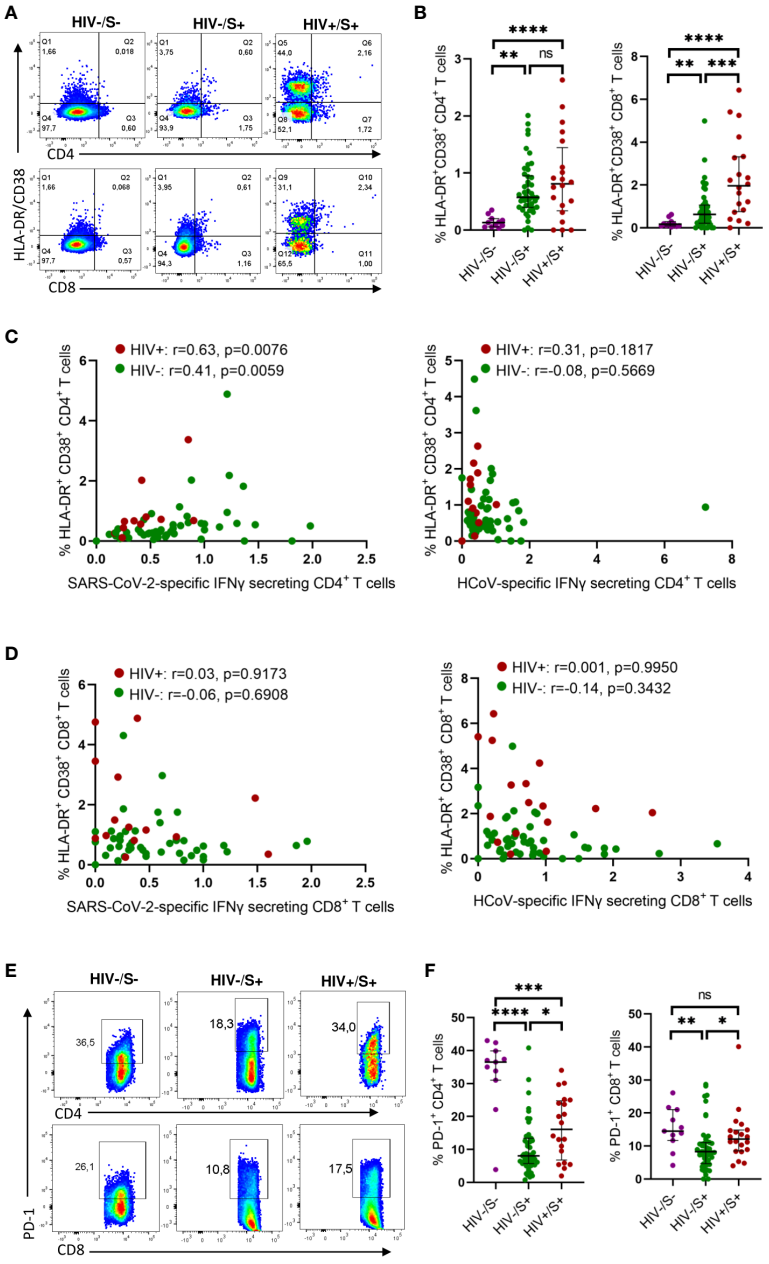

FIGURE 2
Comparison of the activation and exhaustion profile of HCoV-specific CD4$^+$ and CD8$^+$ T cells in COVID-19 convalescent HIV-infected and HIV-uninfected Individuals and healthy controls. Blood samples collected between 1- and 28-days post infection during the second (beta) and third (delta) waves were used to detect activated and exhausted T cells in HIV-uninfected (HIV-, *n* = 46), PLWH (HIV+, *n* = 20) and healthy controls (*n* = 11). **(A)** Representative flow cytometry plots for the identification of activated (HLA-DR$^+$CD38$^+$) CD4$^+$ and CD8$^+$ T cells. **(B)** Summary plots of the frequency of activated CD4$^+$ and CD8$^+$ T cells based on the expression of HLA-DR, CD38. Correlation of T cell activation of SARS-CoV-2 and HCoV-specific **(C)** CD4$^+$ and **(D)** CD8$^+$ T cells in HIV-infected and HIV-uninfected individuals. **(E)** Representative flow cytometry plots and **(F)** summary data for the identification of exhausted (PD-1$^+$) CD4$^+$ and CD8$^+$ T cells. Significance was determined by two-tailed Mann-Whitney test and these two-tailed nonparametric Spearman test was used for correlation analysis, $p < 0.05$ was considered statistically significant. *$p < 0.05$, **$p < 0.01$, ***$p < 0.001$, ****$p < 0.0001$. 'ns' not significant.

antibodies. The aggregate data showed no significant difference in anti-RBD antibody production based on HIV status (Figure 4B).

Virus specific CD4$^+$ T cells responses are known to help B cell responses, but the role of effector CD4$^+$ T cells responses in promoting B cell affinity maturation and antibody class switching during SAR-CoV-2 infection remain unresolved (34). Several studies have reported positive association between SAR-CoV-2 specific CD4$^+$ T cell frequency and the levels of Spike specific antibodies in plasma (12). Others have shown that antibodies generated in the presence and absence of Tfh cells display similar neutralization potency against SARS-CoV-2 (34–36). Here, we investigated the connection between anti-RBD antibody levels

TABLE 2 Description of the subset of samples used to measure cytokine levels and antibody responses.

	Healthy controls (*n* = 8)	HIV-uninfected (*n* = 8)	HIV-infected (*n* = 6)
Age mean (range)	22.4 (18 – 33)	31.8 (20 – 40)	44.4 (25 – 65)
Male, n (%)	2 (25)	5 (62.5)	1 (20)
Female, n (%)	6 (75%)	3 (37.5)	4 (80)
Days since diagnosis, meadian (range)	–	7 (7 – 21)	14 (7 – 22)
CD4 count, median (range)	840 (634 – 1348)	819 (624 – 1131)	260 (133 – 566)
SARS-CoV-2-specific responses	No	Yes	Yes
HCoV-specific responses	Yes	Yes	Yes

Convalescent HIV-infected and HIV-uninfected individuals were infected with either the beta (second wave) or delta (third wave) variants.

and SARS-CoV-2 T-cell responses in both HIV-infected and HIV-uninfected donors. Our analysis revealed no correlation between RBD IgG titers and SARS-CoV-2-specific IFN-γ-secreting $CD4^+$ and $CD8^+$ T cells (Figure 4C). Similarly, TNF-α-secreting SARS-CoV-2-specific $CD4^+$ and $CD8^+$ T cells showed no correlation with RBD IgG titers (Figure 4D). The absence of correlation between antibody responses and $CD4^+$ T cell responses might be attributed to our measurement of overall $CD4^+$ T cell responses instead of follicular helper cells (TFH), which have been linked to anti-spike antibody responses (37, 38).

3.5 Antibody recognition of SARS-CoV-2 antigens and ACE2 binding inhibition by healthy control and SARS-CoV-2 convalescent plasma

Next, we used the SARS-CoV-2 MSD Multi-Spot Assay System (V-PLEX COVID-19 serology assay) to quantify binding and neutralization activity and evaluate anti-spike antibodies in plasma. Specifically, the V-PLEX COVID-19 serology assay allowed us to measure IgG antibody binding activity to multiple antigens such as RBD, nucleocapsid, wildtype, alpha, beta, gamma, delta, and omicron using multi-spot plates (Table 3). Twelve SARS-CoV-2 convalescent participants (6 HIV-infected and 6 HIV-uninfected) and 8 healthy controls were used for these studies based on sample availability (Table 2). We found that most COVID-19 convalescent participants' IgG antibodies were able to bind all SARS-CoV-2 variants except omicron with significantly higher levels of IgG antibodies targeting the SARS-CoV-2 antigens compared to healthy donors (Supplementary Figure 3). The nucleocapsid and beta antigens were most targeted (Figure 5A). There was low-level detection of anti-nucleocapsid antibodies in one of the healthy controls, likely attributable to cross-reactive antibodies (Figure 5A).

Next, we examined the neutralization activity of plasma anti-SARS-CoV-2 Spike antibodies. We used a V-PLEX COVID-19 ACE2 neutralization assay which measures the ability of antibodies to block the binding of ACE2 to its cognate ligands. The V-PLEX COVID-19 ACE2 neutralization assay has been demonstrated to highly correlate with gold standard live microneutralization assays (14). The neutralization assay was performed on samples that had detectable antibodies by V-PLEX COVID-19 serology assay. Almost all COVID-19 participants generated significant RBD-ACE2 binding inhibition of all the variants tested and no significant difference was observed between PLWH and HIV-uninfected participants (Figure 5B). Generally, plasma from healthy subjects did not exhibit ACE2 binding inhibition except 3 donors who exhibited minimal binding activity (ACE2 binding inhibition of< 20%) against the nucleocapsid (Figure 5B). These results indicate that HIV infection has minimal impact on the quality and magnitude of antibody responses against SARS-CoV-2 infection as the SARS-CoV-2-specific antibody responses were similar between PLWH and HIV-uninfected participants. These results are similar to other studies that have shown that antibody responses to SARS-CoV-2 infection did not differ by HIV status (15).

4 Discussion

Enhancing our understanding of both cellular and humoral immune responses to COVID-19 within populations at higher risk of infection or severe illness is crucial for the development of next-generation COVID-19 vaccines, aiming to provide superior protection across all demographic groups. In this study, we aimed to identify the underlying immune deficiencies contributing to weakened immune responses against SARS-CoV-2 in PLWH. We focus on exploring the role of pre-existing cross-reactive responses in SARS-CoV-2 immunity, as various studies have underscored the potential benefits of cross-reactive immunity in both SARS-CoV-2 infection and vaccination (9, 17). Furthermore, the significance of cross-reactive immunity to various coronaviruses is noteworthy in the creation of panCoV T cell-inducing vaccines, designed to safeguard against multiple coronaviruses.

Our study uncovered a notable relationship between pre-existing immunity and the development of cross-reactive responses to SARS-CoV-2. To begin with, we noticed higher occurrences of HCoV-NL63 memory responses in individuals with COVID-19 compared to those who were healthy. Secondly, a strong correlation emerged between HCoV-NL63 memory responses and SARS-CoV-2 responses, suggesting that pre-existing cross-reactive immune responses are present in most individuals. Thirdly, we observed that people living with HIV (PLWH) had lower frequencies of pre-existing memory T cell responses to the endemic human coronavirus (EHC) HCoV-NL63. Fourthly, we noted that HIV infection had a more detrimental impact on cellular immune responses than on antibody immune responses to both HCoV-NL63 and SARS-CoV-2 infections. Overall, our study underscores the need to better understand of how cross-reactive responses influence vaccine-induced immune responses.

Various studies have presented evidence of pre-existing T cells recognizing SARS-CoV-2 in individuals across different geographic regions (13, 39). The idea is that cross-reactive memory T cells,

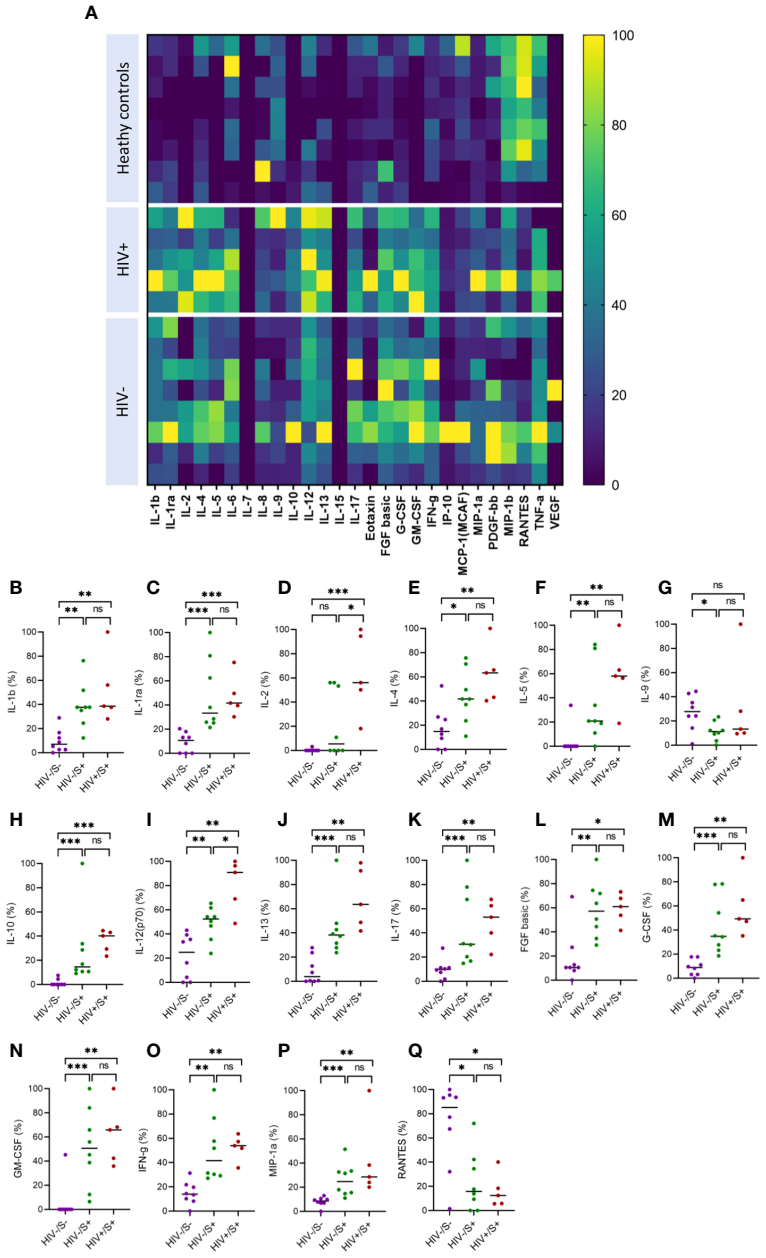

FIGURE 3
Comparison of plasma cytokine and chemokine levels in cells in convalescent HIV-infected and HIV-uninfected individuals and healthy controls. Serum samples collected between 1- and 28-days post infection were used to measure cytokine and chemokine levels by the Bio-Plex assay. **(A)** Heatmap showing normalized cytokine and chemokine levels (in percentages) in convalescent HIV-infected (HIV+/S+, *n* = 5) and HIV-uninfected (HIV-/S+, *n* = 8) individuals and healthy controls (HIV-/S-, *n* = 8). Summary plots of **(B)** IL-1b, **(C)** IL-1ra, **(D)** IL-2, **(E)** IL-4, **(F)** IL-5, **(G)** IL-9, **(H)** IL-10, **(I)** IL-12(p70), **(J)** IL-13, **(K)** IL-17, **(L)** FGF basic, **(M)** G-CSF, **(N)** GM-CSF, **(O)** IFN-g, **(P)** MIP-1a and **(Q)** RANTES. Significance was determined by two-tailed Mann-Whitney test, $p < 0.05$ was considered statistically significant. *$p < 0.05$, **$p < 0.01$, ***$p < 0.001$. 'ns' not significant.

stemming from previous exposure to other circulating coronaviruses, contribute to a baseline immunity against COVID-19 (40, 41). As such, the higher vulnerability of the elderly to severe COVID-19 has been linked to reduced pre-existing cross-reactive CD4+ T cell responses (17). Furthermore, a study by van Rooyen et al. (4) highlighted significant pre-existing T-cell immunity to SARS-CoV-2 in South African individuals who hadn't previously been diagnosed with COVID-19. This immunity might be attributed to pre-existing cross-reactive immune responses to other human coronaviruses or asymptomatic infections. The study also observed that the strength of T cell responses to both SARS-CoV-2 S-proteins and N-proteins was greater in participants with a history of COVID-19 diagnosis, indicating a notable T cell response post-SARS-CoV-2 infection (4).

In our previous study, we focused on comparing individuals infected with the wildtype and beta variant, exploring cross-protection between the first wave virus and the beta variant, and examining the influence of HIV infection on cross-recognition. We

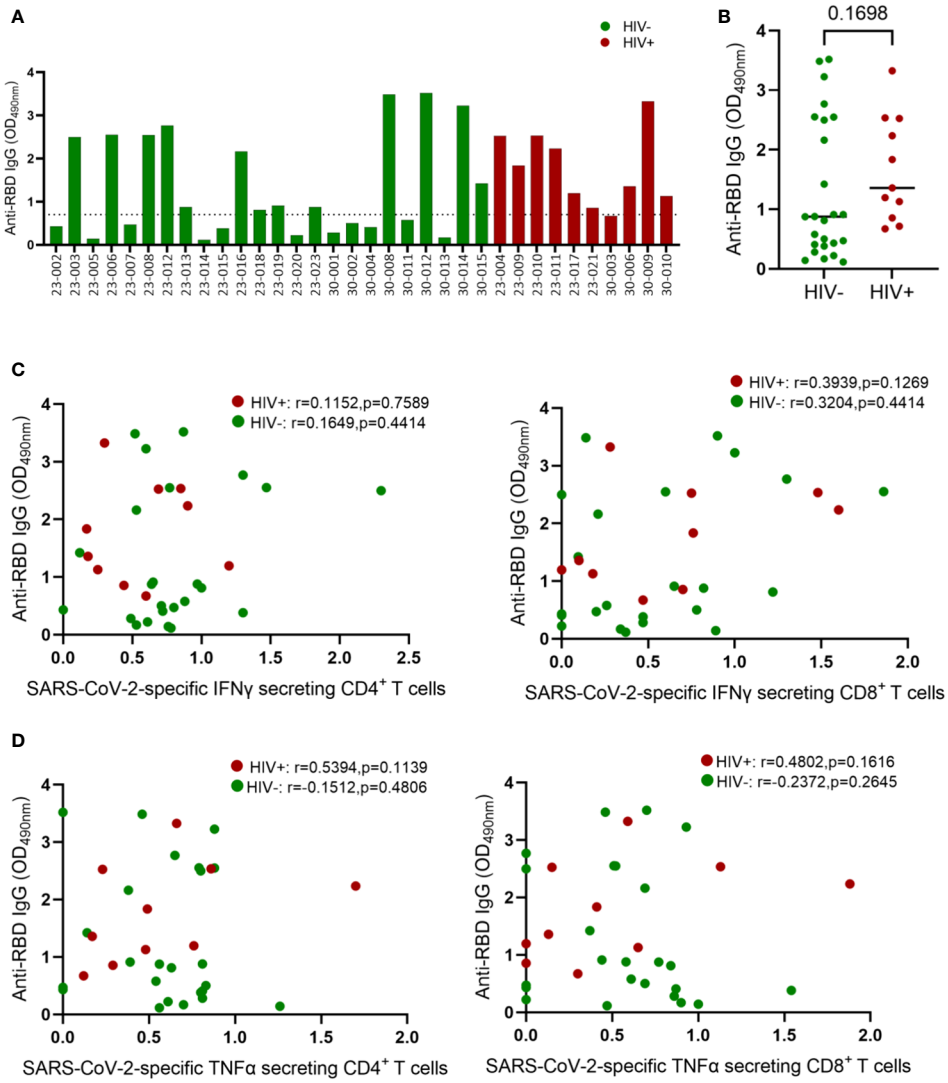

FIGURE 4
Comparison of IgG concentrations in convalescent HIV-infected and HIV-uninfected individuals. Serum samples collected between 1- and 28-days post infection were used to measure spike-specific responses by ELISA. **(A)** Comparison of anti-RBD IgG antibody OD values in convalescent HIV-infected (red bars, n = 10) and HIV-uninfected (green bars, n = 24) individuals. **(B)** Aggregate data of anti-RBD antibodies in HIV infected and HIV-uninfected individuals. **(C)** Correlation of anti-RBD antibodies and SARS-CoV-2 specific IFNγ secreting $CD4^+$ and $CD8^+$ T cells. **(D)** Correlation of anti-RBD antibodies and SARS-CoV-2 specific TNF-α secreting $CD4^+$ and $CD8^+$ T cells. The dotted line denotes OD values ≤ 0.7 that represent a negative ELISA test. ELISA tests are positive if the average OD value is > 0.7. Significance was determined by two-tailed Mann-Whitney test and the two-tailed nonparametric Spearman test was used for correlation analysis, $p< 0.05$ was considered statistically significant.

demonstrated that unsuppressed HIV is linked to weakened immune responses and limited recognition of COVID-19 variants. However, the primary factors contributing to these suboptimal responses were not identified. In this current study, our focus shifted to investigating whether pre-existing immune responses to a common cold coronavirus can cross-recognize and cross-protect against SARS-CoV-2 infection. This current study suggests that the inadequate cross-reactivity of pre-existing memory responses to endemic human coronaviruses (EHCs) might contribute to the overall decline in T cell responses to SARS-CoV-2. It's noteworthy that both studies share a common theme of assessing the impact of HIV infection on the quality and magnitude of pre-existing immunity to SARS-CoV-2 and common cold coronaviruses. These findings are consistent with earlier studies that indicate HIV infection, even when managed with effective antiretroviral therapy, is characterized by chronic immune activation, tissue inflammation, and exhaustion (42, 43).

It has been reported that the severity of clinical disease in COVID-19 patients is associated not only with significant changes in the innate immune system but also with a marked alteration of both humoral and cellular immunity, encompassing SARS-CoV-2–specific and overall T cell function (44). Our immunological analysis revealed that both SARS-CoV-2 and EHC responses were more focused on the CD4 arm of the cellular immune system rather than the CD8 arm, which is consistent with our prior study and other reports (12, 17, 20, 45). Furthermore, HIV infection had a more profound effect on $CD4^+$ T cell responses compared to $CD8^+$ T cell responses and antibody responses. It is not clear why SARS-

10.3389/fimmu.2023.1291048

TABLE 3 List of antigens and their spot assignments on the MULTI-SPOT 96-Well, 10-Spot plate (Plate 24).

Plate description	SARS-CoV-2 antigen	Antigen description
Spot 1	SARS-CoV-2 Spike	Wildtype
Spot 2	Spike (B.1.1.529; BA.1; BA.1.15)	Omicron
Spot 3	SARS-CoV-2 Nucleocapsid	Nucleocapsid
Spot 4	Spike (B.1.617.2; AY.4) Alt Seq 2	Delta
Spot 5	BSA	–
Spot 6	BSA	–
Spot 7	Spike (P.1)	Gamma
Spot 8	Spike (B.1.1.7)	Alpha
Spot 9	Spike (B.1.351)	Beta
Spot 10	SARS-CoV-2 S1 RBD	Receptor binding domain

CoV-2 induces stronger $CD4^+$ T cell responses. One potential explanation is that the most immunogenic SARS-CoV-2 antigens are more readily recognized by $CD4^+$ T cells than $CD8^+$ T cells. Nevertheless, further studies are required to comprehend this phenomenon.

Prior research has demonstrated similar antibody titers against S1 and N proteins of SARS-CoV-2 in individuals with mild COVID-19, regardless of their HIV infection status (46). Other studies have also indicated that there are no discernible differences in antibody responses during the 6-month period following mild COVID-19 based on HIV status. The magnitude, progression, and persistence of anti-SARS-CoV-2 IgM, IgG, and IgA antibodies, as well as neutralization strength, appear to be consistent in PLWH who have well-managed HIV infection (15, 46, 47). In line with these findings, this study reveals that PLWH have comparable levels of neutralizing antibodies in the form of anti-SARS-CoV-2 IgG, compared to individuals without HIV. Additionally, a subset of participants, both HIV-infected and HIV-uninfected, displayed robust neutralization abilities despite having low titers of anti-SARS-CoV-2 binding antibodies. This might be attributed to neutralizing antibodies targeting different viral epitopes and/or elevated levels of non-neutralizing antibodies, or the influence of other antibody isotypes in the neutralizing responses (46).

This study indicates that PLWH have diminished T cell responses to both an endemic human coronavirus (EHC) and SARS-CoV-2. This suggests a potential susceptibility to SARS-CoV-2 infection, and it's plausible that their responses to infections and vaccines might be less robust. Nonetheless, it's important to note that the study has certain limitations, notably a small sample size and the utilization of a cross-sectional design, which restricts the broader generalizability of these observations. To validate these intriguing findings, a more extensive longitudinal analysis of specific T cells and antibodies will be necessary.

In conclusion, our study reveals that the decrease in SARS-CoV-2 specific responses T cell in PLWH may be attributable to

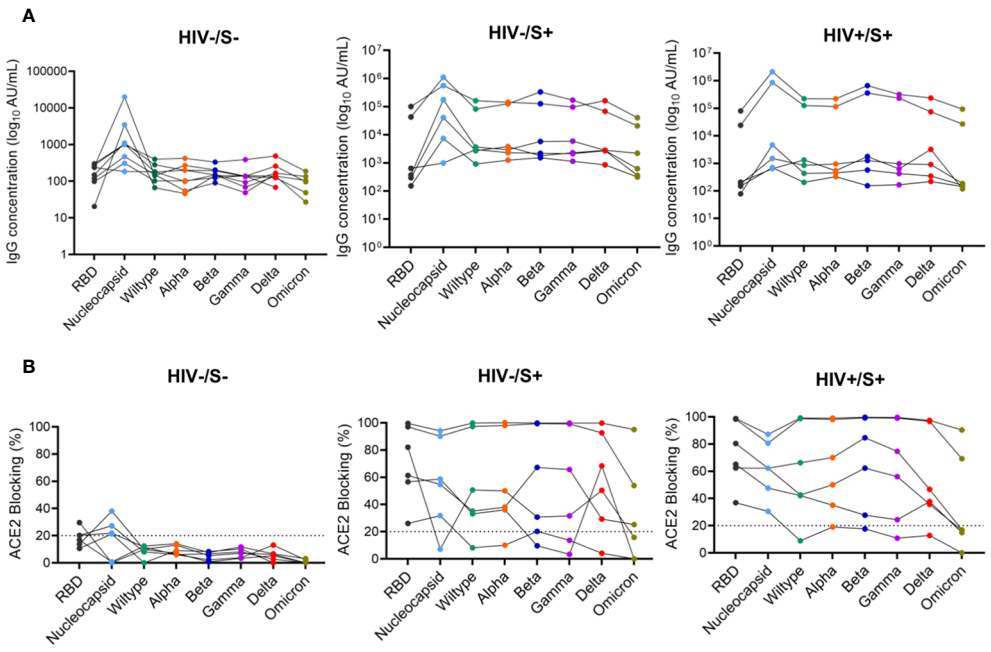

FIGURE 5
Comparison of anti-SARS-CoV-2 IgG antibodies and ACE2 blocking potential in healthy controls and COVID-19 convalescent HIV-infected and HIV-uninfected individuals. Serum samples collected between 1- and 22-days post infection were used to measure anti-SARS-CoV-2 IgG antibodies and ACE2 blocking in HIV-infected (HIV+, n = 6), HIV-uninfected (HIV-, n = 6) and healthy controls (n = 6) by the MSD V=Plex assays. **(A)** Summary plots of SARS-CoV-2-specific IgG antibody concentrations in the three groups. **(B)** Summary plots showing ACE2 blocking of SARS-CoV-2-specific antigens in the three groups.

reduced frequencies of pre-existing cross-reactive responses, heightened T cell activation and systemic inflammation.

Data availability statement

The raw data supporting the conclusions of this article will be made available by the authors, without undue reservation.

Ethics statement

The studies involving humans were approved by University of KwaZulu-Natal Institutional Review Board (approval BREC/00001275/2020) and the National Health Research Authority and University of Zambia Biomedical Research Ethics Committee (REF. No. 1648-2021). The studies were conducted in accordance with the local legislation and institutional requirements. The participants provided their written informed consent to participate in this study.

Author contributions

TNg': Data curation, Formal analysis, Investigation, Writing – original draft, Writing – review & editing, Methodology. VM: Investigation, Writing – review & editing. TNk: Formal analysis, Investigation, Writing – review & editing. JM: Formal analysis, Investigation, Writing – review & editing. MM: Formal analysis, Investigation, Writing – review & editing. CM: Investigation, Writing – review & editing. WK: Writing – review & editing, Conceptualization, Funding acquisition, Project administration, Resources. FK: Project administration, Writing – review & editing, Data curation. MM: Project administration, Writing – review & editing, Resources. KK: Writing – review & editing, Data curation, Project administration. KJ: Writing – review & editing, Formal analysis, Investigation, Resources. WH: Resources, Writing – review & editing, Project administration. AS: Data curation, Funding acquisition, Project administration, Resources, Writing – review & editing. ZN: Conceptualization, Data curation, Formal analysis, Funding acquisition, Investigation, Project administration, Resources, Supervision, Validation, Writing – original draft, Writing – review & editing.

Funding

The author(s) declare financial support was received for the research, authorship, and/or publication of this article. This work was funded by; HHMI International research scholar award (Grant #55008743 to ZN), the Wellcome Trust (Grant# 226137/Z/22/Z Awarded to AS and ZN), the BMGF [Awarded to AS and ZN (INV-018944), awarded to KJ (INV-039481)], and SAMRC (Awarded to WH, # 96838). This work was also partially funded by the Sub-Saharan African Network for TB/HIV Research Excellence (SANTHE) collaborative award (to ZN # SANTHE-COL016), a DELTAS Africa Initiative (grant # DEL-15-006). The DELTAS Africa Initiative is an independent funding scheme of the African Academy of Sciences (AAS)'s Alliance for Accelerating Excellence in Science in Africa (AESA) and supported by the New Partnership for Africa's Development Planning and Coordinating Agency (NEPAD Agency) with funding from the Wellcome Trust (grant # 107752/Z/15/Z) and the UK government. This project was also funded in part with Federal funds from the National Institute of Allergy and Infectious Diseases, National Institutes of Health, Department of Health and Human Services, under Contract No. HHSN272201400004C (NIAID Centers of Excellence for Influenza Research and Surveillance, CEIRS).

Acknowledgments

We would like to thank our study participants, the laboratory and clinic staff at Africa Health Research Institute for collecting the samples and compiling the clinical demographic data for the study. We would like to thank our study participants, the laboratory and clinic staff at Africa Health Research Institute and the Center for Family Health Research in Zambia for collecting the samples and compiling the clinical demographic data for the study.

Conflict of interest

The authors declare that the research was conducted in the absence of any commercial or financial relationships that could be construed as a potential conflict of interest.

Publisher's note

Author disclaimer

The views expressed in this publication are those of the author(s) and not necessarily those of AAS, NEPAD Agency, Wellcome Trust, NIH, NIAID, or the UK government.

Supplementary material

The Supplementary Material for this article can be found online at: https://www.frontiersin.org/articles/10.3389/fimmu.2023.1291048/full#supplementary-material

References

1. Ren LL, Wang YM, Wu ZQ, Xiang ZC, Guo L, Xu T, et al. Identification of a novel coronavirus causing severe pneumonia in human: a descriptive study. *Chin Med J (Engl)* (2020) 133(9):1015–24. doi: 10.1097/CM9.0000000000000722

2. WHO. *COVID-19 timeline 2020*. Available at: https://www.who.int/news-room/detail/29-06-2020-covidtimeline.

3. Shrotri M, van Schalkwyk MCI, Post N, Eddy D, Huntley C, Leeman D, et al. T cell response to SARS-CoV-2 infection in humans: A systematic review. *PloS One* (2021) 16(1):e0245532. doi: 10.1371/journal.pone.0245532

4. van Rooyen C, Brauer M, Swanepoel P, van den Berg S, van der Merwe C, van der Merwe M, et al. Comparison of T-cell immune responses to SARS-CoV-2 spike (S) and nucleocapsid (N) protein using an in-house flow-cytometric assay in laboratory employees with and without previously confirmed COVID-19 in South Africa: nationwide cross-sectional study. *J Clin Pathol* (2022) 76(6):384–390. doi: 10.1136/jclinpath-2021-207556

5. Nomah DK, Reyes-Uruena J, Llibre JM, Ambrosioni J, Ganem FS, Miro JM, et al. HIV and SARS-CoV-2 co-infection: epidemiological, clinical features, and future implications for clinical care and public health for people living with HIV (PLWH) and HIV most-at-risk groups. *Curr HIV/AIDS Rep* (2022) 19(1):17–25. doi: 10.1007/s11904-021-00596-5

6. Ssentongo P, Heilbrunn ES, Ssentongo AE, Advani S, Chinchilli VM, Nunez JJ, et al. Epidemiology and outcomes of COVID-19 in HIV-infected individuals: a systematic review and meta-analysis. *Sci Rep* (2021) 11(1):6283. doi: 10.1038/s41598-021-85359-3

7. Liang M, Luo N, Chen M, Chen C, Singh S, Singh S, et al. Prevalence and mortality due to COVID-19 in HIV co-infected population: A systematic review and meta-analysis. *Infect Dis Ther* (2021) 10(3):1267–85. doi: 10.1007/s40121-021-00447-1

8. Gorse GJ, Patel GB, Vitale JN, O'Connor TZ. Prevalence of antibodies to four human coronaviruses is lower in nasal secretions than in serum. *Clin Vaccine Immunol* (2010) 17(12):1875–80. doi: 10.1128/CVI.00278-10

9. Sette A, Crotty S. Pre-existing immunity to SARS-CoV-2: the knowns and unknowns. *Nat Rev Immunol* (2020) 20(8):457–8. doi: 10.1038/s41577-020-0389-z

10. Meyerholz DK, Perlman S. Does common cold coronavirus infection protect against severe SARS-CoV-2 disease? *J Clin Invest* (2021) 131(1):e144807. doi: 10.1172/JCI144807

11. Sagar M, Reifler K, Rossi M, Miller NS, Sinha P, White LF, et al. Recent endemic coronavirus infection is associated with less-severe COVID-19. *J Clin Invest* (2021) 131(1):e143380. doi: 10.1172/JCI143380

12. Grifoni A, Weiskopf D, Ramirez SI, Mateus J, Dan JM, Moderbacher CR, et al. Targets of T cell responses to SARS-CoV-2 coronavirus in humans with COVID-19 disease and unexposed individuals. *Cell* (2020) 181(7):1489–501 e15. doi: 10.1016/j.cell.2020.05.015

13. Weiskopf D, Schmitz KS, Raadsen MP, Grifoni A, Okba NMA, Endeman H, et al. Phenotype and kinetics of SARS-CoV-2-specific T cells in COVID-19 patients with acute respiratory distress syndrome. *Sci Immunol* (2020) 5(48):eabd2071. doi: 10.1126/sciimmunol.abd2071

14. Lopez E, Haycroft ER, Adair A, Mordant FL, O'Neill MT, Pymm P, et al. Simultaneous evaluation of antibodies that inhibit SARS-CoV-2 variants via multiplex assay. *JCI Insight* (2021) 6(16):e150012. doi: 10.1172/jci.insight.150012

15. Alcaide ML, Nogueira NF, Salazar AS, Montgomerie EK, Rodriguez VJ, Raccamarich PD, et al. A longitudinal analysis of SARS-coV-2 antibody responses among people with HIV. *Front Med (Lausanne)* (2022) 9:768138. doi: 10.3389/fmed.2022.768138

16. Tarke A, Zhang Y, Methot N, Narowski TM, Phillips E, Mallal S, et al. Targets and cross-reactivity of human T cell recognition of common cold coronaviruses. *Cell Rep Med* (2023) 4(6):101088. doi: 10.1016/j.xcrm.2023.101088

17. Loyal L, Braun J, Henze L, Kruse B, Dingeldey M, Reimer U, et al. Cross-reactive CD4(+) T cells enhance SARS-CoV-2 immune responses upon infection and vaccination. *Science* (2021) 374(6564):eabh1823. doi: 10.1126/science.abh1823

18. Day CL, Kaufmann DE, Kiepiela P, Brown JA, Moodley ES, Reddy S, et al. PD-1 expression on HIV-specific T cells is associated with T-cell exhaustion and disease progression. *Nature* (2006) 443(7109):350–4. doi: 10.1038/nature05115

19. Riou C, du Bruyn E, Stek C, Daroowala R, Goliath RT, Abrahams F, et al. Relationship of SARS-CoV-2-specific CD4 response to COVID-19 severity and impact of HIV-1 and tuberculosis coinfection. *J Clin Invest* (2021) 131(12):e149125. doi: 10.1172/JCI149125

20. Nkosi T, Chasara C, Papadopoulos AO, Nguni TL, Karim F, Moosa MS, et al. Unsuppressed HIV infection impairs T cell responses to SARS-CoV-2 infection and abrogates T cell cross-recognition. *Elife* (2022) 11:e78374. doi: 10.7554/eLife.78374.sa2

21. El-Far M, Halwani R, Said E, Trautmann L, Doroudchi M, Janbazian L, et al. T-cell exhaustion in HIV infection. *Curr HIV/AIDS Rep* (2008) 5(1):13–9. doi: 10.1007/s11904-008-0003-7

22. Breton G, Chomont N, Takata H, Fromentin R, Ahlers J, Filali-Mouhim A, et al. Programmed death-1 is a marker for abnormal distribution of naive/memory T cell subsets in HIV-1 infection. *J Immunol* (2013) 191(5):2194–204. doi: 10.4049/jimmunol.1200646

23. Schulte-Schrepping J, Reusch N, Paclik D, Bassler K, Schlickeiser S, Zhang B, et al. Severe COVID-19 is marked by a dysregulated myeloid cell compartment. *Cell* (2020) 182(6):1419–40.e23. doi: 10.1016/j.cell.2020.08.001

24. Shakiba MH, Gemund I, Beyer M, Bonaguro L. Lung T cell response in COVID-19. *Front Immunol* (2023) 14:1108716. doi: 10.3389/fimmu.2023.1108716

25. Bonny TS, Patel EU, Zhu X, Bloch EM, Grabowski MK, Abraham AG, et al. Cytokine and chemokine levels in coronavirus disease 2019 convalescent plasma. *Open Forum Infect Dis* (2021) 8(2):ofaa574. doi: 10.1093/ofid/ofaa574

26. Ibanez-Prada ED, Fish M, Fuentes YV, Bustos IG, Serrano-Mayorga CC, Lozada J, et al. Comparison of systemic inflammatory profiles in COVID-19 and community-acquired pneumonia patients: a prospective cohort study. *Respir Res* (2023) 24(1):60. doi: 10.1186/s12931-023-02352-2

27. Ong SWX, Fong SW, Young BE, Chan YH, Lee B, Amrun SN, et al. Persistent symptoms and association with inflammatory cytokine signatures in recovered coronavirus disease 2019 patients. *Open Forum Infect Dis* (2021) 8(6):ofab156. doi: 10.1093/ofid/ofab156

28. Lucas C, Wong P, Klein J, Castro TBR, Silva J, Sundaram M, et al. Longitudinal analyses reveal immunological misfiring in severe COVID-19. *Nature* (2020) 584(7821):463–9. doi: 10.1038/s41586-020-2588-y

29. Yang Y, Iwasaki A. Impact of chronic HIV infection on SARS-CoV-2 infection, COVID-19 disease and vaccines. *Curr HIV/AIDS Rep* (2022) 19(1):5–16. doi: 10.1007/s11904-021-00590-x

30. Premkumar L, Segovia-Chumbez B, Jadi R, Martinez DR, Raut R, Markmann A, et al. The receptor binding domain of the viral spike protein is an immunodominant and highly specific target of antibodies in SARS-CoV-2 patients. *Sci Immunol* (2020) 5(48):eabc8413. doi: 10.1126/sciimmunol.abc8413

31. Mehdi F, Chattopadhyay S, Thiruvengadam R, Yadav S, Kumar M, Sinha SK, et al. Development of a fast SARS-CoV-2 IgG ELISA, based on receptor-binding domain, and its comparative evaluation using temporally segregated samples from RT-PCR positive individuals. *Front Microbiol* (2020) 11:618097. doi: 10.3389/fmicb.2020.618097

32. Hussein NA, Ali EAA, El-Hakim AE, Tabll AA, El-Shershaby A, Salamony A, et al. Assessment of specific human antibodies against SARS-CoV-2 receptor binding domain by rapid in-house ELISA. *Hum Antibodies* (2022) 30(2):105–15. doi: 10.3233/HAB-220003

33. Suthar MS, Zimmerman MG, Kauffman RC, Mantus G, Linderman SL, Hudson WH, et al. Rapid generation of neutralizing antibody responses in COVID-19 patients. *Cell Rep Med* (2020) 1(3):100040. doi: 10.1016/j.xcrm.2020.100040

34. Chen JS, Chow RD, Song E, Mao T, Israelow B, Kamath K, et al. High-affinity, neutralizing antibodies to SARS-CoV-2 can be made without T follicular helper cells. *Sci Immunol* (2022) 7(68):eabl5652. doi: 10.1126/sciimmunol.abl5652

35. Hoffmann M, Arora P, Gross R, Seidel A, Hornich BF, Hahn AS, et al. SARS-CoV-2 variants B.1.351 and P.1 escape from neutralizing antibodies. *Cell* (2021) 184(9):2384–93 e12. doi: 10.1016/j.cell.2021.03.036

36. Zhou D, Dejnirattisai W, Supasa P, Liu C, Mentzer AJ, Ginn HM, et al. Evidence of escape of SARS-CoV-2 variant B.1.351 from natural and vaccine-induced sera. *Cell* (2021) 184(9):2348–61 e6. doi: 10.1016/j.cell.2021.02.037

37. Chi X, Gu J, Ma X. Characteristics and roles of T follicular helper cells in SARS-coV-2 vaccine response. *Vaccines (Basel)* (2022) 10(10):1623. doi: 10.3390/vaccines10101623

38. Koutsakos M, Lee WS, Wheatley AK, Kent SJ, Juno JA. T follicular helper cells in the humoral immune response to SARS-CoV-2 infection and vaccination. *J Leukoc Biol* (2022) 111(2):355–65. doi: 10.1002/JLB.5MR0821-464R

39. Meckiff BJ, Ramírez-Suástegui C, Fajardo V, Chee SJ, Kusnadi A, Simon H, et al. Imbalance of Regulatory and Cytotoxic SARS-CoV-2-Reactive CD4+ T Cells in COVID-19. *Cell* (2020) 183(5):1340-1353.e16. doi: 10.1016/j.cell.2020.10.001

40. Le Bert N, Tan AT, Kunasegaran K, Tham CYL, Hafezi M, Chia A, et al. SARS-CoV-2-specific T cell immunity in cases of COVID-19 and SARS, and uninfected controls. *Nature* (2020) 584(7821):457–62. doi: 10.1038/s41586-020-2550-z

41. Braun J, Loyal L, Frentsch M, Wendisch D, Georg P, Kurth F, et al. SARS-CoV-2-reactive T cells in healthy donors and patients with COVID-19. *Nature* (2020) 587(7833):270–4. doi: 10.1038/s41586-020-2598-9

42. Serrano-Villar S, Sainz T, Lee SA, Hunt PW, Sinclair E, Shacklett BL, et al. HIV-infected individuals with low CD4/CD8 ratio despite effective antiretroviral therapy exhibit altered T cell subsets, heightened CD8+ T cell activation, and increased risk of non-AIDS morbidity and mortality. *PloS Pathog* (2014) 10(5):e1004078. doi: 10.1371/journal.ppat.1004078

43. Khoury G, Fromentin R, Solomon A, Hartogensis W, Killian M, Hoh R, et al. Human immunodeficiency virus persistence and T-cell activation in blood, rectal, and lymph node tissue in human immunodeficiency virus-infected individuals receiving suppressive antiretroviral therapy. *J Infect Dis* (2017) 215(6):911–9. doi: 10.1093/infdis/jix039

44. Schub D, Klemis V, Schneitler S, Mihm J, Lepper PM, Wilkens H, et al. High levels of SARS-CoV-2-specific T cells with restricted functionality in severe courses of COVID-19. *JCI Insight* (2020) 5(20):e142167. doi: 10.1172/jci.insight.142167

45. Mateus J, Grifoni A, Tarke A, Sidney J, Ramirez SI, Dan JM, et al. Selective and cross-reactive SARS-CoV-2 T cell epitopes in unexposed humans. *Science* (2020) 370(6512):89–94. doi: 10.1126/science.abd3871

46. Alrubayyi A, Gea-Mallorqui E, Touizer E, Hameiri-Bowen D, Kopycinski J, Charlton B, et al. Characterization of humoral and SARS-CoV-2 specific T cell responses in people living with HIV. *Nat Commun* (2021) 12(1):5839. doi: 10.1038/s41467-021-26137-7

47. Snyman J, Hwa SH, Krause R, Muema D, Reddy T, Ganga Y, et al. Similar antibody responses against severe acute respiratory syndrome coronavirus 2 in individuals living without and with human immunodeficiency virus on antiretroviral therapy during the first South African infection wave. *Clin Infect Dis* (2022) 75(1):e249–e56. doi: 10.1093/cid/ciab758

frontiers | Frontiers in Immunology

TYPE Original Research
PUBLISHED 28 March 2024
DOI 10.3389/fimmu.2024.1343716

OPEN ACCESS

EDITED BY
Pedro A. Reche,
Complutense University of Madrid, Spain

REVIEWED BY
Sarah Elizabeth Jackson,
University of Cambridge, United Kingdom
Ricardo Da Silva Antunes,
La Jolla Institute for Immunology (LJI),
United States

*CORRESPONDENCE
Lbachir BenMohamed
Lbenmoha@uci.edu

†These authors have contributed equally to this work

RECEIVED 24 November 2023
ACCEPTED 08 March 2024
PUBLISHED 28 March 2024

CITATION
Coulon P-G, Prakash S, Dhanushkodi NR, Srivastava R, Zayou L, Tifrea DF, Edwards RA, Figueroa CJ, Schubl SD, Hsieh L, Nesburn AB, Kuppermann BD, Bahraoui E, Vahed H, Gil D, Jones TM, Ulmer JB and BenMohamed L (2024) High frequencies of alpha common cold coronavirus/SARS-CoV-2 cross-reactive functional CD4$^+$ and CD8$^+$ memory T cells are associated with protection from symptomatic and fatal SARS-CoV-2 infections in unvaccinated COVID-19 patients. *Front. Immunol.* 15:1343716. doi: 10.3389/fimmu.2024.1343716

High frequencies of alpha common cold coronavirus/SARS-CoV-2 cross-reactive functional CD4$^+$ and CD8$^+$ memory T cells are associated with protection from symptomatic and fatal SARS-CoV-2 infections in unvaccinated COVID-19 patients

Pierre-Gregoire Coulon[1†], Swayam Prakash[1†], Nisha R. Dhanushkodi[1], Ruchi Srivastava[1], Latifa Zayou[1], Delia F. Tifrea[2], Robert A. Edwards[2], Cesar J. Figueroa[3], Sebastian D. Schubl[3], Lanny Hsieh[4], Anthony B. Nesburn[1], Baruch D. Kuppermann[1], Elmostafa Bahraoui[5], Hawa Vahed[6], Daniel Gil[6], Trevor M. Jones[6], Jeffrey B. Ulmer[6] and Lbachir BenMohamed[1,5,6,7*]

[1]Laboratory of Cellular and Molecular Immunology, Gavin Herbert Eye Institute, University of California Irvine, School of Medicine, Irvine, CA, United States, [2]Department of Pathology and Laboratory Medicine, School of Medicine, University of California Irvine, Irvine, CA, United States, [3]Department of Surgery, Divisions of Trauma, Burns and Critical Care, School of Medicine, University of California Irvine, Irvine, CA, United States, [4]Department of Medicine, Division of Infectious Diseases and Hospitalist Program, School of Medicine, University of California Irvine, Irvine, CA, United States, [5]Université Paul Sabatier, Infinity, Inserm, Toulouse, France, [6]Department of Vaccines and Immunotherapies, TechImmune, LLC, University Lab Partners, Irvine, CA, United States, [7]Institute for Immunology, The University of California Irvine, School of Medicine, Irvine, CA, United States

Background: Cross-reactive SARS-CoV-2-specific memory CD4$^+$ and CD8$^+$ T cells are present in up to 50% of unexposed, pre-pandemic, healthy individuals (UPPHIs). However, the characteristics of cross-reactive memory CD4$^+$ and CD8$^+$ T cells associated with subsequent protection of asymptomatic coronavirus disease 2019 (COVID-19) patients (i.e., unvaccinated individuals who never develop any COVID-19 symptoms despite being infected with SARS-CoV-2) remains to be fully elucidated.

Methods: This study compares the antigen specificity, frequency, phenotype, and function of cross-reactive memory CD4$^+$ and CD8$^+$ T cells between common cold coronaviruses (CCCs) and SARS-CoV-2. T-cell responses against genome-wide conserved epitopes were studied early in the disease course in a cohort of 147 unvaccinated COVID-19 patients who were divided into six groups based on the severity of their symptoms.

Results: Compared to severely ill COVID-19 patients and patients with fatal COVID-19 outcomes, the asymptomatic COVID-19 patients displayed

10.3389/fimmu.2024.1343716

significantly: (i) higher rates of co-infection with the 229E alpha species of CCCs (α-CCC-229E); (ii) higher frequencies of cross-reactive functional $CD134^+CD137^+CD4^+$ and $CD134^+CD137^+CD8^+$ T cells that cross-recognized conserved epitopes from α-CCCs and SARS-CoV-2 structural, non-structural, and accessory proteins; and (iii) lower frequencies of CCCs/SARS-CoV-2 cross-reactive exhausted $PD\text{-}1^+TIM3^+TIGIT^+CTLA4^+CD4^+$ and $PD\text{-}1^+TIM3^+TIGIT^+CTLA4^+CD8^+$ T cells, detected both *ex vivo* and *in vitro*.

Conclusions: These findings (i) support a crucial role of functional, poly-antigenic α-CCCs/SARS-CoV-2 cross-reactive memory $CD4^+$ and $CD8^+$ T cells, induced following previous CCCs seasonal exposures, in protection against subsequent severe COVID-19 disease and (ii) provide critical insights into developing broadly protective, multi-antigen, $CD4^+$, and $CD8^+$ T-cell-based, universal pan-Coronavirus vaccines capable of conferring cross-species protection.

KEYWORDS

SARS-CoV-2, symptomatic, asymptomatic, COVID-19, common cold coronavirus, CD4 + T cells, CD8 + T cells, exhaustion α-CCCs/SARS-CoV-2 cross-reactive T cells in asymptomatic COVID-19 infection

Introduction

The coronavirus disease 2019 (COVID-19) pandemic has created one of the largest global health crises in nearly a century (1–3). As of February 2024, the COVID-19 outbreak has affected over 700 million people worldwide, with the number of deaths directly related to severe symptomatic COVID-19 infections reaching 7 million worldwide (1, 2, 4). Some unvaccinated symptomatic COVID-19 patients produce severe symptoms that typically begin with mild upper respiratory syndrome but may further develop into severe respiratory distress and death, particularly in immunocompromised individuals and those with pre-existing co-morbidities (5–8). In contrast, other unvaccinated individuals never develop any COVID-19 symptoms despite being infected with SARS-CoV-2 (5, 9, 10). The underlying mechanisms that lead to protection from symptomatic and fatal SARS-CoV-2 infection in unvaccinated COVID-19 patients remain to be fully elucidated.

There is a growing body of evidence in support of the important role that T-cell responses in protection against COVID-19, as recently reviewed by Wherry and Barouch (11): (i) cross-reactive poly-antigenic $CD4^+$ and $CD8^+$ T-cell responses in COVID-19 patients appear to contribute to the resolution of SARS-CoV-2 infection and reduction in severe symptoms (12–22); (ii) SARS-CoV-2-specific $CD4^+$ and $CD8^+$ T-cell responses reduced viral loads in non-human primates (23, 24); (iii) SARS-CoV-2-infected patients with agammaglobulinemia and B-cell depletion displayed only a small increase in COVID-19 symptoms, indicating that the cross-reactive T cells alone may have protected from severe disease (25–30); and (iv) cancer patients with B-cell deficiencies experience milder COVID-19 disease that correlated with strong SARS-CoV-2-specific $CD8^+$ T-cell responses (22). Conversely, other reports have associated cross-reactive memory $CD4^+$ and $CD8^+$ T cells with poor COVID-19 disease outcomes (16, 31–36). However, the antigen specificity, frequency, phenotype, and function of cross-reactive memory $CD4^+$ and $CD8^+$ T cells that protect against the severity of COVID-19 in unvaccinated asymptomatic patients remain to be determined.

Characterizing the CCCs/SARS-CoV-2 cross-reactive memory $CD4^+$ and $CD8^+$ T cells in unvaccinated COVID-19 patients is a difficult task today because over 85% of adults are currently vaccinated (37–40). Nevertheless, a few studies from our group and others have detected cross-reactive $CD4^+$ and $CD8^+$ T cells, directed toward specific sets of conserved SARS-CoV-2 epitopes, not only from unvaccinated COVID-19 patients but also from a significant proportion (~50%) of unexposed pre-pandemic healthy individuals (UPPHI) who were never exposed to SARS-CoV-2 (1, 16, 18, 20–22, 32, 33, 41–44). Moreover, pre-existing CCCs/SARS-CoV-2 cross-reactive memory $CD4^+$ and $CD8^+$ T cells are also present in unvaccinated UPPHI, suggesting clones of memory T cells induced following previous exposures with seasonal CCCs (1, 16, 21, 31, 41, 43–50). However, it is not yet known whether these cross-reactive memory $CD4^+$ and $CD8^+$ T cells (i) preferentially cross-recognize the alpha CCCs (i.e., α-CCC-229E and α-CCC-NL63) or the beta CCCs (i.e., β-CCC-HKU1 and β-CCC-OC43) and (ii) the antigen specificity, frequency, phenotype, and function of the cross-reactive memory $CD4^+$ and $CD8^+$ T cells associated with protection against COVID-19 severity in unvaccinated asymptomatic patients.

In this study, we hypothesized that different clonal repertoire of CCCs/SARS-CoV-2 cross-reactive memory $CD4^+$ and $CD8^+$ T cells are induced by previous exposures to seasonal alpha CCCs (i.e., α-CCC-229E and α-CCC-NL63) and beta CCCs (i.e., β-CCC-HKU1 and β-CCC-OC43) and that certain clones of T cells are associated with either protective or pathogenic outcomes in SARS-CoV-2 infection. We report that, compared with unvaccinated severely ill COVID-19 patients and unvaccinated patients with fatal COVID-19 outcomes, unvaccinated asymptomatic COVID-19 patients displayed significantly (i) higher rate of the α-CCC species 229E (α-CCC-229E); (ii) higher frequencies of functional memory $CD134^+CD137^+CD4^+$ and $CD134^+CD137^+CD8^+$ T cells directed toward cross-reactive α-CCCs/SARS-CoV-2 epitopes from structural, non-structural, and accessory proteins; and (iii) lower frequencies of cross-reactive exhausted $PD\text{-}1^+TIM3^+TIGIT^+CTLA4^+CD4^+$ and $PD\text{-}1^+TIM3^+TIGIT^+CTLA4^+CD8^+$ T cells. These findings (i) support the crucial role of functional, poly-antigenic α-CCCs/SARS-CoV-2 cross-reactive memory $CD4^+$ and $CD8^+$ T cells, induced following previous exposures to α-CCC species, in protection against subsequent severe disease caused by SARS-CoV-2 infection and (ii) provides a strong rationale for the development of broadly protective, T-cell-based, multi-antigen universal pan-Coronavirus vaccines.

Materials and methods

Human study population cohort and HLA genotyping

Between July 2020 to November 2022, 600 patients were enrolled at the University of California Irvine Medical Center with various severity of COVID-19 disease under an approved Institutional Review Board–approved protocol (IRB No. 2020-5779). Written informed consent was obtained from participants before inclusion. SARS-CoV-2 positivity was defined by a positive RT-PCR on a respiratory tract sample. None of the patients enrolled in this study received any COVID-19 vaccine.

Patient selection based on HLA-A*02:01 and HLA-DRB1*01:01 alleles

We genotyped all the 600 patients enrolled in our study for class I HLA-A*02:01 and class II HLA-DRB1*01:01 by PCR. Out of the 600 COVID-19 patients, 147 patients were positive for HLA-A*02:01 and/or HLA-DRB1*01:01 and were considered in this study (Supplementary Figure 1). The 147 patients were from mixed

TABLE 1 Demographic, age, HLA-genotyping, clinical parameters, and prevalence of comorbidities in unvaccinated COVID-19 patients with various degrees of disease severity.

	Patients' characteristics classified by severity of COVID-19 (n=147)	Severity 5 (SYMP) patients died) (*n* = 26)	Severity 4 (SYMP) (ICU + vent.) (*n* = 15)	Severity 3 (SYMP) (ICU) (n = 21)	Severity 2 (SYMP) (inpatients, Reg. Adm.) (n = 64)	Severity 1 (SYMP) (ED) (n = 12)	Severity 0 (ASYMP) (n = 9)
Demographic features	**Age median**	65 (39–90)	52 (33–85)	53 (26–86)	57 (23–85)	51 (27–91)	27 (19–51)
	Gender (male/female)	19/7 (73%/27%)	9/6 (60%/40%)	13/8 (62%/38%)	37/27 (58%/42%)	5/7 (42%/58%)	5/4 (56%/44%)
Class I & II HLA status	**Race (% White/ non-White)**	6/20 (23%/77%)	8/7 (53%/47%)	13/8 (62%/38%)	25/39 (39%/61%)	7/5 (58%/42%)	2/7 (29%/71%)
	HLA-A*0201$^+$	13 (50%)	8 (53%)	12 (57%)	24 (38%)	7 (58%)	7 (78%)
Clinical parameters	**HLA-DRB1*01:01$^+$**	14 (54%)	11 (73%)	12 (57%)	41 (64%)	7 (58%)	7 (78%)
	Days between onset of symptoms and blood draw (mean)	5.9	5.7	4.6	4.5	4.1	–
	Fever (>38°C)	21 (81%)	11 (73%)	10 (48%)	30 (47%)	4 (33%)	0 (0%)
	Cough	23 (88%)	13 (87%)	16 (76%)	22 (34%)	4 (33%)	0 (0%)
	Shortness of breath/dyspnea	28 (100%)	15 (100%)	6 (29%)	11 (17%)	1 (8%)	0 (0%)
	Fatigue/myalgia	9 (35%)	5 (33%)	6 (29%)	3 (5%)	3 (25%)	0 (0%)
	Headache	5 (19%)	1 (%)	4 (19%)	12 (19%)	4 (33%)	0 (0%)
	Nausea	3 (12%)	3 (20%)	3 (14%)	3 (5%)	0 (0%)	0 (0%)
	Diarrhea	7 (27%)	2 (13%)	2 (10%)	8 (13%)	0 (0%)	0 (0%)

(Continued)

TABLE 1 Continued

	Patients' characteristics classified by severity of COVID-19 (n=147)	Severity 5 (SYMP) patients died) (*n* = 26)	Severity 4 (SYMP) (ICU + vent.) (*n* = 15)	Severity 3 (SYMP) (ICU) (n = 21)	Severity 2 (SYMP) (inpatients, Reg. Adm.) (n = 64)	Severity 1 (SYMP) (ED) (n = 12)	Severity 0 (ASYMP) (n = 9)
	Anosmia/ageusia	6 (23%)	4 (27%)	6 (29%)	17 (27%)	1 (8%)	0 (0%)
	Sore throat	4 (15%)	1 (7%)	1 (5%)	3 (5%)	1 (8%)	0 (0%)
	ICU admission	26 (100%)	15 (100%)	21 (100%)	0 (0%)	0 (0%)	0 (0%)
	Ventilator support	26 (100%)	15 (100%)	0 (0%)	0 (0%)	0 (0%)	0 (0%)
	White blood cells (count: 10^3 cells/μL of blood) (average)	14.3	10.8	10.1	8.4	6.2	8.0
Comorbidities	Lymphocytes (10^3 cells/μL of blood and %) (average)	0.7 (6%)	0.9 (10%)	1.0 (13%)	1.4 (16%)	1.6 (27%)	2.4 (29.3%)
	Average number of all comorbidities	3.5	2.9	2.8	1.9	1.6	0.7
	Diabetes	14 (54%)	9 (60%)	13 (62%)	29 (45%)	4 (33%)	0 (0%)
	Hypertension (HTN)	16 (62%)	6 (40%)	9 (43%)	18 (28%)	4 (33%)	1 (11%)
	Cardiovascular disease (CVD)	17 (65%)	6 (40%)	6 (29%)	13 (20%)	3 (25%)	0 (0%)
	Coronary artery disease (CAD)	12 (46%)	5 (33%)	7 (33%)	12 (19%)	2 (17%)	0 (0%)
	Kidney diseases (CKD/ESRD)	7 (27%)	4 (27%)	6 (29%)	7 (11%)	1 (8%)	0 (0%)
	Asthma/COPD	9 (35%)	1 (7%)	3 (14%)	12 (19%)	0 (0%)	1 (11%)
	Obesity	12 (46%)	12 (80%)	7 (33%)	29 (45%)	4 (33%)	4 (44%)
	Cancer	4(15%)	0(0%)	2(10%)	6(9%)	1(8%)	0 (0%)

Unvaccinated patients (n = 147) were scored on a scale of 0–5 based on the severity of COVID-19 symptoms, regular hospital admission, intensive care unit (ICU) admission and death (severity score). Severity scores 0: asymptomatic patients who had no symptoms despite being tested positive for SARS-CoV-2 (ASYMP). Patients who were SARS-CoV-2 infected and developed symptoms (SYMP) were divided into four categories. Severity 1: patients who were screened at the hospital for COVID-19 but did not stay for regular admission. Severity 2: patients who were screened at the hospital for COVID-19 and went to non-ICU regular admission to treat their symptoms. Severity 3: patients who went to intensive ICU. Severity 4: patients who went to ICU with life support (i.e., mechanical ventilation at any point during their stay). Severity 5: patients who died from direct COVID-19 complications. The parameters displayed in the table (demographic features, HLA genotyping, clinical parameters, and prevalence of comorbidities) represent the number and percentages of patients within each disease severity. For the age parameter, median values are shown for each disease severity along with ranges (between brackets). The time between the onset of symptoms and the blood draw is shown as day-average numbers. The total number of comorbidities is the average of the sum of each patient's comorbidities.

ethnicities (Hispanic (28%), Hispanic Latino (22%), Asian (16%), Caucasian (13%), mixed Afro-American and Hispanic (8%), Afro-American (5%), mixed Afro-American and Caucasian (2%), and Native Hawaiian and Other Pacific Islander descent (1%). Six percent of the patients did not reveal their race/ethnicity. The detailed demographic and clinical data for the 147 patients enrolled in this study are shown in Table 1.

Symptomatic and asymptomatic COVID-19 patient stratification based on disease severity

Following patient discharge, they were divided into six groups depending on the severity of their symptoms and their intensive care unit (ICU) and intubation (mechanical ventilation) status by medical practitioners. The scoring criteria were as follows: severity 5, patients who died from COVID-19 complications; severity 4, infected COVID-19 patients with severe disease who were admitted to the intensive care unit (ICU) and required ventilation support; severity 3, infected COVID-19 patients with severe disease that required enrollment in ICU, but without ventilation support; severity 2, infected COVID-19 patients with moderate symptoms that involved a regular hospital admission; severity 1, infected COVID-19 patients with mild symptoms; and severity 0, infected individuals with no symptoms. Among the 147 COVID-19 patients, subjects with a severity score of 0 were defined as asymptomatic, and subjects with a severity score of 1–5 were defined as symptomatic.

Pre-pandemic healthy controls

Subsequently, we used 15 liquid-nitrogen frozen PBMCs samples (blood collected pre-COVID-19 in 2018) from HLA-

A*02:01$^+$/HLA-DRB1*01:01$^+$ unexposed pre-pandemic healthy individuals (UPPHI, 8 men, 7 women; median age, 54 (20–76)] as controls to measure recalled SARS-CoV-2 cross-reactive T-cell responses. The class-II HLA status of each patient was first screened for HLA-DRB1*01:01 by PCR (Supplementary Figure 1A) (51). For class-I HLA, the screening was first performed (two-digit level) by HLA-A*02 flow cytometry staining (data not shown, mAbs clone BB7.2, BioLegend, San Diego, CA). The four-digit class-I HLA-A*02:01 subtype was subsequently screened by PCR (Supplementary Figure 1B) on blood samples (52).

T-cell epitopes screening, selection, and peptide synthesis

CCCs/SARS-CoV-2 cross-reactive peptide epitopes from 12 SARS-CoV-2 proteins, including 27 9-mer long CD8$^+$ T-cell epitopes ($ORF1ab_{84-92}$, $ORF1ab_{1675-1683}$, $ORF1ab_{2210-2218}$, $ORF1ab_{2363-2371}$, $ORF1ab_{3013-3021}$, $ORF1ab_{3183-3191}$, $ORF1ab_{3732-3740}$, $ORF1ab_{4283-4291}$, $ORF1ab_{5470-5478}$, $ORF1ab_{6419-6427}$, $ORF1ab_{6749-6757}$, S_{2-10}, $S_{691-699}$, $S_{958-966}$, $S_{976-984}$, $S_{1000-1008}$, $S_{1220-1228}$, E_{20-28}, E_{26-34}, M_{52-60}, M_{89-97}, $ORF6_{3-11}$, $ORF7b_{26-34}$, $ORF8a_{31-39}$, $ORF8a_{73-81}$, $ORF10_{3-11}$, and $ORF10_{5-13}$) and 16 13-mer long CD4$^+$ T-cell epitopes ($ORF1a_{1350-1365}$, $ORF1a_{1801-1815}$, $ORF1ab_{5019-5033}$, $ORF1ab_{6088-6102}$, $ORF1ab_{6420-6434}$, S_{1-13}, E_{20-34}, E_{26-40}, $M_{176-190}$, $ORF6_{12-26}$, $ORF7a_{1-15}$, $ORF7a_{3-17}$, $ORF7a_{98-112}$, $ORF7b_{8-22}$, $ORF8b_{1-15}$, and $N_{388-403}$) that we formerly identified were selected as we previously described (1) (Table 2 and Supplementary Table 1). We used the Epitope Conservancy Analysis tool to compute the degree of identity of CD8$^+$ and CD4$^+$ T-cell epitopes within a given protein sequence of SARS-CoV-2 set at 100% identity level (1) (Table 2 and Supplementary Tables 1, 2). Peptides were synthesized (21st Century Biochemicals, Inc., Marlborough, MA), and the purity of peptides determined by both reversed-phase high-performance liquid chromatography and mass spectroscopy was over 95%.

Blood differential test

Total white blood cell (WBC) count and lymphocyte count per microliter of blood were performed by the clinicians at the University of California Irvine Medical Center, using a CellaVision™ DM96 automated microscope. Monolayer smears were prepared from anticoagulated blood and stained using the May Grunwald Giemsa (MGG) technique. Subsequently, slides were loaded onto the DM96 magazines and scanned using a ×10 objective focused on nucleated cells to record their exact position. Images were obtained using the ×100 oil objective and analyzed by artificial neural network (ANN).

Peripheral blood mononuclear cells isolation and T-cell stimulation

Peripheral blood mononuclear cells (PBMCs) from COVID-19 patients were isolated from the blood using Ficoll (GE Healthcare) density gradient media and transferred into 96-well plates at a concentration of 2.5 × 10^6 viable cells per ml in 200 µl (0.5 × 10^6 cells per well) of RPMI-1640 media (Hyclone) supplemented with 10% (v/v) FBS (HyClone), sodium pyruvate (Lonza), L-glutamine, nonessential amino acids, and antibiotics (Corning). A fraction of the blood was kept separated to perform HLA genotyping of the patients and select only the HLA-A*02:01 and/or DRB1*01:01 positive individuals (Supplementary Figure 1). Fresh peripheral blood mononuclear cells (PBMCs) were used in this study, as they generally have higher viability and functionality compared to frozen PBMCs. Freezing and thawing can lead to cell damage and loss of T-cell functionality, which may affect the accuracy and reliability of experimental results. Frozen PBMCs may exhibit altered activation status compared to fresh cells. Cryopreservation can induce stress responses in cells, leading to changes in their activation state and potentially affecting immune response assays. In the context of COVID-19 research, where precise characterization of immune responses is crucial for understanding disease pathogenesis, vaccine development, and treatment strategies, using fresh PBMCs ensures the accuracy and reliability of experimental results. A side-by-side comparison of frozen and fresh PBMCs and pre-pandemic healthy control PBMCs yielded no significant difference. PBMCs were stimulated with 10 µg/ml of each one of the 43 individual CCCs/SARS-CoV-2 cross-reactive peptide epitopes (27 CD8$^+$ T-cell peptides and 16 CD4$^+$ T-cell peptides) and incubated in a humidified chamber with 5% CO_2 at 37°C (Supplementary Figure 2A). Post-incubation, cells were stained by flow cytometry analysis or transferred onto IFN-γ ELISpot plates. The same isolation protocol was followed for HD samples obtained in 2018. Ficoll was kept frozen in liquid nitrogen in FBS DMSO 10%; after thawing, HD PBMCs were stimulated similarly for the IFN-γ ELISpot technique.

ELISpot assay

COVID-19 patients were first screened for their HLA status (DRB1*01:01$^+$ positive = 92 out of 600 tested, HLA-A*02:01$^+$ positive = 71, DRB1*01:01$^+$ and HLA-A*02:01$^+$ positive = 16) (Supplementary Figure 1). The 92 DRB1*01:01 positive individuals were then used to assess the CD4$^+$ T-cell response against CCCs/SARS-CoV-2 cross-reactive class-II restricted epitopes by IFN-γ ELISpot (Supplementary Figure 2). Similarly, we assessed the CD8$^+$ T-cell response against our CCCs/SARS-CoV-2 cross-reactive class-I restricted epitopes in the 71 HLA-A*02:01 positive individuals representing different disease severity categories (Table 1).

All ELISpot reagents were filtered through a 0.22-µm filter. Wells of 96-well Multiscreen HTS Plates (Millipore, Billerica, MA) were pre-wet with 30% ethanol for 60 s and then coated with 100 µl primary anti-IFN-γ antibody solution (10 µg/ml of 1-D1K coating antibody from Mabtech, Cincinnati, OH) OVN at 4°C. After washing, the plate was blocked with 200 µl of RPMI media plus 10% (v/v) FBS for 2 h at room temperature to prevent nonspecific binding. After 24 h, following the blockade, the peptide-stimulated cells from the patient's PBMCs (0.5 × 10^6 cells/well) were

TABLE 2 Percentages of identity and similarity scores (S^s) between CCCs/SARS-CoV-2 cross-reactive $CD4^+$ and $CD8^+$ T cell epitopes.

	Peptide-epitope name/ position	SARS-CoV-2 corresponding protein	SARS-CoV-2 peptide-epitope sequence	Correlation coefficient (R)*	Slope (S)*	Significance (i.e., $p<0.05$)? Y/N	Average IFNγ-SPOTs in HD (measure of observed T-cell cross-reactive response in HD individuals)
CD4+ specific SARS-CoV-2 peptides (class-II HLA-DRB1*01:01 restricted epitopes)	$ORF1a_{1350-1365}$	Non-structural protein NSP3	KSAFYILPSIISNEK	−0.9418	−35.91	Y	52.5
	$ORF1a_{1801-1815}$	Non-structural protein NSP3	ESPFVMMSAPPAQYE	−0.9480	−28.04	Y	20.5
	$ORF1ab_{5019-5033}$	RdRP polymerase NSP12	PNMLRIMASLVLARK	−0.4115	−4.24	N	7.1
	$ORF1ab_{6088-6102}$	Non-structural protein NSP14	RIKIVQMLSDTLKNL	−0.9581	−23.49	Y	10.6
	$ORF1ab_{6420-6434}$	Non-structural protein NSP14	LDAYNMMISAGFSLW	−0.8711	−18.78	Y	3.1
	S_{1-13}	Spike structural protein (Signal peptide)	MFVFLVLLPLVSS	−0.9262	−34.31	Y	39.1
	E_{20-34}	Envelope structural protein	FLAFVVFLLVTLAIL	−0.8348	−18.83	Y	3.6
	E_{26-40}	Envelope structural protein	FLLVTLAILTALRLC	−0.9172	−25.61	Y	12.6
	$M_{176-190}$	Membrane structural protein	LSYYKLGASQRVAGD	−0.9421	−41.26	Y	40.7
	$ORF6_{12-26}$	ORF6 accessory protein	AEILLIIMRTFKVSI	−0.9378	−31.67	Y	41.0
	$ORF7a_{1-15}$	ORF7a accessory protein	MKIILFLALITLATC	−0.9390	−17.96	Y	5.1
	$ORF7a_{3-17}$	ORF7a accessory protein	IILFLALITLATCEL	−0.8915	−17.76	Y	2.8
	$ORF7a_{98-112}$	ORF7a accessory protein	SPIFLIVAAIVFITL	−0.6833	−9.343	N	1.8
	$ORF7b_{8-22}$	ORF7b accessory protein	DFYLCFLAFLLFLVL	−0.8715	−21.66	Y	3.2
	$ORF8b_{1-15}$	ORF8 accessory protein	MKFLVFLGIITTVAA	−0.9191	−29.04	Y	32.4
	$N_{388-403}$	Nucleocapsid structural protein	KQQTVTLLPAADLDDF	−0.8905	−32.13	Y	23.4
CD8+ specific SARS-CoV-2 peptides (class-I HLA-A*02:01 restricted epitopes)	$ORF1ab_{84-92}$	Non-structural protein NSP1	VMVELVAEL	−0.8984	−20.28	Y	1.5
	$ORF1ab_{1675-1683}$	Non-structural protein NSP3	YLATALLTL	−0.9469	−38.91	Y	54.6
	$ORF1ab_{2210-2218}$	Non-structural protein NSP3	CLEASFNYL	−0.7327	−9.93	N	0.7
	$ORF1ab_{2363-2371}$	Non-structural protein NSP3	WLMWLIINL	−0.8962	−14.36	Y	9.9
	$ORF1ab_{3013-3021}$	Non-structural protein NSP4	SLPGVFCGV	−0.5539	−3.89	N	20.4
			FLLNKEMYL	−0.8314	−18.60	Y	15.5

(Continued)

TABLE 2 Continued

	Peptide-epitope name/ position	SARS-CoV-2 corresponding protein	SARS-CoV-2 peptide-epitope sequence	Correlation coefficient (R)*	Slope (S)*	Significance (i.e., $p<0.05$)? Y/N	Average IFNγ-SPOTs in HD (measure of observed T-cell cross-reactive response in HD individuals)
	ORF1ab$_{3783-3790}$	**Non-structural protein NSP6**	SMWALIISV	−0.8909	−19.89	Y	41.0
	ORF1ab$_{4283-4291}$	Non-structural protein NSP10	YLASGGQPI	−0.9269	−30.27	Y	50.2
	ORF1ab$_{5470-5478}$	Non-structural protein NSP13	KLSYGIATV	−0.4496	−7.852	N	55.2
	ORF1ab$_{6419-6427}$	Non-structural protein NSP14	YLDAYNMMI	−0.9026	−25.27	Y	45.7
	ORF1ab$_{6749-6757}$	Non-structural protein NSP15	LLLDDFVEI	−0.9460	−35.39	Y	55.5
	S$_{2-10}$	Spike structural protein (Signal peptide)	FVFLVLLPL	−0.9541	−32.27	Y	43.9
	S$_{691-699}$	Spike structural protein (S1/ S2 cleavage)	SIIAYTMSL	−0.7151	−13.90	N	17.7
	S$_{958-966}$	Spike structural protein (S2: between HR1 and HR2)	ALNTLVKQL	−0.9425	−34.44	Y	40.2
	S$_{976-984}$	Spike structural protein (S2: between HR1 and HR2)	VLNDILSRL	−0.6020	−24.77	N	62.8
	S$_{1000-1008}$	Spike structural protein (S2: between HR1 and HR2)	RLQSLQTYV	−0.9408	−34.98	Y	51.0
	S$_{1220-1228}$	Spike structural protein (CT: cytoplasmic domain)	FIAGLIAIV	−0.9488	−52.81	Y	72.1
	E$_{20-28}$	Envelope structural protein	FLAFVVFLL	−0.8656	−17.72	Y	21.5
	E$_{26-34}$	Envelope structural protein	FLLVTLAIL	−0.9408	−31.78	Y	32.1
	M$_{52-60}$	Membrane structural protein	IFLWLLWPV	−0.9083	−27.55	Y	31.1
	M$_{89-97}$	Membrane structural protein	GLMWLSYFI	−0.9141	−22.70	Y	23.6
	ORF6$_{3-11}$	ORF6 accessory protein	HLVDFQVTI	−0.8881	−18.77	Y	21.9
	ORF7b$_{26-34}$	ORF7b accessory protein	IIFWFSLEL	−0.8960	−18.32	Y	11.9
	ORF8a$_{31-39}$	ORF8 accessory protein	YVVDDPCPI	−0.8756	−16.70	Y	18.6
	ORF8a$_{73-81}$	ORF8 accessory protein	YIDIGNYTV	−0.8775	−15.67	Y	17.1
	ORF10$_{3-11}$		YINVFAFPF	−0.9539	−38.33	Y	44.6

(Continued)

TABLE 2 Continued

	Peptide-epitope name/ position	SARS-CoV-2 corresponding protein	SARS-CoV-2 peptide-epitope sequence	Correlation coefficient (R)*	Slope (S)*	Significance (i.e., $p<0.05$)? Y/N	Average IFNγ-SPOTs in HD (measure of observed T-cell cross-reactive response in HD individuals)
		ORF10 accessory protein					
	$ORF10_{5-13}$	ORF10 accessory protein	NVFAFPFTI	−0.9477	−25.64	Y	41.5

*To assess (for each individual SARS-CoV-2 epitope) the magnitude of the correlation between the breadth of this epitope-specific T-cell response and the protection against severe COVID-19

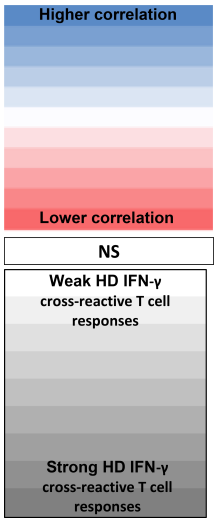

Matching CCCs peptides were chosen after combining both MSA and ECT analysis (see Materials and methods). Each panel represents the alignment of epitopes from SARS-CoV-2 and the four main and seasonal α and β species of common cold coronavirus (CCCs) (i.e., α-CCC-NL63, α-CCC-229E, β-CCC-HKU1, and β-CCC-OC43). The SARS-CoV-2 peptide sequence is set as 100% identity. The amino acids color code was generated with Gecos software (https://gecos.biotite-python.org) using the following parameters: geckos –matrix BLOSUM62 –min 60 –max 75 –f. The distance between two amino acids in the substitution matrix (BLOSUM62) corresponds to the perceptual visual differences in the color scheme. Similarity scores (S^S) based on such matrix are a good predictive measure of potential cross-reactivity (along with % of peptide identity). $S^S \geq 0.80$ and %id ≥ 67% are in red. Identity percentages, similarity scores, conservation, and consensus sequences are indicated in each panel. For each SARS-CoV-2 epitope, the significance ($p < 0.05$) of each correlation is also indicated, along with the magnitude of the T-cell cross-reactive response measured by IFN-γ ELISpots in HD individuals.

transferred into the ELISpot-coated plates. PHA-stimulated or non-stimulated cells (DMSO) were used as positive or negative controls of T-cell activation, respectively. Upon incubation in a humidified chamber with 5% CO_2 at 37°C for an additional 48 h, cells were next washed using PBS and PBS-Tween 0.02% solution. Next, 100 µl of biotinylated secondary anti-IFN-γ antibody (1 µg/ml, clone 7-B6-1, Mabtech) in blocking buffer (PBS 0.5% FBS) was added to each well. Following a 2-h incubation followed by washing, wells were incubated with 100 µl of HRP-conjugated streptavidin (1:1,000) for 1 h at room temperature. Lastly, wells were incubated for 15–30 min with 100 µl of TMB detection reagent at room temperature, and spots were counted both manually and by an automated ELISpot reader counter (ImmunoSpot Reader, Cellular Technology, Shaker Heights, OH).

Flow cytometry analysis

Surface markers detection and flow cytometry analysis were performed on 147 patients after 72 h of stimulation with each CCCs/SARS-CoV-2 cross-reactive class-I or class-II restricted peptide; PBMCs (0.5×10^6 cells) were stained (Supplementary Figure 2). First, the cells were stained with a live/dead fixable dye (Zombie Red dye, 1/800 dilution—BioLegend, San Diego, CA) for 20 min at room temperature, to exclude dying/apoptotic cells. Subsequently, cells were stained for 45 min at room temperature with five different HLA-A*02*01 restricted tetramers and/or five HLA-DRB1*01:01 restricted tetramers (PE labeled) specific toward the CCCs/SARS-CoV-2 cross-reactive $CD8^+$ T-cell epitopes $Orf1ab_{2210-2218}$, $Orf1ab_{4283-4291}$, $S_{976-984}$, $S_{1220-1228}$, and $ORF10_{3-11}$ and toward the CCCs/SARS-CoV-2 cross-reactive $CD4^+$ T-cell epitopes $ORF1a_{1350-1365}$, S_{1-13}, E_{26-40}, $M_{176-190}$, and $ORF6_{12-26}$, respectively. Cells were alternatively stained with the EBV BMLF-$1_{280-288}$-specific tetramer for controls (53) (Supplementary Figure 3). We optimized our tetramer staining according to protocol instructions published by Dolton et al. (54). We stained HLA-A*02*01- HLA-DRB1*01:01-negative patients with our 10 tetramers as a negative control aiming to assess tetramers staining specificity. Subsequently, we used anti-human antibodies for surface-marker staining: anti-CD45 (BV785, clone HI30—BioLegend), anti-CD3 (Alexa700, clone OKT3—BioLegend), anti-CD4 (BUV395, clone SK3—BD), anti-CD8 (BV510, clone SK1—

BioLegend), anti-TIGIT (PercP-Cy5.5, clone A15153G—BioLegend), anti-TIM-3 (BV 711, clone F38-2E2—BioLegend), anti-PD1 (PE-Cy7, clone EH12.1—BD), anti-CTLA-4 (APC, clone BNI3—BioLegend), anti-CD137 (APC-Cy-7, clone 4B4-1—BioLegend), and anti-CD134 (BV650, clone ACT35—BD). mAbs against these various cell markers were added to the cells, either *ex vivo* or *in vitro*, in phosphate-buffered saline (PBS) containing 1% FBS and 0.1% sodium azide [fluorescence-activated cell sorter (FACS) buffer] and incubated for 30 min at 4°C. Cells were then washed twice with FACS buffer and fixed with paraformaldehyde 4% (PFA, Affymetrix, Santa Clara, CA). A total of ~200,000 lymphocyte-gated PBMCs (140,000 alive $CD45^+$) were acquired by Fortessa X20 (Becton Dickinson, Mountain View, CA) and analyzed using FlowJo software (TreeStar, Ashland, OR). The gating strategy is detailed in Supplementary Figure 2B.

TaqMan quantitative polymerase reaction assay for the detection of CCC species in UPPHI and in COVID-19 patients

To detect common cold coronavirus co-infection in COVID-19 patients, Taqman PCR assays were performed on a total of 85 patients distributed into each different category of disease severity (9 ASYMP, 6 patients of category 1, 32 patients of category 2, 9 patients of category 3, 15 patients of category 4, and 14 patients of category 5). Nucleic acid was first extracted from each nasopharyngeal swab sample using Purelink Viral RNA/DNA mini kit (Thermo Fisher Scientific, Waltham, MA) according to the manufacturer's instructions. Subsequently, extracted RNA samples were quantified using Qubit and BioAnalyzer. cDNA was synthesized from 10 µL of RNA eluate using random hexamer primers and SuperScript II Reverse Transcriptase (Applied Biosystems, Waltham, MA). The subsequent RT-PCR screening of the enrolled subjects for the four CCCs was performed using specific sets of primers and probes (55).

CCC-229E, CCC-OC43, and CCC-NL63 RT-PCR assays were performed using the following conditions: 50°C for 15 min followed by denaturation at 95°C for 2 min, 40 cycles of PCR performed at 95°C for 8 s, extending and collecting a fluorescence signal at 60°C for 34 s (56). For CCC-HKU1, the amplification conditions were 48°C for 15 min, followed by 40 cycles of 94°C for 15 s and 60°C for 15 s. For each virus, when the Ct-value generated was <35, the specimen was considered positive. When the Ct-value was relatively high ($35 \leq Ct < 40$), the specimen was retested twice and considered positive if the Ct-value of any retest was <35 (57).

Identity and similarity analysis of CCCs/SARS-CoV-2 cross-reactive epitopes

To assess the % identity (%id) of CCCs/SARS-CoV-2 cross-reactive $CD4^+$ and $CD8^+$ T-cell peptide epitopes, we first identified the best matching CCCs peptide across the CCCs proteomes (Table 2). The full CCCs proteomes sequences were obtained from the National Center for Biotechnology Information (NCBI) GenBank [MH940245.1 (CCC-HUK1), MN306053.1 (CCC-OC43), KX179500.1 (CCC-NL63), and MN306046.1 (CCC-229E)]. We processed this in the following three steps. (1) Corresponding CCCs peptides were determined after protein sequence alignments of all four homologous CCCs proteins plus the SARS-CoV-2 related one using various multiple sequences alignments (MSA) algorithms ran in JALVIEW, MEGA11, and M-coffee software's (i.e., ClustalO, Kalign3, and M-coffee—the latter computing alignments by combining a collection of multiple alignments from a library constituted with the following algorithms: T-Coffee, PCMA, MAFFT, ClustalW, Dialigntx, POA, MUSCLE, and Probcons). Furthermore, we confirmed our results with global and local pairwise alignments (Needle and Water algorithms ran in Biopython) performed to confirm the results. In case of obtaining different results with the various algorithms, the epitope sequence with the highest BLOSUM62-sum score compared to the SARS-CoV-2 epitope set as reference was selected (Table 2 and Supplementary Tables 1, 2). We calculated the % of identity and similarity score S^s with its related SARS-CoV-2 epitope, for each of these CCCs peptides (Supplementary Tables 1-3). The peptide similarity score S^s calculation is based on the method reported by Sune Frankild et al. (58) and the BLOSUM62 matrix to calculate a BLOSUM62 sum (using the Bio.SubsMat.MatrixInfo package in Biopython) between a pair of peptides (peptide "x" from SARS-CoV-2 and "y" from one CCC) and compared their similarity. $0 \leq S^s \leq 1$: the closest S^s is to 1, the highest is the potential for T-cell cross-reactivity response toward the related pair of peptides (58). We used a threshold of $S^s \geq 0.8$ to discriminate between highly similar and non-similar peptides. (2) Then, we examined if other parts of each of the CCCs proteome (without restricting our search only to peptides present in CCCs homologous proteins) could contain better matching peptides than the CCCs peptides reported in Supplementary Tables 1-3. First, for each one of our 16 $CD4^+$ and 27 $CD8^+$ SARS-CoV-2 epitopes, we spanned the entire proteome of each CCCs using the Epitope Conservancy Tool (ECT: http://tools.iedb.org/conservancy/—with a conservancy threshold of 20%). All the CCCs peptides from the top query (i.e., with the highest % of identity) were reported for every four CCCs in Supplementary Tables 1-3. Second, among these returned top queries (peptides with the same highest % identity), we picked the one with the highest similarity score S^s (bolded in Supplementary Tables 1-3—right column). (3) We compared this peptide with the one previously found in Supplementary Table 1 based on MSA. When both methods returned the same peptide (from the same protein), we kept it (peptides highlighted in beige in Supplementary Tables 1-3). When both matching peptides (using the two different methods) were found to be different, we compared (i) $\%id_{MSA}$ with $\%id_{ECT}$ and (ii) S^s_{MSA} with S^s_{ECT}. If $\%id_{MSA} \leq \%id_{ECT}$ but $S^s_{MSA} \geq S^s_{ECT}$, we kept the CCCs peptide found following the MSA method; however, if $\%id_{MSA} \leq \%id_{ECT}$ and $S^s_{MSA} < S^s_{ECT}$, we then picked the CCC peptide found using the ECT instead of the one found using MSA (peptides not highlighted in Supplementary Tables 1-3).

Using the %id and the calculated similarity score with the SARS-CoV-2 epitopes, all related CCCs' best-matching peptides are reported in Supplementary Tables 1-3. They were then evaluated based on their potential to induce a cross-reactive T-cell response (Supplementary Tables 1-3): (0), CCC best matching peptide with low to no potential to induce a cross-reactive response toward the corresponding SARS-CoV-2 epitope and *vice versa* (%id with the corresponding SARS-CoV-2 epitope < 67% and similarity score $S^s < 0.8$); (0.5), CCC best matching peptide that may induce a cross-reactive response (%id with the corresponding SARS-CoV-2 epitope ≥ 67% OR similarity score $S^s \geq 0.8$); and (1), CCC best-matching peptide is very likely to induce a cross-reactive response (%id ≥ 67% and $S^s \geq 0.8$).

Identification of potential cross-reactive peptides in non-CCC human pathogens and vaccines

We took advantage of the database generated by Pedro A. Reche (59). Queries to find matching peptides with our SARS-CoV-2-derived $CD4^+$ and $CD8^+$ epitopes were performed from the data gathered; only peptides sharing a %id ≥ 67% with our corresponding SARS-CoV-2 epitope were selected. The corresponding similarity score S^s was calculated.

Statistical analyses

To assess the linear negative relationship between COVID-19 severity and the magnitude of each SARS-CoV-2 epitope-specific T-cell response, correlation analysis using GraphPad Prism version 8 (La Jolla, CA) was performed to calculate Pearson correlation coefficients (R), coefficient of determination (R^2), and associated *p*-value (correlation statistically significant for $p \leq 0.05$). The slope (S) of the best-fitted line (dotted line) was calculated in Prism by linear regression analysis. The same statistical analysis was performed to compare the cross-reactive pre-existing T-cell response in unexposed pre-pandemic healthy individuals (UPPHI) with the slope S (magnitude of the correlation between this epitope-specific T-cell response in SARS-CoV-2-infected patients and the protection against severe COVID-19). Absolute WBCs and lymphocyte cell numbers (per µL of blood, measured through BDT), corresponding lymphocytes percentages/ratio, flow cytometry data measuring $CD3^+/CD8^+/CD4^+$ cell percentages and the percentages detailing the magnitude ($Tetramer^+$ T cell %), and the quality (% of $PD1^+/TIGIT^+$, $CTLA\text{-}4^+/TIM3^+$ or $AIMs^+$ cells) of the $CD4^+$ and $CD8^+$ SARS-CoV-2-specific T cells, were compared across groups and categories of disease severity by one-way ANOVA multiple tests. ELISpot SFCs data were compared by Student's *t*-tests. Data are expressed as the mean ± SD. Results were considered statistically significant at $p \leq 0.05$. To evaluate whether the differences in frequencies of RT-PCR positivity to the four CCCs across categories of disease severity were significant, we used the Chi-squared test or Fisher's exact test.

Results

Higher magnitudes of common cold coronavirus/SARS-CoV-2 cross-reactive $CD4^+$ T-cell responses detected in unvaccinated asymptomatic COVID-19 patients

We first compared SARS-CoV-2-specific $CD4^+$ T-cell responses in unvaccinated asymptomatic COVID-19 patients (those individuals who never develop any COVID-19 symptoms despite being infected with SARS-CoV-2) to unvaccinated symptomatic (those patients who developed severe to fatal COVID-19 symptoms) (Figure 1). We used 16 recently identified HLA-DR-restricted $CD4^+$ T-cell epitopes that are highly conserved between human SARS-CoVs and CCCs (1). We enrolled 92 unvaccinated $HLA\text{-}DRB1^*01:01^+$ COVID-19 patients, who were genotyped using PCR (Supplementary Figure 1) and divided into six groups, based on the level of severity of their COVID-19 symptoms (from severity 5 to severity 0, assessed at discharge). Clinical and demographic characteristics of this cohort of COVID-19 patients are detailed in Table 1. Fresh PBMCs were isolated from these COVID-19 patients, on average within 4.8 days after reporting a first COVID-19 symptom or a first PCR-positive test (Table 1). PBMCs were then stimulated *in vitro* for 72 h using each of the 16 $CD4^+$ T-cell peptide epitopes, as detailed in *Materials and methods* and illustrated in Supplementary Figure 2. The frequency of responding IFN-γ-producing $CD4^+$ T cells specific to individual epitopes was quantified, in each of the six groups of COVID-19 patients, using ELISpot assay (i.e., number of IFN-γ-spot forming $CD4^+$ T cells or "SFCs") (Figure 1). A positive IFN-γ-producing $CD4^+$ T-cell responses was determined as the mean SFCs > 50 per 0.5×10^6 PBMCs fixed as threshold.

Overall, the highest frequencies of CCCs/SARS-CoV-2 cross-reactive epitope-specific IFN-γ-producing $CD4^+$ T cells were detected in the unvaccinated COVID-19 patients with less severe disease (i.e., severity 0, 1, and 2, Figures 1A, B). In contrast, the lowest frequencies of CCCs/SARS-CoV-2 cross-reactive IFN-γ-producing $CD4^+$ T cells were detected in unvaccinated severely ill COVID-19 patients (severity scores 3 and 4) and in unvaccinated COVID-19 patients with fatal outcomes (severity score of 5, Figures 1A, B).

Pearson correlation analysis was performed to determine the linear correlation between the magnitude of $CD4^+$ T-cell responses directed toward each of the 16 highly conserved SARS-CoV-2 epitopes and the severity of COVID-19 symptoms. A negative correlation is usually considered strong when the coefficient R-value is between −0.7 and −1. Except for the $ORF1ab_{5019–5033}$ and $ORF7a_{98–112}$ epitopes, we found that a strong positive linear correlation existed between the high magnitude of IFN-γ-producing $CD4^+$ T-cell responses specific to 14 $CD4^+$ T-cell epitopes and the "natural protection" observed in unvaccinated asymptomatic COVID-19 patients (Figures 1A, C). This positive correlation existed regardless of whether $CD4^+$ T cells cross-recognized structural, non-structural, or accessory SARS-CoV-2 antigens. Cross-reactive IFN-γ-producing $CD4^+$ T-cell responses, specific to $M_{176–190}$, $ORF1a_{1350–1365}$, $S_{1–13}$, $N_{388–403}$, and $ORF6_{12–26}$,

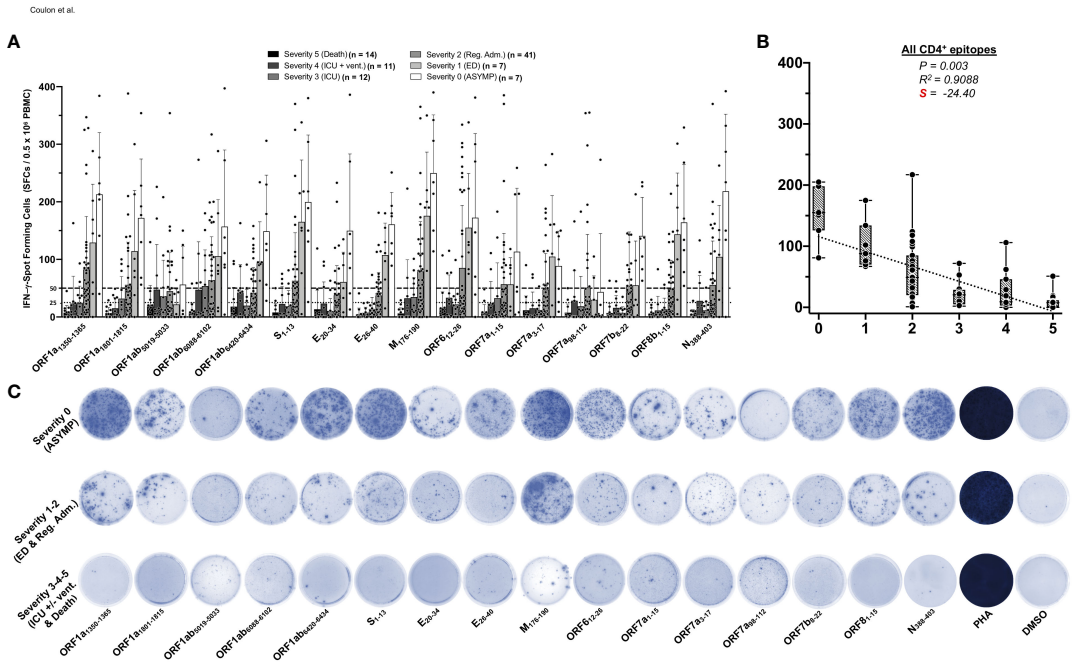

FIGURE 1
IFN-γ-producing CD4$^+$ T-cell responses to CCCs/SARS-CoV-2 cross-reactive epitopes in unvaccinated COVID-19 patients with various degrees of disease severity. PBMCs from HLA-DRB1*01:01-positive COVID-19 patients (n = 92 are HLA-DRB1*01:01-positive out of 600 tested) were isolated and stimulated for a total of 72 h with 10 µg/ml of each of the previously identified 16 CCCs/SARS-CoV-2 cross-reactive CD4$^+$ T cell epitope peptides. The number of IFN-γ-producing CD4$^+$ T cells was quantified in each of the 92 patients using ELISpot assay. **(A)** Average/mean numbers (± SD) of IFN-γ-spot forming cells (SFCs) after CD4$^+$ T-cell peptide-stimulation detected in each of the 92 COVID-19 patients divided into six groups based on disease severity scored 0–5, as described in Materials and methods, and as identified by six columns on a grayscale (black columns = severity 5, to white columns = severity 0) is shown. Dotted lines represent an arbitrary threshold set as a cutoff of the positive response. A mean SFC between 25 and 50 SFCs corresponds to a medium/intermediate response, whereas a strong response is defined for mean SFCs > 50 per 0.5 × 10^6 stimulated PBMCs. **(B)** Correlation between the overall number of IFN-γ-producing CD4$^+$ T cells induced by each of the 16 CCCs/SARS-CoV-2 cross-reactive CD4$^+$ T-cell epitope peptides in each of the six groups of COVID-19 patients with various disease severity. The coefficient of determination (R^2) is calculated from the Pearson correlation coefficients (R). The associated p-value and the slope (S) of the best-fitted line (dotted line) calculated by linear regression analysis are indicated. The gray-hatched boxes in the correlation graphs extend from the 25th to 75th percentiles (hinges of the plots) with the median represented as a horizontal line in each box and the extremity of the vertical bars showing the minimum and maximum values. **(C)** Representative spots images of the IFN-γ-spot forming cells (SFCs) induced by each of the 16 CCCs/SARS-CoV-2 cross-reactive CD4$^+$ T cell epitope peptides in three representative patients, each falling into one of three groups of disease category: the unvaccinated asymptomatic COVID-19 patients (ASYMP, severity score 0), unvaccinated COVID-19 patients who developed mild to moderate disease (severity scores 1 and 2) and unvaccinated severely ill COVID-19 patients and unvaccinated patients with fatal COVID-19 outcomes (severity scores 3–5). PHA was used as a positive control of T-cell activation. Unstimulated negative control SFCs (DMSO—no peptide stimulation) were subtracted from the SFC counts of peptides-stimulated cells. Results are representative of two independent experiments and were considered statistically significant at $p \leq 0.05$.

and to a slightly lesser extent to ORF8b$_{1–15}$ and ORF1a$_{1801–1815}$, were associated with a low COVID-19 severity score (i.e., negatively correlated with an R close to −1) and a very strong negative slope (−41.26 < S < −28.04). Comparatively, the CD4$^+$ T-cell responses against E$_{26–40}$, ORF1ab$_{6088–6102}$, ORF7b$_{8–22}$, E$_{20–34}$, ORF1ab$_{6420–6434}$, ORF7a$_{1–15}$, and ORF7a$_{3–17}$ were also negatively associated with severe disease in patients, but to a lesser degree (relatively less negative slope: −25.61 < S < −17.76) (Figure 1A and Supplementary Figure 4). In contrast, no significant correlation was found between the magnitude of IFN-γ-producing CD4$^+$ T-cell responses directed toward ORF1ab$_{5019–5033}$ and ORF7a$_{98–112}$ epitopes and the disease severity (p > 0.05). For the ORF1ab$_{5019–5033}$ and ORF7a$_{98–112}$ epitopes, the slope was comparatively weak: only slightly negative with S > −10 (Figure 1A and Supplementary Figure 4).

Taken together, these results (i) demonstrate an overall higher magnitude of CCCs/SARS-CoV-2 cross-reactive CD4$^+$ T-cell responses present in unvaccinated asymptomatic COVID-19 patients. In contrast, a lower magnitude of CCCs/SARS-CoV-2 cross-reactive CD4$^+$ T-cell responses were detected in unvaccinated severely ill COVID-19 patients and to patients with fatal COVID-19 outcomes and (ii) suggest a crucial role of CCCs/SARS-CoV-2 cross-reactive CD4$^+$ T cells, directed towards structural, non-structural, and accessory protein antigens, in protection from symptomatic and fatal Infections in unvaccinated COVID-19 patients.

Higher magnitudes of CD8$^+$ T-cell responses to common cold coronavirus/SARS-CoV-2 cross-reactive epitopes detected in unvaccinated asymptomatic COVID-19 patients

We next compared the CCCs/SARS-CoV-2 cross-reactive CD8$^+$ T-cell responses in unvaccinated asymptomatic individuals vs.

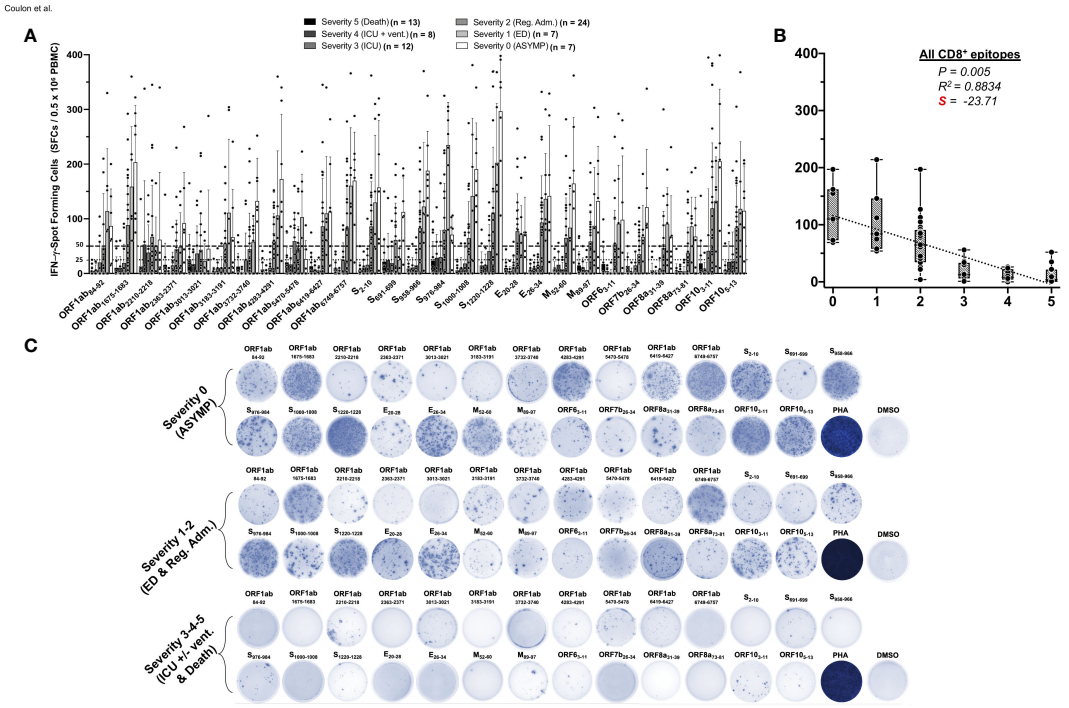

FIGURE 2
IFN-γ-producing CD8$^+$ T-cell responses to CCCs/SARS-CoV-2 cross-reactive epitopes in unvaccinated COVID-19 patients with various degrees of disease severity. PBMCs from HLA-A*02:01-positive COVID-19 patients (n = 71) were isolated and stimulated for a total of 72 h with 10 µg/ml of each of the previously identified 27 CCCs/SARS-CoV-2 cross-reactive CD8$^+$ T-cell epitope peptides. The number of IFN-γ-producing CD8$^+$ T cells was quantified in each of the 71 patients using ELISpot assay. Panel **(A)** shows the average/mean numbers (± SD) of IFN-γ-spot forming cells (SFCs) after CD8$^+$ T-cell peptide stimulation detected in each of the 71 COVID-19 patients divided into six groups based on disease severity scored 0–5, as described in *Materials and methods*, and as identified by six columns on a grayscale (Black columns = severity 5, to white columns = severity 0). Dotted lines represent an arbitrary threshold set as a cutoff of the positive response. A mean SFCs between 25 and 50 SFCs corresponds to a medium/intermediate response, whereas a strong response is defined for mean SFCs > 50 per 0.5 × 10^6 stimulated PBMCs. **(B)** Correlation between the overall number of IFN-γ-producing CD8$^+$ T cells induced by each of the 27 CCCs/SARS-CoV-2 cross-reactive CD8$^+$ T-cell epitope peptides in each of the six groups of COVID-19 patients with various disease severity. The coefficient of determination (R^2) is calculated from the Pearson correlation coefficients (R). The associated p-value and the slope (S) of the best-fitted line (dotted line) calculated by linear regression analysis are indicated. The gray-hatched boxes in the correlation graphs extend from the 25th to 75th percentiles (hinges of the plots) with the median represented as a horizontal line in each box and the extremity of the vertical bars showing the minimum and maximum values. **(C)** Representative spots images of the IFN-γ-spot forming cells (SFCs) induced by each of the 27 CCCs/SARS-CoV-2 cross-reactive CD8$^+$ epitope peptides in three representative patients, each falling into one of three groups of disease category: the unvaccinated asymptomatic COVID-19 patients (ASYMP, severity score 0), unvaccinated COVID-19 patients who developed mild to moderate disease (severity scores 1 and 2), and unvaccinated severely ill COVID-19 patients and unvaccinated patients with fatal COVID-19 outcomes, (severity scores 3–5). PHA was used as a positive control of T-cell activation. Unstimulated negative control SFCs (DMSO—no peptide stimulation) were subtracted from the SFC counts of peptides-stimulated cells. Results are representative of two independent experiments and were considered statistically significant at $p \leq 0.05$.

unvaccinated symptomatic COVID-19 patients (Figure 2). We used 27 recently identified HLA-A*0201-restricted CD8$^+$ T-cell epitopes that are highly conserved between human SARS-CoVs and CCCs (1). We enrolled 71 unvaccinated HLA-A*0201$^+$ COVID-19 patients, who were genotyped using PCR (Supplementary Figure 1) and divided into six groups based on the severity of COVID-19 symptoms (i.e., severity 5 to severity 0, Table 1). Fresh PBMCs were isolated from COVID-19 patients on an average of 4.8 days after reporting initial COVID-19 symptoms or a first PCR-positive test (in the case of asymptomatic). Subsequently, PBMCs were stimulated *in vitro* for 72 h using each of the 27 HLA-A*0201-restricted CD8$^+$ T-cell peptide epitopes (Supplementary Figure 2). The frequency of responding IFN-γ-producing CD8$^+$ T cells specific to individual epitopes was quantified, in each of the six groups of COVID-19 patients, using the ELISpot assay (i.e., number of IFN-γ-spot forming CD8$^+$ T cells or "SFCs") (Figure 2).

Overall, the highest frequencies of CCCs/SARS-CoV-2 cross-reactive epitope-specific functional IFN-γ-producing CD8$^+$ T cells (mean SFCs > 50 per 0.5 × 10^6 PBMCs) were detected in the three groups of unvaccinated COVID-19 patients who presented little to no severe COVID-19 symptoms (i.e., severity 0, 1, and 2, Figures 2A, B). In contrast, significantly lower frequencies of CCCs/SARS-CoV-2 cross-reactive functional IFN-γ-producing CD8$^+$ T cells were detected in the two groups of unvaccinated severely ill symptomatic COVID-19 patients (i.e., severity 3 and 4, mean SFCs < 50) and the unvaccinated COVID-19 patients with fatal outcomes (i.e., severity 5, mean SFCs < 25).

Out of the 27 $CD8^+$ T-cell epitopes, there was a significant positive linear correlation between $CD8^+$ T-cell responses specific to 22 epitopes and little to no severe COVID-19 disease (Figures 2A, B). For these 22 epitopes, the Pearson correlation coefficients (R) ranged from −0.8314 to −0.9541, and slopes (S) of the best-fitted lines comprised between −14.36 and −52.81. For the remaining five epitopes ($ORF1ab_{2210–2218}$, $ORF1ab_{3013–3021}$, $ORF1ab_{5470–5478}$, $S_{691–699}$, and $S_{976–984}$), no significant linear correlation was observed. Nonetheless, among these five epitopes, the slope for $ORF1ab_{2210–2218}$, $ORF1ab_{3013–3021}$, and $ORF1ab_{5470–5478}$ was comparatively less negative (S > −10) (Figures 2A, C and Supplementary Figure 5). Additionally, although we could not establish any significant linear correlation between $S_{691–699}$ and $S_{976–984}$ epitope-specific $CD8^+$ T-cell responses and disease severity, more complex (non-linear) associations might exist. For example, the magnitude of the $S_{976–984}$-specific IFN-γ-producing $CD8^+$ T-cell response followed a clear downside trend, as the disease severity increased in severely ill symptomatic COVID-19 patients and patients with fatal outcomes (i.e., severity 3–5) (Figures 2A, C and Supplementary Figure 5).

Taken together, these results demonstrate that, like SARS-CoV-2-specific $CD4^+$ T cells, an overall higher magnitude of CCCs/SARS-CoV-2 cross-reactive $CD8^+$ T-cell responses were present in asymptomatic COVID-19 patients who never presented any COVID-19 symptoms, despite being infected. In contrast, a lower magnitude of CCCs/SARS-CoV-2 cross-reactive $CD8^+$ T-cell responses was detected in severely ill COVID-19 patients and patients with fatal COVID-19 outcomes. These observations also highlight the importance of rapidly mounting strong CCCs/SARS-CoV-2 cross-reactive $CD8^+$ T-cell responses, directed toward structural, non-structural, and accessory protein antigens, for protection against symptomatic and fatal Infections in unvaccinated COVID-19 patients.

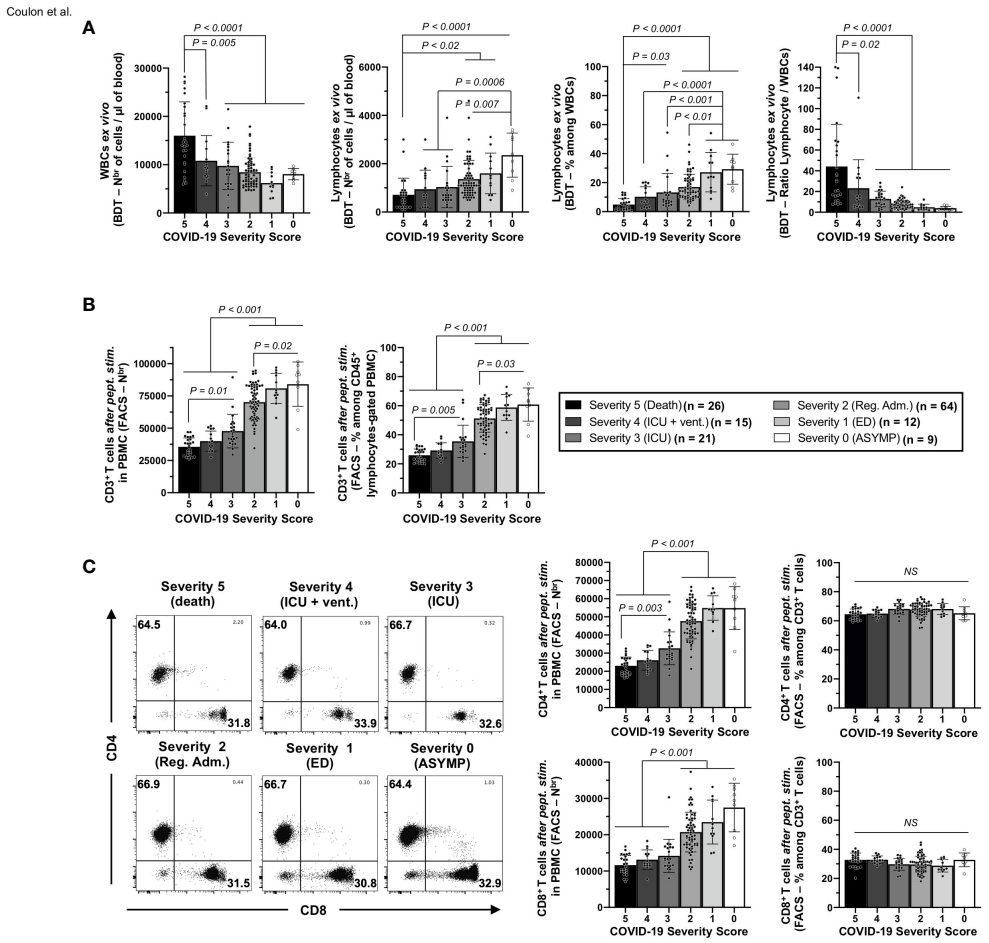

FIGURE 3
Frequencies of white blood cells, lymphocytes, and $CD3^+/CD4^+/CD8^+$ T cells in the blood of unvaccinated COVID-19 patients with various degrees of disease severity. **(A)** numbers of white blood cells (WBCs) and total lymphocytes per µl of blood (left two panels) and percentages and ratios of total lymphocytes among WBCs (right two panels) measured *ex vivo* by blood differential test (BDT) in unvaccinated COVID-19 patients with various degrees of disease severity (n = 147). **(B)** Averages/means of numbers and frequencies of $CD3^+$ T cells and **(C)** of total $CD4^+$, and $CD8^+$ T cells measured by flow cytometry from COVID-19 patients' PBMCs with various severity scores after 72 h of stimulation with a pool of 16 $CD4^+$ and 27 $CD8^+$ CCCs/SARS-CoV-2 cross-reactive epitope peptides. The right panels show representative dot plots from patients with disease severity scores from 0 to 5. Data are expressed as the mean ±SD. Results are representative of two independent experiments and were considered statistically significant at $p \leq 0.05$ (one-way ANOVA).

A broad lymphopenia, leukocytosis, and low frequencies of CD4$^+$ and CD8$^+$ T cells specific to highly conserved CCCs/SARS-CoV-2 cross-reactive epitopes are present in unvaccinated severely ill symptomatic COVID-19 patients

We next determined whether the low magnitudes of CCCs/SARS-CoV-2 cross-reactive CD4$^+$ and CD8$^+$ T-cell responses detected in unvaccinated severely ill and fatal COVID-19 patients was a result of an overall deficit in the frequencies of total CD4$^+$ and CD8$^+$ T cells. Using a blood differential test (BDT), we compared the absolute numbers of white blood cells (WBCs) and blood-derived lymphocytes, *ex vivo*, in the unvaccinated COVID-19 patients (Figure 3A).

A significant increase in the numbers of WBCs was detected in unvaccinated COVID-19 patients with fatal outcomes, (i.e., patients with severity 5, ~1.5- to ~2.6-fold) when compared with all the remaining five groups of unvaccinated COVID-19 patients (i.e., patients with severity 0, 1, 2, 3, and 4; $p \leq 0.02$, Figure 3A—left panel). However, significantly lower absolute numbers of total lymphocytes were detected in the blood of unvaccinated COVID-19 patients with fatal outcomes (i.e., patients with severity 5) compared to unvaccinated COVID-19 patients with mild disease (i.e., patients with severity 1 and 2: ~1.9- to ~2.3-fold decrease—$p < 0.02$) or to asymptomatic patients with no disease (i.e., patients with severity 0: ~3.3-fold decrease—$p < 0.0001$) (Figure 3A—second panel from left). As a result, the more severe the disease, the lower the percentage of blood-derived lymphocytes within WBCs (Figure 3A—third panel from left), and the lower the ratio of lymphocyte/WBCs (Figure 3A—fourth panel from left).

Overall, these results indicate that unvaccinated severely ill COVID-19 patients and unvaccinated COVID-19 patients with fatal outcomes not only had a general leukocytosis but also lymphopenia, which developed as early as 4.8 days after reporting their first symptoms or their first PCR-positive test.

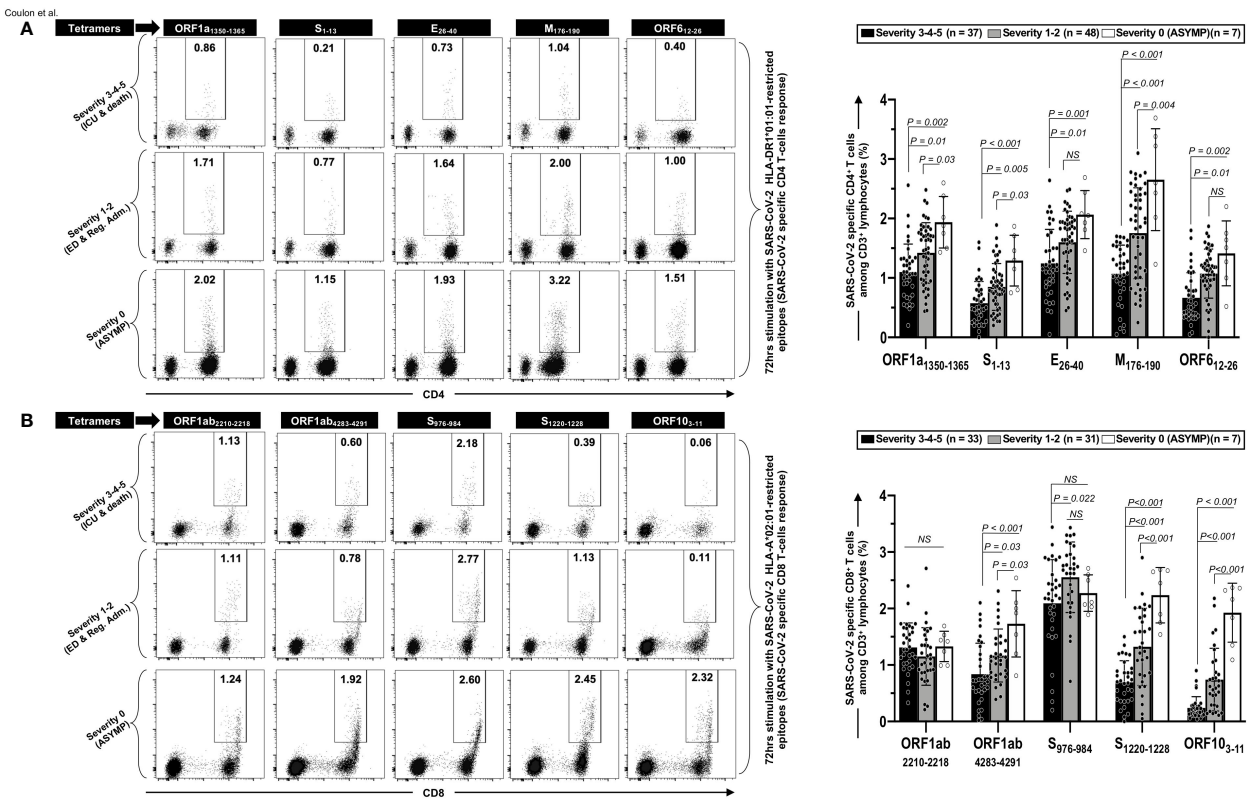

FIGURE 4
Frequencies of CCCs/SARS-CoV-2 cross-reactive CD4$^+$ and CD8$^+$ T cells in unvaccinated COVID-19 patients with various degrees of disease severity. PBMCs from HLA-DRB1*01:01-positive (n = 92) **(A)** or HLA-A*02:01-positive (n = 71) **(B)** unvaccinated COVID-19 patients with various degrees of disease severity were isolated and stimulated for 72 h with 10 µg/ml of indicated CCCs/SARS-CoV-2 cross-reactive CD4$^+$ and CD8$^+$ epitope peptides. The induced CD4$^+$ and CD8$^+$ T cells were then stained and analyzed by flow cytometry. The indicated epitope peptides were chosen among the CCCs/SARS-CoV-2 cross-reactive 16 CD4$^+$ and 27 CD8$^+$ epitope peptides based on tetramer availability. Panel **(A)** shows representative dot plots (left panels) and average frequencies of CCCs/SARS-CoV-2 cross-reactive CD4$^+$ T cells (right panel) detected in three representatives COVID-19 patients, each falling into one of three groups of disease category: the unvaccinated asymptomatic COVID-19 patients (ASYMP, severity score 0), unvaccinated COVID-19 patients who developed mild to moderate disease (severity scores 1 and 2), and unvaccinated severely ill COVID-19 patients and unvaccinated patients with fatal COVID-19 outcomes (severity scores 3–5). Panel **(B)** shows representative dot plots (left panels) and average frequencies of CCCs/SARS-CoV-2 cross-reactive CD8$^+$ T cells (right panel) detected in three representatives of COVID-19 patients and in panel **(A)**. Data are expressed as the mean ± SD. Results are representative of two independent experiments and were considered statistically significant at $p \leq 0.05$ (one-way ANOVA).

Furthermore, we found a significant $CD3^+$ T-cell lymphopenia positively associated with the onset of severe disease in unvaccinated COVID-19 patients (Figure 3B). On average, the two groups of unvaccinated severely ill COVID-19 patients and unvaccinated COVID-19 patients with fatal outcomes (i.e., patients with severity 3, 4, and 5) had a ~1.9-fold decrease in absolute number of $CD3^+$ T cells compared to three groups of unvaccinated asymptomatic COVID-19 patients with low to no severe disease (i.e., patients with severity 0, 1, and 2, Figure 3B, $p < 0.001$). Similarly, the numbers of total $CD4^+$ and $CD8^+$ T cells within $CD3^+$-gated cells were reduced early in the two groups of unvaccinated severely ill COVID-19 patients and unvaccinated COVID-19 patients with fatal outcomes (i.e., patients with severity 3, 4, and 5) compared to the three groups of unvaccinated asymptomatic COVID-19 patients with low to no severe disease (Figure 3C—left column graph).

Finally, we determined the frequencies of SARS-CoV-2-specific $CD4^+$ and $CD8^+$ T cells following a 72-h *in vitro* stimulation with individual $CD4^+$ and $CD8^+$ T epitope peptides (as illustrated in Supplementary Figure 2). We used tetramers specific to five highly conserved CCCs/SARS-CoV-2 cross-reactive DRB1*01:01-restricted $CD4^+$ T-cell epitopes $ORF1a_{1350–1365}$, $S_{1–13}$, $E_{26–40}$, $M_{176–190}$, and $ORF6_{12–26}$ (Figure 4A) and five highly conserved CCCs/SARS-CoV-2 cross-reactive HLA-A*02:01-restricted $CD8^+$ T-cell epitopes $Orf1ab_{2210–2218}$, $Orf1ab_{4283–4291}$, $S_{976–984}$, $S_{1220–1228}$, and $ORF10_{3–11}$ (Figure 4B).

We found a significant decrease in the frequencies of $CD4^+$ T cells specific to all the five highly conserved CCCs/SARS-CoV-2 cross-reactive DRB1*01:01-restricted epitopes in the three groups of unvaccinated severely ill COVID-19 and unvaccinated COVID-19 patients with fatal outcomes (i.e., patients with severity 3, 4, and 5) compared to the remaining three groups of unvaccinated COVID-19 patients with low to no severe disease (i.e., patients with severity 1, 2—$p \leq 0.01$) and to unvaccinated asymptomatic COVID-19 patients (severity 0—$p \leq 0.002$) (Figure 4A). Similarly, we found a significant decrease in the frequencies of $CD8^+$ T cells specific to three out the five highly conserved CCCs/SARS-CoV-2 cross-reactive HLA-A*02:01-restricted $CD8^+$ T-cell epitopes ($Orf1ab_{4283–4291}$, $S_{1220–1228}$, and $ORF10_{3–11}$) in the three groups of unvaccinated severely ill COVID-19 and unvaccinated COVID-19 patients with fatal outcomes (i.e., patients with severity 3, 4, and 5) compared to unvaccinated COVID-19 patients with low to no severe disease (i.e., patients with severity 1 and 2—$p \leq 0.03$) and to unvaccinated asymptomatic COVID-19 patients (severity 0—$p < 0.001$) (Figure 4B). In contrast, similar frequencies of EBV $BMLF\text{-}1_{280–288}$-specific $CD8^+$ T cells were detected across the six groups of unvaccinated COVID-19 patients, regardless of disease severity, indicating that the decrease in the frequencies of T cells in severely ill COVID-19 patients specifically affected highly conserved and CCCs/SARS-CoV-2 cross-reactive T cells (Supplementary Figure 3A).

Taken together, our findings demonstrate that, compared to asymptomatic COVID-19 patients who presented with little to no disease, the severely ill patients and patients with fatal COVID-19 outcomes showed the following: (i) a broad and early lymphopenia (and leukocytosis), (ii) a decrease of bulk $CD3^+$ T-cell lymphocytes number (equally affecting $CD4^+$ and $CD8^+$ T cells), and (iii) a reduction in $CD4^+$ and $CD8^+$ T cells specific to highly conserved CCCs/SARS-CoV-2 cross-reactive epitopes from structural, non-structural, and accessory protein antigens.

Unvaccinated severely ill COVID-19 patients present high frequencies of phenotypically and functionally exhausted CCCs/SARS-CoV-2 cross-reactive $CD4^+$ and $CD8^+$ T cells, detected both *ex vivo* and *in vitro*

We next compared the phenotype and function of $CD4^+$ and $CD8^+$ T cells specific to CCCs/SARS-CoV-2 cross-reactive epitopes in unvaccinated asymptomatic COVID-19 patients, with little to no disease, versus the unvaccinated severely ill COVID-19 patients and the unvaccinated COVID-19 patients with fatal outcomes.

Co-expression of four main exhaustion markers (PD-1, TIM3, TIGIT, and CTLA4) and two activation markers (AIMs) CD137 (4-1BB) and CD134 (OX40) were compared using FACS and tetramers specific to five highly conserved CCCs/SARS-CoV-2 cross-reactive DRB1*01:01-restricted $CD4^+$ T-cell epitopes, $ORF1a_{1350–1365}$, $S_{1–13}$, $E_{26–40}$, $M_{176–190}$, and $ORF6_{12–26}$ both *in vivo* (Figure 5) and *ex vitro* (Supplementary Figure 6) and five highly conserved CCCs/SARS-CoV-2 cross-reactive HLA-A*02:01-restricted $CD8^+$ T-cell epitopes, $Orf1ab_{2210–2218}$, $Orf1ab_{4283–4291}$, $S_{976–984}$, $S_{1220–1228}$, and $ORF10_{3–11}$ both *in vitro* (Figure 6) and *ex vivo* (Supplementary Figure 6).

We detected significantly higher frequencies of phenotypically exhausted SARS-CoV-2-specific $CD4^+$ T cells in unvaccinated symptomatic COVID-19 patients with high severity scores (i.e., patients with severity 3, 4, and 5) compared to unvaccinated asymptomatic COVID-19 patients (i.e., patients with severity 0) (Figure 5A—up to ~6.9-fold increase for $ORF6_{12–26}$-specific PD-1^+TIGIT$^+$CD4$^+$ T cells and up to ~7.8-fold increase for $M_{176–190}$-specific TIM-3^+CTLA-4^+CD4$^+$ T cells). Similarly, there were significantly higher frequencies of phenotypically exhausted $CD8^+$ T cells in unvaccinated severely ill COVID-19 and patients with fatal outcomes compared to unvaccinated asymptomatic COVID-19 patients (Figure 6A—up to ~3.6-fold increase for $S_{1220–1228}$-specific PD-1^+TIGIT$^+$CD8$^+$ T cells and up to ~4.6-fold increase for $S_{1220–1228}$- and $ORF10_{3-11}$-specific TIM-3^+CTLA-4^+CD8$^+$ T cells). Overall, except for $Orf1ab_{2210–2218}$- and $S_{976–984}$-specific-$CD8^+$ T cells, the unvaccinated severely ill and fatal patients (i.e., patients with severity 3, 4, and 5) had significantly higher frequencies of exhausted $CD8^+$ T cells co-expressing PD-1^+TIGIT$^+$ or TIM-3^+CTLA-4 compared to unvaccinated asymptomatic COVID-19 patients with little to no disease (i.e., patients with severity 0, 1, and 2). The $Orf1ab_{2210–2218}$- and $S_{976–984}$-specific-$CD8^+$ T cells did not demonstrate any significantly higher phenotypic exhaustion in unvaccinated severely ill COVID-19 patients. We confirmed *ex vivo* that the unvaccinated severely ill and fatal patients (i.e., patients with severity 3, 4, and 5) had significantly higher frequencies of exhausted $CD8^+$ T cells co-expressing PD-1^+TIGIT$^+$ or TIM-3^+CTLA-4 compared to unvaccinated asymptomatic COVID-19 patients with little to no disease (i.e., patients with severity 0, 1, and 2, $p < 0.05$, Supplementary Figure 6).

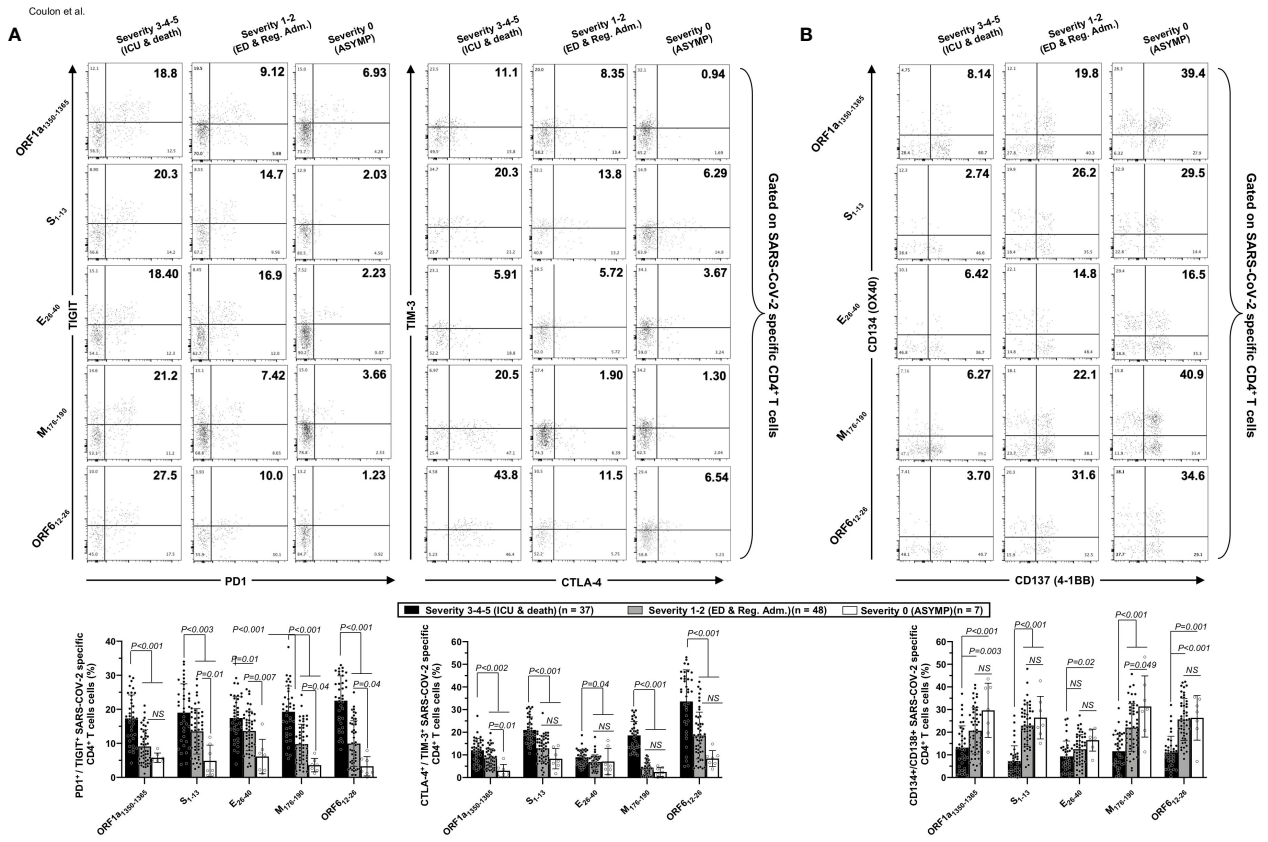

FIGURE 5
Co-expression of exhaustion and activation markers on CCCs/SARS-CoV-2 cross-reactive CD4$^+$ T cells from unvaccinated COVID-19 patients with various degrees of disease severity. PBMCs from HLA-DRB1*01:01-positive unvaccinated COVID-19 patients with various degrees of disease severity were isolated and stimulated for 72 h with 10 µg/ml of five CCCs/SARS-CoV-2 cross-reactive CD4$^+$ T-cell epitope peptides. The induced CD4$^+$ T cells were then stained and analyzed by flow cytometry for the frequency of tetramer-specific CD4$^+$ cells co-expressing exhaustion and activation markers. Panel **(A)** shows representative dot plots (upper panels) and average (lower panels) frequencies of CCCs/SARS-CoV-2 cross-reactive CD4$^+$ T cells expressing exhaustion markers PD1/TIGIT and TIM-3/CTLA-4 detected in three representative groups of unvaccinated COVID-19 patients with various degrees of disease severity. Panel **(B)** shows representative dot plots (upper panels) and average (lower panels) frequencies of CCCs/SARS-CoV-2 cross-reactive CD4$^+$ T cells expressing activation markers (AIMs) CD134/CD137 detected in three representative groups of unvaccinated COVID-19 patients with various degrees of disease severity. Results are representative of two independent experiments, and data are expressed as the mean ± SD and were considered statistically significant at $p \leq 0.05$ calculated using one-way ANOVA.

Accordingly, we also detected low frequencies of functional CD134$^+$CD137$^+$CD4$^+$ T cells (Figure 5B) and low frequencies of functional CD134$^+$CD137$^+$CD8$^+$ T cells (Figure 6B) in unvaccinated severely ill COVID-19 patients and unvaccinated patients with fatal COVID-19 outcomes. This applied to CD134$^+$CD137$^+$CD4$^+$ T cells specific to CCCs/SARS-CoV-2 cross-reactive epitopes from all five structural and non-structural proteins and to CD134$^+$CD137$^+$CD8$^+$ T cells specific to three out of five CCCs/SARS-CoV-2 cross-reactive epitopes from structural and non-structural proteins.

As expected, no differences were observed in phenotypic and functional exhaustion of EBV BMLF-1$_{280–288}$-specific CD8$^+$ T cells across the six groups of COVID-19 patients with various disease severities (Supplementary Figure 3B), suggesting that the exhaustion of CD4$^+$ and CD8$^+$ T cells in severely ill COVID-19 patients and to patients with fatal COVID-19 outcomes was specific to CCCs/SARS-CoV-2 cross-reactive epitopes.

Altogether, these results (i) indicate that phenotypic and functional exhaustion of CD4$^+$ and CD8$^+$ T cells, detected both *ex vivo* and *in vitro*, specific to highly conserved and CCCs/SARS-CoV-2 cross-reactive epitopes from both structural and non-structural antigens was associated with symptomatic and fatal infections in unvaccinated COVID-19 patients and (ii) suggest the importance of functional CCCs/SARS-CoV-2 cross-reactive CD4$^+$ and CD8$^+$ T cells, directed toward structural, non-structural, and accessory protein antigens, for protection against symptomatic and fatal infections in unvaccinated COVID-19 patients.

Higher rates of co-infection with alpha common cold coronavirus 229E present unvaccinated asymptomatic COVID-19 patients

We next compared the co-infection with each of the four main and seasonal α and β CCCs (i.e., α-CCC-NL63, α-CCC-229E, β-

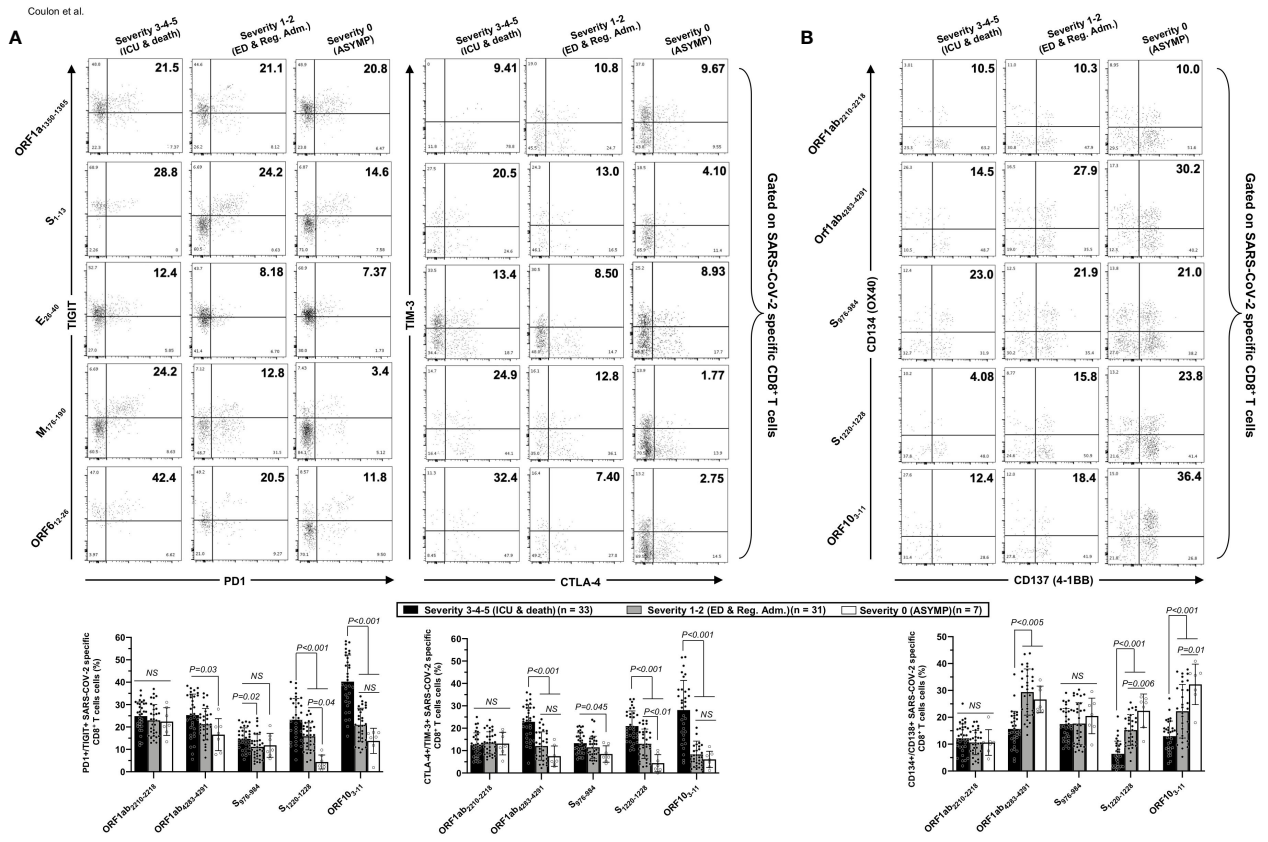

FIGURE 6
Co-expression of exhaustion and activation markers on CCCs/SARS-CoV-2 cross-reactive CD8$^+$ T cells from unvaccinated COVID-19 patients with various degrees of disease severity. PBMCs from HLA-A*02:01-positive unvaccinated COVID-19 patients with various degrees of disease severity were isolated and stimulated for 72 h with 10 µg/ml of five CCCs/SARS-CoV-2 cross-reactive CD8$^+$ T-cell epitope peptides. The induced CD8$^+$ T cells were then stained and analyzed by flow cytometry for the frequency of tetramer-specific CD8$^+$ cells co-expressing exhaustion and activation markers. Panel **(A)** shows representative dot plots (upper panels) and average frequencies of CCCs/SARS-CoV-2 cross-reactive CD8$^+$ T cells (lower panel) expressing exhaustion markers PD1/TIGIT and TIM-3/CTLA-4 detected in three representative groups of unvaccinated COVID-19 patients with various degrees of disease severity. Panel **(B)** shows representative dot plots (upper panels) and average frequencies of CCCs/SARS-CoV-2 cross-reactive CD8$^+$ T cells (lower panel) expressing activation markers (AIMs) CD134/CD137 detected in three representative groups of unvaccinated COVID-19 patients with various degrees of disease severity. Results are representative of two independent experiments, and data are expressed as the mean ± SD and were considered statistically significant at $p \leq 0.05$ (one-way ANOVA).

CCC-HKU1, and β-CCC-OC43) in a cohort of 85 unvaccinated COVID-19 patients divided into six groups based on the severity of COVID-19 symptoms, as above (i.e., patients with severity 5 to severity 0, Figures 7A, B). Using RT-PCR performed on nasopharyngeal swab samples, we found co-infection with the α-CCC species to be more common with significantly higher rates in the asymptomatic COVID-19 patients (i.e. unvaccinated naturally protected from severe symptoms) compared to severely ill COVID-19 patients and to unvaccinated patients with fatal outcomes (i.e., unvaccinated that were not naturally protected from severe symptoms) (Figure 7A—right panel; ~2.6-fold increase in groups 1–2–3 versus groups 4–5–6 of disease severity; $p = 0.0418$ calculated with Fisher's exact test). Co-infection with the CoV-229E α-CCC species was more common with significantly higher rates in the unvaccinated asymptomatic COVID-19 patients compared to unvaccinated severely ill COVID-19 patients and unvaccinated patients with fatal outcomes (Figure 7B, right panels: ~4.2-fold increase between unvaccinated asymptomatic COVID-19 patients and unvaccinated severely ill COVID-19 patients (i.e., patients with severity of 4–5–6; $p = 0.0223$). However, there was no significant difference in the rates of co-infection with β-CCC species (nor with any of the four CCC species) across all six groups of COVID-19 patients with various severity symptoms (Figure 7A, central and left panels, and Figure 7B, left two panels).

As illustrated in Figure 8, these results indicate that (i) compared to severely ill COVID-19 patients and patients with fatal COVID-19 outcomes, the asymptomatic COVID-19 patients presented significantly higher rates of co-infection with the α-CCC species, and with the 229E of α-CCCs, in particular and (*ii*) suggest that co-infection with the α species of CCCs (particularly the 229E species of α-CCCs, but not the β species) was associated with the natural protection from symptomatic and fatal infections in unvaccinated COVID-19 patients with yet-to-be-determined mechanisms(s).

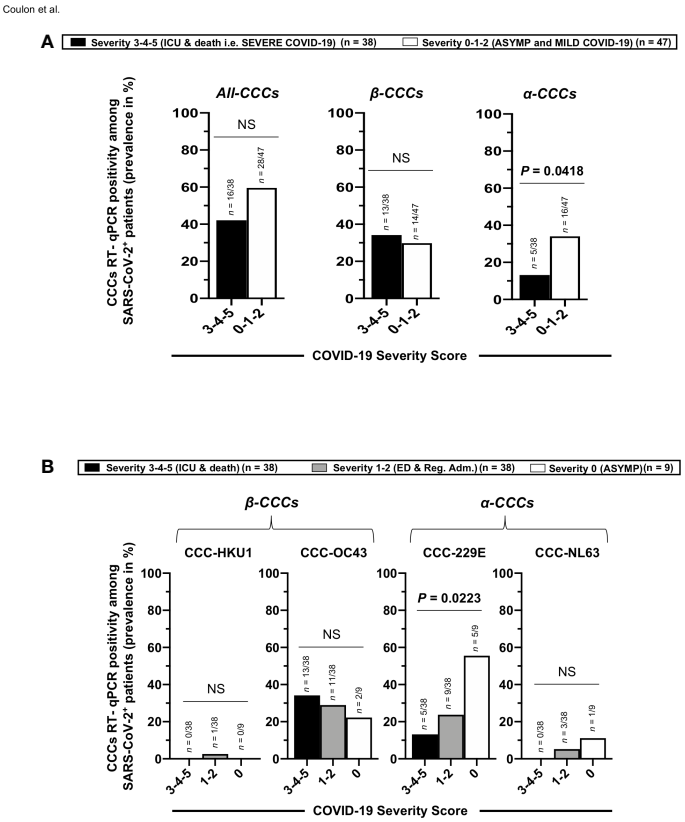

FIGURE 7
Rates (frequency) of co-infection with seasonal common cold coronavirus species α-CCC-NL63, α-CCC-229E, β-CCC HKU1, and β-CCC-OC43 in unvaccinated COVID-19 patients with various degrees of disease severity. Four major human common cold coronaviruses species, CCC-HKU1, CCC-OC43, CCC-229E, and CCC-NL63, were detected using RT-PCR in the nasopharyngeal swabs of COVID-19 patients (n = 85, first column) who developed various disease severity. Panel **(A)** shows all four α-CCCs and β-CCCs species (left panel), β-CCC species alone (middle panel), and α-CCC species alone (right panel), detected in unvaccinated severely ill COVID-19 patients and unvaccinated patients with fatal COVID-19 outcomes (severity scores 3–4–5) vs. unvaccinated COVID-19 patients who developed no, mild, and moderate disease (severity score 1–2–3). **(B)** The rate (%) of co-infection with each one of the four major species, CCC-HKU1, CCC-OC43, CCC-229E, and CCC-NL63, detected in unvaccinated severely ill COVID-19 patients and unvaccinated patients with fatal COVID-19 outcomes (severity scores 3–4–5), in unvaccinated COVID-19 patients who developed mild to moderate disease (severity score 1–2), and in unvaccinated asymptomatic COVID-19 patients (severity score 0). The p-values calculated using the Chi-squared test compare the rate (%) of co-infection with each CCC species between unvaccinated COVID-19 patients with various degrees of disease severity. Results are representative of two independent experiments, and data are expressed as the mean ± SD and were considered statistically significant at $p \leq 0.05$ calculated using Fisher's exact test.

High frequencies of α-CCCs/SARS-CoV-2 cross-reactive memory CD4$^+$ and CD8$^+$ T cells are associated with natural protection from symptomatic and fatal infections in unvaccinated COVID-19 patients

Next, we determined whether (i) the higher rates of co-infection with α-CCC species observed in the unvaccinated asymptomatic COVID-19 patients were associated with high frequencies of CCCs/SARS-CoV-2 cross-reactive CD4$^+$ and CD8$^+$ T cells detected in these asymptomatic COVID-19 groups and (ii) the high frequencies of α-CCCs/SARS-CoV-2 cross-reactive epitope-specific CD4$^+$ and CD8$^+$ T cells were associated with fewer symptoms observed in unvaccinated COVID-19 patients. To this end, we determined the percentage of unvaccinated asymptomatic COVID-19 patients, unvaccinated severely ill COVID-19, and unvaccinated patients with fatal outcomes who presented significant IFN-γ$^+$CD4$^+$ and IFN-γ$^+$CD8$^+$ T-cell responses (i.e., IFN-γ ELISpot SFCs > 50) specific to α-CCCs/SARS-CoV-2 cross-reactive epitopes.

Significantly higher percentages of unvaccinated asymptomatic COVID-19 patients with significant IFN-γ$^+$CD4$^+$ and IFN-γ$^+$CD8$^+$ T-cell responses specific to α-CCCs/SARS-CoV-2 cross-reactive epitopes were observed ($p < 0.001$). Similarly, the α-CCCs/SARS-CoV-2 cross-reactive epitopes were strongly cross-recognized by IFN-γ$^+$CD4$^+$ T cells (SFCs>50) and CD8$^+$ T cells from both unexposed pre-pandemic healthy individuals (UPPHI) and unvaccinated asymptomatic COVID-19 patients. In contrast, low frequencies of unvaccinated severely ill COVID-19 patients and unvaccinated patients with fatal outcomes significant IFN-γ$^+$CD4$^+$, and IFN-γ$^+$CD8$^+$ T-cell responses specific to α-CCCs/SARS-CoV-2 cross-reactive epitopes ($p < 0.001$) (Supplementary Table 4). We also found that unexposed pre-pandemic healthy individuals (UPPHI) who were never exposed to SARS-CoV-2 presented α-CCCs/SARS-CoV-2 cross-reactive IFN-γ$^+$CD4$^+$ and IFN-γ$^+$CD8$^+$ T

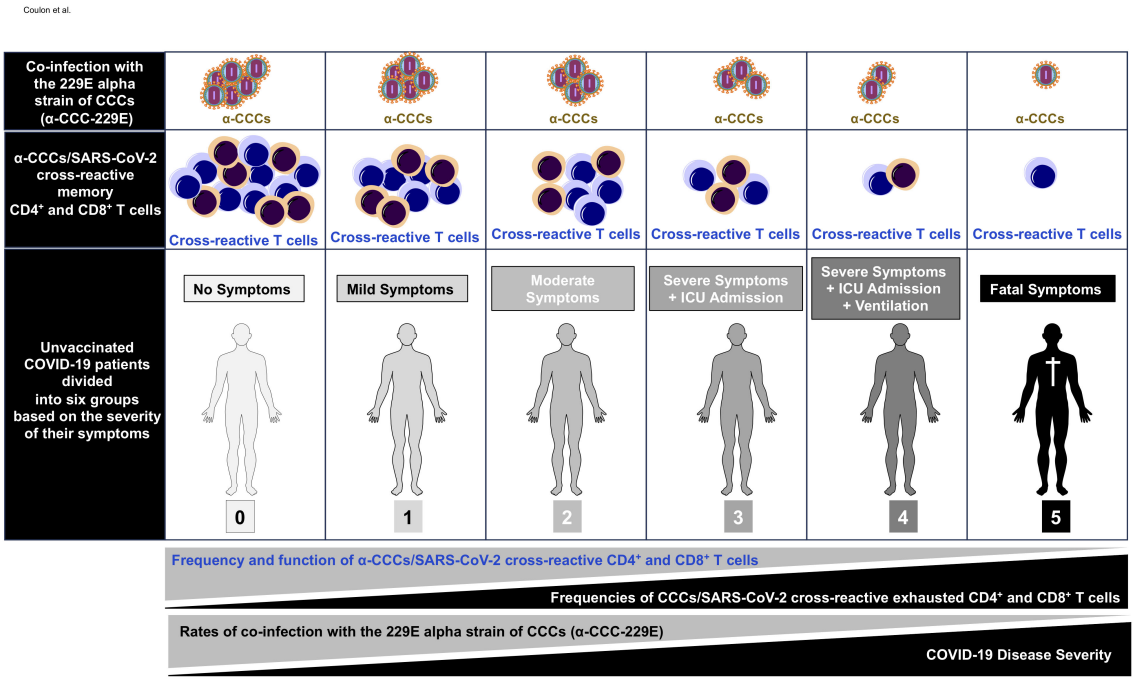

FIGURE 8
Illustration showing higher frequencies of common cold coronavirus/SARS-CoV-2 cross-reactive $CD4^+$ and $CD8^+$ T cells detected in unvaccinated asymptomatic COVID-19 patients is associated with higher rates of co-infection with alpha common cold coronavirus strain 229E (α-CCC-229E). The first row shows increasing copies of α-CCC-229E detected in unvaccinated asymptomatic COVID-19 patients compared to unvaccinated symptomatic COVID-19 patients. The middle row shows increasing numbers of common cold coronavirus/SARS-CoV-2 cross-reactive $CD4^+$ and $CD8^+$ memory T cells detected in unvaccinated asymptomatic COVID-19 patients compared to unvaccinated symptomatic COVID-19 patients. The bottom row shows symptoms detected in unvaccinated COVID-19 patients with symptoms increasing from severity 0 in asymptomatic COVID-19 patients (left) to severity 5 in COVID-19 patients with fatal COVID-19 outcomes (right) as detailed in *Materials and methods*.".

cells specific to highly conserved SARS-CoV-2 epitopes (Supplementary Figure 7), confirming our report and others' previous reports (1, 16, 21, 41, 43, 44).

Taken together, these results demonstrate that, compared to low proportions of severely ill COVID-19 patients and patients with fatal outcomes, significant proportions of both unvaccinated asymptomatic COVID-19 patients and unexposed pre-pandemic healthy individuals (UPPHI) presented significant α-CCCs/SARS-CoV-2 strong cross-reactive $CD4^+$ and $CD8^+$ T-cell responses. These findings suggest a crucial role of functional α-CCCs/SARS-CoV-2 cross-reactive memory $CD4^+$ and $CD8^+$ T cells, induced following previous α-CCC seasonal exposures, in protection against subsequent severe symptomatic SARS-CoV-2 infection, as illustrated in Figure 8.

Cross-reactive $CD4^+$ and $CD8^+$ T-cell epitopes from α-CCCs and SARS-CoV-2 that present high similarity and identity are associated with natural protection from symptomatic and fatal infections in unvaccinated COVID-19 patients

Using both the Multiple Sequences Alignments (MSA) and the Epitope Conservancy Tool (ECT) algorithms and software, we determined the identity (%id) and the similarity scores (S^s) of cross-reactive $CD4^+$ and $CD8^+$ T-cell epitopes, between the four major CCC species (α-hCCC-NL63, α-hCCC-229E, and β-hCCC-HKU1, β-hCCC-OC43), on the one hand, and SARS-CoV-2, on the other hand, as described in *Materials and methods* (58), (Table 2 and Supplementary Tables 1-3).

Of the 16 highly conserved $CD4^+$ T-cell epitopes (Supplementary Figure 8), the $ORF1ab_{5019–5033}$ epitope was highly conserved (%id ≥ 67%) and highly similar ($S^S \geq 0.8$) between SARS-CoV-2 and the two β-CCC species (β-CCC-HKU1 and β-CCC-OC43), while the $ORF1ab_{6088–6102}$ epitope was highly conserved between SARS-CoV-2 and both β-CCC-HKU1 and α-CCC-NL63 species (Table 2 and Supplementary Tables 1-3). Five out of the 27 $CD8^+$ T-cell epitopes ($ORF1ab_{3013–3021}$, $ORF1ab_{6749–6757}$, $S_{958–966}$, $E_{20–28}$, and $M_{52–60}$) were highly conserved (% id ≥67%) and highly similar ($S^S \geq 0.8$) between SARS-CoV-2 and the α-CCCs and/or β-CCC species. Specifically, the $ORF1ab_{3013–3021}$ $CD8^+$ T-cell epitope was highly conserved between SARS-CoV-2 and the two β-CCC species (β-CCC-HKU1 and β-CCC-OC43); the $ORF1ab_{6749–6757}$ epitope was highly conserved between SARS-CoV-2 and all the four CCC species; the $S_{958–966}$ epitope was highly conserved between SARS-CoV-2, the two β-CCC species, and the α-CCC-NL63 species; the $E_{20–28}$ epitope was highly conserved between SARS-CoV-2 and the β-CCC-HKU1 species; and the M_{52-60} epitope was highly conserved between SARS-CoV-2, the two β-CCC species (β-CCC-HKU1 and β-CCC-OC43) and the α-CCC-229E species (Supplementary Figure 9, Table 2, and Supplementary Tables 1-

3). While the E_{20-28} epitope was conserved (%id = 67%) between SARS-CoV-2 and α-CCC-NL63 species, it did not present significant similarity (Table 2 and Supplementary Tables 1-3).

Next, we determined the corresponding NL63 peptide (S^S = 0.76). While the $S_{976-984}$ epitope was conserved between SARS-CoV-2 and three CCC species (%id = 67%), it did not present significant similarity with the corresponding CCC peptides [β-CCC-HKU1 (S^S=0.78), β-CCC-OC43 (S^S=0.78) and α-CCC-NL63 (S^S = 0.73)]. Finally, while the S_{2-10} epitope was highly similar between SARS-CoV-2 and α-CCC-NL63 (S^S = 0.82), it was not significantly identical (id% = 56%) (Table 2 and Supplementary Tables 1-3).

Next, we determined whether the CCCs/SARS-CoV-2-cross-reactive epitopes were cross-recognized preferentially by the $CD4^+$ and $CD8^+$ T cells from either unvaccinated asymptomatic COVID-19 patients, or unvaccinated severely ill COVID-19 patients and unvaccinated patients with fatal outcomes (Supplementary Table 4). No significant differences were detected when the slopes S of the SARS-CoV-2-specific $CD4^+$ and $CD8^+$ T-cell responses were applied towards epitopes that have no significant identity nor similarity to epitopes from the four CCCs. Significant differences were detected when the slopes S of the SARS-CoV-2-specific $CD4^+$ and $CD8^+$ T-cell responses were applied to epitopes that have significant identity and/or similarity to epitopes from at least one of the four CCCs (Supplementary Table 4). In contrast, SARS-CoV-2 $CD4^+$ or $CD8^+$ T cells cross-recognizing epitopes that are highly identical and similar exclusively in β-CCC species, but not in α-CCC species (i.e., epitopes $ORF1ab_{5019-5033}$ and $ORF1ab_{3013-3021}$), presented a significantly lower slope S (p = 0.04) (Supplementary Table 4). The $ORF1ab_{5019-5033}$ and $ORF1ab_{3013-3021}$ epitopes have slopes S close to 0 among all epitopes (Supplementary Table 4).

These data indicated that (i) CCCs/SARS-CoV-2-cross-reactive $CD4^+$ or $CD8^+$ T-cell epitopes that share high identity and similarity exclusively with the α-CCC species were cross-recognized mainly by $CD4^+$ or $CD8^+$ T cells from asymptomatic COVID -19 patients; (ii) in contrast, the CCCs/SARS-CoV-2-cross-reactive $CD4^+$ or $CD8^+$ T cell epitopes that share high identity and similarity exclusively with the β-CCC species were cross-recognized mainly by $CD4^+$ or $CD8^+$ T cells from severely ill symptomatic patients; and (iii) compared to severely ill COVID-19 patients and patients with fatal outcomes, the asymptomatic COVID-19 patients presented significantly higher frequencies of α-CCCs/SARS-CoV-2 cross-reactive $CD4^+$ and $CD8^+$ T cells. The findings suggest a crucial role of functional, poly-antigenic α-CCCs/SARS-CoV-2 cross-reactive memory $CD4^+$ and $CD8^+$ T cells, induced following previous α-CCC seasonal exposures, in protection against subsequent severe symptomatic SARS-CoV-2 infection.

Discussion

Characterizing the underlying T-cell mechanisms associated with protection against COVID-19 severity in unvaccinated asymptomatic patients is a challenging task today, since most individuals have received at least one dose of COVID-19 vaccine (39). Only 15.2% of adults in the United States are unvaccinated (37, 38). This study is one of the few to comprehensively characterize the cross-reactive memory $CD4^+$ and $CD8^+$ T cells in unvaccinated symptomatic and asymptomatic COVID-19 patients. We compared the antigen specificity, frequency, phenotype, and function of CCCs/SARS-CoV-2 cross-reactive memory $CD4^+$ and $CD8^+$ T cells, cross-recognizing genome-wide conserved epitopes in a cohort of 147 unvaccinated COVID-19 patients, divided into six groups based on the severity of their symptoms. The findings demonstrate several relationships between antigen-specific T-cell responses and disease outcome. Specifically, severely ill symptomatic COVID-19 patients who required admission to intensive care units (ICUs) and patients with fatal COVID-19 outcomes, versus unvaccinated asymptomatic COVID-19 patients, displayed significantly (i) higher rates of co-infection with the 229E alpha species of CCCs (α-CCC-229E); (ii) higher frequencies of α-CCCs/SARS-CoV-2 cross-reactive functional memory $CD134^+CD137^+CD4^+$ and $CD134^+CD137^+CD8^+$ T cells, directed toward conserved epitopes from structural, non-structural, and accessory SARS-CoV-2 proteins; and (iii) lower frequencies of CCCs/SARS-CoV-2 cross-reactive and exhausted $PD\text{-}1^+TIM3^+TIGIT^+CTLA4^+CD4^+$ and $PD\text{-}1^+TIM3^+TIGIT^+CTLA4^+CD8^+$ T cells. These observations (i) support a crucial role for functional, poly-antigenic α-CCCs/SARS-CoV-2 cross-reactive memory $CD4^+$ and $CD8^+$ T cells, induced following previous α-CCC seasonal exposures, in protection against subsequent severe symptomatic SARS-CoV-2 infection and (ii) provide critical insights into developing broadly protective, multi-antigen, $CD4^+$ and $CD8^+$ T-cell-based, universal pan-Coronavirus vaccines capable of conferring cross-species protection.

The present comprehensive study of cross-reactive SARS-CoV-2 epitope-specific $CD4^+$ and $CD8^+$ T cells suggests that pre-pandemic exposure to seasonal α-CCC species, but not to β-CCC species, may have conferred protection from symptomatic COVID-19 infections by an as-yet-to-be-determined mechanism(s). It is likely that pre-existing CCCs/SARS-CoV-2 cross-reactive memory $CD4^+$ and $CD8^+$ T cells, induced in UPPHI by seasonal α-CCC species, cross-recognized protective SARS-CoV-2 epitopes. These data are consistent with previous studies showing that high levels of CCCs immunity in convalescent patients are associated with improved survival in COVID-19 patients (60, 61).

In the present study, we detected pre-existing CCCs/SARS-CoV-2 cross-reactive memory $CD4^+$ and $CD8^+$ T cells specific to many conserved SARS-CoV-2 epitopes in UPPHI. These results extend previous reports on the presence of specific repertoires of protective clones of memory $CD4^+$ and $CD8^+$ T cells in UPPHI possibly primed by previous exposure to seasonal CCCs infections and the rapid recall of α-CCCs/SARS-CoV-2 cross-reactive memory $CD4^+$ and $CD8^+$ T cells (1, 21, 41, 43, 62–66). UPPHI likely have different repertoires of protective and pathogenic memory $CD4^+$ and $CD8^+$ T cells targeting cross-reactive CCCs/SARS-CoV-2 epitopes of structural, non-structural, and accessory protein antigens that are associated with different disease outcomes in COVID-19 patients (13, 67–69). Indeed, we discovered that concomitant SARS-CoV-2/β-CCCs species (i.e., β-CCCs-HKU1 and β-CCCs-OC43) co-infection correlated with a trend toward more severe COVID-19 disease, whereas SARS-CoV-2/α-CCCs

species (i.e., α-CCCs-NL63 and mainly α-CCCs-229E) co-infection significantly correlated with less severe COVID-19 disease.

The positive correlation between functional α-CCCs/SARS-CoV-2 cross-reactive memory $CD4^+$ and $CD8^+$ T cells and better disease outcomes in asymptomatic COVID-19 patients supports the importance of developing CoV vaccines that cross-recognize functional α-CCCs/SARS-CoV-2 cross-reactive memory $CD4^+$ and $CD8^+$ T cells (70–72). Pre-existing T cells cross-recognizing conserved SARS-CoV-2 epitopes that cross-react with α-CCCs, but not β-CCCs, may be important in preventing severe COVID-19 symptoms. We are currently assessing whether candidate multi-epitope-based vaccines expressing the epitopes associated with good disease outcomes that cross-react with α-CCC species (in contrast to symptomatic epitopes that cross-react with β-CCC species) would confer cross-species protection in the HLA-A2/DR1/hACE2 triple transgenic mice.

While many SARS-CoV-2 epitopes present high identity and high similarity with the four α-CCCs and β-CCC species, they did not necessarily recall the strongest SARS-CoV-2 epitope-specific $CD4^+$ and $CD8^+$ T-cell responses in UPPHI. For example, the SARS-CoV-2 epitopes $ORF1a_{1350–1365}$, $S_{1–13}$, $M_{176–190}$, and $ORF6_{12–26}$ recalled strong $CD4^+$ T-cell responses in UPPHI but were not identical or similar with any epitopes from the four α-CCCs and β-CCC species. The same observation applies to the $CD8^+$ epitopes $ORF1ab_{1675–1683}$, $S_{1000–1008}$, and $S_{1220–1228}$. This suggests that the SARS-CoV-2-specific $CD4^+$ and $CD8^+$ T-cell responses in UPPHI may have been induced by other non-CCC pathogens, as has been reported by (73–76). Thus, in line with previous reports, we found that not all SARS-CoV-2 T-cell epitopes cross-reacted with CCC epitopes (41, 73–77). For instance, CMV T cells cross-react with SARS-CoV-2 T cells, despite low sequence homology between the two viruses, and this may contribute to the pre-existing immunity against SARS-CoV-2 (74). This is in agreement with our finding that eight of the 27 $CD8^+$ T-cell epitopes ($ORF1ab_{1675–1683}$, $ORF1ab_{5470–5478}$, $ORF1ab_{6749–6757}$, $S_{2–10}$, $S_{958–966}$, $S_{1220–1228}$, $E_{20–28}$, and $E_{26–34}$) shared highly identical sequences (%id equal to 67%–78%) with epitopes from common human pathogens (EBV, *Streptococcus pneumoniae*, *Bordetella pertussis*, and *Corynebacterium diphtheriae*) and to widely distributed BCG and DTa/wP vaccines. Six of those also shared high similarity scores ($S^S \geq 0.8$) with epitopes from EBV, *S. pneumoniae*, *B. pertussis*, and *C. diphtheriae* and widely distributed BCG and DTa/wP vaccines. $CD8^+$ T cells specific to SARS-CoV-2 epitopes that share high identity and similarity with the DTwP vaccine (but not BCG vaccine) epitopes were significantly associated with asymptomatic COVID-19 infection. The most functional $CD8^+$ T cells cross-recognized SARS-CoV-2 common epitopes that are highly similar and identical to epitopes from the DTwP vaccine. These findings are consistent with a previous study that described a correlation between DTwP vaccination and fewer COVID-19 deaths (59). Overall, our findings suggest that the pre-existing SARS-CoV-2-specific $CD4^+$ and $CD8^+$ T-cell responses in UPPHI may be the consequence of heterologous immunity induced by CCCs (31, 44, 75, 78–82), other pathogens (77), and widely administered vaccines (BCG, DTwP) (73–76).

The present comprehensive analysis demonstrates, both *in vitro* and *ex vivo*, that unvaccinated severely ill COVID-19 patients had higher frequencies of phenotypically and functionally exhausted CCCs/SARS-CoV-2 cross-reactive $CD4^+$ and $CD8^+$ T cells. In contrast, higher frequencies of functional $CD4^+$ and $CD8^+$ T cells specific to CCCs/SARS-CoV-2 epitopes were detected in unvaccinated asymptomatic COVID-19 patients. Although older COVID-19 patients tend to be more symptomatic compared to younger COVID-19 patients, the symptomatic COVID-19 patients tend to have less functional SARS-CoV-2-specific T cells, regardless of age. Similar results were obtained when age-matched symptomatic and asymptomatic COVID-19 patients were compared, suggesting that the frequency of functional SARS-CoV-2-specific T cells is age independent (data not shown). Besides CD134 and CD137 functional markers, we recently assessed the expression of additional activation and cytotoxicity markers by CCCs/SARS-CoV-2-cross-reactive $CD4^+$ and $CD8^+$ T cells from COVID-19 patients and healthy individuals (1). Higher frequencies of CCCs/SARS-CoV-2-cross-reactive functional memory $CD8^+$ T cells were detected in both COVID-19 patients and healthy individuals. However, we have observed that COVID-19 patients and unexposed healthy individuals exhibited a different pattern of $CD8^+$ T-cell immunodominance. Unlike for $CD8^+$ T cells, higher frequencies of multifunctional CCCs/SARS-CoV-2-cross-reactive memory $CD4^+$ T cells, expressing CD69, CD107a/b, and TNF-α were detected in COVID-19 patients compared to healthy individuals (1). However, the association of T-cell exhaustion with symptomatic and fatal COVID-19 infections in unvaccinated patients is currently being debated (6, 83). Reports using small cohorts of patients did not identify a link between higher expression of exhaustion markers and impaired function of SARS-CoV-2-specific $CD4^+$ and $CD8^+$ T cells in convalescent patients (84, 85). In contrast, our study used larger cohorts of COVID-19 patients with detailed clinical differentiation of symptomatic and asymptomatic patients. Our data are consistent with previous reports in which a broad T-cell exhaustion with impaired function was found in both the peripheral compartment (PBMCs), the lungs, and the brain of symptomatic patients (15, 86–88) and increased levels of PD-1 in severe cases compared to those in non-severe cases (83, 89).

Moreover, we extended those reports by characterizing the exhausted SARS-CoV-2-specific $CD4^+$ and $CD8^+$ T cells co-expressing multiple markers of exhaustion, TIM3, TIGIT, and CTLA4, besides PD-1. There is no consensus on a specific combination of inhibitory molecules of clusters of exhaustion markers to conclude phenotypic and functional exhaustion of epitope-specific $CD4^+$ and $CD8^+$ T cells. Overall, the major markers (or pathways) described as associated with $CD4^+$ and $CD8^+$ T-cell exhaustion include PD-1, TIGIT, CTLA-4, and TIM-3. While various combinations of these exhaustion have been used to demonstrate T-cell exhaustion, typically the PD-1 and TIM-3 combination is mainly used to demonstrate $CD4^+$ and $CD8^+$ T-cell exhaustion and dysfunction. In this study, we have used the combination of PD-1 and TIGIT exhaustion markers, on the one hand, and the combination of CTLA-4 and TIM-3 exhaustion markers, on the other hand, to demonstrate that increased

frequencies of phenotypically exhausted SARS-CoV-2 epitope-specific $CD4^+$ and $CD8^+$ T cells are associated with severe COVID-19 disease, as previously reported in other systems (90–97). These findings suggest impaired functionality in SARS-CoV-2-specific $CD4^+$ and $CD8^+$ T cells, along with generally lower interferon-gamma (IFN-γ) and tumor necrosis factor-alpha (TNF-α) production, is associated with symptomatic and fatal Infections in unvaccinated COVID-19 patients. Our results also agree with previous reports highlighting that a prior "original antigenic sin" (OAS) potentially linked to prior exposure to seasonal CCCs might skew CCCs/SARS-CoV-2 cross-reactive $CD4^+$ and $CD8^+$ T cells toward an exhausted phenotype (98). Because severely ill patients preferentially developed higher frequencies of co-infection with β-CCC species and higher frequencies of pre-existing β-CCCs/SARS-CoV-2 cross-reactive memory $CD4^+$ and $CD8^+$ T cells, T-cell exhaustion may be related to prior exposure to seasonal β-species of CCCs.

The present study has comprehensively characterized CCCs/SARS-CoV-2 cross-reactive memory $CD4^+$ and $CD8^+$ T cells in blood samples from over 140 unvaccinated symptomatic and asymptomatic COVID-19 patients. However, there remain several gaps in our understanding. First, the study of CCCs/SARS-CoV-2 cross-reactive memory $CD4^+$ and $CD8^+$ T cells in unvaccinated symptomatic and asymptomatic COVID-19 patients has not been adjusted retrospectively to previous CCCs infections, due to the lack of pre-COVID-19 samples. At this point, the vast majority of adults in the United States have been infected and/or received at least one dose of the COVID-19 vaccine (37, 38); thus, going forward, characterizing pre-COVID-19 cross-reactive memory $CD4^+$ and $CD8^+$ T cells in unvaccinated COVID 19 patients will be very difficult (39). Second, the study did not follow up with the COVID-19 patients at later times points after convalescence; hence, the reported CCCs/SARS-CoV-2 cross-reactive memory $CD4^+$ and $CD8^+$ T cell characteristics are reflective of their status shortly after exposure to SARS-CoV-2 or during the symptomatic disease. Although we assessed SARS-CoV-2-specific $CD4^+$ and $CD8^+$ T cell responses at an early stage of the disease (blood sampled on average 5 days after the appearance of the first reported symptoms), the precise timing of the patient's first exposure to SARS-CoV-2 is not known. Third, since the T-cell responses reported in this study were assessed in the peripheral blood, this may not reflect tissue-resident $CD4^+$ and $CD8^+$ T cells in the lungs and the brain. The reduced number of functional CCCs/SARS-CoV-2 cross-reactive memory $CD4^+$ and $CD8^+$ T cells detected in the peripheral blood of symptomatic COVID-19 patients may be due to T-cell redistribution to other organs, such as the lungs and the brain. The asymptomatic infections in unvaccinated COVID-19 patients might be attributed to homing and redistribution of high numbers of functional CCCs/SARS-CoV-2 cross-reactive $CD4^+$ and $CD8^+$ T cells into the lungs of unvaccinated asymptomatic COVID-19 patients, rather than in peripheral blood. In this context, we recently reported that high frequencies of functional lung-resident memory $CD4^+$ and $CD8^+$ T cells contributed to protection against COVID-19-like symptoms and death caused by SARS-CoV-2 infection in a mouse model (2). Thus, future studies should investigate tissue-resident $CD4^+$ and $CD8^+$ T cells in the lungs to determine whether their frequency and function correlate with protection from symptomatic and fatal infections in unvaccinated COVID-19 patients. Finally, while the study enrolled 600 patients overall, the study compared the antigen specificity, frequency, phenotype, and function of common cold coronaviruses (CCCs) and SARS-CoV-2 cross-reactive memory $CD4^+$ and $CD8^+$ T cells, targeting genome-wide conserved epitopes in a cohort of 147 unvaccinated COVID-19 patients screened for two HLA types, HLA-DRB1*01:01 and HLA-A*02:01. Thus, future studies are being conducted to assess T cells from other HLA types. Nevertheless, our results are consistent with the hypothesis that the early presence of high numbers of functional α-CCCs/SARS-CoV-2 cross-reactive $CD4^+$ and $CD8^+$ T cells targeting multiple antigens was associated with protection from symptomatic and fatal SARS-CoV-2 infections in unvaccinated COVID-19 patients (99).

This report also confirms previous reports that (i) early and broad lymphopenia positively correlated with COVID-19 disease severity and mortality (86, 100–102); (ii) broad leukocytosis combined with T cell lymphopenia was present in severe COVID-19 patients and extended those findings by demonstrating that the observed T-cell lymphopenia was particularly prevalent for SARS-CoV-2-specific T cells (86, 100); and (iii) a significant age-dependent and comorbidity-associated susceptibility to COVID-19 disease, with patients over 60 years of age, and those with pre-existing diabetic and hypertension comorbidities being the most susceptible to severe COVID-19 disease (13, 20).

In conclusion, the present comprehensive analysis of specific and cross-reactive SARS-CoV-2 epitope-specific T cells reveals clear relationships between T-cell responses and disease outcomes in unvaccinated COVID-19 patients. Compared to severely ill COVID-19 patients and patients with fatal COVID-19 outcomes, the asymptomatic COVID-19 patients presented high rates of co-infection with the α-CCC species and more functional and less exhausted α-CCCs/SARS-CoV-2 cross-reactive memory $CD4^+$ and $CD8^+$ T cells, targeting structural, non-structural, and accessory proteins. The findings suggest functional, poly-antigenic α-CCCs/SARS-CoV-2 cross-reactive memory $CD4^+$ and $CD8^+$ T cells, induced following CCCs repetitive exposures, are contributing factors in reducing the severity of SARS-CoV-2 infection, as illustrated in Figure 8. Most of the >10 billion doses of first-generation COVID-19 vaccines are based on the Spike antigen alone (103, 104) and function mainly by inducing neutralizing antibodies (105). Because the Spike protein has undergone a substantial number of mutations with each successive viral variant, these first-generation subunit vaccines are susceptible to immune evasion by new variants and subvariants, such as XBB.1.5, EG.5 (Eris), and HV.1 sub-variants of Omicron (71, 72). To overcome this critical limitation, the next generation of COVID-19 vaccines should also target other highly conserved structural and non-structural SARS-CoV-2 antigens capable of inducing protection by cross-reactive $CD4^+$ and $CD8^+$ T cells (1, 106). Herein, the findings of this report provide a roadmap for developing next-generation α-CCCs/SARS-CoV-2 cross-reactive $CD4^+$ and $CD8^+$ T cell-based, multi-antigen, pan-Coronavirus vaccines capable of conferring cross-species protection.

Data availability statement

The raw data supporting the conclusions of this article will be made available by the authors, without undue reservation.

Ethics statement

The studies involving humans were approved by Between July 2020 to November 2023, 600 patients were enrolled at the University of California Irvine Medical Center with mild to severe COVID-19 under an approved Institutional Review Board–approved protocol (IRB#-2020-5779). Written informed consent was obtained from participants before inclusion. The studies were conducted in accordance with the local legislation and institutional requirements. The participants provided their written informed consent to participate in this study.

Author contributions

LB: Conceptualization, Data curation, Formal analysis, Funding acquisition, Investigation, Methodology, Project administration, Resources, Supervision, Validation, Visualization, Writing – original draft, Writing – review & editing. PC: Conceptualization, Data curation, Formal analysis, Investigation, Methodology, Software, Validation, Visualization, Writing – original draft. SP: Conceptualization, Data curation, Formal analysis, Investigation, Methodology, Project administration, Software, Validation, Visualization, Writing – original draft. ND: Conceptualization, Data curation, Formal analysis, Investigation, Methodology, Writing – original draft. RS: Data curation, Formal analysis, Methodology, Project administration, Writing – original draft, Conceptualization. LZ: Data curation, Methodology, Writing – original draft. DT: Data curation, Resources, Writing – original draft. RE: Data curation, Resources, Writing – original draft. CF: Data curation, Resources, Writing – original draft. SS: Resources, Writing – original draft. LH: Resources, Writing – original draft. AN: Writing – review & editing, Writing – original draft. BK: Resources, Writing – original draft. EB: Data curation, Methodology, Writing – original draft. HV: Data curation, Writing – original draft. DG: Conceptualization, Formal analysis, Writing – review & editing. TJ: Conceptualization, Writing – original draft. JU: Conceptualization, Formal analysis, Writing – review & editing, Writing – original draft.

Funding

The author(s) declare that financial support was received for the research, authorship, and/or publication of this article. These studies were supported in part by Public Health Service Research grants AI158060, AI150091, AI143348, AI147499, AI143326, AI138764, AI124911, and AI110902 from the National Institutes of Allergy and Infectious Diseases (NIAID) to LB and by R43AI174383 to TechImmune, LLC. The funder TechImmune, LLC was not involved in the study design, collection, analysis, interpretation of data, the writing of this article or the decision to submit it for publication.

Acknowledgments

The authors would like to thank the NIH Tetramer Facility (Emory University, Atlanta, GA) for providing the Tetramers used in this study. We thank the UC Irvine Center for Clinical Research (CCR) and the Institute for Clinical and Translational Science (ICTS) for providing human blood samples and nasopharyngeal swab samples used in this study. A special thanks to Dr. Alessandro Ghigi and Dr. Kai Zheng for providing patients' clinical information. We also thank those who contributed directly or indirectly to this COVID-19 project: Gavin S. Herbert, Dr. Steven A. Goldstein, Dr. Michael J. Stamos, Dr. Suzanne B. Sandmeyer, Jim Mazzo, Dr. Daniela Bota, Dr. Dan Forthal, Christine Dwight, Janice Briggs, Marge Brannon, Beverley Alberola, Jessica Sheldon, Rosie Magallon, and Andria Pontello.

Conflict of interest

Authors HV, DG, TJ and JU were employed by company TechImmune LLC. LB has an equity interest in TechImmune, LLC., a company that may potentially benefit from the research results and serves on the company's Scientific Advisory Board. LB's relationship with TechImmune, LLC., has been reviewed and approved by the University of California, Irvine by its conflict-of-interest policies.

The remaining authors declare that the research was conducted in the absence of any commercial or financial relationships that could be construed as a potential conflict of interest.

The author(s) declared that they were an editorial board member of Frontiers, at the time of submission. This had no impact on the peer review process and the final decision.

Publisher's note

Supplementary material

The Supplementary Material for this article can be found online at: https://www.frontiersin.org/articles/10.3389/fimmu.2024.1343716/full#supplementary-material

References

1. Prakash S, Srivastava R, Coulon PG, Dhanushkodi NR, Chentoufi AA, Tifrea DF, et al. Genome-wide B cell, CD4(+), and CD8(+) T cell epitopes that are highly conserved between human and animal coronaviruses, identified from SARS-CoV-2 as targets for preemptive pan-coronavirus vaccines. *J Immunol.* (2021) 206:2566–82. doi: 10.4049/jimmunol.2001438

2. Prakash S, Dhanushkodi NR, Zayou L, Ibraim IC, Quadiri A, Coulon PG, et al. Cross-protection induced by highly conserved human B, CD4 (+,) and CD8 (+) T cell epitopes-based coronavirus vaccine against severe infection, disease, and death caused by multiple SARS-CoV-2 variants of concern. *Front Immunol.* (2023) 15:1328905. doi: 10.1101/2023.05.24.541850

3. Pedersen SF, Ho YC. SARS-CoV-2: A storm is raging. *J Clin Invest.* (2020). doi: 10.1172/JCI137647

4. Harris E. Most COVID-19 deaths worldwide were among older people. *JAMA.* (2023) 329:704. doi: 10.1001/jama.2023.1554

5. Bahgat MM, Nadeem R, Nasraa MH, Amer K, Hassan WA, ELGarhy FM, et al. Proinflammatory cytokine profiles in both mild symptomatic and asymptomatic SARS-CoV-2-infected Egyptian individuals and a proposed relationship to post-COVID-19 sequela. *Viral Immunol.* (2023) 36:600–9. doi: 10.1089/vim.2023.0060

6. Wilk AJ, Rustagi A, Zhao NQ, Roque J, Martínez-Colón GJ, McKechnie JL, et al. A single-cell atlas of the peripheral immune response in patients with severe COVID-19. *Nat Med.* (2020) 26:1070–6. doi: 10.1038/s41591-020-0944-y

7. Baek MS, Lee MT, Kim WY, Choi JC, Jung SY. COVID-19-related outcomes in immunocompromised patients: A nationwide study in Korea. *PLoS One.* (2021) 16: e0257641. doi: 10.1371/journal.pone.0257641

8. Helleberg M, Niemann CU, Moestrup KS, Kirk O, Lebech AM, Lane C, et al. Persistent COVID-19 in an immunocompromised patient temporarily responsive to two courses of remdesivir therapy. *J Infect Dis.* (2020) 222:1103–7. doi: 10.1093/infdis/jiaa446

9. Tsang TK, Wang C, Fang VJ, Perera R, So HC, Ip DKM, et al. Reconstructing household transmission dynamics to estimate the infectiousness of asymptomatic influenza virus infections. *Proc Natl Acad Sci U S A.* (2023) 120:e2304750120. doi: 10.1073/pnas.2304750120

10. Bostanci A, Gazi U, Tosun O, Suer K, Unal Evren E, Evren H, et al. Long-COVID-19 in asymptomatic, non-hospitalized, and hospitalized populations: A cross-sectional study. *J Clin Med.* (2023) 12. doi: 10.3390/jcm12072613

11. Wherry EJ, Barouch DH. T cell immunity to COVID-19 vaccines. *Science.* (2022) 377:821–2. doi: 10.1126/science.add2897

12. Perez-Potti A, Lange J, Buggert M. Deciphering the ins and outs of SARS-CoV-2-specific T cells. *Nat Immunol.* (2021) 22:8–9. doi: 10.1038/s41590-020-00838-5

13. Peng Y, Mentzer AJ, Liu G, Yao X, Yin Z, Dong D, et al. Broad and strong memory CD4(+) and CD8(+) T cells induced by SARS-CoV-2 in UK convalescent individuals following COVID-19. *Nat Immunol.* (2020) 21:1336–45. doi: 10.1038/s41590-020-0782-6

14. Schub D, Klemis V, Schneitler S, Mihm J, Lepper PM, Wilkens H, et al. High levels of SARS-CoV-2-specific T cells with restricted functionality in severe courses of COVID-19. *JCI Insight.* (2020) 5:e142167. doi: 10.1172/jci.insight.142167

15. Sette A, Crotty S. Adaptive immunity to SARS-CoV-2 and COVID-19. *Cell.* (2021) 184:861–80. doi: 10.1016/j.cell.2021.01.007

16. Grifoni A, Sidney J, Vita R, Peters B, Crotty S, Weiskopf D, et al. SARS-CoV-2 human T cell epitopes: Adaptive immune response against COVID-19. *Cell Host Microbe.* (2021) 29:1076–92. doi: 10.1016/j.chom.2021.05.010

17. Rydyznski Moderbacher C, Ramirez SI, Dan JM, Grifoni A, Hastie KM, Weiskopf D, et al. Antigen-specific adaptive immunity to SARS-CoV-2 in acute COVID-19 and associations with age and disease severity. *Cell.* (2020) 183:996–1012.e19. doi: 10.1016/j.cell.2020.09.038

18. Tan AT, Linster M, Tan CW, Le Bert N, Chia WN, Kunasegaran K, et al. Early induction of functional SARS-CoV-2-specific T cells associates with rapid viral clearance and mild disease in COVID-19 patients. *Cell Rep.* (2021) 34:108728. doi: 10.1016/j.celrep.2021.108728

19. Tarke A, Zhang Y, Methot N, Narowski TM, Phillips E, Mallal S, et al. Targets and cross-reactivity of human T cell recognition of common cold coronaviruses. *Cell Rep Med.* (2023) 4:101088. doi: 10.1016/j.xcrm.2023.101088

20. Brand I, Gilberg L, Bruger J, Gari M, Wieser A, Eser TM, et al. Broad T cell targeting of structural proteins after SARS-CoV-2 infection: high throughput assessment of T cell reactivity using an automated interferon gamma release assay. *Front Immunol.* (2021) 12:688436. doi: 10.3389/fimmu.2021.688436

21. Nelde A, Bilich T, Heitmann JS, Maringer Y, Salih HR, Roerden M, et al. SARS-CoV-2-derived peptides define heterologous and COVID-19-induced T cell recognition. *Nat Immunol.* (2021) 22:74–85. doi: 10.1038/s41590-020-00808-x

22. Bange EM, Han NA, Wileyto P, Kim JY, Gouma S, Robinson J, et al. CD8(+) T cells contribute to survival in patients with COVID-19 and hematologic cancer. *Nat Med.* (2021) 27:1280–9. doi: 10.1038/s41591-021-01386-7

23. Munoz-Fontela C, Dowling WE, Funnell SGP, Gsell PS, Riveros-Balta AX, Albrecht RA, et al. Animal models for COVID-19. *Nature.* (2020) 586:509–15. doi: 10.1038/s41586-020-2787-6

24. Li Z, Wang Z, Dinh PC, Zhu D, Popowski KD, Lutz H, et al. Cell-mimicking nanodecoys neutralize SARS-CoV-2 and mitigate lung injury in a non-human primate model of COVID-19. *Nat Nanotechnol.* (2021) 16:942–51. doi: 10.1038/s41565-021-00923-2

25. Morita R, Kubota-Koketsu R, Lu X, Sasaki T, Nakayama EE, Liu YC, et al. COVID-19 relapse associated with SARS-CoV-2 evasion from CD4(+) T-cell recognition in an agammaglobulinemia patient. *iScience.* (2023) 26:106685. doi: 10.1016/j.isci.2023.106685

26. Speletas M, Raftopoulou S, Farmaki E, Gatselis N, Germanidis G, Mouchtouri VA, et al. and COVID-19: lessons from patients with agammaglobulinemia and the study of functional B-cell polymorphisms. *J Investig Allergol Clin Immunol.* (2021) 32:53–5. doi: 10.18176/jiaci

27. Soresina A, Moratto D, Chiarini M, Paolillo C, Baresi G, Foca E, et al. Two X-linked agammaglobulinemia patients develop pneumonia as COVID-19 manifestation but recover. *Pediatr Allergy Immunol.* (2020) 31:565–9. doi: 10.1111/pai.13263

28. Quinti I, Lougaris V, Milito C, Cinetto F, Pecoraro A, Mezzaroma I, et al. A possible role for B cells in COVID-19? Lesson from patients with agammaglobulinemia. *J Allergy Clin Immunol.* (2020) 146:211–13.e4. doi: 10.1016/j.jaci.2020.04.013

29. Sabatino JJ Jr., Mittl K, Rowles WM, McPolin K, Rajan JV, Laurie MT, et al. Multiple sclerosis therapies differentially affect SARS-CoV-2 vaccine-induced antibody and T cell immunity and function. *JCI Insight.* (2022) 7. doi: 10.1172/jci.insight.156978

30. Gao Y, Cai C, Wullimann D, Niessl J, Rivera-Ballesteros O, Chen P, et al. Immunodeficiency syndromes differentially impact the functional profile of SARS-CoV-2-specific T cells elicited by mRNA vaccination. *Immunity.* (2022) 55:1732–46.e5. doi: 10.1016/j.immuni.2022.07.005

31. Beretta A, Cranage M, Zipeto D. Is cross-reactive immunity triggering COVID-19 immunopathogenesis? *Front Immunol.* (2020) 11:567710. doi: 10.3389/fimmu.2020.567710

32. Saini SK, Hersby DS, Tamhane T, Povlsen HR, Amaya Hernandez SP, Nielsen M, et al. SARS-CoV-2 genome-wide T cell epitope mapping reveals immunodominance and substantial CD8(+) T cell activation in COVID-19 patients. *Sci Immunol.* (2021) 6. doi: 10.1126/sciimmunol.abf7550

33. Thieme CJ, Anft M, Paniskaki K, Blazquez-Navarro A, Doevelaar A, Seibert FS, et al. Robust T cell response toward spike, membrane, and nucleocapsid SARS-CoV-2 proteins is not associated with recovery in critical COVID-19 patients. *Cell Rep Med.* (2020) 1:100092. doi: 10.1016/j.xcrm.2020.100092

34. Huang P, Zuo Q, Li Y, Oduro PK, Tan F, Wang Y, et al. A vicious cycle: in severe and critically ill COVID-19 patients. *Front Immunol.* (2022) 13:930673. doi: 10.3389/fimmu.2022.930673

35. Tizazu AM, Mengist HM, Demeke G. Aging, inflammaging and immunosenescence as risk factors of severe COVID-19. *Immun Ageing.* (2022) 19:53. doi: 10.1186/s12979-022-00309-5

36. Wratil PR, Schmacke NA, Karakoc B, Dulovic A, Junker D, Becker M, et al. Evidence for increased SARS-CoV-2 susceptibility and COVID-19 severity related to pre-existing immunity to seasonal coronaviruses. *Cell Rep.* (2021) 37:110169. doi: 10.1016/j.celrep.2021.110169

37. Griggs EP, Mitchell PK, Lazariu V, Gaglani M, McEvoy C, Klein NP, et al. Clinical epidemiology and risk factors for critical outcomes among vaccinated and unvaccinated adults hospitalized with COVID-19-VISION Network, 10 States, June 2021-March 2023. *Clin Infect Dis.* (2023). doi: 10.1093/cid/ciad505

38. Johnson AG, Linde L, Payne AB, Ali AR, Aden V, Armstrong B, et al. *Notes from the Field: Comparison of COVID-19 Mortality Rates Among Adults Aged ≥65 Years Who Were Unvaccinated and Those Who Received a Bivalent Booster Dose Within the Preceding 6 Months - 20 U.S. Jurisdictions*, September 18, 2022-April 1, 2023. MMWR Morb Mortal Wkly Rep. (2023) 72(24):667–9. doi: 10.15585/mmwr.mm7224a6

39. Meng L, Masters NB, Lu PJ, Singleton JA, Kriss JL, Zhou T, et al. Cluster analysis of adults unvaccinated for COVID-19 based on behavioral and social factors, National Immunization Survey-Adult COVID Module, United States. *Prev Med.* (2023) 167:107415. doi: 10.1016/j.ypmed.2022.107415

40. Grifoni A, Weiskopf D, Ramirez SI, Mateus J, Dan JM, Moderbacher CR, et al. Targets of T cell responses to SARS-CoV-2 coronavirus in humans with COVID-19 disease and unexposed individuals. *Cell.* (2020) 181:1489–501.e15. doi: 10.1016/j.cell.2020.05.015

41. Tan CCS, Owen CJ, Tham CYL, Bertoletti A, van Dorp L, Balloux F. Pre-existing T cell-mediated cross-reactivity to SARS-CoV-2 cannot solely be explained by prior exposure to endemic human coronaviruses. *Infect Genet Evol.* (2021) 95:105075. doi: 10.1016/j.meegid.2021.105075

42. Sattler A, Angermair S, Stockmann H, Heim KM, Khadzhynov D, Treskatsch S, et al. SARS-CoV-2-specific T cell responses and correlations with COVID-19 patient predisposition. *J Clin Invest.* (2020) 130:6477–89. doi: 10.1172/JCI140965

43. Sekine T, Perez-Potti A, Rivera-Ballesteros O, Stralin K, Gorin JB, Olsson A, et al. Robust T cell immunity in convalescent individuals with asymptomatic or mild COVID-19. *Cell.* (2020) 183:158–68.e14. doi: 10.1016/j.cell.2020.08.017

44. Mateus J, Grifoni A, Tarke A, Sidney J, Ramirez SI, Dan JM, et al. Selective and cross-reactive SARS-CoV-2 T cell epitopes in unexposed humans. *Science.* (2020) 370:89–94. doi: 10.1126/science.abd3871

45. Grifoni E, Vannucchi V, Valoriani A, Cei F, Lamanna R, Gelli AMG, et al. Interleukin-6 added to CALL score better predicts the prognosis of COVID-19 patients. *Intern Med J*. (2021) 51:146–7. doi: 10.1111/imj.14974

46. Diniz MO, Mitsi E, Swadling L, Rylance J, Johnson M, Goldblatt D, et al. Airway-resident T cells from unexposed individuals cross-recognize SARS-CoV-2. *Nat Immunol*. (2022) 23:1324–9. doi: 10.1038/s41590-022-01292-1

47. Le Bert N, Tan AT, Kunasegaran K, Tham CYL, Hafezi M, Chia A, et al. SARS-CoV-2-specific T cell immunity in cases of COVID-19 and SARS, and uninfected controls. *Nature*. (2020) 584:457–62. doi: 10.1038/s41586-020-2550-z

48. Bacher P, Rosati E, Esser D, Martini GR, Saggau C, Schiminsky E, et al. Low-avidity CD4(+) T cell responses to SARS-CoV-2 in unexposed individuals and humans with severe COVID-19. *Immunity*. (2020) 53:1258–71.e5. doi: 10.1016/j.immuni.2020.11.016

49. Yu ED, Narowski TM, Wang E, Garrigan E, Mateus J, Frazier A, et al. Immunological memory to common cold coronaviruses assessed longitudinally over a three-year period pre-COVID19 pandemic. *Cell Host Microbe*. (2022) 30:1269–78.e4. doi: 10.1016/j.chom.2022.07.012

50. An P, Song P, Wang Y, Liu B. Asymptomatic patients with novel coronavirus disease (COVID-19). *Balkan Med J*. (2020). doi: 10.4274/balkanmedj

51. Olerup O, Zetterquist H. HLA-DRB1*01 subtyping by allele-specific PCR amplification: a sensitive, specific and rapid technique. *Tissue Antigens*. (1991) 37:197–204. doi: 10.1111/j.1399-0039.1991.tb01872.x

52. Gatz SA, Pohla H, Schendel DJ. A PCR-SSP method to specifically select HLA-A*0201 individuals for immunotherapeutic studies. *Tissue Antigens*. (2000) 55:532–47. doi: 10.1034/j.1399-0039.2000.550604.x

53. Herr W, Ranieri E, Gambotto A, Kierstead LS, Amoscato AA, Gesualdo L, et al. Identification of naturally processed and HLA-presented Epstein-Barr virus peptides recognized by CD4(+) or CD8(+) T lymphocytes from human blood. *Proc Natl Acad Sci U.S.A*. (1999) 96:12033–8. doi: 10.1073/pnas.96.21.12033

54. Dolton G, Tungatt K, Lloyd A, Bianchi V, Theaker SM, Trimby A, et al. More tricks with tetramers: a practical guide to staining T cells with peptide-MHC multimers. *Immunology*. (2015) 146:11–22. doi: 10.1111/imm.12499

55. Kuypers J, Martin ET, Heugel J, Wright N, Morrow R, Englund JA. Clinical disease in children associated with newly described coronavirus subtypes. *Pediatrics*. (2007) 119:e70–6. doi: 10.1542/peds.2006-1406

56. Gunson RN, Collins TC, Carman WF. Real-time RT-PCR detection of 12 respiratory viral infections in four triplex reactions. *J Clin Virol*. (2005) 33:341–4. doi: 10.1016/j.jcv.2004.11.025

57. Cui L-J, Zhang C, Zhang T, Lu R-J, Xie Z-D, Zhang L-L, et al. Human coronaviruses HCoV-NL63 and HCoV-HKU1 in hospitalized children with acute respiratory infections in Beijing, China. *Adv Virol*. (2011) 2011:129134–4. doi: 10.1155/2011/129134

58. Frankild S, De Boer RJ, Lund O, Nielsen M, Kesmir C. Amino acid similarity accounts for T cell cross-reactivity and for "holes" in the T cell repertoire. *PLoS One*. (2008) 3:e1831. doi: 10.1371/journal.pone.0001831

59. Reche PA. Potential cross-reactive immunity to SARS-CoV-2 from common human pathogens and vaccines. *Front Immunol*. (2020) 11:586984. doi: 10.3389/fimmu.2020.586984

60. Greenbaum U, Klein K, Martinez F, Song J, Thall PF, Ramdial JL, et al. High levels of common cold coronavirus antibodies in convalescent plasma are associated with improved survival in COVID-19 patients. *Front Immunol*. (2021) 12:675679. doi: 10.3389/fimmu.2021.675679

61. Abbasi J. COVID-19 and the common cold-preexisting coronavirus antibodies may hinder SARS-CoV-2 immunity. *JAMA*. (2022) 327:609–10. doi: 10.1001/jama.2022.0326

62. Pedersen J, Koumakpayi IH, Babuadze G, Baz M, Ndiaye O, Faye O, et al. Cross-reactive immunity against SARS-CoV-2 N protein in Central and West Africa precedes the COVID-19 pandemic. *Sci Rep*. (2022) 12:12962. doi: 10.1038/s41598-022-17241-9

63. Kundu R, Narean JS, Wang L, Fenn J, Pillay T, Fernandez ND, et al. Cross-reactive memory T cells associate with protection against SARS-CoV-2 infection in COVID-19 contacts. *Nat Commun*. (2022) 13:80. doi: 10.1038/s41467-021-27674-x

64. Jaago M, Rahni A, Pupina N, Pihlak A, Sadam H, Tuvikene J, et al. Differential patterns of cross-reactive antibody response against SARS-CoV-2 spike protein detected for chronically ill and healthy COVID-19 naive individuals. *Sci Rep*. (2022) 12:16817. doi: 10.1038/s41598-022-20849-6

65. Yin D, Han Z, Lang B, Li Y, Mai G, Chen H, et al. Effect of seasonal coronavirus immune imprinting on the immunogenicity of inactivated COVID-19 vaccination. *Front Immunol*. (2023) 14:1195533. doi: 10.3389/fimmu.2023.1195533

66. Lundgren A, Leach S, Axelsson H, Isakson P, Nystrom K, Scharf L, et al. Plasmablasts in previously immunologically naive COVID-19 patients express markers indicating mucosal homing and secrete antibodies cross-reacting with SARS-CoV-2 variants and other beta-coronaviruses. *Clin Exp Immunol*. (2023) 213:173–89. doi: 10.1093/cei/uxad044

67. Santos MMS, Pereira IJ, Cuboia N, Reis-Pardal J, Adriao D, Cardoso T, et al. Predictors of early and long-term mortality after ICU discharge in critically ill COVID-19 patients: A prospective cohort study. *PLoS One*. (2023) 18:e0293883. doi: 10.1371/journal.pone.0293883

68. Wang S, Zhu R, Zhang C, Guo Y, Lv M, Zhang C, et al. Effects of the pre-existing coronary heart disease on the prognosis of COVID-19 patients: A systematic review and meta-analysis. *PLoS One*. (2023) 18:e0292021. doi: 10.1371/journal.pone.0292021

69. Silva RCD, de Lima SC, Dos Santos Reis WPM, de Magalhaes JJF, Magalhaes RNO, Rathi B, et al. Comparison of DNA extraction methods for COVID-19 host genetics studies. *PLoS One*. (2023) 18:e0287551. doi: 10.1371/journal.pone.0287551

70. Kared H, Redd AD, Bloch EM, Bonny TS, Sumatoh H, Kairi F, et al. SARS-CoV-2-specific CD8+ T cell responses in convalescent COVID-19 individuals. *J Clin Invest*. (2021) 131. doi: 10.1172/JCI145476

71. Polack FP, Thomas SJ, Kitchin N, Absalon J, Gurtman A, Lockhart S, et al. Safety and efficacy of the BNT162b2 mRNA COVID-19 vaccine. *New Engl J Med*. (2020) 383:2603–15. doi: 10.1056/NEJMoa2034577

72. Baden LR, El Sahly HM, Essink B, Kotloff K, Frey S, Novak R, et al. Efficacy and safety of the mRNA-1273 SARS-CoV-2 vaccine. *New Engl J Med*. (2021) 384:403–16. doi: 10.1056/NEJMoa2035389

73. Namuniina A, Muyanja ES, Biribawa VM, Okech BA, Ssemaganda A, Price MA, et al. Proportion of Ugandans with pre-pandemic SARS-CoV-2 cross-reactive CD4+ and CD8+ T-cell responses: A pilot study. *PloS Glob Public Health*. (2023) 3:e0001566. doi: 10.1371/journal.pgph.0001566

74. Pothast CR, Dijkland RC, Thaler M, Hagedoorn RS, Kester MGD, Wouters AK, et al. SARS-CoV-2-specific CD4(+) and CD8(+) T cell responses can originate from cross-reactive CMV-specific T cells. *Elife 11*. (2022). doi: 10.7554/eLife.82050

75. Schmidt KG, Nganou-Makamdop K, Tenbusch M, El Kenz B, Maier C, Lapuente D, et al. SARS-CoV-2-seronegative subjects target CTL epitopes in the SARS-CoV-2 nucleoprotein cross-reactive to common cold coronaviruses. *Front Immunol*. (2021) 12:627568. doi: 10.3389/fimmu.2021.627568

76. Steiner S, Sotzny F, Bauer S, Na IK, Schmueck-Henneresse M, Corman VM, et al. HCoV- and SARS-CoV-2 cross-reactive T cells in CVID patients. *Front Immunol*. (2020) 11:607918. doi: 10.3389/fimmu.2020.607918

77. Ogbe A, Kronsteiner B, Skelly DT, Pace M, Brown A, Adland E, et al. T cell assays differentiate clinical and subclinical SARS-CoV-2 infections from cross-reactive antiviral responses. *Nat Commun*. (2021) 12:2055. doi: 10.1101/2020.09.28.20202929

78. Murray SM, Ansari AM, Frater J, Klenerman P, Dunachie S, Barnes E, et al. The impact of pre-existing cross-reactive immunity on SARS-CoV-2 infection and vaccine responses. *Nat Rev Immunol*. (2023) 23:304–16. doi: 10.1038/s41577-022-00809-x

79. Becerra-Artiles A, Nanaware PP, Muneeruddin K, Weaver GC, Shaffer SA, Calvo-Calle JM, et al. Immunopeptidome profiling of human coronavirus OC43-infected cells identifies CD4 T-cell epitopes specific to seasonal coronaviruses or cross-reactive with SARS-CoV-2. *PLoS Pathog*. (2023) 19:e1011032. doi: 10.1371/journal.ppat.1011032

80. Klompus S, Leviatan S, Vogl T, Mazor RD, Kalka IN, Stoler-Barak L, et al. Cross-reactive antibodies against human coronaviruses and the animal coronavirome suggest diagnostics for future zoonotic spillovers. *Sci Immunol 6*. (2021). doi: 10.1126/sciimmunol.abe9950

81. Johansson AM, Malhotra U, Kim YG, Gomez R, Krist MP, Wald A, et al. Cross-reactive and mono-reactive SARS-CoV-2 CD4+ T cells in prepandemic and COVID-19 convalescent individuals. *PLoS Pathog*. (2021) 17:e1010203. doi: 10.1371/journal.ppat.1010203

82. Lipsitch M, Grad YH, Sette A, Crotty S. Cross-reactive memory T cells and herd immunity to SARS-CoV-2. *Nat Rev Immunol*. (2020) 20:709–13. doi: 10.1038/s41577-020-00460-4

83. Silva BSA, Pereira T, Minuzzi LG, Padilha CS, Figueiredo C, Olean-Oliveira T, et al. Mild to moderate post-COVID-19 alters markers of lymphocyte activation, exhaustion, and immunometabolic responses that can be partially associated by physical activity level- an observational sub-analysis fit- COVID study. *Front Immunol*. (2023) 14:1212745. doi: 10.3389/fimmu.2023.1212745

84. Mazzoni A, Salvati L, Maggi L, Annunziato F, Cosmi L. Hallmarks of immune response in COVID-19: Exploring dysregulation and exhaustion. *Semin Immunol*. (2021) 55:101508. doi: 10.1016/j.smim.2021.101508

85. Zhang JY, Wang XM, Xing X, Xu Z, Zhang C, Song JW, et al. Single-cell landscape of immunological responses in patients with COVID-19. *Nat Immunol*. (2020) 21:1107–18. doi: 10.1038/s41590-020-0762-x

86. Adamo S, Chevrier S, Cervia C, Zurbuchen Y, Raeber ME, Yang L, et al. Profound dysregulation of T cell homeostasis and function in patients with severe COVID-19. *Allergy*. (2021) 76:2866–81. doi: 10.1111/all.14866

87. Wang N, Vuerich M, Kalbasi A, Graham JJ, Csizmadia E, Manickas-Hill ZJ, et al. Limited TCR repertoire and ENTPD1 dysregulation mark late-stage COVID-19. *iScience*. (2021) 24:103205. doi: 10.1016/j.isci.2021.103205

88. Shahbaz S, Xu L, Sligl W, Osman M, Bozorgmehr N, Mashhouri S, et al. The quality of SARS-CoV-2-specific T cell functions differs in patients with mild/moderate versus severe disease, and T cells expressing coinhibitory receptors are highly activated. *J Immunol*. (2021) 207:1099–111. doi: 10.4049/jimmunol.2100446

89. Files JK, Boppana S, Perez MD, Sarkar S, Lowman KE, Qin K, et al. Sustained cellular immune dysregulation in individuals recovering from SARS-CoV-2 infection. *J Clin Invest*. (2021) 131. doi: 10.1172/JCI140491

90. Yin K, Peluso MJ, Luo X, Thomas R, Shin MG, Neidleman J, et al. Long COVID manifests with T cell dysregulation, inflammation and an uncoordinated adaptive immune response to SARS-CoV-2. *Nat Immunol*. (2024) 25:218–25. doi: 10.1038/s41590-023-01724-6

91. Paine SK, Choudhury P, Alam M, Bhattacharyya C, Pramanik S, Tripathi D, et al. Multi-faceted dysregulated immune response for COVID-19 infection explaining clinical heterogeneity. *Cytokine*. (2024) 174:156434. doi: 10.1016/j.cyto.2023.156434

92. Cezar R, Kundura L, Andre S, Lozano C, Vincent T, Muller L, et al. T4 apoptosis in the acute phase of SARS-CoV-2 infection predicts long COVID. *Front Immunol*. (2023) 14:1335352. doi: 10.3389/fimmu.2023.1335352

93. Chentoufi AA, Dhanushkodi NR, Srivastava R, Prakash S, Coulon PA, Zayou L, et al. Combinatorial herpes simplex vaccine strategies: from bedside to bench and back. *Front Immunol*. (2022) 13:849515. doi: 10.3389/fimmu.2022.849515

94. Srivastava R, Roy S, Coulon P, Vahed H, Parkash S, Dhanushkodi N, et al. Therapeutic mucosal vaccination of HSV-2 infected Guinea pigs with the ribonucleotide reductase 2 (RR2) protein boosts antiviral neutralizing antibodies and tissue-resident CD4+ and CD8+ TRM cells associated with protection against recurrent genital herpes. *J Virol In Press*. (2019). doi: 10.1128/JVI.02309-18

95. Srivastava R, Roy S, Coulon PG, Vahed H, Prakash S, Dhanushkodi N, et al. Therapeutic mucosal vaccination of herpes simplex virus 2-infected guinea pigs with ribonucleotide reductase 2 (rr2) protein boosts antiviral neutralizing antibodies and local tissue-resident cd4+ and cd8+ trm cells associated with protection against recurrent genital herpes. *J Virol*. (2019) 93(9):e02309-18. doi: 10.1128/JVI.02309-18

96. Roy S, Coulon PG, Srivastava R, Vahed H, Kim GJ, Walia SS, et al. Blockade of LAG-3 immune checkpoint combined with therapeutic vaccination restore the function of tissue-resident anti-viral CD8(+) T cells and protect against recurrent ocular herpes simplex infection and disease. *Front Immunol*. (2018) 9:2922. doi: 10.3389/fimmu.2018.02922

97. Allen SJ, Hamrah P, Gate D, Mott KR, Mantopoulos D, Zheng L, et al. The role of LAT in increased CD8+ T cell exhaustion in trigeminal ganglia of mice latently infected with herpes simplex virus 1. *J Virol*. (2011) 85:4184–97. doi: 10.1128/JVI.02290-10

98. Aydillo T, Rombauts A, Stadlbauer D, Aslam S, Abelenda-Alonso G, Escalera A, et al. Immunological imprinting of the antibody response in COVID-19 patients. *Nat Commun*. (2021) 12:3781. doi: 10.1038/s41467-021-23977-1

99. Bertoletti A, Le Bert N, Qui M, Tan AT. SARS-CoV-2-specific T cells in infection and vaccination. *Cell Mol Immunol*. (2021) 18:2307–12. doi: 10.1038/s41423-021-00743-3

100. Huang G, Kovalic AJ, Graber CJ. Prognostic value of leukocytosis and lymphopenia for coronavirus disease severity. *Emerg Infect Dis*. (2020) 26:1839–41. doi: 10.3201/eid2608.201160

101. Penaloza HF, Lee JS, Ray P. Neutrophils and lymphopenia, an unknown axis in severe COVID-19 disease. *PLoS Pathog*. (2021) 17:e1009850. doi: 10.1371/journal.ppat.1009850

102. Veiga-Parga T, Suryawanshi A, Mulik S, Gimenez F, Sharma S, Sparwasser T, et al. On the role of regulatory T cells during viral-induced inflammatory lesions. *J Immunol*. (2012) 189:5924–33. doi: 10.4049/jimmunol.1202322

103. Mengist HM, Kombe Kombe AJ, Mekonnen D, Abebaw A, Getachew M, Jin T. Mutations of SARS-CoV-2 spike protein: Implications on immune evasion and vaccine-induced immunity. *Semin Immunol*. (2021) 55:101533. doi: 10.1016/j.smim.2021.101533

104. Ahmad L. Implication of SARS-CoV-2 immune escape spike variants on secondary and vaccine breakthrough infections. *Front Immunol*. (2021) 12:742167. doi: 10.3389/fimmu.2021.742167

105. Sharma S, Vercruysse T, Sanchez-Felipe L, Kerstens W, Rasulova M, Bervoets L, et al. Updated vaccine protects against SARS-CoV-2 variants including Omicron (B.1.1.529) and prevents transmission in hamsters. *Nat Commun*. (2022) 13:6644. doi: 10.1038/s41467-022-34439-7

106. There's no room for COVID complacency in 2023. *Nature*. (2023) 613:7. doi: 10.1038/d41586-022-04476-9

frontiers | Frontiers in Immunology

TYPE Original Research
PUBLISHED 08 May 2024
DOI 10.3389/fimmu.2024.1386586

OPEN ACCESS

EDITED BY
Ahmed Yaqinuddin,
Alfaisal University, Saudi Arabia

REVIEWED BY
Sarah Elizabeth Jackson,
University of Cambridge, United Kingdom
Werner Dammermann,
Brandenburg Medical School Theodor Fontane, Germany

*CORRESPONDENCE
Matthias Unterberg
Matthias.Unterberg@kk-bochum.de

†These authors have contributed equally to this work and share first authorship

‡These authors have contributed equally to this work and share senior authorship

RECEIVED 15 February 2024
ACCEPTED 23 April 2024
PUBLISHED 08 May 2024

CITATION
Ziehe D, Wolf A, Rahmel T, Nowak H, Haberl H, Bergmann L, Rump K, Dyck B, Palmowski L, Marko B, Witowski A, Willemsen KM, Pfaender S, Eisenacher M, Anft M, Babel N, Bracht T, Sitek B, Bayer M, Zarbock A, von Groote T, Putensen C, Ehrentraut SF, Weisheit C, Adamzik M, Unterberg M and Koos B (2024) Exploring the relationship between HCMV serostatus and outcomes in COVID-19 sepsis. *Front. Immunol.* 15:1386586. doi: 10.3389/fimmu.2024.1386586

Exploring the relationship between HCMV serostatus and outcomes in COVID-19 sepsis

Dominik Ziehe[1†], Alexander Wolf[1†], Tim Rahmel[1], Hartmuth Nowak[1], Helge Haberl[1], Lars Bergmann[1], Katharina Rump[1], Birte Dyck[1], Lars Palmowski[1], Britta Marko[1], Andrea Witowski[1], Katrin Maria Willemsen[1], Stephanie Pfaender[2], Martin Eisenacher[3,4], Moritz Anft[5], Nina Babel[5], Thilo Bracht[1,3], Barbara Sitek[1,3], Malte Bayer[1,3], Alexander Zarbock[6], Thilo von Groote[6], Christian Putensen[7], Stefan Felix Ehrentraut[7], Christina Weisheit[7], Michael Adamzik[1], Matthias Unterberg[1*‡] and Björn Koos[1‡]

[1]Klinik für Anästhesiologie, Intensivmedizin und Schmerztherapie, Universitätsklinikum Knappschaftskrankenhaus Bochum, Bochum, Germany, [2]Department of Molecular and Medical Virology, Ruhr University Bochum, Bochum, Germany, [3]Medizinisches Proteom-Center, Ruhr-University Bochum, Bochum, Germany, [4]Medical Proteome Analysis, Center for Proteindiagnostics (PRODI), Ruhr University Bochum, Bochum, Germany, [5]Center for Translational Medicine, Medical Clinic I, Marien Hospital Herne, University Hospital of the Ruhr-University Bochum, Herne, Germany, [6]Klinik für Anästhesiologie, Operative Intensivmedizin und Schmerztherapie, Universitätsklinikum Münster, Münster, Germany, [7]Klinik für Anästhesiologie und Operative Intensivmedizin, Universitätsklinikum Bonn, Bonn, Germany

Background: Sepsis, a life-threatening condition caused by the dysregulated host response to infection, is a major global health concern. Understanding the impact of viral or bacterial pathogens in sepsis is crucial for improving patient outcomes. This study aimed to investigate the human cytomegalovirus (HCMV) seropositivity as a risk factor for development of sepsis in patients with COVID-19.

Methods: A multicenter observational study enrolled 95 intensive care patients with COVID-19-induced sepsis and 80 post-surgery individuals as controls. HCMV serostatus was determined using an ELISA test. Comprehensive clinical data, including demographics, comorbidities, and 30-day mortality, were collected. Statistical analyses evaluated the association between HCMV seropositivity and COVID-19 induced sepsis.

Results: The prevalence of HCMV seropositivity did not significantly differ between COVID-19-induced sepsis patients (78%) and controls (71%, $p = 0.382$) in the entire cohort. However, among patients aged ≤60 years, HCMV seropositivity was significantly higher in COVID-19 sepsis patients compared to controls (86% vs 61%, respectively; $p = 0.030$). Nevertheless, HCMV serostatus did not affect 30-day survival.

Discussion: These findings confirm the association between HCMV seropositivity and COVID-19 sepsis in non-geriatric patients. However, the lack of an independent effect on 30-day survival can be explained by the cross-reactivity of HCMV specific $CD8^+$ T-cells towards SARS-CoV-2 peptides, which might

confer some protection to HCMV seropositive patients. The inclusion of a post-surgery control group strengthens the generalizability of the findings. Further research is needed to elucidate the underlying mechanisms of this association, explore different patient populations, and identify interventions for optimizing patient management.

Conclusion: This study validates the association between HCMV seropositivity and severe COVID-19-induced sepsis in non-geriatric patients, contributing to the growing body of evidence on viral pathogens in sepsis. Although HCMV serostatus did not independently influence 30-day survival, future investigations should focus on unraveling the intricate interplay between HCMV, immune responses, and COVID-19. These insights will aid in risk stratification and the development of targeted interventions for viral sepsis.

KEYWORDS

viral sepsis, COVID-19 risk stratification, human cytomegalovirus, cross-reactive CD8$^+$ T-cells, COVID-19 survival

Introduction

Sepsis is an acute, life-threatening syndrome with millions of incidences each year (1). Up to 2020 the main pathogen inducing sepsis were bacteria (2, 3). However, similarly to bacterial pathogens, viruses are also capable of inducing critical conditions resulting in organ dysfunction and an increased Sequential Organ Failure Assessment (SOFA) Score (4) fulfilling the recent definition of sepsis [Sepsis-3 (5)]. During the COVID-19 pandemic up to 80% of sepsis cases were virally induced (6). In the post-pandemic era, the rate of virally sepsis has decreased; however, COVID-19 sepsis remains prevalent in ICUs worldwide, and it has guided the interest of clinicians towards virally induced sepsis, that was most likely underdiagnosed before (7).

In response to invasive bacterial pathogens, the human immune reaction initially involves the activation of the innate immunity. This consists of the complement-system as a non-cellular component as well as macrophages and neutrophile granulocytes and others as a cellular component, which opsonize, engulf and destroy bacteria. This is followed by the activation of a slower but more specific adaptive immune response. During the adaptive immune response, B-cells start the production of highly specific antibodies. Furthermore, T-cells that specifically target the invading bacteria are expanded.

In contrast, viral pathogens are intracellular and can partly evade from detection by the immune system. Thus, the immune response to viral infections involves the production of cytokines and specific interferons leading to

1. auto- and paracrine cellular effects, inhibiting intracellular viral replication (8) and
2. an activation of cytotoxic T-cells (CD8$^+$) to eliminate infected cells.

Therefore, a virus-specific cascade following an interferon-driven network with type 1 interferon (e.g. IFN-α) leading towards an inhibition of viral replication (9) is described. An inhibition of IL-10 and an upregulation of IL-16 (10) is observed but still incompletely understood and most probably not homogenous in different viral entities. During the pre-pandemic era, influenza was the predominant pathogen, associated to viral sepsis (2, 3).

The virus' ability to evade the host's immune defense and cause continuous inflammatory damage is accompanied by high levels of TNF-α and IL-6 as well as reduced IFN-γ expression (7). However, different viruses will most likely show different approaches to evading the immune defense (7).

In SARS-CoV-2-sepsis, the initially described cytokine storm turned out to be less pronounced, with moderate levels of IL-6 (11, 12) compared to bacterial sepsis.

Furthermore, an imbalance and predominance of non-type-1 cytokines (such as IL-4, or IL-17) is capable to draw the immune system towards an inappropriate response, leading to exhaustion of T-cells with ineffective clearance of viral-infected cells (7).

The immune response in COVID-19 sepsis is believed to differ significantly from bacterial immunity, characterized by a delayed and less severe response, as indicated by IL-6 serum concentrations (11, 12). When compared to Influenza, COVID-19-sepsis also develops with delayed symptoms and a prolonged inflammatory phase (12). The intricate immunological landscape involves a nuanced interplay of cytokines and key immunomodulatory elements, including Type 1 and Type 2 interferons, thereby demarcating a distinct divergence between bacterial and viral

immune responses (12). Specifically, the interferon response in severe COVID-19 is released later and less pronounced than in Influenza-induced sepsis, leading to longer disease duration (12). In this multifaceted milieu, various host-related factors exert influence on immune defenses, encompassing age, genetic predisposition (13) and comorbidities such as pulmonary diseases (14), cardiovascular diseases (15, 16) and obesity (17). Notably, the identification of human cytomegalovirus (HCMV) serostatus as an independent predictor of survival in bacterial sepsis has added a significant layer to our understanding of sepsis risk factors (18).

HCMV is a herpes virus that, subsequent to the primary active infection, remains in the host's body in a latent form detected by seropositivity. The virus re-activates frequently during life priming the immune system towards the anti-viral response. Reactivation of HCMV is mainly recognized during impaired immunity like transplant-related immunosuppression or during severe infection, often focused on sepsis. Here, reactivation is considered as a worsening factor regarding mortality, ICU-and hospital-duration and other secondary complication (19–23). Clear evidence for antiviral prophylaxis in these circumstances is still missing (24). A potential worsening effect of HCMV-reactivation on the clinical course of patients is also described in severe SARS-CoV-2, but this did not impact on patient's mortality (25) except in the very elderly (26). As a mechanistic link between HCMV-reactivation and a propagated SARS-CoV-2 infection, an upregulation of the ACE2-receptor in lung epithelial cells driven by HCMV is discussed (27). Furthermore, a study by Choi et al. (28) describes $CD8^+$ T-cell exhaustion following HCMV-reactivation.

Apart from HCMV-reactivation, HCMV in a controlled stage (latency) continuously concerns the human immunity and, in fact, HCMV seropositive patients have been reported to frequently have up to 20% of $CD8^+$ T-cells specific for HCMV (29–31) a number that only increases with age.

The narrative, however, extends further. In the context of COVID-19, HCMV emerges as a consequential player, associated with heightened hospitalization (32) and ICU admission, particularly in individuals under the age of 60 (33). Despite the relatively modest cohort size in which the association regarding ICU-admission was observed, the findings suggest a complex interplay between SARS-CoV-2 and HCMV.

Moreover, HCMV has the ability to disrupt the antigen presentation process of T- and NK-cells and affect the surface maintenance of TLR4 and TLR5 on HCMV-infected cells, consequently altering immune system cascades (34). Therefore, HCMV-induced impairment of the immune system may have a significant impact on the host's immunity during a subsequent COVID-19 infection and contribute to the development of secondary infections. Additionally, latent HCMV infection may alter the host's response to SARS-CoV-2 vaccination, as has been observed with other viral vaccinations such as influenza (35).

In view of these intriguing observations, our study endeavors to elucidate the impact of HCMV serostatus on 30-day survival and immune response in COVID-19 sepsis, drawing parallels with the established association between HCMV and bacterial sepsis.

Materials and methods

Patient recruitment and study design

This multicenter study was registered at the DRKS (DRKS00026184) and approved by the local ethics board of the Medical Faculty of Ruhr-University Bochum (Protocol No. 18-6606-BR) and the corresponding ethics boards of each study site. As part of the CovidDataNet.NRW project, we enrolled 95 intensive care patients with COVID-19-induced sepsis (severe COVID-19) from three different centers when SEPSIS-3 criteria were met. The recruitment period was from August 1, 2021, to March 31, 2022, and clinical data were collected in an observational approach. To be included in this study, patients had to meet the following criteria: evidence of infection with SARS-CoV-2 and evidence of underlying sepsis with an increased SOFA score of at least two points. Additionally, patients had to be aged 18 or above and provide informed consent. Beyond that, we selected 80 patients who had undergone abdominal surgery as a control group. Blood samples have been collected within 36 h after sepsis diagnosis at the University hospital Knappschaftskrankenhaus Bochum (KKB), University hospital Münster (UKM), and University hospital Bonn (UKB).

Determination of CMV serostatus (IgG) via ELISA

The SERION ELISA classic Cytomegalovirus IgG Kit (Institut Virion\Serion GmbH, Würzburg, Germany) was used to determine the IgG concentration in the patients' blood sera. According to the manufacturer's instructions, 100 µL of diluted samples (1:100) and respective controls were added to microtiter test wells and incubated for 60 minutes at 37°C in a wet chamber. After four washing steps, 100 µL of IgG conjugate solution was added and incubated for 30 minutes at 37°C. Four more washing steps were conducted, followed by the addition of 100 µL substrate solution. After 30 minutes at 37°C, the reactions were stopped by adding 100 µL stopping solution to each well. The optical densities (OD) were determined using a microplate reader (CLARIOstarPLUS, BMG LABTECH, Germany). OD values were measured at a wavelength of 405 nm and analyzed by CLARIOstar Data Analysis software. The values were normalized to a standard curve, and units were calculated. Samples were classified as CMV-IgG positive when 35 or more units were detected.

PBMC isolation

PBMCs of COVID-19 patients were isolated by subjecting the obtained blood samples to Ficoll density gradient centrifugation (GE Healthcare Europe, Freiburg, Germany). Subsequently, the

phase containing the PBMCs was collected. Following erythrocyte lysis, the collected PBMCs were stored at -196°C until use.

Immunophenotyping

Upon thawing, PBMCs were stained with 25 µl master mix, containing the optimal concentrations of each antibody, for 10 min at room temperature in the dark. Erythrocytes were lyzed using RBC Lysis Buffer (BioLegend, San Diego) for 10 min at room temperature in the dark and samples were immediately acquired on a CytoFlex flow cytometer (Beckman Coulter, Brea). Quality control was performed daily using the recommended CytoFlex Daily QC Fluorospheres (Beckman Coulter, Brea). No modification to the compensation matrix was required throughout the study.

Clinical data

Medical data, including laboratory values, vitals, demographics, point-of-care diagnostics, and length of ICU stay, were stored in a comprehensive database (CentraXX software, Kairos GmbH, Bochum, Germany) and pseudonymized according to the obligations of the Ethics Committee.

Statistics

Statistical analyses were performed using SPSS software Version 28 (IBM, Canada). Categorical variables were evaluated using Fisher's exact test, while continuous variables were first subjected to a Kolmogorov-Smirnov test to assess normality. If variables were normally distributed, they were evaluated using Student's t-test for independent samples. If variables were not normally distributed, they were subjected to a Mann-Whitney U test. Kaplan-Meier curves with subsequent log-rank tests were generated to depict 30-day survival as a function of CMV serostatus in COVID-19 patients.

Results

Study design

We systematically assessed the impact of HCMV serostatus on the 30-day mortality in the entire cohort of COVID-19 patients, comparing them to pre-pandemic post-surgery individuals. An additional focus was directed towards the non-geriatric sub-population (patients aged 60 years or younger at study inclusion), as illustrated in Figure 1.

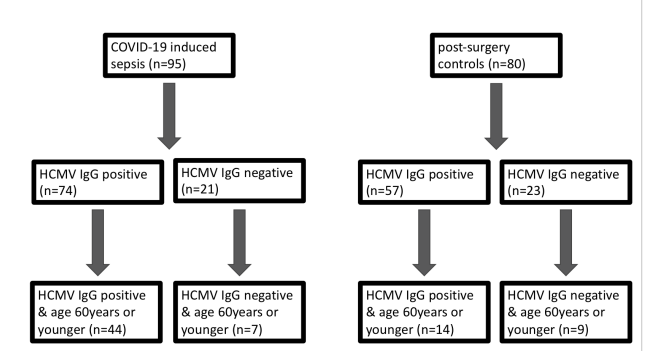

FIGURE 1
Grouping of patients with COVID-19 induced sepsis (left) and control subjects without infection (right) according to their CMV serostatus on day 1 and subsequently according to age (<= vs >60 years).

HCMV serostatus is not different between patients with severe COVID-19 and pre-pandemic patients

95 patients suffering from severe COVID-19 with virus induced sepsis and 80 pre-pandemic, post-surgery individuals without signs of infection (controls) were included in this prospective, observational study. 61% of the COVID-19 patients were male and the median age was 58 years (IQR 49-74years). This was not significantly different to the control cohort in which 38% were male (p=0,112) and the median age was 65 (IQR: 57-76) years (p=0,076).

The median SOFA-score at study inclusion was 9 (IQR 5-12) for the COVID-19 cohort. The 30-day mortality was 42%. Co-morbidities were assessed when available. Comparing the frequency of relevant co-morbidities between the COVID-19 and post-surgical patients, we find diabetes (22% vs. 12% respectively, p=0.023) and obesity (37% vs. 21%, p=0.001) to be more frequent in COVID-19 patients. Malignant diseases (5% vs. 80% p=0.001), alcohol abuse (1% vs. 11%, p=0.017) and nicotine addiction (6% vs. 36% p=0.001) were more frequent in controls. 78% of the COVID-19 patients were seropositive for HCMV-IgG at study inclusion. This was not significantly different than the control cohort (71%, p = 0.382, Figure 2A).

Additional baseline characteristics are presented in Table 1 and immune phenotyping with regard to HCMV-serostatus is shown in Supplementary Table 1.

In patients 60 years or younger, the frequency of HCMV seropositivity is significantly higher than in comparable control patients

The non-geriatric sub-population of these cohorts (i.e. patients under or equal 60 years of age) consisted of 51 patients with severe COVID-19 and 23 post-surgery individuals. In this cohort, 65% of the COVID-19 patients were male, compared to only 39% in the control cohort (p=0.047). The median age in COVID-19 patients and controls was almost equal (49 [IQR:45-56] vs. 50 [IQR: 35-57] years respectively, p = 0.935). The 30-day survival in these COVID-19 patients was 59%. The median SOFA score at study inclusion was 9 (IQR: 5.5 – 12). When comparing co-morbidities, we find significantly more malignant diseases (5% vs. 87%, p=0.001) as well as a higher frequency of nicotine-abuse in post-surgery patients (10% vs. 30%, p=0.043), which aligns with the general cohort. At the

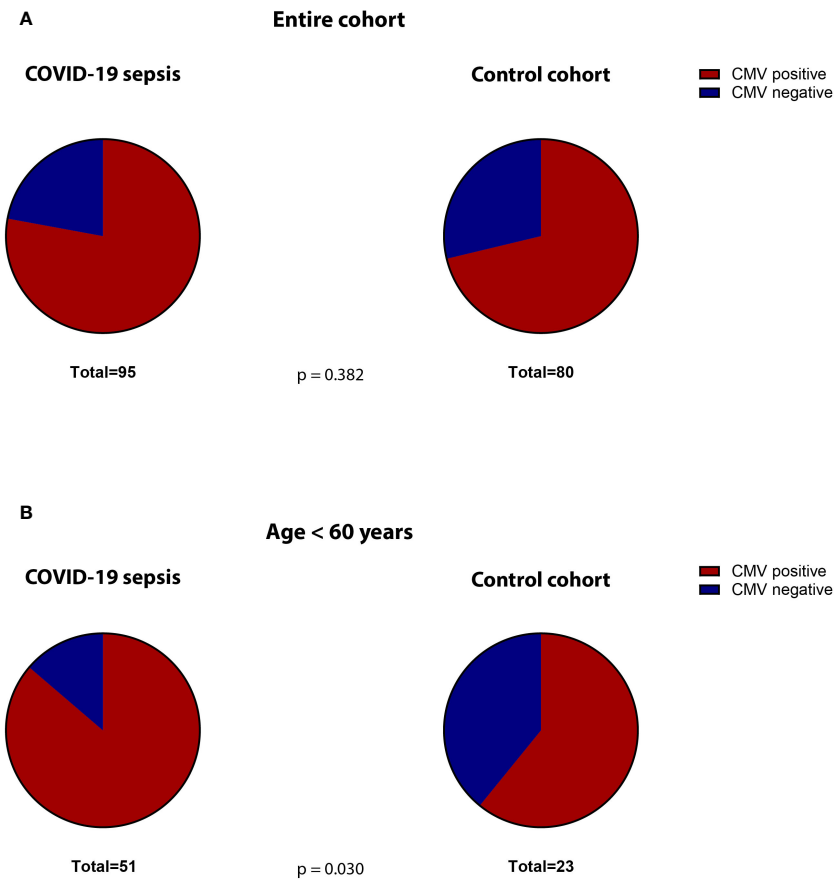

FIGURE 2
Proportion of CMV-seropositive (red) versus -seronegative (blue) patients in the **(A)** total cohorts (COVID-19 versus controls) and **(B)** in the subgroup of non-geriatric patients (COVID-19 versus controls).

time of admission, 86% of the non-geriatric COVID-19 patients presented sero-positive for HCMV-IgG, while only 61% of the post-surgery controls did so (p=0,030, Figure 2B).

Table 2 depicts patients characteristics of the non-geriatric patients.

HCMV serostatus does not affect 30-day mortality

We assessed the effect of the HCMV serostatus on 30-day mortality in the entire cohort of patients with severe COVID-19. We could not identify HCMV seropositivity as a prognostic factor in this cohort. The Kaplan Meier Analysis (Figures 3A, B) shows no significant effect (survival: 57% vs. 58% for HCMV seronegative vs. seropositive respectively, p = 0.721, log rank test).

Discussion

In our study, we observed no significant impact of HCMV serostatus on the 30-day mortality in COVID-19 sepsis. This finding contrasts starkly with bacterial sepsis, where HCMV serostatus was an independent risk factor for mortality (18). The intriguing divergence prompts contemplation on the nuanced interplay between HCMV, T-cell dynamics, and the heterogeneous landscape of COVID-19 sepsis.

The association of HCMV seropositivity with a specialized T-cell pool and diminished naïve T-cell reservoirs, known as T-cell inflation (36), has been postulated to render HCMV-seropositive patients more susceptible to heterologous infections, as their T-cell repertoire is significantly diminished (37). This might well be an explanation for the effects of HCMV on bacterial sepsis patients (18).

However, why does this not translate to COVID-19 sepsis? Interestingly, HCMV specific $CD8^+$ T-cells have been shown to react to SARS-CoV-2 peptides (38) just as SARS-CoV-2 T-cell reacted to HCMV (33). This would grant HCMV seropositive patients a certain protection from COVID-19 induced death, as T-cell function is an important factor when it comes to SARS-CoV-2 immunity (39).

But how does this fit to the findings of others, that have reported that HCMV might be a risk factor for severe COVID-19 in non-geriatric patients (34)? This is especially interesting as we find the same effect of COVID-19 patients under the age of 60 more frequently being HCMV seropositive than post-surgical control patients of the same age group.

We assume, the explanation lies in the characteristic timeline of T-cell inflation, which unfolds over a longer lifetime due to

10.3389/fimmu.2024.1386586

TABLE 1 Baseline characteristics of COVID-19 ICU patients and post-surgery control patients.

	COVID-19 induced sepsis n=95	post-surgery patients; n=80	p-value
gender male	58 (61%)	35 (48%);	0.117
CMV-IgG positive at day one	74 (78%)	57 (71%);	0.382
age in years median (IQR)	58 (49-74)	65 (57-76);	0.076
SOFA score at day one median (IQR)	9 (5-12)	n.a.	n.a.
Median Oxygenation-Index (paO_2/FiO_2) day 1 (median ± IQR)	157 (115-191) n=49	n.a.	n.a.
Mean arterial blood pressure (MAP) day 1 (median ± IQR)	84 (79-92) n=53	n.a.	n.a.
Number of patients receiving adrenalin on day 1	1	n.a.	n.a.
Number of patients receiving dobutamin on day 1	3	n.a.	n.a.
Number of patients receiving noradrenalin on day 1	27	n.a.	n.a.
Platelet count day 1 (lowest value, median ± IQR)	217 (130-283) n=58	n.a.	n.a.
Serum creatinin (mg/dl) day 1 (highest value, median ± IQR)	0,54 (0,34-0,78) n=58	n.a.	n.a.
Serum bilirubine (mg/dl) day 1 (highest value, median ± IQR)	0,88 (0,73-1,33) n= 56	n.a.	n.a.
Co-Morbidities			
- pulmonal (non copd)	10 (11%)	11 (15%)	0.818
- copd	5 (5%)	12 (16%)	0.076
- nicotin	6 (6%)	26 (36%)	0.001
- diabetes	21 (22%)	9 (12%)	0.023
- hypertension	42 (44%)	46 (63%)	0.502
- obesity	35 (37%)	15 (21%)	0.001
- cardiovascular	16 (17%)	23 (32%)	0.195
- malignant	5 (5%)	58 (80%)	0.001
- alcohol	1 (1%)	8 (11%)	0.017
- transplantation	7 (7%)	1 (1%)	0.063
- Kidney (non rrt)	11 (12%)	4 (6%)	0.100
- renal replacement therapy (rrt)	0 (0%)	0 (0%)	n.a.
length of stay on ICU days median (IQR)	18 (6-29,5)	n.a.	n.a.
length of stay in hospital median (IQR)	21 (12-31,5)	11 (6-21)	0.001
30-day survival	55 (57,9%)	80 (100%)	0.001
Leukocyte count (cells*1000/µl) median (IQR) day 1	10,3 (7,2-13,7)	8,5 (6,3-12,5)	0.225

(Continued)

TABLE 1 Continued

n.a., not applicable.

TABLE 2 Baseline characteristics of COVID-19 ICU patients and post-surgery control patients aged 18-60years.

	COVID-19 induced sepsis <60years; n=51	postoperative patients <60years; n=23	p-value
gender male	33 (65%)	9 (39%)	0.047
CMV-IgG positive at day one	44 (86%)	14 (61%)	0.030
age in years median (IQR)	49 (45-56)	50 (35-57)	0.935
SOFA score at day one median (IQR)	9 (5,5-12)	n.a.	
Co-Morbidities			
- pulmonal (non copd)	3 (7%)	3 (13%)	0.657
- copd	2 (5%)	4 (17%)	0.174
- nicotin	4 (10%)	7 (30%)	0.043
- diabetes	11 (26%)	3 (13%)	0.345
- hypertension	18 (43%)	9 (39%)	0.799
- obesity	24 (57%)	6 (26%)	0.021
- cardiovascular	4 (10%)	2 (8%)	1.000
- malignant	2 (5%)	20 (87%)	0.001
- alcohol	1 (2%)	3 (13%)	0.123
- transplantation	3 (7%)	1 (4%)	1.000
- Kidney (non rrt)	5 (12%)	1 (4%)	0.411
- renal replacement therapy	0 (0%)	0 (0%)	n.a.
length of stay on ICU days median (IQR)	21 (6-35)	n.a.	n.a.
length of stay in hospital median (IQR)	23 (10,5-42,5)	13 (6-22)	0.025
30-day survival	30 (59%)	23 (100%)	0.001

n.a., not applicable.

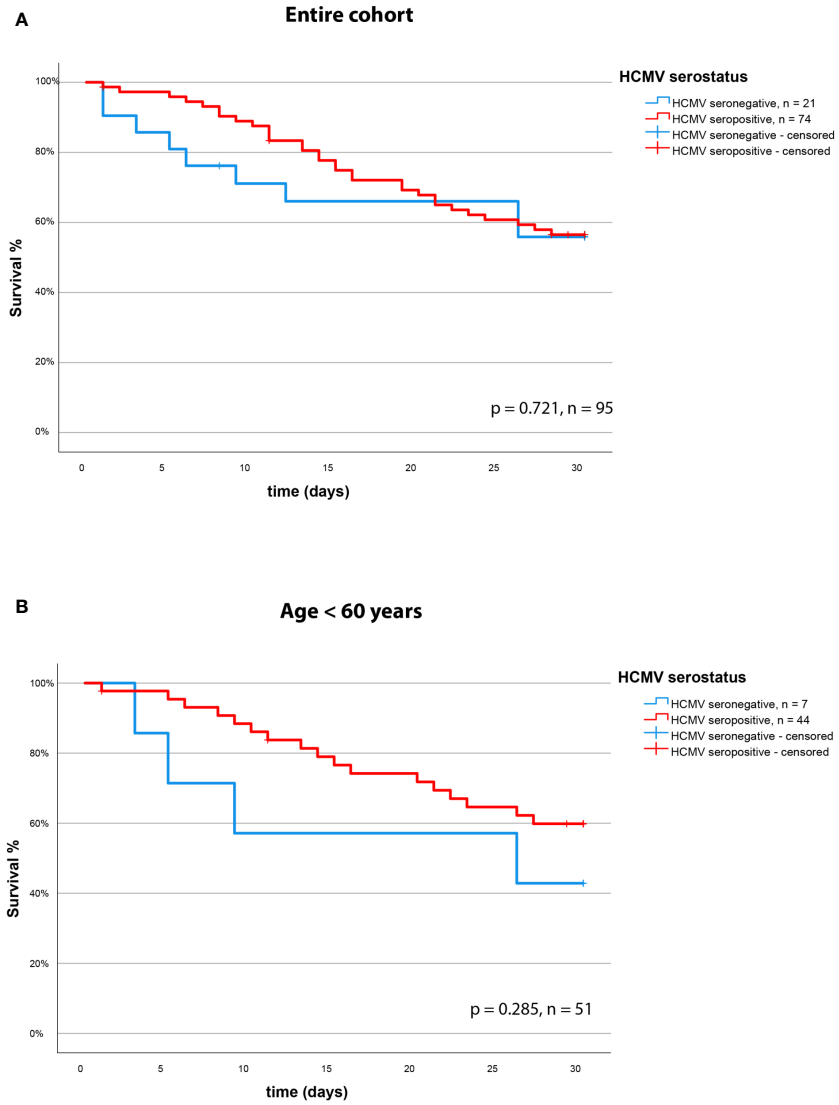

FIGURE 3
30-day survival (Kaplan-Meier curve) based on HCMV serostatus in **(A)** the overall cohort and **(B)** in the subgroup of non-geriatric patients.

recurrent HCMV reactivations (37). Consequently, any discernible effects on the immune system may be more pronounced in older patients, thereby explaining the association of HCMV with COVID-19 sepsis in younger adults.

Crucially, our study's design deviates from previous works, such as Weber et al. (34), by contrasting severe COVID-19 cases with a pre-pandemic cohort of post-surgery patients devoid of infection or sepsis development. This approach enhances the generalizability of our findings beyond specific COVID-19 patient subsets, thereby augmenting the external validity of our results. This becomes particularly crucial when considering potential interventions or preventive measures based on our observations. What needs to be discussed at this point, is the main and obvious condition, distinguishing our post-surgery cohort from the COVID-19 patients under the age of 60 years: One main reason for surgery were malignant diseases. Thus, we cannot exclude that the known association between HCMV and malignancies (40) (41) plays further role. In this light the association does not contradict our interpretation, as we find even higher rates of HCMV-seropositivity in the COVID-19 patients than in the post-surgery cohort.

Future investigations should delve into the intricate interactions among HCMV, the immune system, and the pathogenesis of COVID-19-induced sepsis, with a specific focus on delineating the role of T-cell function and its implications for disease outcomes. By unraveling the underlying mechanisms, exploring associations in diverse patient populations, and scrutinizing potential interventions, we can deepen our understanding of HCMV's impact on COVID-19 and potentially enhance patient management strategies.

Nevertheless, our study harbors limitations that warrant acknowledgment. Despite a relatively larger COVID-19 cohort compared to previous studies, the sample size remains modest, particularly when undertaking subgroup analyses. Thus, we advocate for retrospective assessments of HCMV serostatus in

larger observational COVID-19 trials to validate our findings rigorously. The prevalence of HCMV seropositivity in the non-geriatric COVID-19 cohort introduces another constraint, diminishing the size of the seronegative cohort. As such, caution is warranted, and we refrain from definitively ruling out an effect of HCMV serostatus on the 30-day mortality in the non-geriatric cohort, given our limited statistical power.

In conclusion, our investigation unveils that HCMV seropositivity does not exert a discernible effect on the 30-day mortality in COVID-19 patients. However, a nuanced association surfaces, suggesting HCMV as a potential risk factor for severe disease, particularly in younger patients. This dichotomy underscores the complexity of viral-bacterial interactions within the immune landscape and underscores the need for further extensive studies to refine our comprehension.

Data availability statement

The raw data supporting the conclusions of this article will be made available by the authors, without undue reservation.

Ethics statement

The studies involving humans were approved by Ethics Committee of the Medical Faculty of Ruhr-University Bochum. The studies were conducted in accordance with the local legislation and institutional requirements. The participants provided their written informed consent to participate in this study.

Author contributions

DZ: Investigation, Writing – original draft, Writing – review & editing. AWo: Conceptualization, Data curation, Validation, Writing – original draft, Writing – review & editing. TR: Project administration, Writing – review & editing. HN: Software, Validation, Writing – review & editing. HH: Data curation, Writing – original draft. LB: Resources, Writing – review & editing. KR: Methodology, Resources, Writing – original draft. BD: Investigation, Writing – review & editing. LP: Data curation, Investigation, Writing – original draft. BM: Data curation, Writing – original draft. AWi: Data curation, Writing – review & editing. KW: Data curation, Writing – review & editing. SP: Supervision, Writing – review & editing. ME: Conceptualization, Investigation, Writing – review & editing. MoA: Conceptualization, Writing – review & editing. NB: Conceptualization, Writing – review & editing. TB: Conceptualization, Data curation, Methodology, Writing – review & editing. BS: Conceptualization, Methodology, Writing – review & editing. MB: Data curation, Writing – original draft. AZ: Conceptualization, Data curation, Writing – review & editing. TV: Data curation, Writing – review & editing. CP: Conceptualization, Writing – review & editing. SE: Data curation, Formal Analysis, Writing – original draft. CW: Data curation, Writing – review & editing. MiA: Conceptualization, Data curation, Funding acquisition, Project administration, Resources, Supervision, Writing – review & editing. MU: Data curation, Investigation, Methodology, Resources, Visualization, Writing – original draft. BK: Conceptualization, Formal Analysis, Funding acquisition, Investigation, Methodology, Project administration, Supervision, Writing – original draft, Writing – review & editing.

Funding

The author(s) declare that financial support was received for the research, authorship, and/or publication of this article. The CovidDataNet.NRW project was supported by the Ministerium für Wirtschaft, Innovation, Digitalisierung und Energie (MWIDE), Federal State of North Rhine-Westphalia. The SepsisDataNet.NRW study was supported by the European Regional Development Fund (EFRE.NRW, reference number LS-1-2-012).

Acknowledgments

We acknowledge support by the Open Access Publication Funds of the Ruhr-Universität Bochum.

Conflict of interest

The authors declare that the research was conducted in the absence of any commercial or financial relationships that could be construed as a potential conflict of interest.

Publisher's note

Supplementary material

The Supplementary Material for this article can be found online at: https://www.frontiersin.org/articles/10.3389/fimmu.2024.1386586/full#supplementary-material

SUPPLEMENTARY FIGURE 1
(A) Proportion of CMV-seropositive (red) versus -seronegative (blue) patients in the geriatric (>=60years) cohort (COVID-19 and controls). **(B)** 30-day survival (Kaplan-Meier curve) based on HCMV serostatus in the geriatric COVID-19 cohort (>=60years).

References

1. Fleischmann-Struzek C, Schwarzkopf D, Reinhart K. [Sepsis incidence in Germany and worldwide: Current knowledge and limitations of research using health claims data]. *Med Klin Intensivmed Notfmed*. (2022) 117:264–8. doi: 10.1007/s00063-021-00777-5

2. Umemura Y, Ogura H, Takuma K, Fujishima S, Abe T, Kushimoto S, et al. Current spectrum of causative pathogens in sepsis: A prospective nationwide cohort study in Japan. *Int J Infect Dis*. (2021) 103:343–51. doi: 10.1016/j.ijid.2020.11.168

3. Sakr Y, Jaschinski U, Wittebole X, Szakmany T, Lipman J, Namendys-Silva SA, et al. Sepsis in intensive care unit patients: worldwide data from the intensive care over nations audit. *Open Forum Infect Dis*. (2018) 5:ofy313. doi: 10.1093/ofid/ofy313

4. Vincent JL, Moreno R, Takala J, Willatts S, De Mendonca A, Bruining H, et al. The SOFA (Sepsis-related Organ Failure Assessment) score to describe organ dysfunction/failure. On behalf of the Working Group on Sepsis-Related Problems of the European Society of Intensive Care Medicine. *Intensive Care Med*. (1996) 22:707–10. doi: 10.1007/BF01709751

5. Singer M, Deutschman CS, Seymour CW, Shankar-Hari M, Annane D, Bauer M, et al. The third international consensus definitions for sepsis and septic shock (Sepsis-3). *JAMA*. (2016) 315:801–10. doi: 10.1001/jama.2016.0287

6. Karakike E, Giamarellos-Bourboulis EJ, Kyprianou M, Fleischmann-Struzek C, Pletz MW, Netea MG, et al. Coronavirus disease 2019 as cause of viral sepsis: A systematic review and meta-analysis. *Crit Care Med*. (2021) 49:2042–57. doi: 10.1097/CCM.0000000000005195

7. Lin GL, McGinley JP, Drysdale SB, Pollard AJ. Epidemiology and immune pathogenesis of viral sepsis. *Front Immunol*. (2018) 9:2147. doi: 10.3389/fimmu.2018.02147

8. Schoggins JW, Rice CM. Interferon-stimulated genes and their antiviral effector functions. *Curr Opin Virol*. (2011) 1:519–25. doi: 10.1016/j.coviro.2011.10.008

9. Levy DE, Marie IJ, Durbin JE. Induction and function of type I and III interferon in response to viral infection. *Curr Opin Virol*. (2011) 1:476–86. doi: 10.1016/j.coviro.2011.11.001

10. Ludwiczek O, Kaser A, Koch RO, Vogel W, Cruikshank WW, Tilg H. Activation of caspase-3 by interferon alpha causes interleukin-16 secretion but fails to modulate activation induced cell death. *Eur Cytokine Netw*. (2001) 12:478–86.

11. Remy KE, Brakenridge SC, Francois B, Daix T, Deutschman CS, Monneret G, et al. Immunotherapies for COVID-19: lessons learned from sepsis. *Lancet Respir Med*. (2020) 8:946–9. doi: 10.1016/S2213-2600(20)30217-4

12. Gallo CG, Fiorino S, Posabella G, Antonacci D, Tropeano A, Pausini E, et al. COVID-19, what could sepsis, severe acute pancreatitis, gender differences, and aging teach us? *Cytokine*. (2021) 148:155628. doi: 10.1016/j.cyto.2021.155628

13. Schenz J, Rump K, Siegler BH, Hemmerling I, Rahmel T, Thon JN, et al. Increased prevalence of clonal hematopoiesis of indeterminate potential in hospitalized patients with COVID-19. *Front Immunol*. (2022) 13:968778. doi: 10.3389/fimmu.2022.968778

14. Rognvaldsson KG, Eythornorsson ES, Emilsson OI, Eysteinsdottir B, Palsson R, Gottfreethsson M, et al. Obstructive sleep apnea is an independent risk factor for severe COVID-19: a population-based study. *Sleep*. (2022) 45(3):1–7. doi: 10.1093/sleep/zsab272

15. Harrison SL, Buckley BJR, Rivera-Caravaca JM, Zhang J, Lip GYH. Cardiovascular risk factors, cardiovascular disease, and COVID-19: an umbrella review of systematic reviews. *Eur Heart J Qual Care Clin Outcomes*. (2021) 7:330–9. doi: 10.1093/ehjqcco/qcab029

16. Mustroph J, Hupf J, Baier MJ, Evert K, Brochhausen C, Broeker K, et al. Cardiac fibrosis is a risk factor for severe COVID-19. *Front Immunol*. (2021) 12:740260. doi: 10.3389/fimmu.2021.740260

17. Sattar N, Valabhji J. Obesity as a risk factor for severe COVID-19: summary of the best evidence and implications for health care. *Curr Obes Rep*. (2021) 10:282–9. doi: 10.1007/s13679-021-00448-8

18. Unterberg M, Ehrentraut SF, Bracht T, Wolf A, Haberl H, von Busch A, et al. Human cytomegalovirus seropositivity is associated with reduced patient survival during sepsis. *Crit Care*. (2023) 27:417. doi: 10.1186/s13054-023-04713-1

19. Limaye AP, Kirby KA, Rubenfeld GD, Leisenring WM, Bulger EM, Neff MJ, et al. Cytomegalovirus reactivation in critically ill immunocompetent patients. *JAMA*. (2008) 300:413–22. doi: 10.1001/jama.300.4.413

20. Kalil AC, Florescu DF. Prevalence and mortality associated with cytomegalovirus infection in nonimmunosuppressed patients in the intensive care unit. *Crit Care Med*. (2009) 37:2350–8. doi: 10.1097/CCM.0b013e3181a3aa43

21. Lachance P, Chen J, Featherstone R, Sligl WI. Association between cytomegalovirus reactivation and clinical outcomes in immunocompetent critically ill patients: A systematic review and meta-analysis. *Open Forum Infect Dis*. (2017) 4:ofx029. doi: 10.1093/ofid/ofx029

22. Osawa R, Singh N. Cytomegalovirus infection in critically ill patients: a systematic review. *Crit Care*. (2009) 13:R68. doi: 10.1186/cc7875

23. Walton AH, Muenzer JT, Rasche D, Boomer JS, Sato B, Brownstein BH, et al. Reactivation of multiple viruses in patients with sepsis. *PloS One*. (2014) 9:e98819. doi: 10.1371/journal.pone.0098819

24. Imlay H, Limaye AP. Current understanding of cytomegalovirus reactivation in critical illness. *J Infect Dis*. (2020) 221:S94–S102. doi: 10.1093/infdis/jiz638

25. Shen HC, Feng JY, Sun CY, Huang JR, Chen YM, Chen WC, et al. Analysis of the effect of cytomegalovirus infection in clinical outcomes and prolonged duration of SARS-CoV-2 shedding in intensive care unit patients with COVID-19 pneumonia. *Ther Adv Respir Dis*. (2023) 17:17534666231209150. doi: 10.1177/17534666231209150

26. Giacconi R, Cardelli M, Piacenza F, Pierpaoli E, Farnocchia E, Di Rosa M, et al. Effect of cytomegalovirus reactivation on inflammatory status and mortality of older COVID-19 patients. *Int J Mol Sci*. (2023) 24(7):6832. doi: 10.3390/ijms24076832

27. Perera MR, Greenwood EJD, Crozier TWM, Elder EG, Schmitt J, Crump CM, et al. Human cytomegalovirus infection of epithelial cells increases SARS-coV-2 superinfection by upregulating the ACE2 receptor. *J Infect Dis*. (2023) 227:543–53. doi: 10.1093/infdis/jiac452

28. Choi YJ, Kim SB, Kim JH, Park SH, Park MS, Kim JM, et al. Impaired polyfunctionality of CD8(+) T cells in severe sepsis patients with human cytomegalovirus reactivation. *Exp Mol Med*. (2017) 49:e382. doi: 10.1038/emm.2017.146

29. Gillespie GM, Wills MR, Appay V, O'Callaghan C, Murphy M, Smith N, et al. Functional heterogeneity and high frequencies of cytomegalovirus-specific CD8(+) T lymphocytes in healthy seropositive donors. *J Virol*. (2000) 74:8140–50. doi: 10.1128/JVI.74.17.8140-8150.2000

30. Lang KS, Moris A, Gouttefangeas C, Walter S, Teichgraber V, Miller M, et al. High frequency of human cytomegalovirus (HCMV)-specific CD8+ T cells detected in a healthy CMV-seropositive donor. *Cell Mol Life Sci*. (2002) 59:1076–80. doi: 10.1007/s00018-002-8488-5

31. Khan N, Shariff N, Cobbold M, Bruton R, Ainsworth JA, Sinclair AJ, et al. Cytomegalovirus seropositivity drives the CD8 T cell repertoire toward greater clonality in healthy elderly individuals. *J Immunol*. (2002) 169:1984–92. doi: 10.4049/jimmunol.169.4.1984

32. Alanio C, Verma A, Mathew D, Gouma S, Liang G, Dunn T, et al. Cytomegalovirus latent infection is associated with an increased risk of COVID-19-related hospitalization. *J Infect Dis*. (2022) 226:463–73. doi: 10.1093/infdis/jiac020

33. Weber S, Kehl V, Erber J, Wagner KI, Jetzlsperger AM, Burrell T, et al. CMV seropositivity is a potential novel risk factor for severe COVID-19 in non-geriatric patients. *PloS One*. (2022) 17:e0268530. doi: 10.1371/journal.pone.0268530

34. Zheng L, Li H, Fu L, Liu S, Yan Q, Leng SX. Blocking cellular N-glycosylation suppresses human cytomegalovirus entry in human fibroblasts. *Microb Pathog*. (2020) 138:103776. doi: 10.1016/j.micpath.2019.103776

35. Goodier MR, Rodriguez-Galan A, Lusa C, Nielsen CM, Darboe A, Moldoveanu AL, et al. Influenza vaccination generates cytokine-induced memory-like NK cells: impact of human cytomegalovirus infection. *J Immunol*. (2016) 197:313–25. doi: 10.4049/jimmunol.1502049

36. Derhovanessian E, Maier AB, Hahnel K, Beck R, de Craen AJM, Slagboom EP, et al. Infection with cytomegalovirus but not herpes simplex virus induces the accumulation of late-differentiated CD4+ and CD8+ T-cells in humans. *J Gen Virol*. (2011) 92:2746–56. doi: 10.1099/vir.0.036004-0

37. Redeker A, Remmerswaal EBM, van der Gracht ETI, Welten SPM, Hollt T, Koning F, et al. The contribution of cytomegalovirus infection to immune senescence is set by the infectious dose. *Front Immunol*. (2017) 8:1953. doi: 10.3389/fimmu.2017.01953

38. Pothast CR, Dijkland RC, Thaler M, Hagedoorn RS, Kester MGD, Wouters AK, et al. SARS-CoV-2-specific CD4(+) and CD8(+) T cell responses can originate from cross-reactive CMV-specific T cells. *Elife*. (2022) 11:e82050. doi: 10.7554/eLife.82050

39. Moss P. The T cell immune response against SARS-CoV-2. *Nat Immunol*. (2022) 23:186–93. doi: 10.1038/s41590-021-01122-w

40. Cobbs C. Cytomegalovirus is a tumor-associated virus: armed and dangerous. *Curr Opin Virol*. (2019) 39:49–59. doi: 10.1016/j.coviro.2019.08.003

41. Herbein G. Tumors and Cytomegalovirus: An Intimate Interplay. *Viruses*. 14 (4):812. doi: 10.3390/v14040812

frontiers | Frontiers in Immunology

TYPE Original Research
PUBLISHED 10 May 2024
DOI 10.3389/fimmu.2024.1394429

OPEN ACCESS

EDITED BY
Aristo Vojdani,
Immuno Sciences Lab Inc., United States

REVIEWED BY
Stelvio Tonello,
University of Eastern Piedmont, Italy
Suguru Saito,
Cedars Sinai Medical Center, United States

*CORRESPONDENCE
Yanli Kang
kangyanli614279133@163.com
Liangyuan Chen
liangyuan039083@163.com

†These authors have contributed equally to this work

RECEIVED 01 March 2024
ACCEPTED 23 April 2024
PUBLISHED 10 May 2024

CITATION
You J, Huang R, Zhong R, Shen J, Huang S, Chen J, Chen F, Kang Y and Chen L (2024) Serum AXL is a potential molecular marker for predicting COVID-19 progression. *Front. Immunol.* 15:1394429. doi: 10.3389/fimmu.2024.1394429

Serum AXL is a potential molecular marker for predicting COVID-19 progression

Jianbin You[1,2†], Rong Huang[1†], Ruifang Zhong[1], Jing Shen[2], Shuhang Huang[3], Jinhua Chen[2], Falin Chen[2], Yanli Kang[1,2*] and Liangyuan Chen[1,2*]

[1]Department of Clinical Laboratory, Shengli Clinical Medical College of Fujian Medical University, Fuzhou, Fujian, China, [2]Department of Clinical Laboratory, Fujian Provincial Hospital, Fuzhou, Fujian, China, [3]The School of Basic Medical Sciences, Fujian Medical University, Fuzhou, Fujian, China

Background: The severity, symptoms, and outcome of COVID-19 is thought to be closely linked to how the virus enters host cells. This process involves the key roles of angiotensin-converting enzyme 2 (ACE2) and the Tyrosine protein kinase receptor UFO (AXL) receptors. However, there is limited research on the circulating levels of ACE2 and AXL and their implications in COVID-19.

Methods: A control group of 71 uninfected individuals was also included in the study. According to the Guidance for Corona Virus Disease 2019 (10th edition), a cohort of 358 COVID-19 patients were categorized into non-severe and severe cases. Serum ACE2/AXL levels in COVID-19 patients were detected by enzyme-linked immunosorbent assay (ELISA) at different time points post-COVID-19 infection, including days 0-7, 8-15, 31-179 and >180 days. Serum SARS-CoV-2 IgG/IgM antibodies in COVID-19 patients at the same intervals were assessed by using an iFlash 3000 Chemiluminescence Immunoassay Analyzer. The receiver operating characteristic (ROC) curves were used to assess the diagnostic value of the biological markers, and the association between laboratory parameters and illness progression were explored.

Results: Compared with the uninfected group, the levels of ACE2 and AXL in the COVID-19 group were decreased, and the SARS-COV-2 IgG level was increased. AXL (AUC = 0.774) demonstrated a stronger predictive ability for COVID-19 than ACE2. In the first week after infection, only the level of AXL was statistically different between severe group and non-severe group. After first week, the levels of ACE2 and AXL were different in two groups. Moreover, in severe COVID-19 cases, the serum ACE2, AXL, and SARS-COV-2 IgM levels reached a peak during days 8–15 before declining, whereas serum SARS-COV-2 IgG levels continued to rise, reaching a peak at day 31-180 days before decreasing. In addition, the AXL level continued to decrease and the SARS-COV-2 IgG level continued to increase in the infected group after 180 days compared to the uninfected group.

Conclusions: The levels of serum ACE2 and AXL correlate with COVID-19 severity. However, AXL can also provide early warning of clinical deterioration in the first week after infection. AXL appears to be a superior potential molecular marker for predicting COVID-19 progression.

KEYWORDS

AXL, ACE2, SARS-CoV-2 IgG/IgM antibodies, COVID-19, biomarker

1 Introduction

The COVID-19 pandemic, resulting from SARS-CoV-2 infection, has imposed a significant global burden since its initial report in December 2019 (1, 2). The COVID-19 vaccination programs have been implemented worldwide, and have effectively prevented numerous deaths from SARS-CoV-2 infection (2). However, the rise of persistent viral immune evasion has led to waves of new SARS-CoV-2 variants, such as the Delta and Omicron strains. They are more deadly or contagious, which make existing vaccines less effective (3). The clinical spectrum of the disease ranges from asymptomatic or mild cases to severe manifestations like acute hepatitis or liver failure (4). A substantial portion of individuals with COVID-19 experience severe illness and require intensive care, particularly in the elder (5).

The severity, symptoms, and outcome of COVID-19 is thought to be linked to virus-induced damage to cells and the ability of the virus to evade the host immune system. It has been established that SARS-CoV-2 gains cellular entry by binding to angiotensin-converting enzyme 2 (ACE2) via its spike protein (6, 7). ACE2 expression is detected in various human organs, including the liver, lung, stomach, kidney, and colon, albeit at relatively low levels, especially in the lung (8). Despite sharing the same receptor (ACE2) for cell entry as SARS-CoV, SARS-CoV-2 is more infectious and transmissible. It is plausible that SARS-CoV-2 might rely on additional receptors for effective infection. Tyrosine protein kinase receptor UFO (AXL) functions as a receptor tyrosine kinase transmitting signals from the extracellular matrix to the cytoplasm (9). It has also been identified as a potential receptor for SARS-CoV-2. It interacts directly with the N-terminal domain of SARS-CoV-2 spike glycoprotein to facilitate infection of pulmonary and bronchial epithelial cells (10).

The roles of ACE2 and AXL receptors are crucial in the context of COVID-19. Both of them exist in membrane-bound form and soluble form, and the distinct forms elicit varying impacts (11). Metallo-endopeptidase A and Metalloproteinasesadam are responsible for their hydrolysis, yielding soluble ACE2 and soluble AXL. Researchers have linked elevated levels of soluble AXL to various cancers and have identified it as a cancer biomarker (12). Nonetheless, research on circulating levels of soluble ACE2 and AXL and their implications in COVID-19 patients remains limited.

Our study aimed to analyze the serum levels of ACE2 and AXL in individuals during the acute phase of COVID-19, in comparison to healthy individuals. In addition, we sought to investigate the serum levels of ACE2 and AXL in patients at different time points post-COVID-19 infection and determine if these levels correlate with COVID-19 progression.

2 Methods

2.1 Study design

Between December 2022 to October 2023, a total of 358 patients with COVID-19 were enrolled in Fujian Provincial hospitals in Fujian Province. COVID-19 was diagnosed through a nasopharyngeal reverse-transcription polymerase chain reaction (RT-PCR) assay or SARS-CoV-2 antigen rapid test. All patients were subdivided into mild or moderate or severe or critical according to the Guidance for Corona Virus Disease 2019 (10th edition) released by the National Health Commission of China (https://www.chinacdc.cn/jkzt/crb/zl/szkb_11803/jszl_11815/202301/t20230107_263257.html). During the study period, effective genomic sequences of COVID-19 cases correspond to the Omicron variant, according to investigation and announcement of the Chinese Center for Disease Control and Prevention (https://www.chinacdc.cn/jkzt/crb/zl/szkb_11803/jszl_13141/).

In our study, patients with mild or moderate COVID-19 were categorized as the non-severe group, and patients with severe or critical COVID-19 were categorized as the severe group. The starting point for all analyses was the day of the positive nucleic acid test or SARS-CoV-2 antigen rapid test (Day 0). Patients were divided into four groups according to different time points: 0-7 days, 8-15 days, 31-179 days, and >180 days. After the patient's serum is collected, a detailed medical history or telephone return visit must be conducted. If the patient gets another COVID-19 infection, or if the PCR or antigen test taken on the day the serum was collected is positive, the specimen will be excluded.

TABLE 1 Clinical characteristics of COVID-19 patients and uninfected individuals.

Characteristics	Uninfected(n=71)	Non-severe(n=209)	Severe(n=149)	p-value
Age, y, median(IQR)	45(33~62)	63.00 (49.00~75.00)	75.50(68.00~83.00)	<0.001
Gender, n(%)				<0.001
Male	28(39.4)	118(56.5)	103(69.1)	
Female	43(60.6)	91(43.5)	46(30.9)	
Comorbidities, n(%)				
Hypertension	–	78 (37.3)	102 (68.5)	<0.001
Diabetes	–	40 (19. 1)	56 (37.6)	<0.001
Cancer	–	39 (18.7)	34 (22.8)	0.336
Nephropathy	–	10 (4.8)	17 (11.4)	0.019
Autoimmune disease	–	36 (17.2)	10 (6.7)	0.003

The data conforming to non normal distribution are described as medians and 25th–75th percentile quartile intervals (IQRs) and are compared using the Mann-Whitney U or Kruskal Wallis test. Categorical variables are expressed as numbers and percentages [n (%)], and are compared using contingency table analysis and $\chi 2$ tests or Fisher's exact test.

2.2 Participants

A control group of 71 uninfected individuals was also included in the study. The median age of participants was 45 years (IQR 33-62 years), including 28 men and 43 women. Among the 358 cases of patients with COVID-19, 209 non-severe patients and 149 severe patients were included in our study. Severe patients were older than non-severe patients (75 years [IQR 68-83 years] vs. 63 years [IQR 49-75 years]). The study recorded the data for each patient, including age, gender, and comorbidities (e.g. hypertension, diabetes mellitus (DM), chronic cardiovascular disease, chronic pulmonary disease, chronic kidney disease, and tumor). This data were shown in Table 1. Informed consent was obtained from all participants, and the experimental protocol was approved by the Institutional Review Board of Fujian Provincial Hospital(Fuzhou, China; No. KY2021-03-013).

2.3 Detection of serum markers

To prepare human serum, blood is drawn from participants, and allowed to clot at room temperature for at least 30 minutes. Then, after centrifugation (8min, 3500 rpm), the supernatant part, the serum, was collected and stored at -80°C.

Serum ACE2/AXL levels were detected through an ELISA assay by using the ACE2/AXL quantitative detection kit (Shanghai Nibei Bio-pharmaceutical Technology Co., Ltd, China). Based on the instructions provided by the kit manufacturer, the ELISA protocol was followed. Briefly, the standards (50 μl; provided by the kit), samples to be tested (10 μl serum samples and 40 μl sample diluent), and blanks were added to a microplate, which precoated with human ACE2/AXL antibody. Then it was incubated at 37°C for 30min. After washing the plate 5 times with phosphate buffer saline (PBS) with Tween, horseradish peroxidase was added to form an immune complex. The unbound substances were washed away, and a substrate solution containing tetramethylbenzidine and urea hydrogen peroxide was added to the microplate. The reaction was stopped by a sulfuric acid solution, and absorbance values were measured by an enzyme-labeled instrument at 450 nm using an enzyme-labelled instrument (Bio-Rad, Hercules, CA, USA). The concentration of ACE2/AXL in serum samples was calculated using its calibration curve. Serum IgM and IgG against SARS-CoV-2 spike 1 protein or nucleocapsid protein were detected by using SARS-CoV-2 antibody reagent kits (YHLO Biotech Co, Ltd, Shenzhen, China) on an iFlash 3000 Chemiluminescence Immunoassay Analyzer (Shenzhen YHLO Biotech Co, Ltd, Shenzhen, China, http://en.szyhlo.com). The kits have catalog numbers C86095M and C86095G for IgM and IgG. The normal reference values were as follows: SARS-COV-2 IgG < 10 AU/ml, SARS-COV-2 IgM < 10 AU/ml.

2.4 Statistical analysis

Statistical analyses were performed using SPSS 25.0 software package (SPSS Inc. Chicago, USA) and GraphPad Prism 9.0 (GraphPad Software, USA). Continuous variables were presented as median and interquartile range (IQR). Independent continuous variables were compared using the Mann-Whitney U test or Kruskal-Wallis test, and paired variables with the Wilcoxon matched-pairs signed rank tests or Friedman test. Categorical variables are expressed as numbers and percentages [n (%)], and are compared using contingency table analysis and $\chi 2$ tests or Fisher's exact test. The receiver operating characteristic (ROC) curves were used to assess the diagnostic value of the biological markers, and the association between laboratory parameters and the risk of developing critical disease were explored. A p-value < 0.05 was considered statistically significant.

3 Results

3.1 Expression of ACE2, AXL and SARS-COV-2 IgG/IgM and their diagnostic value for COVID-19

The serum ACE2, AXL, and SARS-COV-2 IgG/IgM were compared between a cohort of 71 uninfected individuals and 148 COVID-19 patients with positive nucleic acid in 0-7days. As shown in the Figures 1A, B, the levels of ACE2 and AXL in the COVID-19 group were significantly lower than in the non-infected group, while SARS-COV-2 IgG was significantly higher in the COVID-19 group (Figure 1C). There was no significant difference in the SARS-COV-2 IgM between the two groups (Figure 1D). The ROC curve analysis show that the area under the curve (AUC) of serum ACE2, AXL, and SARS-COV-2 IgG were 0.714, 0.752, and 0.631, respectively (Figure 1E). However, the AUC of a combination of ACE2 + AXL (0.741) was not higher than AXL alone, suggesting that AXL had a better ability to predict the risk of COVID-19 (Figure 1F).

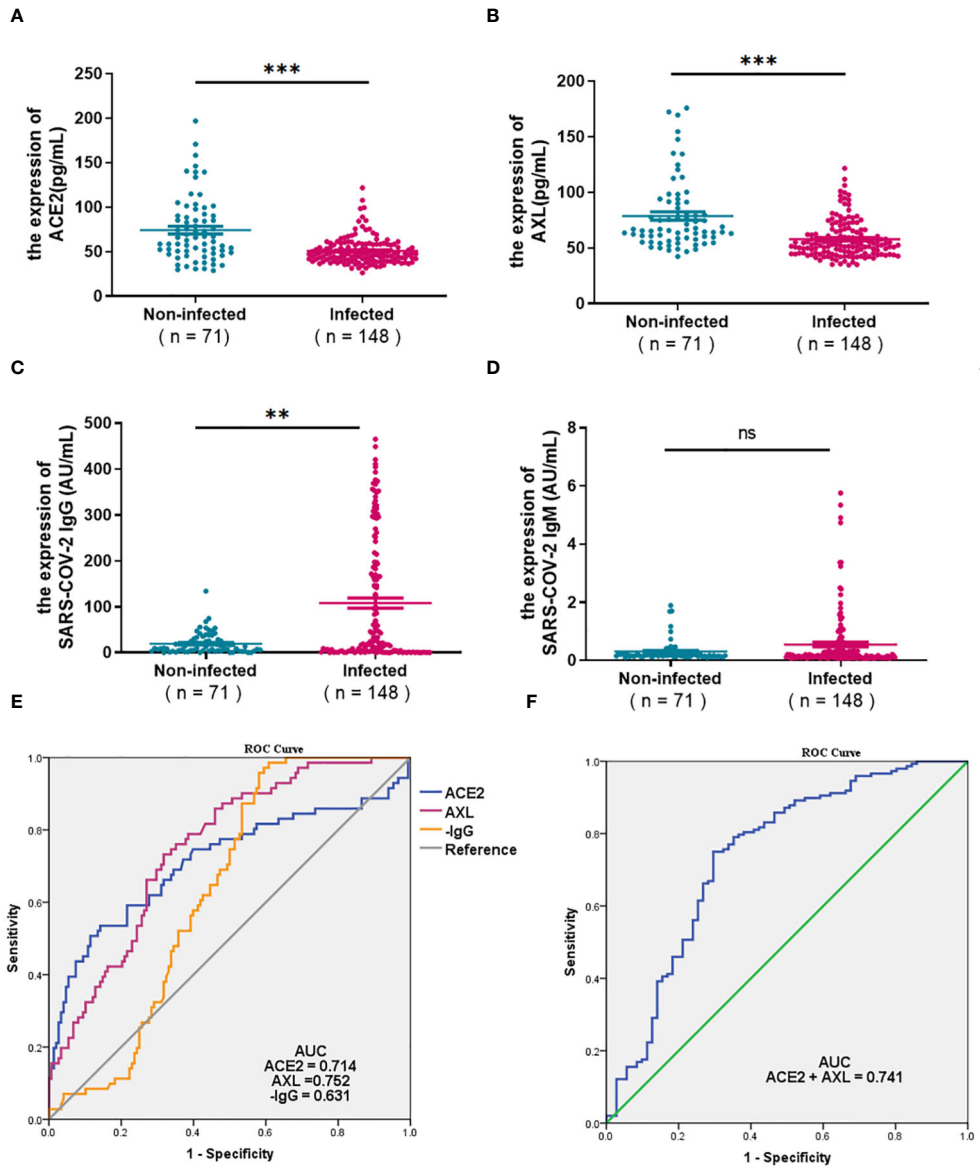

FIGURE 1
Expression of ACE2, AXL and SARS-COV-2 IgG/IgM and their diagnostic value for COVID-19. The differential expression of serum ACE2, AXL, andSARS-COV-2 IgG/IgM between 71 uninfected individuals and 148 COVID-19 patients with positive nucleic acid in 0-7days were compared withMann Whitney test **(A–D)**. The diagnostic value of ACE2, AXL, minus SARS-COV-2 IgG **(E)** and a combination of ACE2 + AXL **(F)** for COVID-19 wereperformed by ROC curve (***P* <0.01; ****P* <0.001; ns, not statistically significant).

3.2 Expression of serum ACE2, AXL and SARS-COV-2 IgG/IgM in severe and non-severe patients

3.2.1 Days 0-7 after laboratory-confirmed COVID-19

The levels of ACE2, AXL, SARS-COV-2 IgG/IgM were analyzed in patients with early COVID-19 (first week after laboratory-confirmed COVID-19), including 84 cases of non-severe and 64 cases of severe. The results showed that AXL in the severe group was significantly lower than in the non-severe group, while there were no significant differences in the levels of ACE2, SARS-COV-2 IgG/IgM between the two groups (Figures 2A-D).

3.2.2 Days 8-15 after laboratory-confirmed COVID-19

In the second week after laboratory-confirmed COVID-19, the levels of serum ACE2 and AXL in the severe group (n=93) were significantly higher than that in the non-severe group (n=67), while SARS-COV-2 IgG was significantly lower (Figures 2E-G). No significant differences were observed in the levels of serum SARS-COV-2 IgM between the two groups (Figure 2H).

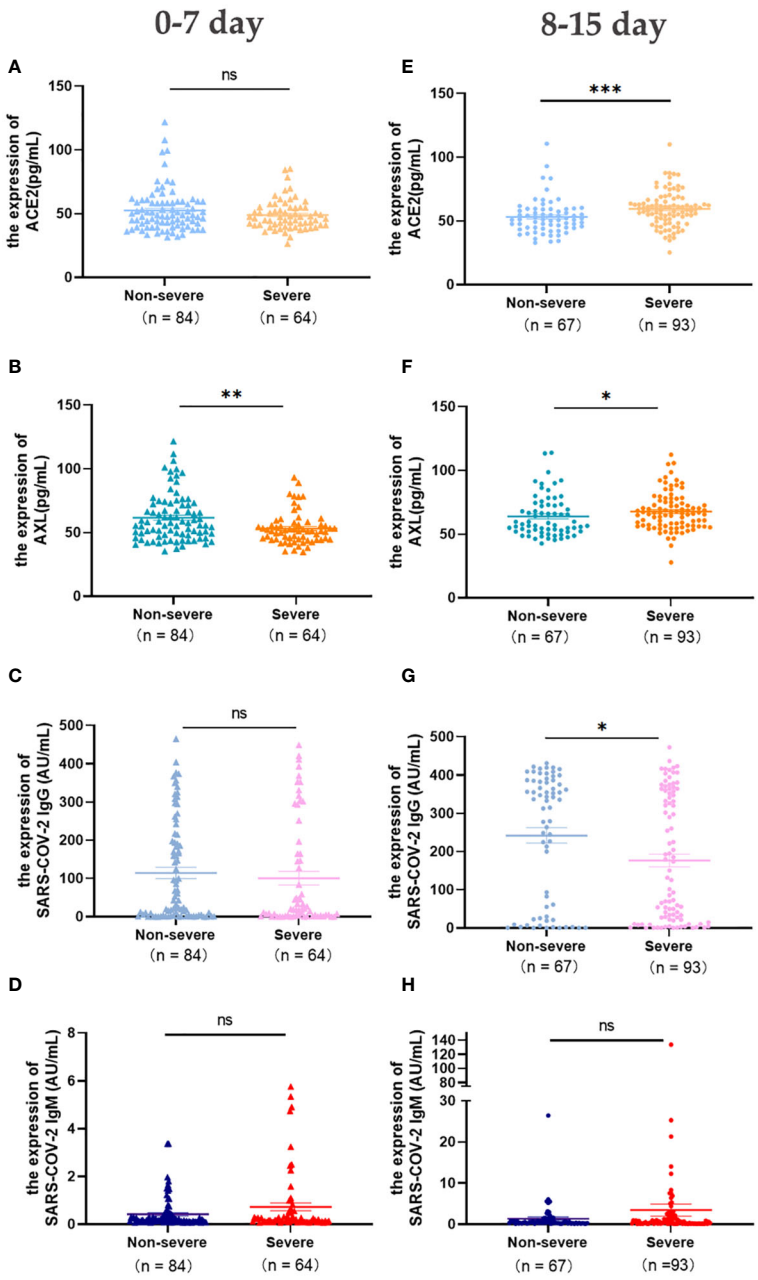

FIGURE 2
Expression of serum ACE2, AXL and SARS-COV-2 IgG/IgM in severe and non-severe groups at intervals of 0-7 days and 8-15 days were compared with Mann Whitney test **(A-H)** (*P <0.05; **P <0.01; ***P <0.001; ns, not statistically significant).

3.2.3 Days 31-179 and more than 180 days after laboratory-confirmed COVID-19

The change in these indicators were concerned within a half year and more than 180 days after laboratory-confirmed COVID-19. The levels of serum ACE2 and SARS-COV-2 IgG in the severe group were significantly lower than those in the non-severe group (Days 31-179) (Figures 3A, C). After 6 months, SARS-COV-2 IgG was still higher in the non-severe group than in the severe group (Figure 3G), and there were no significant differences in the other three indicators between the two groups(>180 days) (Figures 3E-F, H).

3.3 Evolution of serum ACE2, AXL and SARS-COV-2 IgG/IgM levels over time

The study illustrated the overall profile of serum ACE2, AXL, SARS-COV-2 IgG/IgM at different time points after

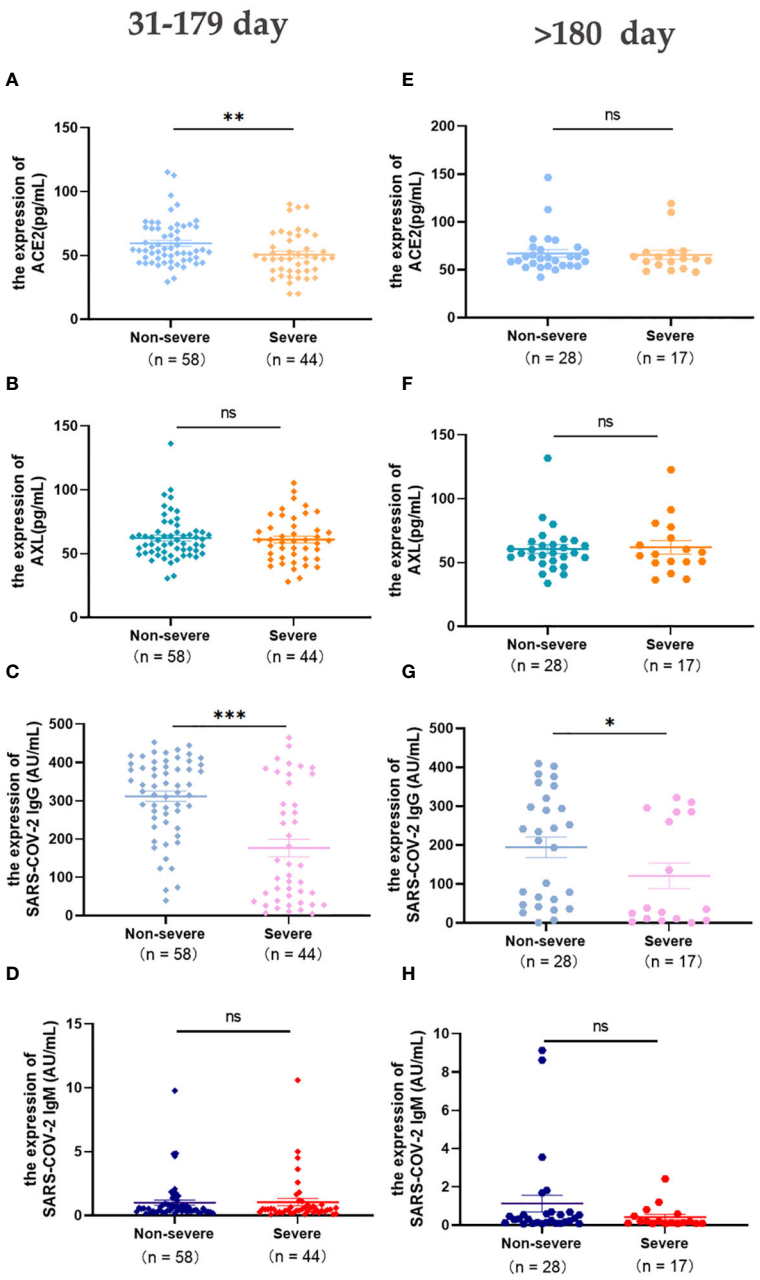

FIGURE 3
Expression of serum ACE2, AXL and SARS-COV-2 IgG/IgM in severe and non-severe groups at intervals of 31-179 days and >180 days were compared with Mann Whitney test **(A-H)** (*P <0.05; **P <0.01; ***P <0.001; ns, not statistically significant).

infection. In the non-severe group, the level of ACE2 increased over time (Figure 4A). While the levels of SARS-COV-2 IgG and IgM were on the rise in the 0–179 days interval but declined after 180 days (Figures 4C, D). No statistically significant increase in the level of serum AXL was observed (Figure 4B). In the severe group, the serum levels of ACE2, AXL, and SARS-COV-2 IgM all reached a peak during 8–15 days, but subsequently decreased (Figures 4A, B, D). Moreover, the serum level of SARS-COV-2 IgG rapidly increased after infection but declined after 180 days (Figure 4C).

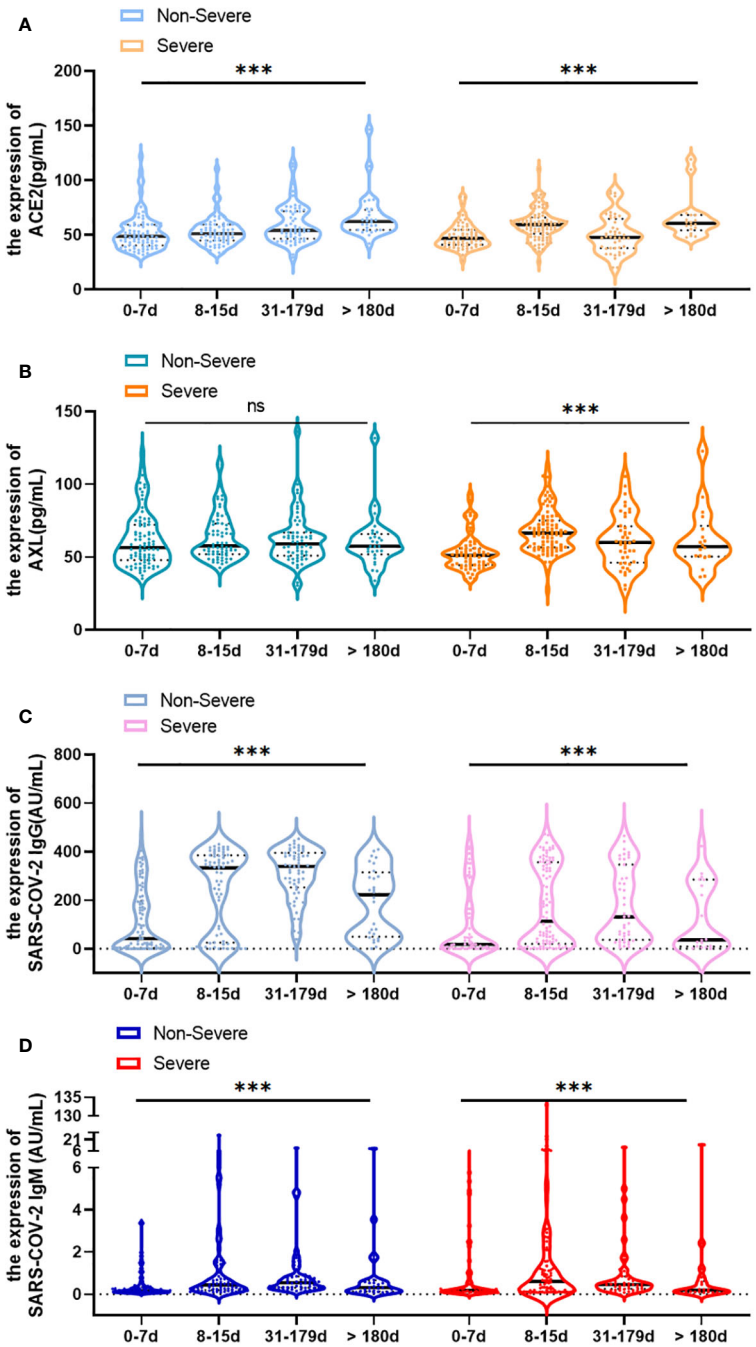

FIGURE 4
Change of serum ACE2, AXL and SARS-COV-2 IgG/IgM levels over time (0-7 days, 8-15 days, 31-179 days and >180 days) in severe and non-severegroups, respectively **(A–D)**. Data were presented as violin plots (median, quartiles and all points). The data do not follow normal distribution, statisticalsignificance of the difference was evaluated by Kruskal-Wallis test (***P <0.001; ns, not statistically significant).

10.3389/fimmu.2024.1394429

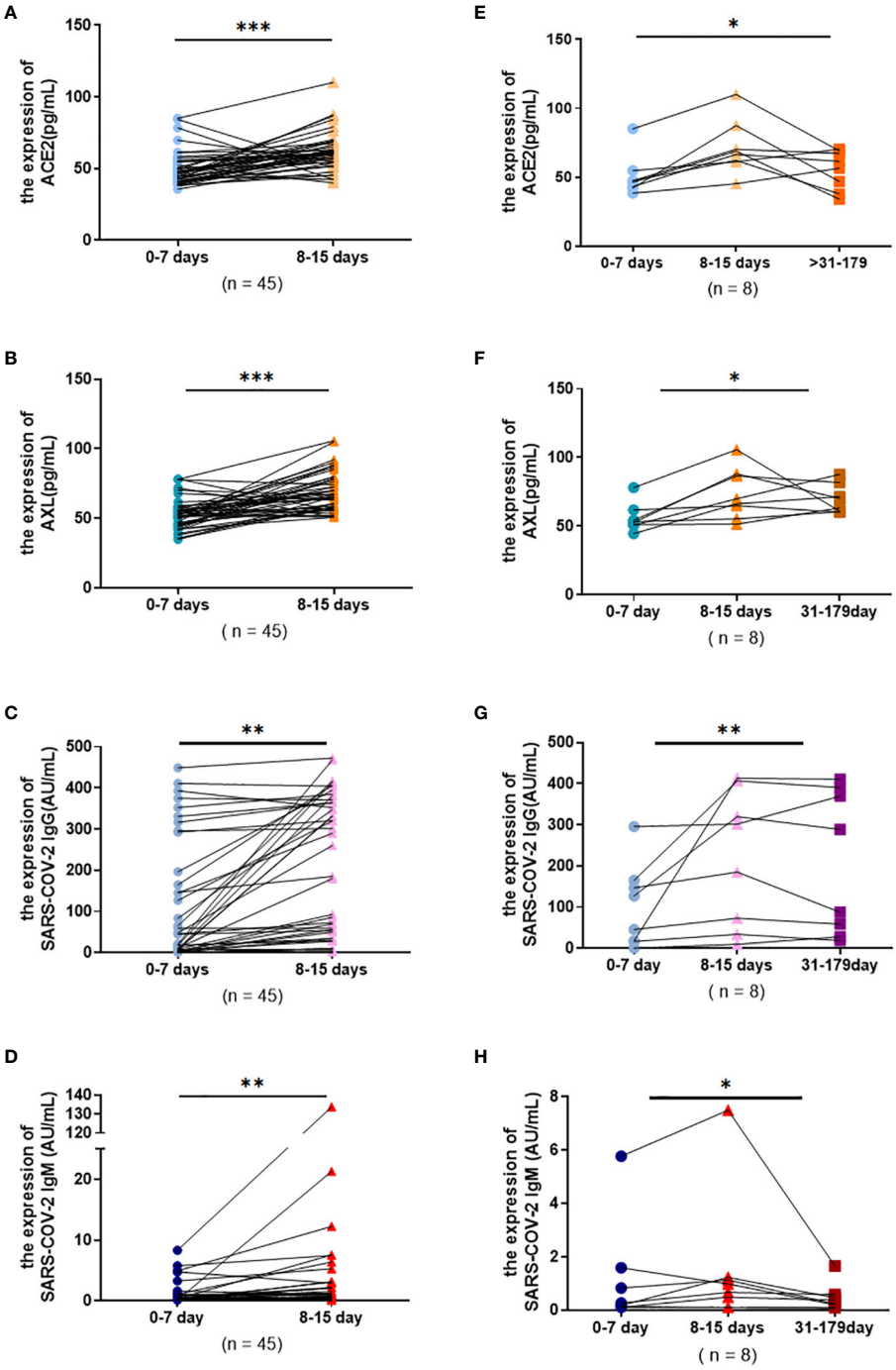

FIGURE 5
Serum ACE2, AXL and SARS-COV-2 IgG/IgM levels in severe group were compared among different temporal periods by using paired data. Wilcoxon matched-pairs signed rank tests were used to compare the changes of ACE2, AXL and SARS-COV-2 IgG, SARS-COV-2 IgM levels from 0-7 days and 8-15 days **(A-D)**. Friedman test were used to compare the changes of ACE2, AXL and SARS-COV-2 IgG, SARS-COV-2 IgM levels among 0-7 days, 8-15 days and 31-180 days **(E-H)** (*P <0.05; **P <0.01; ***P <0.001).

3.4 Changes of serum ACE2, AXL and SARS-COV-2 IgG/IgM by using paired Data

The paired data from severe patients with COVID-19 were conducted to investigate the change pattern of serum antibodies more precisely. The results showed that the levels of serum ACE2, AXL, SARS-COV-2 IgG and IgM all had a significant rise during 8-14 days (Figures 5A-D). In addition, the levels of ACE2, AXL, and SARS-COV-2 IgM were significantly decreased after 30 days, while SARS-COV-2 IgG was not obviously altered (Figures 5E-H).

10.3389/fimmu.2024.1394429

3.5 Do the levels of ACE2, AXL and SARS-COV-2 IgG/IgM in COVID-19 patients return to an uninfected state after 180 days?

To answer this question, the levels of serum ACE2, AXL, SARS-COV-2 IgG/IgM between 45 patients (>180 days) and 71 uninfected individuals were analyzed. The results showed that there were no significant differences in ACE2 and SARS-COV-2 IgM between the two groups (Figures 6A, D), indicating that the serum levels of ACE2 and SARS-COV-2 IgM returned to an uninfected stage. However, AXL was sustained at a lower level, and SARS-COV-2 IgG was still at a higher level in the infected group after 180 days compared with the uninfected group (Figures 6B, C).

4 Discussion

Based on the experience gained during the COVID-19 pandemic, new indicators need to be developed at an early stage to predict the emergence and severity of new pathogens, especially those associated with severe cases. Many studies have demonstrated that serum ACE2 activity correlated with COVID-19 severity and predicted mortality (13–15). In our study, not only ACE2, but also serum AXL, derived from another receptor of COVID-19, also seem to be a potential molecular marker for predicting COVID-19 progression.

Compared with the non-infected group, the initial cohort of COVID-19 patients showed with higher levels of SARS-COV-2 IgG/IgM. However, ACE2 in the COVID-19 group were significantly lower than those in the non-infected group, which is consistent with the result reported by María del (16). The level of AXL also decreased in the initial cohort of COVID-19 patients, which was first noted in our research. A previous comprehensive study on SARS-CoV had established that the binding of the S glycoprotein to ACE2 receptor down-regulated ACE2 expression (17). The SARS-COV-2 enters the cytoplasm through ACE2 and AXL-mediated endocytosis, which may cause the decrease in serum ACE2 and AXL levels in the initial cohort of COVID-19 patients. Surprisingly, the ROC curve analysis showed that the combined AUC of ACE2 and AXL did not exceed the AUC of AXL alone. Therefore, serum AXL seems to be a better predictor for COVID-19.

During the first week after infection with COVID-19, there is no obvious difference in symptoms and the levels of SARS-COV-2 IgG/IgM between non-severe and severe patients. However, better management can be achieved to prevent deaths by capturing early warning signs and timely intervention in critically ill patients. Fortunately, our results show that AXL, but not ACE2, can provide early warning of clinical deterioration. Then the changes of serum ACE2, AXL and SARS-COV-2 IgG/IgM between the non-severe and severe groups over time were observed. Serum ACE2 and AXL levels peaked at 8-15 days in the severe group compared to the non-severe group. Although the serum SARS-COV-2 IgG level in the severe group was always lower than in the non-severe group, it reached a significant peak at 31-179 days in both groups.

The main manifestations of SARS-CoV-2 infection were respiratory symptoms, but single-cell sequencing data showed that ACE2 expression was low in human tissues (18, 19). AXL is widely expressed in almost all human organs. In particular, in

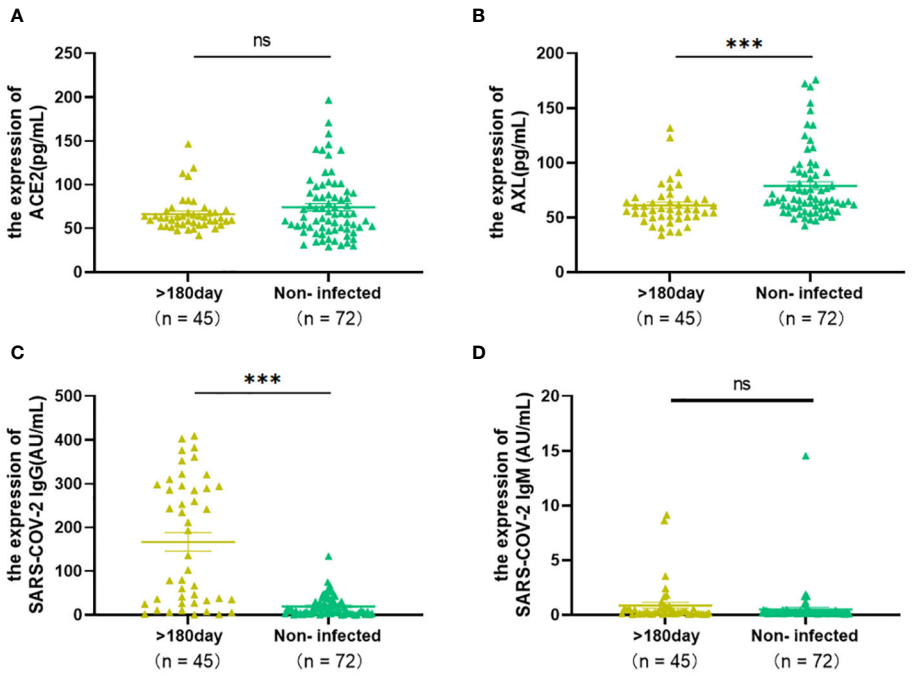

FIGURE 6
The Levels of ACE2, AXL and SARS-COV-2 IgG/IgM of COVID-19 patients (>180 days) were compared with those of uninfected individuals by using Mann Whitney test **(A–D)** (*P <0.05; **P <0.01; ***P <0.001; ns, not statistically significant).

human pulmonary and bronchial epithelial tissue and cells, AXL expression is much higher than ACE2 expression (20). AXL is known to regulate various intracellular signaling pathways, including Ras/ERK, PI3K, and p38 (21, 22). SARS-CoV-2 activated the PI3K/Akt/mTOR signaling during the initial phases of infection (23, 24), which supported the theory of AXL as an early warning indicator for clinical deterioration. Another study found that the p38/MAPK signaling was promoted by SARS-CoV-2 infection leading to the overproduction of inflammatory cytokines (25). As is well known, SARS-CoV-2 triggers a strong immune response that can cause cytokine storm syndrome in severe COVID-19 patients (26). Hypoxia inducible factor-1 (HIF-1) binds to the AXL promoter, and then promotes SARS-CoV-2 infection and exacerbates inflammatory responses to COVID-19 (27, 28). Moreover, serum AXL has been reported to interact with two vitamin K-dependent protein ligands, growth arrest-specific factor 6 (GAS6) and protein S, forming a complex. Elevated levels of AXL complex have been detected in a variety of pathologies including specific inflammatory conditions and various tumors (29–33). Numerous studies have reported that plasma Gas6 levels are directly related to the severity and outcome of COVID-19 (34–36), and the Gas6/AXL axis is involved in regulating inflammation and fibrosis in COVID-19 patients (37). In our results, a significant change in serum AXL levels were found in the severe group but not in the non-severe group. Considering serum AXL plays a major role in regulating inflammation, AXL may play an important role in the severe progression of COVID-19.

After half a year, the serum levels of ACE2 and SARS-CoV-2 IgM returned to levels seen in uninfected individuals. Interestingly, AXL sustained lower levels, and SARS-CoV-2 IgG remained at higher levels in the infected group after 180 days. Some patients recovering from COVID-19 may develop a group of new onset or aggravated sequelae known as long COVID (38). The prevalence of long COVID is still uncertain, but evidence is emerging that it is relatively common (39, 40). There was a study indicated that ACE2 activity is substantially attenuated at 8 months post-infection and has not been associated with long COVID symptoms (41). Long COVID-19 can occur as part of the process of COVID-19. The major contributory mechanistic factor is the persistent cytokine storm that may last longer in long COVID patients than in others, probably triggered by aggregates of SARS-Co-2 discovered recently in the adrenal cortex, kidney and brain (42). AXL, playing an important role in regulating inflammation, which may correlated with the long COVID symptoms. However, further exploration and additional experimental validation are needed.

It should be pointed out that there were some shortcomings of this study. Firstly, we didn't record the patient's symptoms in detail in the telephone follow-up, so we can't confirm whether the patients have post COVID-19 condition. Secondly, according to investigation and announcement of the Chinese Center for Disease Control and Prevention, the analysis of the novel coronavirus genome of COVID-19 cases in China showed that all were Omicron from 2022.9 to 2023.11, so all findings above apply only to Omicron infection.

Nevertheless, a study indicated that AXL could independently mediate the omicron infection (43). In our study, the level of serum AXL not only is correlated with the development of COVID-19, but also can provide early warning of clinical deterioration in the first week after infection, suggesting that it is a superior biomarker for COVID-19. Our results offer a new perspective for early management of COVID-19.

5 Conclusions

Previous study demonstrated serum ACE2 can be used as a protective biomarker for rapid test screening and even as one of the treatment strategies. In our study, AXL and ACE2 were compared in patient serum for the first time. Firstly, serum AXL appears to be a better predictor for COVID-19, with the highest AUC. Secondly, only AXL can provide early warning of clinical deterioration in the first week after infection with COVID-19. Thirdly, AXL and ACE2 play important roles in the severe progression of COVID-19. Lastly, AXL may be related to the development of long COVID symptoms. In summary, serum AXL seems to be a superior biomarker for COVID-19. However, further studies are needed to understand the immune mechanism involved.

Data availability statement

The raw data supporting the conclusions of this article will be made available by the authors, without undue reservation.

Ethics statement

The studies involving humans were approved by the Institutional Review Board of Fujian Provincial Hospital. The studies were conducted in accordance with the local legislation and institutional requirements. Written informed consent for participation in this study was provided by the participants' legal guardians/next of kin.

Author contributions

JY: Formal Analysis, Methodology, Software, Writing – original draft. RH: Software, Writing – original draft. RZ: Software, Writing – original draft, Data curation, Formal Analysis, Methodology. JS: Data curation, Writing – review & editing. SH: Formal Analysis, Methodology, Software, Writing – review & editing. YK: Formal Analysis, Software, Data curation, Writing – original draft. FC: Investigation, Validation, Writing – review & editing. JC:

Methodology, Project administration, Visualization, Writing – review & editing. LC: Project administration, Conceptualization, Supervision, Writing – review & editing.

Funding

The author(s) declare financial support was received for the research, authorship, and/or publication of this article. This research was funded by Joint Funds for the innovation of science and Technology, Fujian province (Grant number: 2023Y9279); and Startup Fund for scientific research, Fujian Medical University, Grant number (2021QH1316) and Sponsored by Fujian provincial health technology project, Grant number (2022QNA011).

Conflict of interest

The authors declare that the research was conducted in the absence of any commercial or financial relationships that could be construed as a potential conflict of interest.

Publisher's note

References

1. Zhang JJ, Dong X, Cao YY, Yuan YD, Yang YB, Yan YQ, et al. Clinical characteristics of 140 patients infected with SARS-CoV-2 in Wuhan, China. *Allergy*. (2020) 75:1730–41. doi: 10.1111/all.14238

2. Hall V, Foulkes S, Insalata F, Kirwan P, Saei A, Atti A, et al. Protection against SARS-CoV-2 after Covid-19 Vaccination and Previous Infection. *New Engl J Med*. (2022) 386:1207–20. doi: 10.1056/NEJMoa2118691

3. Hadj Hassine I. Covid-19 vaccines and variants of concern: A review. *Rev Med Virol*. (2022) 32:e2313. doi: 10.1002/rmv.2313

4. Hu B, Guo H, Zhou P, Shi ZL. Characteristics of SARS-coV-2 and COVID-19. *Nat Rev Microbiol*. (2021) 19:141–54. doi: 10.1038/s41579-020-00459-7

5. O'Driscoll M, Ribeiro Dos Santos G, Wang L, Cummings DAT, Azman AS, Paireau J, et al. Age-specific mortality and immunity patterns of SARS-CoV-2. *Nature*. (2021) 590:140–5. doi: 10.1038/s41586-020-2918-0

6. Beyerstedt S, Casaro EB, Rangel É.B. COVID-19: angiotensin-converting enzyme 2 (ACE2) expression and tissue susceptibility to SARS-CoV-2 infection. *Eur J Clin Microbiol Infect diseases: Off Publ Eur Soc Clin Microbiol*. (2021) 40:905–19. doi: 10.1007/s10096-020-04138-6

7. Saengsiwaritt W, Jittikoon J, Chaikledkaew U, Udomsinprasert W. Genetic polymorphisms of ACE1, ACE2, and TMPRSS2 associated with COVID-19 severity: A systematic review with meta-analysis. *Rev Med Virol*. (2022) 32:e2323. doi: 10.1002/rmv.2323

8. Ziegler CGK, Allon SJ, Nyquist SK, Mbano IM, Miao VN, Tzouanas CN, et al. SARS-coV-2 receptor ACE2 is an interferon-stimulated gene in human airway epithelial cells and is detected in specific cell subsets across tissues. *Cell*. (2020) 181:1016–1035.e19. doi: 10.1016/j.cell.2020.04.035

9. Braunger J, Schleithoff L, Schulz AS, Kessler H, Lammers R, Ullrich A, et al. Intracellular signaling of the Ufo/Axl receptor tyrosine kinase is mediated mainly by a multi-substrate docking-site. *Oncogene*. (1997) 14:2619–31. doi: 10.1038/sj.onc.1201123

10. Wang S, Qiu Z, Hou Y, Deng X, Xu W, Zheng T, et al. AXL is a candidate receptor for SARS-CoV-2 that promotes infection of pulmonary and bronchial epithelial cells. *Cell Res*. (2021) 31:126–40. doi: 10.1038/s41422-020-00460-y

11. Yalcin HC, Sukumaran V, Al-Ruweidi MKAA, Shurbaji S. Do changes in ACE-2 expression affect SARS-coV-2 virulence and related complications: A closer look into membrane-bound and soluble forms. *Int J Mol Sci*. (2021) 22:6703. doi: 10.3390/ijms22136703

12. van Aalen EA, Wouters SFA, Verzijl D, Merkx M. Bioluminescent RAPPID sensors for the single-step detection of soluble axl and multiplex analysis of cell surface cancer biomarkers. *Analytical Chem*. (2022) 94:6548–56. doi: 10.1021/acs.analchem.2c00297

13. Fagyas M, Fejes Z, Sütő R, Nagy Z, Székely B, Pócsi M, et al. Circulating ACE2 activity predicts mortality and disease severity in hospitalized COVID-19 patients. *Int J Infect Dis*. (2022) 115:8–16. doi: 10.1016/j.ijid.2021.11.028

14. Fagyas M, Kertész A, Siket IM, Bánhegyi V, Kracskó B, Szegedi A, et al. Level of the SARS-CoV-2 receptor ACE2 activity is highly elevated in old-aged patients with aortic stenosis: implications for ACE2 as a biomarker for the severity of COVID-19. *Geroscience*. (2021) 43:19–29. doi: 10.1007/s11357-020-00300-2

15. Fagyas M, Bánhegyi V, Úri K, Enyedi A, Lizanecz E, Mányiné IS, et al. Changes in the SARS-CoV-2 cellular receptor ACE2 levels in cardiovascular patients: a potential biomarker for the stratification of COVID-19 patients. *Geroscience*. (2021) 43:2289–304. doi: 10.1007/s11357-021-00467-2

16. Maza MDC, Úbeda M, Delgado P, Horndler L, Llamas MA, van Santen HM, et al. ACE2 serum levels as predictor of infectability and outcome in COVID-19. *Front Immunol*. (2022) 13:836516. doi: 10.3389/fimmu.2022.836516

17. Kuba K, Imai Y, Rao S, Gao H, Guo F, Guan B, et al. A crucial role of angiotensin converting enzyme 2 (ACE2) in SARS coronavirus-induced lung injury. *Nat Med*. (2005) 11:875–9. doi: 10.1038/nm1267

18. Lukassen S, Chua RL, Trefzer T, Kahn NC, Schneider MA, Muley T, et al. SARS-CoV-2 receptor ACE2 and TMPRSS2 are primarily expressed in bronchial transient secretory cells. *EMBO J*. (2020) 39:e105114. doi: 10.15252/embj.2020105114

19. Sungnak W, Huang N, Bécavin C, Berg M, Queen R, Litvinukova M, et al. SARS-CoV-2 entry factors are highly expressed in nasal epithelial cells together with innate immune genes. *Nat Med*. (2020) 26:681–7. doi: 10.1038/s41591-020-0868-6

20. Zhang Z, Cui F, Cao C, Wang Q, Zou Q. Single-cell RNA analysis reveals the potential risk of organ-specific cell types vulnerable to SARS-CoV-2 infections. *Comput Biol Med*. (2022) 140:105092. doi: 10.1016/j.compbiomed.2021.105092

21. Allen MP, Linseman DA, Udo H, Xu M, Schaack JB, Varnum B, et al. Novel mechanism for gonadotropin-releasing hormone neuronal migration involving Gas6/Ark signaling to p38 mitogen-activated protein kinase. *Mol Cell Biol*. (2002) 22:599–613. doi: 10.1128/MCB.22.2.599-613.2002

22. Antony J, Huang RY. AXL-driven EMT state as a targetable conduit in cancer. *Cancer Res*. (2017) 77:3725–32. doi: 10.1158/0008-5472.CAN-17-0392

23. Appelberg S, Gupta S, Svensson Akusjärvi S, Ambikan AT, Mikaeloff F, Saccon E, et al. Dysregulation in Akt/mTOR/HIF-1 signaling identified by proteo-transcriptomics of SARS-CoV-2 infected cells. *Emerg Microbes Infect*. (2020) 9:1748–60. doi: 10.1080/22221751.2020.1799723

24. Basile MS, Cavalli E, McCubrey J, Hernández-Bello J, Muñoz-Valle JF, Fagone P, et al. The PI3K/Akt/mTOR pathway: A potential pharmacological target in COVID-19. *Drug Discovery Today*. (2022) 27:848–56. doi: 10.1016/j.drudis.2021.11.002

25. Bouhaddou M, Memon D, Meyer B, White KM, Rezelj VV, Correa Marrero M, et al. The global phosphorylation landscape of SARS-coV-2 infection. *Cell*. (2020) 182:685–712.e19. doi: 10.1016/j.cell.2020.06.034

26. Salton F, Confalonieri P, Campisciano G, Cifaldi R, Rizzardi C, Generali D, et al. Cytokine profiles as potential prognostic and therapeutic markers in SARS-coV-2-induced ARDS. *J Clin Med*. (2022) 11:2951. doi: 10.3390/jcm11112951

27. Tian M, Liu W, Li X, Zhao P, Shereen MA, Zhu C, et al. HIF-1α promotes SARS-CoV-2 infection and aggravates inflammatory responses to COVID-19. *Signal transduction targeted Ther*. (2021) 6:308. doi: 10.1038/s41392-021-00726-w

28. Nalwoga H, Ahmed L, Arnes JB, Wabinga H, Akslen LA. Strong expression of hypoxia-inducible factor-1α (HIF-1α) is associated with axl expression and features of aggressive tumors in african breast cancer. *PloS One*. (2016) 11:e0146823. doi: 10.1371/journal.pone.0146823

29. Bellan M, Cittone MG, Tonello S, Rigamonti C, Castello LM, Gavelli F, et al. Gas6/TAM system: A key modulator of the interplay between inflammation and fibrosis. *Int J Mol Sci*. (2019) 20:5070. doi: 10.3390/ijms20205070

30. Ekman C, Stenhoff J, Dahlbäck B. Gas6 is complexed to the soluble tyrosine kinase receptor Axl in human blood. *J Thromb haemostasis: JTH*. (2010) 8:838–44. doi: 10.1111/j.1538-7836.2010.03752.x

31. Lu Q, Lemke G. Homeostatic regulation of the immune system by receptor tyrosine kinases of the Tyro 3 family. *Sci (New York N.Y.)*. (2001) 293:306–11. doi: 10.1126/science.1061663

32. Ekman C, Gottsäter A, Lindblad B, Dahlbäck B. Plasma concentrations of Gas6 and soluble Axl correlate with disease and predict mortality in patients with critical limb ischemia. *Clin Biochem*. (2010) 43:873–6. doi: 10.1016/j.clinbiochem.2010.04.006

33. Lee IJ, Hilliard BA, Ulas M, Yu D, Vangala C, Rao S, et al. Monocyte and plasma expression of TAM ligand and receptor in renal failure: Links to unregulated immunity and chronic inflammation. *Clin Immunol*. (2015) 158:231–41. doi: 10.1016/j.clim.2015.01.012

34. Tonello S, Rizzi M, Matino E, Costanzo M, Casciaro GF, Croce A, et al. Baseline plasma gas6 protein elevation predicts adverse outcomes in hospitalized COVID-19 patients. *Dis Markers*. (2022) 2022:1568352. doi: 10.1155/2022/1568352

35. Huckriede J, Anderberg SB, Morales A, de Vries F, Hultström M, Bergqvist A, et al. Evolution of NETosis markers and DAMPs have prognostic value in critically ill COVID-19 patients. *Sci Rep*. (2021) 11:15701. doi: 10.1038/s41598-021-95209-x

36. Şik N, Duman M, Küme T, Gürsoy Doruk Ö., Yilmaz D, Ören H. Roles of vitamin-K-dependent factors protein S and GAS6 with TAM receptors and HMGB1 in pediatric COVID-19 disease. *J Pediatr hematology/oncology*. (2023) 45:e298–303. doi: 10.1097/MPH.0000000000002528

37. Rizzi M, Tonello S, D'Onghia D, Sainaghi PP. Gas6/TAM axis involvement in modulating inflammation and fibrosis in COVID-19 patients. *Int J Mol Sci*. (2023) 24:951. doi: 10.3390/ijms24020951

38. Al-Aly Z, Xie Y, Bowe B. High-dimensional characterization of post-acute sequelae of COVID-19. *Nature*. (2021) 594:259–64. doi: 10.1038/s41586-021-03553-9

39. Nehme M, Braillard O, Alcoba G, Aebischer Perone S, Courvoisier D, Chappuis F, et al. COVID-19 symptoms: longitudinal evolution and persistence in outpatient settings. *Ann Intern Med*. (2021) 174:723–5. doi: 10.7326/M20-5926

40. Petersen MS, Kristiansen MF, Hanusson KD, Danielsen ME, Á Steig B, Gaini S, et al. Long COVID in the Faroe Islands: A longitudinal study among nonhospitalized patients. *Clin Infect Dis*. (2021) 73:e4058–63. doi: 10.1093/cid/ciaa1792

41. Phetsouphanh C, Darley DR, Wilson DB, Howe A, Munier CML, Patel SK, et al. Immunological dysfunction persists for 8 months following initial mild-to-moderate SARS-CoV-2 infection. *Nat Immunol*. (2022) 23:210–6. doi: 10.1038/s41590-021-01113-x

42. Szabo S, Zayachkivska O, Hussain A, Muller V. What is really 'Long COVID'? *Inflammopharmacology*. (2023) 31:551–7. doi: 10.1007/s10787-023-01194-0

43. Zhang WN, Li XP, Wang PF, Zhu L, Xiao XH, Dai YJ. Comprehensive analysis of the novel omicron receptor AXL in cancers. *Comput Struct Biotechnol J*. (2022), 20:3304–12. doi: 10.1016/j.csbj.2022.06.051

frontiers | Frontiers in Immunology

TYPE Original Research
PUBLISHED 23 May 2024
DOI 10.3389/fimmu.2024.1396603

OPEN ACCESS

EDITED BY
Pedro A. Reche,
Complutense University of Madrid, Spain

REVIEWED BY
Divya Jha,
Icahn School of Medicine at Mount Sinai, United States
Sneh Lata Gupta,
Emory University, United States

*CORRESPONDENCE
Silvia Beatriz Boscardin
sbboscardin@usp.br

†These authors have contributed equally to this work

RECEIVED 06 March 2024
ACCEPTED 07 May 2024
PUBLISHED 23 May 2024

CITATION
Adami FL, de Castro MV, Almeida BdS, Daher IP, Yamamoto MM, Souza Santos K, Zatz M, Naslavsky MS, Rosa DS, Cunha-Neto E, de Oliveira VL, Kalil J and Boscardin SB (2024) Anti-RBD IgG antibodies from endemic coronaviruses do not protect against the acquisition of SARS-CoV-2 infection among exposed uninfected individuals. *Front. Immunol.* 15:1396603. doi: 10.3389/fimmu.2024.1396603

Anti-RBD IgG antibodies from endemic coronaviruses do not protect against the acquisition of SARS-CoV-2 infection among exposed uninfected individuals

Flávia Lopes Adami[1], Mateus Vidigal de Castro[2,3], Bianca da Silva Almeida[1], Isabela Pazotti Daher[1,4], Márcio Massao Yamamoto[1], Keity Souza Santos[4,5,6], Mayana Zatz[2,3], Michel Satya Naslavsky[2,3], Daniela Santoro Rosa[6,7], Edecio Cunha-Neto[4,5,6], Vivian Leite de Oliveira[4†], Jorge Kalil[4,5,6] and Silvia Beatriz Boscardin[1,6*†]

[1]Departamento de Parasitologia, Instituto de Ciências Biomédicas, Universidade de São Paulo, São Paulo, Brazil, [2]Centro de Estudos do Genoma Humano e Células Tronco, Universidade de São Paulo, São Paulo, Brazil, [3]Departamento de Genética e Biologia Evolutiva, Instituto de Biociências, Universidade de São Paulo, São Paulo, Brazil, [4]Laboratório de Imunologia, LIM19, Instituto do Coração (InCor), Hospital das Clínicas da Faculdade de Medicina da Universidade de São Paulo (HCFMUSP), São Paulo, Brazil, [5]Departamento de Clínica Médica, Disciplina de Alergia e Imunologia Clínica, Faculdade de Medicina da Universidade de São Paulo (FMUSP), São Paulo, SP, Brazil, [6]Instituto de Investigação em Imunologia-Instituto Nacional de Ciências e Tecnologia (iii-INCT), São Paulo, Brazil, [7]Departamento de Microbiologia, Imunologia e Parasitologia, Disciplina de Imunologia, Universidade Federal de São Paulo (UNIFESP), São Paulo, Brazil

Background: The Coronaviridae family comprises seven viruses known to infect humans, classified into alphacoronaviruses (HCoV-229E and HCoV-NL63) and betacoronaviruses (HCoV-OC43 and HCoV-HKU1), which are considered endemic. Additionally, it includes SARS-CoV (severe acute respiratory syndrome), MERS-CoV (Middle East respiratory syndrome), and the novel coronavirus SARS-CoV-2, responsible for COVID-19. SARS-CoV-2 induces severe respiratory complications, particularly in the elderly, immunocompromised individuals and those with underlying diseases. An essential question since the onset of the COVID-19 pandemic has been to determine whether prior exposure to seasonal coronaviruses influences immunity or protection against SARS-CoV-2.

Methods: In this study, we investigated a cohort of 47 couples (N=94), where one partner tested positive for SARS-CoV-2 infection via real-time PCR while the other remained negative. Plasma samples, collected at least 30 days post-PCR reaction, were assessed using indirect ELISA and competition assays to measure specific antibodies against the receptor-binding domain (RBD) portion of the Spike (S) protein from SARS-CoV-2, HCoV-229E, HCoV-NL63, HCoV-OC43, and HCoV-HKU1.

Results: IgG antibody levels against the four endemic coronavirus RBD proteins were similar between the PCR-positive and PCR-negative individuals, suggesting that IgG against endemic coronavirus RBD regions was not associated with protection from infection. Moreover, we found no significant IgG antibody cross-reactivity between endemic coronaviruses and SARS-CoV-2 RBDs.

Conclusions: Taken together, results suggest that anti-RBD antibodies induced by a previous infection with endemic HCoVs do not protect against acquisition of COVID-19 among exposed uninfected individuals.

KEYWORDS

seasonal coronavirus, COVID-19, humoral immunity, cross-reactivity, RBD protein

1 Introduction

Human coronaviruses (HCoVs) are zoonotic viruses of the Coronaviridae family that can cause severe respiratory infections (1)and rank as the second cause of the common cold after rhinoviruses (2). There are currently seven known human-infecting coronaviruses: seasonal alphacoronaviruses HCoV-229E and HCoV-NL63, betacoronaviruses HCoV-OC43 and HCoV-HKU1, and the emergent severe acute respiratory syndrome coronavirus (SARS-CoV), Middle East respiratory syndrome coronavirus (MERS-CoV), and the novel severe acute respiratory syndrome coronavirus 2 (SARS-CoV-2) (3). Typically, seasonal or common coronaviruses cause mild upper-respiratory tract infections in immunocompetent individuals, although severe lower-respiratory tract disease can affect children, the elderly, and immunocompromised individuals (4). HCoV-229E (5) and HCoV-OC43 (6) were isolated over 50 years ago, while HCoV-NL63 (7) and HCoV-HKU1 (8) were identified after the 2002 SARS-CoV outbreak in China. These viruses are endemic, contributing to an estimated 15–30% of respiratory tract infections each year (4). However, the real clinical importance of these viruses remains undefined due to conflicting data in the literature and the lack of studies specially designed to directly address their infection prevalence.

HCoV-229E was the first coronavirus to be discovered in 1966 (5), belongs to the Duvinacovirus subgenus, and causes common colds in healthy individuals and susceptible populations like children and the elderly. Despite its association to common colds, HCoV-229E has been detected in severe infections of the lower-respiratory tract among healthy adults with no comorbidities, leading to cases of pneumonia or bronchiolitis. The precise reasons behind the varying clinical manifestations observed in different patient groups remain unclear (9, 10). HCoV-OC43, discovered in 1967 (6), is the most prevalent coronavirus related to infections and was the second coronavirus identified. Named with the prefix 'OC' from organ culture, it belongs to the Embecovirus subgenus and can infect both humans and cattle (11). Discovered in the Netherlands in 2004 (7), HCoV-NL63 is directly associated with common cold manifestations but can also lead to more serious infections of the lower-respiratory tract. Similar to the virus causing COVID-19 (SARS-CoV-2), HCoV-NL63 is the only seasonal coronavirus known to use the human angiotensin-converting enzyme 2 (ACE2) as cell penetration receptor, although studies suggest that the Spike (S) protein from HCoV-NL63 has a weaker interaction with human ACE2 than SARS-CoV-2 (12, 13). HCoV-HKU1 was the last seasonal coronavirus to be discovered in Hong Kong in 2005 (8), and it seems to have originated from infected mice. Among all seasonal coronaviruses, HCoV-HKU1 infection is associated with more severe symptoms such as chills, tonsillar hypertrophy and febrile seizures. Infections with this virus are usually self-limiting, with only two reported pneumonia-related deaths in patients with serious underlying conditions like cancer (8, 14).

SARS-CoV-2 was identified in Wuhan, Hubei province, China, in individuals exposed at a seafood market that also commercialized live animals, suggesting zoonotic transmission. However, until now, it is not known how the virus spilled over from its original host to the market and, consequently, to people. SARS-CoV-2 infection causes COVID-19, declared a global public health emergency, displaying symptoms ranging from mild colds (80% of symptomatic cases) to more severe manifestations (5–10% of cases) such as pneumonia, respiratory failure, heart failure, sepsis and multi-organ failure, as well as, asymptomatic cases (15).

The main protein of coronaviruses, Spike (S), is a glycoprotein of approximately 180 kilodaltons (kDa), located on the viral surface. Its sequence encodes a signal peptide at the N-terminus and the S1 and S2 subunits, responsible for receptor binding and membrane fusion, respectively (16). Mutations in the gene encoding Spike enable its adaptation to new tissues and hosts (17–19). Given its role in virus entry into host cells, the S protein is the primary target for neutralizing antibodies and a focus for therapeutic and vaccine strategies. Potent neutralizing antibodies usually target the receptor-binding domain (RBD) located in the S1 subunit, blocking viral entry by preventing the interaction of the S1 subunit with the ACE2 receptor (20, 21).

Cross-immunity occurs when an immune response triggered by one pathogen confers partial or complete protection against a related pathogen, relying on common antigens shared by both pathogens. Cross-reactivity to seasonal coronaviruses may be significant for COVID-19, as studies indicate the presence of SARS-CoV-2 specific $CD4^+$ T cells in individuals not previously exposed. Thus, cross-reactivity in T cell recognition is plausible, since there are homologous sequences among the different types of human-infecting coronaviruses (22).

However, while extensive exploration has been conducted on the degree of antibody cross-reactivity between endemic HCoVs and SARS-CoV-2, findings remain controversial. A study reported 2.3% seropositivity (53 out of 1938 samples) in immunoassays against nucleoprotein (NP) and RBD protein in individuals likely unexposed to the virus, suggesting potential cross-reactivity against SARS-CoV-2 (23). Other studies revealed pre-existing antibodies against SARS-CoV-2 in unexposed individuals directed specifically to the S2 subunit of the Spike protein, but not the S1 subunit which includes the RBD (24), lacking neutralizing or protective activity against SARS-CoV-2 infection (24–26). In addition, cross-reactive antibodies potentially induced by previous endemic HCoV infections were also detected against ORF1 and, to a lesser extent, Spike and NP (27).

Evidence also suggests that an immune response against seasonal coronaviruses might correlate to a better prognosis in COVID-19 progression (28). Moreover, previous responses to endemic HCoVs might influence the functionality of the anti-SARS-CoV-2 antibody repertoire responses (29, 30).

In order to evaluate the endemic HCoVs' anti-RBD IgG response profile, its association with COVID-19 acquisition, and the cross-reactivity of endemic HCoV RBD with SARS-CoV-2 RBD, we tested plasma samples from couples living together, where one individual acquired COVID-19, while the other remained uninfected despite exposure in the same household. Our results showed that anti-RBD IgG responses to endemic HCoVs did not predict protection against infection, discarding the potential cross-reactive effect from previous endemic coronavirus exposure on the antibody repertoire against SARS-CoV-2 infections.

2 Materials and methods

2.1 Volunteers' recruitment, blood collection, and sample processing

For this study, we selected a cohort of 47 Brazilian couples who showed discordant results in real-time PCR tests for SARS-CoV-2 detection, during the first wave of COVID-19 in Brazil in 2020, as detailed in Supplementary Table 1. In each selected couple, one partner tested positive for COVID-19 via PCR, while the other tested negative. The infected partner exhibited symptoms of COVID-19, while the other partner remained uninfected (as confirmed by a negative PCR result), despite sharing the same living space and sleeping arrangements throughout the period of infection. The couples did not maintain social distance during the course of the illness, did not wear masks and did not take any protective measures at home. The members of each couple were of similar age (between 24 and 79 years, with an average age of 44.4 years) and had access to the same health insurance plan. Also, individuals with pre-existing diseases and/or comorbidities that could influence the course of the disease were not included in this cohort.

Members infected within the cohort were classified into subgroups according to their COVID-19 clinical conditions, based on the severity scales proposed by the World Health Organization (WHO-2019-nCoV-clinical-2020.5) and elaborated upon by Gandhi et al. (31). The classifications are as follows: Mild illness: characterized by the presence of common symptoms such as fever, cough, and changes in smell (anosmia) and taste (dysgeusia), but not shortness of breath (dyspnea). No hospitalization is required; Moderate illness: defined by the presence of common symptoms, including dyspnea, and either clinical or radiographic evidence of lower respiratory tract disease, but without hypoxemia (blood oxygen saturation of 94% or higher). Hospitalization may be warranted. In this study, none of the participants were hospitalized, and all infected participants recovered without any complications or sequelae.

Blood samples were collected in vacutainer tubes containing EDTA (BD Biosciences) from both partners at least one month after the initial illness (to detect SARS-CoV-2 antibodies) prior to the availability of COVID-19 vaccines in Brazil, and before the appearance of new SARS-CoV-2 variants (between June and October 2020). To ensure that the partners who tested negative had not contracted the virus asymptomatically, we conducted serological tests to confirm their seronegative status. Plasma was separated by centrifuging the samples at 2000 x g for 10 minutes at room temperature, performed within 30 minutes of venipuncture. Subsequently, the supernatant was aliquoted into 1.5 mL cryovials (Corning®, USA). These samples were then stored at -80°C until further analysis.

Each couple had their sample for real-time PCR testing collected on the same day the partner was confirmed positive, and his/her plasma sample was collected on the same day as the positive partner was collected.

2.2 Production of the RBD from HCoVs and SARS-CoV-2

Plasmids containing nucleic acid sequences encoding the RBD protein sequences of four seasonal human coronaviruses (HCoV-OC43, HCoV-NL63, HCoV-229E, and HCoV-HKU1) were kindly provided by Dr. Aravinda M. de Silva (University of North Carolina School of Medicine, Chapel Hill, USA) and are described in (32). Additionally, the RBD protein sequence from SARS-CoV-2 Wuhan Hu-1 strain was kindly provided by Dr. Florian Krammer (Icahn School of Medicine at Mount Sinai, New York, USA) and is described in (33).

The plasmids were transformed by heat shock into TOP10 competent *Escherichia coli* bacteria (ThermoFisher Scientific). A single colony was cultured for 16–18 hours in 200 mL of LB medium (Merck) supplemented with 100 µg/mL of ampicillin. Plasmid DNA extraction was performed using the PureLink™ HiPure Plasmid MaxiPrep kit (ThermoFisher Scientific) exactly as

advised by the manufacturer. The concentrations of the purified plasmids were determined by spectrophotometry (NanoDrop 2000, ThermoFisher Scientific), and their integrity was analyzed using 0.8% agarose gels.

Expi293F™ cells (ThermoFisher Scientific) were grown at a concentration of 1–3x10^6 cells/mL. The cells were thawed in a water bath and then fed into a flask containing 30 mL of pre-warmed Expi293™ expression medium (ThermoFisher Scientific). The cells were diluted every 2–3 days, depending on the density found, and at least 3 passages were made with the addition of a new medium, before transfection. Transfections were performed exactly as described in (34).

2.3 Purification of RBD Proteins by affinity chromatography

On day 5, transfected cell cultures were harvested after the addition of 100 mM of phenylmethylsulfonyl fluoride (PMSF, ThermoFisher Scientific). After centrifugation at 3.000 xg for 20 min, the supernatants were collected and an equivalent volume of cold 1x PBS (Phosphate Buffered Saline) was added. Five mL plastic columns were set up with 1 mL of HisPur™ Ni-NTA resin (ThermoFisher Scientific) for each 100 mL of culture supernatant. After two washes with 5 mL of cold 1x PBS, each column was adapted to a peristaltic pump (Mini-Peristaltic Pump II, Harvard Apparatus), and the cold supernatant was passed slowly twice. Subsequently, the columns were washed with 100 mL of cold 1x PBS containing 5mM imidazole (Merck). Elution was carried out initially with 50 mL of cold 1x PBS containing 25 mM imidazole followed by 10 mL of cold PBS 1x containing 250 mM of imidazole, collected in 1 mL-fractions. Protein presence in each fraction was evaluated using Bradford reagent (ThermoFisher Scientific). Protein-containing tubes were pooled together and dialyzed against cold 1x PBS to remove imidazole. Protein concentration was quantified by spectrophotometry (NanoDrop 2000, ThermoFisher Scientific), and protein integrity was confirmed via 12% polyacrylamide gel electrophoresis and Coomassie blue staining (BioRad) (Supplementary Figure 1).

2.4 Indirect ELISA

To assess plasma reactivity against RBD proteins from seasonal HCoVs and SARS-CoV-2, and against the nucleoprotein (NP, kindly provided by Dr. Ricardo T. Gazzinelli, Federal University of Minas Gerais, Brazil (35)), an Enzyme Linked Immunosorbent Assay (ELISA) was performed. High binding 96-well ELISA plates (Costar) were incubated with 100 ng/well of each RBD or NP protein diluted in 1x PBS at room temperature (RT) for 18 hours. The plates were then washed 3x with 1x PBS+0.02% Tween (Synth, PBS-T). Blocking was performed for 1 hour at RT with 150 µL/well of PBS-T containing 1% bovine serum albumin (BSA, Merck) and 5% powdered skim milk (Nestle). After 3 more washes with PBS-T, plasma samples were diluted 1:100, in duplicates, in 100 µL/well of PBS-T containing 0.25% BSA and 5% powdered skim milk, and incubated at 37 °C for 2 hours. Following three additional washes with PBS-T, plates were incubated with 50 µL/well of a secondary anti-human IgG-HRP antibody (1:15,000, KPL) for 1-hour incubation at RT. After three washes with PBS-T, plates were developed using a solution containing 1mg/mL ortho-phenylenediamine dihydrochloride (OPD, Amresco), 0.2 M sodium phosphate and 0.1 M citric acid (pH 4.7) plus 30% H_2O_2. The reaction was stopped with 50 µL of 4N H_2SO_4 (Merck) solution after 15 minutes, and plates were read at a wavelength of 492 nm using the BioTek ELx800 reader (Biotek).

2.5 Competition ELISA

To examine the cross-reactivity of antibodies present in the plasma of each patient, competition ELISA assays were conducted. Plasma from each patient was adsorbed or not with 20 µg/mL of each recombinant RBD for 2 hours at 37°C. Then, the plasmas were diluted 1:100, in duplicates, in 100 µL/well of PBS-T containing 0.25% BSA and 5% powdered skim milk, and transferred to high binding 96-well ELISA plates (Costar) containing 100 ng/well of each RBD (previously diluted in 1x PBS at RT for 18 hours, and washed 3x with 1x PBS-T). Diluted plasmas were then incubated at 37 °C for 2 hours. Following three additional washes with PBS-T, plates were incubated with 50 µL/well of a secondary anti-human IgG-HRP antibody (1:15,000, KPL) for 1-hour incubation at RT. After three washes with PBS-T, plates were developed using a solution containing 1mg/mL ortho-phenylenediamine dihydrochloride (OPD, Amresco), 0.2 M sodium phosphate and 0.1 M citric acid (pH 4.7) plus 30% H_2O_2. The reaction was stopped with 50 µL of 4N H_2SO_4 (Merck) solution after 15 minutes, and plates were read at a wavelength of 492 nm using the BioTek ELx800 reader (Biotek). The O.D. readings obtained for each duplicate without or with RBD adsorption were recorded. The ratio was obtained by dividing the mean values of the O.D. readings obtained without and with RBD adsorption.

2.6 Statistical data analysis

Normality testing was performed using the D'Agostino & Pearson test. For data not passing normality test, non-parametric Kruskal-Wallis test followed by Dunn's multiple comparisons test were utilized. Non-parametric Mann-Whitney test was used when two groups were compared. One-way ANOVA for repetitive measures was used for data passing the normality test. The GraphPad Prism 9 software was used for data analysis and significance was set at $P < 0.05$.

3 Results

3.1 Plasma reactivity to SARS-CoV-2 RBD and nucleocapsid protein

Initially, we tested plasma reactivity against SARS-CoV-2 Wild-type (Wuhan-Hu-1) strain by ELISA (Figure 1). All PCR-negative

10.3389/fimmu.2024.1396603

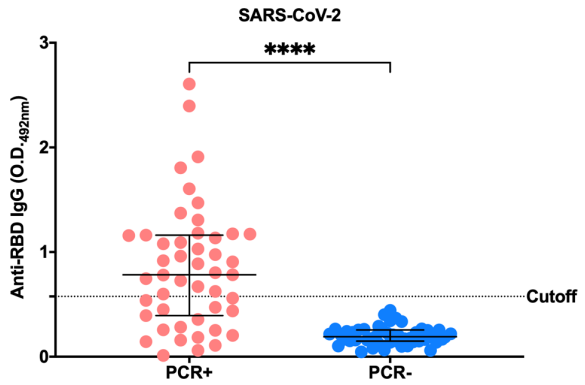

FIGURE 1
SARS-CoV-2 anti-RBD IgG serology profile. Indirect ELISA performed in order to identify the IgG response profile of PCR+ or PCR- individuals against the RBD portion of SARS-CoV-2 Spike protein. Plasma samples were used at a concentration of 1:100 and recombinant RBD at 2 µg/ml (100 ng/well). The test was read at a wavelength of 492 nm. The horizontal black lines represent the medians ± interquartile intervals. Cutoff = Average O.D. of known negative individuals (pre-pandemic samples) + 3 standard deviations. Mann-Whitney test, ****p<0.0001.

(PCR-) individuals presented reactivities below the set cut-off (calculated using 8 pre-pandemic plasma samples plus 3 standard deviations, cutoff= 0.576). Notably, 17 out of 47 PCR-positive (PCR+) individuals failed to seroconvert IgG antibodies against SARS-CoV-2 RBD 30 days after infection, despite the confirmation of infection by real-time PCR. The detailed data are presented in Supplementary Table 1. Although 30 days is generally sufficient for most individuals to develop detectable IgG antibodies, there are significant individual variations in the immune response. These individuals may have generated antibodies against distinct components of the virus, besides the RBD. To test if this was the case, we conducted serological testing for the nucleocapsid protein (NP). Among the 17 individuals without antibodies against SARS-CoV-2 RBD, 9 of them exhibited antibodies to SARS-CoV-2 NP (Supplementary Table 1). Notably, all seven volunteers diagnosed with moderate COVID-19 exhibited detectable levels of SARS-CoV-2 antibodies, targeting the receptor binding domain (RBD) or the nucleocapsid protein (NP).

3.2 Plasma reactivity to HCoV RBDs

We further investigated plasma reactivity against a panel of HCoV RBDs produced in eukaryotic cells (Supplementary Figure 1). Figure 2 shows the reactivity of PCR-positive and negative individuals' plasmas against a panel of recombinant HCoV RBD proteins (HCoV-229E, HCoV-NL63, HCoV-OC43 and HCoV-HKU1). The analysis revealed robust IgG-specific antibody responses to HCoVs among most individuals in the cohort, irrespective of COVID-19 status, displaying relatively high O.D. values (Figures 2B-D), except for HCoV-229E

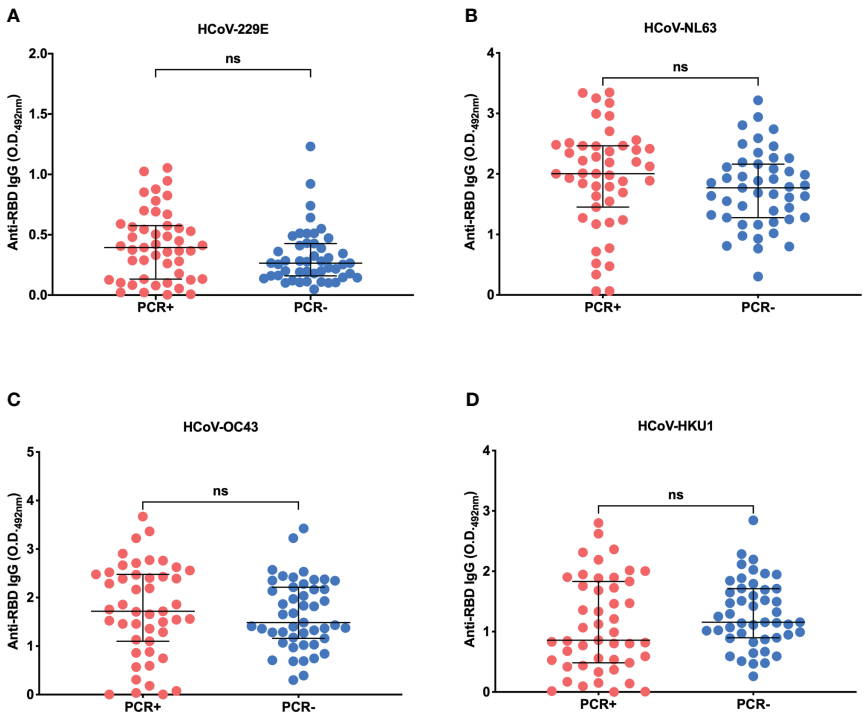

FIGURE 2
Anti-RBD IgG serology profile of HCoV-229E, HCoV-OC43, HCoV-NL63 and HCoV HKU1. IgG response profile of PCR+ or PCR- individuals for SARS-CoV-2 against RBD proteins derived from alphacoronaviruses HCoV-229E **(A)** and HCoV-NL63 **(B)**, and betacoronaviruses HCoV-OC43 **(C)** and HCoV-HKU1 **(D)**. For this assay, the subjects' plasma was used at a concentration of 1:100, and the recombinant RBD in 2 µg/ml (100 ng/well). The test was read in the wavelength of 492 nm and each graph shows the O.D. obtained for the PCR+ (red) or PCR- (blue) individuals for SARS-CoV-2. The horizontal black lines represent the medians ± interquartile intervals. Mann-Whitney test. ns, not significant.

which showed lower reactivity compared to the other HCoVs (Figure 2A). However, more importantly, no statistically significant differences were detected when comparing anti-RBD responses between SARS-CoV-2 PCR-positive and negative individuals (p=0.1054 for HCoV-229E, p=0.1022 for HCoV-NL63, p=0.3347 for HCoV-OC43 and p=0.1113 for HCoV-HKU1). Additionally, when dividing the individuals into groups based on their PCR results and gender, no statistical differences were observed (Supplementary Figures 2A-D). Regarding the reactivity to SARS-CoV-2, both PCR-positive males and females exhibited statistically significant differences in comparison to PCR-negative subjects, but not between PCR-positive or PCR-negative individuals (Supplementary Figure 2E).

3.3 Competition ELISAs to detect anti-HCoV RBD-specific antibodies

The lack of negative controls, i.e. plasma samples that were known to be negative for each HCoV, did not allow us to calculate a cut-off for each HCoV RBD protein, as we did for SARS-CoV-2 in Figure 1. To overcome this limitation and indeed check if we could detect anti-HCoV RBD specific antibodies, plasma samples were pre-incubated with each HCoV RBD, followed by testing on ELISA plates containing the same HCoV RBD. A reduction in response to each HCoV RBD was observed upon previous incubation with the respective HCoV RBD (Figure 3). However, no differences were detected between SARS-CoV-2 PCR-positive and negative individuals regarding plasma reactivity to HCoV-229E (Figure 3A), HCoV-NL63 (Figure 3B), HCoV-OC43 (Figure 3C) or HCoV-HKU1 (Figure 3D), in both non-adsorbed or previously adsorbed samples. As expected, significant differences were detected when comparing PCR-positive and negative plasma samples tested against SARS-CoV-2 RBD (Figure 3E), in line with the clinical and molecular diagnostics.

3.4 Adsorption of plasma samples and evaluation of cross reactivity against each previously tested RBD

We proceeded to adsorb or not the plasma samples from PCR-positive and negative individuals to each HCoVs or SARS-CoV-2 RBD protein and tested them against each HCoV RBD in competition ELISA assays (Figure 4). The normalization of the data involved calculating a ratio of O.D. values obtained without adsorption to those obtained after adsorption. Notably, no statistical differences were found when we compared the ratios of PCR-positive and negative samples for HCoV-229E or the other HCoVs (Figures 4A-D), except a small difference observed for PCR-positive and negative individuals adsorbed against HCoV-OC43 and tested to itself (Figure 4C). It is important to mention that when the samples were adsorbed to a specific protein and subsequently tested with the same protein, we expected an increase in the ratios. As previously observed in Figure 3, adsorption resulted in the removal of the anti-RBD specific antibodies, leading to lower O.D. values when compared to non-adsorbed samples. This is precisely what we observed when the plasma samples from PCR-positive and negative individuals were adsorbed and tested against the same protein.

4 Discussion

In this study, we conducted a comparative analysis of antibody responses to the RBD from the four endemic coronaviruses - HCoV-OC43, HCoV-NL63, HCoV-229E and HCoV-HKU1 – as well as the SARS-CoV-2 RBD. The focus was on individuals in intimate relationships, specifically couples (n=47), who either had symptomatic COVID-19 (SARS-CoV-2 PCR positive) or had not (SARS-CoV-2 PCR negative spouses). Among the infected participants, the majority exhibited mild symptoms (n=40) and were predominantly male, supporting other studies that suggested men were more prone to symptomatic presentations of COVID-19 than females during the first outbreak (2020) of the disease (36, 37). Here, our results indicate that both SARS-CoV-2 infected and uninfected individuals exhibit similar levels of IgG antibodies against the RBD portion of endemic coronaviruses. Furthermore, IgG antibodies against the RBD of different endemic coronaviruses did not show cross-reactivity with the SARS-CoV-2 RBD or with each other.

Our initial results revealed that not every individual who tested positive for SARS-CoV2 infection via PCR (17 out of 47) underwent RBD seroconversion within 30 days following the PCR positive test. In some cases, seroconversion may occur later than expected. Alternatively, these individuals might have developed antibodies targeting different viral components, such as the nucleocapsid protein (NP), a highly immunogenic protein also used in the serological diagnosis of SARS-CoV-2 infection (35, 38). Among those 17 individuals showing reactivity to SARS-CoV-2 below the threshold, 9 had developed antibodies to the SARS-CoV-2 NP. The remaining 8 PCR+ participants who did not show seroconversion for either SARS-CoV-2 RBD or NP might require additional time post-infection to produce anti-RBD/NP antibodies or might be relying on different immune responses that do not involve antibody production. Instead, these mechanisms could include the activation of T cells (39). It is important to mention that further monitoring of seroconversion in these participants was not possible at subsequent time points, as all volunteers received vaccinations shortly after the initial blood sample collection.

Regarding IgG antibody responsiveness to endemic coronavirus RBDs, most individuals, regardless of SARS-CoV-2 PCR status, displayed relatively high O.D. values against RBDs of different HCoVs. This was corroborated by the results of IgG homologous competition ELISAs, indicating that the majority of individuals in the PCR+ and PCR- groups showed similar ratios prior exposure to all HCoVs. However, results on homologous adsorption with HCoV-OC43 RBD did reveal a difference between ratios of non-adsorbed/adsorbed plasmas observed in PCR+ and PCR- subjects. This was unexpected since it was not apparent when comparing O.D. values of HCoV-OC43 RBD between the PCR+ and PCR- groups. Currently, we do not have a clear explanation for this difference. This may suggest that patients with COVID-19 could

10.3389/fimmu.2024.1396603

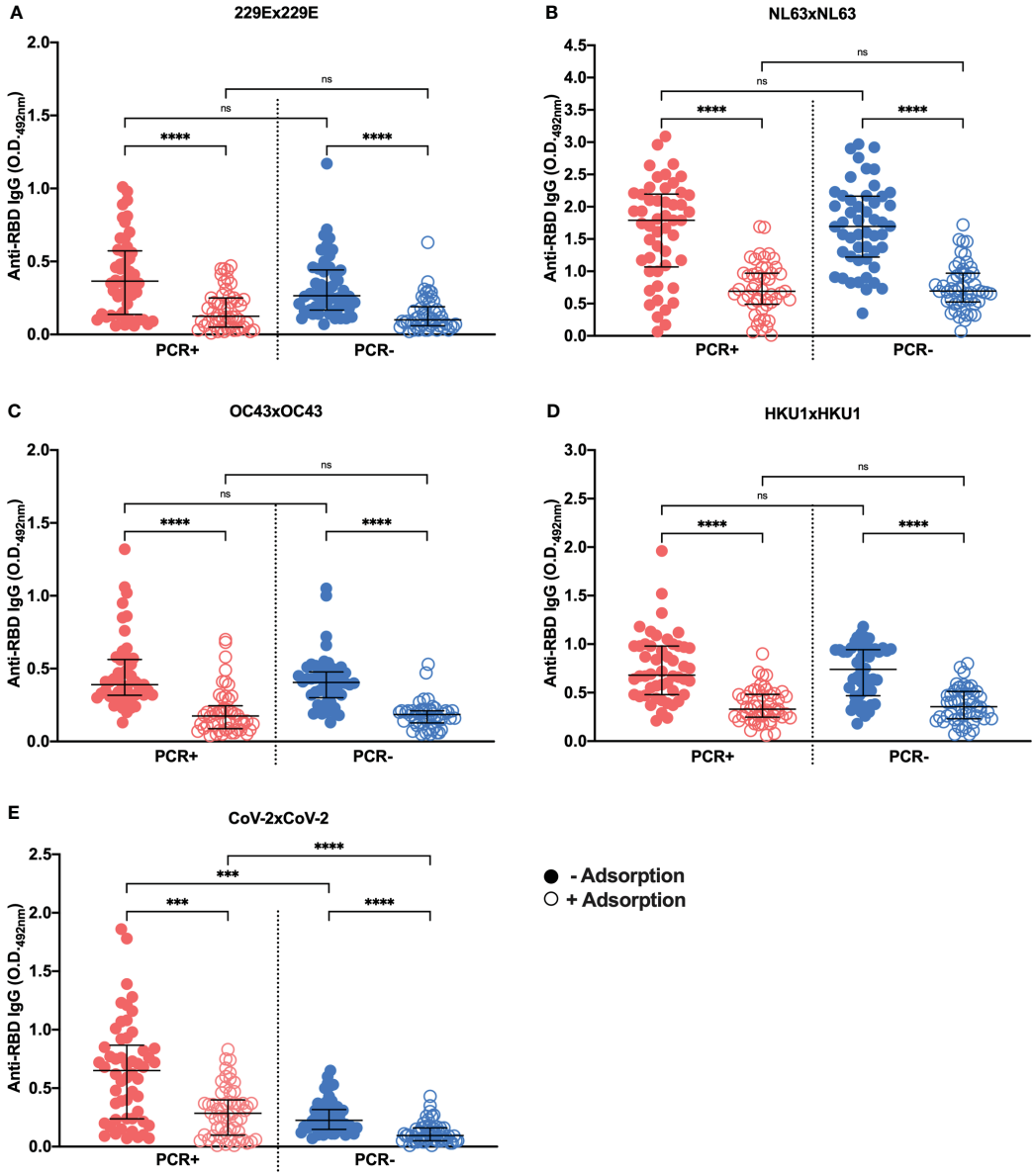

FIGURE 3
Cross-reactivity testing using SARS-CoV-2 PCR-positive (PCR+) and negative (PCR-) samples adsorbed or not against each RBD protein. Graphs show ELISA assays with samples of SARS-CoV-2 PCR+ or PCR- individuals against RBD proteins from HCoV-229E **(A)**, HCoV-NL63 **(B)**, HCoV-OC43 **(C)**, HCoV-HKU1 **(D)** and SARS-CoV-2 **(E)** adsorbed (open circles) or not (filled circles) to their respective proteins. Plasma from the subjects was used at a concentration of 1:500 and the recombinant RBD for coating diluted to 2 µg/mL (100 ng/well) and for adsorption at 20 µg/mL. The assay read-out was performed at a wavelength of 492 nm. The graphs show O.D. values for SARS-CoV-2 PCR+ (red) or PCR- (blue) individuals, with and without adsorption with the respective RBD protein. The horizontal black lines represent the medians ± interquartile intervals. Kruskal-Wallis followed by the Dunn's test. ***p<0.001 and ****p<0.0001; ns, not significant.

have increased antibody levels against HCoV-OC43 RBD and therefore could have been more exposed, or more recently exposed to it. A previous report using samples from the United States noticed an increase in reactivity against S protein of HCoV-HKU1 among individuals who developed COVID-19 disease as compared to COVID-19 negative subjects (40). At any event, our interpretation is that anti-RBD antibodies acquired in a previous infection with endemic coronaviruses play no role in the non-acquisition of SARS-CoV-2 infection of the PCR negative partner, thus having no protective effect. This conclusion is supported by previous data, where no significant differences were observed in the reactivity of sera from COVID-19 patients compared to individuals from the pre-pandemic period for the S proteins of HCoV-229E, HCoV-OC43 and HCoV-NL63 (40). Taken together, these findings suggest that SARS-CoV-2 infection might not induce the expansion of B cell clones with RBD-specific memory exhibiting cross-reactivity to any of the HCoVs, possibly due to the limited amino acid similarity (19 to 21%) between the RBDs of HCoVs and SARS-CoV-2 (32).

In terms of cross-reactivity between endemic coronavirus RBDs and SARS-CoV-2 RBD, as measured by the heterologous competition RBD ELISA assays, no cross-reactivity was observed

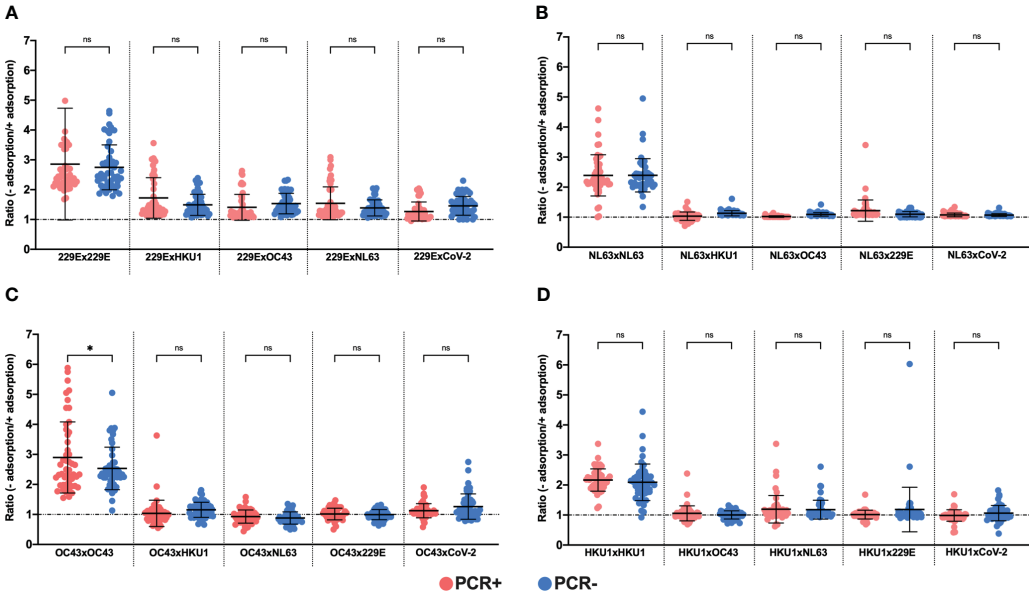

FIGURE 4
Ratio between O.D. values of plasma samples not adsorbed and adsorbed to recombinants RBDs of seasonal coronavirus. To assess cross-reactivity between proteins seasonal coronavirus RBDs were performed in competition ELISA assays, using 100 plasma samples from PCR+ (red) and PCR- (blue) individuals to COVID-19. The charts show the data normalized from non-adsorbed and adsorbed plasma samples against RBDs proteins from HCOV-229E **(A)**, HCOV-NL63 **(B)**, HCOV-OC43 **(C)** and HCOV-HKU1 **(D)**. The individual plasma was used in a title of 1:500 and the recombinant RBD for the coating was diluted in 2 µg/mL (100 ng/well) and for adsorption at 20 µg/mL. The assay reading was performed at a wavelength of 492 nm and each symbol shows the value of the ratio between the O.D. values without adsorption/with adsorption. The horizontal black lines represent the mean ± SD. One-way ANOVA for repetitive measures. *p<0.01; ns, not significant.

between endemic coronaviruses and SARS-CoV-2 RBDs, as well as no cross-reactivity among different endemic coronaviruses themselves, while homologous competition ELISAs showed the expected reduction of reactivity after absorption. It is worth noting that, as a control, we included the SARS-CoV-2 RBD, for which the homologous competition ELISA was validated.

These findings suggest that SARS-CoV-2 infection may not induce the expansion of memory B cell clones previously activated with endemic coronavirus RBDs, possibly due to limited amino acid homology between the RBDs of SARS-CoV-2 and those of HCoVs (32). However, it is critical to clarify that our findings do not suggest a complete absence of cross-reactivity between HCoVs and SARS-CoV-2. Indeed, several studies analyzing pre-pandemic serum or plasma samples have identified a significant fraction showing reactivity with the S protein of SARS-CoV-2 (24, 40–42). Notably, Majdoubi et al. showed that over 90% of non-infected adults exhibited antibody reactivity against the S protein, its RBD, its N-terminal domain (NTD), or the NP of SARS-CoV-2 (41). Conversely, others have shown that the cross-reactive antibody responses against the S protein were predominantly targeted to the S2 fragment, a region of the S protein that is significantly more conserved (24, 42). Moreover, Song et al. provided limited evidence for the existence of pre-pandemic cross-reactive serum antibodies against SARS-CoV-2. However, they detected pre-existing cross-reactive memory B cells that underwent further expansion upon SARS-CoV-2 infection (40). A cross-reactive peptide within the S2 fragment of the S protein was subsequently identified (43). Following SARS-CoV-2 infection and vaccination, a 2- to 4-fold increase in antibodies that bind to seasonal HCoVs was observed in sera, compared to those from pre-pandemic healthy donors, with the S2 fragment being the main target of cross-reactivity (44). More recently, broadly neutralizing monoclonal antibodies targeting not the RBD but the S2 fragment were also developed (45, 46). Thus, the absence of cross-reactivity between the RBDs of various endemic HCoVs and SARS-CoV-2 observed in our study is consistent with these previous findings.

It should also be noted that the major limitation of our study was that we used ELISA readings as the only read-out for our experiments. Nonetheless, competition assays and the absence of statistical differences in antibody responses between PCR-positive and negative individuals suggest that pre-existing antibodies against HCoV RBDs may not confer protection against SARS-CoV-2 infection.

Data availability statement

The original contributions presented in the study are included in the article/Supplementary Material. Further inquiries can be directed to the corresponding author.

Ethics statement

The study was approved by the Committee for Ethics in Research of the Institute of Biosciences at the University of São

Paulo (CAAE 34786620.2.0000.5464) following the Declaration of Helsinki principles, ICH06 Good Clinical Practices, and Brazilian Health Regulatory Agency (ANVISA) resolution number 466 from 2012 that regulates research with humans. Participants were enrolled in the study between June 24 and October 1, 2020, during which time blood samples were collected. The researchers in this study also had access to demographic and clinical data of the participants, which was necessary to integrate these findings with the serological results. However, the data remained anonymized and confidential to anyone unauthorized outside of this study. All participants were >18 years old and provided written informed consent prior to participation.

Author contributions

FA: Formal analysis, Investigation, Methodology, Validation, Visualization, Writing – original draft. MC: Data curation, Resources, Writing – review & editing. BA: Investigation, Validation, Writing – review & editing. ID: Investigation, Validation, Writing – review & editing. MY: Investigation, Validation, Writing – review & editing. KS: Writing – review & editing. MZ: Funding acquisition, Resources, Writing – review & editing. MN: Data curation, Resources, Writing – review & editing. DR: Conceptualization, Methodology, Writing – review & editing. EC-N: Funding acquisition, Writing – review & editing. VO: Methodology, Project administration, Resources, Validation, Visualization, Writing – review & editing. JK: Funding acquisition, Resources, Writing – review & editing. SB: Conceptualization, Formal analysis, Funding acquisition, Methodology, Resources, Supervision, Validation, Visualization, Writing – review & editing.

Funding

The author(s) declare financial support was received for the research, authorship, and/or publication of this article. This research was supported by the Brazilian National Research Council (CNPq, grants 465434/2014-2 and 404134/2020-3), the Sao Paulo State Research Funding Agency (FAPESP, grants 2018/07142-9, 2014/50890-5, 2014/50931-3 and 2020/09702-1), the Coordination for the Improvement of Higher Education Personnel (CAPES, Finance code 001 and grant 23038.000776/2017-54), the Funding Authority for Studies and Projects (FINEP, contract 01.20.0009.00) and JBS S.A (grant 69004).

Acknowledgments

We thank all individuals in the cohort and the medical and multidisciplinary team involved. The funders had no role in study design, data collection and analysis, decision to publish, or preparation of the manuscript.

Conflict of interest

The authors declare that the research was conducted in the absence of any commercial or financial relationships that could be construed as a potential conflict of interest.

The author(s) declared that they were an editorial board member of Frontiers, at the time of submission. This had no impact on the peer review process and the final decision.

Publisher's note

Supplementary material

The Supplementary Material for this article can be found online at: https://www.frontiersin.org/articles/10.3389/fimmu.2024.1396603/full#supplementary-material

References

1. Garbino J, Crespo S, Aubert JD, Rochat T, Ninet B, Deffernez C, et al. A prospective hospital-based study of the clinical impact of non-severe acute respiratory syndrome (Non-sars)-related human coronavirus infection. *Clin Infect Dis*. (2006) 43:1009–15. doi: 10.1086/507898

2. Makela MJ, Puhakka T, Ruuskanen O, Leinonen M, Saikku P, Kimpimaki M, et al. Viruses and bacteria in the etiology of the common cold. *J Clin Microbiol*. (1998) 36:539–42. doi: 10.1128/JCM.36.2.539–542.1998

3. Jonassen CM, Kofstad T, Larsen IL, Lovland A, Handeland K, Follestad A, et al. Molecular identification and characterization of novel coronaviruses infecting graylag geese (Anser anser), feral pigeons (Columbia livia) and mallards (Anas platyrhynchos). *J Gen Virol*. (2005) 86:1597–607. doi: 10.1099/vir.0.80927–0

4. Liu DX, Liang JQ, Fung TS. Human Coronavirus-229e, -Oc43, -Nl63, and -Hku1 (Coronaviridae). In: Bamford DH, Zuckerman M, editors. *Encyclopedia of Virology*, *4th ed*. Oxford, UK: Academic Press (2021). p. 428–40.

5. Hamre D, Procknow JJ. A new virus isolated from the human respiratory tract. *Proc Soc Exp Biol Med*. (1966) 121:190–3. doi: 10.3181/00379727–121-30734

6. Almeida JD, Tyrrell DA. The morphology of three previously uncharacterized human respiratory viruses that grow in organ culture. *J Gen Virol*. (1967) 1:175–8. doi: 10.1099/0022–1317-1–2-175

7. van der Hoek L, Pyrc K, Jebbink MF, Vermeulen-Oost W, Berkhout RJ, Wolthers KC, et al. Identification of a new human coronavirus. *Nat Med*. (2004) 10:368–73. doi: 10.1038/nm1024

8. Woo PC, Lau SK, Chu CM, Chan KH, Tsoi HW, Huang Y, et al. Characterization and complete genome sequence of a novel coronavirus, coronavirus hku1, from patients with pneumonia. *J Virol*. (2005) 79:884–95. doi: 10.1128/JVI.79.2.884–895.2005

9. Pene F, Merlat A, Vabret A, Rozenberg F, Buzyn A, Dreyfus F, et al. Coronavirus 229e-related pneumonia in immunocompromised patients. *Clin Infect Dis*. (2003) 37:929–32. doi: 10.1086/377612

10. Vassilara F, Spyridaki A, Pothitos G, Deliveliotou A, Papadopoulos A. A rare case of human coronavirus 229e associated with acute respiratory distress syndrome in a healthy adult. *Case Rep Infect Dis*. (2018) 2018:6796839. doi: 10.1155/2018/6796839

11. Lau SK, Lee P, Tsang AK, Yip CC, Tse H, Lee RA, et al. Molecular epidemiology of human coronavirus oc43 reveals evolution of different genotypes over time and recent emergence of a novel genotype due to natural recombination. *J Virol*. (2011) 85:11325–37. doi: 10.1128/JVI.05512–11

12. Abdul-Rasool S, Fielding BC. Understanding human coronavirus hcov-nl63. *Open Virol J*. (2010) 4:76–84. doi: 10.2174/1874357901004010076

13. Mathewson AC, Bishop A, Yao Y, Kemp F, Ren J, Chen H, et al. Interaction of severe acute respiratory syndrome-coronavirus and nl63 coronavirus spike proteins with angiotensin converting enzyme-2. *J Gen Virol*. (2008) 89:2741–5. doi: 10.1099/vir.0.2008/003962–0

14. Lau SK, Woo PC, Yip CC, Tse H, Tsoi HW, Cheng VC, et al. Coronavirus hku1 and other coronavirus infections in Hong Kong. *J Clin Microbiol*. (2006) 44:2063–71. doi: 10.1128/JCM.02614–05

15. Zhu N, Zhang D, Wang W, Li X, Yang B, Song J, et al. A novel coronavirus from patients with pneumonia in China, 2019. *N Engl J Med*. (2020) 382:727–33. doi: 10.1056/NEJMoa2001017

16. Huang Y, Yang C, Xu XF, Xu W, Liu SW. Structural and functional properties of sars-cov-2 spike protein: potential antivirus drug development for covid-19. *Acta Pharmacol Sin*. (2020) 41:1141–9. doi: 10.1038/s41401–020-0485–4

17. Lu W, Zhao Z, Huang YW, Wang B. Review: A systematic review of virus-like particles of coronavirus: assembly, generation, chimerism and their application in basic research and in the clinic. *Int J Biol Macromol*. (2022) 200:487–97. doi: 10.1016/j.ijbiomac.2022.01.108

18. Rota PA, Oberste MS, Monroe SS, Nix WA, Campagnoli R, Icenogle JP, et al. Characterization of a novel coronavirus associated with severe acute respiratory syndrome. *Science*. (2003) 300:1394–9. doi: 10.1126/science.1085952

19. Wu XD, Shang B, Yang RF, Yu H, Ma ZH, Shen X, et al. The spike protein of severe acute respiratory syndrome (Sars) is cleaved in virus infected vero-E6 cells. *Cell Res*. (2004) 14:400–6. doi: 10.1038/sj.cr.7290240

20. Taguchi F. The S2 subunit of the murine coronavirus spike protein is not involved in receptor binding. *J Virol*. (1995) 69:7260–3. doi: 10.1128/JVI.69.11.7260–7263.1995

21. Xiao X, Chakraborti S, Dimitrov AS, Gramatikoff K, Dimitrov DS. The sars-cov S glycoprotein: expression and functional characterization. *Biochem Biophys Res Commun*. (2003) 312:1159–64. doi: 10.1016/j.bbrc.2003.11.054

22. da Silva Antunes R, Pallikkuth S, Williams E, Dawen Yu E, Mateus J, Quiambao L, et al. Differential T-cell reactivity to endemic coronaviruses and sars-cov-2 in community and health care workers. *J Infect Dis*. (2021) 224:70–80. doi: 10.1093/infdis/jiab176

23. To KK, Cheng VC, Cai JP, Chan KH, Chen LL, Wong LH, et al. Seroprevalence of sars-cov-2 in hong kong and in residents evacuated from Hubei Province, China: A multicohort study. *Lancet Microbe*. (2020) 1:e111–e8. doi: 10.1016/S2666–5247(20)30053–7

24. Nguyen-Contant P, Embong AK, Kanagaiah P, Chaves FA, Yang H, Branche AR, et al. S protein-reactive igg and memory B cell production after human sars-cov-2 infection includes broad reactivity to the S2 subunit. *mBio*. (2020) 11(5):e01991-20. doi: 10.1128/mBio.01991-20

25. Anderson EM, Goodwin EC, Verma A, Arevalo CP, Bolton MJ, Weirick ME, et al. Seasonal human coronavirus antibodies are boosted upon sars-cov-2 infection but not associated with protection. *Cell*. (2021) 184:1858–64 e10. doi: 10.1016/j.cell.2021.02.010

26. Poston D, Weisblum Y, Wise H, Templeton K, Jenks S, Hatziioannou T, et al. Absence of severe acute respiratory syndrome coronavirus 2 neutralizing activity in prepandemic sera from individuals with recent seasonal coronavirus infection. *Clin Infect Dis*. (2021) 73:e1208–e11. doi: 10.1093/cid/ciaa1803

27. Shrock E, Fujimura E, Kula T, Timms RT, Lee IH, Leng Y, et al. Viral epitope profiling of covid-19 patients reveals cross-reactivity and correlates of severity. *Science*. (2020) 370z:eabd4250. doi: 10.1126/science.abd4250

28. Henss L, Scholz T, von Rhein C, Wieters I, Borgans F, Eberhardt FJ, et al. Analysis of humoral immune responses in patients with severe acute respiratory syndrome coronavirus 2 infection. *J Infect Dis*. (2021) 223:56–61. doi: 10.1093/infdis/jiaa680

29. Morgenlander WR, Henson SN, Monaco DR, Chen A, Littlefield K, Bloch EM, et al. Antibody responses to endemic coronaviruses modulate covid-19 convalescent plasma functionality. *J Clin Invest*. (2021) 131(7):e146927. doi: 10.1172/JCI146927

30. Sagar M, Reifler K, Rossi M, Miller NS, Sinha P, White LF, et al. Recent endemic coronavirus infection is associated with less-severe covid-19. *J Clin Invest*. (2021) 131(1):e143380. doi: 10.1172/JCI143380

31. Gandhi RT, Lynch JB, Del Rio C. Mild or moderate covid-19. *N Engl J Med*. (2020) 383:1757–66. doi: 10.1056/NEJMcp2009249

32. Premkumar L, Segovia-Chumbez B, Jadi R, Martinez DR, Raut R, Markmann A, et al. The receptor binding domain of the viral spike protein is an immunodominant and highly specific target of antibodies in sars-cov-2 patients. *Sci Immunol*. (2020) 5(48):eabc8413. doi: 10.1126/sciimmunol.abc8413

33. Amanat F, Stadlbauer D, Strohmeier S, Nguyen THO, Chromikova V, McMahon M, et al. A serological assay to detect sars-cov-2 seroconversion in humans. *Nat Med*. (2020) 26:1033–6. doi: 10.1038/s41591–020-0913–5

34. Stadlbauer D, Amanat F, Chromikova V, Jiang K, Strohmeier S, Arunkumar GA, et al. Sars-cov-2 seroconversion in humans: A detailed protocol for a serological assay, antigen production, and test setup. *Curr Protoc Microbiol*. (2020) 57:e100. doi: 10.1002/cpmc.100

35. Bagno FF, Sergio SAR, Figueiredo MM, Godoi LC, Andrade LAF, Salazar NC, et al. Development and validation of an enzyme-linked immunoassay kit for diagnosis and surveillance of covid-19. *J Clin Virol Plus*. (2022), 100103. doi: 10.1016/j.jcvp.2022.100103

36. Abate BB, Kassie AM, Kassaw MW, Aragie TG, Masresha SA. Sex difference in coronavirus disease (Covid-19): A systematic review and meta-analysis. *BMJ Open*. (2020) 10:e040129. doi: 10.1136/bmjopen-2020–040129

37. Silva MVR, de Castro MV, Passos-Bueno MR, Otto PA, Naslavsky MS, Zatz M. Men are the main covid-19 transmitters: behavior or biology? *Discovery Ment Health*. (2022) 2:1. doi: 10.1007/s44192–022-00004–3

38. Hachim A, Kavian N, Cohen CA, Chin AWH, Chu DKW, Mok CKP, et al. Orf8 and orf3b antibodies are accurate serological markers of early and late sars-cov-2 infection. *Nat Immunol*. (2020) 21:1293–301. doi: 10.1038/s41590–020-0773–7

39. Sette A, Crotty S. Adaptive immunity to sars-cov-2 and covid-19. *Cell*. (2021) 184:861–80. doi: 10.1016/j.cell.2021.01.007

40. Song G, He WT, Callaghan S, Anzanello F, Huang D, Ricketts J, et al. Cross-reactive serum and memory B-cell responses to spike protein in sars-cov-2 and endemic coronavirus infection. *Nat Commun*. (2021) 12:2938. doi: 10.1038/s41467–021-23074–3

41. Majdoubi A, Michalski C, O'Connell SE, Dada S, Narpala S, Gelinas J, et al. A majority of uninfected adults show preexisting antibody reactivity against sars-cov-2. *JCI Insight*. (2021) 6(8):e146316. doi: 10.1172/jci.insight.146316

42. Ng KW, Faulkner N, Cornish GH, Rosa A, Harvey R, Hussain S, et al. Preexisting and *de novo* humoral immunity to sars-cov-2 in humans. *Science*. (2020) 370:1339–43. doi: 10.1126/science.abe1107

43. Jia L, Weng S, Wu J, Tian X, Zhang Y, Wang X, et al. Preexisting antibodies targeting sars-cov-2 S2 cross-react with commensal gut bacteria and impact covid-19 vaccine induced immunity. *Gut Microbes*. (2022) 14:2117503. doi: 10.1080/19490976.2022.2117503

44. Grobben M, van der Straten K, Brouwer PJ, Brinkkemper M, Maisonnasse P, Dereuddre-Bosquet N, et al. Cross-reactive antibodies after sars-cov-2 infection and vaccination. *Elife*. (2021) 10:e70330. doi: 10.7554/eLife.70330

45. Ko SH, Chen WY, Su SC, Lin HT, Ke FY, Liang KH, et al. Monoclonal Antibodies against S2 Subunit of Spike Protein Exhibit Broad Reactivity toward Sars-Cov-2 Variants. *J BioMed Sci*. (2022) 29:108. doi: 10.1186/s12929–022-00891–2

46. Zhou P, Song G, Liu H, Yuan M, He WT, Beutler N, et al. Broadly neutralizing anti-S2 antibodies protect against all three human betacoronaviruses that cause deadly disease. *Immunity*. (2023) 56:669–86 e7. doi: 10.1016/j.immuni.2023.02.005

frontiers | Frontiers in Immunology

TYPE Original Research
PUBLISHED 18 July 2024
DOI 10.3389/fimmu.2024.1425374

OPEN ACCESS

EDITED BY
Erez Bar-Haim,
Israel Institute for Biological Research (IIBR), Israel

REVIEWED BY
Jane Homan,
ioGenetics LLC, United States
Marsia Gustiananda,
Indonesia International Institute for Life-Sciences (i3L), Indonesia

*CORRESPONDENCE
Pedro A. Reche
parecheg@med.ucm.es

†These authors have contributed equally to this work

RECEIVED 29 April 2024
ACCEPTED 02 July 2024
PUBLISHED 18 July 2024

CITATION
Fernandez SA, Pelaez-Prestel HF, Fiyouzi T, Gomez-Perosanz M, Reiné J and Reche PA (2024) Tetanus-diphtheria vaccine can prime SARS-CoV-2 cross-reactive T cells. *Front. Immunol.* 15:1425374. doi: 10.3389/fimmu.2024.1425374

Tetanus-diphtheria vaccine can prime SARS-CoV-2 cross-reactive T cells

Sara Alonso Fernandez[1†], Hector F. Pelaez-Prestel[1†], Tara Fiyouzi[1†], Marta Gomez-Perosanz[1], Jesús Reiné[2,3] and Pedro A. Reche[1*]

[1]Department of Immunology & O2, Faculty of Medicine, Complutense University of Madrid, Ciudad Universitaria, Madrid, Spain, [2]Clinical Sciences, Liverpool School of Tropical Medicine, Liverpool, United Kingdom, [3]Oxford Vaccine Group, University of Oxford, Oxford, United Kingdom

Vaccines containing tetanus-diphtheria antigens have been postulated to induce cross-reactive immunity to severe acute respiratory syndrome coronavirus 2 (SARS-CoV-2), which could protect against coronavirus disease (COVID-19). In this work, we investigated the capacity of Tetanus-diphtheria (Td) vaccine to prime existing T cell immunity to SARS-CoV-2. To that end, we first collected known SARS-CoV-2 specific $CD8^+$ T cell epitopes targeted during the course of SARS-CoV-2 infection in humans and identified as potentially cross-reactive with Td vaccine those sharing similarity with tetanus-diphtheria vaccine antigens, as judged by Levenshtein edit distances (≤ 20% edits per epitope sequence). As a result, we selected 25 potentially cross-reactive SARS-CoV-2 specific $CD8^+$ T cell epitopes with high population coverage that were assembled into a synthetic peptide pool (TDX pool). Using peripheral blood mononuclear cells, we first determined by intracellular IFNγ staining assays existing $CD8^+$ T cell recall responses to the TDX pool and to other peptide pools, including overlapping peptide pools covering SARS-CoV-2 Spike protein and Nucleocapsid phosphoprotein (NP). In the studied subjects, $CD8^+$ T cell recall responses to Spike and TDX peptide pools were dominant and comparable, while recall responses to NP peptide pool were less frequent and weaker. Subsequently, we studied responses to the same peptides using antigen-inexperienced naive T cells primed/stimulated *in vitro* with Td vaccine. Priming stimulations were carried out by co-culturing naive T cells with autologous irradiated peripheral mononuclear cells in the presence of Td vaccine, IL-2, IL-7 and IL-15. Interestingly, naive $CD8^+$ T cells stimulated/primed with Td vaccine responded strongly and specifically to the TDX pool, not to other SARS-CoV-2 peptide pools. Finally, we show that Td-immunization of C57BL/6J mice elicited T cells cross-reactive with the TDX pool. Collectively, our findings support that tetanus-diphtheria vaccines can prime SARS-CoV-2 cross-reactive T cells and likely contribute to shape the T cell responses to the virus.

KEYWORDS

COVID-19, SARS-CoV-2, epitope, T cell cross-reactivity, tetanus-diphtheria toxoid vaccines

1 Introduction

Severe acute respiratory syndrome coronavirus 2 (SARS-CoV-2) is an emergent β-coronavirus identified in late 2019, causing pneumonia as well as a wide array of ailments and symptoms under the umbrella of coronavirus disease 2019 (COVID-19) (1). The rapid spread and pathogenesis of SARS-CoV-2 resulted in a global pandemic and health crisis that urged the mass deployment of novel COVID-19 vaccines (2). However, SARS-CoV-2 remains a public health concern since COVID-19 vaccines do not provide sterile immunity (3) and new SARS-CoV-2 variants have emerged (4). Hence, effective and universal measures against COVID-19 are still in demand. Fortunately, we now know much about SARS-CoV-2 infection and immune responses, which should help in this endeavor.

It is now clear that exposure to SARS-CoV-2 does not always result in infection, nor does infection follow the same course in everyone (5). Several factors have been identified to increase the severity of COVID-19, most notably old age, but also obesity, male gender and the presence of conditions like diabetes and vascular diseases (6). The immune response to SARS-CoV-2 plays itself a major role in the course of infection. The most severe cases of COVID-19 are characterized by significant immunopathology, resulting from a disproportionate anti-viral innate immune response, concomitant with a poor adaptive immune response (7, 8). In contrast, COVID-19 severity and duration are reduced in individuals developing a coordinated adaptive immune response, involving SARS-CoV-2-specific $CD4^+$ and $CD8^+$ T cells and neutralizing antibodies (9). However, anti-SARS-CoV-2 neutralizing antibodies are short-lived (10) and long-term immunity to SARS-CoV-2 appears to be mediated by memory T cells (11–13). Moreover, there is evidence indicating that T cell immunity alone, in the absence of neutralizing antibodies, may protect from SARS-CoV-2 (14). SARS-CoV-2-specific T cell immunity is characterized by $CD4^+$ T cells with a typical T cell helper type 1 (Th1) phenotype (11, 13) but displaying a lower IFNγ/TNFα ratio than influenza-specific Th1 responses (15). Th1 cells promote the activation and differentiation of SARS-CoV-2 specific cytotoxic $CD8^+$ T cells, which are crucial for resolving the infection by killing infected cells (16, 17). In fact, delayed $CD8^+$ T cell responses have been linked to severe COVID-19, since viral replication in the lungs is not controlled sufficiently fast (18).

Adaptive immune responses to SARS-CoV-2 induced by both infection and vaccines are surely influenced by pre-existing cross-reactive immunity (19–22). Cross-reactive immunity occurs when memory T and B cells elicited by a primary encounter with pathogens/antigens recognize and respond to different pathogens/antigens (23, 24). The first evidence of pre-existing cross-reactive immunity to SARS-CoV-2 came from the extensive T cell and antibody responses to the virus detected in unexposed individuals prior to or early in the outbreak (25–28). T cells are by nature more cross-reactive than B cells (29) and about 20–85% of unexposed individuals have been shown to present T cell reactivity to SARS-CoV-2 (25, 30). Interestingly, while pre-existing B-cell cross-reactivity can enhance SARS-CoV-2 pathogenesis (31, 32), cross-reactive memory T cells contribute to host protection (33).

Immune cross-reactivity is more likely to occur, and easy to detect, between related pathogens/antigens. SARS-CoV-2 shares sequence and structure similarity with common cold human coronavirus (ccHCoVs), comprising two α-coronaviruses (299E and NL63) and two β-coronaviruses (HKU1, OC43) (34), which cause seasonal and prevalent infections in humans (35, 36). Therefore, immune cross-reactivity between SARS-CoV-2 and ccHCoVs has received major attention and is widely documented (37, 38). It has been reported that up to 50% of T cell clones generated from unexposed subjects against SARS-CoV-2 peptides can cross-react with ccHCoVs peptides (39). However, other studies point out that the cross-reactive T cell epitope repertoire between SARS-CoV-2 and ccHCoVs is much smaller (40, 41). Moreover, T cell cross-reactivity has also been identified between SARS-CoV-2 and unrelated pathogens/antigens, including bacteria (42) and common viruses like human cytomegalovirus (43, 44) and influenza virus (44). Therefore, the priming sources of cross-reactive T cells to SARS-CoV-2 and contribution to protection are still unclear.

Adaptive immunity develops early during childhood from exposure to environmental antigenic challenges (e.g. microbes and vaccines) (45), and so does cross-reactive immunity to SARS-CoV-2. Interestingly, small children, who are generally vulnerable to new pathogens, are particularly resilient to SARS-CoV-2 infection (46). Since children receive multiple vaccinations from infancy to puberty, we investigated in a seminal *in silico* work common vaccines as potential sources of cross-reactive immunity to SARS-CoV-2 (47, 48). We concluded that vaccines containing tetanus-diphtheria antigens could induce cross-reactive protective immunity to SARS-CoV-2 (47, 48). Evidence of such protection was confirmed latter (49) and it has been shown that T cells expanded with SARS-CoV-2 antigens and Tdap vaccine, which includes tetanus-diphtheria antigens and acellular *Bordetella pertussis* antigens, exhibit overlapping T cell receptor (TCR) repertoires (50). It is worth noting that vaccines containing tetanus-diphtheria toxoids include far more proteins than the inactivated toxins. As revealed by proteomics analysis, diphtheria and tetanus toxoids only account for ~50–70% of the total protein content in these vaccines, being accompanied by hundreds of additional proteins from the relevant bacteria (51–53). All these tetanus-diphtheria antigens can be immunogenic and were taken into consideration in our former *in silico* analysis. Given the relevance of $CD8^+$ T cells in clearing viral infections, in this work, we experimentally studied SARS-CoV-2 $CD8^+$ T cell cross-reactivity from tetanus-diphtheria Td vaccines. We report that stimulation of naive T cells with autologous irradiated peripheral mononuclear cells pulsed with a tetanus-diphtheria Td vaccine renders them cross-reactive with a peptide pool consisting of 25 known SARS-CoV-2-specific $CD8^+$ T cell epitopes related by similarity with antigens in Td vaccines (TDX pool). In contrast, these same T cells seldom responded to control peptides, including other SARS-CoV-2 peptide pools from Spike protein and Nucleocapsid phosphoprotein (NP). In addition, we also found that Td immunization of C57BL/6J mice induced T cell responses to the TDX pool. These results support that tetanus-diphtheria vaccines

can prime SARS-CoV-2 cross-reactive T cells and likely contribute to shape the T cell responses to the virus.

2 Methods

2.1 Selection of cross-reactive SARS-CoV-2-specific CD8$^+$ T cell epitopes, prediction of binding to MHC I molecules and computation of population coverage

SARS-CoV-2-specific CD8$^+$ T cell epitopes potentially cross-reactive with tetanus-diphtheria antigens were selected upon experimentally verified SARS-CoV-2-specific CD8$^+$ T cell epitopes targeted by humans infected with SARS-CoV-2. Such SARS-CoV-2-specific CD8$^+$ T cell epitopes were obtained from the Immune Epitope Database (IEDB)[(54) after the following search criteria: 1) Peptide, linear; 2) Host, human; 3) Source, SARS-CoV-2; 4) T cell assay, positive results only; 5) Restriction, Class I and 6) Disease, infection. T cell epitope assays were downloaded and processed, and a dataset consisting of the amino acid sequences of 1153 distinct SARS-CoV-2-specific CD8$^+$ T cell epitopes with their reported restriction elements was assembled (Supplementary Dataset 1). Subsequently, a PERL script for fuzzy matching based on Levenshtein edit distances (String: Approx perl extension) was used to select CD8$^+$ T cell epitopes whose sequences matched those of antigens identified in tetanus-diphtheria vaccines. Approximate matches of up to 20% edits per epitope sequence (insertions, deletions or substitutions) were allowed. A 20% Levenshtein distance for a peptide of 10 residues means that two editions are required to produce a match, while a peptide matching exactly has 0 Levenshtein distance. The Levenshtein distance between sequences is related to their similarity but it does not align with a fixed percentage of similarity. Protein antigens in diphtheria and tetanus toxoid vaccines were those identified through proteomics studies and available in proteome datasets PXD012806 (51), PXD013804 (52) and PXD009289 (53) at the Proteomics Identification Database (PRIDE). Protein sequences were retrieved from UniProt and assembled into a single file in FASTA format including 210 antigens from *Corynebacterium diphtheriae* (diphtheria) and 548 from *Clostridium tetani* (tetanus). Antigen sequences and PERL script for fuzzy matching can be obtained from the corresponding author upon written request.

Binding of CD8$^+$ T cell peptide epitopes to human and mouse major histocompatibility complex class I (MHC I) molecules was predicted using standalone versions of RANKPEP (55, 56) and NetMHCpan (57, 58). The targeted MHC I molecules included 22 human leukocyte antigens class I (HLA I) molecules (HLA-A*01:01, HLA-A*02:01, HLA-A*02:03, HLA-A*02:06, HLA-A*03:01, HLA-A*11:01, HLA-A*23:01, HLA-A*24:02. HLA-A*26:01, HLA-A*30:01, HLA-A*30:02, HLA-A*31:01, HLA-A*32:01, HLA-A*33:01, HLA-A*68:01, HLA-A*68:02, HLA-B*07:02, HLA-B*08:01, HLA-B*15:01, HLA-B*35:01, HLA-B*40:01 and HLA-B*44:02) and 9 mouse class I H2 alloantigens (H2-Db, H2-Dd, H2-Dq, H2-Kb, H2-Kd, H2-Kk, H2-Kq, H-2-Ld and H-2-Lq). RANKPEP and NetMHCpan prediction models were selected to match the size of the peptides that had 8 or 9 residues. For longer peptides, the % rank of all nested 9mer peptides was analyzed and the best rank assigned to the peptide. Peptides were considered to bind to any given MHC I molecule if they were reported to have a % rank ≤ 2 by either RANKPEP or NetMHCpan. Human population coverage of CD8$^+$ T cell epitopes was computed after HLA I binding profiles using a standalone version of EPISOPT (59).

2.2 Synthetic peptides and peptide pools

Synthetic peptides corresponding to SARS-CoV-2-specific CD8$^+$ T cell epitopes cross-reactive with tetanus-diphtheria antigens were obtained from ProteoGenix at 2 mg scale and ≥ 90% purity. Peptides were dissolved in 80% dimethyl sulfoxide (DMSO), diluted to a final stock concentration of 5 mM (40% DMSO) and stored at -80°C. A custom peptide pool (TDX pool) was prepared by combining an equal volume of all these peptides (final concentration 200 µM). Commercial SARS-CoV-2 peptide pools consisting of overlapping peptides spanning the entire SARS-CoV-2 nucleocapsid phosphoprotein (NP pool) and S1 immunogenic region of Spike protein (Spike pool) were purchased from Miltenyi: PepTivator® SARS-CoV-2 Prot_N and PepTivator® SARS-CoV-2 Prot_S, respectively (reference Wuhan strain). CEF peptide pool consisting of immunodominant CD8$^+$ T cell peptide epitopes from Human Cytomegalovirus, Epstein-Barr and Influenza A viruses was purchased from Mabtech. PepTivators® pools were reconstituted in sterile H_2O (30 µM final concentration) and CEF pool in DMSO plus phosphate-buffered saline (PBS) buffer (200 µg/ml final concentration), following the manufacturer's instructions.

2.3 Culture media and reagents

Human cells were cultured in RPMI complete medium consisting of RPMI 1640 medium (Gibco) supplemented with 10% of heat-inactivated human serum (Gibco), 2 mM L-glutamine (Lonza), and 100 U/ml penicillin (Lonza) and 100 µg/ml streptomycin (Lonza). Splenocytes from mice were also incubated in RPMI complete medium, but including 10% of heat inactivated fetal bovine serum (FBS)(Gibco), instead of human serum. Cytokines for cell cultures were obtained from Immunotools GmbH. DIFTAVAX® Tetanus-diphtheria (Td) toxoids vaccine (Sanofi-Pasteur) was used for *in vitro* stimulations and *in vivo* immunizations. DIFTAVAX® (Td) contains no less than 2.5 Lf (2 IU) of purified diphtheria toxoid and 5 Lf (20 IU) of purified tetanus toxoid per dose (0.5 ml).

2.4 Isolation of peripheral blood mononuclear cells and naive T cells

Peripheral blood mononuclear cells (PBMCs) were isolated from buffy coats by a density gradient on Ficoll-Paque™ PLUS (Fisher Scientific). PBMCs in the interface layer were collected,

washed twice with cold PBS, resuspended in complete RPMI medium and counted. Buffy coats were provided by the regional blood transfusion center (Centro de Transfusión de la Comunidad de Madrid, Spain), and were obtained from healthy donors after written informed consent. Naive T cells were isolated from PBMCs by negative selection using a magnetic separation kit (EasySepTM Human Naive Pan T Cell Isolation, StemcellTM Technologies). Briefly, freshly isolated PBMCs (~5x10^7 cells) were incubated in PBS containing 2% of heat-inactivated human serum and 1 mM EDTA (1ml) with T cell isolation and TCR Gamma/Delta depletion antibody cocktails (50 µl each) for 5 minutes, and then with magnetic beads (60 µl) capturing antibody-labeled cells for 3 minutes. Magnetic-labeled cells were then pulled out with the help of a magnet, leaving untouched isolated naive T cells in the media. All isolation steps were performed at room temperature. To control the purification, freshly isolated naive T cells (~10^5 cells) were stained with anti-human CD3-APC (UCHT1, BD Biosciences), anti-human CD45RA-PE (HI100, BD Biosciences) and anti-human CD45RO-FITC (UCHL1, Miltenyi Biotec) antibodies, and analyzed by flow cytometry. On average, 5x10^6 cells were isolated from 5x10^7 PBMCs.

2.5 T cell proliferation assay

Proliferation of T cells was determined by Carboxyfluorescein Diacetate Succinimidyl Ester (CFSE)(Biolegend) dilution assay, which was used as a criterium to select an optimal working concentration of Td vaccine. About 10^7 PBMCs were incubated with CSFE (0.5 µM final concentration) for 20 min in PBS at 37°C. Cells were washed twice using complete RPMI and plated on 96-well cell-culture plates (10^5 cells/well) with IL-2 (20 ng/ml) and varying concentrations of Td vaccine as determined by the content of diphtheria toxoid (0.0012, 0.004 and 0.04 Lf/ml of diphtheria toxoid). Plates were incubated at 37°C and 5% CO_2 for 5 days. As controls, PBMCs were incubated with 25 ng/ml phorbol 12-myristate 13-acetate (PMA)(Merck) or media alone. CFSE-labeled cells were then stained with anti-human CD3-APC antibody (UCHT-1, BD Biosciences) and analyzed by flow cytometry.

2.6 Stimulation of naive T cells with Td vaccine

Naive T cells were primed with diphtheria-tetanus antigens using irradiated PBMCs pulsed with Td vaccine. About 10^7 PBMCs at a density of 5x10^6 cells/ml were incubated with Td vaccine (0.0012 Lf/ml) for 30 min in a sterile 15 ml tube with 2 ml of complete RMPI media. PBMCs were then homogenously irradiated with 30 Gy (Gammacell 1000 irradiator, Nordion). Td-pulsed irradiated PBMCs were disposed in p24 plates (4x10^5 cells/well) along with 4x10^5 of autologous naive T cells per well in complete RPMI (800 µl) supplemented with Td vaccine (0.0012 lf/ml) plus IL-2 (20 ng/ml), IL-7 (25 ng/ml) and IL-15 (25 ng/ml) (cytokines from ImmunoTools) and were incubated for 13 days at 37°C and 5% CO_2. Td vaccine and cytokines were renewed every 2 days and 200 µl of growth medium replenished.

2.7 Mice immunizations and preparation of splenocytes

All mice procedures included in this study were reviewed and approved by the Ethics Board Committee at the Universidad Complutense de Madrid and by the Division of Animal Protection of the Comunidad de Madrid. C57BL/6J mice (male, 6 weeks old, Charles River) received 3 intramuscular (IM) immunizations at 3-week intervals with 1/25 dose of Td vaccine diluted in 100 µl of PBS (Td vaccinated group, n = 5) or with PBS alone (control group, n = 5). Seven days after the last immunization, mice were sacrificed by cervical dislocation, under general anesthesia with 1–2% isoflurane/O_2. At termination, blood was obtained from mice via cardiac puncture, collecting 0.2 ml in 1.5 ml microcentrifuge tubes (Eppendorf). The samples were then centrifuged at 10,000 rpm for 10 minutes at room temperature. Afterward, serum was carefully collected and stored at -80°C for subsequent analysis. To examine mice immunization with Td vaccine, the concentration of specific tetanus toxoid (TT) IgG was quantified by an indirect ELISA assay using Tetanus Toxoid Coated Plates (Biomat). The plates were incubated with serum samples (1:400) for 1 hour at room temperature, and after 3 washes with PBS containing Tween 20 (Sigma-Aldrich), incubated with HRP-conjugated IgG1 secondary anti-mouse antibody (PA1–74421, Invitrogen) (1:4000) followed by the addition of TMB substrate. The reaction was stopped with 1 M HCl stop solution and optical density (OD) was measured at 492 nm using a BioTek plate reader (Agilent). The average blank corrected value was calculated for each sample, and the data was analyzed using BioTek Gen5 software (Agilent). Spleens were also collected and processed as follows. Spleens were minced and filtered through 70 µm nylon cell strainers (Corning) to obtain a single-cell suspension. Cells were washed with cold PBS containing 2% FBS and red blood cells lysed in ammonium-chloride-potassium (ACK) lysis buffer (Gibco). The remaining splenocytes were washed 2 times with cold PBS containing 2% FBS, counted and resuspended in complete RPMI at a density of 2x10^6 cells/ml.

2.8 Detection of peptide-specific $CD8^+$ T cell responses

$CD8^+$ T cell responses to peptides pools (SARS-CoV-2 TDX, NP and Spike pools, and control CEF pool) were determined by intracellular IFNγ staining using human PBMCs (recall response), Naive T cells stimulated with Td vaccine and splenocytes from mice (Td immunized and controls). Human cells (PBMCs and T cells) in complete fresh RPMI were plated in 24-well plates (1x10^6 cells/well), rested for 30 minutes and then cultured at 37°C and 5% CO2 for 16 hours with the relevant peptide pools and a Golgi inhibitor (Brefeldin A) at 2.5 µg/mL (Thermo Fisher Scientific). A negative control condition consisting of media alone with DMSO (0.3%) was also included. Mouse splenocytes in complete RPMI (2x10^6 cells/well) were cultured in 24-well plates with the relevant peptides or media with DMSO (0.3%) for 36 hours at 37°C and 5% CO_2. Brefeldin A (2.5 µg/ml) was added the last 16 hours of

culture. SARS-CoV-2 TDX pool in cell cultures was at 2.0 µM (each peptide) and SARS-CoV-2 NP and Spike pools were at 0.6 µM (each peptide, as recommended by the manufacturer). CEF pool was used at a final concentration of 2 µg/ml, following the manufacturer's recommendations. After peptide stimulations, cells were stained with anti-human CD3-PE (UCHT1, Biolegend) or anti-mouse CD3-PE (17A2, Biolegend) and anti-human CD8-FITC (SK1, Biolegend) or anti-mouse CD8-FITC (Ssa1, ImmunoTools). Subsequently, cells were permeabilized and stained intracellularly with anti-human IFNγ-APC (B27, Biolegend) or anti-mouse IFNγ-APC (XMG1.2, BD Biosciences). Finally, cells were acquired and analyzed by flow cytometry, and $CD3^+CD8^+IFN\gamma^+$ cells quantified. In these intracellular IFNγ staining assays, the positive $IFN\gamma^+$ gate was set utilizing Fluorescence Minus One (FMO) controls. These controls and the delimitation of the gate were obtained after stimulating human PBMCs and mouse splenocytes with Phytohemagglutinin-L as a positive control (PHA-L, Sigma)(Supplementary Figure S1).

2.9 Flow cytometry general procedures

Cells were washed twice with PBS prior to any staining and with ZombieAqua for live/dead cell discrimination (Biolegend). For surface staining, Fc receptors were first blocked with 200 µg/ml of human IgG from human serum (Merck). Next, cells were stained with the relevant antibodies diluted 1:25 in PBS supplemented with 0.5% of FBS and 1 mM EDTA (50 µL of final volume/sample), incubating for 30 minutes at room temperature. Finally, cells were fixed with BD CytofixTM (BD Biosciences), containing 4.2% formaldehyde, unless intracellular staining for IFNγ detection was performed (described earlier). After staining, cell samples were washed twice in PBS and resuspended in PBS with 1 mM EDTA (200 µl of final volume/sample). Cells were acquired on BD FACSCelesta and FACSCalibur flow cytometers (BD Biosciences) (human samples and mouse samples, respectively), and analyzed using FlowJo software (version 10, Treestar). Compensation matrices were set using compensation beads (BD Biosciences) and ArC™ Amine Reactive Compensation beads (Thermofisher). For data analysis, we performed live/dead cell discrimination on single cells, and subsequently gated on the relevant staining.

2.10 Statistical analyses

Kruskal-Wallis tests were used for comparing T cell responses to different peptide pools and media in human and mice samples. Wilcoxon signed-rank tests were applied to compare recall and Td-primed T cell responses to the same peptide pools in the same subjects. Mann-Whitney U tests were used to compare T cell responses to the same peptides between groups of immunized and control mice. $p < 0.05$ was considered significant. Statistic calculations were performed on GraphPad Prism 8.

3 Results

3.1 SARS-CoV-2-specific $CD8^+$ T cell epitopes with similarity to tetanus-diphtheria vaccine antigens

We identified $CD8^+$ T cells epitopes potentially cross-reactive with tetanus-diphtheria vaccine antigens within a set of known SARS-CoV-2-specific $CD8^+$ T cell epitopes (Supplementary Dataset 1). This set consisted of 1153 experimentally verified $CD8^+$ T cell epitopes, recognized by humans infected with SARS-CoV-2 (details in Methods). To identify potentially cross-reactive $CD8^+$ T cell epitopes, we relied on Levenshtein edit distances to detect sequence similarity to tetanus-diphtheria vaccine antigens. In particular, SARS-CoV-2-specific $CD8^+$ T cell epitopes matching tetanus-diphtheria vaccine antigens with ≤ 20% edit distances were considered as potentially cross-reactive. We found that 66 SARS-CoV-2-specific $CD8^+$ T cell epitopes met this criterion (Supplementary Dataset 2) and selected 25 for experimental analyses (Table 1). The selection of $CD8^+$ T cell epitopes was made to cover the maximum number of SARS-CoV-2 antigens and HLA I molecules. The selected $CD8^+$ T cell epitopes span over 10 distinct SARS-CoV-2 mature antigens with the majority lying on the Spike (8 epitopes) and Polymerase (POL)(5 epitopes) proteins. These epitopes are collectively noted to be restricted by 13 distinct HLA I molecules. Judging by the phenotypic frequency of these HLA I molecules, over 85% of the population, regardless of ethnicity, could respond to any of these $CD8^+$ T cell epitopes (See Methods). This population coverage is likely to be much greater and to reach the entire population because many more HLA I molecules are predicted to present these $CD8^+$ T cell epitopes (Table 1). We also predicted that some of these $CD8^+$ T cell epitopes could be presented by mouse class I H2 alloantigens (Table 1). To experimentally address cross-reactivity, the selected SARS-CoV-2-specific T cell epitopes were synthesized and combined in a peptide pool (TDX pool).

3.2 Detection of existing T cell responses to SARS-CoV-2 TDX pool

Given the dimensions of COVID-19 pandemics and vaccination programs, SARS-CoV-2 specific memory T cells are now present in most individuals. Therefore, we first determined existing T cell recall responses to the TDX pool using PBMCs from 10 subjects (healthy blood donors) and compared them with those to SARS-CoV-2 peptide pools from spike (Spike pool) and nucleocapsid phosphoprotein (NP pool). To that end, we stimulated PBMCs with the noted peptide pools for 16 hours and subsequently analyzed intracellular IFNγ expression in $CD8^+$ T cells by flow cytometry. As controls, we stimulated PBMCs with CEF pool and media alone (0.3% DMSO). In these experiments, we surely detect responses by memory $CD8^+$ T cells although effector T cells could also respond in the case of recent vaccination or infection. We found dominant and statistically significant memory $CD8^+$ T cells recall responses to TDX and Spike pools

TABLE 1 Potentially cross-reactive SARS-CoV-2-specific CD8$^+$ T cell epitopes with tetanus-diphtheria vaccine antigens.

Epitope Sequence	Antigen [NCBI Accession]	HLA I Presentation (experimental)	HLA I presentation (Predicted)	H2 I presentation (Predicted)	Td Peptide[1]	Td antigen[2] ACC|[T/D]	Td peptide HLA I presentation[3] (Predicted)
IIWVATEGA	NP [YP_009724397]	HLA-A*02:01	NN	NN	IIKVATEDG	Q897I8|T	NN
QLNRALTGI	SPIKE [YP_009724390]	HLA-A*02:03	HLA-A*02:01, HLA-A*02:03	NN	QLREALTGI	Q895W2|T	HLA-A*02:01, HLA-A*02:03, HLA-A*02:06, HLA-A*30:01
FERDISTEI	SPIKE [YP_009724390]	HLA-B*40:01	HLA-B*40:01, HLA-B*44:02, HLA-B*44:03, HLA-B*51:01	H-2-Kk, H-2-Kq, H-2-Lq	FMRDIDAEI	Q894X4|T	HLA-A*02:01, HLA A*02:03, HLA-A*02:06, HLA-B*08:01, HLA-B*15:01, HLA-B*44:03
SFELLHAPATV	SPIKE [YP_009724390]	HLA-A*02:01	HLA-A*02:01, HLA-A*02:03, HLA-A*02:06, HLA-A*68:02, HLA-B*40:01	H-2-Kd, H-2-Kk	AFELLHACPQV	Q6NJ45|D	HLA-A*02:01, HLA-A*02:03, HLA-A*02:06, HLA-A*68:02
ATVVIGTSK	POL [YP_009725307]	HLA-A*11:01	HLA-A*03:01, HLA-A*11:01, HLA-A*30:01, HLA-A*31:01, HLA-A*68:01	NN	ATVAEGTKK	Q6NF63|D	HLA-A*03:01, HLA-A*11:01, HLA-A*30:01, HLA-A*68:01
AQALNTLVKQL	SPIKE [YP_009724390]	HLA class I	HLA-A*02:01, HLA-A*02:03, HLA-A*02:06, HLA-A*03:01, HLA-A*11:01, HLA-A*30:01, HLA-A*32:01, HLA-B*08:01	H-2-Db, H-2-Kd	VAALNGLVKQG	Q6NG46|D	HLA-A*03:01, HLA-A*11:01, HLA-B*51:01
IVAGGIVAI	NSP4 [YP_00972530]	HLA-A*02:01	HLA-A*02:01, HLA-A*02:03, HLA-A*02:06, HLA-A*26:01, HLA-A*32:01, HLA-A*68:02, HLA-B*51:01	NN	IVAGGGVAL	Q891Q6|T	HLA-A*02:01, HLA-A*02:03, HLA-A*02:06, HLA-A*26:01, HLA-A*32:01, HLA-A*68:02, HLA-B*07:02, HLA-B*15:01, HLA-B*35:01
FVFKNIDGY	SPIKE [YP_009724390]	HLA-A*29:02, HLA-A*26:01	HLA-A*01:01, HLA-A*26:01, HLA-A*30:02, HLA-A*32:01, HLA-A*68:01, HLA-B*15:01, HLA-B*35:01, HLA-B*53:01	NN	QKFVNIDGY	Q891E4|T	HLA-A*30:02
IMASLVLAR	POL [YP_009725307]	HLA-A*33:01	HLA-A*03:01, HLA-A*11:01, HLA-A*31:01, HLA-A*33:01, HLA-A*68:01	NN	IFASLYLAR	Q895E4|T	HLA-A*31:01, HLA-A*33:01
ILRGHLRIA	MP [YP_009724393]	HLA-A*02:03	HLA-A*02:03, HLA-A*30:01	NN	KLALHLRIA	Q6NH14|D	HLA-A*02:03, HLA-A*30:01
MASLVLARK	POL [YP_009725307]	HLA-A*68:01	HLA-A*03:01, HLA-A*11:01, HLA-A*30:01, HLA-A*33:01, HLA-A*68:01	NN	VASLVSALK	Q899H3|T	HLA-A*03:01, HLA-A*11:01, HLA-A*30:01, HLA-A*68:01, HLA-B*51:01
LVKPSFYVY	ENV [YP_00972439]	HLA-C*07:02	HLA-A*01:01, HLA-A*03:01, HLA-A*11:01, HLA-A*26:01, HLA-A*30:01, HLA-A*30:02, HLA-A*32:01, HLA-B*15:01, HLA-B*35:01, HLA-B*53:01, HLA-B*57:01, HLA-B*58:01	NN	EVKPSSYVY	Q893Q3|T	HLA-A*01:01, HLA-A*26:01, HLA-A*30:02, HLA-A*32:01, HLA-A*33:01, HLA-A*68:01, HLA-A*68:02, HLA-B*15:01, HLA-B*35:01, HLA-B*44:02, HLA-B*44:03, HLA-B*53:01
FVAAIFYLI	NSP4 [YP_00972530]	HLA-A*02:01	HLA-A*02:01, HLA-A*02:03, HLA-A*02:06, HLA-A*68:02, HLA-B*51:01	H-2-Db, H-2-Dd, H-2-Kb	IFAAIMYLI	Q895R4|T	HLA-A*23:01, HLA-A*24:02, HLA-B*51:01
TLADAGFIK	SPIKE [YP_009724390]	HLA-A*03:01	HLA-A*03:01, HLA-A*11:01, HLA-A*68:01	NN	TLDAGFIPR	Q6NG84|D	HLA-A*03:01, HLA-A*11:01, HLA-A*31:01, HLA-A*33:01, HLA-A*68:01

(Continued)

10.3389/fimmu.2024.1425374

TABLE 1 Continued

Epitope Sequence	Antigen [NCBI Accession]	HLA I Presentation (experimental)	HLA I presentation (Predicted)	H2 I presentation (Predicted)	Td Peptide[1]	Td antigen[2] ACC|[T/D]	Td peptide HLA I presentation[3] (Predicted)
LLDRLNQL	NP [YP_009724397]	HLA class I	HLA-A*02:01, HLA-A*02:03, HLA-B*08:01	NN	NLDKLNQL	Q897F3|T	HLA-B*08:01
AYSNNSIAI	SPIKE [YP_009724390]	HLA-A*24:02	HLA-A*23:01, HLA-A*24:02	H-2-Db, H-2-Kd	AYSHYSIAI	Q6NJH2|D	HLA-A*23:01, HLA-A*24:02, HLA-B*51:01
IPTITQMNL	POL [YP_009725307]	HLA-B*07:02	HLA-B*07:02, HLA-B*08:01, HLA-B*35:01, HLA-B*51:01, HLA-B*53:01	H-2-Dq, H-2-Ld, H-2-Lq	IPTIFQDNL	Q6NFM0|D	HLA-B*07:02, HLA-B*35:01, HLA-B*51:01, HLA-B*53:01
TDLEGNFY	3CPR [YP_009725301]	HLA-A*01:01	HLA-A*01:01, HLA-A*26:01, HLA-A*30:02	NN	LDDEGNFY	Q893J1|T	HLA-A*01:01
VTNNTFTLK	NSP2 [YP_009725298]	HLA-A*03:01, HLA-A*11:01	HLA-A*03:01, HLA-A*11:01, HLA-A*30:01, HLA-A*31:01, HLA-A*68:01	H-2-Db, H-2-Dd, H-2-Kb	DATNTFTLK	Q6NF84|D	HLA-A*03:01, HLA-A*11:01, HLA-A*33:01, HLA-A*68:01, HLA-B*51:01
TYVPAQEKNFT	SPIKE [YP_009724390]	HLA-A*24:02	HLA-A*23:01, HLA-A*24:02, HLA-A*26:01, HLA-B*35:01, HLA-B*53:01	H-2-Dd, H-2-Dq, H-2-Kd, H-2-Ld H-2-Lq	TNVHAQEKNFN	Q899V7|T	HLA-A*26:01
TDNYITTY	NSP3 [YP_009725299]	HLA-A*01:01	HLA-A*01:01, HLA-B*44:02	H-2-Kq	TINYITEY	Q898F9|T	HLA-A*01:01, HLA-A*26:01, HLA-A*30:02, HLA-B*15:01, HLA-B*35:01
KRVDWTIEY	35EXON [YP_009725309]	HLA-B*07:02	HLA-A*01:01, HLA-A*26:01, HLA-A*30:02, HLA-A*32:01, HLA-B*44:03	NN	KRVDWDIEY	Q899B2|T	HLA-A*01:01, HLA-A*30:02
TLIGDCATV	2ORMT [YP_009725311]	HLA class I	HLA-A*02:01, HLA-A*02:03, HLA-A*02:06, HLA-A*68:02	NN	TLIIDATCV	Q890S3|T	HLA-A*02:01, HLA-A*02:03, HLA-A*02:06
VLAWLYAAV	3CPR [YP_009725301]	HLA class I	HLA-A*02:01, HLA-A*02:03, HLA-A*02:06, HLA-B*51:01	H-2-Kb	VLAALGAAA	Q6NFZ1|T	HLA-A*02:03
LRIMASLVL	POL [YP_009725307]	HLA-C*07:02	NN	NN	LRAMASEVL	P62411|D	NA

NN, None predicted. Underlined epitopes lie within antigen regions covered by the Spike peptide pool. [1]Td peptide equivalent to SARS-CoV-2 $CD8^+$ T cell epitope. [2]UniProt accession number (ACC) of Td peptide protein source followed by T or D, indicating a Tetanus or Diphtheria antigen,respectively. [3]Predicted HLA I presentation profile of Td peptide.

10.3389/fimmu.2024.1425374

10.3389/fimmu.2024.1425374

compared to CEF and NP pool (Figure 1). Moreover, all 10 subjects have detectable responses to the TDX pool, confirming the high population coverage of the CD8$^+$ T cell epitopes included in the pool, outnumbering those responding to other peptide pools, including the Spike peptide pool. However, overall there was no statistical difference between the detected T cell recall responses to TDX and Spike pools. The detection of dominant and prevalent memory/effector responses to SARS-CoV-2 spike protein in the studied subjects is likely the result of COVID-19 vaccination. COVID-19 vaccines rely on inducing immunity to SARS-CoV-2 Spike protein (4) and over 85% of people in Spain aged 12 and above are fully vaccinated against COVID-19 (60). The TDX pool does also include 8 CD8$^+$ T cell epitopes from SARS-CoV-2 spike protein but only 4 of them lie within the regions covered by the Spike peptide pool (underlined in Table 1). Therefore, it is unlikely that these epitopes can fully account for the comparable memory/effector T cell responses to TDX pool and Spike pool. Hence, the strong memory/effector T cell responses to TDX pool detected in most subjects are likely the result of SARS-CoV-2 infections and may also be impacted by pre-existing cross-reactive memory T cells elicited by vaccines with tetanus-diphtheria antigens. However, T cells are cross-reactive by nature and T cell immunity dynamic, which makes challenging to identify the source of pre-existing SARS-CoV-2 cross-reactive memory T cells. Therefore, in this work, we resorted to non-antigen experienced naive T cells, and examined whether Td-stimulations could activate them to respond to the SARS-CoV-2 TDX pool.

3.3 Td-stimulated responses of naive T cells to SARS-CoV-2 TDX pool

Tetanus-diphtheria vaccines must be capable of priming T cells cross-reactive with SARS-CoV-2 to have had an impact in the existing T cell immunity to the virus. To verify this point, we resorted to *in vitro* immunizations in which we stimulated antigen-inexperienced naive T cells from 7 subjects (healthy blood donors) with autologous irradiated PBMCs pulsed with Td vaccine, and then analyzed responses to SARS-CoV-2 peptide pools (Figure 2A). We found that Td vaccine can be toxic to cells and so we first worked out a dose of Td vaccine that was not toxic and foster proliferation of T cells in PBMCs (See Methods for details). As a result, we selected a dose of Td vaccine containing 0.0012 Lf/ml of diphtheria toxoid (Supplementary Figure S2) to pulse irradiated PBMCs. To enable priming conditions, autologous naive T cells were co-cultured with irradiated Td-pulsed PBMCs for 13 days in the

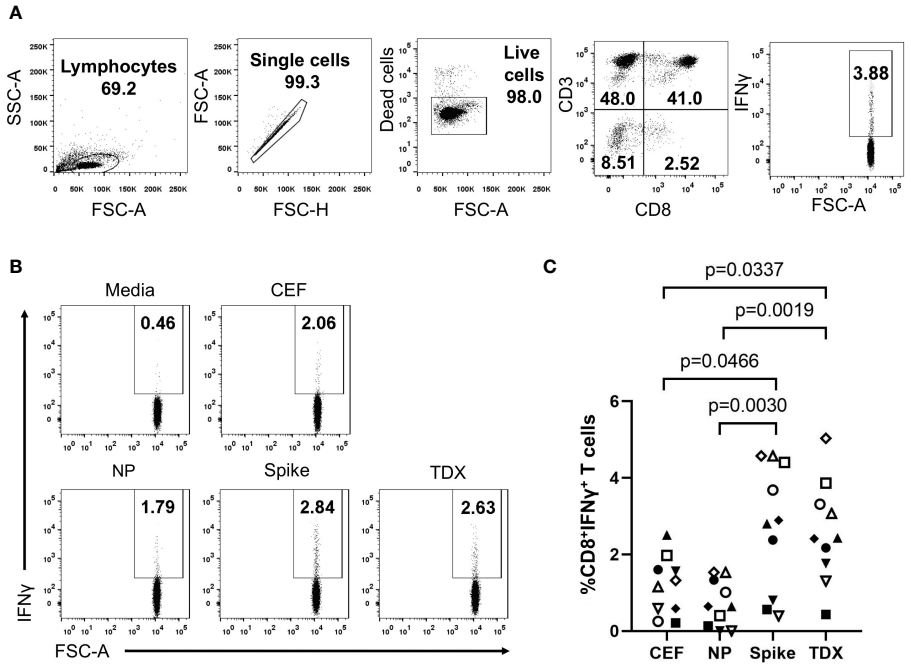

FIGURE 1
Existing T cell responses to SARS-CoV-2 peptide pools. PBMCs from 10 healthy subjects were stimulated with SARS-CoV-2 peptide pools (Spike, NP and TDX), CEF pool or media (complete RPMI with 0.3% DMSO) during 16 hours and CD8$^+$ T cell responses detected by intracellular IFNγ staining assays **(A)** Gating strategy for the detection of intracellular IFNγ expression within the CD8$^+$ T cell population by flow cytometry using a representative PBMC sample stimulated with the TDX peptide pool. IFNγ$^+$CD3$^+$CD8$^+$ cells were identified after the following steps: a) Adequate adjustment of the gate of the lymphocytes using the light scatter parameters (FSC and SSC-A), b) Exclusion of doublets with the identification of singlets improving the accuracy of the analysis, c) Selection of the viable lymphocytes, d) Identification of the CD3$^+$CD8$^+$ cell subset and e) IFNγ$^+$ cells within the CD3$^+$CD8$^+$ cells. IFNγ$^+$ gate was set after FMO stainings with PHA-L stimulation (see Supplementary Figure S1). **(B)** Representative dot plot showing IFNγ$^+$ cells on CD3$^+$CD8$^+$ gated cells in response to the different stimuli (Media, CEF, Spike, NP and TDX). Percentage of IFNγ$^+$ cells are indicated **(C)** Graph depicting the percentage of CD8$^+$ T cells expressing IFNγ (y-axis) in response to peptide pools (x-axis) after subtracting response to media (n = 10). Individual values are plotted. Statistically significant differences were obtained by applying Kruskal-Wallis tests. Significant differences are indicated and *p*-values shown.

10.3389/fimmu.2024.1425374

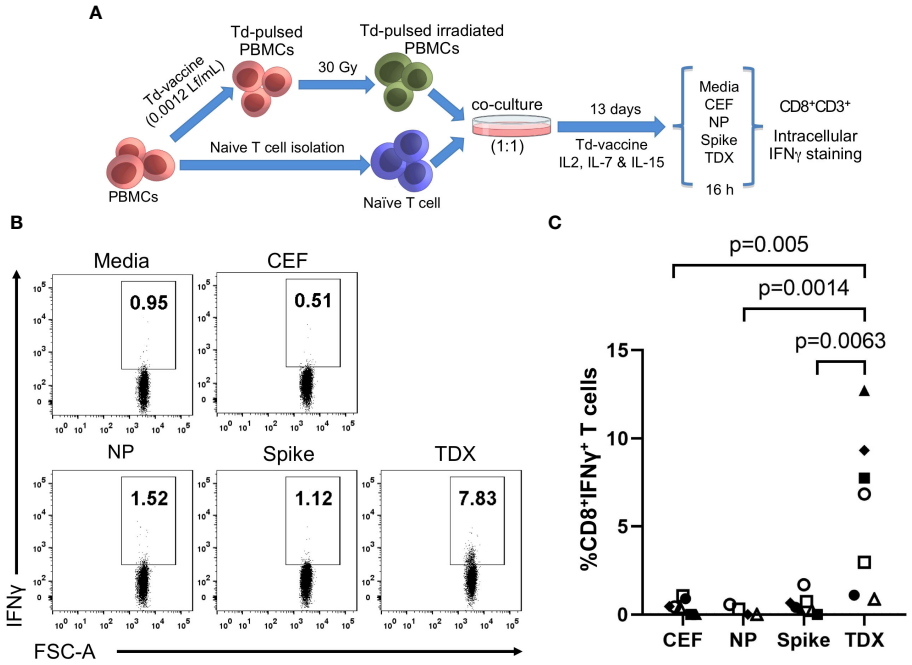

FIGURE 2
Cross-reactive responses of naive T cells stimulated with Td vaccine to SARS-CoV-2 peptide pools. **(A)** Experimental design to stimulate/prime T cells against Td vaccine. PBMCs were pulsed with Td vaccine (0.0012 Lf/ml of diphtheria toxoid) and homogenously irradiated at 30 Gy. Td-pulsed irradiated PBMCs were co-cultured with autologous naive T cells (ratio 1:1) for 13 days in the presence of IL-2, IL-7, IL-15 and Td vaccine (details in Methods). Subsequently, T cell responses to peptide pools (TDX pool, Spike pool, NP pool and CEF pool) and media (0.3% DMSO) were determined by intracellular IFNγ staining assays. IFNγ positive gate was set after FMO staining with PHA stimulation. **(B)** Representative dot plot showing the $IFN\gamma^+CD8^+$ T cells after stimulation with the relevant peptide pools **(C)** Percentage of $CD8^+$ T cells expressing IFNγ after subtracting value from control media. Individual values were plotted (n = 7, except for NP with n = 5). Statistically significant differences were obtained by applying Kruskal-Wallis tests. Significant differences are indicated and *p*-values shown.

presence of Td-vaccine, IL-2, IL-7 and IL-15 (details in Methods). Naive T cells used in these experiments were purified from PBMCs and had a purity of over 91% (Supplementary Figure S3). Subsequently, we investigated the responses of Td-stimulated T cells to SARS-CoV-2 peptide pools (Spike, NP and TDX), as previously described by intracellular IFNγ staining assays (details in Methods). As controls, the responses of Td-stimulated T cells to media and CEF pool was also determined. As shown in Figures 2B, C, Td-primed T cells from all subjects responded strongly to TDX pool (n = 7), while responses to Spike pool, CEF pool and NP pool were seldom detected (Figure 2C). It is worth noting that naive T cells stimulated with irradiated PBMCs in the absence of Td vaccine did not respond to TDX (see Supplementary Figure S4).

The fact that Td-stimulated naive T cells responded only to SARS-CoV-2 $CD8^+$ T cell epitopes that were anticipated as cross-reactive (TDX pool) with comparable strength than existing memory/effector T cells is truly outstanding. One could wonder if Td-stimulated T cell responses are due to contaminating TDX-specific memory/effector T cells or differentiated effector T cells ($CD45RA^+$ TEMRA cells). However, this scenario is very unlikely. On the one hand, naive T cells used in the experiments were highly enriched (see Supplementary Figure S3) and did not respond to the TDX pool prior to Td stimulation (Supplementary Figure S4). On the other hand, if such contamination had occurred, Td-stimulated naive T cells should have also responded to the Spike pool but they did not. Further support of Td-priming of T cells cross-reactive with SARS-CoV-2 TDX pool is very noticeable in those individuals in which T cell responses were measured using PBMCs and Td-stimulated naive T cells (Figure 3). Statistical differences in matched responses to the different peptide pools mirrored those described previously, but were fewer given the smaller sample size (n = 5). Td-stimulated naive T cells only responded to the TDX pool. Moreover, it is worth noting that naive T cells from individuals with weak memory/effector T cell recall responses to the TDX pool responded strongly to this peptide pool after Td-stimulation. At the same time, Td-stimulated naive T cells from individuals with strong memory/effector T cell responses to the Spike pool did not respond to the Spike pool, only to the TDX pool. Overall, these results strongly support that Td vaccine can prime T cells to precisely recognize SARS-CoV-2-specific $CD8^+$ T cell epitopes that were anticipated as cross-reactive with tetanus-diphtheria vaccines.

3.4 Immunization of mice with Td vaccine induces SARS-CoV-2 cross-reactive T cells

We also analyzed $CD8^+$ T cell cross-reactivity to SARS-CoV-2 peptide pools in C57BL/6J mice immunized with Td vaccine. C57BL/6J mice express two H2 class I alloantigens, H2-Kb and H2-Db, that are predicted to present 5 of the cross-reactive $CD8^+$ T cell epitopes (Table 1). We immunized mice with 3 IM injections of Td vaccine (0.01 Lfu of diphtheria toxoid)(n = 5) or PBS (control group, n = 5)

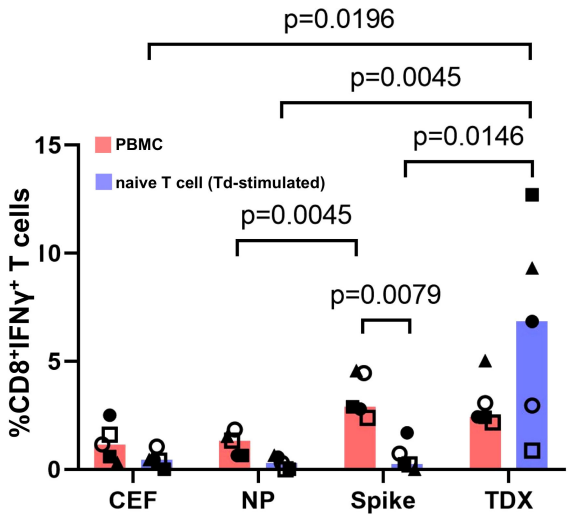

FIGURE 3
Responses to SARS-CoV-2 peptide pools from matched PBMCs and Td-stimulated native T cells. T cell responses to SARS-CoV-2 peptide pools (NP, Spike and TDX) and CEF pool determined using PBMCs (pink) and Td-stimulated naive T cells (blue) from the same five subjects. PBMCs and Td-stimulated naive T cells were incubated with peptide pools or media for 16 hours and responses were detected by intracellular IFNγ staining assays. All responses (value from media control subtracted) are plotted and bars represent median values. Statistically significant differences between conditions are indicated and *p*-values shown. Kruskal-Wallis tests were used for comparing responses to peptide pools from PBMC recall and Td-stimulated naive T cells. Wilcoxon signed-rank tests were carried out to compare T cell responses between PBMCs and Td-stimulated naive T cells in the same individuals to the same peptide pools.

at3-week intervals, and sacrificed them one week after the last immunization to isolate splenocytes (Figure 4A). Appropriated immunization of mice with Td vaccine was confirmed by the detection of high levels of tetanus toxoid–specific IgG in blood serum (Supplementary Figure S5). Subsequently, we incubated splenocytes from Td-vaccinated and control mice for 36 hours with SARS-CoV-2 TDX, Spike and NP peptide pools. As controls, splenocytes were incubated with CEF pool and media (RMPI with 0.3% DMSO). Subsequently, we analyzed IFNγ production in $CD8^+$ T cells by flow cytometry (Figures 4B, C). We observed that Td-vaccinated mice responded strongly to the TDX pool, with up to 8-fold increase in IFNγ-producing $CD8^+$ T cells compared to non-vaccinated mice. Moreover, the response to the TDX pool in Td-vaccinated mice was significantly larger than that to CEF and Spike peptide pools, which were negligible. It is worth noting that Td-vaccinated mice also exhibited significant responses to the NP pool (Figure 4C). Overall, these results clearly show that Td-vaccination of mice induces SARS-CoV-2 specific $CD8^+$ T cells recognizing the selected epitopes with similarity with tetanus-diphtheria vaccine antigens.

4 Discussion

There is increasing evidence that pre-existing cross-reactive T cell immunity contributes to protect against SARS-CoV-2 infection (33). Given the structural similarity between SARS-CoV-2 and ccHCoVs, it has become widely accepted that ccHCoVs are the sources of pre-existing cross-reactive immunity to SARS-CoV-2 (22). That ccHCoVs cause seasonal infections in humans with higher incidence in children (35) supports this view. However, evidence of exposure to ccHCoVs is seen in 95% of adults (35) and why cross-reactive immunity from ccHCoVs could be more protective in children than in young adults is open to speculation. On the other hand, it has also been reported that prior infection by seasonal ccHCoVs does not prevent SARS-CoV-2 infection in children (61). Moreover, it has been noted that pre-existing SARS-CoV-2 cross-reactive T immunity cannot be solely explained by ccHCoVs infections (62). Hence, there must be additional sources of T cell cross-reactivity to SARS-CoV-2.

T cell cross-reactivity is actually quite common. During maturation in the thymus, individual T cells are required to recognize numerous peptides presented by the same MHC molecules, which render them cross-reactive by nature (29). In fact, it has been reported that a single T cell receptor can recognize about a million different peptides (63). Therefore, it is not surprising that T cell cross-reactivity to SARS-CoV-2 had been found beyond ccHCoVs, reaching to unrelated viruses (43, 44), vaccines such as MMR and Tdap (50), and bacteria (42). However, until now and to our knowledge none of these candidates have been shown to prime antigen-inexperienced naive T cells cross-reacting with SARS-CoV-2. Such priming ought to be necessary to regard a candidate as responsible of pre-existing cross-reactive T cell immunity. Following the tracks of an early study proposing tetanus-diphtheria vaccine antigens as sources of protective cross-reactive immunity to SARS-CoV-2 (47, 48), in this exploratory work we show proof that Td vaccine can prime T cells cross-reacting with known SARS-CoV-2-specific $CD8^+$ T cell epitopes.

Vaccines with tetanus-diphtheria toxoids include hundreds of additional antigens (51–53) and are widely used. During infancy children receive three immunizations with DTP vaccine (diphtheria and tetanus toxoids combined with antigens from *Bordetella persussis*), alone or combined with other vaccines like Polio vaccine, hepatitis B vaccine and conjugated *Haemophilus influenzae* type B vaccine (Hib vaccine) (64). Children receive one additional DTP vaccination at 4–6 years of age and a boost in puberty with versions containing a lower dose of diphtheria antigens (d), with or without a low dose of antigens from acellular *B. pertussis* (ap): Tdap or Td vaccine, respectively (64). Td vaccines are also given in the case of severe or unclean wounds (64) and immunization with Tdap vaccine is recommended for pregnant women (65). Moreover, conjugated pneumococcal vaccines and Hib vaccines also use diphtheria or tetanus toxoids for conjugation (66, 67). In sum, T cell immunity and memory to tetanus-diphtheria vaccine antigens develop early during childhood through repeated vaccinations and can be present in adults (64, 68).

Memory T cells elicited by tetanus-diphtheria antigens ought to imprint existing T cell responses to SARS-CoV-2, provided that cross-recognition occurs. Therefore, we sought for evidence of cross-reactivity from tetanus-diphtheria vaccine antigens in experimentally verified SARS-CoV-2 $CD8^+$ T cell epitopes, recognized by humans during the course of infection. We

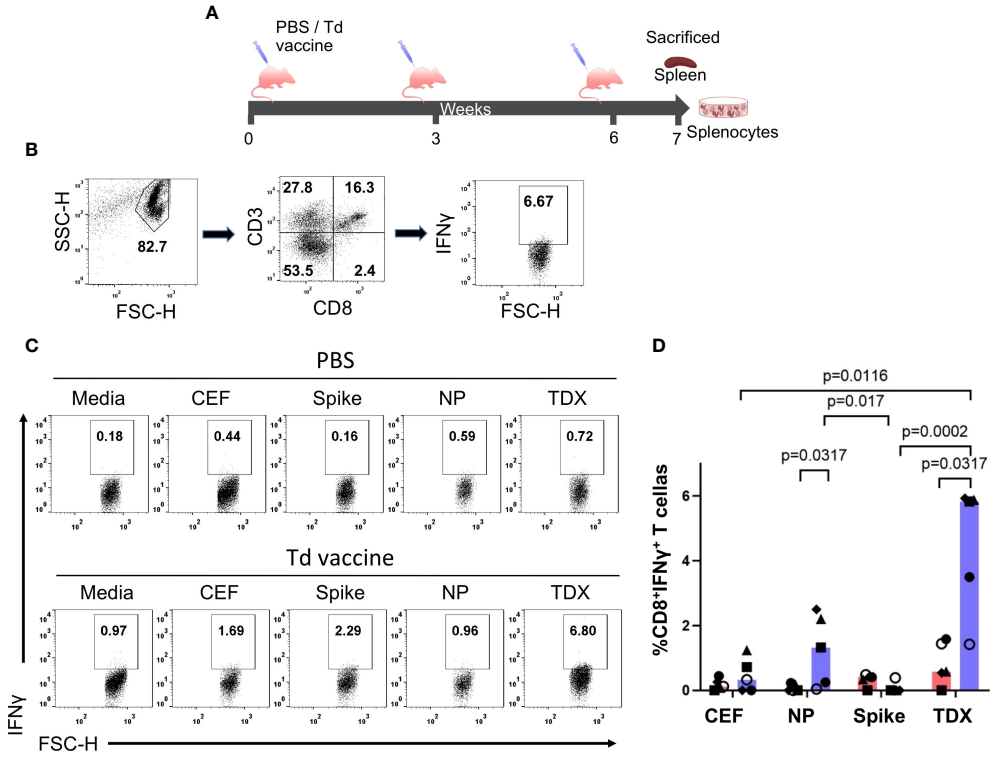

FIGURE 4
Cross-reactive T cell responses to SARS-CoV-2 peptide pools in Td-vaccinated mice. **(A)** Immunization schedule. Mice were immunized intramuscularly (IM) at 3-week intervals with Td vaccine (0.1 Lf diphtheria toxoid)(Td-vaccine group, n = 5) or PBS (PBS control group, n=5). Mice were sacrificed seven days after the last immunization, spleens were collected and splenocytes prepared and responses to SARS-CoV-2 peptide pools (NP, Spike and TDX), CEF pool and media (complete RPMI with 0.3% DMSO) after 36-hour stimulations determined by intracellular IFNγ staining assays **(B)** Gating strategy for intracellular IFNγ detection within the $CD8^+$ T cell population by flow cytometry using mouse splenocytes stimulated with the TDX peptide pool. $IFN\gamma^+CD3^+CD8^+$ cells were identified after the following steps: a) Adequate selection of cells using the light scatter parameters (FSC, SSC), b) Selection of $CD3^+CD8^+$ cells, c) Selection of $IFN\gamma^+$ cells within the $CD3^+CD8^+$ cells. $IFN\gamma^+$ gate set after FMO stainings with PHA-L stimulation (see Supplementary Figure S1) **(C)** Representative dot plot showing $IFN\gamma^+CD8^+$ T cells responding to SARS-CoV-2 peptide pools (TDX, Spike and NP), CEF pool or media in both, PBS and Td-vaccine groups. **(D)** Percentage of $CD8^+$ T cells producing IFNγ (value from control media subtracted) in both, PBS control group (pink) and Td-vaccine group (blue). All values are plotted and bars represent median values. Statistically significant differences between responses are shown with *p*-values. Kruskal-Wallis tests were used for comparing T cell responses to peptide pools in Td-vaccinated and control mice. Mann-Whitney U tests were carried out to compare T cell responses to the same peptides (CEF, NP, Spike and TDX pools) between Td-vaccinated mice and control mice.

identified 66 SARS-CoV-2-specific $CD8^+$ T cell epitopes sharing sequence similarity (≤ 20% Levenshtein distance edits) with tetanus-diphtheria vaccine antigens, suggesting cross-reactivity. Subsequently, we investigated T cell responses to 25 of these potentially cross-reactive SARS-CoV-2 $CD8^+$ T cell epitopes (TDX pool) that were selected for covering most of SARS-CoV-2 antigens and for their presentation by 13 distinct HLA I molecules (Table 1). In the studied subjects (healthy blood donors), we observed dominant memory/effector T cell responses to the selected, potentially cross-reactive, SARS-CoV-2 $CD8^+$ T cell epitopes (TDX pool) that were comparable to those against a peptide pool covering the Spike protein (Figures 1, 3). We had no information on COVID-19 vaccination status of participants or if they have been infected by SARS-CoV-2 but presumably all participants had been vaccinated for COVID-19 and passed the infection. In this context, strong and prevalent memory T cell recall responses to SARS-CoV-2 spike peptides are likely due to T cell immunity elicited by both, COVID-19 vaccinations and infection. On the other hand, the comparable memory/effector T cell responses to the TDX pool can be attributed to SARS-CoV-2 infections and may also be compatible with pre-existing T cell immunity elicited by tetanus-diphtheria vaccine antigens. This latter possibility is supported by the fact that stimulating naive T cells with autologous irradiated PBMCs pulsed with Td vaccine resulted in T cells that responded strongly to TDX pool but not to control peptides, including other SARS-CoV-2 peptide pools (Figures 2, 3). We are aware that we worked with a very small donor sample size, which could limit the generalizability of our findings. However, our results are not only statistically significant, but also quite compelling. Td-primed T cells from every single donor responded to TDX pool using Td-stimulated naive T cells, while the same cells did not respond to other peptide pools. It has been reported that immunogenic $CD8^+$ T cell epitopes are characterized by the presence of short motifs that are highly represented in the human proteome (69). Interestingly, the 25 SARS-CoV-2 $CD8^+$ T cell epitopes included in the TDX pool displayed an average identity to human proteins of 66.1 ± 5.9, which may indicate the presence of such motifs. None of the

selected epitopes were however identical to human proteins (see Supplementary Dataset 2).

Similar results were reproduced *in vivo* using C57BL/6J mice immunized with Td vaccine. Td-vaccination elicited in mice induced SARS-CoV-2 cross-reactive $CD8^+$ T cells responding strongly to TDX pool (Figure 4). However, unlike Td-primed T cells from humans, Td-vaccinated mice also responded to SARS-CoV-2 NP pool. All together these results show that i) vaccines with tetanus-diphtheria toxoids can be a priming source of cross-reactive T cell immunity to SARS-CoV-2 and ii) SARS-CoV-2-specific $CD8^+$ T cell epitopes in TDX pool are indeed cross-reactive with tetanus-diphtheria antigens, as predicted by Levenshtein edit distances. We should point that not necessarily all SARS-CoV-2-specific $CD8^+$ T cell epitopes in TDX pool are cross-reactive with tetanus-diphtheria antigens. Conversely, there might be may other SARS-CoV-2 T cell epitopes cross-reactive with tetanus-diphtheria vaccine antigens. Indeed, the TDX pool only included 25 of the 66 SARS-CoV-2 $CD8^+$ T epitopes that were predicted to be cross-reactive with tetanus-diphtheria antigens (Supplementary Dataset 2). Moreover, T cell cross-reactivity is not always predictable and epitopes without or very little sequence similarity can be cross-reactive (70). Therefore, further work is required to confirm individually SARS-CoV-2 cross-reactive T cell epitopes, as well as their counterparts in Td vaccines. Selecting SARS-CoV-2 $CD8^+$ T cell epitopes related by similarity with tetanus-diphtheria vaccine antigens is not an unbiased method to detect cross-reactivity, but it provides an objective and reproducible manner to detect cross-reactive epitopes. Therefore, we believe that this same approach could be applied to investigate cross-reactivity between other vaccines and pathogens, saving much time and resources. Moreover, our approach to detect cross-reactive epitopes could be enhanced by taking in consideration if amino acid edits occur in anchor or exposed amino acid positions. However, it is worth noting that cross-reactivity may involve changes in both, anchor or non-anchor positions (71). Taking in consideration HLA binding profiles of epitopes and matching peptides could also serve to improve the selection of potentially cross-reactive T cell epitopes.

Through a completely different approach, Mysore et al. (50) identified T cell cross-reactivity between SARS-CoV-2 and Tdap vaccine, which contains tetanus and diphtheria antigens. In their study, Mysore et al. stimulated total human T cells with MMR or Tdap vaccines on the one hand and on the other with SARS-CoV-2 antigens, and subsequently carried out single cell RNA sequencing and TCR clonotyping. The authors found that T cells stimulated with these vaccines and SARS-CoV-2 antigens displayed overlapping TCRs (CD3 regions), which is sign of cross-reactivity. In addition, these authors found that COVID-19 disease severity was reduced in Tdap-vaccinated individuals by 20%–23%. However, Mysore et al. did not show that Tdap vaccine can prime/stimulate naive T cells nor investigated the responses of Tdap activated T cells to SARS-CoV-2 epitopes. Although we determined SARS-CoV-2 T cell epitopes that are cross-reactive with Td vaccines, we did not explore if these particular epitopes mediate protective immunity. Moreover, we did not characterize cross-reactive T cells but our results will facilitate the design of tetramers to label antigen-specific $CD8^+$ T cells and show the presence of cross-reactive T cells.

5 Conclusions

Naive T cell cells stimulated *in vitro* with Td vaccine are cross-reactive with known SARS-CoV-2 $CD8^+$ T cell epitopes sharing similarity to tetanus-diphtheria vaccine antigens. Similarly, C57BL/6J mice immunized with Td vaccine respond to SARS-CoV-2-specific $CD8^+$ T cell epitopes. Therefore, we conclude that tetanus-diphtheria vaccines can prime SARS-CoV-2 cross-reactive T cells, likely shaping existing T cell responses to the virus. Whether the selected SARS-CoV-2 $CD8^+$ T cell epitopes that are cross-reactive tetanus-diphtheria mediate protective immunity remains to be determined. We only studied immune responses in a controlled environment and the clinical relevance of these findings needs further investigation. Nonetheless, pre-existing SARS-CoV-2 cross-reactive memory T cells have been shown to be protective (33) and there is already mounting evidence indicating that vaccines with tetanus-diphtheria antigens can make a contribution: 1) as shown here, naive T cells stimulated with tetanus-diphtheria vaccine respond strongly to SARS-CoV-2 epitopes; 2) tetanus-diphtheria vaccinations are associated with lower chances of developing severe COVID-19, even in the elderly (49); and 3) T cell immunity to tetanus-diphtheria antigens wanes with age (72), correlating inversely with the incidence of SARS-CoV-2 infections (46). Currently, immunizations with Td vaccine are recommended for adults every 10 years and, although we cannot correlate the data presented here with real clinical implications, our results strongly support staying up to date with Td boosters.

Data availability statement

The original contributions presented in the study are included in the article/Supplementary Material. Further inquiries can be directed to the corresponding author.

Ethics statement

The studies involving humans were approved by Comité de Evaluación de Investigación y Docencia del Centro de Transfusión de Madrid. The human samples used in this study were acquired from Buffy coats from healthy blood donors. Written informed consent for participation was not required from the participants or the participants' legal guardians/next of kin in accordance with the national legislation and institutional requirements. The studies were conducted in accordance with the local legislation and institutional requirements. The participants provided their written informed consent to participate in this study. The animal study was approved by Ethics Board Committee at the Universidad Complutense de Madrid. The study was conducted in accordance with the local legislation and institutional requirements.

Author contributions

SAF: Formal analysis, Methodology, Validation, Visualization, Writing – review & editing. HFP-P: Formal analysis, Methodology, Validation, Visualization, Writing – original draft. TF: Formal analysis, Methodology, Validation, Visualization, Writing – review & editing. MG-P: Methodology, Writing – review & editing. JR: Formal analysis, Methodology, Writing – review & editing. PAR: Conceptualization, Funding acquisition, Investigation, Methodology, Software, Supervision, Writing – original draft, Writing – review & editing.

Funding

The author(s) declare financial support was received for the research, authorship, and/or publication of this article. This study was funded by a REACT-EU grant from the Comunidad de Madrid to the ANTICIPA project of Complutense University of Madrid (UCM) and by a Spanish MCI research grant (PID2022-136662OB-I00) to PAR. The funders had no role in study design, data collection and analysis, preparation of the manuscript or decision to publish.

Acknowledgments

We wish to thank Dr. Ellis L. Reinherz and Dr. Esther M. Lafuente for comments and revisions, Dr. Edgar Fernandez-Malave for providing anti-mouse CD3-PE antibody and Alvaro Ras-Carmona for computing assistance. We thank CAM for support provided through REACT-EU grant to UCM ANTICIPA project. PAR also thanks CAM for keeping Madrid operative in difficult times.

Conflict of interest

The authors declare that the research was conducted in the absence of any commercial or financial relationships that could be construed as a potential conflict of interest.

The author(s) declared that they were an editorial board member of Frontiers, at the time of submission. This had no impact on the peer review process and the final decision.

Publisher's note

Supplementary material

The Supplementary Material for this article can be found online at: https://www.frontiersin.org/articles/10.3389/fimmu.2024.1425374/full#supplementary-material

SUPPLEMENTARY DATA SHEET 1
Excel file including 1153 experimentally verified SARS-CoV-2-specific $CD8^+$ T cell epitopes reported to be targeted in humans infected by the virus.

SUPPLEMENTARY DATA SHEET 2
Excel file including 66 experimentally verified SARS-CoV-2-specific $CD8^+$ T cell epitopes related by similarity with tetanus-diphtheria vaccine antigens, as judged by Levenshtein edit distances.

SUPPLEMENTARY FIGURE S1
Fluorescence minus one (FMO) controls for intracellular cytokine staining assays.

SUPPLEMENTARY FIGURE S2
T cell proliferation upon Td vaccine stimulation.

SUPPLEMENTARY FIGURE S3
Quality control of isolated naive T cells.

SUPPLEMENTARY FIGURE S4
Control T cell responses.

SUPPLEMENTARY FIGURE S5
Tetanus Toxoid (TT)– specific IgG.

References

1. Viruses, CSGotICoTo. The species Severe acute respiratory syndrome-related coronavirus: classifying 2019-nCoV and naming it SARS-CoV-2. *Nat Microbiol.* (2020) 5:536–44. doi: 10.1038/s41564-020-0695-z

2. Barbour V. COVID-19: no longer a global health emergency, now a long term challenge. *Med J Aust.* (2023) 218:437. doi: 10.5694/mja5692.51976

3. Yewdell JW. Individuals cannot rely on COVID-19 herd immunity: Durable immunity to viral disease is limited to viruses with obligate viremic spread. *PloS Pathog.* (2021) 17:e1009509. doi: 10.1001371/journal.ppat.1009509

4. Ballesteros-Sanabria L, Pelaez-Prestel HF, Ras-Carmona A, Reche PA. Resilience of spike-specific immunity induced by COVID-19 vaccines against SARS-coV-2 variants. *Biomedicines.* (2022) 10:996. doi: 10.3390/biomedicines10050996

5. Li R, Tian J, Yang F, Lv L, Yu J, Sun G, et al. Clinical characteristics of 225 patients with COVID-19 in a tertiary Hospital near Wuhan, China. *J Clin Virol.* (2020) 127:104363. doi: 10.1016/j.jcv.2020.104363

6. Solimando AG, Bittrich M, Shahini E, Albanese F, Fritz G, Krebs M. Determinants of COVID-19 disease severity-lessons from primary and secondary immune disorders including cancer. *Int J Mol Sci.* (2023) 24:8746. doi: 10.3390/ijms24108746

7. Yongzhi X. COVID-19-associated cytokine storm syndrome and diagnostic principles: an old and new Issue. *Emerg Microbes Infect.* (2021) 10:266–76. doi: 10.1080/22221751.22222021.21884503

8. Lowery SA, Sariol A, Perlman S. Innate immune and inflammatory responses to SARS-CoV-2: Implications for COVID-19. *Cell Host Microbe.* (2021) 29:1052–62. doi: 10.1016/j.chom.2021.1005.1004

9. Unterman A, Sumida TS, Nouri N, Yan X, Zhao AY, Gasque V, et al. Single-cell multi-omics reveals dyssynchrony of the innate and adaptive immune system in progressive COVID-19. *Nat Commun.* (2022) 13:440. doi: 10.1038/s41467–41021-27716–41464

10. Iyer AS, Jones FK, Nodoushani A, Kelly M, Becker M, Slater D, et al. Persistence and decay of human antibody responses to the receptor binding domain of SARS-CoV-

2 spike protein in COVID-19 patients. *Sci Immunol*. (2020) 5:1–12. doi: 10.1126/sciimmunol.abe0367

11. Moss P. The T cell immune response against SARS-CoV-2. *Nat Immunol*. (2022) 23:186–93. doi: 10.1038/s41590–41021-01122-w

12. Aleksova M, Todorova Y, Emilova R, Baymakova M, Yancheva N, Andonova R, et al. Virus-specific stem cell memory CD8+ T cells may indicate a long-term protection against evolving SARS-coV-2. *Diagn (Basel)*. (2023) 13:1280. doi: 10.3390/diagnostics13071280

13. Sette A, Sidney J. and crotty, S. T cell responses to SARS-coV-2. *Annu Rev Immunol*. (2023) 41:343–73. doi: 10.1146/annurev-immunol-101721-061120

14. Kingstad-Bakke B, Lee W, Chandrasekar SS, Gasper DJ, Salas-Quinchucua C, Cleven T, et al. Vaccine-induced systemic and mucosal T cell immunity to SARS-CoV-2 viral variants. *Proc Natl Acad Sci U.S.A*. (2022) 119:e2118312119. doi: 10.1073/pnas.2118312119

15. Law JC, Koh WH, Budylowski P, Lin J, Yue F, Abe KT, et al. Systematic examination of antigen-specific recall T cell responses to SARS-coV-2 versus influenza virus reveals a distinct inflammatory profile. *J Immunol*. (2021) 206:37–50. doi: 10.4049/jimmunol.2001067

16. van den Dijssel J, Hagen RR, de Jongh R, Steenhuis M, Rispens T, Geerdes DM, et al. Parallel detection of SARS-CoV-2 epitopes reveals dynamic immunodominance profiles of CD8(+) T memory cells in convalescent COVID-19 donors. *Clin Transl Immunol*. (2022) 11:e1423. doi: 10.1002/cti1422.1423

17. Weiskopf D, Schmitz KS, Raadsen MP, Grifoni A, Okba NMA, Endeman H, et al. Phenotype and kinetics of SARS-CoV-2-specific T cells in COVID-19 patients with acute respiratory distress syndrome. *Sci Immunol*. (2020) 5:eabd2071. doi: 10.1126/sciimmunol.abd2071

18. Sette A, Crotty S. Adaptive immunity to SARS-coV-2 and COVID-19. *Cell*. (2021) 184:861–80. doi: 10.1016/j.cell.2021.1001.1007

19. Casado JL, Vizcarra P, Martin-Hondarza A, Blasco M, Grandal-Platero M, Haemmerle J, et al. Impact of Previous Common Human Coronavirus Exposure on SARS-CoV-2-Specific T-Cell and Memory B-Cell Response after mRNA-Based Vaccination. *Viruses*. (2023) 15:627. doi: 10.3390/v15030627

20. Dan J, da Silva Antunes R, Grifoni A, Weiskopf D, Crotty S, Sette A. Observations and perspectives on adaptive immunity to severe acute respiratory syndrome coronavirus 2 (SARS-coV-2). *Clin Infect Dis*. (2022) 75:S24–9. doi: 10.1093/cid/ciac1310

21. Jia L, Weng S, Wu J, Tian X, Zhang Y, Wang X, et al. Preexisting antibodies targeting SARS-CoV-2 S2 cross-react with commensal gut bacteria and impact COVID-19 vaccine induced immunity. *Gut Microbes*. (2022) 14:2117503. doi: 10.2111080/19490976.19492022.12117503

22. Murray SM, Ansari AM, Frater J, Klenerman P, Dunachie S, Barnes E, et al. The impact of pre-existing cross-reactive immunity on SARS-CoV-2 infection and vaccine responses. *Nat Rev Immunol*. (2023) 23:304–16. doi: 10.1038/s41577–41022-00809-x

23. Agrawal B. Heterologous immunity: role in natural and vaccine-induced resistance to infections. *Front Immunol*. (2019) 10:2631. doi: 10.3389/fimmu.2019.02631

24. Welsh RM, Selin LK. No one is naive: the significance of heterologous T-cell immunity. *Nat Rev Immunol*. (2002) 2:417–26. doi: 10.1038/nri820

25. Grifoni A, Weiskopf D, Ramirez SI, Mateus J, Dan JM, Moderbacher CR, et al. Targets of T cell responses to SARS-coV-2 coronavirus in humans with COVID-19 disease and unexposed individuals. *Cell*. (2020) 20:30610–3. doi: 10.31016/j.cell.32020.30605.30015

26. Le Bert N, Tan AT, Kunasegaran K, Tham CYL, Hafezi M, Chia A, et al. SARS-CoV-2-specific T cell immunity in cases of COVID-19 and SARS, and uninfected controls. *Nature*. (2020) 584:457–62. doi: 10.1038/s41586–41020-42550-z

27. Ng KW, Faulkner N, Cornish GH, Rosa A, Harvey R, Hussain S, et al. Preexisting and *de novo* humoral immunity to SARS-CoV-2 in humans. *Science*. (2020) 370:1339–43. doi: 10.1126/science.abe1107

28. Woldemeskel BA, Kwaa AK, Garliss CC, Laeyendecker O, Ray SC, Blankson JN. Healthy donor T cell responses to common cold coronaviruses and SARS-CoV-2. *J Clin Invest*. (2020) 130:6631–8. doi: 10.1172/JCI143120

29. Sewell AK. Why must T cells be cross-reactive? *Nat Rev Immunol*. (2012) 12:669–77. doi: 10.1038/nri3279

30. Namuniina A, Muyanja ES, Biribawa VM, Okech BA, Ssemaganda A, Price MA, et al. High proportion of Ugandans with pre-pandemic SARS-CoV-2 cross-reactive CD4+ and CD8+ T-cell responses. *PLOS Glob Public Health*. (2023) 3:e0001566:1-11. doi: 10.1371/journal.pgph.0001566

31. Wratil PR, Schmacke NA, Karakoc B, Dulovic A, Junker D, Becker M, et al. Evidence for increased SARS-CoV-2 susceptibility and COVID-19 severity related to pre-existing immunity to seasonal coronaviruses. *Cell Rep*. (2021) 37:110169. doi: 10.111016/j.celrep.112021.110169

32. Lin CY, Wolf J, Brice DC, Sun Y, Locke M, Cherry S, et al. Pre-existing humoral immunity to human common cold coronaviruses negatively impacts the protective SARS-CoV-2 antibody response. *Cell Host Microbe*. (2022) 30:83–96.e84. doi: 10.1016/j.chom.2021.1012.1005

33. Kundu R, Narean JS, Wang L, Fenn J, Pillay T, Fernandez ND, et al. Cross-reactive memory T cells associate with protection against SARS-CoV-2 infection in COVID-19 contacts. *Nat Commun*. (2022) 13:80. doi: 10.1038/s41467–41021-27674-x

34. Coutard B, Valle C, de Lamballerie X, Canard B, Seidah NG, Decroly E. The spike glycoprotein of the new coronavirus 2019-nCoV contains a furin-like cleavage site absent in CoV of the same clade. *Antiviral Res*. (2020) 176:104742. doi: 10.1016/j.antiviral.2020.104742

35. Nickbakhsh S, Ho A, Marques DFP, McMenamin J, Gunson RN, Murcia PR. Epidemiology of seasonal coronaviruses: establishing the context for the emergence of coronavirus disease 2019. *J Infect Dis*. (2020) 222:17–25. doi: 10.1093/infdis/jiaa1185

36. Gorse GJ, Patel GB, Vitale JN, O'Connor TZ. Prevalence of antibodies to four human coronaviruses is lower in nasal secretions than in serum. *Clin Vaccine Immunol*. (2010) 17:1875–80. doi: 10.1128/CVI.00278–00210

37. Sealy RE, Hurwitz JL. Cross-reactive immune responses toward the common cold human coronaviruses and severe acute respiratory syndrome coronavirus 2 (SARS-coV-2): mini-review and a murine study. *Microorganisms*. (2021) 9:1643. doi: 10.3390/microorganisms9081643

38. Grifoni A, Sidney J, Vita R, Peters B, Crotty S, Weiskopf D, et al. SARS-CoV-2 human T¬†cell epitopes: Adaptive immune response against COVID-19. *Cell Host Microbe*. (2021) 29:1076–92. doi: 10.1016/j.chom.2021.1005.1010

39. Mateus J, Grifoni A, Tarke A, Sidney J, Ramirez SI, Dan JM, et al. Selective and cross-reactive SARS-CoV-2 T cell epitopes in unexposed humans. *Science*. (2020) 370:89–94. doi: 10.1126/science.abd3871

40. Ferretti AP, Kula T, Wang Y, Nguyen DMV, Weinheimer A, Dunlap GS, et al. Unbiased screens show CD8(+) T cells of COVID-19 patients recognize shared epitopes in SARS-coV-2 that largely reside outside the spike protein. *Immunity*. (2020) 53:1095–1107 e1093. doi: 10.1016/j.immuni.2020.10.006

41. Rha MS, Jeong HW, Ko JH, Choi SJ, Seo IH, Lee JS, et al. PD-1-expressing SARS-coV-2-specific CD8(+) T cells are not exhausted, but functional in patients with COVID-19. *Immunity*. (2021) 54:44–52.e43. doi: 10.1016/j.immuni.2020.1012.1002

42. Eggenhuizen PJ, Ng BH, Chang J, Cheong RMY, Yellapragada A, Wong WY, et al. Heterologous immunity between SARS-coV-2 and pathogenic bacteria. *Front Immunol*. (2022) 13:821595. doi: 10.3389/fimmu.2022.821595

43. Pothast CR, Dijkland RC, Thaler M, Hagedoorn RS, Kester MGD, Wouters AK, et al. SARS-CoV-2-specific CD4(+) and CD8(+) T cell responses can originate from cross-reactive CMV-specific T cells. *Elife*. (2022) 11:e82050. doi: 10.7554/eLife.82050

44. Mahajan S, Kode V, Bhojak K, Karunakaran C, Lee K, Manoharan M, et al. Immunodominant T-cell epitopes from the SARS-CoV-2 spike antigen reveal robust pre-existing T-cell immunity in unexposed individuals. *Sci Rep*. (2021) 11:13164. doi: 10.11038/s41598–13021-92521–13164

45. Simon AK, Hollander GA, McMichael A. Evolution of the immune system in humans from infancy to old age. *Proc Biol Sci*. (2015) 282:20143085. doi: 10.20141098/rspb.20142014.20143085

46. Bhopal SS, Bagaria J, Olabi B, Bhopal R. Children and young people remain at low risk of COVID-19 mortality. *Lancet Child Adolesc Health*. (2021) 5:e12–3. doi: 10.1016/S2352–4642(1021)00066–00063

47. Reche PA. Potential cross-reactive immunity to SARS-coV-2 from common human pathogens and vaccines. *Front Immunol*. (2020) 11:586984. doi: 10.3389/fimmu.2020.586984

48. Reche P. Cross-reactive immunity from combination DTP vaccines could protect against COVID-19. *Osf Preprints*. (2020). doi: 10.31219/osf.io/sbgy3

49. Monereo-Sanchez J, Luykx JJ, Pinzon-Espinosa J, Richard G, Motazedi E, Westlye LT, et al. Diphtheria and tetanus vaccination history is associated with lower odds of COVID-19 hospitalization. *Front Immunol*. (2021) 12:749264. doi: 10.3389/fimmu.2021.749264

50. Mysore V, Cullere X, Settles ML, Ji X, Kattan MW, Desjardins M, et al. Protective heterologous T¬†cell immunity in COVID-19 induced by the trivalent MMR and Tdap vaccine antigens. *Med*. (2021) 2:1050–1071.e1057. doi: 10.1016/j.medj.2021.1008.1004

51. Moller J, Kraner M, Sonnewald U, Sangal V, Tittlbach H, Winkler J, et al. Proteomics of diphtheria toxoid vaccines reveals multiple proteins that are immunogenic and may contribute to protection of humans against Corynebacterium diphtheriae. *Vaccine*. (2019) 37:3061–70. doi: 10.1016/j.vaccine.2019.3004.3059

52. Moller J, Kraner ME, Burkovski A. Proteomics of Bordetella pertussis whole-cell and acellular vaccines. *BMC Res Notes*. (2019) 12:329. doi: 10.1186/s13104–13019-14373–13102

53. Moller J, Kraner ME, Burkovski A. More than a Toxin: Protein Inventory of Clostridium tetani Toxoid Vaccines. *Proteomes*. (2019) 7:15. doi: 10.3390/proteomes7020015

54. Zhang Q, Wang P, Kim Y, Haste-Andersen P, Beaver J, Bourne PE, et al. Immune epitope database analysis resource (IEDB-AR). *Nucleic Acids Res*. (2008) 36:W513–518. doi: 10.1093/nar/gkn1254

55. Reche PA, Glutting JP, Reinherz EL. Prediction of MHC class I binding peptides using profile motifs. *Hum Immunol*. (2002) 63:701–9. doi: 10.1016/S0198-8859(02)00432-9

56. Reche PA, Glutting JP, Zhang H, Reinherz EL. Enhancement to the RANKPEP resource for the prediction of peptide binding to MHC molecules using profiles. *Immunogenetics*. (2004) 56:405–19. doi: 10.1007/s00251-004-0709-7

57. Hoof I, Peters B, Sidney J, Pedersen LE, Sette A, Lund O, et al. NetMHCpan, a method for MHC class I binding prediction beyond humans. *Immunogenetics*. (2009) 61:1–13. doi: 10.1007/s00251-008-0341-z

58. Reynisson B, Alvarez B, Paul S, Peters B, Nielsen M. NetMHCpan-4.1 and NetMHCIIpan-4.0: improved predictions of MHC antigen presentation by concurrent

motif deconvolution and integration of MS MHC eluted ligand data. *Nucleic Acids Res*. (2020) 48:W449–54. doi: 10.1093/nar/gkaa379

59. Molero-Abraham M, Lafuente EM, Flower DR, Reche PA. Selection of conserved epitopes from hepatitis C virus for pan-populational stimulation of T-cell responses. *Clin Dev Immunol*. (2013) 2013:601943. doi: 10.1155/2013/601943

60. Fontan-Vela M, Gullon P, Bilal U, Franco M. Social and ideological determinants of COVID-19 vaccination status in Spain. *Public Health*. (2023) 219:139–45. doi: 10.1016/j.puhe.2023.1004.1007

61. Sermet-Gaudelus I, Temmam S, Huon C, Behillil S, Gajdos V, Bigot T, et al. Prior infection by seasonal coronaviruses, as assessed by serology, does not prevent SARS-CoV-2 infection and disease in children, France, April to June 2020. *Euro Surveill*. (2021) 26:2001782. doi: 10.2002807/2001560–2007917.ES.2002021.2001726.2001713.2001782

62. Tan CCS, Owen CJ, Tham CYL, Bertoletti A, van Dorp L, Balloux F. Pre-existing T cell-mediated cross-reactivity to SARS-CoV-2 cannot solely be explained by prior exposure to endemic human coronaviruses. *Infect Genet Evol*. (2021) 95:105075. doi: 10.1016/j.meegid.2021.105075

63. Wooldridge L, Ekeruche-Makinde J, van den Berg HA, Skowera A, Miles JJ, Tan MP, et al. A single autoimmune T cell receptor recognizes more than a million different peptides. *J Biol Chem*. (2012) 287:1168–77. doi: 10.1074/jbc.M1111.289488

64. Prygiel M, Mosiej E, Gorska P, Zasada AA. Diphtheria-tetanus-pertussis vaccine: past, current & future. *Future Microbiol*. (2022) 17:185–97. doi: 10.2217/fmb-2021-0167

65. Lu PJ, O'Halloran A, Ding H, Liang JL, Williams WW. National and state-specific td and tdap vaccination of adult populations. *Am J Prev Med*. (2016) 50:616–26. doi: 10.1016/j.amepre.2015.1009.1033

66. Daniels CC, Rogers PD, Shelton CM. A review of pneumococcal vaccines: current polysaccharide vaccine recommendations and future protein antigens. *J Pediatr Pharmacol Ther*. (2016) 21:27–35. doi: 10.5863/1551–6776-5821.5861.5827

67. Goldblatt D. Conjugate vaccines. *Clin Exp Immunol*. (2000) 119:1–3. doi: 10.1046/j.1365-2249.2000.01109.x

68. Okhrimenko A, Grun JR, Westendorf K, Fang Z, Reinke S, von Roth P, et al. Human memory T cells from the bone marrow are resting and maintain long-lasting systemic memory. *Proc Natl Acad Sci U S A*. (2014) 111:9229–34. doi: 10.1073/pnas.1318731111

69. Koncz B, Balogh GM, Papp BT, Asztalos L, Kemeny L, Manczinger M. Self-mediated positive selection of T cells sets an obstacle to the recognition of nonself. *Proc Natl Acad Sci U S A*. (2021) 118:e2100542118. doi: 10.1073/pnas.2100542118

70. Riley TP, Hellman LM, Gee MH, Mendoza JL, Alonso JA, Foley KC, et al. T cell receptor cross-reactivity expanded by dramatic peptide-MHC adaptability. *Nat Chem Biol*. (2018) 14:934–42. doi: 10.1038/s41589–41018-40130–41584

71. Petrova GV, Naumov YN, Naumova EN, Gorski J. Role of cross-reactivity in cellular immune targeting of influenza A M1(58–66) variant peptide epitopes. *Front Immunol*. (2022) 13:956103. doi: 10.3389/fimmu.2022.956103

72. Hammarlund E, Thomas A, Poore EA, Amanna IJ, Rynko AE, Mori M, et al. Durability of vaccine-induced immunity against tetanus and diphtheria toxins: A cross-sectional analysis. *Clin Infect Dis*. (2016) 62:1111–8. doi: 10.1093/cid/ciw1066

frontiers | Frontiers in Immunology

TYPE Original Research
PUBLISHED 27 August 2024
DOI 10.3389/fimmu.2024.1434291

OPEN ACCESS

EDITED BY
Guido Ferrari,
Duke University, United States

REVIEWED BY
Yaping Sun,
Yale University, United States
Ashley Nelson,
NewYork-Presbyterian, United States

*CORRESPONDENCE
Almut Meyer-Bahlburg
almut.meyer-bahlburg@med.uni-greifswald.de
Dina Raafat
dina.raafat@med.uni-greifswald.de

†These authors have contributed equally to this work and share first authorship

RECEIVED 17 May 2024
ACCEPTED 05 August 2024
PUBLISHED 27 August 2024

CITATION
Kuthning D, Raafat D, Holtfreter S, Gramenz J, Wittmann N, Bröker BM and Meyer-Bahlburg A (2024) Variant-specific antibody profiling for tracking SARS-CoV-2 variant infections in children and adolescents. *Front. Immunol.* 15:1434291. doi: 10.3389/fimmu.2024.1434291

Variant-specific antibody profiling for tracking SARS-CoV-2 variant infections in children and adolescents

Daniela Kuthning[1†], Dina Raafat[2,3*†], Silva Holtfreter[2], Jana Gramenz[1], Nico Wittmann[1], Barbara M. Bröker[2] and Almut Meyer-Bahlburg[1*]

[1]Pediatric Rheumatology, Department of Pediatric and Adolescent Medicine, University Medicine Greifswald, Greifswald, Germany, [2]Institute of Immunology, University Medicine Greifswald, Greifswald, Germany, [3]Department of Microbiology and Immunology, Faculty of Pharmacy, Alexandria University, Alexandria, Egypt

Monitoring the seroprevalence of SARS-CoV-2 in children and adolescents can provide valuable information for effective SARS-CoV-2 surveillance, and thus guide vaccination strategies. In this study, we quantified antibodies against the spike S1 domains of several SARS-CoV-2 variants (wild-type, Alpha, Delta, and Omicron variants) as well as endemic human coronaviruses (HCoVs) in 1,309 children and adolescents screened between December 2020 and March 2023. Their antibody binding profiles were compared with those of 22 pre-pandemic samples from children and adolescents using an in-house Luminex®-based Corona Array (CA). The primary objectives of this study were to (i) monitor SARS-CoV-2-specific antibodies in children and adolescents, (ii) evaluate whether the S1-specific antibody response can identify the infecting variant of concern (VoC), (iii) estimate the prevalence of silent infections, and (iv) test whether vaccination or infection with SARS-CoV-2 induce HCoV cross-reactive antibodies. Both SARS-CoV-2 infection and vaccination induced a robust antibody response against the S1 domain of WT and VoCs in children and adolescents. Antibodies specific for the S1 domain were able to distinguish between SARS-CoV-2 VoCs in infected children. The serologically identified VoC was typically the predominant VoC at the time of infection. Furthermore, our highly sensitive CA identified more silent SARS-CoV-2 infections than a commercial ELISA (12.1% vs. 6.3%, respectively), and provided insights into the infecting VoC. Seroconversion to endemic HCoVs occurred in early childhood, and vaccination or infection with SARS-CoV-2 did not induce HCoV S1 cross-reactive antibodies. In conclusion, the antibody response to the S1 domain of the spike protein of SARS-CoV-2 is highly specific, providing information about the infecting VoC and revealing clinically silent infections.

KEYWORDS

SARS-CoV-2, children, adolescents, variants of concern, silent infections, antibody, spike S1

1 Introduction

The global spread of the severe acute respiratory syndrome coronavirus 2 (SARS-CoV-2) and the continuous emergence of new variants of concern (VoCs) have resulted in over 676 million infections and a death toll of approximately 6.9 million (as of 10/03/23) due to the associated coronavirus disease 2019 (COVID-19) (1). In Northern Germany, there have been four epidemic waves of COVID-19, caused respectively by the original SARS-CoV-2 strain Wu01 (March – December 2020), the Alpha variant (December 2020 – June 2021), the Delta variant (June 2021 – January 2022), and the Omicron variants BA.1, BA.2, BA.4 and BA.5 (from January 2022) (2).

Epidemiological data indicate that children are less prone to develop COVID-19 upon exposure to SARS-CoV-2 and, when infected, the symptoms are less severe than those in adults (3, 4). These milder disease courses are attributed to several factors, including earlier and more rapid type 1 interferon responses, increased cytokine production and differences in immune cell numbers (5, 6).

Asymptomatic, i.e. silent infections (SI) represent a significant potential driver of SARS-CoV-2 epidemics, as they can facilitate uncontrollable transmission. The role of asymptomatic children in viral transmission was a highly debated topic at the beginning of the pandemic. Recent studies, however, indicate that children are less frequently identified as index cases than adults in household and school settings (3), and that asymptomatic SARS-CoV-2-infected children are less likely to transmit the virus to other household members than symptomatic individuals (7). Knowledge of SI prevalence is essential for more accurately estimating transmission dynamics, improving epidemiological modelling, and guiding effective public health measures (8, 9).

Monitoring SI relies on the detection of viral RNA (PCR) or proteins (lateral flow tests) in swab samples, or on serological assays (e.g. ELISA). In the early stages of the pandemic, PCR testing was primarily focused on symptomatic cases and their direct contacts (10). Subsequently, the advent of lateral flow tests for public use in March 2021 facilitated mass testing, particularly in educational institutions such as schools and kindergartens (11). Serological assays are frequently employed in surveillance studies to ascertain the prevalence of SI (12, 13). Seroconversion to spike S1 protein is more common than to nucleocapsid (NC) protein (14), and serves as a marker for previous infection in unvaccinated cohorts.

The infection with the SARS-CoV-2 virus results in the formation of antibodies against a number of antigens, including the Spike (S) protein and NC. The Spike protein is composed of two domains, S1 and S2, which are responsible for mediating receptor binding and virus-host membrane fusion, respectively (15). The S2 domain is highly conserved amongst SARS-CoV-2 and closely related coronaviruses, and shares numerous antibody epitopes. Neutralizing antibodies primarily target the more variable S1 domain. The human immune response against SARS-CoV-2 drives viral evolution, leading to the emergence and global spread of VoCs with Spike variants that are less well recognized by vaccine-induced antibodies (16–18). The majority of amino acid exchanges are located in the spike S1 domain (18). Consequently, vaccine-induced antibodies and also therapeutic neutralizing antibodies are largely ineffective against the Omicron variant.

In addition to SARS-CoV-2, children frequently contract the closely related common cold human coronaviruses (HCoVs), including the alphacoronaviruses 229E and NL63 and the betacoronaviruses HKU1 and OC43. The vast majority of children experience their first HCoV infection at an early age and are subsequently re-exposed throughout their lives (19–21). Due to conserved epitopes, pre-existing antibodies from prior infections with HCoVs can cross-react with SARS-CoV-2 S and NC proteins (20, 22, 23). Nevertheless, it seems that seasonal HCoV infection does not confer cross-protection against SARS-CoV-2 infection (20, 22, 23).

Here, a total of 1,309 children aged six months to 17 years were sampled in North-Eastern Germany between December 2020 and March 2023. SARS-CoV-2 antibody profiling was performed using both commercial ELISA-based assays and an in-house Luminex®-based approach. The Luminex®-based Corona Array (CA) demonstrated greater sensitivity, resulting in an under-ascertainment rate of 12.1% among children and adolescents. Moreover, antibody profiles against the spike S1 domain from wild-type (WT) and VoCs were highly discriminatory and reflected the kinetics of VoC waves in Northern Germany. This approach enabled us to attribute the identified SI to the infecting variant with the highest probability. Finally, seroconversion to endemic HCoVs occurred at an early age. With regard to the variable S1 domain, COVID-19 vaccination or SARS-CoV-2 infection did not induce HCoV-cross-reactive antibodies.

2 Methods

2.1 Patient recruitment

Serum or plasma samples were collected from 22 pre-pandemic children and adolescents (aged 4-17 years) as well as from 1,309 children and adolescents (aged six months to 17 years; COVIDKID cohort) attending medical care in one of six participating hospitals and two private pediatric practices in North-Eastern Germany between December 2020 and March 2023. Repeated participation was permitted after a minimum interval of two months. Additionally, the families of the participants were requested to complete a questionnaire concerning the children's SARS-CoV-2-vaccination status, previous SARS-CoV-2 infections, demographic data and socioeconomic background.

The study was approved by the Ethics Committee of the University Medicine Greifswald (BB188/20, and its amendment BB188/20a; BB 014/18) and entered in the German Clinical Trial Register on 09/03/2021 (Trial ID: DRKS00024635; https://drks.de/search/de/trial/DRKS00024635). All research was conducted in accordance with the tenets of the Declaration of Helsinki. All requirements of data protection and confidentiality were fully respected.

The study period was divided into distinct SARS-CoV-2 waves based on publicly available data from CoMV-Gen (24). Turning points of a new dominant VoC were interpolated from weekly proportions of challenging variants (interpolated proportion >50% for respective VoC). This resulted in the delineation of the following

pandemic waves: I) Alpha wave (10/12/2020 – 19/06/2021), II) Delta wave (20/06/2021 – 05/01/2022), BA.1 wave (06/01/2022 – 16/02/2022), BA.2 wave (17/02/2022 – 07/06/2022) and BA.5 wave (08/06/2022 – 13/03/2023).

2.2 ELISA for the detection of SARS-CoV-2-specific IgG antibodies

The presence of SARS-CoV-2-specific IgG antibodies against the spike S1 domain and the nucleocapsid protein (Anti-SARS-CoV-2-ELISA (IgG) using the Spike S1 protein from the wild type strain and Anti-SARS-CoV-2-NCP-ELISA, respectively) was determined using commercially available kits (EI 2606-9601 G, EI 2606-9601-2 G; EUROIMMUN, Lübeck, Germany) according to the manufacturer's instructions. Antibodies were detected semi-quantitatively and the results were interpreted as recommended by the manufacturer: positive at a ratio ≥1.1; negative at a ratio < 0.8; borderline at a ratio between 0.8 and 1.1. In brief, serum or plasma samples were diluted 1:101, and the levels of IgG antibodies against S1 or NC were analyzed using an Immunomat (Virion/Serion, Würzburg, Germany) or Tecan infinite M200 Pro microplate reader (Tecan Group Ltd., Männedorf, Switzerland), respectively.

2.3 12-plex Corona Array for the detection of SARS-CoV-2 and HCoV-specific IgG antibodies

The Corona Array (CA) is an in-house bead-based 12-plex suspension array based on the xMAP® technology (Luminex®, Austin, USA) (25). The CA was designed for the simultaneous analysis of antibodies against different recombinant coronavirus antigens. Twelve recombinant proteins were procured from Sino Biological Europe GmbH (Eschborn, Germany), comprising seven recombinant His-tagged proteins/protein subunits of SARS-CoV-2; four recombinant spike S1 proteins of the endemic HCoVs, and the recall antigen tetanus toxoid (Table 1). The proteins were covalently coupled to MagPlex® magnetic microspheres at a concentration of 100 µg per 1.25×10^7 beads. The coupling efficiency (coupling factor) was determined via the His-tag as previously described in detail (26).

The CA was performed with serum or plasma samples as previously described (26, 27). The plasma dilution was optimized based on 7-point dilution series (1:20 to 1:312,500) of 19 representative plasma samples of various anti-S1_WT IgG levels as determined by a commercial S1 IgG ELISA, in order to be able to detect both low and high antibody levels in a single measurement (Supplementary Figure 1). Based on this pretest, we selected a sample dilution of 1:10,000 to ensure a reliable detection of both high and low antibody levels. Plasma samples with a raw median fluorescence intensity (MFI) > 15.000 (n=46) were once more analyzed using 7-dilution series, to avoid saturation effects, and a single dilution within the linear range was selected for the analysis. A plasma pool (prepared from plasma samples of 13 donors with previous SARS-CoV-2 infection (COV^+) and/or COVID-19 vaccination (VAC^+)) was included on each plate for data normalization. The antibody binding was determined using the BioPlex 200 system (Bio-Rad Laboratories GmbH, Feldkirchen, Germany) with bead buffer serving as the blank. The following instrument settings were used: bead type: MagPlex beads, beads: 100 beads per region, sample timeout: 60 sec, sample volume: 80 µL,

TABLE 1 Recombinant proteins used in this study for the construction of the CA.

	Recombinant protein/protein domain*	Abbreviation	Company	Catalog Number
SARS-CoV-2 (2019-nCoV)				
1	SARS-CoV-2 (2019-nCoV) Spike S1	S1_WT	Sino Biological	40591-V08H
2	SARS-CoV-2 (2019-nCoV) Nucleocapsid	NC_WT	Sino Biological	40588-V08B
3	SARS-CoV-2 (2019-nCoV) Spike S1 (Alpha variant)	S1_Alpha	Sino Biological	40591-V08H12
4	S1 Delta (B.1.617.2)	S1_Delta	Sino Biological	40591-V08H23
5	S1 Omicron (B.1.1.529)	S1_ BA.1	Sino Biological	40591-V08H41
6	S1 Omicron (BA.2)	S1_ BA.2	Sino Biological	40591-V08H43
7	S1 Omicron (BA.4/BA.5)	S1BA.4/5	Sino Biological	40591-V08H46
Human coronaviruses				
8	Human coronavirus (HCoV-229E) Spike/S1 Protein	S1_229E	Sino Biological	40601-V08H
9	Human coronavirus (HCoV-HKU1) Spike/S1 Protein	S1_HKU1	Sino Biological	40021-V08H
10	Human coronavirus (HCoV-NL63) Spike/S1 Protein	S1_NL63	Sino Biological	40600-V08H
11	Human coronavirus (HCoV-OC43) Spike/S1 Protein	S1_OC43	Sino Biological	40607-V08H1
Recall antigen				
12	Tetanus Toxoid	TT	Sigma Aldrich	582231

*all recombinant proteins/protein domains, except for the tetanus toxoid, were His-tagged.

gate settings: 7,500–15,000 (BioPlex Manager 5.0 software; Bio-Rad Laboratories GmbH, Feldkirchen, Germany).

The relative IgG concentrations measured in the plasma pool were employed to normalize inter-plate variations. The coupling factor was utilized for correction between antigens. Serum samples were considered seropositive for SARS-CoV-2 when antibody binding to at least one S1 variant (WT or VoCs) was above the cut-off value of the respective antigen. Serum samples with only anti-NC antibodies above the cut-off value were not considered seropositive for SARS-CoV-2, as cross-reactivity to other coronaviruses can result in increased NC antibody levels.

2.4 Statistics

Statistical testing and data visualization were conducted using GraphPad Prism (v9) and R (v4.2.0; https://www.R-project.org/) in combination with the tidyverse package (v2.0.0) (28) and the patchwork package (v1.1.2; https://CRAN.R-project.org/package=patchwork). Cutoff values for the CA were defined based on MFI values of 22 pre-pandemic samples from children and calculated as mean + 5× standard deviation (SD).

The significance of differences between groups was tested by one-way analysis of variance (ANOVA; Kruskall-Wallis test) with *post-hoc* Dunn's multiple-comparison test. Statistical significance was defined as a p-value <0.05. The correlation between the ELISA and CA was calculated using Spearman's correlation coefficient.

3 Results

The dynamics of the antibody response to several SARS-CoV-2 variants were traced in 1,309 serum/plasma samples obtained from children and adolescents in North-Eastern Germany between December 2020 and March 2023 (median age: 10 years, range: 0.5-17 years). Serum samples from a pre-pandemic cohort of 22 individuals (pre-COVID; median age: 12 years; range 4-17 years) served as controls and for the calculation of the cut-off values (WT_S1: 50.4; WT_NC: 545.65; Alpha_S1: 74.58; Delta_S1: 63.46; BA.1_S1: 64.1; BA.2_S1: 60.3; BA.4/5_S1: 51.2). Questionnaires were employed to ascertain previous SARS-CoV-2 infections (COV^+ or COV^-) and/or COVID-19 vaccinations (VAC^+ or VAC^-). Among the 1,309 study subjects, 271 reported infection with SARS-CoV-2 (COV^+) and 177 reported vaccination (VAC^+) (Table 2). Serum/plasma samples were assigned to five distinct SARS-CoV-2 waves (Alpha, Delta, BA.1, BA.2, BA.5), based on the time point of study inclusion. A SARS-CoV-2 wave was defined as the period in which the respective VoC was responsible for more than 50% of the reported cases (Table 2).

3.1 SARS-CoV-2 infection and vaccination induce high levels of S1-specific antibodies

The presence of SARS-CoV-2-specific serum antibodies (seroconversion) against NC and the S1 subunits of SARS-CoV-2

TABLE 2 Patient characteristics of the COVIDKID cohort.

	Total (n=1,309)	Unvaccinated, VAC^- (n=1,107)	Vaccinated, VAC^+ (n=177)	Unknown (n=25)
Female, no. (%)	668 (51.0)	549 (49.6)	104 (58.8)	15 (60.0)
Age [years] median (range)	10 (0.5 - 17)	9 (0.5 – 17)	15 (2 – 17)	13 (1 – 17)
Study inclusion during[1]				
Alpha wave (10/12/2020 – 19/06/2021)	496	481	4	11
Delta wave (20/06/2021 – 05/01/2022)	343	303	34	6
BA.1 wave (06/01/2022 – 16/02/2022)	99	62	37	–
BA.2 wave (17/02/2022 – 07/06/2022)	188	138	47	3
BA.5 wave (08/06/2022 – 13/03/2023)	183	123	55	5
SARS-CoV-2 infection status (COV)[2]				
Undiagnosed (COV^-)	1009	876	120	13
At least one diagnosis (COV^+)	271	210[3]	55	6
Unknown	29	21	2	6

[1]SARS-CoV-2 waves were defined as the period in which the respective VoC was responsible for more than 50% of the reported cases.
[2]Information about SARS-CoV-2 exposure at the time of study inclusion were evaluated from a questionnaire.
[3]including n=190 of COV^+/VAC^- with a single diagnosis, of which n=143 with known date of diagnosis and analyzed for SARS-CoV-2 IgG profiles in Figure 3.

WT and VoCs was quantified using a bead-based in-house CA. The levels of anti-NC antibodies (NC_WT; Figure 1; panel 1) were found to be highest in children and adolescents who reported a previous COVID-19 infection (COV^+; median log(MFI) 2.60). In contrast, the majority of vaccinated individuals without prior infection (COV^-/VAC^+; median log(MFI) 1.55), participants with neither infection nor vaccination (COV^-/VAC^-; median log(MFI) 1.28) and pre-COVID samples (median log(MFI) 1.44) lacked anti-NC antibodies. This is not unexpected, given that all SARS-CoV-2 vaccines approved for children and adolescents in Germany during the study period contained mRNA or DNA encoding the SARS-CoV-2 WT spike protein.

Vaccinated children and adolescents with (COV^+/VAC^+) or without infection (COV^-/VAC^+) mounted a robust serum IgG response against the S1 subunit of the SARS-CoV-2 spike protein. Their antibodies bound to the S1-domains of the SARS-CoV-2 strain Wu01 (wild-type, WT) and the five VoCs that circulated in the study region (Figure 1). The highest antibody levels were observed in children and adolescents who had experienced both infection and vaccination (COV^+/VAC^+), while infection alone induced significantly lower amounts of anti-S1 IgG serum antibodies (median log(MFI) 1.3- to 1.6-times lower in COV^+/VAC^- than in COV^+/VAC^+ individuals; $p < 0.001$ in Kruskall-Wallis test for all S1 antigens; not shown). As anticipated, pre-COVID- and most COV^-/VAC^- samples lacked anti-S1 antibodies. However, some COV^-/VAC^- subjects exhibited high anti-S1 IgG levels, suggesting the possibility of silent SARS-CoV-2 infections.

Furthermore, the antibody binding patterns to the S1 from WT and circulating VoCs (Alpha, Delta, Omicron BA.1, BA.2, and BA.4/5) differed between vaccinated and infected subjects. In the vaccinated group (COV^-/VAC^+), antibody binding to the closely-related S1_WT and S1_Alpha (median log(MFI) 4.01 and 4.24, respectively) exhibited a tendency to be stronger than to S1 of the other VoCs (median log(MFI) 3.59 to 3.91). In the COV^+/VAC^- group, the anti-S1 antibody binding patterns exhibited considerable inter-individual variability (median log(MFI) 2.7 to 3.3).

In conclusion, our CA data demonstrate that both vaccination and infection elicit robust anti-S1 antibody responses.

3.2 The Corona Array is more sensitive than a commercially available ELISA

To assess the performance of our in-house CA, we compared its results (antibody binding to NC_WT, S1_WT, S1 of five circulating VoCs) with the data obtained with commercial ELISAs (anti-nucleocapsid (NCP) IgG and anti-S1 IgG). Both methods yielded concordant results, as evidenced by Spearman's correlation coefficients between 0.69 and 0.71 for the individual S1 antigens (Figure 2). However, regarding the S1_WT antigen, the CA exhibited greater sensitivity than the commercial ELISA (lower right quadrant, with samples positive in CA but negative in ELISA assay), and its dynamic range was considerably larger, spanning 5-6 logs as compared to two logs for the ELISA (upper right quadrant).

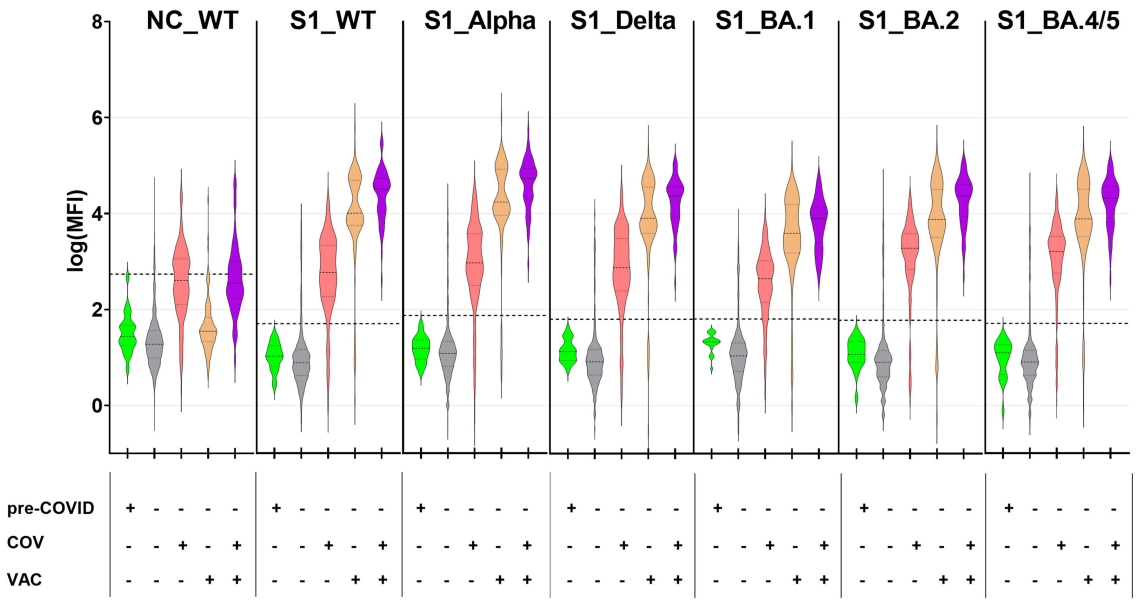

FIGURE 1
SARS-CoV-2-exposed children and adolescents exhibit a robust antibody response against SARS-CoV-2 antigens from wild-type SARS-CoV-2 and its VoCs. SARS-CoV-2-specific antibodies were quantified with the CA in 1261 pediatric samples with known SARS-CoV-2 vaccination and infection status as well as 22 pre-COVID samples, against nucleocapsid protein from SARS-CoV-2 wild-type (NC_WT), spike S1 domain from WT (S1_WT) and circulating VoCs (S1_Alpha, S1_Delta, S1_BA.1, S1_BA.2 and S1_BA.4/5). Data are displayed as log-transformed MFI values. Samples were categorized based on sampling time point (pre-$COVID^+$/pre-$COVID^-$), anamnestic SARS-CoV-2 infection (COV^+/COV^-) and COVID-19 vaccination status (VAC^+/VAC^-). Horizontal dotted lines represent the cut-off values for each of the tested antigens (mean (MFI) +5xSD). The dotted lines within the violin plots depict the median and the quartiles. Sub-cohorts: pre-COVID, n=22; COV^-/VAC^-, n=876; COV^+/VAC^-, n=210; COV^-/VAC^+, n= 120; COV^+/VAC^+, n=55.

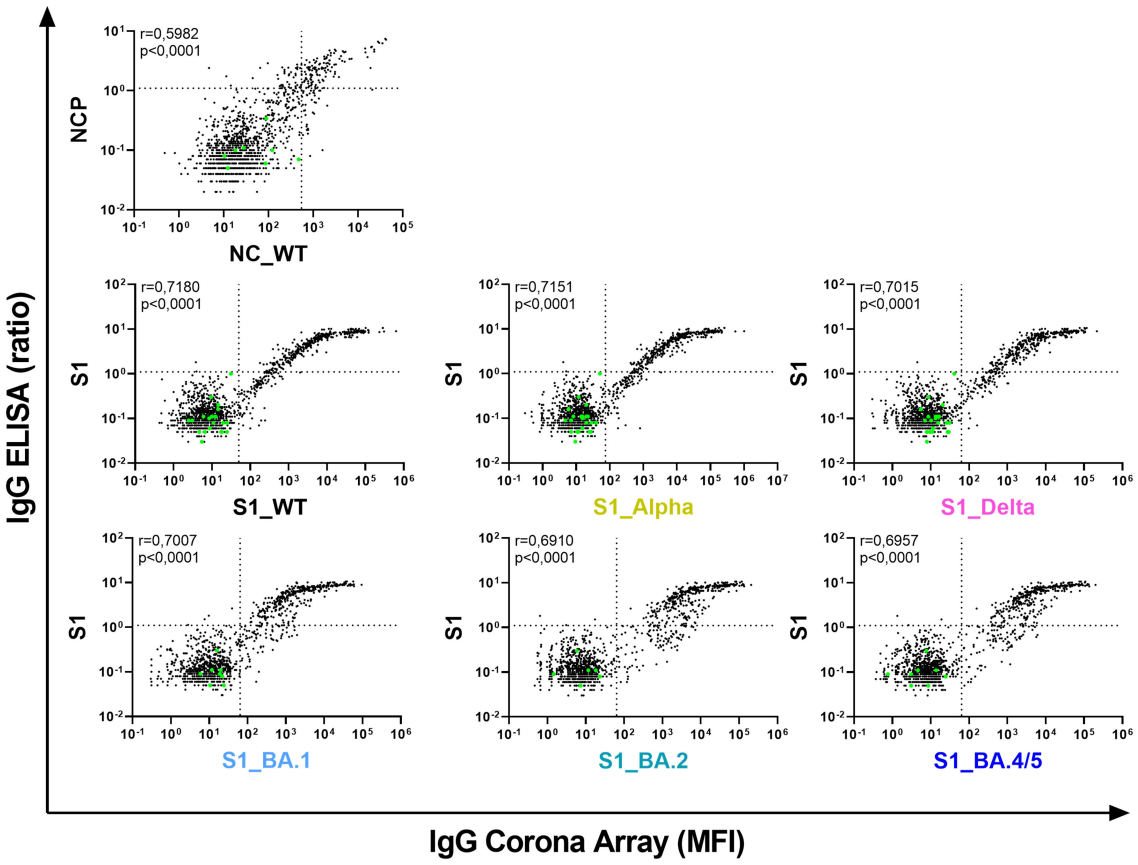

FIGURE 2
The Corona Array (CA) is more sensitive and covers a broader range than commercially available ELISAs. Serum IgG against nucleocapsid protein (NC) as well as S1 from SARS-CoV-2 WT and circulating VoCs (Alpha, Delta, BA.1, BA.2 and BA.4/5) were quantified in 1331 pediatric samples using the CA and are plotted on the x-axis. Pre-COVID samples (n=22; green dots) were also used for calculation of cut-off values for the CA (mean (MFI) +5×SD; indicated by vertical dotted lines). Serum IgG against nucleocapsid protein (NCP) and S1_WT were determined by commercial ELISA. Results are indicated as ratio of $OD_{sample}/OD_{calibrator}$, and are plotted on the y-axis. The cut-off values recommended by the manufacturer are indicated by horizontal dotted lines. Spearman´s correlation coefficient r is depicted. NC/NCP, nucleocapsid protein; MFI, median fluorescence intensity; S1, Spike S1 domain.

3.3 Anti-NC antibodies alone are not a reliable indicator of SARS-CoV-2 infections

As both COVID-19 vaccination and SARS-CoV-2 infection induce anti-S1 antibody responses, we investigated whether seroconversion to NC could serve as a reliable marker for previous COVID-19 infection(s). Consequently, the CA (NC_WT) or ELISA (NCP) were used to determine the prevalence of anti-NC antibodies among unvaccinated children and adolescents (n=1,086), of whom n=210 had reported a SARS-CoV-2 infection (COV^+/VAC^-).

Less than 50% of individuals with anamnestic COVID-19 infections were seropositive for NC, regardless of the applied method (sensitivities of 0.44 and 0.49, for CA and ELISA respectively) (Table 3). This remained consistent throughout the pandemic waves, with the exception of the BA.5 wave, where only 29.9% of infected individuals showed a positive NC result with either method (data not shown). The specificity of both the CA and ELISA assays was 0.96. Consequently, a negative NC test does not rule out a SARS-CoV-2 infection, while a positive NC test reliably indicates a (silent) infection.

In contrast, a positive CA result for at least one S1 antigen (WT or VoCs) identified a previous SARS-CoV-2 infection in unvaccinated children with a superior sensitivity of 0.93, compared to a sensitivity of 0.61 for the ELISA. Therefore, we used the CA-based detection of antibodies against at least one S1 of either WT or VoC as a marker for (silent) SARS-CoV-2 infection in the subsequent analyses.

3.4 The S1-specific antibody response discriminates between SARS-CoV-2 VoCs

We hypothesized that the immune system is capable of discriminating between the S1 allelic variants of the circulating VoCs, with the strongest antibody response directed against S1 of the infecting VoC. To test this hypothesis, we analyzed the antibody profiles in children and adolescents with a single SARS-CoV-2 infection with known date of diagnosis (COV^+/VAC^-; n=143) (Table 2). We then calculated the MFI ratio of antibody binding to each S1_VoC to that to S1_WT, which we subsequently refer to as the VoC-to-WT ratio.

10.3389/fimmu.2024.1434291

TABLE 3 SARS-CoV-2-specific anti-S1 and anti-nucleocapsid IgG-antibodies in a cohort of VAC$^-$ children and adolescents (n=1,086).

	n	CA[1]				ELISA[2]			
		S1		NC_WT		S1		NCP	
		+	–	+	–	+	–	+	–
COV^{+3}	210	195	15	92	118	129	81	103	107
COV^{-3}	876	106	770	36	840	49	827	36	840
PPV		0.65		0.72		0.72		0.74	
NPV		0.98		0.88		0.91		0.89	
Sensitivity		0.93		0.44		0.61		0.49	
Specificity		0.88		0.96		0.94		0.96	

[1]cut-off values for CA were defined as mean (MFI) +5×SD from 22 pre-COVID samples.
[2]cut-off values for commercial anti-S1 and -NCP ELISAs were defined as ratio ($OD_{sample}/OD_{calibrator}$) ≥1.1, as per manufacturer´s instructions.
[3]self-reported SARS-CoV-2 infection status.
CA, Corona Array; NC/NCP, nucleocapsid protein; S1, Spike S1 domain; PPV, positive predictive value; NPV, negative predictive value; +, positive test result; -, negative test result.

Samples were assigned to five distinct SARS-CoV-2 waves (Alpha, Delta, BA.1, BA.2 and BA.4/5) based on the time of diagnosis. In Figure 3A, the VoC with the highest ratio is highlighted as a colored dot for each individual, hinting towards the most probable infecting variant.

In subjects diagnosed with COVID-19 during the Alpha, Delta, BA.2 and BA.4/5 waves, the highest VoC-to-WT ratio was found to correspond closely with the dominant variant (Figures 3B, C, E, F). For example, during the Alpha wave, 24/30 study participants exhibited the strongest antibody binding to the S1 of the Alpha variant (Figure 3B, highlighted in gold), while three exhibited the strongest antibody binding to the Delta variant (pink dots). This does not contradict our assumption, as during each wave, there were also infections with non-dominant VoCs. Unexpectedly, three COV$^+$ children who reported a SARS-CoV-2 infection during the Alpha wave exhibited the strongest binding ratios for Omicron variants BA.2 or BA.4/5, which were not yet present during the Alpha wave. These samples were obtained at a late stage of the pandemic, which might reflect additional Omicron infections that went undiagnosed (Figure 3B).

Of the 35 subjects diagnosed during the Delta wave, 27 (75%) exhibited the highest VoC-to-WT ratio for the Delta variant, while the remaining 8 samples demonstrated a strong reaction with the Alpha variant (Figure 3C). In individuals diagnosed during the BA.1 wave (n=13, Figure 3D), the results were inconclusive. The majority of samples diagnosed during the BA.2 and BA.5 waves presented with a BA.2- or BA.4/5-specific serological signature, respectively (Figures 3E, F).

In conclusion, antibody profiles against the VoC-S1 domains were highly discriminatory and reflected the kinetics of the VoC waves in Northern Germany.

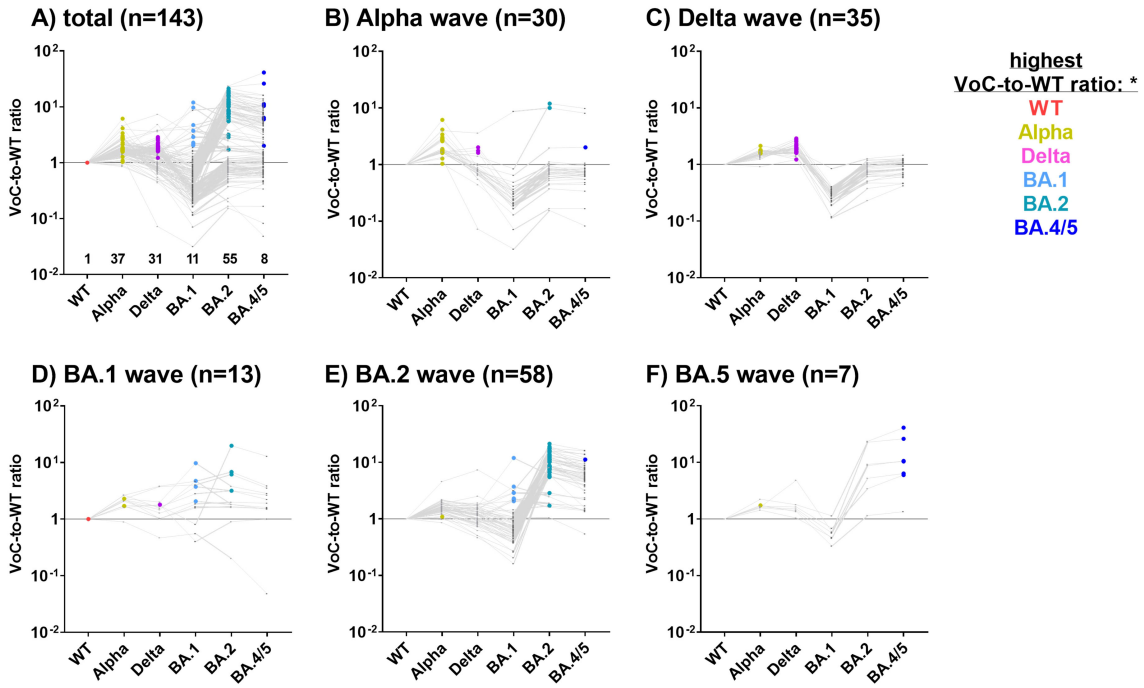

FIGURE 3
S1 variant-specific serological signatures can be used to identify the most probable infecting VoC. For 143 COV$^+$/VAC$^-$ SARS-CoV-2 CA_S1$^+$ children and adolescents with a single SARS-CoV-2 diagnosis, antibody levels against S1 are depicted as ratios of MFI_{VoC} to MFI_{WT} (VoC-to-WT ratio) **(A)**. Subsequently, samples were assigned to the SARS-CoV-2 Alpha **(B)**, Delta **(C)**, BA.1 **(D)**, BA.2 **(E)** or BA.4/5 **(F)** waves based on the time of diagnosis. VoCs-to-WT ratios for each study subject are connected by a grey line. The VoC with the highest ratio is highlighted as a colored dot, likely reflecting the infecting VoC. Samples where all VoC-to-WT ratios were below 1 were assigned to the WT.

3.5 Detection of silent SARS-CoV-2 infections

Seroconversion to S1 is a commonly used marker for previous SARS-CoV-2 infections in unvaccinated individuals. However, the sensitivity of this approach depends on the method of detection. Figure 4 depicts the antibody binding to S1_WT. While the commercial ELISA detected known SARS-CoV-2 infections in 136/210 unvaccinated children and adolescents (COV^+/VAC^-), CA was positive for at least one S1 allele in 195 of the 210 COV^+/VAC^- participants (Figure 4, left panel). This results in 64.8% and 92.9% seropositivity for the ELISA and CA, respectively. The anti-S1_WT antibody levels in CA-positive (CA^+) samples that were ELISA-negative ($ELISA^-$) were found to be lower than in samples that were positive with both methods.

Using the same methods to identify unnoticed (silent) infections (SI), the commercial ELISA revealed anti-S1 antibodies in 6.3% (55 of 876 samples) of COV^-/VAC^- children and adolescents. In contrast, the CA identified twice as many SI (106 of 876 samples; 12.1%). The positive samples that were missed by the ELISA (6.3%) exhibited lower S1-specific antibody levels against all tested S1 antigens than $ELISA^+$ samples (Figure 4, right panel).

Looking at the whole COVIDKID cohort, a total of 301 of the 1,086 unvaccinated children had been exposed to SARS-CoV-2 based on the CA-S1 results. Of these, only 210 cases were diagnosed (COV^+/VAC^-). This results in a 1.43-fold higher SARS-CoV-2 exposure rate than reported.

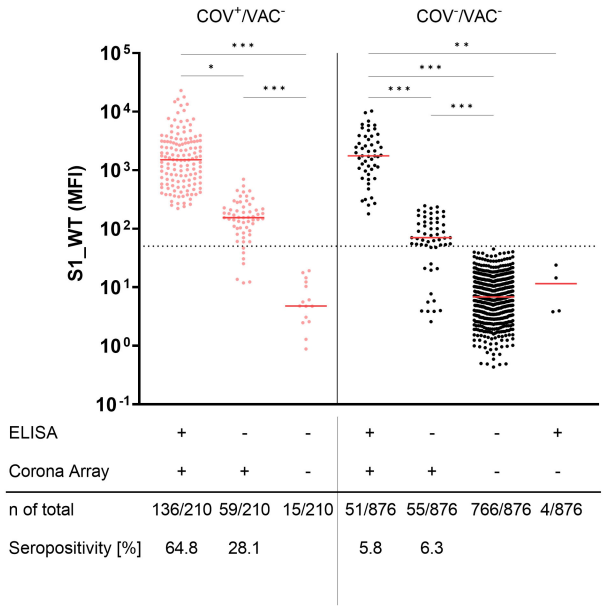

FIGURE 4
Corona Array (CA) detects SARS-CoV-2 infections with high sensitivity and unveils silent infections in 12.1% of anamnestically SARS-CoV2-naïve children and adolescents. Seroconversion to Spike S1 was determined by commercial ELISA and CA in pediatric COV^+/VAC^- samples (red, left panel) and COV^-/VAC^- samples (black, right panel). Samples were stratified by being positive in ELISA (S1_WT) and/or CA (S1 from WT or VoCs). $ELISA^-$ but CA_S1^+ samples from both groups show significantly lower levels of antibodies against S1_WT. The median is shown in red. The dashed line indicates the cut-off value for S1_WT. Significance between groups was tested by Kruskall-Wallis test and *post-hoc* Dunn´s correction. *, p<0.05; **, p < 0.01; ***, p<0.001.

3.6 Antibody signatures specific to the S1-variant provide insights into the contact variant in children with silent infections

We next calculated the VoC-to-WT ratio to determine the most probable infecting VoC in children and adolescents with SI (Figure 5), as the immune system of COV^+ patients was able to discriminate between the S1 allelic variants of the circulating VoCs (Figure 3). Since the time of infection was unknown in this cohort, probands were assigned to the VoC waves based on the date of recruitment.

Out of 106 SI identified using the CA (Figure 4, right panel), 47 (44.3%) exhibited the highest VoC-to-WT ratio for the Alpha variant, indicating an infection with this variant (Figure 5A). For WT, Delta and Omicron variants BA.1, BA.2 and BA.4/5, these proportions were lower (n=5 (4.7%), n=10 (9.4%), n=15 (14.2%), n=18 (17.0%), and n=11 (10.4%), respectively).

During the Alpha wave, 16 of 26 CA^+ subjects exhibited the highest VoC-to-WT antibody ratio for S1_Alpha (Figure 5B), suggesting that they were indeed in contact with the Alpha variant of SARS-CoV-2. It was unexpected to observe the highest VoC-to-WT antibody ratio for the BA.1 or BA.4/5 S1 domains in eight children recruited during the Alpha wave, despite the fact that these VoCs were not circulating at that time. The majority of these samples, however, had S1_BA.4/5 antibody levels just above the cut-off and displayed no reactivity to the other tested SARS-CoV-2 S1 antigens (data not shown). This may have caused a distortion of the VoC-to-WT ratios.

The majority of subjects recruited during the Delta wave (n=26) were most likely exposed to the Alpha variant (n=18), followed by the Delta variant (n=4), the WT strain (n=3), and the BA.1 variant (n=1) (Figure 5C). For subjects recruited during the Omicron waves, S1 antibody signatures pointed to infecting variants that again matched the currently or previously prevailing variants (Figures 5D–F).

The VoC-specific antibody profiling of children with SI often indicated the prevailing SARS-CoV-2 variants as the likely cause of infection. However, as expected, the correlation between antibody binding and recruitment into the study (COV^-) was less stringent than that between antibody binding and known time point of infection (COV^+).

3.7 Seroconversion to endemic HCoVs occurs in early childhood and was not affected by the SARS-CoV-2 pandemic

One of the objectives of this study was to assess whether the SARS-CoV-2 pandemic altered the seroconversion rate to endemic HCoVs in children and adolescents. To this end, antibodies against the S1 domains of the four endemic HCoVs, namely 229E, HKU1,

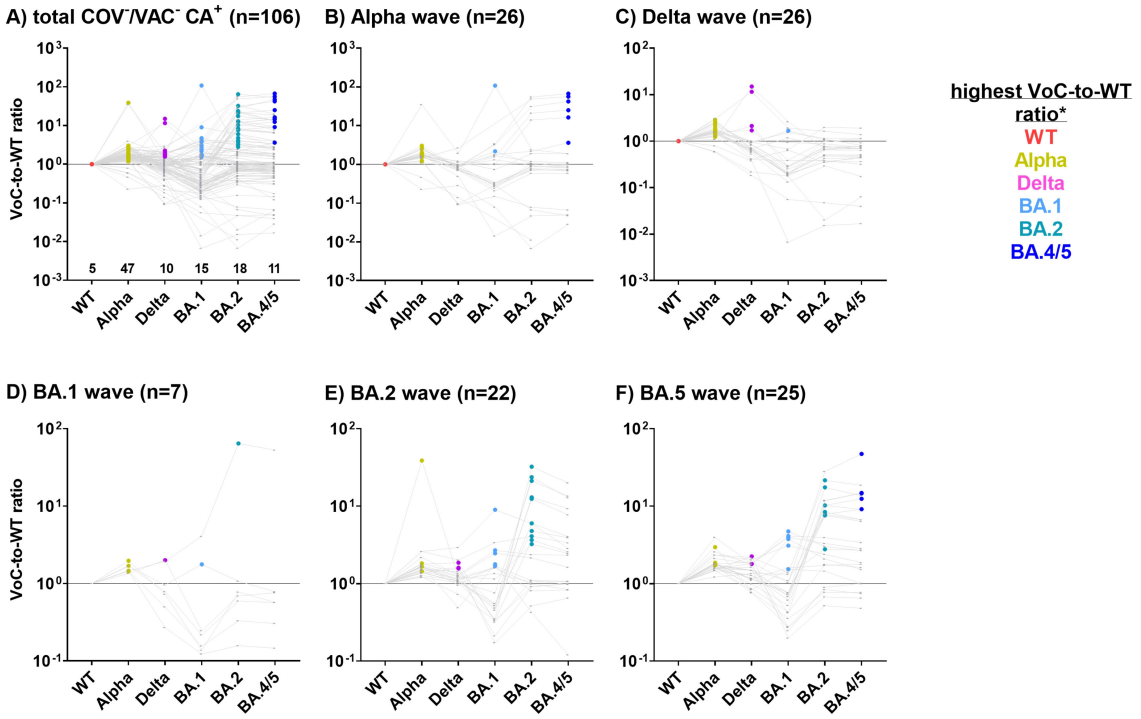

FIGURE 5
Children and adolescents silently infected with SARS-CoV-2 can be allocated to the most probable infecting variant using the Corona Array (CA). For 106 COV^-/VAC^- children and adolescents with SI (CA^+, **(A)** recruited during **(B)** Alpha, **(C)** Delta, **(D)** BA.1, **(E)** BA.2 or **(F)** BA.4/5 waves, ratios of MFI_{VoC} to MFI_{WT} (VoC-to-WT ratio) were calculated as a surrogate marker for the detection of the most probable infecting VoC. Samples with highest antibody levels against S1_WT and therefore with VoC-to-WT ratios below 1 were classified as infected with the WT virus. Samples were assumed to be infected with a variant when the VoC-to-WT ratio was highest.

NL63 and OC43, were measured in 1,309 children and adolescents. As a positive control, antibodies against the recall antigen tetanus toxoid were also measured (Figure 6). For all four HCoVs, seroconversion occurred during early childhood. Antibody levels increased sharply in the first years of life and plateaued at approximately eight years for 229E, four years for HCoV-HKU1 and NL63, and five years for OC43 (Figures 6A, C, E, G, respectively). The kinetics of anti-TT antibodies reflected the German vaccination recommendations, which include a baseline vaccination at two months of age and booster vaccinations at an age of 5 – 6 years (29). This resulted in a first antibody peak at 1 year of age and another steep increase around the age of six years (Figure 6I).

To ascertain the impact of the hygiene measures implemented during the SARS-CoV-2 pandemic on antibody titers to HCoVs in our cohort, we compared anti-HCoV-S1 antibody levels during a pre-pandemic period with an age-adjusted subsample of the COVIDKID cohort. Our findings revealed no significant differences throughout the pandemic waves in comparison to pre-pandemic levels (Figures 6B, D, F, H).

Finally, to investigate whether vaccination or infection with SARS-CoV-2 induces or enhances HCoV-cross-reactive antibodies, we also compared HCoV-S1-specific antibody levels in naive vs. SARS-CoV-2-exposed (VAC^+ and/or COV^+) children and adolescents, matched by age and time of study inclusion (median age 10 and 12 years, respectively). Neither VAC^+ nor COV^+ children exhibited higher HCoV-S1-specific antibody levels compared to the naïve children (COV^-/VAC^-; seronegative for SARS-CoV-2 S1) (Figure 7), suggesting that the SARS-CoV-2 serostatus had no influence on HCoV-S1-specific antibody titers in this age stratum.

In conclusion, seroconversion to endemic HCoVs occurs in early childhood and, in terms of S1-specific antibodies, was not affected by the SARS-CoV-2 pandemic.

4 Discussion

Seroconversion to circulating SARS-CoV-2 variants can provide valuable information for SARS-CoV-2 surveillance. In this study, we performed extensive anti-SARS-CoV-2 antibody profiling in more than 1,300 children and adolescents screened between December 2020 and March 2023, covering several SARS-CoV-2 waves. Both SARS-CoV-2 infection and vaccination induced high levels of specific antibodies against the S1 domains from SARS-CoV-2 WT and VoCs. The antibody profiles against the spike S1 domain from WT and VoCs were highly discriminatory and reflected the kinetics of VoC waves in the study region. Furthermore, our highly sensitive Luminex®-based approach discovered more SI than a conventional ELISA and, additionally, provided hints at the infecting VoC. Finally, vaccination or infection with SARS-CoV-2 did not induce HCoV S1-cross-reactive antibodies in children and adolescents.

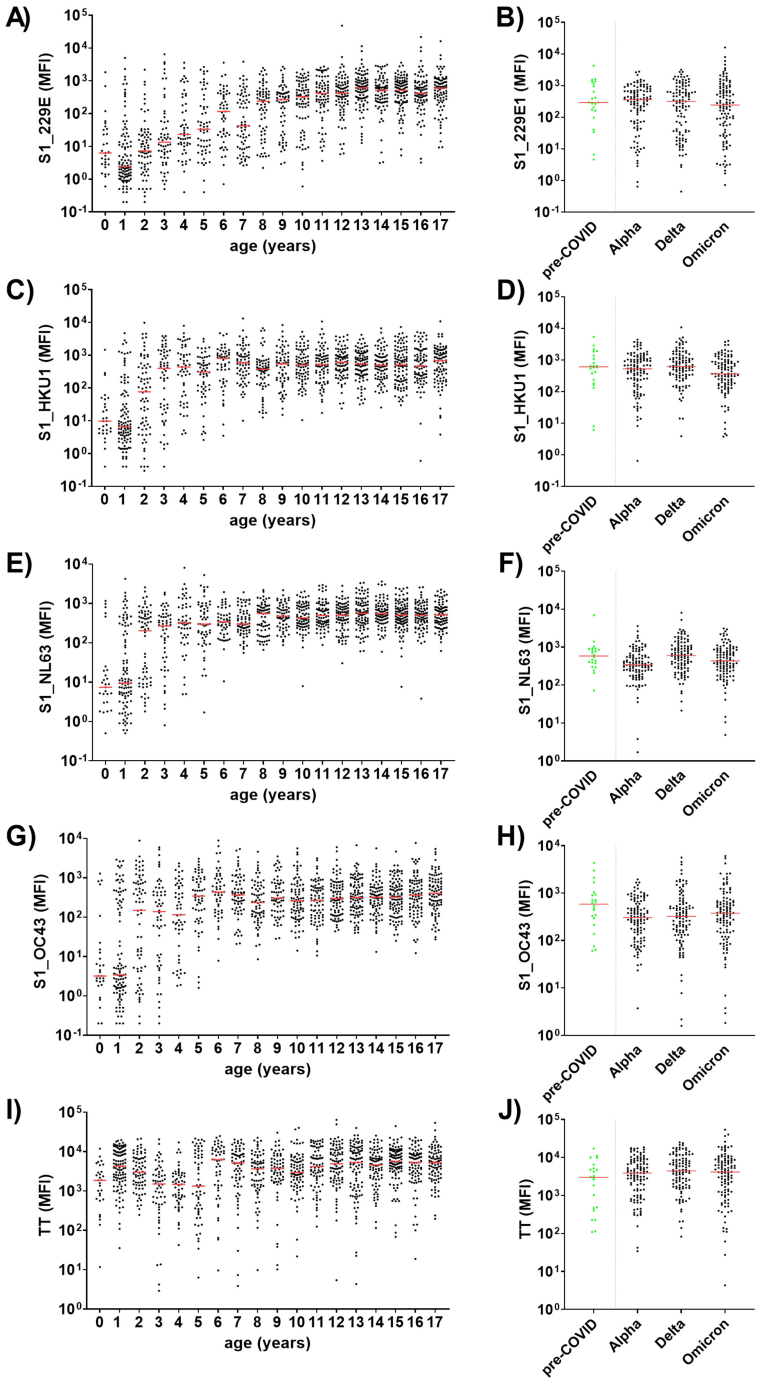

FIGURE 6
HCoV-specific antibody levels are age-dependent and are not affected by the SARS-CoV-2 pandemic. Age-dependent serum IgG levels were determined against the S1 domain of the four endemic HCoVs 229E **(A)**, HKU1 **(C)**, NL63 **(E)** and OC43 **(G)**, as well as tetanus toxoid (TT) as positive control **(I)** among 1,309 children and adolescents recruited during the SARS-CoV-2 pandemic. HCoV-specific antibody levels from pre-COVID (n=22; green) children and adolescents (median age 12 years) were compared to age-matched samples from three SARS-CoV-2 waves **(B, D, F, H)**. Matching was conducted regarding age and study site (all samples were from the University Medicine Greifswald, Germany): for each pre-COVID control five samples from one of three defined time frames (Alpha, Delta or Omicron) were matched (1:5 ratio). Significance between pre-COVID and Alpha, Delta or Omicron waves was tested with Kruskall-Wallis test with *post-hoc* Dunn´s correction. Median values are shown in red.

Our in-house, Luminex®-based CA exhibited a higher sensitivity and a broader detection range than commercial ELISA kits. The assay sensitivity for anti-S1 antibodies increased from 61% (ELISA) to 93% (CA), resulting in a reduction in false-negative cases of SARS-CoV-2 infections and, conversely, a 1.43-fold increase in correctly identified COV^+ cases. Similarly, other research groups have reported a sensitivity of 98% for a Luminex®-based SARS-CoV-2 6-plex for an adult cohort (30).

Moreover, the CA was more suitable for detecting SI in COV^- children and adolescents, with detection rates of 12.1% for CA as

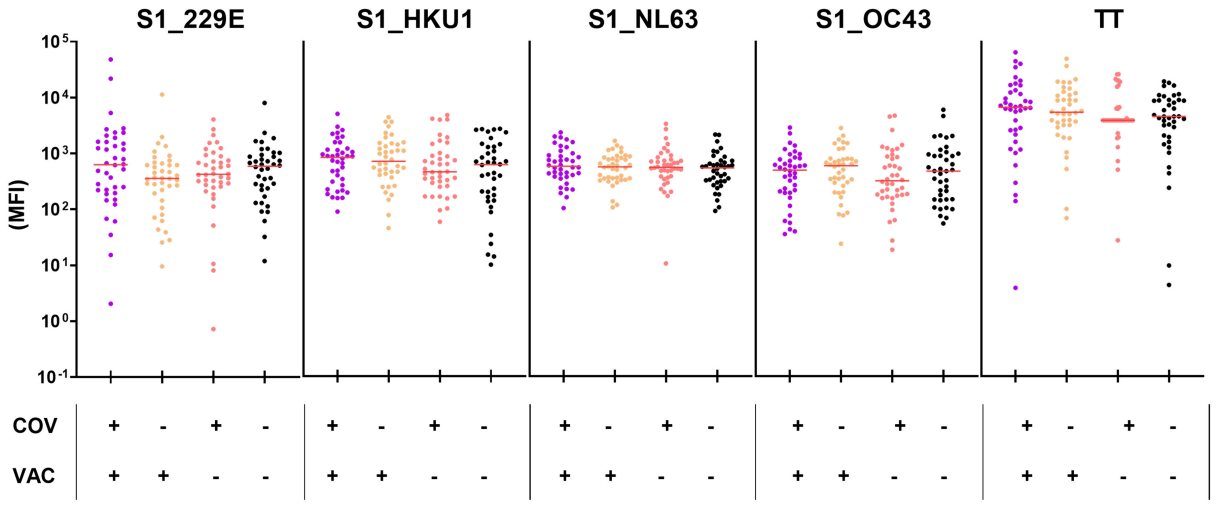

FIGURE 7
Neither SARS-CoV-2-infection nor vaccination elicits higher titers for HCoV-S1 domains in children and adolescents. Anti-HCoV-S1 antibody levels were compared in naïve (COV^-/VAC^-), COV^+ and/or VAC^+ children and adolescents (n=40 per group, matched by age and time of study inclusion in a 1:1 ratio). Antibodies against tetanus toxoid (TT) were included as control. The median is shown in red. Significance between all four groups was tested by Kruskall-Wallis test with *post-hoc* Dunn´s correction.

compared to 6.3% using the commercial ELISA. Two other studies conducted in Germany during the initial SARS-CoV-2 waves (2020 – 2021) reported lower rates of seroconversion. Specifically, 0.87% of the total cohort for the year 2020 (13) and 4.4% of children without SARS-CoV-2 infections in 2020 – 2021 were seropositive (12). As our study recruited subjects up until March 2023, it is reasonable to anticipate a higher seroprevalence. The ratio of seropositive cases (CA-based) to diagnosed and recalled infections was 1.43 (301 CA-positive cases/210 COV^+/VAC^-) in our study. The proportion of silent infection was considerably higher in earlier studies, with rates of 3.9 (12) and 6 (13), respectively. This highlights the significant advancement in the clinical diagnosis of COVID-19 during the pandemic.

Luminex®-based seroprevalence studies can serve as an invaluable component of SARS-CoV-2 surveillance. Despite the fact that SARS-CoV-2 has now entered the endemic phase (31), monitoring the humoral immunity to SARS-CoV-2 remains vital not only to gain insights into the impact of circulating VoCs, but also to monitor waning immunity, identify immune escape variants and inform vaccination programs. Given that vaccination against COVID-19 is no longer recommended for healthy children in Germany (32), it is likely that primary SARS-CoV-2 infections will occur at an early age. In this endemic scenario, monitoring the S1 seroprevalence will be the most informative marker for SARS-CoV-2 exposure in infants and children. The Luminex®-based approach can be utilized to monitor the kinetics of SARS-CoV-2 infection in infants and children, with the objective of determining whether they will converge with those of endemic HCoVs, which plateau at approximately five to six years of age (as discussed below). In addition to its implications for the current pandemic, our Luminex®-based approach offers an efficient and easily expandable tool for the surveillance of future outbreaks with other pathogens.

As both COVID-19 vaccination and SARS-CoV-2 infection induce S1-specific antibodies, we investigated whether seroconversion to NC could serve as a reliable marker for previous COVID-19 infection(s). However, anti-NC antibodies alone were not sufficient to reliably detect (silent) SARS-CoV-2 infections in children and adolescents. In contrast to the S1 antigen, the CA did not improve the sensitivity for the detection of anti-NC antibodies (ELISA: 49%; CA: 44%). Conversely, the assay specificity for both the CA and ELISA was 96%. Consequently, a positive NC test result can be taken as an indication of an (unnoticed) infection.

The low assay sensitivity can be attributed to the presence of low-level, cross-reactive anti-NC antibodies in children and adolescents who had not been exposed to SARS-CoV-2, exemplified by our pre-pandemic cohort (22, 23, 27, 33). This basal antibody binding required a much higher cut-off value (NC: 545.7; S1_WT: 50.4), which reduced sensitivity. Nevertheless, higher sensitivities might be achieved with different detection systems, such as the double-antigen sandwich assay format utilized in Elecsys® anti-SARS-CoV-2 immunoassays (sensitivity: 97.8%; specificity: 98.5%) (34). Another reason for the lower sensitivity of NC versus S1 antibody detection systems could be the relatively swift decay of NC- versus S-specific antibody levels (35). Moreover, the immune response of children to SARS-CoV-2 infection is predominantly directed towards the S protein, rather than the NC (14). Consequently, the absence of anti-NC antibodies is not suitable to exclude previous SARS-CoV-2 infection in children and adolescents.

The results of this study clearly demonstrated that the S1-specific antibody response can discriminate between different SARS-CoV-2 VoCs. To enhance the CA's discriminatory power, the analysis was focused on the more variable S1 domain, rather than using the full-length S protein. Indeed, several studies have demonstrated that the more conserved S2 domain contains numerous cross-reactive epitopes, not only with other SARS-CoV-2 VoCs, but also with the closely related HCoVs (23, 27, 36,

37). The presence of cross-reactive antibodies directed at the S2 domain would have blurred our results. In contrast, antibodies cross-reacting to the RBD/S1 domain have only rarely been reported (23, 33, 36, 37).

Our multiplex approach demonstrated that antibody binding patterns for the S1 domains of SARS-CoV-2 WT and VoCs are highly individual and allele-specific. In most cases, the strongest antibody response was detected against the most likely infecting VoC, e.g. the prevailing VoC at the time of diagnosis. This demonstrates that in terms of the spike S1/RBD domain, the antibody response is highly VoC-specific, as previously reported (16, 27, 33, 38, 39). However, in each SARS-CoV-2 wave we also observed subjects that showed a specific antibody response to other VoCs. This is not unexpected and actually reflects the pandemic situation in Northern Germany with several variants circulating in parallel (3; personal communication Meyer-Bahlburg). Consequently, the S1-specific antibody profiling can provide insights into the causative VoC.

To the best of our knowledge, allele-specific antibody profiles have not been investigated on a large scale until now. Some studies have conducted RBD-specific antibody profiling and performed correlation analyses for comparing antibody binding to WT versus Alpha, Beta and Delta variants. These studies demonstrated comparable IgG binding to RBD from both WT and Alpha variant, but reduced binding to RBD from the Beta variant in children and/or adults recruited in the first wave of the pandemic (16, 38). The Omicron variant exhibits an even more pronounced immune escape, as evidenced by the markedly reduced antibody binding to the Omicron Spike protein in vaccinated individuals (17, 18). Our study is distinctive in two ways: Firstly, the study spanned a considerable period of time (December 2020 – March 2023), allowing the subjects to be allocated to six distinct SARS-CoV-2 waves (WT, Alpha, Delta, and Omicron BA.1, BA.2 and BA.4/5). Secondly, the conversion of S1 domain-specific antibody responses into VoC-to-WT ratios enabled a comparison of antibody profiles against all VoCs on an individual level. This approach proved to be a robust tool for estimating exposure to SARS-CoV-2 on a variant-specific level.

Furthermore, S1 variant-specific serological signatures can also provide insights into the infecting VoC in silent SARS-CoV-2 infections. In our study cohort, 12.1% of children and adolescents experienced SI, as determined by an antibody response against the S1 domain from the WT virus or VoCs. We again employed the S1 variant-specific antibody signatures to determine the most likely infecting VoC in these children. Since the time of infection is unknown in this cohort, probands were assigned to the VoC waves based on the date of recruitment. Consequently, they might have been infected with the prevailing VoC or previously circulating variants, which is clearly reflected in our data. For instance, children and adolescents recruited during the Delta wave showed the highest antibody binding for S1 from the Alpha or Delta VoCs, but not from BA.2 and BA.4/5. The majority of detected SI presented with an antibody signature for the Alpha variant, which dominated in North-Eastern Germany between December 2020 and June 2021. Overall, S1-variant specific antibody signatures can provide valuable insights into the contact variant in children with SI. However, it should be noted that the reliability of our analysis is contingent upon the absence of a prior SARS-CoV-2 vaccination or infection, as both of these conditions induce high titers of SARS-CoV-2 S1-specific antibodies.

Endemic HCoVs are a common cause of acute respiratory infections, leading to a wide range of disease severity, especially during the winter months. A meta-analysis attributed 5.9% (range: 0.9 – 18.4%) of respiratory infections in children to HCoVs on a global scale (19). In order to gain further insight into the epidemiology of these viruses, we profiled the antibody binding to the S1 domain of endemic HCoVs. Our findings confirmed that seroconversion occurs in early childhood. The antibody levels against HCoV-S1 domains exhibited a marked increase with age, reaching a plateau at approximately four to eight years of age. This pattern aligns with the findings of other seroprevalence studies in Germany and France, which reported that many infants experienced HCoV infections in their first two years of life (16, 20).

Remarkably, seroconversion to endemic HCoVs was not affected by the SARS-CoV-2 pandemic, despite reduced contact rates and implemented hygiene measures. However, our pandemic and pre-pandemic cohorts consisted primarily of older participants (median age of 12 and 10 years, respectively). This limits the sensitivity for the discovery of changes caused by the pandemic, as anti-HCoV antibody levels had already plateaued at 4-8 years of age. Indeed, Sikkema et al. observed a reduction in S1 seroprevalence during the SARS-CoV-2 pandemic only in very young Dutch children (aged <1 year, for all four HCoVs), and only for NL63 also in older age groups (up to 18 years) (40).

Finally, we investigated whether vaccination or infection with SARS-CoV-2 induces HCoV-cross-reactive antibodies, focusing our analysis on the highly variable spike S1 domain. Our data demonstrated that there was no increase in antibodies specific to the S1 domain of HCoVs following SARS-CoV-2 infection or vaccination. Other research groups employed the full-length spike protein or the S2 domain, and reported elevated HCoV antibodies (particularly against OC43 and HKU1) post-infection and -vaccination (36, 41, 42). Consequently, infection and vaccination elicit cross-reactive antibodies, although these antibodies predominantly recognize epitopes on the more conserved S2 domain.

A limitation of our study is the use of a single dilution for plasma samples for the CA. Indeed, serum/plasma titrations are in general a more accurate approach to obtain quantitative information on antibody reactivity (27, 43). For incorporation into the clinical routine, however, diagnostic tests should ideally provide information from a single serum/plasma dilution, thus enabling sufficient throughput. This is the reason why a significant number of published studies using Luminex-based assays employ a single dilution, ranging from 1:100 to 1:2000 (44–47). In our study, a 1:10,000 plasma dilution was identified as the optimal dilution for our semi-quantitative readout, enabling accurate detection by avoiding saturation effects at high antibody levels, while ensuring the proper detection of low antibody levels in the majority of cases. Given the relatively large sample size of 1,309 subjects in this study, this approach enabled the conservation of reagents and time, while maintaining data quality. The larger dynamic range of the CA compared to the ELISA approach proved advantageous in this context.

In conclusion, our highly sensitive Luminex®-based Corona Array represents a valuable tool for monitoring the S1-specific antibody response against SARS-CoV-2 WT and VoCs as well as HCoVs in children and adolescents, and has the potential to serve as a surveillance tool. By focusing on the variable S1 domain, we were able to identify the most likely SARS-CoV-2 contact variant in children with diagnosed and silent infections. This has opened up new possibilities for addressing underreporting during pandemics.

Data availability statement

The raw data supporting the conclusions of this article will be made available by the authors, without undue reservation.

Ethics statement

The study was approved by the Ethics Committee of the University Medicine Greifswald. The study was conducted in accordance with the local legislation and institutional requirements. Written informed consent for participation in this study was provided by the participants' legal guardians/next of kin.

Author contributions

DK: Conceptualization, Data curation, Formal Analysis, Investigation, Methodology, Project administration, Supervision, Validation, Visualization, Writing – original draft, Writing – review & editing. DR: Conceptualization, Data curation, Investigation, Methodology, Project administration, Supervision, Validation, Writing – original draft, Writing – review & editing. SH: Conceptualization, Project administration, Supervision, Visualization, Writing – original draft, Writing – review & editing. JG: Data curation, Investigation, Methodology, Writing – review & editing. NW: Data curation, Formal Analysis, Investigation, Methodology, Writing – review & editing. BB: Conceptualization, Funding acquisition, Project administration, Supervision, Writing – review & editing. AM: Conceptualization, Funding acquisition, Project administration, Supervision, Writing – review & editing.

Funding

The author(s) declare that financial support was received for the research, authorship, and/or publication of this article. This study was funded by the University Medicine Greifswald and by the Ministry of Social Affairs, Health and Sport, State of Mecklenburg-Western Pomerania, Germany (406-00000-2020/002-018). This work was funded by grants to BMB from the Federal State of Mecklenburg-Western Pomerania ("COVIDPROTECT", grant no. GW-20-0004) and to SH from the Research Network Molecular Medicine (FVMM) of the University Medicine Greifswald (grant no. FOVB-2021-01). DR was supported by the MV-Schutzfonds of the Federal State of Mecklenburg-Western Pomerania ("PoCoReCONNECT", grant no. LAGuS-MV-6-SF915-0002-23).

Acknowledgments

We thank all study participants and their families for participating in the COVIDKID study. We thank the teams of physicians and nurses in all participating clinics for their support in sample acquisition. We also thank the Friedrich Loeffler-Institute for Medical Microbiology (Head: Prof. Dr. Karsten Becker, Dr. Kathrin Lehmann, Kathrin Hollmann, Maria Schuparis) for sample analysis, and the Institute of Clinical Chemistry and Laboratory Medicine (especially Dr. Theresa Winter) as well as IMD Greifswald for sample transport. We would also like to thank Stefan Weiss for assistance in data processing.

Conflict of interest

The authors declare that the research was conducted in the absence of any commercial or financial relationships that could be construed as a potential conflict of interest.

Publisher's note

Supplementary material

The Supplementary Material for this article can be found online at: https://www.frontiersin.org/articles/10.3389/fimmu.2024.1434291/full#supplementary-material

References

1. Johns Hopkins University & Medicine. COVID-19 Dashboard by the Center for Systems Science and Engineering (CSSE) at Johns Hopkins University (JHU): (data collected from 1/22/20 to 3/10/23). Available at: https://coronavirus.jhu.edu/map.html. [cited 2024 May 13].

2. Kohler C, King J, Stacker L, Goller KV, Moritz J, Pohlmann A, et al. Neighbourhood watch: genomic epidemiology of SARS-CoV-2 variants circulating in a German federal state, Mecklenburg-Western Pomerania, in 2020–2022. *Emerg Microbes Infect.* (2023) 12. doi: 10.1080/22221751.2023.2245916

3. Viner RM, Mytton OT, Bonell C, Melendez-Torres GJ, Ward J, Hudson L, et al. Susceptibility to SARS-CoV-2 infection among children and adolescents compared with adults: A systematic review and meta-analysis. *JAMA Pediatr*. (2021) 175:143–56. doi: 10.1001/jamapediatrics.2020.4573

4. Xu W, Li X, Dozier M, He Y, Kirolos A, Lang Z, et al. What is the evidence for transmission of COVID-19 by children in schools? A living systematic review. *J Glob Health*. (2020) 10:21104. doi: 10.7189/jogh.10.021104

5. Vono M, Huttner A, Lemeille S, Martinez-Murillo P, Meyer B, Baggio S, et al. Robust innate responses to SARS-CoV-2 in children resolve faster than in adults without compromising adaptive immunity. *Cell Rep*. (2021) 37:109773. doi: 10.1016/j.celrep.2021.109773

6. Yoshida M, Worlock KB, Huang N, Lindeboom RG, Butler CR, Kumasaka N, et al. Local and systemic responses to SARS-CoV-2 infection in children and adults. *Nature*. (2022) 602:321–7. doi: 10.1038/s41586-021-04345-x

7. Vardavas CI, Nikitara K, Aslanoglou K, Kamekis A, Puttige Ramesh N, Symvoulakis E, et al. Systematic review of outbreaks of COVID-19 within households in the European region when the child is the index case. *BMJ Paediatr Open*. (2023) 7(1):e001718. doi: 10.1136/bmjpo-2022-001718

8. Mangel M. Operational analysis for COVID-19 testing: Determining the risk from asymptomatic infections. *PLoS One*. (2023) 18:e0281710. doi: 10.1371/journal.pone.0281710

9. Frutos AM, Kuan G, Lopez R, Ojeda S, Shotwell A, Sanchez N, et al. Infection-induced immunity is associated with protection against severe acute respiratory syndrome coronavirus 2 infection and decreased infectivity. *Clin Infect Dis*. (2023) 76:2126–33. doi: 10.1093/cid/ciad074

10. Bundesministerium für Gesundheit. Coronavirus-Pandemie: Was geschah wann? . Available online at: https://www.bundesgesundheitsministerium.de/coronavirus/chronik-coronavirus.html (Accessed November 23, 2023).

11. Bundesministerium für Gesundheit. *Verordnung zur Änderung der Medizinprodukte-Abgabeverordnung im Rahmen der epidemischen Lage von nationaler Tragweite*. Germany: Bundesministerium der Justiz und für Verbraucherschutz (2020).

12. Sorg A-L, Bergfeld L, Jank M, Corman V, Semmler I, Goertz A, et al. Cross-sectional seroprevalence surveys of SARS-CoV-2 antibodies in children in Germany, June 2020 to May 2021. *Nat Commun*. (2022) 13:3128. doi: 10.1038/s41467-022-30482-6

13. Hippich M, Holthaus L, Assfalg R, Zapardiel-Gonzalo J, Kapfelsperger H, Heigermoser M, et al. A public health antibody screening indicates a 6-fold higher SARS-CoV-2 exposure rate than reported cases in children. *Med*. (2021) 2:149–63.e4. doi: 10.1016/j.medj.2020.10.003

14. Weisberg SP, Connors TJ, Zhu Y, Baldwin MR, Lin W-H, Wontakal S, et al. Distinct antibody responses to SARS-CoV-2 in children and adults across the COVID-19 clinical spectrum. *Nat Immunol*. (2021) 22:25–31. doi: 10.1038/s41590-020-00826-9

15. Huang Y, Yang C, Xu X-F, Xu W, Liu S-W. Structural and functional properties of SARS-CoV-2 spike protein: Potential antivirus drug development for COVID-19. *Acta Pharmacol Sin*. (2020) 41:1141–9. doi: 10.1038/s41401-020-0485-4

16. Renk H, Dulovic A, Seidel A, Becker M, Fabricius D, Zernickel M, et al. Robust and durable serological response following pediatric SARS-CoV-2 infection. *Nat Commun*. (2022) 13:128. doi: 10.1038/s41467-021-27595-9

17. Planas D, Saunders N, Maes P, Guivel-Benhassine F, Planchais C, Buchrieser J, et al. Considerable escape of SARS-CoV-2 Omicron to antibody neutralization. *Nature*. (2022) 602:671–5. doi: 10.1038/s41586-021-04389-z

18. Gruell H, Vanshylla K, Tober-Lau P, Hillus D, Schommers P, Lehmann C, et al. mRNA booster immunization elicits potent neutralizing serum activity against the SARS-CoV-2 Omicron variant. *Nat Med*. (2022) 28:477–80. doi: 10.1038/s41591-021-01676-0

19. Park S, Lee Y, Michelow IC, Choe YJ. Global seasonality of human coronaviruses: A systematic review. *Open Forum Infect Dis*. (2020) 7:ofaa443. doi: 10.1093/ofid/ofaa443

20. Woudenberg T, Pelleau S, Anna F, Attia M, Donnadieu F, Gravet A, et al. Humoral immunity to SARS-CoV-2 and seasonal coronaviruses in children and adults in north-eastern France. *EBioMedicine*. (2021) 70:103495. doi: 10.1016/j.ebiom.2021.103495

21. Edridge AW, Kaczorowska J, Hoste AC, Bakker M, Klein M, Loens K, et al. Seasonal coronavirus protective immunity is short-lasting. *Nat Med*. (2020) 26:1691–3. doi: 10.1038/s41591-020-1083-1

22. Ng KW, Faulkner N, Cornish GH, Rosa A, Harvey R, Hussain S, et al. Preexisting and *de novo* humoral immunity to SARS-CoV-2 in humans. *Science*. (2020) 370:1339–43. doi: 10.1126/science.abe1107

23. Anderson EM, Goodwin EC, Verma A, Arevalo CP, Bolton MJ, Weirick ME, et al. Seasonal human coronavirus antibodies are boosted upon SARS-CoV-2 infection but not associated with protection. *Cell*. (2021) 184:1858–64.e10. doi: 10.1016/j.cell.2021.02.010

24. Becker K, Hübner N-O. Available online at: https://www.comv-gen.de/. (Accessed January 17, 2024).

25. Angeloni S, Das S, Dunbar S, Stone V, Swift S. xMAP cookbook. In: *A Collection of Methods and Protocolls for Developing Multiplex Assays with xMAP Technology*. US: Luminex Corporation (2018).

26. Lucchese G, Vogelgesang A, Boesl F, Raafat D, Holtfreter S, Bröker BM, et al. Anti-neuronal antibodies against brainstem antigens are associated with COVID-19. *EBioMedicine*. (2022) 83:104211. doi: 10.1016/j.ebiom.2022.104211

27. Wietschel KA, Fechtner K, Antileo E, Abdurrahman G, Drechsler CA, Makuvise MK, et al. Non-cross-reactive epitopes dominate the humoral immune response to COVID-19 vaccination – kinetics of plasma antibodies, plasmablasts and memory B cells. *Front Immunol*. (2024) 15:1382911. doi: 10.3389/fimmu.2024.1382911

28. Wickham H, Averick M, Bryan J, Chang W, McGowan L, François R, et al. Welcome to the tidyverse. *JOSS*. (2019) 4:1686. doi: 10.21105/joss.01686

29. Robert Koch-Institut. Impfkalender (Standardimpfungen) für Säuglinge, Kinder, Jugendliche und Erwachsene; 2023 (2023). Available online at: https://www.rki.de/DE/Content/Kommissionen/STIKO/Empfehlungen/Aktuelles/Impfkalender.pdf?:blob=publicationFile (Accessed January 23, 2024).

30. Fisher M, Levy H, Fatelevich E, Afrimov Y, Ben-Shmuel A, Rosenfeld R, et al. A serological snapshot of COVID-19 initial stages in Israel by a 6-plex antigen array. *Microbiol Spectr*. (2021) 9:e0087021. doi: 10.1002/bimj.200410135

31. Agrawal K, Broad A. Can we predict the future? Modelling SARS-CoV-2 epidemic to endemic transition. *J Stud Res*. (2022) 11. doi: 10.47611/jsrhs.v11i3.2898

32. Ständige Impfkommission. Implementierung der COVID-19- Impfung in die allgemeinen Empfehlungen der STIKO 2023 (Aktualisierung Epid Bull 4/2023). *Epidemiologisches Bull*. (2023) 21:3–6.

33. Brewer RC, Ramadoss NS, Lahey LJ, Jahanbani S, Robinson WH, Lanz TV. BNT162b2 vaccine induces divergent B cell responses to SARS-CoV-2 S1 and S2. *Nat Immunol*. (2021) 23:33–9. doi: 10.1038/s41590-021-01088-9

34. Inés RM, Gabriela HT, Paula CM, Magdalena TM, Jimena A, Salome KB, et al. Performance of elecsys anti-SARS CoV-2 (Roche) and VIDAS anti-SARS CoV-2 (Biomérieux) for SARS-CoV-2 nucleocapsid and spike protein antibody detection. *EJIFCC*. (2022) 33:159–65.

35. Joshi D, Nyhoff LE, Zarnitsyna VI, Moreno A, Manning K, Linderman S, et al. Infants and young children generate more durable antibody responses to SARS-CoV-2 infection than adults. *iScience*. (2023) 26:107967. doi: 10.1002/cpim.116

36. Anderson EM, Li SH, Awofolaju M, Eilola T, Goodwin E, Bolton MJ, et al. SARS-CoV-2 infections elicit higher levels of original antigenic sin antibodies compared with SARS-CoV-2 mRNA vaccinations. *Cell Rep*. (2022) 41:111496. doi: 10.1016/j.celrep.2022.111496

37. Song G, He W-T, Callaghan S, Anzanello F, Huang D, Ricketts J, et al. Cross-reactive serum and memory B-cell responses to spike protein in SARS-CoV-2 and endemic coronavirus infection. *Nat Commun*. (2021) 12:2938. doi: 10.1038/s41467-021-23074-3

38. Becker M, Dulovic A, Junker D, Ruetalo N, Kaiser PD, Pinilla YT, et al. Immune response to SARS-CoV-2 variants of concern in vaccinated individuals. *Nat Commun*. (2021) 12:3109. doi: 10.1038/s41467-021-23473-6

39. La Prados de Torre E, Obando I, Vidal M, de Felipe B, Aguilar R, Izquierdo L, et al. SARS-CoV-2 seroprevalence study in pediatric patients and health care workers using multiplex antibody immunoassays. *Viruses*. (2022) 14(9):2039. doi: 10.3390/v14092039

40. Sikkema RS, Bruin Ed, Ramakers C, Bentvelsen R, Li W, Bosch B-J, et al. Reduced seasonal coronavirus antibody responses in children following COVID-19 mitigation measures, the Netherlands. *Viruses*. (2023) 15:212. doi: 10.3390/v15010212

41. Dowell AC, Butler MS, Jinks E, Tut G, Lancaster T, Sylla P, et al. Children develop robust and sustained cross-reactive spike-specific immune responses to SARS-CoV-2 infection. *Nat Immunol*. (2022) 23:40–9. doi: 10.1038/s41590-021-01089-8

42. Tamminen K, Salminen M, Blazevic V. Seroprevalence and SARS-CoV-2 cross-reactivity of endemic coronavirus OC43 and 229E antibodies in Finnish children and adults. *Clin Immunol*. (2021) 229:108782. doi: 10.1016/j.clim.2021.108782

43. Meyer TC, Schmidt F, Steinke J, Bröker BM, Völker U, Michalik S. Technical report: xMAPr - High-dynamic-range (HDR) quantification of antigen-specific antibody binding. *J Proteomics*. (2020) 212:103577. doi: 10.1016/j.jprot.2019.103577

44. Cameron A, Porterfield CA, Byron LD, Wang J, Pearson Z, Bohrhunter JL, et al. A multiplex microsphere IgG assay for SARS-CoV-2 using ACE2-mediated inhibition as a surrogate for neutralization. *J Clin Microbiol*. (2021) 59(2):e02489-20. doi: 10.1128/JCM.02489-20

45. Becker M, Strengert M, Junker D, Kaiser PD, Kerrinnes T, Traenkle B, et al. Exploring beyond clinical routine SARS-CoV-2 serology using MultiCoV-Ab to evaluate endemic coronavirus cross-reactivity. *Nat Commun*. (2021) 12:1152. doi: 10.1038/s41467-021-20973-3

46. Ayouba A, Thaurignac G, Morquin D, Tuaillon E, Raulino R, Nkuba A, et al. Multiplex detection and dynamics of IgG antibodies to SARS-CoV2 and the highly pathogenic human coronaviruses SARS-CoV and MERS-CoV. *J Clin Virol*. (2020) 129:104521. doi: 10.1016/j.jcv.2020.104521

47. Abela IA, Pasin C, Schwarzmüller M, Epp S, Sickmann ME, Schanz MM, et al. Multifactorial seroprofiling dissects the contribution of pre-existing human coronaviruses responses to SARS-CoV-2 immunity. *Nat Commun*. (2021) 12:6703. doi: 10.1038/s41467-021-27040-x

frontiers | Frontiers in Immunology

TYPE Case Report
PUBLISHED 29 August 2024
DOI 10.3389/fimmu.2024.1404542

OPEN ACCESS

EDITED BY
Pedro A Reche,
Complutense University of Madrid, Spain

REVIEWED BY
Ann Auma,
Case Western Reserve University,
United States
Neeta Gade,
All India Institute of Medical Sciences Nagpur,
India

*CORRESPONDENCE
Zhao-shou Yang
yangzhsh3@gdpu.edu.cn

†These authors have contributed equally to this work

RECEIVED 21 March 2024
ACCEPTED 12 August 2024
PUBLISHED 29 August 2024

CITATION
Zhong Q, Lin Q-m, Long H-b, Liao C-x, Sun X-x, Yang M-d, Zhang Z-h, Huang Y-h, Wang S-m and Yang Z-s (2024) Bacterial pneumonia patients with elevated globulin levels did not get infected with SARS-CoV-2: two case reports.
Front. Immunol. 15:1404542.
doi: 10.3389/fimmu.2024.1404542

Bacterial pneumonia patients with elevated globulin levels did not get infected with SARS-CoV-2: two case reports

Qi Zhong[1†], Qiu-mei Lin[1†], Hong-bin Long[1†], Cai-xia Liao[1], Xiao-xiao Sun[1], Miao-du Yang[1], Zhi-hao Zhang[1], Yi-hua Huang[1], Shi-min Wang[2] and Zhao-shou Yang[1*]

[1]The First Affiliated Hospital/The First School of Clinical Medicine of Guangdong Pharmaceutical University, Guangdong Pharmaceutical University, Guangzhou, Guangdong, China, [2]Zhongshan School of Medicine, Sun Yat-Sen University, Guangzhou, China

Background: COVID-19 began in December 2019, rapidly spreading worldwide. China implemented a dynamic zero-COVID strategy and strict control measures after the outbreak. However, Guangzhou city ended closed-off management by the end of November 2022, leading to exposure to SARS-CoV-2. Despite most hospitalized patients being infected or co-infected with SARS-CoV-2, some remained uninfected. We report two cases of bacterial pneumonia with elevated globulin levels not infected with SARS-CoV-2, aiming to identify protection factors of SARS-CoV-2 infection and provide a scientific basis for SARS-CoV-2 prevention.

Case presentation: Case 1, a 92-year-old male, admitted on October 21, 2022, developed worsening cough and sputum after aspiration, diagnosed with bacterial pneumonia with Pseudomonas aeruginosa, Escherichia coli (CRE) and carbapenem-resistant Acinetobacter baumannii (CRAB) infections. He was treated with imipenem anti-infective therapy and mechanical ventilation, then switched to a combination of meropenem, voriconazole and amikacin anti-infective therapy due to recurrent infections and septic shock, and died of sepsis on 8 January 2023. Case 2 is an 82-year-old male admitted on 30 September 2022, with recurrent cough, sputum, and shortness of breath, diagnosed with bacterial pneumonia with carbapenem-resistant Klebsiella pneumoniae (CRKP) and Mycobacterium pneumoniae infections. He was treated with ventilator-

Abbreviations: ALB, Albumin; ALT, Alanine aminotransferase; APTT, Activated Partial Thromboplastin Time; AST, Aspartate aminotransferase; BCG: Bacillus Calmette-Guerin; BUN, Blood Urea Nitrogen; COVID-19, Coronavirus Disease 2019; CRAB, Carbapenem-Resistant Acinetobacter Baumannii; CRE, Carbapenem-Resistant Enterobacteriaceae; CREA, Creatinine; CRKP, Carbapenem-Resistant Klebsiella Pneumoniae; CRP, C-reactive Protein; CRRT, Continuous Renal Replacement Therapy; CXR, Chest X-Ray; EGG, Electroencephalogram; ELISA, Enzyme Linked Immunosorbent Assay; FIB, Fibronectin; GLB, Globulin; Hb, Hemoglobin; ICU, Intensive Care Unit; IL-6, Interleukin 6; IVIG, Intravenous Immunoglobulin; PCR, Polymerase Chain Reaction; PCT, Procalcitonin; PT/INR, Prothrombin Time/International Normalized Ratio; PT, Prothrombin Time; PT-A, Prothrombin Activity; RBC, Red Blood Cell; RBD, Receptor-Binding Domain; RT-qPCR, Quantitative Reverse Transcription PCR; SAA, Serum Amyloid A; SARS-CoV-2, Severe Acute Respiratory Syndrome Coronavirus 2; TP, Total Protein; TT, Thrombin Time; WBC, White Blood Cell.

assisted ventilation, meropenem, amikacin, tigecycline and mucomycin nebulization and discharged with improvement on 26 October. He was readmitted on 21 November 2022 and diagnosed with bacterial pneumonia. He was treated with cefoperazone sulbactam, amikacin, meropenem and fluconazole and discharged on 31 December. Neither patient was infected with SARS-CoV-2 during hospitalization. Notably, their globulin levels were elevated before SARS-CoV-2 exposure, gradually decreasing afterward.

Conclusions: Patients with bacterial pneumonia with high globulin levels likely have large amounts of immunoglobulin, and that immunoglobulin cross-reactivity causes this protein to be involved in clearing SARS-CoV-2 and preventing infection. Therefore, bacterial pneumonia patients with high globulin levels included in this study were not infected with SARS-CoV-2. After exposure to SARS-CoV-2, the amount of globulin in the patient's body was reduced because it was used to clear SARS-CoV-2. The results of this study are expected to provide a theoretical basis for the study of the mechanism of prevention and treatment of SARS-CoV-2 infection.

KEYWORDS

bacterial pneumonia, globulin protein, SARS-CoV-2, cross-reactivity, case reports

1 Introduction

COVID-19, caused by SARS-CoV-2, first emerged in Wuhan, China, in late 2019 and then rapidly spread worldwide to become a pandemic (1, 2). China adopted a dynamic zero-COVID strategy to prevent and control the outbreak by the end of November 2022 (3). Subsequently, China optimized its control measures, including implementing '20 measures' (4) and lifting closed-off management measures (5). Guangzhou ended closed-off management on 30 November 2022 (6). This led to hospitalized patients beginning to be exposed to an environment filled with SARS-CoV-2, ultimately leading to an outbreak of SARS-CoV-2 infections in December 2022 in Guangzhou (7, 8). However, the results of our previous study found that some of the patients with bacterial pneumonia in December 2022 were not infected with SARS-CoV-2 during their hospitalization (7).

Bacterial pneumonia is a lung disease caused by bacterial infection, and common pathogens include Streptococcus pneumoniae, Staphylococcus aureus, Pseudomonas aeruginosa, Klebsiella pneumoniae, and Haemophilus influenzae (9, 10). Typical clinical symptoms include fever, chills, cough (may cough up purulent sputum), chest pain, and shortness of breath and dyspnoea. Diagnosis can be made by physical examination, medical history, chest X-ray (CXR) and laboratory tests (sputum culture and blood tests). Treatment is initially based on empirical antibiotics, with subsequent adjustments to the regimen based on sputum culture and drug susceptibility testing, supplemented by supportive therapy such as adequate hydration, oxygenation, and physical expectoration. While the prognosis for most patients is good, if the prognosis is poor, sepsis and infectious shock may develop. Currently, though many studies focused on co-infection with bacteria in patients with COVID-19 (11, 12), there are relatively few studies and reports on the susceptibility of patients with bacterial pneumonia to SARS-CoV-2.

This study describes two hospitalized patients with bacterial pneumonia who were not infected with SARS-CoV-2. Their globulin levels were above the upper limit of the reference value, but gradually decreased and remained above the lower limit of the reference value after lifting closed-off management. This study is expected to identify protection factors of SARS-CoV-2 infection and provide a scientific basis for its prevention and treatment.

2 Case presentation

2.1 Case 1 presentation

On 21 October 2022, a 92-year-old male was admitted to our Rehabilitation Unit with progressive memory loss, diagnosed with Alzheimer's disease and treated with olanzapine, electroencephalogram (EGG) biofeedback, and cognitive training. He was transferred to ICU on 17 November 2022, with worsening cough and sputum and shortness of breath due to aspiration of bloody fluid from the nasal passage. He had a history of left-sided nosebleed, malignant melanoma with multiple metastases in the left nasal cavity for over 2 years, hypertension, diabetes mellitus, and history of transfusion of AB Rh+ red blood cell suspension without transfusion reaction. He denied history of infectious diseases such as hepatitis and tuberculosis, drug

and food allergies. He denied any close contact with history of SARS-CoV-2 infection.

He was diagnosed with bacterial pneumonia with the presence of Pseudomonas aeruginosa, Escherichia coli (CRE), and carbapenem-resistant Acinetobacter baumannii (CRAB) infections. His physical examination revealed coarse breath sounds in both lungs, accompanied by a significant amount of dry and moist rales. Some of the clinical laboratory findings are shown in Figure 1. The examination results suggested leukocytosis, neutrophilia, elevated infection markers, sputum smear suggestive of gram-negative bacilli, and sputum culture suggestive of Pseudomonas aeruginosa, *Escherichia coli* (CRE), and CRAB. The patient's CXR showed thickening and blurring of the texture of both lungs, and scattered few patches of patchy, reticulated, or flocculent slightly dense blurred shadows were seen in both lungs. Sputum smear and CXR supported the diagnosis of pneumonia. The ORF1ab Gene and N Gene assays for the 2019-nCoV-RNA were performed using RT-qPCR, and he was tested negative for the SARS-CoV-2 during hospitalization.

He was treated with piperacillin sodium sulbactam sodium for anti-infection, ambroxol for sputum, and intensive bedside suctioning. Later, considering the recurrent infection, he was switched to imipenem anti-infective treatment, mechanical ventilation, and continuous renal replacement therapy (CRRT) if necessary. On 19 December, due to the patient's recurrent infection and septic shock, the anti-infective treatment regimen was adjusted, and he was given a combination of meropenem, voriconazole, and amikacin for anti-infective treatment. Unfortunately, the patient died of sepsis on 8 January 2023.

It is worth noting that the patient was not infected with SARS-CoV-2 during hospitalization. When he was admitted to the hospital, his peripheral blood globulin level was significantly elevated, exceeding the upper limit of the reference range. During hospitalization, although his globulin levels occasionally fell below the upper limit, they remained high. On November 30, 2022, the day of the lifting of closed-off management, his peripheral blood globulin level was still above the upper limit of the reference range. Following that, the level gradually decreased but remained above the lower limit of the reference range.

2.2 Case 2 presentation

On 30 September 2022, an 82-year-old male was admitted to our respiratory department with recurrent cough, sputum, and shortness of breath. Over a year ago, he coughed up sputum for no apparent cause and was diagnosed with a lung infection, which was ultimately diagnosed as severe pneumonia and treated at several hospitals. He had a history of cerebral infarction for more than 6 years, with inability to cough up sputum autonomously; history of various chronic diseases and hypertension. He denied the history of tuberculosis, surgery, trauma, blood transfusion, and allergy. He denied any close contact with history of SARS-CoV-2 infection. His personal and family history, medication history and social history were normal.

He was diagnosed with bacterial pneumonia with carbapenem-resistant Klebsiella pneumoniae (CRKP) and Mycobacterium pneumoniae infections. His physical examination showed hyperresonance on percussion in bilateral lungs, increased breath sounds, audible moist rales, and no dry rales. Some of the clinical laboratory findings are shown in Figure 2. The examination results suggested leukocytosis, neutrophilia and elevated infection markers, and sputum culture and alveolar lavage fluid genetic testing showed CRKP (sensitive to ceftazidime avibactam, mediated to colistin), Mycobacterium tuberculosis complex group 747 sequences, and Mycobacterium abscessus 1035 sequences. He was treated with ventilator-assisted ventilation, sputum reduction, bronchoscopic aspiration and was also given meropenem, amikacin, tigecycline and mucomycin nebulization to fight infection. During treatment, there was impairment of liver function, which might be a side effect of tigecycline drug therapy. He was discharged on 26 October 2022.

He was readmitted to the hospital on 21 November 2022, due to cough, sputum, and decreased blood oxygen saturation. His diagnosis was bacterial pneumonia with CRKP, CRAB and Mycobacterium tuberculosis infection. Some of laboratory findings are also shown in the Figure 2. Sputum culture and genetic testing of alveolar lavage showed CRKP, CRAB (mediated to colistin), and Mycobacterium pneumoniae. CXR showed thickened, increased, and blurred texture in both lungs, localized grid-like changes, with multiple scattered speckled and flocculent slightly hyperdense blurred shadows in bilateral lungs, predominantly in the left lung. The ORF1ab Gene and N Gene assays for the 2019-nCoV-RNA were performed using RT-qPCR, and he was tested negative for the SARS-CoV-2 during hospitalization. He was treated with cefoperazone sulbactam, amikacin, meropenem and fluconazole and was discharged on 31 December 2022.

During hospitalization, the patient was also not infected with SARS-CoV-2. Interestingly, during hospitalization, the patient's globulin level was above the upper reference limit before 30 November 2022, and then the globulin level gradually decreased but was still above the lower limit of the reference value. A follow-up phone call after discharge from the hospital revealed that he remained uninfected with SARS-CoV-2.

3 Discussion

We report two hospitalized cases of bacterial pneumonia with high globulin levels who were not infected with SARS-CoV-2 in Guangzhou, China. At the end of the closed-off management in Guangzhou city on November 30, 2022, their globulin levels were above the upper limit of the reference value. After ending of closed-off management, *i.e.*, exposure to SARS-CoV-2, their globulin levels all gradually decreased but remained above the lower reference limit.

When the lungs are invaded by bacteria causing pneumonia, the body's immune response, particularly the mucosal immune response, is triggered to fight off the infection (13, 14). The innate immune response acts as the initial defense, without requiring prior

10.3389/fimmu.2024.1404542

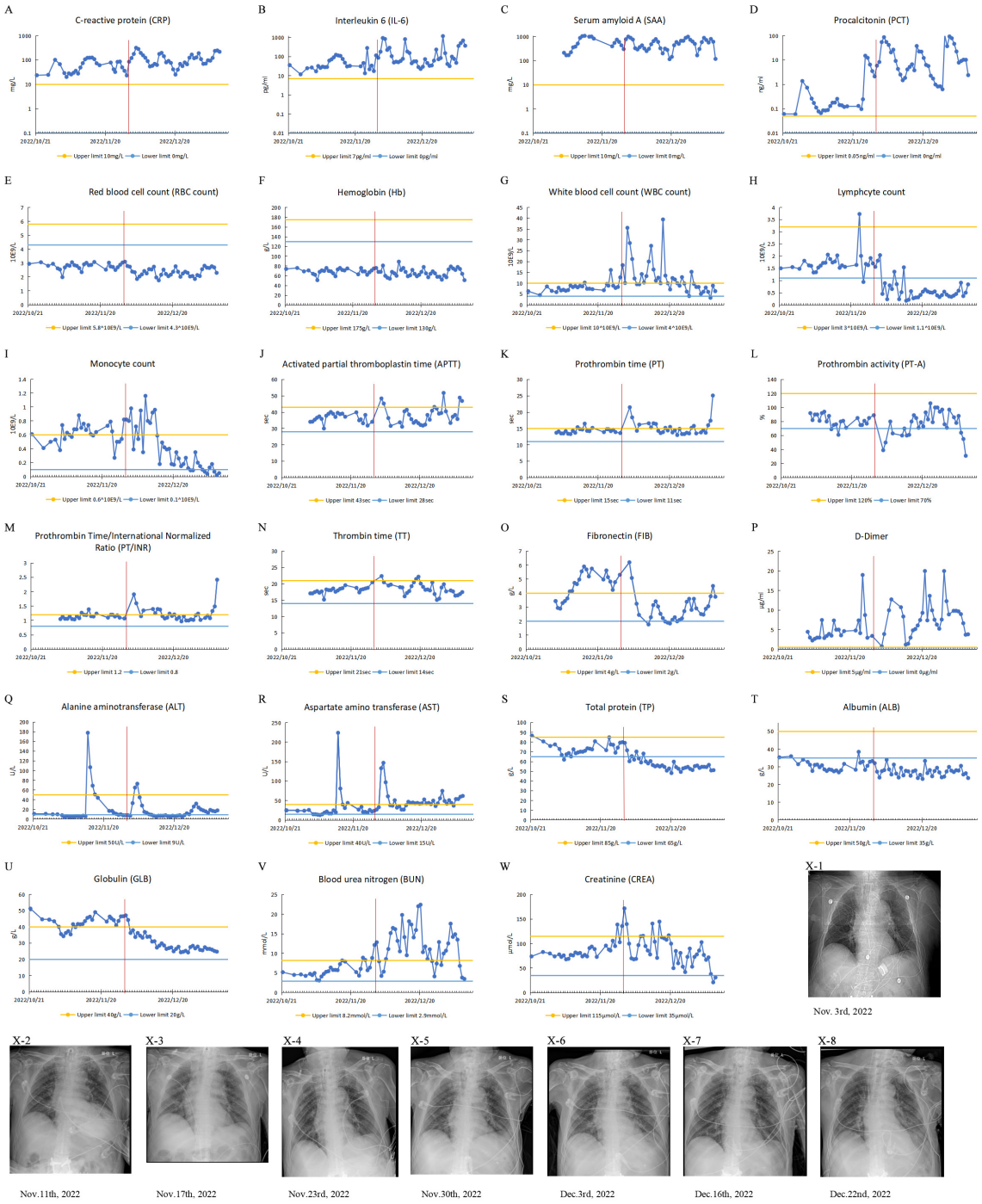

FIGURE 1
Clinical test results of case 1 from October 21, 2022, to January 9, 2023. The patient's IL-6 and PCT were measured with a Roche cobas e 601. CRP, SAA, TP, Alb, Glob, AST and ALT were measured with a BECKMAN COULTER AU5800. The patient's Routine blood tests were measured with a Mindray BC-6900 instrument. **(A-W)** Test results of patient's blood specimens. The horizontal axis represents the dates, and the solid blue dots indicate the test results at the corresponding time points. The red vertical line in the figure corresponds to November 30, 2022, when the city of Guangzhou ended closed-off management. **(A-D)** Infection-related test results: CRP, IL-6, PCT and SAA. **(E-I)** Routine blood test results: RBC, Hb, WBC, monocyte count, lymphocyte count. **(J-P)** Coagulation-related test results: APTT, PT, PT-A, PT/INR, TT, FIB and D-Dimer. **(Q, R)** Liver function-related test results: ALT and AST. **(S-U)** Serum protein-related test results: TP, ALB and GLB. **(V, W)** Renal function-related test results: BUN and CREA. **(X1-8)** CXR test results.

recognition of specific pathogens, while the mucosal barrier prevents pathogen entry. In response to invasion, the immune system triggers inflammation, releasing cytokines and chemokines to recruit other immune cells. Macrophages, neutrophils, and other cells are mobilized to engulf and destroy bacteria through phagocytosis, aided by enzyme release and reactive oxygen species. The adaptive immune system, involving T cells and B cells, also contributes. T cells help regulate the immune response

FIGURE 2
Clinical test results of case 2 from September 30, 2022, to December 31, 2022. **(A-W)** Test results of patient's blood specimens. The horizontal axis represents the dates, and the solid orange dots indicate the test results at the corresponding time points. The red vertical line in the figure corresponds to November 30, 2022, when the city of Guangzhou ended closed-off management. **(A-D)** Infection-related test results: CRP, IL-6, PCT and SAA. **(E-I)** Routine blood test results: RBC, Hb, WBC, monocyte count, lymphocyte count. **(J-P)** Coagulation-related test results: APTT, PT, PT-A, PT/INR, TT, FIB and D-Dimer. **(Q, R)** Liver function-related test results: ALT and AST. **(S-U)** Serum protein-related test results: TP, ALB and GLB. **(V, W)** Renal function-related test results: BUN and CREA. **(X)** CXR test result.

and activate immune cells, while B cells produce antibodies that bind to bacteria, marking them for destruction through opsonized phagocytosis or complement-mediated lysis, thus limiting pathogen spread.

The body's immune system mounts a complex and fine-tuned response to the infection of SARS-CoV-2 (15–17). Upon infection with SARS-CoV-2 via the respiratory tract, the body initiates a local immune response. Immune cells such as macrophages and monocytes are recruited to respond to the infection by releasing cytokines and generating an adaptive T-cell and B-cell immune response. CD8+ T-cells are able to directly attack and kill virus-infected cells, whereas CD4+ T-cells are essential for turning on the function of CD8+ T-cells and B-cells. In addition, CD4+ T-cells are responsible for the production of cytokines that drive the recruitment of immune cells. Activated B-cells produce specific antibodies to neutralize SARS-CoV-2.

Antibodies against other viruses, such as human immunodeficiency virus (HIV), middle east respiratory syndrome coronavirus (MERS-CoV), and dengue virus, can also neutralize SARS-CoV-2 due to cross-reactivity (18–21). Interestingly, BCG vaccination (attenuated strain of tubercle bacillus Mycobacterium) improves the patient's immunity against SARS-CoV-2 infection and improves prognosis (22). Several peptides of BCG proteins are highly homologous to that of the SARS-CoV-2 spike protein (22). BCG

vaccination increases IgG antibodies in mice, which could neutralize the SARS-CoV-2 leading to the blocking of the SARS-CoV-2 infection (22). In this study, we also predicted antigenic epitopes in the RBD region of the SARS-CoV-2 spike protein, which is closely associated with viral invasion (22), using online software, and compared the predicted antigenic epitopes ("NGVGYQ" and "KIADYNYKLP") (Supplementary Figures 1, 2) with the protein sequences of Escherichia coli and Klebsiella pneumoniae. Many peptides of protein sequences of *Escherichia coli* and *Klebsiella pneumoniae* were found to be highly homologous to the predicted antigenic epitopes of the RBD region of the SARS-CoV-2 spike protein (Supplementary Tables 1-3). Further ELISA results showed that the monoclonal antibody against SARS-CoV-2 could bind the antigens of *Escherichia coli* and *Klebsiella pneumoniae* (Supplementary Figure 3). Therefore, the above reports and results suggest that antibodies produced by the body induced by bacterial infections or bacterial antigens, may neutralize SARS-CoV-2 viruses and hence blocks its invasion.

Elevated levels of Infection-associated tests include SAA, PCT, CRP, and IL-6 indicate the presence of infection (23). Two patients we studied had consistently high levels of infection-related tests, suggesting the presence of a persistent infection. Persistent existence of microorganisms on mucosal surfaces can lead to robust adaptive immunity including producing antibodies (24, 25). Hence, we hypothesized that the high globulin levels in the patients by the end of November 2022 were due to the body's production of immunoglobulins induced by the persistent presence of infection in the body. And after exposure to SARS-CoV-2, the induced immunoglobulins, *i.e.* antibodies, cross-reacted with SARS-CoV-2, blocking the invasion and infection of SARS-CoV-2. A large amount of immunoglobulins in the body of patients are consumed to neutralize SARS-CoV-2, leading to a decrease in immunoglobulins and ultimately a corresponding decrease in the patient's globulins.

This study also has limitations. With only two cases reported, the sample size is too small to draw conclusions that are generally applicable, and therefore not representative of the entire population of patients with bacterial pneumonia. Subsequent analyses are warranted to involve a larger number of cases, which will be retrospectively analyzed in collaboration with several healthcare centers to investigate the relationship between bacterial pneumonia, globulin levels, and SARS-CoV-2 infection, considering various factors such as age, gender, and others.

4 Conclusion

Bacterial pneumonia patients with high globulin levels were less susceptible to SARS-CoV-2. The immunoglobulins induced by bacterial infection could neutralize SARS-CoV-2 blocking the virus's invasion and preventing infection. The results of the study are expected to provide new ideas for the prevention and treatment of SARS-CoV-2 infection. For example, when IVIG therapy is given to COVID-19 patients (26), the effect of using immunoglobulin extracted from patients with bacterial pneumonia may be more effective in treating SARS-CoV-2 infection compared to immunoglobulin sourced from healthy individuals.

Data availability statement

The raw data supporting the conclusions of this article will be made available by the authors, without undue reservation.

Ethics statement

The study was approved by the Ethics Committee of the First Affiliated Hospital of Guangdong Pharmaceutical University (Approval Document No. [2023] (11)). The studies were conducted in accordance with the local legislation and institutional requirements. The participants provided their written informed consent to participate in this study. Written informed consent was obtained from the participant/patient(s) for the publication of this case report.

Author contributions

QZ: Conceptualization, Data curation, Formal Analysis, Investigation, Methodology, Software, Validation, Writing – original draft, Writing – review & editing. QL: Conceptualization, Data curation, Formal Analysis, Investigation, Methodology, Software, Writing – original draft, Writing – review & editing. HL: Conceptualization, Data curation, Formal Analysis, Investigation, Methodology, Software, Writing – original draft, Writing – review & editing. CL: Data curation, Formal Analysis, Investigation, Methodology, Software, Writing – original draft, Writing – review & editing. XS: Data curation, Formal Analysis, Investigation, Methodology, Resources, Writing – original draft, Writing – review & editing. MY: Methodology, Software, Writing – original draft, Writing – review & editing. ZZ: Methodology, Software, Writing – original draft, Writing – review & editing. YH: Methodology, Software, Writing – original draft, Writing – review & editing. SW: Resources, Software, Writing – original draft, Writing – review & editing. ZY: Conceptualization, Formal Analysis, Funding acquisition, Project administration, Supervision, Writing – original draft, Writing – review & editing.

Funding

The author(s) declare financial support was received for the research, authorship, and/or publication of this article. This work was financially supported in by the Science and Technology Program of Guangzhou (grant no. 202103000051). The founder has no role in the study design and collection, analysis, and interpretation of the results.

Acknowledgments

We would like to thank Miss Bao-yi Liang and Mr. Rui Ye, two students at Guangdong Pharmaceutical University, and Mr. Shuo-qi Jiang, a student at Jining Medical University, for their technical support in data analysis.

Conflict of interest

The authors declare that the research was conducted in the absence of any commercial or financial relationships that could be construed as a potential conflict of interest.

Publisher's note

Supplementary material

The Supplementary Material for this article can be found online at: https://www.frontiersin.org/articles/10.3389/fimmu.2024.1404542/full#supplementary-material

References

1. Li Q, Guan X, Wu P, Wang X, Zhou L, Tong Y, et al. Early transmission dynamics in Wuhan, China, of novel coronavirus-infected pneumonia. *N Engl J Med*. (2020) 382:1199–207. doi: 10.1056/NEJMoa2001316

2. WHO. WHO Director-General's opening remarks at the media briefing on COVID-19 - 11 March 2020. Available online at: https://www.who.int/director-general/speeches/detail/who-director-general-s-opening-remarks-at-the-media-briefing-on-covid-19—11-march-2020.

3. Liu J, Liu M, Liang W. The dynamic COVID-zero strategy in China. *China CDC weekly*. (2022) 4:74–5. doi: 10.46234/ccdcw2022.015

4. ChinaDaily. Q&A: Details of implementing '20 measures' explained China Daily: China Daily. November 28, 2022. Available online at: https://www.Chinadaily.com.cn/a/202211/28/WS63833a2ea31057c47eba1469_4.html.

5. Xinhua. China actively optimizes COVID-19 response measures Xinhua2022-12-01. December 1, 2022. Available online at: https://english.news.cn/20221201/1fa2f59184144123af7266aa2f1b16d2/c.html.

6. ChinaDaily. Temporary controls in Guangzhou lifted. December 1, 2022. Available online at: http://guangdong.Chinadaily.com.cn/2022-12/01/c_835621.htm.

7. Yue W, Xiao-xiao S, Xiao-qi Z, Ke-liang Y, Han-wei L, Xiao-rong Y, et al. Analysis of SARS-CoV-2 infection among inpatients in a tertiary hospital in Guangzhou during the Covid-19 pandemic. *J OF SUN YAT-SEN UNIVERSITY(MEDICAL SCIENCES)*. (2023) 44:878–85. doi: 10.13471/j.cnki.j.sun.yat-sen.univ(med.sci).2023.0522

8. ChinaDaily. Guangzhou scrambles to treat COVID patients. December 16, 2022. Available online at: http://guangdong.Chinadaily.com.cn/2022-12/16/c_840132.htm.

9. Brooks WA. Bacterial pneumonia. In: *Hunter's Tropical Medicine and Emerging Infectious Diseases*. Amsterdakm, Netherlands: Elsevier (2020). p. 446–53.

10. Eshwara VK, Mukhopadhyay C, Rello J. Community-acquired bacterial pneumonia in adults: An update. *Indian J Med Res*. (2020) 151:287–302. doi: 10.4103/ijmr.IJMR_1678_19

11. Fazel P, Sedighian H, Behzadi E, Kachuei R, Imani Fooladi AA. Interaction between SARS-CoV-2 and pathogenic bacteria. *Curr Microbiol*. (2023) 80:223. doi: 10.1007/s00284-023-03315-y

12. Westblade LF, Simon MS, Satlin MJ. Bacterial coinfections in coronavirus disease 2019. *Trends Microbiol*. (2021) 29:930–41. doi: 10.1016/j.tim.2021.03.018

13. Korkmaz FT, Traber KE. Innate immune responses in pneumonia. *Pneumonia (Nathan)*. (2023) 15:4. doi: 10.1186/s41479-023-00106-8

14. Kumar V. Pulmonary innate immune response determines the outcome of inflammation during pneumonia and sepsis-associated acute lung injury. *Front Immunol*. (2020) 11:1722. doi: 10.3389/fimmu.2020.01722

15. Qi H, Liu B, Wang X, Zhang L. The humoral response and antibodies against SARS-CoV-2 infection. *Nat Immunol*. (2022) 23:1008–20. doi: 10.1038/s41590-022-01248-5

16. Tay MZ, Poh CM, Renia L, MacAry PA, Ng LFP. The trinity of COVID-19: immunity, inflammation and intervention. *Nat Rev Immunol*. (2020) 20:363–74. doi: 10.1038/s41577-020-0311-8

17. Ni L, Ye F, Cheng ML, Feng Y, Deng YQ, Zhao H, et al. Detection of SARS-CoV-2-specific humoral and cellular immunity in COVID-19 convalescent individuals. *Immunity*. (2020) 52:971–7.e3. doi: 10.1016/j.immuni.2020.04.023

18. Mishra N, Kumar S, Singh S, Bansal T, Jain N, Saluja S, et al. Cross-neutralization of SARS-CoV-2 by HIV-1 specific broadly neutralizing antibodies and polyclonal plasma. *PloS Pathog*. (2021) 17:e1009958. doi: 10.1371/journal.ppat.1009958

19. Tajuelo A, Lopez-Siles M, Mas V, Perez-Romero P, Aguado JM, Briz V, et al. Cross-recognition of SARS-CoV-2 B-cell epitopes with other betacoronavirus nucleoproteins. *Int J Mol Sci*. (2022) 23:2977. doi: 10.3390/ijms23062977

20. Dutta D, Ghosh A, Dutta C, Sukla S, Biswas S. Cross-reactivity of SARS-CoV-2 with other pathogens, especially dengue virus: A historical perspective. *J Med Virol*. (2023) 95:e28557. doi: 10.1002/jmv.28557

21. Wang C, van Haperen R, Gutierrez-Alvarez J, Li W, Okba NMA, Albulescu I, et al. A conserved immunogenic and vulnerable site on the coronavirus spike protein delineated by cross-reactive monoclonal antibodies. *Nat Commun*. (2021) 12:1715. doi: 10.1038/s41467-021-21968-w

22. Jackson CB, Farzan M, Chen B, Choe H. Mechanisms of SARS-CoV-2 entry into cells. *Nat Rev Mol Cell Biol*. (2022) 23:3–20. doi: 10.1038/s41580-021-00418-x

23. Zhu S, Zeng C, Zou Y, Hu Y, Tang C, Liu C. The clinical diagnostic values of SAA, PCT, CRP, and IL-6 in children with bacterial, viral, or co-infections. *Int J Gen Med*. (2021) 14:7107–13. doi: 10.2147/IJGM.S327958

24. Cerutti A, Chen K, Chorny A. Immunoglobulin responses at the mucosal interface. *Annu Rev Immunol*. (2011) 29:273–93. doi: 10.1146/annurev-immunol-031210-101317

25. McCoy KD, Ronchi F, Geuking MB. Host-microbiota interactions and adaptive immunity. *Immunol Rev*. (2017) 279:63–9. doi: 10.1111/imr.12575

26. Mazeraud A, Jamme M, Mancusi RL, Latroche C, Megarbane B, Siami S, et al. Intravenous immunoglobulins in patients with COVID-19-associated moderate-to-severe acute respiratory distress syndrome (ICAR): multicentre, double-blind, placebo-controlled, phase 3 trial. *Lancet Respir Med*. (2022) 10:158–66. doi: 10.1016/S2213-2600(21)00440-9

Frontiers in Immunology

Explores novel approaches and diagnoses to treat immune disorders.

The official journal of the International Union of Immunological Societies (IUIS) and the most cited in its field, leading the way for research across basic, translational and clinical immunology.

Discover the latest Research Topics

See more →

Frontiers

Avenue du Tribunal-Fédéral 34
1005 Lausanne, Switzerland
frontiersin.org

Contact us

+41 (0)21 510 17 00
frontiersin.org/about/contact